

DET KGL. DANSKE VIDENSKABERNES SELSKAB  
MATEMATISK-FYSISKE MEDDELELSER, BIND XXII, Nr. 1

---

THE ORBIT OF COMET  
DU TOIT-NEUJMIN-DELPORTE  
(1941 e)

BY

PETER NAUR



KØBENHAVN

I KOMMISSION HOS EJNAR MUNKSGAARD

1945





Comet 1941 e was discovered by DU TOIT on July 18th, 1941, by NEUJMIN on July 25th and by DELPORTE on August 19th. It was observed until October 20th, and 54 accurate observations are available. Several provisional orbits have been computed; the basis of this improvement is the following system, computed by GROSCH:

$$\left. \begin{array}{l}
 \text{Osculation 1941 Aug. 29.0 U.T.} \\
 T = 1941 \text{ July } 21.18766 \text{ U.T.} \\
 \omega = 69^{\circ}10'33''.3 \\
 \Omega = 229 \ 37 \ 7 \ .2 \\
 i = 3 \ 14 \ 49 \ .4 \\
 e = 0.5789569 \\
 \mu = 0^{\circ}.18099891 \\
 a = 3.0951760 \\
 P = 5^y.4456
 \end{array} \right\} \text{I}$$

From these elements I computed the following ephemeris. The perturbations from Jupiter were taken into account with the aid of ENCKE's method. It gives  $\alpha_{1950.0}$  and  $\delta_{1950.0}$  when  $t$ —light time is used as argument.

1941		0 <sup>h</sup> U. T.		$r$	$\Delta$	Light time
	$\alpha_{1950.0}$	$\delta_{1950.0}$				
July 20	20 <sup>h</sup> 1 <sup>m</sup> 28 <sup>s</sup> .87	— 6°44'52".7		1.303	0.294	0. 0017
	21	2 57 .44	35 14 .8			
	22	4 25 .82	26 1 .8			
	23	5 54 .03	17 14 .0			
	24	7 22 .09	8 51 .9			
	25	8 50 .03	6 0 55 .4	1.304	0.295	0 .0017
	26	20 10 17 .86	— 5 53 25 .1			

1941	$\alpha_{1950.0}$	$\delta_{1950.0}$	$r$	$\Delta$	Light time
Aug. 16	20 <sup>h</sup> 40 <sup>m</sup> 52 <sup>s</sup> .76	- 4°48'31".9			
17	42 19 .65	49 6 .7			
18	43 46 .52	49 56 .0			
19	45 13 .40	50 58 .5	1.344	0.345	0.0020
20	46 40 .32	52 13 .3			
21	48 7 .26	53 39 .7			
22	49 34 .30	55 16 .5			
23	51 1 .41	57 2 .8			
24	52 28 .63	4 58 57 .6	1.359	0.365	0.0021
25	53 55 .98	5 1 0 .1			
26	55 23 .47	3 9 .2			
27	56 51 .13	5 23 .9			
28	58 18 .94	7 43 .5			
29	20 59 46 .95	10 7 .0	1.376	0.388	0.0022
30	21 1 15 .12	12 33 .5			
31	2 43 .48	15 2 .3			
Sept. 1	4 12 .01	17 32 .7			
2	5 40 .72	20 3 .7			
3	21 7 9 .57	- 5 22 35 .2	1.395	0.414	0.0024
<hr/>					
Sept. 7	21 13 6 .40	- 5 32 29 .3			
8	14 35 .92	34 52 .3	1.416	0.444	0.0026
9	16 5 .58	37 11 .9			
10	17 35 .37	39 27 .6			
11	19 5 .28	41 39 .0			
12	20 35 .31	43 45 .7			
13	22 5 .49	45 47 .1	1.438	0.476	0.0027
14	23 35 .82	47 42 .9			
15	25 6 .30	49 32 .6			
16	26 36 .92	51 16 .0			
17	28 7 .71	52 52 .7			
18	29 38 .67	54 22 .3	1.462	0.513	0.0030
19	31 9 .80	55 44 .3			
20	32 41 .11	56 58 .8			
21	34 12 .62	58 5 .2			
22	35 44 .33	59 3 .4			
23	37 16 .25	5 59 53 .0	1.487	0.553	0.0032
24	38 48 .39	6 0 33 .7			
25	40 20 .74	1 5 .6			
26	41 53 .30	1 28 .3			
27	43 26 .07	1 41 .9			
28	44 59 .07	1 46 .1	1.514	0.596	0.0034
29	21 46 32 .20	- 6 1 40 .8			

1941		$\alpha_{1950.0}$	$\delta_{1950.0}$	$r$	$\Delta$	Light time
Oct. 11	22 <sup>h</sup>	5 <sup>m</sup> 21 <sup>s</sup> .40	- 5°48'19".2			
	12	6 56 .25	46 11 .5			
	13	8 31 .21	43 54 .6	1.600	0.747	0.0043
	14	10 6 .28	41 28 .5			
	15	11 41 .44	38 53 .4			
	16	13 16 .72	36 9 .1			
	17	14 52 .10	33 16 .1			
	18	22 16 27 .59	- 5 30 14 .0	1.631	0.805	0.0046

The following table gives the observations. The weights  $p$  were found from curves drawn with  $\Delta\alpha$  and  $\Delta\delta$  as ordinates and times as abscissae.

No.	$t$ —light time	$\alpha_{1950.0}$	$\delta_{1950.0}$	O—C		$p$	
				$\Delta\alpha \cos \delta$	$\Delta\delta$		
1	July 21.94483	20 <sup>h</sup> 4 <sup>m</sup> 21 <sup>s</sup> .18	- 6°26'28".0	+ 6 <sup>s</sup> .23	+ 3".9	1	Würzburg
2	22.00337	4 26 .5-	25 56 .-	+ 0 .4-	+ 4 .-	0	Sonneberg
3	22.03198	4 27 .58	25 25 .9	- 1 .06	+ 18 .6	1	Würzburg
4	24.91471	8 41 .82	1 24 .3	- 0 .71	+ 10 .7	1	—
5	24.98025	8 47 .69	0 45 .8	- 0 .60	+ 18 .8	1	—
6	25.03649	8 50 .7-	6 0 50 .-	- 2 .5-	- 12 .-	0	Sonneberg
7	Aug. 17.97581	43 45 .6-	4 49 59 .-	+ 1 .2-	- 4 .-	2	—
8	19.85465	46 27 .84	52 4 .5	+ 0 .16	- 2 .8	4	Uccle
9	19.89066	46 30 .43	52 4 .3	- 0 .38	+ 0 .2	4	—
10	20.85883	47 54 .59	53 27 .3	- 0 .40	- 0 .5	4	—
11	20.88549	47 57 .20	53 32 .4	- 0 .10	- 3 .2	4	—
12	20.90261	47 58 .80	53 32 .5	+ 0 .01	- 1 .7	4	—
13	22.87201	50 49 .81	56 51 .1	- 0 .45	- 2 .4	4	—
14	22.89635	50 52 .17	57 54 .3	- 0 .21	- 3 .0	4	—
15	22.90210	50 52 .79	57 6 .9	- 0 .09	- 14 .9	4	—
16	23.96282	52 26 .0-	4 59 17 .-	+ 0 .6-	- 24 .-	0	Torino
17	24.86235	53 43 .50	5 0 42 .5	- 0 .45	+ 0 .3	4	Uccle
18	24.90509	53 47 .80	0 39 .0	+ 0 .12	+ 9 .1	1	Torino
19	26.92494	56 44 .48	5 15 .5	- 0 .06	- 1 .8	4	Uccle
20	27.17961	57 6 .8-	5 53 .-	- 0 .1-	- 4 .-	3	Yerkes
21	27.86642	58 6 .6-	7 15 .-	- 0 .6-	+ 10 .-	2	Barcelona
22	27.95347	58 14 .67	7 36 .9	- 0 .18	0 .0	4	Uccle
23	28.11264	58 28 .67	8 0 .5	- 0 .17	- 1 .0	3	Washington
24	28.26938	58 42 .6-	8 22 .-	0 .0-	0 .-	3	Yerkes
25	28.90777	20 59 38 .56	9 56 .1	- 0 .26	- 2 .5	4	Uccle
26	30.90056	21 2 35 .10	14 41 .5	+ 0 .42	+ 5 .9	1	Torino
27	31.92046	4 4 .31	17 20 .7	- 0 .65	0 .0	2	Posen
28	Sept. 1.85346	5 29 .87	19 58 .8	+ 2 .16	- 17.3	0	—
29	8.82855	15 50 .02	36 45 .1	- 0 .18	+ 3 .1	4	Uccle
30	9.82287	21 17 19 .30	- 5 38 59 .2	- 0 .16	+ 4 .6	1	Torino

No.	$t$ —light time	$\alpha_{1950.0}$	$\delta_{1950.0}$	O—C		$p$	
				$\Delta\delta \cos\delta$	$\Delta\delta$		
31	Sept. 11.05975	21 <sup>h</sup> 19 <sup>m</sup> 10 <sup>s</sup> .24	— 5°41'52".9	— 0 <sup>s</sup> .42	— 6 .2	3	Yerkes
32	11.81540	20 20 .76	43 20 .1	+ 2 .08	+ 2 .6	0	Uccle
33	11.84068	20 22 .30	43 22 .5	+ 1 .34	+ 3 .3	0	—
34	12.06600	20 41 .05	43 56 .5	— 0 .21	— 2 .6	3	Yerkes
35	15.81748	26 19 .57	50 34 .5	— 0 .80	+ 23 .1	0	Uccle
36	15.84882	26 23 .57	50 50 .3	+ 0 .36	+ 10 .5	1	Torino
37	16.85134	27 53 .87	52 49 .0	— 0 .33	— 10 .3	1	—
38	17.81158	29 21 .17	54 3 .7	— 0 .35	+ 2 .3	4	Uccle
39	17.83023	29 22 .78	54 4 .6	— 0 .44	+ 3 .0	4	—
40	19.82196	32 24 .67	56 41 .8	— 0 .17	+ 4 .3	4	—
41	19.84004	32 26 .75	56 57 .2	+ 0 .26	— 9 .8	1	Torino
42	21.83026	35 28 .10	58 50 .2	— 0 .65	+ 3 .9	4	Uccle
43	21.86139	35 31 .24	58 54 .3	— 0 .37	+ 1 .5	2	Posen
44	22.87949	37 5 .48	59 55 .8	+ 0 .32	— 8 .4	1	Torino
45	22.91306	37 8 .00	5 59 46 .5	— 0 .25	+ 2 .5	3	Wien
46	23.81120	38 30 .41	6 0 27 .8	— 0 .57	— 1 .1	4	Uccle
47	23.84927	38 34 .55	0 36 .7	+ 0 .06	— 8 .6	1	Torino
48	23.89737	38 38 .45	0 28 .1	— 0 .47	+ 1 .8	3	Wien
49	24.92442	40 13 .23	1 2 .5	— 0 .52	+ 1 .0	3	—
50	25.83195	41 37 .23	1 20 .3	— 0 .50	+ 4 .8	4	Uccle
51	26.99327	43 14 .49	1 41 .6	— 10 .96	+ 0 .2	0	Wien
52	27.84472	21 44 43 .56	6 1 48 .1	— 1 .07	— 2 .0	4	Uccle
53	Oct. 12.79599	22 8 10 .14	5 44 25 .8	— 1 .69	— 2 .5	4	—
54	15.79004	22 12 54 .58	— 5 36 47 .4	— 2 .13	— 3 .0	4	—

Then the following normal-places were formed:

No.	$t$ —light time	$\alpha_{1950.0}$	$\delta_{1950.0}$	O — C		$\sqrt{p}$	Observations
				$\Delta\alpha \cos\delta$	$\Delta\delta$		
I	July 23.96660	20 <sup>h</sup> 7 <sup>m</sup> 18 <sup>s</sup> .61	— 6° 8'55".3	— 0 <sup>s</sup> .54	+ 13".0	2.0	1— 6
II	Aug. 21.70963	20 49 8 .89	— 4 54 50 .1	— 0 .13	— 2 .8	6.3	7—18
III	28.67058	20 59 17 .77	— 5 9 19 .7	— 0 .17	— 0 .4	5.1	19—27
IV	Sept. 10.44429	21 18 15 .06	— 5 40 27 .4	— 0 .25	— 0 .9	3.3	28—34
V	18.00066	21 29 38 .49	— 5 54 20 .5	— 0 .24	+ 1 .9	3.9	35—41
VI	23.96431	21 38 44 .57	— 6 0 31 .6	— 0 .53	+ 0 .8	5.4	42—52
VII	Oct. 14.26302	22 10 29 .49	— 5 40 51 .4	— 1 .91	— 2 .8	2.8	53—54

and the equations of condition were found to be:

$$\begin{aligned}
 &+ 19.8224dM_0 + 41.0626du + 0.51675de - 0.04082dp + 1.01137dq + 4.31135dr = - 8''.1 \\
 &+ 15.7863 + 313.934 + 4.02330 - 0.45481 + 0.94913 + 3.55031 = - 2 .0 \\
 &+ 14.3172 + 346.377 + 4.43659 - 0.52502 + 0.87727 + 3.27142 = - 2 .6 \\
 &+ 11.6652 + 375.150 + 4.79515 - 0.61045 + 0.72435 + 2.76488 = - 3 .8 \\
 &+ 10.23307 + 377.840 + 4.82050 - 0.63687 + 0.63137 + 2.48949 = - 3 .6 \\
 &+ 9.20276 + 374.803 + 4.77272 - 0.64718 + 0.56032 + 2.29043 = - 8 .0
 \end{aligned}$$



+ 6.40185	+ 346.345	+ 4.36920	- 0.63363	+ 0.34979	+ 1.74653	= -28 .7
+ 4.57092	+ 186.914	+ 2.11522	+ 0.17072	- 4.22992	+ 1.00660	= +13 .0
+ 4.69369	+ 225.102	+ 2.65361	+ 1.55773	- 3.25082	+ 1.15823	= - 2 .8
+ 4.44765	+ 218.084	+ 2.59019	+ 1.73256	- 2.89496	+ 1.12026	= - 0 .4
+ 3.86734	+ 198.156	+ 2.38399	+ 1.89444	- 2.24793	+ 1.00705	= - 0 .9
+ 3.49852	+ 184.847	+ 2.23945	+ 1.91311	- 1.89657	+ 0.92817	= + 1 .9
+ 3.21337	+ 174.481	+ 2.12452	+ 1.89822	- 1.64344	+ 0.86535	= + 0 .8
+ 2.36517	+ 143.986	+ 1.77517	+ 1.73495	- 0.95776	+ 0.67534	= - 2 .8

In solving this system I obtained the result:

$$\begin{aligned}
 dM_0 &= - 9''.342 \\
 d\mu &= - 8.4836 \\
 de &= + 661.46 \\
 dp &= - 7.05 \\
 dq &= - 44.94 \\
 dr &= + 52.63
 \end{aligned}$$

and the new elements:

$$\left. \begin{aligned}
 &\text{Osculation 1941 Aug. 29.0 U.T.} \\
 &T = 1941 \text{ July 21.20200 U.T.} \\
 &\omega = 69^\circ 17' 2''.0 \\
 &\Omega = 229 \ 39 \ 2 \ .9 \\
 &i = 3 \ 15 \ 26 \ .5 \\
 &e = 0.5821638 \\
 &\mu = 0^\circ.17864235 \\
 &a = 3.1223369
 \end{aligned} \right\} 1950.0 \quad \text{II}$$

Although the substitution of the improvements in the equations of condition were in good accordance with the normal-places this did not apply to the direct computation from the new elements, as the improvements were too great. The new residuals were:

	O - C	
No.	$\Delta\alpha \cos \delta$	$\Delta\delta$
I.....	+ 0 <sup>s</sup> .17	+ 4'' .8
II.....	+ 0 .59	+ 5 .5
III.....	+ 0 .55	+ 7 .0
IV.....	+ 0 .63	+ 3 .9
V.....	+ 0 .82	+ 5 .7
VI.....	+ 0 .76	+ 4 .4
VII.....	+ 0 .68	+ 4 .1

Therefore I computed the following new equations of condition from the elements II:

+ 19.98787	$dM_0$	+ 41.1398	$d\mu$	+ 0.51493	$de$	- 0.04044	$dp$	+ 1.00704	$dq$	+ 4.29344	$dr$	= + 2'' .4
+ 15.93193		+ 316.770		+ 4.03241		- 0.45270		+ 0.94600		+ 3.53893		= + 8 .9
+ 14.45154		+ 349.583		+ 4.44802		- 0.52274		+ 0.87456		+ 3.26146		= + 8 .3
+ 11.77827		+ 378.797		+ 4.80981		- 0.60802		+ 0.72250		+ 2.75767		= + 9 .5
+ 10.33399		+ 381.586		+ 4.83633		- 0.63447		+ 0.62995		+ 2.48351		= + 12 .3
+ 9.29457		+ 378.589		+ 4.78933		- 0.64484		+ 0.55924		+ 2.28537		= + 11 .4
+ 6.46903		+ 350.152		+ 4.38825		- 0.63164		+ 0.34962		+ 1.74401		= + 10 .2
+ 4.60872		+ 188.335		+ 2.12035		+ 0.16916		- 4.21253		+ 1.00231		= + 4 .8
+ 4.73383		+ 226.981		+ 2.66001		+ 1.55099		- 3.24107		+ 1.15390		= + 5 .5
+ 4.48611		+ 219.919		+ 2.59658		+ 1.72556		- 2.88689		+ 1.11621		= + 7 .0
+ 3.90173		+ 199.885		+ 2.39038		+ 1.88755		- 2.24296		+ 1.00376		= + 3 .9
+ 3.53017		+ 186.466		+ 2.24546		+ 1.90662		- 1.89304		+ 0.92527		= + 5 .7
+ 3.24289		+ 176.039		+ 2.13050		+ 1.89177		- 1.64065		+ 0.86281		= + 4 .4
+ 2.38812		+ 145.364		+ 1.78105		+ 1.73030		- 0.95775		+ 0.67376		= + 4 .1

These gave the new improvements and elements:

$$\begin{aligned}
 dM_0 &= - 3'' .647 \\
 d\mu &= - 0 .1432 \\
 de &= + 12 .35 \\
 dp &= - 0 .91 \\
 dq &= - 1 .17 \\
 dr &= + 17 .73
 \end{aligned}$$

$$\left. \begin{aligned}
 &\text{Osculation 1941 Aug. 29.0 U. T.} \\
 &T = 1941 \text{ July 21.20767 U. T.} \\
 &\omega = 69^\circ 17' 41'' .3 \\
 &\Omega = 229 \ 38 \ 41 \ .2 \\
 &\dot{i} = 3 \ 15 \ 27 \ .3 \\
 &e = 0.5822237 \\
 &a = 3.1228007 \\
 &\mu = 0^\circ .17860256 \\
 &P = 5^y .519
 \end{aligned} \right\} \text{III}$$

Hence we get the following residuals between the elements III and the normal-places:



No.	O — C			
	Differentially		Direct	
	$\Delta\alpha \cos \delta$	$\Delta\delta$	$\Delta\alpha \cos \delta$	$\Delta\delta$
I . . . . .	— 0'' .1	— 0'' .2	— 0'' .6	— 0'' .2
II . . . . .	+ 0 .5	— 0 .4	+ 0 .6	— 0 .4
III . . . . .	— 0 .9	+ 1 .2	— 1 .2	+ 1 .2
IV . . . . .	— 1 .3	— 1 .5	— 1 .2	— 1 .4
V . . . . .	+ 1 .1	+ 0 .7	+ 1 .0	+ 0 .8
VI . . . . .	— 0 .1	— 0 .4	— 0 .1	— 0 .4
VII . . . . .	— 1 .3	+ 0 .1	— 1 .3	+ 0 .1

An ephemeris for the opposition in 1946—47 will be published later.



DET KGL. DANSKE VIDENSKABERNES SELSKAB  
MATEMATISK-FYSISKE MEDDELELSER, BIND XXII, NR. 2

---

# INVESTIGATIONS ON THE GLYCOSIDASES OF MILK-SUGAR YEAST EMULSIN

BY

STIG VEIBEL,  
CHRISTIAN MØLLER, AND JØRGEN WANGEL



KØBENHAVN

I KOMMISSION HOS EJNAR MUNKSGAARD

1945

Printed in Denmark  
Bianco Lunos Bogtrykkeri A/S

NEUBERG and HOFMANN (1932) and HOFMANN (1932) have shown that milk-sugar yeast emulsin, in contrast to almond emulsin, provokes a quicker hydrolysis of  $\beta$ -galactosides than of  $\beta$ -glucosides.

Using an enzyme preparation from milk-sugar yeast (*saccharomyces fragilis Jørgensen*, one of the strains investigated by HOFMANN) we have to our astonishment found that  $\beta$ -galactosides were not hydrolysed at all, while on the contrary  $\beta$ -glucosides were hydrolysed, even if slowly, at a measurable velocity. Starting from this fact we have made a more thorough investigation of milk-sugar yeast emulsin in order to try to elucidate some problems concerning enzymic specificity. We are here presenting some results of this investigation.

The problem of the identity or non-identity of  $\beta$ -glucosidase and  $\beta$ -galactosidase has not yet been solved. For emulsin from almonds we know, principally from the close study made by HELFERICH and his co-workers (1938), that the two enzymes are, if not identical, at least so nearly related that all purifying or damaging manipulations which have been carried out have not been able to bring about a modification of the ratio between the  $\beta$ -glucosidatic and the  $\beta$ -galactosidatic effect. From this HELFERICH (1938) has drawn the conclusion that at any rate in almond emulsin the two enzymes are identical.

When emulsin from other sources than almond is used it is, however, no longer so. Through the investigations of NEUBERG and HOFMANN (see HOFMANN 1934, 1935) it was proved that the ratio between the  $\beta$ -glucosidatic and the  $\beta$ -galactosidatic effect of emulsin from milk-sugar yeast, from hip, from different *aspergillus*-species as well as of emulsin of animal origin (liver, kidney) is different from that found for almond emulsin. As an example may be mentioned that the  $\beta$ -glucosidatic effect, which

is the preponderant effect in almond emulsin, can barely be demonstrated in hip emulsin.

Later on HILL (1934) and HELFERICH and VORSATZ (1935) found that there is a still greater difference in alfalfa seed emulsin and in coffee emulsin, so that no  $\beta$ -glucosidatic effect at all is to be found. From this fact HELFERICH (1938, s. 96) draws the conclusion that there must exist two different  $\beta$ -galactosidases. One of them, which is present in almond emulsin, is identical with  $\beta$ -glucosidase, the other, which has been found e. g. in alfalfa seed emulsin, is different from  $\beta$ -glucosidase.

From the investigations hitherto mentioned no doubt has arisen as to the uniformity of the  $\beta$ -glucosidase from different sources.

ANTONIANI (1935), on the other hand, is of opinion that an enzyme preparation from the ungerminated seeds of *sorghum saccharatum* has only  $\beta$ -glucosidatic properties and no  $\beta$ -galactosidatic effect at all. This creates a doubt as to the uniformity of the  $\beta$ -glucosidase, which, according to HELFERICH, should be identical with one of the  $\beta$ -galactosidases, whereas ANTONIANI's  $\beta$ -glucosidase is obviously different from either of the two  $\beta$ -galactosidases.

HELPERICH is of opinion that the two  $\beta$ -galactosidases may be distinguished from each other by their behaviour toward o-cresol- $\beta$ -d-galactoside and phenol- $\beta$ -d-galactoside as expressed in the "Wertigkeit" of the two galactosides. (Wertigkeit =  $k_{50\%}/e$  (log. 2)). For the  $\beta$ -galactosidase of the type found in almond emulsin the Wertigkeit of o-cresol- $\beta$ -d-galactoside is considerably (some 8 times) greater than that of phenol- $\beta$ -d-galactoside, just as it has been found for the two corresponding glucosides. For the  $\beta$ -galactosidase of the type found in alfalfa seed emulsin, on the contrary, the two Wertigkeits are nearly alike, that of o-cresol- $\beta$ -d-galactoside being somewhat inferior to that of phenol- $\beta$ -d-galactoside.

The significance of this is, however, reduced by the fact that MIWA and co-workers (1937) found similar differences for  $\beta$ -glucosidase from different sources. They use more dilute solutions than HELFERICH, hoping that possible differences in the affinities between the substrates and the enzyme will thereby better manifest themselves than in the more concentrated



solutions used by HELFERICH. From their investigations we learn that for emulsin from different *prunus*-species the ratio between the Wertigkeits of o-cresol- $\beta$ -d-glucoside and phenol- $\beta$ -d-glucoside is 25:1, for emulsin from *glucine hispada* it is 0.97:1, from *cucumbita moschata* 0.46:1 and for emulsin from different *aspergillus*-species the ratio drops to 0.025:1. These differences are greater than those stated for the two presumed  $\beta$ -galactosidases, and the findings of MIWA and co-workers render the assumption of only one  $\beta$ -glucosidase, common to all enzyme preparations with  $\beta$ -glucosidatic faculties, very unlikely.

The experiments described below prove that with emulsin from *saccharomyces fragilis Jørgensen* the finding of ANTONIANI that there exists a  $\beta$ -glucosidase which does not at the same time catalyse the hydrolysis of  $\beta$ -galactosides, as well as the findings of MIWA and co-workers, that for some  $\beta$ -glucosidase-preparations the Wertigkeit of phenol- $\beta$ -d-glucoside is greater than that of o-cresol- $\beta$ -d-glucoside, are corroborated.

One of the present authors (VEIBEL and ERIKSEN, 1937) has previously shown that velocity constants,  $k_{\text{obs}}$ , or Wertigkeits, as calculated directly from the hydrolysis experiments, are not suitable as a means of comparing the facility of hydrolysis of different substrates, since differences of  $k_{\text{obs}}$  may be caused either by differences of  $K_m$ , the dissociation constant of the enzyme-substrate compound, or by differences of  $k_3$ , the real unimolecular velocity constant for the fission of the enzyme-substrate compound into the products of hydrolysis, glucose, aglucone and enzyme. This will appear from the expression used for the calculation of  $k_3$  (VEIBEL and LILLELUND 1938, 1940 1, 2):

$$k_3 = \frac{k_{\text{obs}}}{e(\text{sal.f.})} (K_m + c + (K_m/K_{m_1} + K_m/K_{m_2} - 1) x)$$

or, in the initial stage of the hydrolysis,

$$k_3 = \frac{k'_{\text{obs}}}{e(\text{sal.f.})} (K_m + c)$$

$k_3$  and  $K_m$  having the signification mentioned above,  $k_{\text{obs}}$  and  $k'_{\text{obs}}$  being the directly calculated unimolecular velocity con-



stants of the hydrolysis,  $k_{\text{obs}}$  calculated from point to point,  $k'_{\text{obs}}$  from time zero to time  $t$ ,  $K_{m_1}$  and  $K_{m_2}$  being the dissociation constants of the compounds formed by the enzyme with the products of hydrolysis,  $e$  conventionally being  $g$  enzyme in 50 ml reaction mixture and  $\text{sal.f.} = k_{\text{obs } 50\%}/e$  for a 0.139 n salicin solution in acetate buffer at  $p_{\text{H}} 4.4$ .  $\text{Sal.f.}$  may be calculated also from the velocity constant of hydrolysis of e. g. o-cresol- $\beta$ -d-glucoside, see VEIBEL and LILLELUND (1938).

Also when enzyme preparations of different origin are compared it seems likely that a comparison of the  $k_3$ -values of a deliberately chosen substrate is to be preferred to the comparison of the  $k_{\text{obs}}$ -values, as it may be presumed that  $K_m$  is determined not only by the prostetic group of the enzyme, but that it is also influenced by the nature of the colloidal carrier, and even if it is presumed that the prostetic group of the  $\beta$ -glucosidase is identical in all enzyme preparations with a  $\beta$ -glucosidatic effect, it will surely not be true that the colloidal carriers are also identical. The differences found by MIWA and co-workers may possibly be explained as differences in  $K_m$  caused by different colloidal carriers.

In the above-mentioned paper (VEIBEL and LILLELUND, 1940, 2)  $K_m$ ,  $K_{m_1}$ ,  $K_{m_2}$  and  $k_3$  were determined for o-cresol- $\beta$ -d-glucoside, using almond emulsin as enzyme. The determinations were made in different buffer solutions and at different  $p_{\text{H}}$ . In order to find an answer to the question as to the identity or non-identity of almond emulsin and milk-sugar yeast emulsin we have, with milk-sugar yeast emulsin as a catalyst, tried to determine  $K_m$ ,  $K_{m_1}$ ,  $K_{m_2}$  and  $k_3$  for o-cresol- $\beta$ -d-glucoside, this time confining ourselves to the use of phosphate-citrate buffer (Mc. ILVAINE, 1921). The result of the investigation may be summarized as follows:

The  $p_{\text{H}}$ -optimum which, using almond emulsin, was found at  $p_{\text{H}} 4.4$  (phosphate-citrate buffer) is, when milk-sugar yeast emulsin is used, at  $p_{\text{H}} 5.7-5.9$ .

The affinity constant of the o-cresol- $\beta$ -d-glucoside  $K_m$  was determined at 0.050, using almond emulsin at  $p_{\text{H}} 6.0$ . When milk-sugar yeast emulsin is used the affinity between enzyme and substrate is appreciably greater, all of the enzyme being

combined with the substrate even in 0.01 m solutions of the substrate.

These differences may possibly be explained as being due to differences in the nature of the colloidal carrier. If the view put forward above is correct, the  $k_3$ -value is independent of the colloidal carrier, and if the two  $\beta$ -glucosidases are identical, we should find the same  $k_3$ -value in both cases. We have previously found (VEIBEL and LILLELUND, 1940, 2)  $k_3 = 42.5 \cdot 10^{-2}$  (phosphate-citrate buffer,  $p_H$  6.0, almond emulsin). Now we find, under identical experimental conditions, values for  $\frac{k'_{obs}}{e} (K_m + c) = k_3$  (sal.f.) between  $0.012 \cdot 10^{-2}$  and  $0.0012 \cdot 10^{-2}$ . In order to obtain a  $k_3$ -value of  $42.5 \cdot 10^{-2}$  we must presume sal.f.-values between 0.0003 and 0.00003 for the milk-sugar yeast emulsin preparations examined. Calculation of sal.f. from the  $k_{obs}$ -values of 0.04 m solutions of o-cresol- $\beta$ -d-glucoside have, however, given values between 0.0007 and 0.00007, and the  $k_3$ -value, when milk-sugar yeast is used, is consequently only about half of the value found when using almond emulsin, thus indicating a difference between the two  $\beta$ -glucosidases. Other peculiarities are, however, still more difficult to reconcile with the assumption of only one  $\beta$ -glucosidase, identical with one of the two  $\beta$ -galactosidases.

In almond emulsin the  $\beta$ -galactosidatic effect at the  $p_H$ -optimum of the  $\beta$ -glucosidase is usually about 1/6—1/13 of the  $\beta$ -glucosidatic effect. With the preparation of almond emulsin used by us we have found  $k_{obs \text{ glucoside}}/k_{obs \text{ galactoside}}$  for 0.04 m solutions of o-cresol- $\beta$ -d-glycosides (phosphate-citrate buffer) 7.1 at  $p_H$  4.4, 6.3 at  $p_H$  6.0. (VEIBEL and co-workers, not yet published). If the  $\beta$ -glycosidase in milk-sugar yeast emulsin were identical with the  $\beta$ -glucosidase of almond emulsin we should, therefore, expect a  $k_{obs}$ -value for the galactoside about 1/6—1/7 of the  $k_{obs}$ -value of the glucoside, presuming that the affinity constants of o-cresol- $\beta$ -d-glucoside and of o-cresol- $\beta$ -d-galactoside are not very different, for milk-sugar yeast emulsin as well as for almond emulsin. As we tried, however, to determine the velocity constant of the hydrolysis of o-cresol- $\beta$ -d-galactoside with milk-sugar yeast emulsin as a catalyst, we



found that no measurable hydrolysis took place, even though the change in rotation was expected to be some  $0.06^\circ$ . This result was obtained with all milk-sugar yeast emulsin preparations examined, and it is, in our opinion, very difficult to explain, if the  $\beta$ -glucosidase present is identical with one of the  $\beta$ -galactosidases presumed by HELFERICH.

HOFMANN (1932), on the other hand, states that milk-sugar yeast emulsin hydrolyses  $\beta$ -galactosides more rapidly than  $\beta$ -glucosides. The only  $\beta$ -galactoside of which an investigation has been reported is, however, milk-sugar. We have, therefore, tried our preparations of milk-sugar yeast emulsin against milk-sugar. The result was the same as that obtained in trying it against o-cresol- $\beta$ -d-galactoside, no hydrolysis whatever could be detected.

From these findings it results that, even if in accordance with HELFERICH we assume the  $\beta$ -glucosidase of almond emulsin to be identical with the  $\beta$ -galactosidase of the same enzyme preparation, we must admit that at least two  $\beta$ -glucosidases exist, since the  $\beta$ -glucosidase of the milk-sugar yeast emulsin has no  $\beta$ -galactosidatic properties.

Possibly, however, two different types of milk-sugar yeast emulsin may be isolated, since the preparation of HOFMANN is in several respects different from our preparations. A closer study may perhaps show whether it will be possible to indicate procedures by which milk-sugar yeast emulsin with or without  $\beta$ -galactosidatic properties can be prepared at will.

NEUBERG and HOFMANN (1932) mention that their preparation of milk-sugar yeast emulsin is capable of hydrolysing raffinose, 1- $\alpha$ -galactosido < 1,5 > 6- $\alpha$ -glucosidose < 1,5 > 2-fructose. Our preparations, too, hydrolyse raffinose and the hydrolysis presumably leads to the formation of melibiose and fructose, this assumption according better with the changes in rotation observed than the assumption of the formation of galactose and sucrose or the complete splitting of the trisaccharide into 3 molecules of monosaccharide. A more thorough study of the action of milk-sugar yeast emulsin upon raffinose will be published elsewhere.

As mentioned above, HELFERICH is of opinion that a characteristic of the  $\beta$ -glucosidase of almond emulsin is that o-cresol-

$\beta$ -d-glucoside is hydrolysed at a greater velocity than phenol- $\beta$ -d-glucoside. In this respect too there is a difference between almond emulsin and milk-sugar yeast emulsin. We find that the  $k_{\text{obs}}$  of a 0.04 m solution of phenol- $\beta$ -d-glucoside is about twice as great as the  $k_{\text{obs}}$  of a 0.04 m solution of o-cresol- $\beta$ -d-glucoside. Much the same must be the case with the  $k_3$ -values of the two glucosides, if the  $K_m$ -values of o-cresol- $\beta$ -d-glucoside and phenol- $\beta$ -d-glucoside against milk-sugar yeast emulsin are not very different. (For a peculiarity concerning phenol- $\beta$ -d-glucoside see the experimental part).

### Experimental part.

Preparation of substrates. 1. Phenol- $\beta$ -d-glucoside. Phenol- $\beta$ -d-glucoside-tetracetate was prepared according to the method of HELFERICH and SCHMITZ-HILLEBRECHT (1933), which is quoted also in a paper by ZEMPLÉN (1938). Yield 42 % as stated by HELFERICH and SCHMITZ-HILLEBRECHT. F. 125.5°;  $[\alpha]_{\text{D}}^{20} = -23.0^\circ$  ( $\text{CHCl}_3$ ,  $c = 0.999$ ,  $\alpha^{20} = -0.460^\circ$ , all measurements in 2 dm tubes) in fairly good accordance with the findings of HELFERICH and SCHMITZ-HILLEBRECHT, F. = 124–125°,  $[\alpha]_{\text{D}}^{20} = -22.0^\circ$  ( $\text{CHCl}_3$ ). In the paper of ZEMPLÉN  $[\alpha]_{\text{D}}$  is erroneously given at  $-71^\circ$ , the value found by HELFERICH and SCHMITZ-HILLEBRECHT for the free glucoside, not for the tetracetate.

The acetyl-groups were removed by means of sodium methylate in methyl alcohol (ZEMPLÉN and PASCU (1929)). The glucoside isolated showed F. 173–174° (capillary tube),  $[\alpha]_{\text{D}}^{20} = -64.1^\circ$  (water,  $c = 0.963$ ,  $\alpha^{20} = -1.235^\circ$ ). HELFERICH and SCHMITZ-HILLEBRECHT indicate F. = 144–145°,  $[\alpha]_{\text{D}}^{20} = -64.8^\circ$ . As we tried to determine the melting point on bloc maquette we observed that at 145° the substance melted and after a moment solidified again and then melted at 173–174°. 145° is, therefore, the melting point of the glucoside with crystal water, 173–174° the melting point of the anhydrous glucoside. The water content of the glucoside was determined by drying it in vacuum over  $\text{P}_2\text{O}_5$  at 78°. 1.2007 g lost 0.1483 g = 12.35 %. Kept at room temperature in an atmosphere saturated with water vapour 0.1465 g was regained in 4 days. No further water uptake could



be registered during the following 7 days. For  $C_6H_{11}O_5OC_6H_5$ ,  $2H_2O$  is calculated a water content of 12.33 %.

$[\alpha]_D^{20}$  of the anhydrous glucoside is  $-72.6^\circ$  (water,  $c = 0.992$ ,  $\alpha^{20} = -1.440^\circ$ ). HELFERICH and SCHMITZ-HILLEBRECHT indicate  $[\alpha]_D^{20} = -71.0^\circ$  (water).

o-Cresol- $\beta$ -d-glucoside, o-cresol- $\beta$ -d-galactoside and phenol- $\beta$ -d-glucoside were prepared analogically and showed the constants indicated in the literature.

Salicin, milk-sugar and raffinose were commercial preparations (MERCK).

Preparation and estimation of the enzymic force of emulsin from *saccharomyces fragilis* Jørgensen.

The emulsin preparations I—III described below are derived from a culture of *saccharomyces fragilis* Jørgensen which had kindly been placed at the disposal of one of the authors some years ago by Professor NEUBERG, Berlin-Dahlem, and which had since then been preserved at Alfred Jørgensens gæringsfysiologiske Laboratorium, Copenhagen. Preparations IV and V are derived from a culture of *saccharomyces fragilis* Jørgensen, strain 14, and preparations VI and VII from a Dutch strain of the same fungus, both belonging to the said laboratory and kindly placed at our disposal.

All cultures were grown on beer wort containing  $\frac{1}{2}$  % milk-sugar. After some 3 weeks the cultures were filtered by suction. The cultivation and the filtration were carried out at the laboratory mentioned above. We are glad to take the opportunity of thanking the director of the laboratory, Mr. ALBERT HANSEN, and the head of the fermentation department, Mr. F. de FONTENAY, most cordially for all help in preserving and cultivating the yeast preparations.

The procedure adopted in isolating an emulsin preparation from the yeast cells was that described by NEUBERG and HOFMANN (1932) and by HOFMANN (1932) for the preparations I—IV. For the preparations V—VII we have examined the activity of the centrifuged and filtered plasmolysate and then from this solution prepared a dry preparation, using the method indicated by HELFERICH (1932) for the purification of almond emulsin, precipitating the enzyme by tannin.

The activities of the preparations examined are indicated in Table I (substrate *o*-cresol- $\beta$ -*D*-glucoside).

Table I.

Emulsin prp. nr. ....	I	II	III	IV	V	VI	VII	V	VI	VII
								Plasmolysate		Dry preparation
$10^2 \cdot k/e$ .....	0.34	0	0.04	0	0.02	—	0.2	0.03	0	0.12

These figures were obtained by carrying out hydrolysis experiments at  $30^\circ$  in phosphate-citrate buffer ( $p_H = 6.0$ ). It was found later on that the emulsin powder loses in activity, rapidly at first, more slowly later on. These initial determinations carried out immediately after the preparation of the emulsin have, therefore, only a limited value.

0.1–0.3 g emulsin was dissolved in 25–45 ml of water. 2 ml were added, at  $30^\circ$ , to a 25 ml measuring flask containing a solution of *o*-cresol- $\beta$ -*D*-glucoside in phosphate-citrate buffer ( $p_H 6.0$ ), previously placed in a  $30^\circ$ -thermostat. Water was added to the mark, the glucoside concentration thus being regulated to 0.040 m.

At convenient intervals 5 ml samples were taken and added to 1 ml of a 20%  $K_2CO_3$ -solution, all enzymic action being thus suppressed. The progress of the hydrolysis was followed polarimetrically, the measurements not being carried out till the mutarotation had been given time to come to an end (2–3 hours) and attention being paid to the sources of error pointed out by VEIBEL and ERIKSEN (1936). The actual content of emulsin in 50 ml of the solution in consideration ( $e$  in Table I) was determined by drying 10 ml of the emulsin solution at  $105^\circ$  and dividing the weight of dry material by 2.5.

Table II summarizes the results obtained.

It will be seen that within the first 24–33 hours the inactivation in solution is some 25–40% but in the next 24 hours it is rather negligible. It will also be seen, on comparison of the values of  $k/e$  for the fresh emulsin-preparations and for the same preparations some days old, that these preparations, which lost a considerable part of their activity during the first few days, have conserved most of the remaining activity for a much longer period of time (some 30–50 days).

Table II.

	$10^2 \cdot k/e$				
	freshly prepared	some days old	30—50 days old	24—33 h. in solution at 30°	48 h. in solution at 30°
Prp. I .....	0.9	0.34	0.29	0.22	—
Prp. II .....	0	—	—	—	—
Prp. III .....	0.2	0.04	0.028	0.016	0.015
Prp. IV .....	0	—	—	—	—
Prp. V Plasmolysate .....	0.02	—	—	—	—
Prp. V Dry prp. ....	—	0.03	—	—	—
Prp. VI Dry prp. ....	0	—	—	—	—
Prp. VII Plasmolysate ...	0.2	—	—	—	—
Prp. VII Dry prp. ....	—	0.12	—	—	—

Determination of the  $p_H$ -optimum for milk-sugar yeast emulsin.

The velocity constants of hydrolysis of 0.04 m solutions of *o*-cresol- $\beta$ -*D*-glucoside in phosphate-citrate buffer at  $p_H$  5.0, 5.4, 5.8, 6.2, 6.6 and 7.0 (6.0 ml buffer solution in 25 ml reaction mixture) were determined. To each measuring flask were added 2 ml of an emulsin solution (preparation I).  $e$  was determined to be 0.0217, The hydrolysis was followed during some 6000 minutes, the degree of hydrolysis being then 45–65 %.

Table III and figure 1 show that the  $p_H$ -optimum is at  $p_H$  5.7–5.9.

Table III.

$p_H$ .....	5.0	5.4	5.8	6.2	6.6	7.0
$10^2 \cdot k/e$ .....	0.29	0.31	0.32	0.29	0.26	0.20

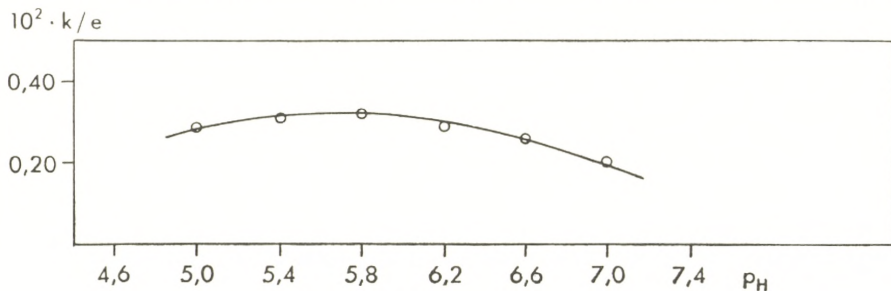


Figure 1.

This agrees fairly well with the statement of NEUBERG and HOFMANN (1932) that the optimal effect is obtained at  $p_H$  6.3–6.0,



but is rather different from the  $p_H$ -optimum of almond emulsin, for which VEIBEL and LILLELUND (1940, 2) found  $p_H$  4.4 in phosphate-citrate buffer.

Determination of  $K_m$ , the dissociation constant of the enzyme-substrate-complex. *o*-Cresol- $\beta$ -d-glucoside, phosphate-citrate buffer,  $p_H$  6.0.

The affinity between milk-sugar yeast emulsin and *o*-cresol- $\beta$ -d-glucoside is so great that a determination by the method usually adopted by VEIBEL and co-workers (VEIBEL and LILLELUND 1940, I) could not be carried through, this method not being sufficiently sensitive. From the experiments registered in Table IV it will be seen, however, that the enzyme is practically completely bound to the substrate, even at a substrate concentration of 0.01 m. Table IV indicates, for a series of glucoside solutions of different concentrations containing emulsin in identical concentration, the change of rotation after 4 different intervals of time. The identity of these changes of rotation, within the limits of error, indicates that for all 6 concentrations the concentration of the enzyme-substrate compound, which is the velocity-determining substance, is identical.

Table IV.

Changes in rotation  $\alpha$  of solutions of *o*-cresol- $\beta$ -d-glucoside.

Time min.	Concentration of glucoside solution					
	0.01	0.02	0.04	0.06	0.08	0.10
Emulsin preparation I.						
150	0.060°	0.055°	0.055°	0.045°	0.045°	0.060°
300	0.105°	0.100°	0.095°	0.085°	0.085°	0.100°
480	0.155°	0.155°	0.125°	0.125°	0.140°	0.150°
1440	0.355°	0.380°	0.375°	0.365°	0.365°	0.390°
Emulsin preparation V. Plasmolysate.						
1440	0.18°	0.19°	0.12°	0.14°	0.11°	
2880	0.31°	0.33°	0.31°	0.28°	0.28°	
4320	0.38°	—	0.45°	0.43°	0.42°	
5760	* 0.45°	0.58°	0.58°	0.57°	0.58°	

\* For 0.01 m solution the maximum change in rotation by complete hydrolysis is 0.49°.

From this it may be concluded that 0.001 is a maximum value for  $K_m$ , as the fraction of the emulsin present in the solution, which has combined with the substrate, is  $c/K_m + c$ ,  $c$  being the concentration of the substrate. At the concentration 0.01 m a  $K_m$ -value of 0.001 indicates that 90 % of the enzyme have combined with the substrate, and a difference of combination from 90 % to 99 % is to be detected, even here where the exactitude of the readings is diminished owing to the darkness of the solutions of milk-sugar yeast emulsin.

For *o*-cresol- $\beta$ -*D*-glucoside and almond emulsin VEIBEL and LILLELUND (1940, 2) found the  $K_m$ -value 0.050 in phosphate-citrate buffer at  $p_H$  6.0. The affinity between the glucoside and milk-sugar yeast emulsin is, therefore, at least 50 times as great as that between the glucoside and almond emulsin, and a difference between the two enzymes is seen to exist in this respect as well as in regard to the  $p_H$ -optimum (see above).

Determination of  $K_{m_1}$ , the dissociation constant of the enzyme-glucose-compound, in phosphate-citrate buffer at  $p_H$  6.0.

Here the usual technique was used, i. e. determination of the velocity constants of the hydrolysis of 0.04 m solutions of *o*-cresol- $\beta$ -*D*-glucoside which at the same time are 0.00, 0.02, 0.04 or 0.08 m respectively with regard to glucose. The concentration of the enzyme (preparation I) was the same in all 4 solutions.  $K_{m_1}$  is then usually determined from the expression

$$K_{m_1} = \frac{K_m \cdot c_{\text{glucose}}}{(K_m + c) (k/k_H - 1)}$$

(VEIBEL 1937),  $k$  and  $k_H$  being the velocity constants for the hydrolysis of solutions without and with glucose respectively. Here no definite value of  $K_m$  is obtainable, but at all events  $K_m$  is negligible as compared with  $c$  and the above expression may be written

$$K_{m_1} = \frac{K_m \cdot c_{\text{glucose}}}{c \cdot (k/k_H - 1)}$$

Table V gives the result, which is  $K_{m_1} = 7 K_m$ . For almond emulsin VEIBEL and LILLELUND (1940, 2) found  $K_m = 0.050$ ,

$K_{m_1} = 0.35$ , i. e.  $K_{m_1} = 7 K_m$ . In this respect there is, consequently, no difference between the two enzymes.

Table V.

$C_{\text{glucose}}$ .....	0.00	0.02	0.04	0.08
$10^4 \cdot k'$ .....	0.51	0.48	0.45	0.38
$k/k_H - 1$ .....	—	0.07	0.13	0.34
$K_{m_1}$ .....	—	$6 K_m$	$8 K_m$	$6 K_m$
Average value of $K_{m_1} \dots 7 K_m$				

Attempts at determination of  $K_{m_2}$ , the dissociation constant of the enzyme-o-cresol-compound, in phosphate-citrate buffer at  $p_H 6.0$ .

While the determination of  $K_{m_1}$  presented no difficulties whatever, the determination of  $K_{m_2}$  met with some anomalies which we did not encounter in the determination of  $K_{m_2}$  in the case of almond emulsin. The technique was exactly the same as that used in determining  $K_{m_1}$ , only with o-cresol instead of glucose. The results are indicated in Table VI (preparation I) and Table VII (preparation III).

Table VI.

Determination of  $K_{m_2}$  for o-cresol. Emulsin preparation I.

t	c-x	$10^4 \cdot k'$	c-x	$10^4 \cdot k'$	c-x	$10^4 \cdot k'$	c-x	$10^4 \cdot k'$
	0.00 m		0.02 m		0.04 m		0.08 m o-cresol	
0	2.245	—	2.245	—	2.245	—	2.245	—
533	2.105	0.53	2.110	0.51	2.155	0.34	2.185	0.22
1440	1.940	0.44	1.870	0.55	1.915	0.48	2.145	0.14
2880	1.665	0.45	1.555	0.55	1.685	0.43	2.175	—
5810	1.250	0.44	1.130	0.52	1.335	0.39	2.175	—
average...	0.46		0.53		0.41		—	

Table VII.

Determination of  $K_{m_2}$  for o-cresol. Emulsin preparation III.

t in.	c-x	$10^4 \cdot k'$	c-x	$10^4 \cdot k'$	c-x	$10^4 \cdot k'$	c-x	$10^4 \cdot k'$	c-x	$10^4 \cdot k'$	c-x	$10^4 \cdot k'$
	0.000 m		0.005 m		0.010 m		0.015 m		0.020 m		0.040 m o-cresol	
0	1.945	—	1.945	—	1.945	—	1.945	—	1.945	—	1.945	—
440	1.820	0.200	1.810	0.217	1.820	0.200	1.810	0.217	1.790	0.250	1.830	0.183
380	1.710	0.194	1.705	0.199	1.705	0.199	1.710	0.194	1.700	0.203	1.720	0.185
320	1.650	0.165	1.610	0.190	1.615	0.187	1.670	0.153	1.615	0.187	1.660	0.159
760	1.570	0.161	1.530	0.181	1.510	0.191	1.550	0.171	1.575	0.159	1.640	0.129
average...	0.18		0.20		0.19		0.18		0.20		0.16	



Both experiments show concordantly that *o*-cresol in small concentrations not only has no inhibiting effect but that, on the contrary, it seems to accelerate the hydrolysis of the glucoside. At higher concentrations, however, the inhibition is very considerable and it seems to be non-competitive, as the hydrolysis comes completely to a stand-still (see Table VI, 0.08 m *o*-cresol).

It was clearly seen that *o*-cresol in not too low concentrations has a special effect, for the addition of the enzyme-solution to the *o*-cresol-containing solution at once caused a turbidity, most distinct in the solution richest in *o*-cresol.

On account of these difficulties it has been impossible to determine any  $K_{m_1}$ -value.

#### Determination of $k_3$ for *o*-cresol- $\beta$ -*D*-glucoside.

In previous papers (VEIBEL and collaborators 1937, 1938, 1940, 1) it was pointed out that the directly determined velocity constants of hydrolysis of glucosides are not very convenient as a basis of comparison. Instead it was recommended to use  $k_3$ , determined by the expression  $k_3 = k_{\text{obs}} (K_m + c + (K_m/K_{m_1} + K_m/K_{m_2} - 1) x)/e$  (sal.f.), which is independent of the concentration of substrate used in the experiment, and in which the inhibiting effect of the products of hydrolysis are to a great extent accounted for.

As, however, it has not been possible to determine a  $K_{m_2}$ -value for *o*-cresol- $\beta$ -*D*-glucoside and milk-sugar yeast emulsin, we must confine ourselves to the use of an approximative expression for the calculation of  $k_3$ :  $k_3 = k'_{\text{obs}} (K_m + c)/e$  (sal.f.) or, if an inhibiting substance with dissociation constant of its enzyme-compound  $K_{m_h}$  is present in a concentration  $c_h$ ,  $k_3 = k'_{\text{obs}} (K_m + c + K_m/K_{m_h} \cdot c_h)/e$  (sal.f.). These approximative formulae are valid for the initial stage of the hydrolysis only, where the effect of the products of hydrolysis is not considerable.

In Table VIII we have calculated the  $k_3$ -values for all hydrolysis experiments at  $p_H$  6.0, using the values  $K_m = 0.001$  and  $K_{m_1} = 7 K_m$  in the calculations.

The mean value of all  $k_3$ -determinations is  $19.2 \cdot 10^{-2}$ . The values found with substrate concentrations 0.01 m and 0.02 m

are considerably higher than the mean value. This may mean that the  $K_m$ -value 0.001 is too high, but, as was pointed out above (p. 14), this value is a maximum value.

For the hydrolysis of *o*-cresol- $\beta$ -*D*-glucoside catalysed by almond emulsin we previously found (VEIBEL and LILLELUND 1940, 2)  $k_3 = 42.5 \cdot 10^{-2}$  (phosphate-citrate buffer,  $p_H = 6.0$ ). The velocity of hydrolysis of the enzyme-substrate compound is, therefore, in the case of milk-sugar yeast emulsin only about half the value in the case of almond emulsin, another feature showing the difference between the two glucosidases.

Table VIII.  
 $k_3$ -values of *o*-cresol- $\beta$ -*D*-glucoside.

$c_{\text{glucoside}}$	$c_{\text{glucose}}$	$k' \cdot 10^4$	e	sal. f.	$k_3 \cdot 10^2$	Enzyme prp. nr.
0.0390	0.00	3.73	0.1104	0.0007	19.3	I
0.0098	0.00	3.76	0.0245	0.0007	23.7	I
0.0197	0.00	1.61	0.0245	0.0007	19.6	I
0.0394	0.00	0.70	0.0245	0.0007	17.0	I
0.0590	0.00	0.43	0.0245	0.0007	15.3	I
0.0789	0.00	0.33	0.0245	0.0007	15.5	I
0.0983	0.00	0.30	0.0245	0.0007	17.7	I
0.0460	0.00	0.51	0.0192	0.0007	17.8	I
0.0460	0.02	0.48	0.0192	0.0007	17.9	I
0.0460	0.04	0.45	0.0192	0.0007	17.7	I
0.0460	0.08	0.38	0.0192	0.0007	16.4	I
0.0400	0.00	0.59	0.0256	0.0004	20.5	III fresh
0.0400	0.00	0.18	0.0600	0.00007	17.6	III old
0.0400	0.00	0.26	0.0930	0.00007	16.4	III old
0.0100	0.00	2.49	0.1296	0.00006	35.2	V Plasmolysate
0.0200	0.00	1.05	0.1296	0.00006	28.4	V Plasmolysate
0.0400	0.00	0.40	0.1296	0.00006	21.1	V Plasmolysate
0.0600	0.00	0.27	0.1296	0.00006	21.2	V Plasmolysate
0.0800	0.00	0.21	0.1296	0.00006	21.9	V Plasmolysate
0.1000	0.00	0.18	0.1296	0.00006	23.4	V Plasmolysate
0.0400	0.00	0.09	0.0262	0.00007	20.1	V dry prp.
0.0400	0.00	3.1	0.1572	0.00004	20.0	VII Plasmolysate
0.0400	0.00	0.70	0.0584	0.00003	16.4	VII dry prp.
average value...					19.2	

### Investigation of the hydrolysability of milk-sugar.

HOFMANN (1932) has investigated the hydrolysis of milk-sugar, catalysed by milk-sugar yeast emulsin. He finds that at



37° and  $p_H$  6.7 (phosphate buffer) a 0.045 m solution of milk-sugar is hydrolysed to 63 % in 105 min., to 82 % in 284 min. As his  $e$ -value is 0.05,  $10^2 \cdot k_{obs}/e$  is 9.20 or 5.20. At 30° and  $p_H$  6.0 a value for  $k_{obs}/e$  of about  $8 \cdot 10^{-2}$  is to be expected for a 0.040 m solution, at least for hydrolysis to some 50 %.

We have placed a 0.1000 m milk-sugar solution (phosphate-citrate buffer,  $p_H$  6.0) containing milk-sugar yeast emulsin (preparation I) at 30°.  $e = 0.0217$ . Even after 2980 minutes no change in rotation of the solution could be observed. This means that no greater change than 0.02° has taken place. As the change in rotation for complete hydrolysis of a 0.1000 m milk-sugar solution is 7.04° this means that  $k_{obs}/e$  as a maximum value is  $0.002 \cdot 10^{-2}$ , i. e. 1/4000 of the value found by HOFMANN for a 0.045 m solution.

For a 0.0400 m solution of *o*-cresol- $\beta$ -*D*-galactoside containing milk-sugar yeast emulsin (preparation I,  $e = 0.0112$ ) no change in rotation was observed during 2665 min. Assuming again 0.02° as the limit of change in rotation not observed, a maximum value for  $k_{obs}$  is  $0.04 \cdot 10^{-4}$ , for  $k_{obs}/e$  (sal. f.)  $24 \cdot 10^{-2}$ , i. e. 1/20 of the value found for *o*-cresol- $\beta$ -*D*-glucoside.

We have repeated this experiment with other preparations of milk-sugar yeast emulsin, both plasmolysates and dry preparations. In no case have we observed any change in rotation of the milk-sugar solution. Practically, therefore, these enzyme preparations are inactive towards milk-sugar.

#### Investigation of the hydrolysis of raffinose.

NEUBERG and HOFMANN (1932) state that raffinose is hydrolysed by milk-sugar yeast emulsin. Their experiments were carried out at 22° in acetate buffer ( $p_H$  4.7), the solution being 0.057 m as regards raffinose. The result was a  $k_{obs}/e$ -value of about  $1.5 \cdot 10^{-2}$ , assuming a hydrolysis to melibiose and fructose, i. e. the action of an  $\alpha$ -glucosidase or a fructosidase.

We have examined the hydrolysis of a 0.0400 m solution of raffinose in phosphate-citrate buffer at  $p_H$  6.0. Table IX gives the result.

It will be seen that the result is practically the same as that obtained by NEUBERG and HOFMANN. With other prepara-

tions of milk-sugar yeast emulsin we have obtained quite analogous results, but a more detailed description of the results will be published elsewhere.

Table IX.  
Hydrolysis of raffinose (to melibiose and fructose).

t min		x	c-x	k · 10 <sup>4</sup>
0	+ 4.105	—	1.955	—
235	+ 3.410	0.695	1.260	8.1
1433	+ 2.080	2.025	—	—

$$c = 0.048. \quad k/e = 1.7 \cdot 10^{-2}.$$

Investigations of the hydrolysis of phenol- $\beta$ -d-glucoside.

Table X records the determination of the velocity of hydrolysis of phenol- $\beta$ -d-glucoside catalysed by milk-sugar yeast emulsin.

Table X.

Hydrolysis of phenol- $\beta$ -d-glucoside.  $c = 0.0400$ .  $e = 0.0217$ .  
 $\alpha_{\text{beg}} = -1.275^\circ$ .  $\alpha_{\text{end}} = +0.620^\circ$ .  $\alpha_{\text{Emulsin}} = 0^\circ$  Phosphate-citrate  
buffer.  $p_{\text{H}} 6.0$ . Enzyme preparation I.

t min	$\alpha$	c-x	10 <sup>4</sup> · k'
0	-1.275	1.895	—
240	-1.100	1.720	1.76
521	-0.950	1.570	1.57
1440	-0.535	1.155	1.46
2980	-0.110	0.730	1.39
6157	+0.355	0.265	1.39

average... 1.51

$$10^2 \cdot k'/e = 0.70.$$

By comparison with e. g. Table III (p. 12) it is seen that a 0.04 m solution of phenol- $\beta$ -d-glucoside is hydrolysed somewhat more than twice as quickly as an equimolar solution of o-cresol- $\beta$ -d-glucoside, whereas HELFERICH and co-workers (1935) state that with almond emulsin as a catalyst o-cresol- $\beta$ -d-glucoside is hydrolysed 13 times as quickly as phenol- $\beta$ -d-glucoside. In order to find out whether this difference is due to a difference



in affinity between the two glucosidases and the substrates (different  $K_m$ -values) or possibly to a difference in the velocity of fission of the enzyme-substrate compounds of the two glucosides (different  $k_3$ -values) we have attempted to determine the  $K_m$ -values of phenol- $\beta$ -d-glucoside, with almond emulsin as well as with milk-sugar yeast emulsin as catalyst.

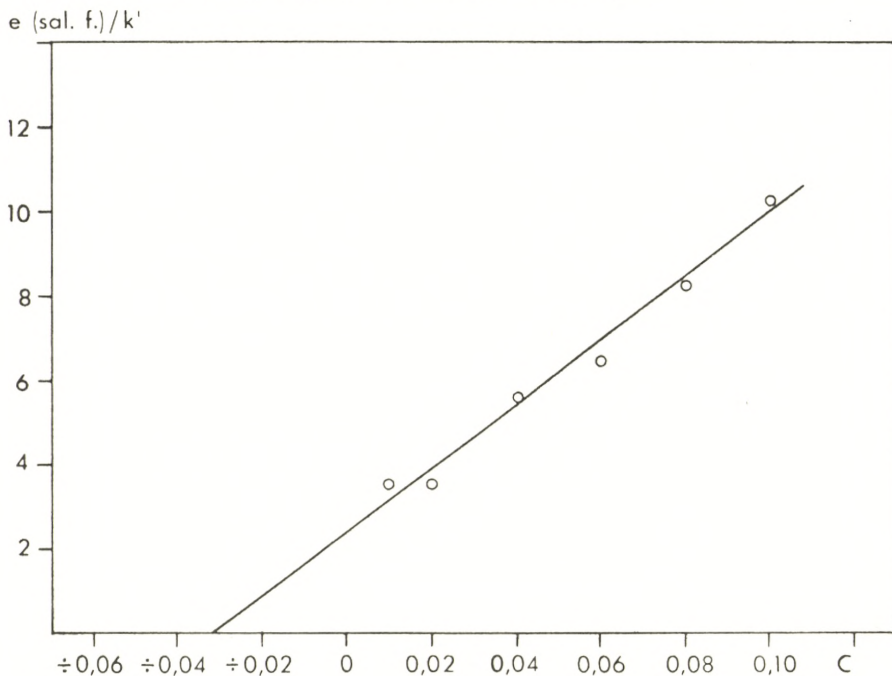


Fig. 2. Determination of  $K_m$ . Phenol- $\beta$ -d-glucoside.  $p_H$  6.0. Almond emulsin.

The determination of  $K_m$ , using almond emulsin, met with no difficulty whatever, the value found, 0.033 (for material see Table XI and fig. 2), shows that the affinity of phenol- $\beta$ -d-glucoside to almond emulsin is somewhat greater than the affinity of o-cresol- $\beta$ -d-glucoside to almond emulsin ( $K_m = 0.050$ ).

A determination of  $K_m$  using milk-sugar yeast emulsin was, however, not possible as phenol- $\beta$ -d-glucoside apparently has an inhibiting effect on the enzyme. The velocity of hydrolysis decreases rapidly with time, as will be seen from Table XII, which indicates the changes in rotation of 6 different glucoside solutions after 4 different intervals of time. For the more concentrated solutions the reaction comes to a complete standstill.

Table XI.

Determination of  $K_m$ . Phenol- $\beta$ -d-glucoside. Almond emulsin.  
Phosphate-citrate buffer.  $p_H$  6.0.  $30^\circ$ .

$c_{\text{glucoside}}$	$10^2 \cdot k'/e$ (sal. f.)	$e$ (sal. f.)/ $k'$	$10^2 \cdot k_3$
0.0100	28.2	3.55	1.21
0.0200	28.2	3.55	1.49
0.0400	18.1	5.54	1.31
0.0600	15.6	6.43	1.45
0.0800	12.2	8.22	1.38
0.1000	9.7	10.29	1.29
		average...	1.36

$$K_m = 0.033.$$

Table XII.

Changes in rotation  $\alpha$  of solutions of phenol- $\beta$ -d-glucoside.  
Milk-sugar yeast emulsin.

Time min	Concentration of glucoside solution					
	0.01	0.02	0.04	0.06	0.08	0.10
	Emulsin preparation I					
213	0.060°	0.085°	0.045°	0.050°	0.100°	0.015°
465	0.085°	0.120°	0.120°	0.100°	0.105°	0.075°
1440	0.320°	0.390°	0.295°	0.225°	0.205°	0.150°
2865	0.455°	0.540°	0.385°	0.300°	0.605° (?)	0.190°
	Emulsin preparation III					
1440	0.275°	0.280°	0.225°	0.190°	0.195°	0.205°
2880	0.375°	0.395°	0.300°	0.285°	0.280°	0.275°
4320	0.465°	0.505°	0.340°	0.285°	0.255°	0.250°
5760	0.455°	0.595°	0.385°	—	—	—

### Discussion.

During this and previous investigations we have found the following values of  $k'_{\text{obs}}/e$  (sal. f.), valid for 0.0400 m glucoside solutions in phosphate-citrate buffer at  $p_H$  6.0.

o-Cresolglucoside, almond emulsin  $468 \cdot 10^{-2}$

o-Cresolglucoside, milk-sugar yeast emulsin  $456 \cdot 10^{-2}$

Phenolglucoside, almond emulsin  $18.1 \cdot 10^{-2}$

Phenolglucoside, milk-sugar yeast emulsin  $1000 \cdot 10^{-2}$ .

From these values we have calculated the  $k_3$ -values.

o-Cresolglucoside, almond emulsin  $42.5 \cdot 10^{-2}$ .

o-Cresolglucoside, milk-sugar yeast emulsin  $19.2 \cdot 10^{-2}$ .

Phenolglucoside, almond emulsin  $1.36 \cdot 10^{-2}$   
 (Phenolglucoside, milk-sugar yeast emulsin  $31 \cdot 10^{-2}$ ).

The value for  $k_3$  for phenolglucoside, milk-sugar yeast emulsin is calculated, assuming a  $K_m$ -value not exceeding 0.001, as was the case for o-cresolglucoside. It was shown above that a determination of the  $K_m$ -value is impossible.

The constants found for o-cresol- $\beta$ -d-glucoside does not render impossible the identity of the glucosidases found in almonds and in milk-sugar. If, however, the constants found for phenol- $\beta$ -d-glucoside also are compared, the differences are so great that it seems improbable that the two glucosidases can be identical. This is very clearly seen from Table XIII.

Table XIII.

Comparison of emulsin from almond and from milk-sugar yeast.

$$\frac{k_{\text{obs cresol almond}}}{k_{\text{obs cresol milk-sugar yeast}}} = 1.0 \quad \frac{k_{\text{obs phenol almond}}}{k_{\text{obs phenol milk-sugar yeast}}} = 0.02$$

$$\frac{k_3 \text{cresol a.}}{k_3 \text{cresol m.}} = 2.1 \quad \frac{k_3 \text{phenol a.}}{k_3 \text{phenol m.}} = 0.04$$

$$\left[ \frac{k_{\text{obs cresol}}}{k_{\text{obs phenol}}} \right]_{\text{almond}} = 26 \quad \left[ \frac{k_{\text{obs cresol}}}{k_{\text{obs phenol}}} \right]_{\text{milk-sugar yeast}} = 0.5$$

$$\left[ \frac{k_3 \text{cresol}}{k_3 \text{phenol}} \right]_{\text{almond}} = 31 \quad \left[ \frac{k_3 \text{cresol}}{k_3 \text{phenol}} \right]_{\text{milk-sugar yeast}} = 0.6.$$

### Summary.

An investigation of a milk-sugar yeast emulsin preparation (from *saccharomyces fragilis* Jørgensen) has proved that by this enzyme

- 1) o-Cresol- $\beta$ -d-glucoside is hydrolysed
- 2) o-Cresol- $\beta$ -d-galactoside and milk-sugar are not hydrolysed
- 3) Raffinose is hydrolysed
- 4) Phenol- $\beta$ -d-glucoside is hydrolysed twice as quickly as o-cresol- $\beta$ -d-glucoside.



This is in partial disagreement with the findings of NEUBERG and HOFMANN who state that

- 1) Milk-sugar, salicin and raffinose are all hydrolysed
- 2) Milk-sugar is hydrolysed much more rapidly than  $\beta$ -d-glucosides.

Preliminary determinations of  $k_{\text{obs}}$ ,  $K_m$ ,  $K_{m_2}$  and  $k_3$  for o-cresol- $\beta$ -d-glucoside and  $k_{\text{obs}}$ ,  $K_m$  and  $k_3$  for phenol- $\beta$ -d-glucoside have been given.

The results obtained are hardly reconcilable with the assumption of HELFERICH that there only exists one  $\beta$ -glucosidase, which is identical with one of the two galactosidases assumed by HELFERICH, as the  $\beta$ -glucosidase examined by us does not hydrolyse  $\beta$ -galactosides. Another difference from the  $\beta$ -glucosidase examined by HELFERICH is that it hydrolyses phenol- $\beta$ -d-glucoside more rapidly than o-cresol- $\beta$ -d-glucoside, whereas the  $\beta$ -glucosidase examined by HELFERICH hydrolyses o-cresol- $\beta$ -d-glucoside some 13 times as quickly as phenol- $\beta$ -d-glucoside.

Thanks are due to the Carlsberg Foundation for a grant which enabled one of us (J. W.) to take part in this work.

*From the Chemical Laboratory,  
University of Copenhagen.*

---

### References.

- ANTONIANI (1935) R. Inst. Lomb. Sc. e. Lettere, Rendiconti [2], 68, 355.  
HELPERICH (1938) *Ergebn. Enzymf.* 7, 95. Here other references.  
HELPERICH, GOOTZ, PETERS and GÜNTHER (1932) *Z. physiol. Chem.* 208, 91.  
HELPERICH, SCHEIBER, STREECK and VORSATZ (1935) *Liebigs Ann.* 518, 213.  
HELPERICH and SCHMITZ-HILLEBRECHT (1933) *Ber. dtsh. Chem. Ges.* 66, 378.  
HELPERICH and VORSATZ (1935) *Z. physiol. Chem.* 237, 254.  
HILL (1934) *Ber. Verh. Sächs. Akad. Wiss.* 86, 115.  
HOFMANN (1932) *Biochem. Z.* 256, 462.  
HOFMANN (1934) *Naturwiss.* 22, 406.  
HOFMANN (1935) *Biochem. Z.* 281, 438.  
JOSEPHSON (1925) *Z. physiol. Chem.* 147, 1.  
MC ILVAINE (1921) *J. biol. Chem.* 49, 183.  
MIWA, CHENG, FUJISAKE and TOISCHI (1937) *Acta Phytochim. (jap.)* 10, 155.  
NEUBERG and HOFMANN (1932) *Biochem. Z.* 256, 450.  
VEIBEL (1937) *Enzymol.* 3, 147.  
VEIBEL and ERIKSEN (1936) *Biochem. J.* 30, 163.  
VEIBEL and ERIKSEN (1937) *D. Kgl. Danske Vidensk. Selskab, Math.-fys. Medd.* XIV, 15.  
VEIBEL and LILLELUND (1938) *Enzymol.* 5, 129.  
VEIBEL and LILLELUND (1940, 1) *D. Kgl. Danske Vidensk. Selskab. Math.-fys. Medd.* XVII, 6.  
VEIBEL and LILLELUND (1940, 2) *Enzymol.* 9, 161.  
WEIDENHAGEN (1929) *Z. Verein dtsh. Zuckerind.* 79, 591.  
ZEMPLÉN (1938) *Fortschr. Chem. org. Naturst.* I p. 18.  
ZEMPLÉN and PASCU (1929) *Ber. dtsh. Chem. Ges.* 62, 1613.

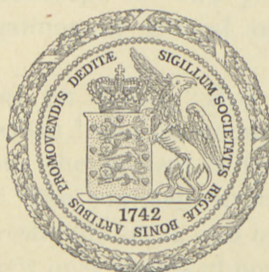
DET KGL. DANSKE VIDENSKABERNES SELSKAB  
MATEMATISK-FYSISKE MEDDELELSER, BIND XXII, NR. 3

---

# THE STRUCTURE OF $\text{BaCl}_2 \cdot 2\text{H}_2\text{O}$

BY

AKSEL TOVBORG JENSEN



KØBENHAVN

I KOMMISSION HOS EJNAR MUNKSGAARD

1945



THE POLYMERIZATION OF VINYL MONOMERS  
BY FREE RADICAL MECHANISM

# THE STRUCTURE OF POLYMER

BY  
J. V. FITZPATRICK



Printed in Denmark.  
Bianco Lunos Bogtrykkeri A/S

## INTRODUCTION

The structural differences between  $\text{CuCl}_2, 2\text{H}_2\text{O}^1$  and  $\text{SrCl}_2, 2\text{H}_2\text{O}^2$  are readily explained by the fact that the bonds of the Cupric ion are directional while the bonds of the Strontium ion are not. The reason why there exist a considerable number of different structures of compounds  $\text{AX}_2, 2\text{H}_2\text{O}$  (A being an alkaline earth metal, X a halogen) is less obvious. Usually a compound type with only one "variable", the radius ratio  $\frac{R_{\text{cation}}}{R_{\text{anion}}}$ , is not expected to exhibit such a variety of different crystal structures. However, it must be borne in mind that  $R_{\text{H}_2\text{O}}$  is probably constant, so that we have two variables,  $\frac{R_{\text{cation}}}{R_{\text{anion}}}$  and  $\frac{R_{\text{anion}}}{R_{\text{H}_2\text{O}}}$ , each of which on alteration tend to alter the structure.

In other words, we have a definition interval which is a rectangle and not a straight line. The only way to an understanding of the dynamics of a group of compounds is through a detailed knowledge of their geometry. The present paper and the preceding one<sup>2</sup> provide this knowledge for two points of the definition interval, but investigations of several other points would be desirable.

X-ray investigations on  $\text{BaCl}_2, 2\text{H}_2\text{O}$  were commenced by NÁRAY-SZABÓ and SASVÁRI,<sup>3</sup> who abandoned it. After a considerable amount of labour the present author also had to leave the problem unsolved. The complete structure of  $\text{SrCl}_2, 2\text{H}_2\text{O}^2$ , however, shed some fresh light on it, and by utilizing all the scattered data and some new ones it proved possible to determine the complete structure of  $\text{BaCl}_2, 2\text{H}_2\text{O}$ .

<sup>1</sup> D. HARKER, Z. Krist. **93** (1936) 136.

<sup>2</sup> A. TOVBORG JENSEN. D. Kgl. Danske Vidensk. Selskab, Mat.-fys. Medd. XX (1942) Nr. 5.

<sup>3</sup> ST. V. NÁRAY-SZABÓ and K. SASVÁRI, Z. Krist. **97** (1937) 235.



### Crystallography of $\text{BaCl}_2, 2\text{H}_2\text{O}$ .

The crystal class of  $\text{BaCl}_2, 2\text{H}_2\text{O}$  was shown by WYROUBOFF and GROTH<sup>1</sup> to be  $2/m$  ( $C_{2h}$ ), the monoclinic holohedral class. The space group was found by NÁRAY-SZABÓ and SASVÁRI to be  $P2_1/n$  ( $C_{2h}^5$ ). The systematic absences in diagrams indexed by the author are in agreement with  $P2_1/n$ , and the structure finally arrived at proves the assignment of  $\text{BaCl}_2, 2\text{H}_2\text{O}$  to the holohedral class to be correct.

The space group  $C_{2h}^5$  in the orientation  $P2_1/n$  has the following special points:

$$2: (a) \ 000; \frac{1}{2} \frac{1}{2} \frac{1}{2}$$

$$(b) \ \frac{1}{2} 00; \ 0 \frac{1}{2} \frac{1}{2}$$

$$(c) \ \frac{1}{2} \frac{1}{2} 0; \ 00 \frac{1}{2}$$

$$(d) \ \frac{1}{2} 0 \frac{1}{2}; \ 0 \frac{1}{2} 0$$

and the general point

$$4: (e) \ xyz; \ \bar{x}\bar{y}\bar{z}; \ \frac{1}{2} + x, \ \frac{1}{2} - y, \ \frac{1}{2} + z; \ \frac{1}{2} - x, \ \frac{1}{2} + y, \ \frac{1}{2} - z.$$

The structure factor is

$$A = 4 \cos 2\pi \left( hx + lz + \frac{h+k+l}{4} \right) \cos 2\pi \left( ky - \frac{h+k+l}{4} \right)$$

$$B = 0$$

separated

$$h + k + l = 2n \quad \left| \begin{array}{l} A = -4 \cos 2\pi (hx + lz) \cos 2\pi ky \\ B = 0 \end{array} \right.$$

$$h + k + l = 2n + 1 \quad \left| \begin{array}{l} A = -4 \sin 2\pi (hx + lz) \sin 2\pi ky \\ B = 0. \end{array} \right.$$

The lattice constants given in<sup>2</sup> and a set of accurate values obtained by the author are given in Table 1. The agreement is

<sup>1</sup> GMELINS Handbuch d. anorg. Ch. System Nr. 30. Ba.

<sup>2</sup> ST. V. NÁRAY-SZABÓ and K. SASVÁRI. Z. Krist. **97** (1937) 235.



good. The second set is considered the more accurate, since they are determined from powder photographs (Phragmén focussing camera and circular Bradley camera, 191 mm. diameter), while the first set are from oscillation photographs.

$\text{BaCl}_2 \cdot 2\text{H}_2\text{O}$  is the well known hydrate of  $\text{BaCl}_2$ .  $\text{BaCl}_2 \cdot \text{H}_2\text{O}$  has never been obtained from an aqueous solution. KIRSCHNER (<sup>1</sup> p. 180) prepared  $\text{BaCl}_2 \cdot \text{H}_2\text{O}$  by treating solid  $\text{BaCl}_2 \cdot 2\text{H}_2\text{O}$  with methyl alcohol. The solubility curve of  $\text{BaCl}_2 \cdot 2\text{H}_2\text{O}$  is known from the cryohydratic point  $-7.8^\circ$  and upwards. The temperature at which this curve and the solubility curve of the lower hydrate (monohydrate) intersect is not known, but it has been stated to be above  $60^\circ\text{C}$ . *Vide*<sup>1</sup> p. 180. Incidentally this temperature has been found to lie between  $108^\circ$  and  $110^\circ\text{C}$ ., in the course of experiments to prepare mixed crystals of  $\text{BaCl}_2 \cdot 2\text{H}_2\text{O}$  and  $\text{BaBr}_2 \cdot 2\text{H}_2\text{O}$  with a maximum of  $\text{BaBr}_2 \cdot 2\text{H}_2\text{O}$ . Below  $108^\circ\text{C}$ . crystals of  $\text{BaCl}_2 \cdot 2\text{H}_2\text{O}$  under mother liquor will keep indefinitely; above  $110^\circ\text{C}$ ., they deteriorate rapidly.

### Catalogues of Reflections.

The following lists of reflections were applied in deducing the structure.

(1) Complete set of  $30^\circ$  oscillation diagrams of [001] zone, camera diameter 100 mm,  $\text{CuK}_\alpha$  radiation.

(2) Complete series of  $30^\circ$  oscillation diagrams of [100] zone,  $\text{FeK}_\alpha$  radiation.

(3)  $hk0$ ,  $hk1$ ,  $h0l$ ,  $h1l$ ,  $h2l$ ,  $h3l$  Weissenberg diagrams, Buerger goniometer,  $\text{CrK}_\alpha$  radiation.

(4) Full rotation photograph of a cylindrical crystal, [001] axis.

(5) Powder photographs, Phragmén focussing camera,  $\text{CrK}_\alpha$  and  $\text{K}_\beta$  radiation. Powder photograph,  $\text{CoK}_\alpha$  radiation, circular camera 191 mm. diameter.

(1) and (2) were indexed by Bernal's method.

The equatorial intensities of (1), (2), and (4) were used for Fourier syntheses. (3) afforded an easy check on the space group, (5) were used for lattice constant determination, and the intensities applied to check the complete structure.

<sup>1</sup> GMELINS Handbuch d. anorg. Ch. System Nr. 30. Ba.

### Fourier syntheses.

The difficulties in determining the complete structure of  $\text{BaCl}_2 \cdot 2\text{H}_2\text{O}$  already realized by NÁRAY-SZABÓ and SASVÁRI<sup>1</sup> are easily seen. The Ba atom contains so many electrons that it obscures the Cl and O atoms. The number of electrons in  $\text{Ba}^{++}$ ,  $\text{Cl}^-$  and O are 54, 18, and 8, or as 100:32:15. At high reflection angles the effective numbers of electrons in  $\text{Cl}^-$  and O are even smaller

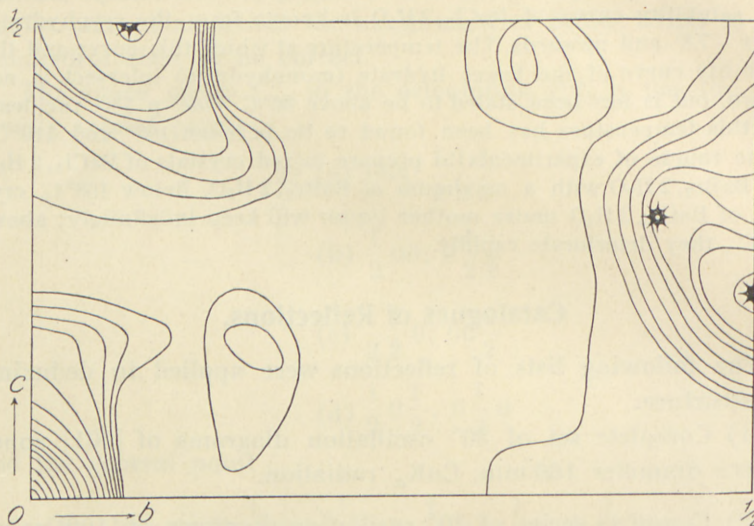


Fig. 1. Patterson-Fourier projection on 100 in  $\text{BaCl}_2 \cdot 2\text{H}_2\text{O}$ . Visually estimated intensities. Ba-Ba peaks shown as stars.

fractions of the number for  $\text{Ba}^{++}$ . At  $\sin \theta/\lambda = 0.5$  the figures are 100:25:8. These figures pertain to atoms at rest. At room temperature the figures are still more unfavourable since thermal movements tend to decrease the effective number of electrons in lighter atoms more strongly than in heavy ones.

The observed spot intensities  $hk0$  and  $0hk$  were converted into series of approximate F's by the aid of appropriate charts. Such charts are described in.<sup>2</sup>

Patterson-Fourier projections on 100 and 001 were computed and drawn (Fig. 1 and Fig 3). Fig. 2 shows the projection unit, its symmetry elements and the calculation area in the two strictly analogous cases. The space group  $P2_1/n(C_{2h}^5)$  projects

<sup>1</sup> ST. V. NÁRAY-SZABÓ and K. SASVÁRI, Z. Krist. **97** (1937) 235.

<sup>2</sup> A. TOVBORG JENSEN, D. Kgl. Danske Vidensk. Selskab, Mat.-fys. Medd. XX (1942) Nr. 5.



on to 100 as well as on 001 in the plane group Pba, *vide*<sup>1</sup> and <sup>2</sup>. An atomic arrangement of Pba symmetry gives a Patterson vector map of Pmm symmetry.

The Ba-Ba peaks on Fig. 1 and Fig. 3 are very conspicuous and easily found. It is seen at once from the figures that the Ba atom is in general position. The special

two-fold positions  $00, \frac{1}{2}\frac{1}{2}$  and  $\frac{1}{2}0, 0\frac{1}{2}$  are ruled out. Atoms at these special positions should give rise to peaks in the vector map at  $00$  and  $\frac{1}{2}\frac{1}{2}$ , and the vector maps contain no outstanding peak at  $\frac{1}{2}\frac{1}{2}$ .

One atom in general position  $xy; \frac{1}{2}-x, \frac{1}{2}+y; \bar{x}\bar{y}; \frac{1}{2}+x, \frac{1}{2}-y$  produces a set of peaks situated as shown in Fig. 4.

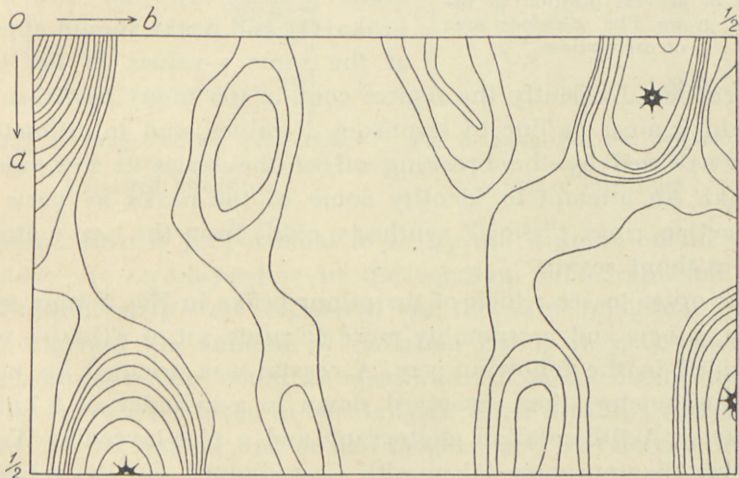


Fig. 3. Patterson-Fourier projection on 001 in BaCl<sub>2</sub>, 2 H<sub>2</sub>O. Visually estimated intensities. Ba-Ba peaks shown as stars.

Fig. 1 and Fig. 3 correspond exactly to Fig. 4, and finally prove the Ba atom to be in general position. Ba-coordinates found from

<sup>1</sup> A. L. PATTERSON, Z. Krist. **90** (1935) 543

<sup>2</sup> W. L. BRAGG and H. LIPSON, Z. Krist. **95** (1936) 323.

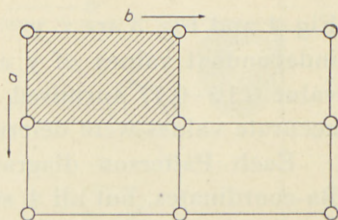


Fig. 2. Unit of projection and symmetry elements in 100 and 001 Patterson-Fourier projections in BaCl<sub>2</sub>, 2 H<sub>2</sub>O. Shaded: area of calculation.



Fig. 1 and Fig. 3 are  $x, y = 0.04, 0.22$ ;  $y, z = 0.22, 0.15$ . The two independent values of  $y$  agree, but are rather different from the value 0.16–0.17 surmised by NÁRAY-SZABÓ and SASVÁRI.<sup>1</sup> More accurate values were determined later.

Each Patterson diagram yields 4 different sets of the two Ba-coordinates, but all 4 sets are really identical, differing only in choice of origin and axis orientation.

The Ba-coordinates obtained suffice to fix the signs of all reflections. With the  $F$  values already employed and the signs

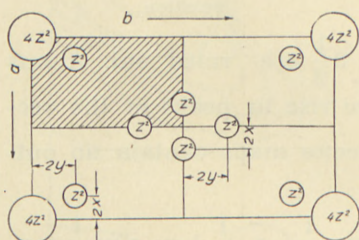


Fig. 4. Interatomic vectors (Patterson peaks) corresponding to one atom in general position in the plane group  $Pba$ . Shaded: area of calculation.

now obtained the corresponding Bragg-Fourier projections were computed. They are shown in Fig. 5 and Fig. 6. Heavy Ba atoms appear where they were expected, but the remaining peaks are not capable of immediate interpretation. The projection area, one quarter of the unit cell, should contain two medium peaks (Cl), and two low peaks (O), and peaks should appear at the same  $y$ -values in the two

projections. Evidently the figures contain too many peaks, some of which must be due to erroneous  $F$ -values, and to diffraction effects caused by the breaking off of the series at low values of  $hkl$ . An attempt to identify some of the peaks as parts of diffraction rings ("ghost"-synthesis, *vide*<sup>2</sup>) from the heavy atoms was without result.

In order to see which of the minor peaks in Fig. 5 were spurious, a new and presumably more accurate set of  $F(hk0)$ 's was provided in the following way. A crystal was oriented by optical goniometry, then dissolved down to a cylinder of 0.7 mm. diameter. A full rotation photograph and a zero-layer-line Weissenberg diagram were taken with Cu-radiation. On the rotation photograph a calibration strip was printed by exposing the film to the direct beam through a rotating disk in which is cut a sector limited by a radius and a logarithmic spiral curve. The amount of radiation falling at a distance  $X$  from the end of the

<sup>1</sup> ST. V. NÁRAY-SZABÓ and K. SASVÁRI, *Z. Krist.* **97** (1937) 235.

<sup>2</sup> A. TOVBORG JENSEN, *D. Kgl. Danske Vidensk. Selskab, Mat.-fys. Medd.* **XX** (1942) Nr. 5.

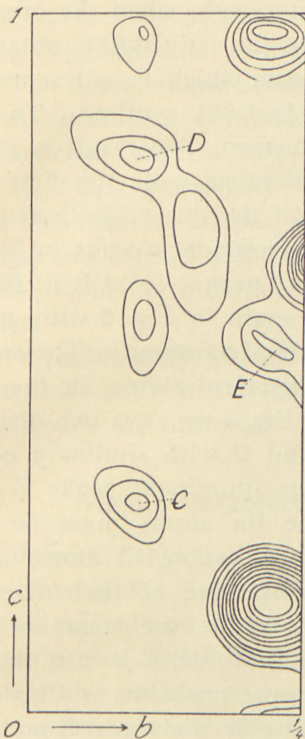


Fig. 5. Bragg-Fourier projection on 100 in  $\text{BaCl}_2, 2 \text{H}_2\text{O}$ . Visually estimated intensities.

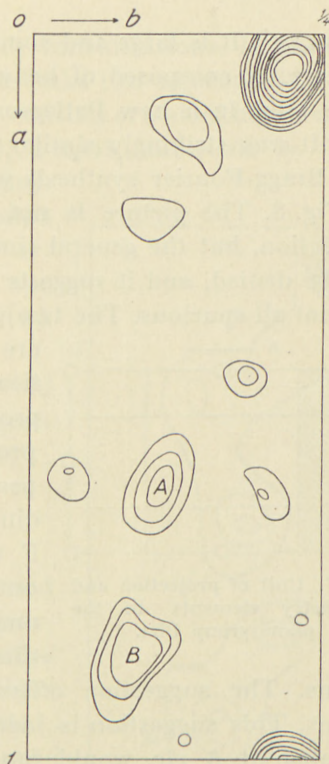


Fig. 6. Bragg-Fourier projection on 001 in  $\text{BaCl}_2, 2 \text{H}_2\text{O}$ . Visually estimated intensities.

exposed strip is proportional to  $X$ . By the Kipp automatic photometer the zero-layer-line in the rotation photograph and the calibration strip were registered on the same diagram. From this diagram the amount of radiation falling in each spot on the zero-layer line could be measured. All peaks on the photometer curve were taken to be triangles. Their breadths were measured at the bottom and at half heights, and by referring to the calibration curve the amounts of radiation falling on each spot were calculated in arbitrary units. The amounts of radiation were divided by the polarisation and Lorentz factors and the absorption factor. The quotient gives  $F^2(hk0)$  in arbitrary units. The polarization and Lorentz factors were taken from *Internationale Tabellen zur Bestimmung von Kristallstrukturen* p. 567. The absorption factor was calculated according to



BRADLEY<sup>1</sup>. It is large and somewhat uncertain when the crystal, as here, is composed of heavy atoms. The  $F^2(hk0)$ 's obtained were used in a new Patterson synthesis which is not reproduced. It was strikingly similar to the first 001 synthesis. Then a 001 Bragg-Fourier synthesis was performed. The result is given in Fig. 8. The picture is not quite identical with the first 001 projection, but the general similarity of the two projections cannot be denied, and it suggests that the secondary peaks in Fig. 6

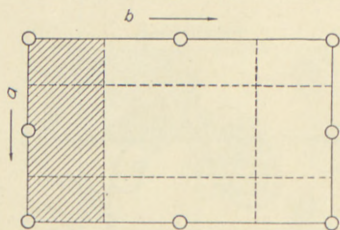


Fig. 7. Unit of projection and symmetry elements in the plane group Pba.

are found again in Fig. 8 with practically identical coordinates. They most probably represent atoms. In the 100 projection Fig. 5 we have two distinct peaks C and D with similar y coordinates. The prominent peaks E and F near the Ba atoms must be left out of consideration. Cl atoms at E and F irrespective of their X-coordinates would be too near the Ba

atoms. The suggestion offers itself, that A-B-C-D are the Cl atoms. This suggestion is made the more probable as Cl atoms situated at A etc. would have reasonable distances from two adjacent Ba atoms (whose coordinates we know accurately). The proposed Cl atoms would link the Ba atoms in sheets parallel with the developed face of our crystal. A similar arrangement has previously been found in  $\text{SrCl}_2 \cdot 2\text{H}_2\text{O}$ .

A calculation showed that this arrangement of Cl atoms would also explain quite nicely all secondary peaks in the 001 Patterson projection as due to interaction between Ba and Cl.

The projections discussed give few or no indications of the O-coordinates. The projection Fig. 8, which must be considered more accurate than Fig. 5 and Fig. 6, however, seems to indicate that O atoms must be somewhere on the "high ground" in the upper half of the picture.

A model to scale of the proposed structure was built of plasticine and glass rods. Combination of the two projections to a structure in space involves no difficulties. The model suggested one and only one position for each of the water molecules rea-

<sup>1</sup> A. J. BRADLEY, Proc. Phys. Soc. 47 (1935) 879.



sonably to be expected from space considerations. In the positions suggested each water molecule links two adjacent Ba atoms.

The entire atomic arrangement consists of a stacking of sheets. Each sheet is a complete  $(\text{BaCl}_2, 2\text{H}_2\text{O})_n$  molecule as far as geometrical aspects are concerned.  $\text{SrCl}_2, 2\text{H}_2\text{O}$  previously investigated contains similar sheets, but the arrangement of  $\text{H}_2\text{O}$  and Cl around the metal atoms is different in the two cases.

A preliminary calculation of 0kl intensities showed satisfactory agreement with the observed values.

### Atomic Parameters.

Before subjecting the proposed structure to the final test of comparing calculated and observed intensities of the general type hkl, the best values of atomic parameters were selected. Parameter values from different projections are undoubtedly of varying accuracy. All intensities employed are not equally accurate, thus data with Cu radiation are to be preferred to Fe radiation data. Photometric estimation is considered better than visual estimation. But it is not easy to see which of the two independent sets of values obtained from each Patterson diagram is the better, nor to estimate whether figures obtained by Patterson synthesis are more accurate than the slightly different values obtained from subsequent Bragg synthesis on the same data. Hence it was decided to take for final values the averages from all projections. The figures and averages are given in Table 2. Table 2 gives some idea of the accuracy which may be attached to the averages. Each set of parameter values has been obtained from

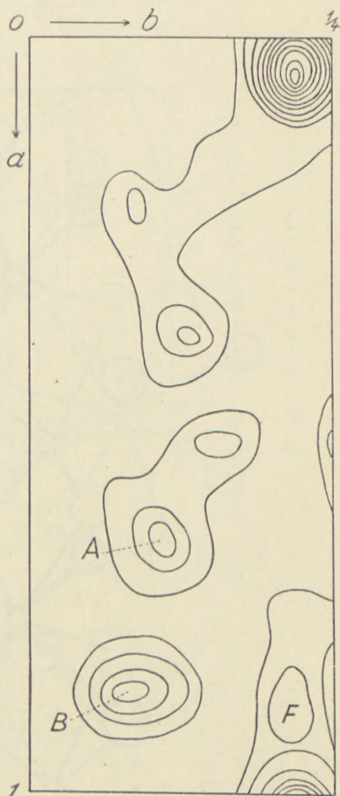


Fig. 8. Bragg-Fourier projection on 001 in  $\text{BaCl}_2, 2\text{H}_2\text{O}$ . Photometric intensities.

a carefully drawn detail map of the peak in question. These maps, 15 in all, are not reproduced.

The final water parameters were chosen in the following way. It was assumed that the water molecules link two Ba atoms at

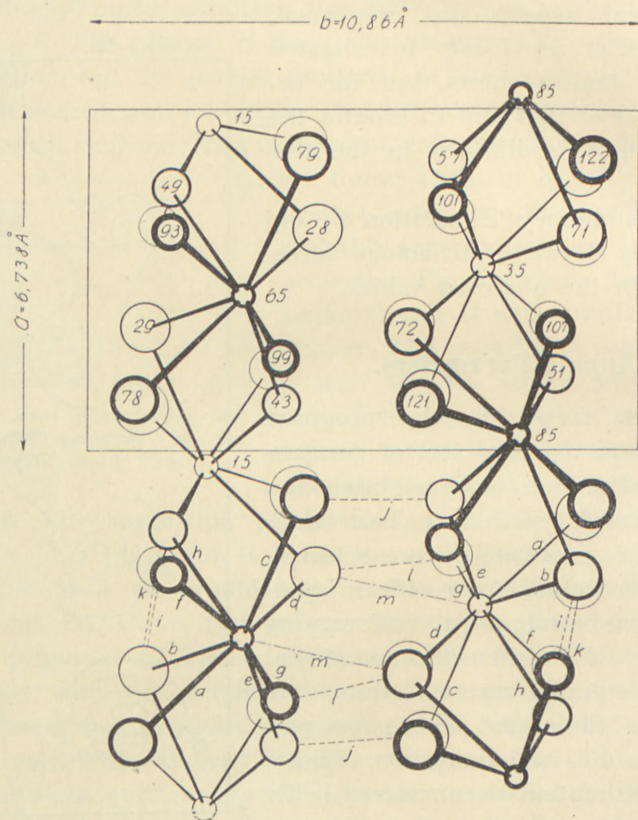


Fig. 9.  $\text{BaCl}_2 \cdot 2\text{H}_2\text{O}$  projected on 001.  $\circ$  Ba,  $\bigcirc$   $\text{H}_2\text{O}$ ,  $\bullet$  Cl.

distances of about  $2.85 \text{ \AA}$ , and that all distances from other neighbouring atoms are not much below the sums of corresponding radii. A few trials gave parameters involving reasonable distances from all neighbouring atoms and causing the water molecule to make two distinct contacts with Cl atoms apart from the two contacts with Ba atoms originally assumed. Four such contacts, two negative and two positive, show that the water molecule is of Bernal's "tetrahedral" type.<sup>1</sup>

<sup>1</sup> J. D. BERNAL and R. H. FOWLER. *J. chem. Phys.* **1** (1933) 515.



The atomic parameters are tabulated in Table 3. Interatomic distances are given in Table 4. The distances in the last column of Table 4 are the corresponding radius sums.

The letters in the first column of Table 4 refer to Fig. 9 and

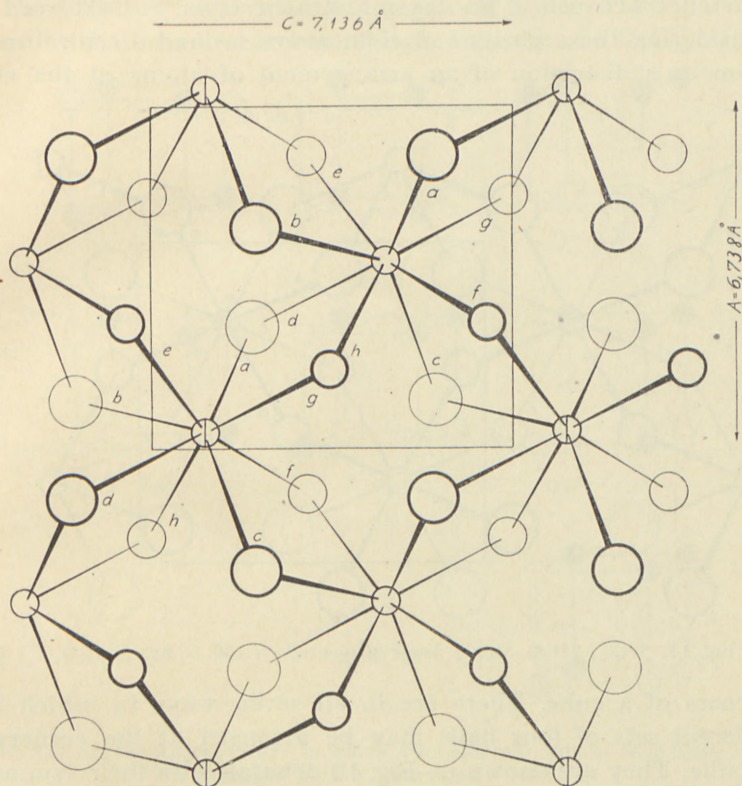


Fig. 10.  $\text{BaCl}_2 \cdot 2\text{H}_2\text{O}$ . Single layer projected on 010.

⊕ Ba above plane of drawing. ○ Ba below plane of drawing. ○  $\text{H}_2\text{O}$ . ○ Cl.

Fig. 10, which depict the structure. It is scarcely possible to denote all the distances in a complicated structure like the one in hand, in such a way that their position in space can be visualized without the aid of a diagram or a model.

### Description of the Structure.

The structure consists of identical  $(\text{BaCl}_2 \cdot 2\text{H}_2\text{O})_{n^2}$  layers of which one is shown in Fig. 10. The layer is projected on



010. The figure should be compared with Fig. 11, the corresponding picture of a  $(\text{SrCl}_2, 2\text{H}_2\text{O})_{n2}$  layer which is taken from the preceding paper.<sup>1</sup> The two layers are similar in so far as a metal atom in each is surrounded by 4 Cl and 4  $\text{H}_2\text{O}$ . The chief difference between a Ba layer and a Sr layer is best seen by considering these clusters of eight atoms around a central metal atom as a distortion of an arrangement of atoms at the eight

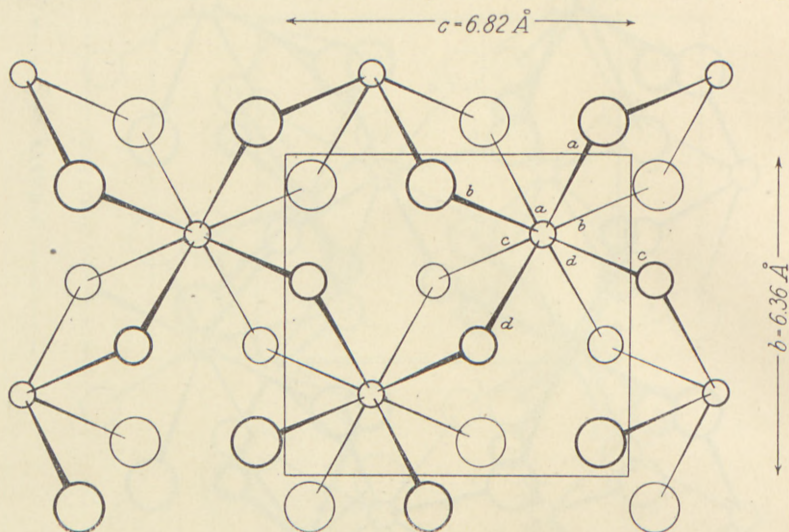


Fig. 11.  $\text{SrCl}_2, 2\text{H}_2\text{O}$ . Single layer projected on 100.  $\bigcirc$  Sr,  $\bigcirc$   $\text{H}_2\text{O}$ ,  $\bigcirc$  Cl.

corners of a cube. There are in all seven ways in which two different sets of four balls may be arranged at the corners of a cube. They are shown in Fig. 12 denoted with their symmetry symbols in the Hermann-Mauguin shorthand.

The  $\text{SrCl}_2, 2\text{H}_2\text{O}$  layer is built by distortion and linking of  $4mm$  units, while  $\text{BaCl}_2, 2\text{H}_2\text{O}$  is derived from  $mmm$  units. Possibly several others of these arrangements may be found in other crystals of  $\text{AX}_2\text{Y}_2$  compounds built of neutral layers, or even in crystals containing electrically charged layers of this formula.

Another noteworthy difference between the two kinds of layer is that while in  $\text{SrCl}_2, 2\text{H}_2\text{O}$  the Sr atoms of one layer all lie in a plane, in  $\text{BaCl}_2, 2\text{H}_2\text{O}$  they form a puckered layer. This puckering causes each Ba atom to be rather close to one Cl

<sup>1</sup> A. TOVBORG JENSEN, D. Kgl. Dansk Vidensk. Selskab, Mat.-fys Medd. XX (1942) Nr. 5.

atom in the adjacent layer. The corresponding line is called  $m$  in Fig. 9. The distance is  $3.38 \text{ \AA}$  as compared with  $3.20$  for a contact. A similar feature is not present in  $\text{SrCl}_2, 2\text{H}_2\text{O}$ , where Sr atoms on all sides are completely screened by adjacent Cl and  $\text{H}_2\text{O}$ .

The distances between atoms in adjacent layers in  $\text{SrCl}_2, 2\text{H}_2\text{O}$  were all well above the corresponding radius sums. In  $\text{BaCl}_2, 2\text{H}_2\text{O}$

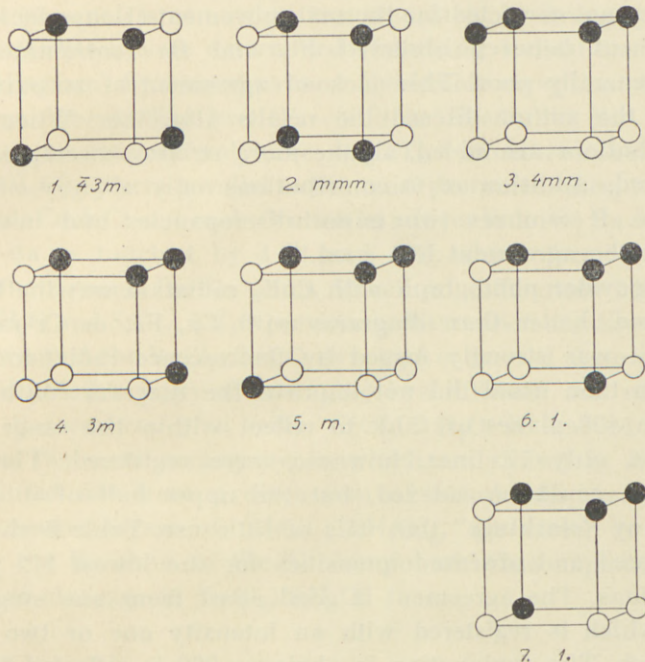


Fig. 12. The seven different ways in which two different sets of four balls may be arranged at the corners of a cube.

several distances between Cl atoms and  $\text{H}_2\text{O}$  molecules in different layers are equal to the corresponding radius sum. Hence the electrostatic attraction between adjacent layers is probably considerable. This attraction seems to be the reason why  $\text{BaCl}_2, 2\text{H}_2\text{O}$  although a layer lattice, does not easily cleave parallelly to the layers.

### Comparison between Calculated and Observed Intensities.

Table 5 gives a comparison between observed and calculated values of  $F(hk0)$ . The observed  $F$ 's are the set photometrically



registered. They are given in the arbitrary units in which they were obtained. The calculated values employ the final set of parameters as given in Table 2. The  $f$  curves applied were James's and Brindley's. The agreement is considered satisfactory. Observed  $F$ 's at high glancing angles are much lower than the calculated values in accordance with the fact that the calculated  $F$ 's are not corrected for thermal movement (Debye factor). The agreement between observed  $F$ 's and *Ba contributions alone* was generally poor. This lack of agreement at an early stage made the author discard the results altogether. When the  $Cl$  contributions are added, all the more striking discrepancies are removed. Addition of  $O$  contributions only slightly alters the picture. It removes two minor discrepancies and in no case makes the agreement less good.

A powder photograph with  $CoK_{\alpha}$  radiation was the best one obtained, better than diagrams with  $Cu$ ,  $Fe$ , or  $Cr$  radiation. Still, it was strongly fogged by fluorescence radiation. Lower tension than usual did not improve the diagram. With  $Co$  radiation 408 planes are able to reflect within the range of the camera, only 77 lines, however, were registered. The entire diagram could be indexed, but the upper half of it contains so many "clashings" that it is of little use. Table 6 shows the calculated and observed intensities for the lowest 112 possible reflections. The agreement is good apart from one single line, 020, which is registered with an intensity one or two classes too high. The explanation is obvious: 020 is reflected from the only face developed on small flaky crystals and hence apt to give too strong reflections because of preferential orientation in the powder specimen. The  $BaCl_2 \cdot 2H_2O$  powder had been precipitated from a strong aqueous solution by alcohol. No attempt was made to remove the effect by grinding the powder. Moderate grinding of soft hydrate crystals spoils the quality of their powder-diagram. As previously noted for the  $hk0$  intensities, it was seen that the  $Ba$  contribution alone is quite insufficient to account for the observed intensities. The  $Ba$  and  $Cl$  contributions suffice, and the  $O$  contributions make but little difference.



### Summary.

The complete structure of  $\text{BaCl}_2, 2\text{H}_2\text{O}$ , which is determined by 15 independent parameters, has been worked out by an extensive use of Patterson- and Bragg-Fourier-synthesis on visually and photometrically estimated intensities. Ba parameters were determined very accurately by Patterson and Bragg synthesis, Cl parameters somewhat less accurately by Bragg synthesis. O parameters were determined (following indications on a Fourier diagram) by consideration of plausible coordination and space requirement. The two O's could be fitted into the  $\text{BaCl}_2$  framework in one and only one way. The structure consists of  $(\text{BaCl}_2, 2\text{H}_2\text{O})_n$  layers parallel to the most prominent face, 010, of the crystal. Each Cl and each O atom in a layer link two Ba atoms, so each Ba is touched by 4 Cl and 4 O, which form a compact cluster around the Ba atom. Structural differences between  $\text{BaCl}_2, 2\text{H}_2\text{O}$  and  $\text{SrCl}_2, 2\text{H}_2\text{O}$  previously determined are discussed. It is shown that the  $\text{BaCl}_2, 2\text{H}_2\text{O}$  structure is derived from one of the seven possible ways of arranging two different sets of four balls at the corners of a cube.  $\text{SrCl}_2, 2\text{H}_2\text{O}$  is derived from another of the seven arrangements, which are shown in Fig. 12. It is pointed out from a discussion of atomic distances that the consecutive layers of  $(\text{MeCl}_2, 2\text{H}_2\text{O})_n$  are closer to each other in the Ba than in the Sr compound. This explains the absence of cleavage in  $\text{BaCl}_2, 2\text{H}_2\text{O}$ .

### Acknowledgements.

I am highly indebted to Professor NIELS BJERRUM for his unflinching interest in these studies and for the excellent working conditions in the laboratory; to Professor GUNNAR HÄGG of Uppsala, in whose laboratory part of the work was done in the spring of 1940, for his constant aid and encouragement, and to the Carlsberg Foundation and K. A. Larssens Legat for grants.

*Copenhagen.*

*Royal Veterinary and Agricultural College.  
Chemical Laboratory.*

Table 1.  
Lattice constants of  $\text{BaCl}_2 \cdot 2\text{H}_2\text{O}$ .

a	b	c	$\beta$	
6.69 Å	10.86 Å	7.15 Å	91°.05	(Náray-Szabó and Sasvári)
6.738 Å	10.86 Å	7.136 Å	90°.57	(Author)

Table 2.  
All parameter values obtained and their averages.

	Fig. 1 a	Fig. 3 a	Fig. 3 b	X a	X b	Fig. 5	Fig. 6	Fig. 8	Average
Ba x ...	..	0.050	0.037	0.050	0.042	..	0.047	0.043	0.045
y ...	0.216	0.217	0.219	0.216	0.215	0.217	0.218	0.218	0.217
z ...	0.145	..	..	..	..	0.150	..	..	0.147
Cl <sub>I</sub> x ...	..	..	..	..	..	..	0.838	0.864	0.851
y ...	..	..	..	..	..	0.087	0.088	0.077	0.084
z ...	..	..	..	..	..	0.781	..	..	0.781
Cl <sub>II</sub> x ...	..	..	..	..	..	..	0.622	0.660	0.641
y ...	..	..	..	..	..	0.094	0.113	0.107	0.105
z ...	..	..	..	..	..	0.289	..	..	0.289

The columns marked a contain values read off from special point peaks in the Patterson diagrams. Values in columns marked b are read off from general point peaks. There are no Fig 1 b data, because the general point peak in Fig. 1 is too near a special point peak and too blurred to be of any use. X a and X b are from a Patterson x-y diagram based on photometric data, which is not reproduced.

Table 3.  
Atomic parameters in  $\text{BaCl}_2 \cdot 2\text{H}_2\text{O}$ .

	x	y	z
Ba .....	0.045	0.217	0.147
Cl <sub>I</sub> .....	0.851	0.084	0.781
Cl <sub>II</sub> .....	0.641	0.105	0.289
O <sub>I</sub> .....	0.36	0.15	0.93
O <sub>II</sub> .....	0.23	0.15	0.49



Table 4.  
Interatomic distances in  $\text{BaCl}_2 \cdot 2\text{H}_2\text{O}$ .

No.	Kind	Distance	Radius Sum
a . . . . .	Ba—Cl <sub>I</sub>	3.11 Å	3.20 Å
b . . . . .	Ba—Cl <sub>I</sub>	3.27 -	"
c . . . . .	Ba—Cl <sub>II</sub>	3.16 -	"
d . . . . .	Ba—Cl <sub>II</sub>	3.24 -	"
e . . . . .	Ba—O <sub>I</sub>	2.78 -	2.77 Å
f . . . . .	Ba—O <sub>I</sub>	2.81 -	"
g . . . . .	Ba—O <sub>II</sub>	2.82 -	"
h . . . . .	Ba—O <sub>II</sub>	2.80 -	"
i . . . . .	O <sub>I</sub> —Cl <sub>II</sub>	3.18 -	3.19 Å
j . . . . .	O <sub>I</sub> —Cl <sub>II</sub>	3.22 -	"
k . . . . .	O <sub>II</sub> —Cl <sub>II</sub>	3.17 -	"
l . . . . .	O <sub>II</sub> —Cl <sub>I</sub>	3.19 -	"
(m . . . . .)	Ba—Cl <sub>I</sub>	3.38 -	3.20 Å)

Table 5.  
Calculated and observed F's in the hk0 zone of  
 $\text{BaCl}_2 \cdot 2\text{H}_2\text{O}$ .  $\text{CuK}_\alpha$  radiation.

hk	sin $\theta$	F calc.	F obs.	Obs. Int.	hk	sin $\theta$	F calc.	F obs.	Obs. Int.
11	.132	7.6	0	0	25	.414	6.6	0	0
02	.140	33.1	29.5	m	06	.418	25.1	15.7	w-m
12	.179	2.5	0	0	16	.432	9.8	0	0
20	.225	27.4	14.1	w-m	34	.437	23.6	14.0	w
21	.235	22.3	10.1	w-m	40	.450	0.0	0	0
13	.237	21.3	21.4	m	41	.455	32.8	12.9	w, w-m
22	.264	36.9	25.1	m	42	.471	22.0	12.4	w
04	.278	3.5	0	0	26	.473	9.4	0	0
14	.300	25.2	14.1	w	35	.484	18.8	9.1	w
23	.307	21.9	13.9	w	43	.495	24.2	12.3	w
31	.345	6.7	0	0	17	.500	40.5	36.0	m-s
24	.358	32.4	15.7	w-m	44	.528	21.9	11.4	w
32	.365	2.5	0	0	27	.536	4.4	0	0
15	.366	37.3	25.4	m	36	.537	27.0	8.5	v,w
33	.396	20.4	10.1	w	08	.556	1.2	0	0



Table 5 (continued).

hk	sin $\theta$	F calc.	F obs.	Obs Int.	hk	sin $\theta$	F calc.	F obs.	Obs. Int.
51	.566	4.2	0	0	211	.797	16.2	0	0
18	.568	5.4	0	0	73	.807	12.2	0	0
45	.569	18.5	9.8	v, w	74	.827	19.7	0	0
52	.580	27.6	10.5	w	410	.828	4.3	0	0
37	.592	15.3	7.1	v	67	.832	0.3	0	0
53	.600	6.1	0	0	012	.835	15.6	9.2	w
28	.600	3.8	0	0	311	.837	16.8		
46	.613	8.1	0	0	59	.842	5.6	0	0
54	.627	13.5	0	0	112	.843	12.2	0	0
19	.636	23.3	16.5	w-m	75	.854	7.1	0	0
38	.651	19.2	8.8	v	212	.865	19.0	7.7	w
55	.661	2.1	0	0	68	.875	0.5	0	0
47	.663	3.2	0	0	76	.884	24.4	8.4	w-m
29	.665	0.9	0	0	411	.888	12.0	5.5	w
60	.676	5.8	0	0	510	.895	17.1	6.1	v
61	.679	31.9	13.4	w-m	80	.900	7.5	0	0
62	.689	10.2	0	0	312	.900	12.1	0	0
010	.696	22.1	8.5	v	81	.903	19.1	6.7	w
56	.700	23.8	11.8	w	82	.911	17.2	6.3	w
110	.704	12.2	0	0	113	.911	16.6		
63	.707	24.1	13.8	w-m.	77	.920	2.9	0	0
39	.711	26.1	13.8		69	.920	6.9	0	0
48	.716	3.4	0	0	83	.924	20.5	5.5	w
64	.730	9.3	0	0	213	.933	8.6	0	0
210	.731	11.7	0	0	84	.943	18.1	*	v
57	.745	3.2	0	0	412	.948	11.3	*	v
65	.759	15.0	0	0	511	.950	3.3	0	0
49	.770	10.0	0	0	78	.957	23.6	7.7	w-m
310	.773	19.4	12.4	w	85	.965	9.4	0	0
111	.773	18.3	12.4	w	313	.965	2.2	0	0
71	.783	4.5	0	0	610	.969	5.2	0	0
58	.791	37.6	18.0	m	014	.974	23.0	7.0	m-s
72	.791	8.1	0	0	114	.980	3.6	0	0
66	.793	8.2	0	0					

\* visible but not strong enough to show up on photometer curve.

Table 6.

Calculated and observed intensities in a powder diagram of  $\text{BaCl}_2 \cdot 2\text{H}_2\text{O}$ .  $\text{CoK}_\alpha$  radiation.

hkl	$10^4 \times \sin^2 \theta$	$\theta$ F <sup>2</sup>	Obs. Int.	hkl	$10^4 \times \sin^2 \theta$	$\theta$ F <sup>2</sup>	Obs. Int.
011	0368	19	0	$\bar{1}41$	2307	38	w
110	0400	24	0	141	2325	3.2	0
020	0442	250	m	132	2328	6.7	0
$\bar{1}01$	0537	226	w	212	2329	37	v
101	0555	50	0	$\bar{2}31$	2390	49	w
$\bar{1}11$	0648	132	0	013	2420	3.5	0
111	0666	316	w	231	2426	0	0
021	0699	56	0	$\bar{1}03$	2571	44	v
120	0731	0.8	0	$\bar{2}22$	2588	2.3	0
$\bar{1}21$	0979	146	v	103	2625	47	v
121	0997	43	0	222	2660	36	} v
002	1026	27	0	$\bar{1}13$	2682	49	
012	1137	152	v	310	2712	1.3	0
200	1156	92	0	113	2736	2.9	0
031	1252	21	0	023	2751	0.3	0
210	1267	60	} w	042	2796	0	0
130	1284	50		$\bar{3}01$	2831	29.5	v
$\bar{1}12$	1408	0.4	0	301	2885	0.6	0
112	1444	10.2	0	240	2926	31.6	w
022	1468	29	0	$\bar{3}11$	2942	2.1	0
$\bar{2}11$	1506	77	v	311	2996	94	w-m
$\bar{1}31$	1532	108	w-m	$\bar{1}23$	3013	21.3	0
211	1542	21.3	} m	051	3022	13.0	0
131	1550	173		320	3043	0.5	0
220	1598	98	w-m	150	3054	44	} w-m
$\bar{1}22$	1739	5.0	0	$\bar{1}42$	3067	45	
040	1770	1.5	0	123	3067	47	} 0
122	1775	110	w-m	142	3103	11.4	
$\bar{2}21$	1837	18	v?	$\bar{2}32$	3141	27	v?
221	1873	5.8	0	241	3165	2.0	0
032	2021	118	} m-s	241	3201	28	v
041	2027	51		232	3213	12	0
140	2059	31	w	$\bar{3}21$	3273	44	v
$\bar{2}02$	2146	5.7	0	$\bar{1}51$	3302	2.5	0
230	2151	26	v	033	3304	11	v?
$\bar{2}02$	2218	29	0	151	3320	9	0
$\bar{2}12$	2257	102	v	321	3327	0.6	0
$\bar{1}32$	2292	0	0	$\bar{2}13$	3522	4.3	0



Tabel 6 (continued).

hkl	$10^4 \times \sin^2 \theta$	$\theta$ F <sup>2</sup>	Obs. Int.	hkl	$10^4 \times \sin^2 \theta$	$\theta$ F <sup>2</sup>	Obs. Int.
$\bar{1}33$	3566	2.3	0	004	4104	3.3	0
330	3596	1.0	0	322	4123	1.8	0
133	3620	1.0	0	$\bar{2}51$	4160	4.8	0
213	3630	0	0	251	4196	9.0	} v?
$\bar{3}12$	3684	1.9	0	014	4215	5.2	
052	3791	10.6	0	061	4239	12.9	
312	3792	1.4	0	160	4271	3.2	0
$\bar{3}31$	3826	3.0	0	$\bar{1}43$	4341	11.9	} v
$\bar{2}23$	3853	0	0	340	4371	12.8	
331	3880	4.4	0	143	4395	8.4	
$\bar{2}42$	3916	1.4	0	$\bar{2}33$	4406	3.1	0
250	3921	1.0	0	$\bar{1}14$	4468	6.4	} v
223	3961	0.5	0	233	4514	7.7	
060	3982	7.5	} v?	$\bar{1}61$	4519	4.7	
242	3988	8.7		161	4537	0.4	0
$\bar{3}22$	4015	0.9	0	114	4540	0.9	0
$\bar{1}52$	4062	0.4	0	024	4546	23.1	v
043	4079	1.2	0	332	4568	2.0	0
152	4098	3.3	0				

Indleveret til Selskabet den 11. November 1944.  
Færdig fra Trykkeriet den 12. Juni 1945.



DET KGL. DANŠKE VIDENSKABERNES SELSKAB  
MATEMATISK-FYSISKE MEDDELELSER, BIND XXII, NR. 4

---

# ON A NEW APPARATUS FOR GAS ANALYSIS

BY

J. A. CHRISTIANSEN AND INGER WULFF



KØBENHAVN

I KOMMISSION HOS EJNAR MUNKSGAARD

1945

Printed in Denmark.  
Bianco Lunos Bogtrykkeri A/S

It is well known that gas analysis is widely used in science and industry and especially in the hands of physiologists has been developed to a high degree of precision. But from a constructive point of view the current modern apparatuses, Orsat's for technical gas analysis and HALDANE'S (1) for physiological purposes (respiration studies), in some respects are not quite so elegant as Doyère's apparatus from 1850 (2), the difference being that Doyère used gas siphons and no stop-cocks at all and consequently could avoid any dead space, while both Orsat's and Haldane's apparatuses are based on the use of stop-cocks involving the occurrence of dead spaces. On the other hand it is obvious that the modern apparatuses are faster in operation than Doyère's, and it must be said at once that for technical and many physiological purposes, respectively, the two constructions mentioned will probably retain their dominating positions as standard apparatuses.

Orsat's apparatus usually has a capacity of about 100 ml., while that of Haldane's is designed for quantities of about 10 ml. At the other end of the scale of capacities we have the renowned KROGH (3) burette for quantities from 10 to 100  $\mu$ l. and for instance the construction proposed by CHRISTIANSEN (4) and CHRISTIANSEN and HUFFMANN (5) (6) for quantities of a similar order of magnitude, the gap between 100 and 10.000  $\mu$ l. remaining uncovered. The aim of what follows is to describe an apparatus covering this gap, i. e. an apparatus with the capacity of about 1000  $\mu$ l.

The principle of the above mentioned apparatus of Christiansen and Huffmann may be described as a combined application of Krogh's mercury screw and Doyère's gas siphon with the modification that the siphon is placed on the gas burette,



and not as proposed by Doyère on the absorption pipettes, which renders the construction of these utterly simple.

It seemed obvious that the increased capacity could be reached simply by increasing the dimensions of the different parts of the apparatus, but experiments immediately revealed that operations with these larger quantities of gas required reconstruction of several details, especially the absorption pipettes, to make the absorptions sufficiently fast.

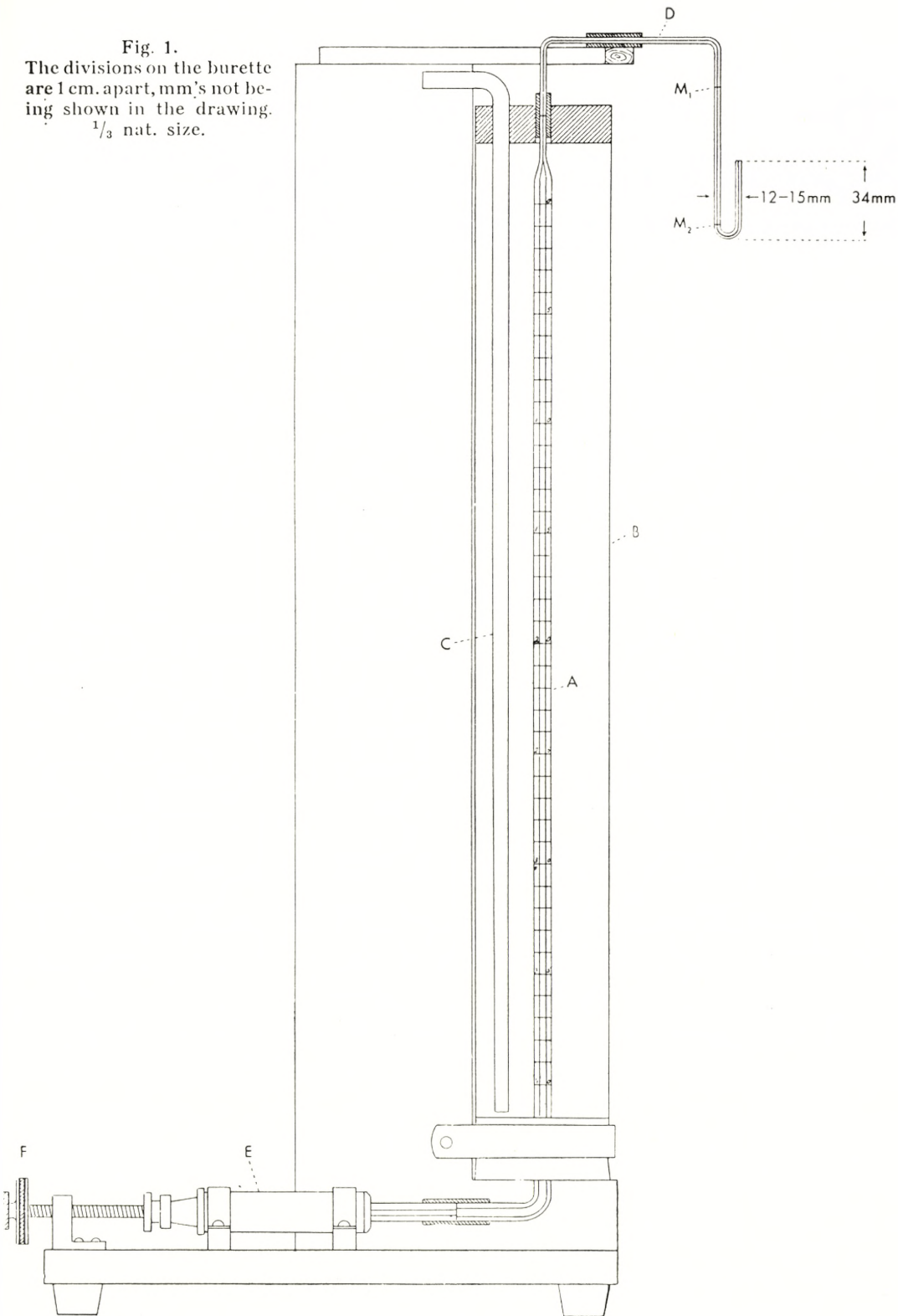
### **The Gas Burette without Compensator.**

The construction of the burette appears from the diagram in fig. 1. It should be mentioned that we have chosen a scale of 400 mm. on the burette as a convenient height, but 500 mm. might be chosen without serious inconvenience.

A is the measuring tube divided in millimetres. The inner diameter of the burette has been chosen at about 1.8 mm., which means a total capacity of about 1000  $\mu$ l., and the accessories, especially the absorption pipettes, are designed for this volume. If desired, the capacity may according to calculations be chosen up to 2000  $\mu$ l. without redimensioning of the accessories. For a length of 400 mm. a tube of 2.5 mm. diameter contains about 2000  $\mu$ l., and as it is sometimes difficult to get capillary tubing of diameters prescribed within narrow limits, a diameter between 1.8 and 2.5 mm., preferably nearer to the former, may be prescribed in ordering the tubing.

The graduated tube is surrounded by water contained in the mantle B equipped with a tube C and a thermometer (not shown in the figure) divided in  $0.1^\circ$  or  $0.2^\circ$ . During the measurements air is bubbled through the water-bath by means of tube C to equalize the temperature. It is advisable to use a rubber stopper at the lower end of the mantle and a cork at the upper end. D is a capillary connected to A by means of a narrow but thick-walled piece of rubber tubing. Care should be taken to make the two glass ends meet inside the tubing. It is essential that D and the narrow tip of A should have nearly the same outer and inner diameters. A convenient outer diameter is about 3 mm. The inner one should be between 0.3 and 0.5 mm. preferably nearer to the former, the idea being that the error arising from

Fig. 1.  
The divisions on the burette  
are 1 cm. apart, mm's not be-  
ing shown in the drawing.  
 $\frac{1}{3}$  nat. size.



a difference in temperature between D and A of not more than  $3^{\circ}$  should not amount to more than 0.1 mm. on the scale. Besides it is desirable that D is so narrow that mercury does not enter the siphon too easily, and furthermore that the volume between  $M_2$  and the tip is as small as possible. It may be added that for several obvious reasons it would be preferable to avoid the rubber connection altogether, but according to experience this makes the apparatus a little too rigid and liable to break. D has two marks,  $M_1$  and  $M_2$ ,  $M_1$  being conveniently placed 13.7 or 27.4 mm. higher than the tip of D. Usually the gas is confined between a mercury surface in A and a column of water extending to  $M_1$ , so that the volume between zero on the scale and  $M_1$  must be known. Volumes smaller than this may be measured from zero, confined as before between water (meniscus at zero) and mercury.

E is an all-glass syringe connected as shown to the graduated tube by means of stout rubber tubing. Care should again be taken to make the ends meet inside the rubber tubing. If it is intended to use combustion by explosion, a short piece of steel tubing, about 2 cm., must be inserted between the syringe and tube A. The piston should have a diameter between 8 and 12 mm., if shorter, the apparatus is too tedious to operate, if longer, the mercury is apt to move in jumps. It is operated by means of the screw F and a pair of springs, not shown in the figure. Rubber bands may be used, but springs of steel wire are to be preferred.

The apparatus, as shown, is mounted on a wooden support.

The burette is filled with mercury through the siphon by suction with the syringe. By suitable tilting of the whole apparatus and operation of the piston, air bubbles in the syringe are removed. To calibrate the graduations the tip is provided with an inverted U-formed capillary tube, one branch of the U being about twice as long as the other. The short branch is connected to the tip by means of a piece of rubber tubing. The other end is left free. A few  $\mu$ l. of air followed by a column of mercury is sucked in, and the calibration is performed by weighing mercury sucked in or pressed out, the upper end of the short air column being used as an index. We perform the calibration for whole values of the centimetres and it is recommended to tabulate the corrections on a piece of cardboard. The volumes (expressed in centimetres



on the scale) between zero and  $M_1$  and  $M_2$  and the tip together with the volume in  $\mu\text{l}$ . corresponding to 1 cm. on the scale, are tabulated on the same piece of cardboard.

### Accessories.

The accessories include an adjustable table and a number of absorption pipettes.

The table must have a maximum height of about 1 cm. below the height from the laboratory desk to the lower bend of the tip D, thus minimizing the risk of breaking the siphon. It is convenient to fix this table on the same base as the burette. The top of the table is preferably rectangular and so mounted that it may easily, although with some friction, be swung round the centre. Its length must be so great, that it nearly touches the mantle B. The breadth may be chosen at about 8 cm. In the vertical direction it must be moved by rack and pinion, length of the movement 8—10 cm.

The absorption pipettes are T-shaped as shown in fig. 2.

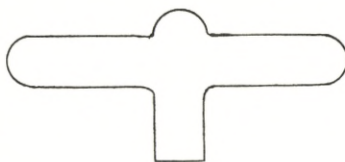


Fig. 2.  
 $\frac{2}{3}$  nat. size.

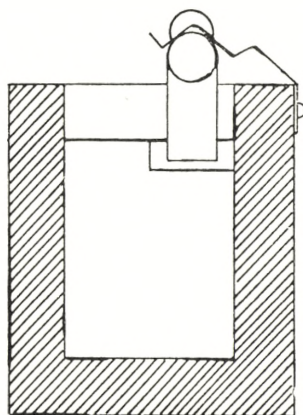


Fig. 3 a.

$\frac{2}{3}$  nat. size.

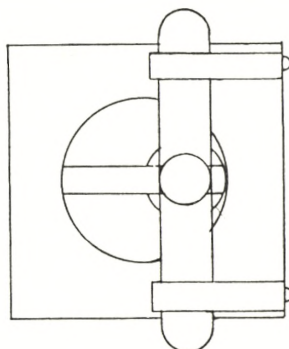


Fig. 3 b.

By means of springs they are placed horizontally on wooden blocks (figs. 3 a, 3 b) 6 cm. high, cross-section  $5 \times 5$  cm. The blocks are provided with two circular holes, one with its centre in the middle of the block, diameter 3 cm. and depth 1 cm.,

and one eccentric, diameter 1.5 cm., extending 0.5 cm. below the larger hole. As it is convenient always to use a depth of the holes of 1 cm., it is the diameter of the larger hole which determines the capacity. A slit 5 cm. deep reckoned from the upper face of the block is extending from the bottom of the holes. The breadth of this slit is 0.5 cm., just allowing the gas-siphon to pass, and the length 3 cm. This somewhat complicated inner form of the block has been chosen to economize mercury, partly on account of the cost and partly to decrease the weight of the block when filled. For a complete analysis 8 of these pipettes are necessary, viz. 2 for  $\text{CO}_2$ , 2 for  $\text{O}_2$ , 1 for  $\text{C}_2\text{H}_4$ , 2 for  $\text{CO}$  and 1 for explosion or combustion. The pairs for  $\text{CO}_2$  and  $\text{O}_2$  are necessary because on account of the different compositions of the gases it is not permissible to use the same absorption liquid for the first absorptions of  $\text{CO}_2$  and  $\text{O}_2$  and for the absorptions after combustion. As, however, it is sometimes desirable to have one or two extra pipettes, one or two spare blocks should be at hand making 10 in all.

In this connection we want to emphasize that we have tried to unite the whole battery of absorption pipettes in one mercury trough, but this proved much less convenient than the use of separate blocks. Besides the blocks with absorption pipettes at least 2 and preferably 3 are necessary as containers for  $\text{O}_2$  and the gas to be analyzed, but these must be somewhat larger. We have found the following dimensions convenient: Height of the block 6 cm., cross section  $7 \times 7$  cm. Depth of the slit 5 cm., breadth 0.5 cm., length 5 cm. Diameter of the holes 5, and 2.5 cm., respectively, depths as described above for the smaller blocks. Of course the T-formed containers must also be larger, preferably with a capacity of about 10—12 ml. But it should be remembered that it must be possible to reach the highest point of the T (the bulb just above the opening) with the gas-siphon.

If it is intended to use the explosion method, one of the smaller containers (the absorption pipettes) must be stoppered inside with a short piece of rubber tubing (0.5—1.0 cm. in length), which just allows the tip of the gas-siphon to pass without or nearly without friction.

Finally 2 or 3 gas containers of the type described by CHRISTIANSEN and HUFFMANN and a small device for filling and

emptying the absorption pipettes are necessary. For the sake of convenience the drawings are repeated here, figs. 4, 5. For sanitary reasons it is recommended to keep objects with uncovered mercury surfaces not in use in a box with a tightly closing lid.

For the explosions an induction-coil is needed. We have used a Ford induction-coil connected through a switch to a 2 volt

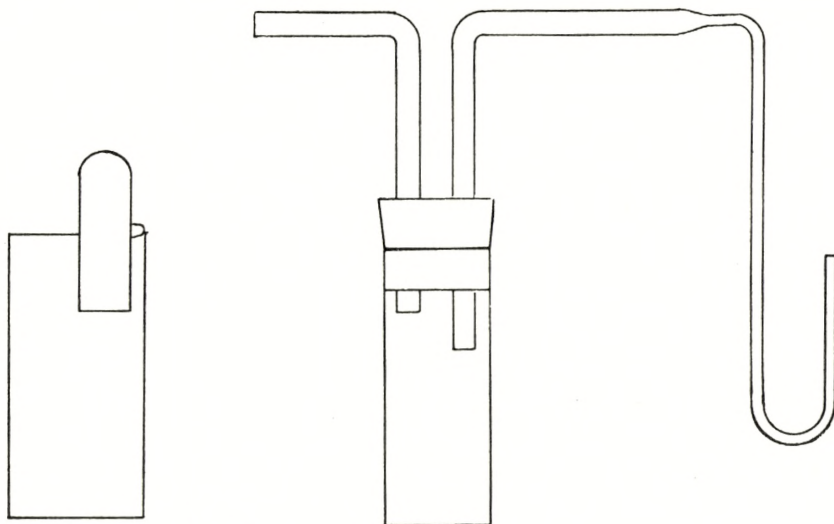


Fig. 4.

 $\frac{2}{3}$  nat. size.

Fig. 5.

accumulator, the oscillator of the coil being put out of action by means of a piece of match. By this means a single spark is produced when the switch is operated once on and off, the spark appearing at the "off" stroke. The high-tension terminal of the induction-coil is connected to the mercury in the graduated tube through the above mentioned short steel tube, while the low-tension terminal binding post is connected to the mercury in the explosion pipette through a steel wire. In this way the tip of the gas-siphon acts as a sparking-plug when introduced just above the mercury surface in the pipette, the terminals being a small globe of mercury made to appear on the tip and the surrounding mercury, respectively.

The operation of the apparatus is as follows: From the T-shaped container a suitable amount of the gas to be analyzed is drawn into the burette and sealed with mercury in the siphon. (It should be noted here, that the tip of the siphon must always



be wet when dipped under dry mercury. If not, a trace of air will be drawn in. The tip should be cleaned at intervals with chromic acid mixture.) Now one of the gas containers (fig. 4) is filled completely with water and placed round the siphon. Air above the outer branch of mercury is expelled and then the tip of the siphon is put into the inverted glass tube (the bell). Next the mercury is expelled, at which it cannot be avoided that some gas escapes into the bell. This is drawn back into the burette and the whole specimen sealed with a column of water. The table is now so adjusted that the tip is on a level with the free surface of the water and the meniscus in the capillary is placed at  $M_1$ , after which the volume is read. It should be noted, that if the gas contains high percentages of relatively soluble gases, such as  $CO_2$  or  $N_2O$ , the gas escaping when the mercury is expelled must not be collected as its composition will have changed. On the other hand there is no risk of serious errors by sealing even mixtures rich in those gases with water in the narrow tubing of the siphon on account of the small surface involved. It is mainly for this reason, that adjustment of the water meniscus at  $M_1$  and not at the zero mark of the burette proper is to be preferred.

Next the absorptions are brought about in the usual order.

As absorption liquids we recommend: For  $CO_2$ : a solution of 50 g. KOH in 50 ml. of water. For  $O_2$  a solution of 10 g.  $Na_2S_2O_4$  and 7 g. KOH in 50 ml. of water.

For  $C_2H_4$ : 100 per cent.  $H_2SO_4$ , which does not seriously attack mercury, while fuming acid (containing  $H_2S_2O_7$ ) evolves  $SO_2$ . 100 per cent.  $H_2SO_4$  is easily prepared by mixing ordinary conc.  $H_2SO_4$  with fuming acid in suitable amounts. It is tested by means of the melting point, which should be  $+9^\circ$  or higher.

For CO the ammoniacal solution of CuCl known from macro gas-analysis must be used, as the acid solution attacks mercury. As is well-known, two pipettes of this reagent must be used in series, when considerable amounts of CO are to be expected. It must be said that immediately after the use of this solution it is sometimes necessary to clean tube D with water, conc. sulphuric acid, and water in the order mentioned.

The absorption pipettes are filled somewhat less than half with the solutions. As they are stored over mercury there is no

danger of their deteriorating by contact with air. For this reason the  $\text{CO}_2$  and  $\text{CO}$  reagents keep indefinitely when not in use. But the  $\text{O}_2$ -reagent is intrinsically unstable and must be renewed at intervals and the pipette with 100 per cent.  $\text{H}_2\text{SO}_4$  should be emptied as soon as circumstances permit. For the absorptions the gas is transferred to the pipette and absorption effected by suitable rhythmic shaking of the block. The gas-siphon is not removed during this operation. The  $\text{CO}_2$ -absorption is very fast, 30 strokes (about 30 sec.) being amply sufficient. The velocity of the  $\text{O}_2$ -absorption depends on the age of the reagent. If 200 strokes (about 2—3 min.) do not suffice it will be convenient to renew the reagent. The  $\text{C}_2\text{H}_4$ - and  $\text{CO}$ -reagents seem to work somewhat faster than the  $\text{O}_2$ -reagent and the user is advised to work out for himself the times necessary for the different absorptions.

After the absorption the gas is drawn back into the burette, the last part collecting as a small bubble in the bulb just above the tip of the siphon, where it is easily caught and drawn into the burette. It must be avoided to get detached drops of the liquid into the siphon. At last the gas is sealed with the absorption liquid, the absorption pipette removed from the siphon, and one of the containers (fig. 4) filled with water placed with the bell around the tip. By operating the screw the absorption liquid is replaced by water and the capillary washed several times to remove traces of the liquid. Any gas bubbles lost during these operations collect in the top of the bell and are easily drawn back without any detached drops of water in the gas column. The volume is read as at the reading of the original volume.

If there is any reason to suppose that the rest after the absorptions contains combustible gases ( $\text{H}_2$  and  $\text{CH}_4$ ), it is collected in the explosion pipette and mixed with a measured amount of oxygen. After the measurements both gases (the rest and the added  $\text{O}_2$ ) are sealed with columns of water extending only from  $\text{M}_2$  to the tip of the siphon. The explosion is brought about as described above. Usually it occurs at the first spark; if not, the reason probably is that the mixture is not explosive. In that case a measured amount of hydrogen is added and the explosion thus effected. It may, however, happen that the spark gap is short-circuited by a drop of water adhering to the tip. In that case the explosion pipette is raised a little so that the tip dis-



appears under the mercury. The water drop then remains on the mercury surface, just above the tip, from where it is removed by shaking the pipette.

After the explosion the gas is drawn back into the burette, by which operation first the gas, next, most of the water (twice the volume contained between  $M_2$  and the tip) and finally some mercury as sealing liquid passes the siphon. To replace the mercury by water (this is necessary as it has proved too difficult in the long run to use mercury as confining liquid) the siphon is introduced into a container (fig. 4) filled mainly with mercury, but with a small amount of water, about 5 mm. in height, on the top of it. The mercury is now pressed out, some gas also escaping into the bell. This is united with the main portion in the burette and sealed with water.

With gases rich in  $CH_4$  this operation is the only one which is a little difficult, as it is essential here that the gas bubble in the bell should be in contact with the water for the shortest possible time on account of the risk of loss of  $CO_2$  by absorption. For the same reason it is recommended to saturate the water over the mercury in the bell with the gas resulting after explosion from the first analysis, whose result is then disregarded, and to repeat the analysis with the same ratio between gas and added oxygen.

After the sealing with water the bell with mercury is replaced by the one with water and the volume read as before.

During this replacement it sometimes happens that mercury enters the tip of the siphon, which is very inconvenient as it necessitates the repetition of the operation. If the siphon is not too wide this can be remedied by reducing the difference in level between the outer and the inner surface of mercury in the water-containing bell.

When only one of the gases  $H_2$  or  $CH_4$  is present, the analysis may be considered as finished; if not, and if an independent control is wanted, first  $CO_2$  and then  $O_2$  are absorbed as above. As the compositions of the remaining gases are completely different from those at the first absorptions of  $CO_2$  and  $O_2$ , a second set of absorption pipettes should be at hand.

It is a matter of course that the most scrupulous cleanliness must be observed at the filling of the absorption pipettes and



at all the operations, especially the washings of the siphon after the absorptions and before the combustion, as traces of alkali remaining in the capillary or still worse at the rubber connections,

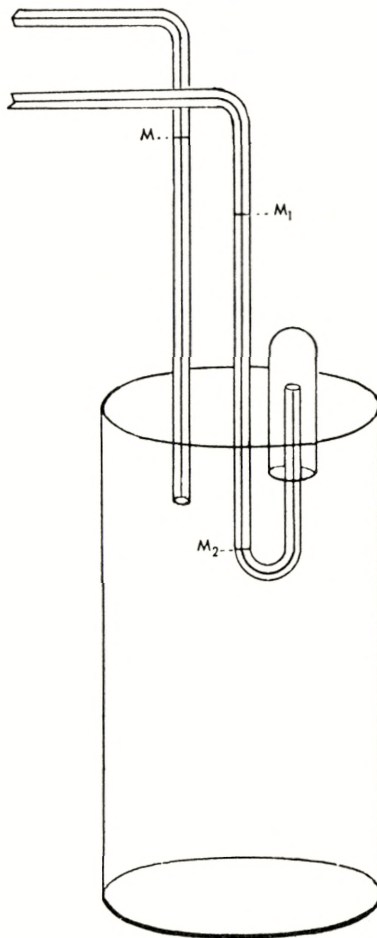


Fig. 6.  
 $\frac{2}{3}$  nat. size.

if any, may give rise to serious errors in the  $\text{CO}_2$ -determination after combustion. On the other hand this danger should not be exaggerated, and care taken to avoid unnecessary time-consuming manipulations. F. inst. we have found by experiment that in working with the burette with compensator, which necessitates the use of an especially large wash-beaker (see fig. 6), there is no objection to using the same wash-water for one complete analysis. We add that we take advantage of the fact that the

absorption liquid has specific gravities exceeding that of water, so that water layers a few millimetres above the tip are practically pure even if concentrated KOH solution has recently passed out. Concerning the filling of the pipettes with the absorption liquids the siphon (fig. 5) used for this purpose should be cleaned with chromic acid mixture just before use, as traces of impurities (grease?) suffice to alter the surface conditions inside the pipette so that the gas splits up into bubbles, which do not unite before a certain lapse of time, making the withdrawal from the pipette into the burette a rather time-consuming procedure. Of course also the flasks containing the absorbents should be held scrupulously clean.

For specimens rich in combustible gases we have found the explosion method convenient on account of its rapidity, and with access to pure hydrogen it may of course be used in all cases. But in the case of small contents of combustible gases the result becomes uncertain, the final result being a small difference between relatively large quantities.

It should be added that the explosion method has a still more serious drawback, as one must be careful to ascertain that no oxidation of nitrogen takes place. This can be attained by increasing the amount of oxygen, but if the gas specimen is too small to allow a second analysis to be performed, this is inconvenient. If rapidity is not essential, we therefore recommend slow combustion in a heated quartz capillary. In this way oxidation of nitrogen is avoided and the method has this further advantage that combustible gases are burnt, however small their concentrations.

For this purpose a hairpin-shaped quartz capillary (about 0.5 mm. inside diameter, the branches being 50 mm. long) is inserted on the top of the burette or on a separate combustion pipette by means of rubber tubing. Here, too, the siphon is preferably made from quartz, but we have found it sufficient to use a second rubber connection to the glass siphon about the middle of its horizontal part. To heat the "hairpin" a small removable electric furnace wound from nichrome wire on an unglazed porcelain tube (about 10 mm. inside diameter) on a length of about 50 mm. and insulated with two or three layers of asbestos card is recommended. Our furnace uses 1 amp. at 50 volt, this

giving a bright yellow heat. If the apparatus is intended to give the highest attainable accuracy of the absorptions, it is preferable to use a separate pipette for the combustion as the insertion of the quartz capillary between the burette proper and the gas-siphon increases the volume containing gas at an ill-defined temperature. The use of a separate combustion pipette of course necessitates an extra transfer of the gas, thus increasing the duration of the analysis by about 1 min., which is not very essential. It is more important that it is cheaper to mount the "hairpin" and the furnace on the same support as the burette, thus avoiding not only the extra support but also an extra glass syringe and generally making the apparatus more compact. Fig. 7 shows the construction of the separate combustion pipette. It has a quartz hairpin made in one piece with the siphon. Outer and inner diameters of the capillary are as usual 3 mm. and 0.3—0.5 mm., respectively. It may be remarked that we have been unable to purchase quartz capillaries with inside diameters less than 0.5 mm. If desired, f. inst. after a break, the siphon may be made of glass from G to the tip, the glass and quartz capillaries being connected by means of rubber tubing. If necessary, the ends are ground fairly plane by means of a file or a carborundum stone.

The tube H of a capacity somewhat larger than the burette serves as gas container at the operation. I is the furnace wound on the end of the unglazed porcellain tube (inside diameter 10 mm.). The tube is cramped in one end of the wooden bar K, the other end of which is fastened on the brass tube L, through which the electric leads for the furnace pass. This tube is so mounted on the back of the wooden stand that it may be swung round its axis and lifted about 6 cm. so as to allow the furnace to be placed round the hairpin and to be removed after use. Suitable stops prevent undesired movements of the furnace.

For the combustion the gas mixed with oxygen is collected in the explosion pipette, after which the combustion is performed by screwing the mercury backwards and forwards some times, the minimum number, usually about 4, being determined by experiments. If the quartz capillary is narrow enough, explosions hardly occur, even with strongly explosive mixtures. Further-



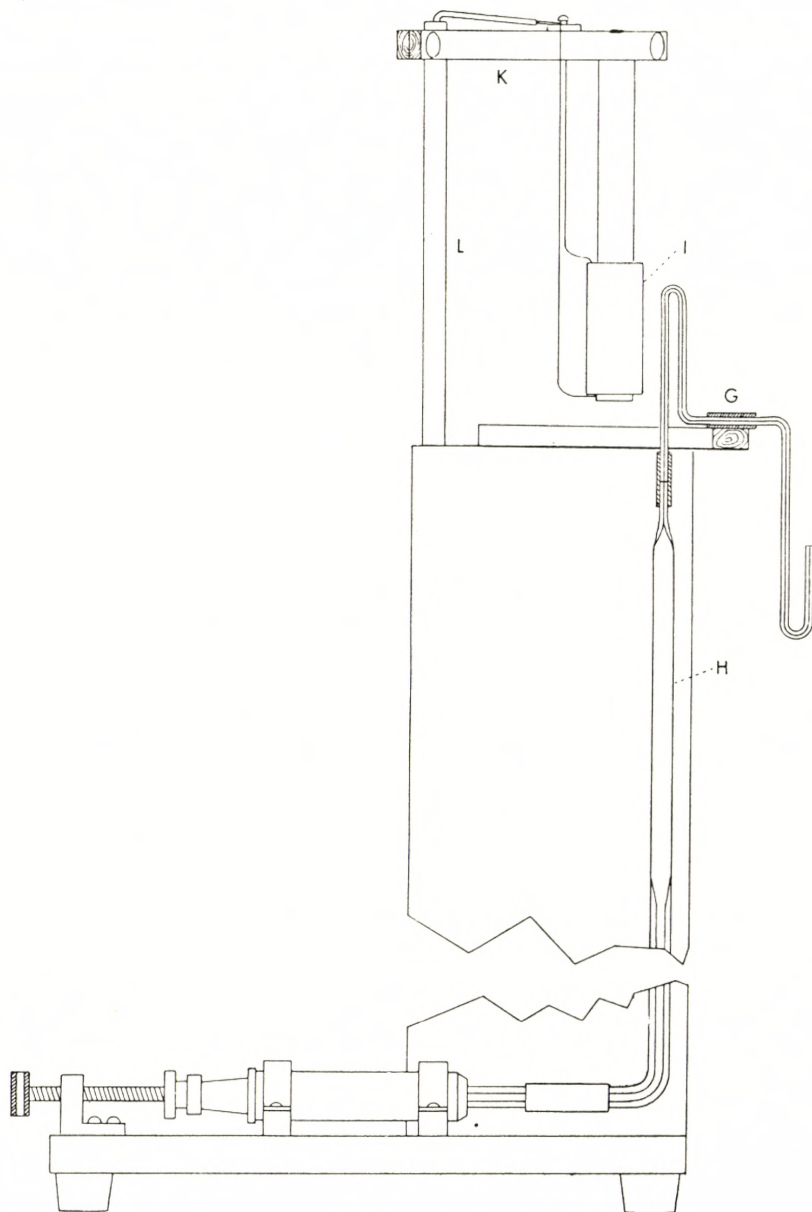


Fig. 7.  
 $\frac{1}{3}$  nat. size.

more an explosion is harmless, when the stoppered explosion pipette is used as container.

The treatment after combustion is exactly as after an explosion.

It is obvious that the combustion takes more time than the explosion as it is necessary to pass the gas several times through the combustion tube to ensure complete combustion, not to speak of the time of heating and cooling the "hairpin." It is especially difficult to burn the last traces of  $\text{CH}_4$ . In this connection it should be mentioned that at first we worked for some time with a platinum capillary about 0.5 mm. inside diameter instead of the quartz tube. But this gave rise to troubles probably arising from spluttering during the combustion. At least they seemed especially to occur after we had tried to fractionate a mixture of  $\text{H}_2$  and  $\text{CH}_4$  by burning  $\text{H}_2$  at low temperatures. These experiments in so far seemed successful, but after we had tried a few times, the flow of mercury through the capillary was rendered more and more difficult and eventually stopped completely. For this reason and of course also on account of its transparency quartz is to be preferred. Concerning the combustion of  $\text{CH}_4$  it must be emphasized that it is at least as difficult to burn  $\text{CH}_4$  quantitatively in a platinum as in a quartz tube, the only remedy being to choose the highest temperature the furnace will stand.

### Calculations.

The principle of the calculations is too obvious to be given here, but a few details may be mentioned. It is of course necessary to reduce the "wet" volumes corrected for errors of calibration to standard conditions. All volumes are preferably measured in centimetres on the scale, as the absolute volumes are of interest in exceptional cases only. If  $M_1$  is placed, as proposed, 13.7 mm. above the tip, the pressure obviously is always 1 mm. less than that read on the barometer. The volume after combustion must be corrected for  $\text{CO}_2$  dissolved in the water introduced together with the gas and the oxygen, viz. in twice the volume of water contained between  $M_2$  and the tip. If  $c$  is the volume of  $\text{CO}_2$ ,  $a$  the total volume after combustion and  $w$  the volume between

$M_2$  and the tip, the correction will be  $\left(2 w \cdot \frac{c}{a} 0.942\right)$ .

0.942 is the Ostwald solubility of  $\text{CO}_2$  in water at  $20^\circ$ . At other temperatures the solubilities are

at $15^\circ$	$16^\circ$	$17^\circ$	$18^\circ$	$19^\circ$	$20^\circ$	$21^\circ$	$22^\circ$	$23^\circ$	$24^\circ$	$25^\circ$
1.074	1.043	1.015	0.989	0.965	0.942	0.920	0.896	0.872	0.850	0.829

The correction thus calculated will be a minimum value as some extra moisture will get into the explosion pipette from the outer surface of the wet gas-siphon.

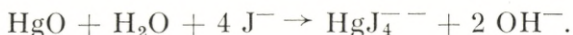
### Accuracy.

The accuracy of the results is about 0.1 per cent. absolute on the absorptions, depending somewhat on the total volume. But of course it should be remembered that the first analysis on a gas mixture can never be quite correct, as saturation of the absorption liquids with the mixture at hand must be accomplished before the results are reliable. The error on the combustion is somewhat greater, especially when a mixture rich in  $\text{CH}_4$  is to be analyzed. As far as we have been able to ascertain, the error is chiefly due to the solubility of  $\text{CO}_2$ . The correction for dissolved  $\text{CO}_2$  mentioned above may easily amount to 2 mm. or more (on the scale), and as the amount of water in the explosion pipette certainly is somewhat greater than that known to be introduced with the gases, it is no wonder that the values for  $\text{CH}_4$  (calculated from the  $\text{CO}_2$  found after explosion or combustion) always tend to be low. We should say that a defect in  $\text{CH}_4$  of 0.5 per cent. on values about 100 per cent. is rather the rule than the exception. By skilful operation and especially by using a large excess of  $\text{O}_2$ , thus reducing the  $\text{CO}_2$ -content in the gas after combustion, the error may be reduced, but it will be difficult to avoid it completely. For this reason the determination of small amounts of hydrogen in gases rich in methane is nearly impossible. We have made some experiments to ascertain if also oxidation of mercury might play a rôle. To this end we proceeded as follows: A certain amount, about 200  $\mu\text{l}$ . of 10 per cent. KJ solution was measured in the burette, 0.1 n HCl added from a microburette of the REHBERG (7) type, after which the  $\text{CO}_2$  was expelled with a stream of  $\text{CO}_2$ -free air and the acid titrated back with 0.1 n NaOH, phenolphthalein being used as an indicator. Next, an ex-



plosion was brought about and a similar amount of KJ-solution sucked into the explosion pipette, shaken for a short time and then drawn back and delivered into the beaker used for titration. The rest of the solution was delivered into the same beaker by repeating the operation twice with water and the titration performed as mentioned above.

In this way we performed a series of experiments both with explosions and combustion. We found indications of a slight formation of base according to the equation



The amount of  $\text{O}_2$  consumed by oxidation was rather variable, usually less than  $0.4 \mu\text{l.}$ , which on our burette corresponded to  $0.2 \text{ mm.}$  May be the oxidation was slightly greater in the combustion experiments, but on the whole it must be said that an error corresponding to more than  $0.2 \text{ mm.}$  on our burette is exceptional, an error which is barely perceptible. And even this must be considered as a maximum, as our KJ-solution seemed to attack mercury under formation of base.

### The Burette with Compensator.

As is well-known, the reduction of gas volumes to standard conditions is rather time-consuming. F. inst. Haldane's apparatus for that reason is provided with a compensator containing moist air. The same principle was used by L. DOYÈRE (2) nearly a century ago.

We have found it convenient to use it also in our apparatus. To this end the mantle containing the temperature bath is made about  $55 \text{ mm.}$  wide, the burette and the compensator being placed about  $30 \text{ mm.}$  apart. The water in the bath must be stirred continually by means of air bubbles during the analysis.

The compensator is a glass tube, whose inner diameter is not important, about twice the inner diameter of the burette being suitable. At the upper end it is constricted to about  $0.3\text{--}0.5 \text{ mm.}$  inside and about  $3 \text{ mm.}$  outside diameter. At the lower end it is somewhat extended so as to accomodate a mercury screw according to A. Krogh (a hard rubber nut with a steel screw about  $3 \text{ mm.}$  in diameter). The mercury screw is made

mercury-tight by means of tap grease and is cemented into the glass tubing by means of picein or de Khotinsky cement. It is covered with mercury and a few drops of water. By means of rubber tubing the upper end is connected to a narrow glass tube similar to the one used at the top of the burette, only without the part from  $M_2$  to the tip. For use the narrow tube is cleaned with chromic acid mixture, which is drawn in and squeezed out by means of the mercury screw and afterwards cleaned by water. We recommend this to be done immediately before the start of a series of analyses. By suitably screwing back and forth any detached water drops are removed. The arrangement of the two tips is shown in fig. 6.

The method of reading the volumes is as follows: The tips of the burette and the compensator both dip into the same beaker filled with water. This should be of the same type as the one in fig. 4 but of larger dimensions, height about 8—9 cm., diameter about 6 cm. The gas bell, which is of the same dimensions as the one in fig. 4, may be cemented on to the wall of the beaker with de Khotinsky cement. At the start of the analysis the water in the compensator is placed at the mark  $M$  by means of the mercury screw, the adjustable table being set at a suitable height, and the screw  $F$  on the burette is operated so as to place the level in the gas-siphon at the mark  $M_1$ . For the subsequent readings the mercury screw of the compensator must be left untouched, but the water level in the compensator-tip is placed at the mark  $M$  by adjustment of the table, after which the burette screw is operated so as to place the water level in the gas-siphon at  $M_1$ . Thus the reduction factor obviously remains constant during the whole analysis and therefore can be omitted from the calculations. For cases where comparison with measurements from other burettes are needed, a thermometer in the temperature bath is provided.

As it is inconvenient to make the range of movement of the adjustable table greater than 8—10 cm., which corresponds to a temperature difference of less than  $1.5^\circ \text{C.}$ , a place with not too variable temperature should be chosen for the apparatus. If nevertheless necessary, the mantle may be heated slightly by the hand or cooled with a wet cloth.



### Advisory Remarks.

In conclusion we should add a few remarks on the choice between the different possibilities of construction mentioned above, this choice of course depending on the purpose. First of all we should recommend the use of the compensator in all cases. The extra complication in construction and use is not essential, and it saves hours spent on tedious calculations.

If the apparatus is intended for absorptions only, or if the highest possible accuracy is aimed at, no combustion device should be arranged on the top of the burette. Combustion may then be carried out by explosion, the devices for this being easily improvised. As mentioned above, the explosion method often gives rise to errors, which may be avoided by increasing the amount of oxygen added, or decreasing the amount of gas to be analyzed, or both. If a series of analyses of similar gases is to be carried out, in which case the amount of oxygen necessary may be found once for all by experiments, the explosion method must be preferred on account of its rapidity.

In all other cases, however, combustion in the heated quartz capillary is preferable, and if the highest possible accuracy of the absorptions of  $\text{CO}_2$  and  $\text{O}_2$  is desired, as will be the case in physiological investigations, the separate combustion pipette should be used. It should be added that if the adjustable table is fixed on the same base as the burette, which is convenient, the mirror image of fig. 7 should be used for the design. Furthermore, in this case the table should be amply large and care should be taken that the siphons of the burette and the combustion pipette, respectively, are being placed at the same height above the laboratory desk. In this way the cost of an extra adjustable table for the combustion pipette can be avoided.

For ordinary use, however, it is more convenient in use and much cheaper to mount the quartz hairpin and the furnace on the burette and its stand. No drawing of this arrangement is given as its design is practically self-evident.

It should perhaps be mentioned that for physiological purposes the accuracy may be increased by the well-known device of enlarging the upper part of the burette, so that it contains



700 out of 1000 parts of the whole volume on a length of about 100 mm., while 300 parts occupy a length of 300 mm., the total volume of the compensator being distributed in a similar way. In that case, however, an adjustment of the mercury in the burette finer than that to be obtained with the syringe will be found necessary. Presumably the best plan will be to move the syringe about 15 mm. from the bottom end of the graduated tube and then to connect the ends with stout rubber tubing, which can be compressed by means of a pinchcock whose base is fixed on the board behind. By this means it ought to be possible to obtain an absolute accuracy of nearly 0.01 per cent. abs., but it should be added that the authors have not tried out this possibility, as the extreme accuracy obtainable by such means has been unnecessary in their current work.

*Chemical Laboratory A*  
*Royal Technical High-School, Copenhagen.*

---

### References.

- (1) See f. inst. the article by A. KROGH in Abderhaldens Handb. der Biochemischen Arbeitsmethoden 8 (1915) 532.
  - (2) L. DOYÈRE: Annales de chim. et de phys. (3) 28 (1850) 1.
  - (3) A. KROGH: Abderhaldens Handb. der Biochemischen Arbeitsmethoden 8 (1915) 495.
  - (4) Journ. Am. Chem. Soc. 47 (1925) 109.
  - (5) Z. anal. Chem. 80 (1930) 435.
  - (6) For other constructions especially of American origin see f. inst. W. D. TREADWELL: Tabellen und Vorschriften zur quantitativen Analyse (Leipzig und Wien, FRANZ DEUTICKE, 1938) p. 222.
  - (7) P. B. REHBERG: Biochemical Journ. 19 (1925) 270.
-





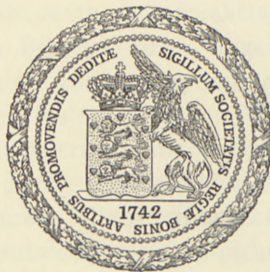
DET KGL. DANSKE VIDENSKABERNES SELSKAB  
MATEMATISK-FYSISKE MEDDELELSER, BIND XXII, NR. 5

---

ÜBER LINEARE  
UND QUADRATISCHE ABBILDUNGEN  
DES RAUMES AUF EINE EBENE

VON

FR. FABRICIUS-BJERRE



KØBENHAVN

I KOMMISSION HOS EJNAR MUNKSGAARD

1945

Printed in Denmark.  
Bianco Lunos Bogtrykkeri A/S

## EINLEITUNG

Die vorliegende Untersuchung hat als Ausgangspunkt eine Abhandlung von L. ECKHART [3], in der gezeigt wird, wie man aus zwei gegebenen axonometrischen Bildern einer Raumfigur andere axonometrische Bilder konstruieren kann. Die Methode ist, kurz gesagt, die, dass man durch entsprechende Punkte der beiden Bilder (d. h. Bilder desselben Raumpunktes) parallel zu zwei gegebenen Richtungen Geraden legt, deren Schnittpunkt dann eine neue Figur durchläuft, die sich als ein neues axonometrisches Bild der Raumfigur erweist.

Im ersten Kapitel haben wir diese Methode aufs neue untersucht, indem wir nicht nur reguläre, sondern auch singuläre axonometrische Abbildungen betrachten. Dadurch ist z. B. ermöglicht worden, aus Grundriss und Aufriss allein, ohne Verwendung von Ähnlichkeit oder Kongruenz, beliebige axonometrische Bilder zu konstruieren. Wir beenden dieses Kapitel mit einer algebraischen Darstellung der behandelten Abbildungen nebst einigen Bemerkungen über orthogonale Axonometrie.

Im zweiten Kapitel, (das sich unabhängig vom ersten lesen lässt), wird die erwähnte Methode projektivisch verallgemeinert. Aus zwei perspektiven Bildern eines Gegenstandes konstruiert man ein neues Bild, indem man entsprechende Punkte der gegebenen Bilder aus zwei festen Punkten der Ebene projiziert, wobei der Schnittpunkt korrespondierender Strahlen ein drittes Bild durchläuft. Die dadurch erzeugte Abbildung des Raumes auf die Ebene wird allgemein nicht perspektivisch. Wir werden nachweisen, dass man entweder eine Abbildung, die aus STEINERS »schiefer Projektion«<sup>1)</sup> und einer Kollineation besteht, oder eine rationale quadratische Abbildung eines Geradenbündels auf eine Ebene oder schliesslich eine neue perspektive Abbildung erhält.

1) Siehe S. 20.



Wir untersuchen dann besonders, unter welchen Bedingungen die Abbildung perspektivisch wird. Indem wir sowohl reguläre als singuläre Abbildungen einführen, werden wir zu Konstruktionen ähnlich denjenigen von G. HAUCK [7, 8] geführt. Wir schließen dieses Kapitel mit einigen Bemerkungen über imaginäre Abbildungen und mit einer algebraischen Darstellung der verschiedenen Transformationen.

---

Die oben definierte quadratische Abbildung des Raumes auf eine Ebene lässt sich unmittelbar auf Räume mehrerer Dimensionen verallgemeinern. Im vierdimensionalen Raum z. B. müssen wir drei perspektive Abbildungen von diesem Raum auf einen  $R^3$  betrachten, und im  $R^3$  müssen ausserdem drei Geraden vorgelegt sein. Aus diesen Geraden projiziert man entsprechende Punkte der drei Bilder, und der Schnittpunkt korrespondierender Ebenen durchläuft dann ein neues Bild der gegebenen vierdimensionalen Figur. Diese Abbildung wird von drittem Grade, und man erhält dadurch eine Verallgemeinerung der Steinerschen schiefen Projektion. Die Abbildung, die hierdurch zwischen zwei dreidimensionalen Räumen allgemeiner Lage erzeugt wird, ist von anderen Gesichtspunkten aus z. B. von R. STURM (Geom. Verwandtsch. IV, S. 394) untersucht worden.

Im Raum von  $n + 1$  Dimensionen müssen  $n$  perspektive Abbildungen des Raumes auf einen  $R^n$  vorgelegt sein, und die erzeugte Abbildung wird in diesem Fall von  $n$ 'tem Grade.

Im folgenden werden wir auf die Abbildungen in höheren Räumen nicht eingehen.

---

## 1. KAPITEL

### Axonometrische Abbildungen.

#### § 1. Reguläre und singuläre Abbildungen.

Unter einer axonometrischen Abbildung versteht man eine affine (lineare) Abbildung des Raumes  $R^3$  auf eine Ebene  $\alpha$ , die Bildebene. Eine solche Abbildung  $T$  lässt sich aus einer Parallelprojektion in einer Richtung  $r$  auf eine Ebene  $\beta$  und einer affinen Abbildung von  $\beta$  auf  $\alpha$  zusammensetzen. Falls diese Affinität den Rang 2 hat, nennt man  $T$  regulär. Ist der Rang gleich 1, wird  $T$  als singulär (einfach-singulär) bezeichnet, und ist schliesslich der Rang gleich 0, nennt man  $T$  doppel-singulär, und  $R^3$  wird in einen einzelnen Punkt abgebildet. Diesen letzteren Fall werden wir gewöhnlich ausser Betracht lassen.

Wenn  $T$  regulär ist, werden Geraden mit der Richtung  $r$  in Punkte abgebildet, während andere Geraden wieder in Geraden transformiert werden. Entsprechende Punktreihen sind ähnlich. Ist  $T$  dagegen singulär, lässt sich die Abbildung von  $\beta$  auf  $\alpha$  aus einer Parallelprojektion in einer Richtung  $r'$  in  $\beta$  auf eine Gerade  $b$  und einer linearen Abbildung von  $b$  auf  $\alpha$  zusammensetzen. Es ist danach klar, dass eine Ebene  $\rho$  parallel zu  $r$  und  $r'$  in einen einzelnen Punkt von  $\alpha$  abgebildet wird. Die Projektionsrichtung  $r$  hat dann keine besondere Stellung vor anderen Richtungen der Ebene  $\rho$ , und  $T$  ergibt sich in diesem Fall durch eine »Ebenenprojektion« mit der »Ebenenrichtung«  $\rho$  auf  $b$ , gefolgt von einer linearen Abbildung von  $b$  auf  $\alpha$ .

Es seien  $T_1$  und  $T_2$  zwei gegebene axonometrische Abbildungen von  $R^3$  auf  $\alpha$ . Einen beliebigen Punkt in  $R^3$  bezeichnen wir mit  $P$ , eine von  $P$  durchlaufene Figur mit  $(P)$ , die Bilder von  $P$  bei  $T_1$  und  $T_2$  mit  $P_1$  und  $P_2$  und die Bilder der Figur mit  $(P_1)$



und  $(P_2)$ . Wir nehmen an, dass die Bilder  $O_1$  und  $O_2$  eines Punktes  $O$  zusammenfallen (in  $O_{12}$ ). Wenn dies für keinen Punkt des Raumes der Fall ist, fügen wir zu  $T_2$  die Parallelverschiebung  $\vec{O_2O_1}$  hinzu.

Wenn  $T_1$  und  $T_2$  beide regulär sind, bezeichnen wir mit  $r_1$  und  $r_2$  Strahlen durch  $O$  in den gegebenen Projektionsrichtungen. Falls  $r_1$  und  $r_2$  zusammenfallen, werden zwei beliebige Bilder  $(P_1)$  und  $(P_2)$  affin sein. Sind dagegen die Richtungen verschieden, sind die Bilder nicht affin. Dies folgt z. B. daraus, dass die Gerade  $r_1$  bei  $T_1$  in einen Punkt, bei  $T_2$  in eine Gerade abgebildet wird.

Wenn  $T_1$  regulär ist,  $T_2$  dagegen singulär (mit der Ebenenrichtung  $\varrho_2$  durch  $O$ ), werden zwei willkürliche Bilder  $(P_1)$  und  $(P_2)$  dann und nur dann affin sein, wenn  $r_1$  in der Ebene  $\varrho_2$  liegt. Und sind schliesslich sowohl  $T_1$  als auch  $T_2$  singulär (mit Ebenenrichtungen  $\varrho_1$  und  $\varrho_2$  durch  $O$ ), werden die Bilder  $(P_1)$  und  $(P_2)$  einer beliebigen Figur  $(P)$  in  $R^3$  affin sein oder nicht, je nachdem  $\varrho_1$  und  $\varrho_2$  zusammenfallen oder nicht. Die Beweise dieser einfachen Sätze werden hier übergangen.

Falls  $T_1$  und  $T_2$  beide regulär mit verschiedenen Projektionsrichtungen  $r_1$  und  $r_2$  sind, wird die Ebene  $\pi_{12} = r_1r_2$  bei  $T_1$  in eine Gerade  $s_1^*$ , bei  $T_2$  in eine Gerade  $s_2^*$  abgebildet. Diese Geraden (durch  $O_{12}$ ) bestimmen die sogenannten singulären Richtungen in  $\alpha$ , und man sagt, dass  $T_1$  und  $T_2$  allgemeine oder spezielle Lage haben, je nachdem  $s_1^*$  und  $s_2^*$  verschieden oder zusammenfallend sind.

## § 2. Die Abbildung $T_3$ .

Wir betrachten nun zwei willkürliche axonometrische Abbildungen  $T_1$  und  $T_2$  und konstruieren eine neue Abbildung  $T_3$  folgendermassen:

Durch  $O_{12}$  legen wir zwei verschiedene Geraden  $s_1$  und  $s_2$ . Ein beliebiger Punkt  $P$  in  $R^3$  hat bei  $T_1$  und  $T_2$  die Bilder  $P_1$  und  $P_2$ . Durch  $P_1$  legt man eine zu  $s_1$  parallele Gerade  $p_1$ , durch  $P_2$  eine zu  $s_2$  parallele Gerade  $p_2$ . Den Schnittpunkt von  $p_1$  und  $p_2$  bezeichnen wir mit  $P_3$ . Somit ist eine Abbildung  $T_3$  von  $R^3$  auf die Ebene  $\alpha$  festgelegt, die  $P$  in  $P_3$  überführt (Fig. 1).



$T_3$  hängt ausser von  $T_1$  und  $T_2$  auch von den Richtungen  $s_1$  und  $s_2$  ab, im ganzen von 14 Parametern, da  $T_1$  und  $T_2$  je von 6 Parametern abhängig sind (vgl. § 4). Der Punkt  $O_3$ , das Bild von  $O$  bei  $T_3$ , fällt, wie man unmittelbar sieht, in  $O_{12}$ . Von  $T_3$  gilt übrigens:

Die Abbildung  $T_3$  ist ebenfalls eine axonometrische Abbildung. Für diesen Satz werden wir im § 4 einen allgemeinen analytischen Beweis geben.

Wir wollen zunächst die verschiedenen möglichen Fälle näher untersuchen:

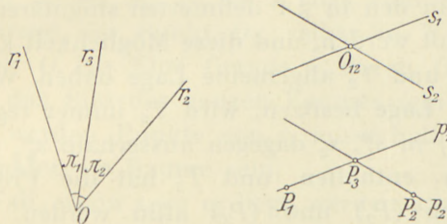


Fig 1.

### A. Die Abbildungen $T_1$ und $T_2$ sind beide regulär.

Die Geraden  $s_1$  bzw.  $s_2$  sind bei  $T_1$  bzw.  $T_2$  Bilder von zwei Ebenen  $\pi_1$  bzw.  $\pi_2$  durch  $r_1$  bzw.  $r_2$ . Wenn diese Ebenen nicht zusammenfallen (in  $\pi_{12}$ ), gibt es eine Schnittgerade  $r_3$ , und jeder Punkt einer Geraden  $p$  durch  $P$  parallel zu  $r_3$  wird bei  $T_3$  in denselben Punkt  $P_3$  abgebildet. Punkte ausserhalb  $p$  werden dagegen in Punkte ausserhalb  $P_3$  abgebildet. Falls  $P$  eine Gerade  $q$  durchläuft, die nicht zu  $r_1, r_2$  oder  $r_3$  parallel ist, wird  $P_1$  eine Gerade  $q_1, P_2$  eine Gerade  $q_2$  so durchlaufen, dass entsprechende Punktreihen ähnlich sind. Die zur Konstruktion der Punkte  $P_3$  gehörigen Büschel paralleler Geraden werden dann auch ähnlich, also perspektiv, und  $P_3$  durchläuft eine neue Gerade  $q_3$  in  $\alpha$ .  $q_3$  fällt speziell in  $p_1$ , wenn  $q$  zu der Ebene  $\pi_1$  parallel ist; dies hat auch Gültigkeit, wenn  $q$  zu  $r_1$  parallel wird. — Die Abbildung  $T_3$  ist somit eine reguläre axonometrische Abbildung mit der Projektionsrichtung  $r_3$ .

Falls die oben eingeführten Ebenen  $\pi_1$  und  $\pi_2$  in  $\pi_{12}$  zusammenfallen, werden sämtliche Punkte in einer Ebene durch  $P$  parallel zu  $\pi_{12}$  in denselben Punkt  $P_3$  abgebildet, während Punkte ausser-

halb der Ebene ausserhalb  $P_3$  abgebildet werden. Eine Gerade  $g$ , die nicht zu  $\pi_{12}$  parallel ist, wird wie oben in eine neue Gerade abgebildet, woraus folgt, dass  $T_3$  in diesem Fall eine singuläre axonometrische Abbildung mit  $\pi_{12}$  als Ebenenrichtung ist.

Wenn  $T_1$  und  $T_2$  dieselbe Projektionsrichtung  $r_1 = r_2$  haben, folgt aus obigem, dass man allgemein wieder eine Abbildung  $T_3$  mit derselben Projektionsrichtung erhält, so dass die drei Bilder  $(P_1)$ ,  $(P_2)$ ,  $(P_3)$  eines Objekts affin sind.

Sind  $r_1$  und  $r_2$  verschieden, wird  $T_3$  nur dann singulär sein, wenn  $s_1$  und  $s_2$  in den in § 1 definierten singulären Richtungen  $s_1^*$  und  $s_2^*$  gewählt werden, und diese Möglichkeit kann nur entstehen, wenn  $T_1$  und  $T_2$  allgemeine Lage haben. Wenn also  $T_1$  und  $T_2$  spezielle Lage besitzen, wird  $T_3$  immer regulär.

Wenn man  $s_1$  in  $s_1^*$ ,  $s_2$  dagegen ausserhalb  $s_2^*$ , wählt, ist  $r_2$  in der Ebene  $\pi_1$  enthalten, und  $T_3$  hat die Projektionsrichtung  $r_2$ , wodurch  $(P_2)$  und  $(P_3)$  affin werden. Wählt man sowohl  $s_1$  ausserhalb  $s_1^*$  als  $s_2$  ausserhalb  $s_2^*$ , haben  $\pi_1$  und  $\pi_2$  eine Schnittgerade  $r_3$ , welche nicht in der Ebene  $\pi_{12}$  liegt.  $T_3$  wird also eine reguläre Abbildung mit der Projektionsrichtung  $r_3$ .

Verschiedenen Wahlen von  $s_1$  und  $s_2$  entsprechend erhält man verschiedene Richtungen  $r_3$ . Man kann jedoch nicht alle Richtungen  $r_3$  erhalten. Erstens muss  $r_3$  ausserhalb der Ebene  $\pi_{12}$  liegen, und ferner muss man die Forderung stellen, dass die Bilder  $s_1$  von  $\pi_1$  (bei  $T_1$ ) und  $s_2$  von  $\pi_2$  (bei  $T_2$ ) nicht zusammenfallen. Wenn nun eine Gerade  $s$  den Strahlenbüschel mit dem Scheitel  $O_{12}$  durchläuft, so durchlaufen die (in  $T_1$  und  $T_2$ ) entsprechenden Ebenen projektive Ebenenbüschel mit den Achsen  $r_1$  und  $r_2$ . Diese Ebenenbüschel werden nur in dem Fall perspektiv, wenn die Ebene  $\pi_{12}$  dasselbe Bild sowohl bei  $T_1$  als auch bei  $T_2$  hat, also wenn  $T_1$  und  $T_2$  spezielle Lage haben.

Wenn also  $T_1$  und  $T_2$  allgemeine Lage haben, können wir als Projektionsrichtung jede Richtung ausserhalb der Ebene  $\pi_{12}$  und der durch die projektiven Ebenenbüschel erzeugten Kegelfläche zweiter Ordnung haben. Falls die Abbildungen spezielle Lage haben, muss die Kegelfläche durch einen von den perspektiven Ebenenbüscheln erzeugten (ebenen) Geradenbüschel ersetzt werden.

Unabhängig davon, ob  $T_1$  und  $T_2$  allgemeine oder spezielle Lage haben, haben  $T_1$  und  $T_3$  (und ebenso  $T_2$  und  $T_3$ ) in jedem



Fall spezielle Lage. Der Strahl  $s_1$  entspricht nämlich sowohl in  $T_1$  wie in  $T_3$  der Ebene  $\pi_1$ . Zum Abbildungspaar  $(T_1, T_3)$  gehört somit nur die eine singuläre Richtung  $s_1$ , und dementsprechend zu  $(T_2, T_3)$  nur die singuläre Richtung  $s_2$ .

Wir gehen nun zum zweiten Fall über:

### B. Die Abbildung $T_1$ ist regulär, die Abbildung $T_2$ singulär.

Bei  $T_1$  wird der Raum  $R^3$  in die ganze Ebene  $\alpha$  abgebildet, während  $T_2$  den Raum in eine Gerade  $a_2$  durch  $O_{12}$  abbildet. Eine Gerade  $s_1$  durch  $O_{12}$  ist in  $T_1$  das Bild einer Ebene  $\pi_1$  durch  $r_1$ , während der Punkt  $O_{12}$  selber in  $T_2$  das Bild der Ebene  $\varrho_2$  durch  $O$  ist. Eine Gerade  $s_2$  durch  $O_{12}$  wird, wenn sie in  $a_2$  fällt, das Bild des ganzen Raumes sein; im entgegengesetzten Fall werden Punkte von  $s_2$  ausserhalb  $O_{12}$  gar nicht Bilder von Punkten im Raume sein.

Im ersten Fall, wenn  $s_2$  in  $a_2$  liegt, werden alle Punkte einer Ebene  $\pi$  durch  $P$ , parallel zu  $\pi_1$ , bei  $T_3$  in denselben Punkt  $P_3$  (auf  $a_2$ ) abgebildet, und da übrigens Gerade wie oben in Gerade überführt werden, ist  $T_3$  eine singuläre axonometrische Abbildung von  $R^3$  auf  $a_2$  mit der Ebenenrichtung  $\pi_1$ . Wenn  $s_1$  variiert, erzeugt  $\pi_1$  einen Ebenenbüschel mit der Achse  $r_1$ .

Sind dagegen  $s_2$  und  $a_2$  verschieden — und fällt  $r_1$  nicht in  $\varrho_2$  — wird die Schnittgerade  $r_3$  der Ebenen  $\pi_1$  und  $\varrho_2$  Projektionsrichtung für eine reguläre Abbildung  $T_3$ . Wenn  $s_1$  den Strahlenbüschel ( $O_{12}$ ) in  $\alpha$  durchläuft, wird  $r_3$  einen Strahlenbüschel in  $\varrho_2$  durchlaufen, dessen Strahlen alle Projektionsrichtungen für  $T_3$  sein können. Zu jeder Richtung  $s_1$  kann man unendlich viele Richtungen  $s_2$  wählen, so dass man zu jeder Projektionsrichtung  $r_3$  unendlich viele unter sich affine Bilder erhalten kann. Der Strahl  $s_1$  bestimmt somit die Projektionsrichtung  $r_3$ , während  $s_2$  bestimmt, welches von den affinen Bildern entstehen wird.

Der Fall, wo  $r_1$  in  $\varrho_2$  liegt, hat nichts von Interesse aufzuweisen. Schliesslich soll der letzte Fall betrachtet werden:

### C. Die Abbildungen $T_1$ und $T_2$ sind beide singulär.

$R^3$  wird bei  $T_1$  in die Gerade  $a_1$  durch  $O_{12}$ , bei  $T_2$  in die Gerade  $a_2$  durch  $O_{12}$  abgebildet. Der Punkt  $O_{12}$  ist bei  $T_1$  (bzw.  $T_2$ )



das Bild einer Ebene  $\varrho_1$  (bzw.  $\varrho_2$ ) durch  $O$ . Je nachdem die gewählten Strahlen  $s_1$  und  $s_2$  in  $a_1$  bzw.  $a_2$  fallen oder nicht, entstehen, vorausgesetzt dass  $\varrho_1$  und  $\varrho_2$  nicht zusammenfallen, drei verschiedene Fälle:

1°.  $s_1 = a_1$ ,  $s_2 = a_2$ . Der ganze  $R^3$  wird in den Punkt  $O_{12}$  abgebildet.  $T_3$  ist somit eine doppel-singuläre axonometrische Abbildung.

2°.  $s_1 = a_1$ ,  $s_2$  verschieden von  $a_2$ . Der ganze  $R^3$  wird auf  $a_1$  abgebildet, so dass sämtliche Punkte in einer Ebene durch  $P$  parallel mit  $\varrho_2$  in denselben Punkt von  $a_1$  abgebildet werden.

Da sich im übrigen Strahlen als Strahlen abbilden, wird  $T_3$  eine (einfach-)singuläre axonometrische Abbildung.

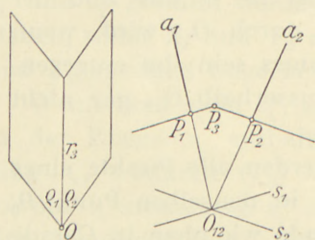


Fig. 2.

3°.  $s_1$  ist verschieden von  $a_1$ ,  $s_2$  von  $a_2$  (Fig. 2.). Sämtliche Punkte einer Geraden  $p$  durch  $P$  parallel zu der Schnittgeraden  $r_3$  der Ebenen  $\varrho_1$  und  $\varrho_2$  werden bei  $T_3$  in denselben Punkt  $P_3$  abgebildet. Deshalb wird hier  $T_3$

eine reguläre Abbildung mit der Projektionsrichtung  $r_3$ . — Man beachte, dass die Projektionsrichtung  $r_3$  unabhängig von den gewählten Richtungen  $s_1$  und  $s_2$  ist. Wir erhalten durch Variation von  $s_1$  und  $s_2$  eine doppelte Unendlichkeit von unter sich affinen, derselben Projektionsrichtung entsprechenden Bildern.

Indem wir uns besonders für die regulären Abbildungen  $T_3$  interessieren, können wir den folgenden Satz aussprechen:

Je nachdem  $T_1$  und  $T_2$  beide regulär, die eine oder beide singulär sind, entstehen durch Variation der Geraden  $s_1$  und  $s_2$  Bilder, die  $\infty^2$ ,  $\infty^1$  und einer Projektionsrichtung entsprechen. Die Zahl der unter sich affinen, jeder Projektionsrichtung entsprechenden Bilder ist 1,  $\infty^1$  und  $\infty^2$ .

### § 3. Erzeugung einer vorgelegten $T_3$ aus gegebenen $T_1$ und $T_2$ .

Es seien  $T_1$  und  $T_2$  gegebene reguläre axonometrische Abbildungen mit den Projektionsrichtungen  $r_1$  und  $r_2$ , und  $T_3$  sei eine neue reguläre Abbildung mit der Projektionsrichtung  $r_3$ . Die Bilder des Gegenstandes ( $P$ ) werden wie früher mit  $(P_1)$ ,  $(P_2)$ ,  $(P_3)$  bezeichnet.

Allgemein lässt sich  $(P_3)$  nicht aus  $(P_1)$  und  $(P_2)$  durch Wahl der Richtungen  $s_1$  und  $s_2$  bilden. Wenn bei  $T_3$  die Richtung  $r_3$  Projektionsrichtung werden soll, muss man nämlich  $s_1$  und  $s_2$  als Bilder der Ebene  $r_1 r_3$  bzw.  $r_2 r_3$  in  $T_1$  bzw.  $T_2$  wählen, und das aus  $(P_1)$  und  $(P_2)$  und den Richtungen  $s_1, s_2$  entstehende Bild wird dann im allgemeinen nur mit dem gegebenen  $(P_3)$  affin sein.

Man könnte sich nun die Aufgabe stellen, zu  $T_1$  und  $T_2$  solche ebenen affinen Abbildungen hinzufügen, wodurch  $(P_1)$  in  $(P'_1)$  und  $(P_2)$  in  $(P'_2)$  übergehen, dass sich  $(P_3)$  nun durch die gewöhnliche Konstruktion aus den neuen Bildern  $(P'_1)$  und  $(P'_2)$  bilden lässt. Mit den drei Projektionsrichtungen  $r_1, r_2, r_3$  sind auch die Richtungen  $s_1, s_2$  gegeben, da wir ja früher gezeigt haben (S. 9), dass auch in  $T_3$  die Gerade  $s_1 (s_2)$  das Bild der Ebene  $r_1 r_3 (r_2 r_3)$  ist. Indem wir annehmen, dass  $r_3$  ausserhalb der Ebene  $r_1 r_2$  liegt, sind  $s_1$  und  $s_2$  verschiedene Geraden.

Hiermit ist unsere Aufgabe darauf reduziert worden, eine Affinität zu finden, die  $(P_1)$  in  $(P'_1)$  überführt, so dass entsprechende Punkte in  $(P'_1)$  und  $(P_3)$  auf Geraden parallel zu  $s_1$  liegen, und analog für  $(P_2)$ . Da eine Affinität durch zwei entsprechende Dreiecke bestimmt ist, brauchen wir nur auf zu  $s_1$  parallelen Geraden durch drei Punkte  $P_3, Q_3, R_3$  drei andere Punkte  $P'_1, Q'_1, R'_1$ , zu wählen, wodurch die Affinität festgelegt wird. Entsprechend für  $(P_2)$ . Wenn man nun das neue Bild  $(P'_3)$  aus  $(P'_1)$  und  $(P'_2)$  mit den Richtungen  $s_1, s_2$  konstruiert, wird  $(P'_3)$  der Projektionsrichtung  $r_3$  entsprechen, also mit  $(P_3)$  affin sein, und da drei entsprechende Punkte von  $(P_3)$  und  $(P'_3)$  zusammenfallen, werden die beiden Bilder identisch.

Unsere Aufgabe ist hiermit gelöst, und zwar, wie man sieht, mit unendlich vielen Lösungen. Man könnte ferner die Forderung stellen, die Figur  $(P'_1)$  solle der Figur  $(P_1)$  ähnlich sein. Wir



gelangen dann zu der elementaren Aufgabe, ein Dreieck, einem gegebenen ähnlich, so zu legen, dass ein Eckpunkt in einem gegebenen Punkte und die beiden anderen auf gegebenen parallelen Geraden liegen. Wenn die Orientierung beibehalten wird, hat diese Aufgabe eine und nur eine Lösung. Wir haben somit:

Aus zwei axonometrischen Bildern kann man, einer willkürlichen Projektionsrichtung entsprechend, die ausserhalb der Ebene der gegebenen Projektionsrichtungen liegt, jedes axonometrische Bild auf eine und nur eine Weise allein durch

Anwendung von Ähnlichkeit aus den vorgelegten Bildern erhalten.

Es seien danach  $T_1$  und  $T_2$  beide singuläre axonometrische Abbildungen mit den Ebenenrichtungen  $e_1$  und  $e_2$ , deren Schnittgerade mit  $r_3$  bezeichnet ist.  $T_1$  bilde den Raum auf die Gerade  $a_1$ ,  $T_2$  auf  $a_2$  ab. Wie auch  $s_1$  und  $s_2$  gewählt werden, führt die früher beschriebene Kon-

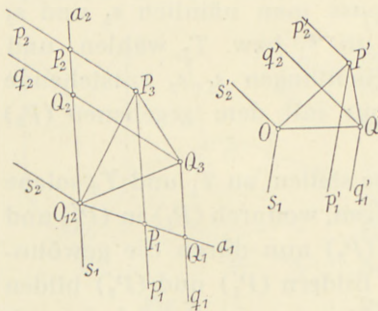


Fig. 3.

struktion zu unter sich affinen Bildern, der Projektionsrichtung  $r_3$  entsprechend. In diesem Fall gilt folgender Satz:

Durch passende Wahl von  $s_1$  und  $s_2$  kann man im allgemeinen bis auf Ähnlichkeit jedes axonometrische Bild der Richtung  $r_3$  entsprechend erhalten.

Beweis. — Drei Punkte  $O, P, Q$  sollen eine Ebene bestimmen, die  $r_3$  nicht enthält. Die Bilder von  $P$  und  $Q$  werden wie üblich mit  $P_1, Q_1, P_2, Q_2$  bezeichnet. Durch  $P_1$  und  $Q_1$  werden Geraden  $p_1$  und  $q_1$  parallel zu einer vorgelegten Richtung  $s_1$  gelegt, analog durch  $P_2$  und  $Q_2$  Geraden  $p_2$  und  $q_2$  parallel zu  $s_2$ ;  $p_1$  und  $p_2$  schneiden sich in  $P_3$ ,  $q_1$  und  $q_2$  in  $Q_3$ . Wir wollen nun beweisen, dass  $s_1$  und  $s_2$  im allgemeinen so gewählt werden können, dass das Dreieck  $O_{12}P_3Q_3$  ähnlich einem beliebigen Dreieck  $O'P'Q'$  wird.

Dies wird dadurch bewiesen, dass man eine Ähnlichkeitstransformation findet, welche die Punkte  $O_{12}P_1Q_1P_2Q_2$  so in Punkte  $O'P'_1Q'_1P'_2Q'_2$  überführt, dass die Geraden  $P'P'_1$  und  $Q'_1Q'$  und ebenso  $P'_2P'$  und  $Q'_2Q'$  parallel werden.



Die Lage der parallelen Strahlen  $s'_1, p'_1 = P'_1P'$  und  $q'_1 = Q'_1Q'$  lässt sich dadurch bestimmen, dass ihre Abstände sich wie  $O_{12}P_1 : P_1Q_1$  verhalten müssen. Analog findet man die parallelen Geraden  $s'_2, p'_2, q'_2$  durch  $O', P', Q'$ , indem ihre Abstände das Verhältnis  $O_{12}P_2 : P_2Q_2$  haben. Da die Punkte  $O, P, Q$  weder auf einer Geraden noch in einer zu der Richtung  $r_3$  parallelen Ebene liegen, sind die genannten Verhältnisse ungleich, und die beiden Systeme von parallelen Geraden haben folglich verschiedene Richtung.

Man hat nun noch ein dem Dreieck  $O_{12}P_1P_2$  ähnliches Dreieck so zu legen, dass  $P'_1$  auf  $p'_1$  und  $P'_2$  auf  $p'_2$  liegen. Denn wenn dieses erfüllt ist, werden von selbst  $Q'_1$  auf  $q'_1$  und  $Q'_2$  auf  $q'_2$  liegen. Wir sind somit zu der elementaren Aufgabe geführt worden, ähnlich einem gegebenen Dreieck ein Dreieck zu legen, welches einen Eckpunkt in einem gegebenen Punkt und die beiden anderen auf gegebenen sich schneidenden Geraden hat. Es gibt im allgemeinen nur eine Lösung unter Bewahrung der Orientierung, doch keine oder unendlich viele in dem Sonderfall, wo  $\angle(a_1, a_2) = \angle(s'_1, s'_2)$ . — Somit ist der aufgestellte Satz bewiesen.

Die zuletzt erwähnte Möglichkeit kommt nicht in Frage, wenn  $a_1$  und  $a_2$  mit einander den Winkel null bilden, also parallel (zusammenfallend) sind. Wir heben hervor, dass in diesem Fall der obige Satz unbeschränkt gilt.

Die Eckhart'sche Methode — Parallelkonstruktion aus eigentlichen axonometrischen Bildern — hat in der Praxis den Nachteil, dass Ähnlichkeits- und Kongruenztransformationen der gegebenen Figuren notwendig sind, um bestimmte axonometrische Bilder hervorzubringen. Diesem Nachteil ist, wie wir jetzt zeigen werden, durch Anwendung von singulären axonometrischen Abbildungen abzuhelfen. Hierdurch wird es dann ermöglicht, z. B. allein aus Grundriss und Aufriss einer Figur, ohne Anwendung der erwähnten Transformationen, beliebige axonometrische Bilder zu konstruieren.

Wir betrachten drei reguläre axonometrische Abbildungen  $T_1, T_2, T_3$  mit den Projektionsrichtungen  $r_1, r_2, r_3$ , die nicht in derselben Ebene liegen. Objekt und Bilder werden wie gewöhnlich bezeichnet. Den Ebenen  $r_1r_3$  und  $r_2r_3$  entsprechen in  $T_1$  und  $T_2$  die Strahlen  $s_1$  und  $s_2$ ; diese Geraden können zusammenfallend (parallel) sein oder nicht. Durch entsprechende Punkte

$P_1$  und  $P_2$  legt man jetzt Geraden  $p_1$  und  $p_2$  parallel zu  $s_1$  und  $s_2$ . Man sucht aber nicht den Schnittpunkt dieser Geraden, sondern lässt neue Geraden  $a_1$  bzw.  $a_2$  die Geraden  $p_1$  bzw.  $p_2$  schneiden (Fig. 4). Mit anderen Worten: Wir parallelprojizieren die Figur ( $P_1$ ) auf die Gerade  $a_1$  in der Richtung  $s_1$ , und analog für ( $P_2$ ).

Die neuen Bilder auf  $a_1$  und  $a_2$ , ( $P'_1$ ) und ( $P'_2$ ), sind axonometrische Bilder von ( $P$ ) in den singulären Abbildungen  $T'_1$  und  $T'_2$ , wo  $T'_1$  bzw.  $T'_2$  die Ebenenrichtung  $r_1r_3$  bzw.  $r_2r_3$  hat. Falls

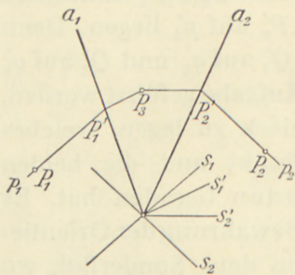


Fig. 4.

wir auf diese neuen Bilder die gewöhnliche Parallelkonstruktion anwenden, werden reguläre axonometrische, der Projektionsrichtung  $r_3$  entsprechende Bilder entstehen, und durch passende Wahl der neuen Richtungen  $s'_1$  und  $s'_2$  kann man, wie oben gezeigt ist, bis auf Ähnlichkeit jedes axonometrische Bild hervorbringen.

#### § 4. Algebraische Darstellung. Orthogonale Axonometrie.

Eine axonometrische Abbildung  $T_1$  lässt sich durch zwei Gleichungen folgender Form definieren

$$(1) \quad \begin{aligned} y'_1 &= a_1x_1 + a_2x_2 + a_3x_3 = \alpha\bar{x} \\ y'_2 &= b_1x_1 + b_2x_2 + b_3x_3 = \bar{b}\bar{x}, \end{aligned}$$

oder kürzer

$$(1) \quad \eta' = (y'_1, y'_2) = (\alpha\bar{x}, \bar{b}\bar{x}),$$

wo  $\bar{x} = (x_1, x_2, x_3)$  affine Koordinaten eines Punktes  $P$  in  $R^3$  und  $\eta' = (y'_1, y'_2)$  affine Koordinaten des Bildpunktes  $P_1$  in der Ebene  $\alpha$  sind.

Wenn  $\alpha = \bar{b} = 0$ , wird der ganze Raum in dem Punkt  $(0,0)$  abgebildet; diesen Fall lassen wir hier ausser Betracht. In anderen Fällen wird die Matrix

$$\begin{vmatrix} a_1a_2\bar{a}_3 \\ b_1b_2b_3 \end{vmatrix}$$

den Rang 2 oder 1 haben, je nachdem die Abbildung regulär oder singulär ist. Der Vektor  $(a_2b_3 - a_3b_2, a_3b_1 - a_1b_3, a_1b_2 - a_2b_1)$ ,



den wir mit  $\widehat{ab}$  bezeichnen<sup>1)</sup>, wird entsprechend ein eigentlicher Vektor, der die Projektionsrichtung  $r_1$  bestimmt, oder der Nullvektor sein.  $\widehat{ab}$  befriedigt nämlich die Gleichungen  $ax = 0$  und  $bx = 0$ .

Wenn  $\widehat{ab} = 0$ , existiert ein eigentliches Zahlenpaar  $(p, q)$ , wo  $pa + qb = 0$ . Der Raum wird auf die Gerade  $py'_1 + qy'_2 = 0$  abgebildet, und die Ebenenrichtung  $\varrho$  wird durch eine der Gleichungen  $ax = 0$  oder  $bx = 0$  bestimmt.

Es sei nun die axonometrische Abbildung  $T_2$  durch

$$(2) \quad \eta'' = (y''_1, y''_2) = (cx, dx)$$

bestimmt, wo  $c$  und  $d$  gegebene Vektoren, nicht beide Nullvektoren, sind.

Wenn  $T_1$  und  $T_2$  beide regulär sind, werden die durch  $T_1$  und  $T_2$  bestimmten Bilder affin sein oder nicht, je nachdem die beiden eigentlichen Vektoren  $\widehat{ab}$  und  $\widehat{cd}$  linear abhängig sind oder nicht. Die zu  $T_1, T_2$  gehörigen singulären Richtungen  $s_1^*$  und  $s_2^*$  werden Bilder der Ebene  $\xi = \alpha\widehat{ab} + \beta\widehat{cd}$  in  $T_1$  bzw.  $T_2$ . Die Richtungen werden dann durch  $(|acd|, |bcd|)$  und  $(|abc|, |abd|)$  bestimmt, und die beiden Abbildungen haben allgemeine oder spezielle Lage, je nachdem die Determinante von Null

$$\begin{vmatrix} |acd| & |bcd| \\ |abc| & |abd| \end{vmatrix}$$

verschieden oder gleich Null ist.

Es seien zwei Richtungen  $s_1$  und  $s_2$  in der Bildebene  $\alpha$  durch  $(\lambda_1, \lambda_2)$  und  $(\mu_1, \mu_2)$ , wo  $\lambda_1\mu_2 - \lambda_2\mu_1 \neq 0$ , gegeben. Wir wollen die Gleichungen für die aus  $T_1, T_2, s_1$  und  $s_2$  abgeleitete Abbildung  $T_3$  aufstellen. Wenn der Punkt  $P_3$  den Koordinatenvektor  $\eta''' = (y'''_1, y'''_2)$  hat, wird  $P_3$  durch die Gleichungen

$$\begin{aligned} \lambda_2 y'''_1 - \lambda_1 y'''_2 &= \lambda_2 y'_1 - \lambda_1 y'_2 \\ \mu_2 y'''_1 - \mu_1 y'''_2 &= \mu_2 y''_1 - \mu_1 y''_2 \end{aligned}$$

bestimmt. Setzen wir hier (1) und (2) ein, erhalten wir Ausdrücke der Form

<sup>1)</sup> Wenn das Koordinatensystem in  $R^3$  rechtwinklig ist, bedeutet  $\widehat{ab}$  das Vektorprodukt  $a \times b$ .



$$\eta''' = (y_1''', y_2''') = (e\zeta, f\zeta),$$

wo  $e$  und  $f$  aus den Gleichungen

$$(3) \quad \begin{aligned} \lambda_2 e - \lambda_1 f &= \lambda_2 a - \lambda_1 b \\ \mu_2 e - \mu_1 f &= \mu_2 c - \mu_1 d \end{aligned}$$

gefunden werden können.

Man sieht daraus, dass  $T_3$  eine neue axonometrische Abbildung ist. Die in den obigen Paragraphen gefundenen geometrischen Eigenschaften kann man jetzt durch Rechnung nachweisen<sup>1)</sup>. Beispielsweise sei hier erwähnt, dass man aus (3) die Gleichung

$$(4) \quad (\lambda_1 \mu_2 - \lambda_2 \mu_1) \widehat{ef} = \lambda_2 \mu_2 \widehat{ac} - \lambda_2 \mu_1 \widehat{ad} - \lambda_1 \mu_2 \widehat{bc} + \lambda_1 \mu_1 \widehat{bd}$$

erhalten kann. Falls sowohl  $T_1$  als  $T_2$  singular sind, d. h. sowohl  $a$  und  $b$  als auch  $c$  und  $d$  linear abhängig sind, zeigt die obige Gleichung (4), dass  $T_3$  im allgemeinen regulär ist und dass die Projektionsrichtung  $\widehat{ef}$  von der Wahl der Richtungen  $s_1$  und  $s_2$  unabhängig ist, da nämlich die Vektoren  $\widehat{ac}$ ,  $\widehat{ad}$ ,  $\widehat{bc}$ ,  $\widehat{bd}$  alle linear abhängig sind.

Schließlich erwähnen wir einige einfache Bedingungen, die erforderlich sind, wenn ein axonometrisches Bild eine orthogonale Projektion des Gegenstandes sein soll. Wir nehmen hier an, dass  $(x_1, x_2, x_3)$  rechtwinklige Koordinaten bezeichnen, dass die  $x_1 x_2$ -Ebene Bildebene ist, und dass  $(y'_1, y'_2)$  rechtwinklige Koordinaten dieser Ebene bezeichnen.

Falls das Bild ( $P_1$ ) eine orthogonale Projektion des Objektes ( $P$ ) sein kann, muss man ( $P$ ) so drehen können, dass der Punkt  $P(x_1, x_2, x_3)$  in den Punkt  $P'(y'_1, y'_2, y'_3)$ , wo  $y'_3$  eine zu  $y'_1, y'_2$  gehörige passende  $x_3$ -Koordinate ist, kommt. Folglich sollen die Gleichungen

$$y'_1 = a\zeta, \quad y'_2 = b\zeta, \quad y'_3 = c\zeta$$

eine Drehung im Räume bestimmen, d. h.  $a$  und  $b$  müssen orthogonale Einheitsvektoren (und  $c = \widehat{ab} = a \times b$ ) sein. Daraus folgt:

1) Siehe [5].

Die Abbildung  $\eta' = (ax, by)$  ist dann und nur dann eine orthogonale axonometrische Abbildung, wenn  $a$  und  $b$  orthogonale Einheitsvektoren sind.

Die Einheitsvektoren  $i(1, 0, 0)$ ,  $j(0, 1, 0)$  und  $k(0, 0, 1)$  werden durch (1) in die Vektoren  $i'(a_1, b_1)$ ,  $j'(a_2, b_2)$  und  $k'(a_3, b_3)$  abgebildet. Ein solches Vektorensystem ist somit orthogonale Projektion eines rechtwinkligen Koordinatensystems, wenn

$$(5) \quad a^2 = b^2 \text{ und } ab = 0,$$

indem man nicht gerade fordert, dass die gegebenen Vektoren Einheitsvektoren sein sollen.

Betrachtet man die Vektoren  $i', j'$  und  $k'$  als Ortsvektoren komplexer Zahlen der Ebene, und setzt

$$z_1 = a_1 + ib_1, \quad z_2 = a_2 + ib_2, \quad z_3 = a_3 + ib_3,$$

sieht man, dass die Bedingungen (5) sich in die einzige Gleichung

$$z_1^2 + z_2^2 + z_3^2 = 0$$

umschreiben lassen. Die Bedingungen in dieser Form sind GAUSS [6] zu verdanken.

Die erwähnten Bedingungen kann man so aufstellen, dass nur die Vektoren  $i', j', k'$  eingehen. Man erhält<sup>1)</sup>

$$(j'k') (j' \times k') = (k'i') (k' \times i') = (i'j') (i' \times j'),$$

welches sich durch Rechnen leicht nachweisen lässt. Diese letzteren Bedingungen sind notwendig, aber nur hinreichend, wenn keine der erhaltenen skalaren oder vektoriiellen Produkte verschwinden.

1) Vergl. [5], S. 14–15.



## 2. KAPITEL

### Perspektive und quadratische Abbildungen.

#### § 5. Reguläre und singuläre Abbildungen.

Unter einer perspektiven Abbildung versteht man eine lineare Abbildung des projektiven Raumes auf eine projektive Ebene  $\alpha$ , die Bildebene. Eine solche Abbildung  $T$  lässt sich aus einer Zentralprojektion mit dem Zentrum  $O$  auf eine Ebene  $\beta$  und einer projektiven Abbildung von  $\beta$  auf  $\alpha$  zusammensetzen. Ist diese Abbildung regulär, wird  $T$  selbst als regulär bezeichnet. Wenn dagegen die ganze Ebene auf eine Gerade  $a$  in  $\alpha$  abgebildet wird, sagt man, dass  $T$  singulär ist, und falls der ganze  $R^3$  in einen Punkt abgebildet wird, ist  $T$  ganz ausgeartet. Diesen letzteren Fall werden wir im Folgenden ausser Betracht lassen.

Ist  $T$  regulär, werden Geraden durch  $O$  in Punkte abgebildet, während andere Geraden projektiv auf Geraden in  $\alpha$  abgebildet werden. Der Punkt  $O$  selber hat kein Bild. Ist  $T$  singulär, lässt sich die Abbildung von  $\beta$  auf  $\alpha$  aus einer Zentralprojektion der Ebene  $\beta$  aus einem Punkt  $O_1$  von  $\beta$  auf eine Gerade  $b$  und einer projektiven Abbildung von  $b$  auf  $a$  zusammensetzen. Jede Ebene durch den Strahl  $OO_1$  wird dann in einen Punkt von  $a$  abgebildet; die Gerade selber, die Achse der Abbildung, hat kein Bild.

Man kann kurz sagen, dass eine reguläre perspektive Abbildung eine projektive Abbildung eines Strahlenbündels auf eine Ebene ist; eine singuläre perspektive Abbildung dagegen ist eine projektive Abbildung eines Ebenenbüschels auf eine Gerade.

Es seien jetzt  $T_1$  und  $T_2$  gegebene perspektive Abbildungen. Ein beliebiger Punkt des Raumes wird mit  $P$  bezeichnet, seine Bilder bei  $T_1$  und  $T_2$  werden mit  $P_1$  und  $P_2$  bezeichnet. Eine



von  $P$  durchlaufene Raumfigur wird mit  $(P)$  und ihre Bilder werden mit  $(P_1)$  und  $(P_2)$  bezeichnet.

Wenn  $T_1$  und  $T_2$  beide regulär sind, werden die beiden Bilder  $(P_1)$  und  $(P_2)$  von  $(P)$  dann und nur dann projektiv, wenn die Projektionszentren  $O_1$  und  $O_2$  zusammenfallen. Der letzte Teil des Satzes folgt daraus, dass  $O_2$  einen Bildpunkt in  $T_1$ , aber nicht in  $T_2$  hat, wenn  $O_1$  und  $O_2$  verschieden sind.

Falls  $T_1$  regulär mit dem Zentrum  $O_1$  und  $T_2$  singulär mit der Achse  $o_2$  sind, wird  $(P_2)$  nur dann ein projektives (singuläres) Bild von  $(P_1)$ , wenn  $O_1$  auf  $o_2$  liegt. Sind endlich  $T_1$  und  $T_2$  beide singulär mit den Achsen  $o_1$  und  $o_2$ , werden  $(P_1)$  und  $(P_2)$  dann und nur dann projektiv, wenn die Achsen  $o_1$  und  $o_2$  zusammenfallen. Die Beweise dieser einfachen Satze werden hier übergangen.

## § 6. Die Abbildung $T_3$ .

Wir betrachten jetzt zwei willkürliche, reguläre oder singuläre Abbildungen  $T_1$  und  $T_2$ , bei welchen der Punkt  $P$  in  $P_1$  bzw.  $P_2$  abgebildet wird. Eine neue Abbildung  $T_3$  des Raumes wird folgendermassen gebildet:

In der Ebene  $\alpha$  wählen wir zwei feste Punkte  $U_1$  und  $U_2$ . Wir nehmen an, dass die Geraden  $U_1P_1$  und  $U_2P_2$  sich in einem Punkt  $P_3$  schneiden. Dadurch ist eine neue Abbildung  $T_3$  festgelegt, die  $P$  in  $P_3$  überführt.

Diese aus  $T_1$ ,  $T_2$ ,  $U_1$  und  $U_2$  abgeleitete Abbildung wird, wie wir sehen werden, im allgemeinen nicht eine perspektive, sondern eine quadratische Abbildung des Raumes auf  $\alpha$  (oder auf eine Gerade oder einen Kegelschnitt in  $\alpha$ ) sein. Da eine perspektive Abbildung von der Wahl des Zentrums und von einer ebenen Kollineation, d. h. von  $3 + 8 = 11$  Parametern, abhängig ist, wird  $T_3$  von  $2 \cdot 11 + 2 \cdot 2 = 26$  Parametern abhängen. Im folgenden sollen die verschiedenen Formen von  $T_3$ , je nachdem  $T_1$  und  $T_2$  regulär oder singulär sind, nebst verschiedenen Lagen von  $U_1$  und  $U_2$  untersucht werden. Wir interessieren uns besonders für die Fälle, wo  $T_1$  und  $T_2$  entweder beide regulär oder beide singulär sind, während der »schiefe« Fall, wo die eine regulär, die andere singulär ist, nur kurz behandelt werden wird.

### A. Die Abbildungen $T_1$ und $T_2$ sind beide regulär.

Der Punkt  $U_1$  ist in  $T_1$  das Bild einer Geraden  $u_1$  durch  $O_1$ , entsprechend  $U_2$  das Bild in  $T_2$  einer Geraden  $u_2$  durch  $O_2$ . Für  $T_3$  ist es jetzt entscheidend, ob die Geraden  $u_1$  und  $u_2$  windschief liegen, sich schneiden oder zusammenfallen.

#### A<sub>1</sub>. Die Geraden $u_1$ und $u_2$ schneiden sich nicht.

Es sei  $P$  ein Punkt im  $R^3$  ausserhalb  $u_1$  und  $u_2$ . Der Ebene  $u_1P$  entspricht in  $T_1$  die Gerade  $U_1P_1$ , der Ebene  $u_2P$  in  $T_2$  die Gerade  $U_2P_2$ . Wenn  $P_1$  und  $P_2$  nicht beide auf der Geraden  $u = U_1U_2$  liegen, hat  $P$  in  $T_3$  einen bestimmten Bildpunkt  $P_3$ , den Schnittpunkt der Geraden  $U_1P_1$  und  $U_2P_2$ , und alle Punkte der Schnittgeraden  $p$  der Ebenen  $u_1P$  und  $u_2P$ , d. h. alle Punkte auf der Geraden durch  $P$ , die  $u_1$  und  $u_2$  schneiden (die Punkte auf  $u_1$  und  $u_2$  ausgenommen), haben denselben Bildpunkt  $P_3$ . — Die

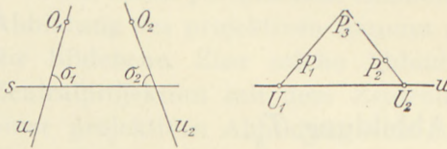


Fig. 5.

Gerade  $u = U_1U_2$  ist in  $T_1$  das Bild einer Ebene  $\sigma_1$  durch  $u_1$ , in  $T_2$  das Bild einer Ebene  $\sigma_2$  durch  $u_2$ . Liegt  $P$  auf der Schnittgeraden  $s$  dieser Ebenen, so hat  $P$  kein bestimmtes Bild. Liegt endlich  $P$  auf  $u_1$ , wird  $P_1$  in  $U_1$  fallen, die Gerade  $U_1P_1$  ist deshalb unbestimmt, und  $P$  hat kein Bild bei  $T_3$ . Wir haben somit (Fig. 5):

Bei  $T_3$  hat jeder Punkt  $P$  ausserhalb der Geraden  $u_1$ ,  $u_2$  und  $s$  einen Bildpunkt.

Die Geraden  $u_1$  und  $u_2$  sind Leitgeraden einer Geradenkongruenz  $G$ , der  $s$  angehört. Indem wir im folgenden nur auf die ausserhalb  $u_1$ ,  $u_2$  und  $s$  liegenden Punkte  $P$  im  $R^3$  Rücksicht nehmen, gilt der Satz:

Bei  $T_3$  werden sämtliche Strahlen der Kongruenz  $G$  (ausser  $s$ ) in Punkte der Ebene  $\alpha$  abgebildet.

Umgekehrt ist ein Punkt  $P_3$  in der Ebene  $\alpha$  ausserhalb der Geraden  $u$  das Bild einer Geraden der Kongruenz. Der Punkt  $U_1$  kann als Schnittpunkt der Geraden  $u$  und einer beliebigen von  $u$  verschiedenen Geraden durch  $U_1$  aufgefasst werden.  $U_1$  ist deshalb in  $T_3$  das Bild der Ebene  $\sigma_2$ ,  $U_2$  das Bild von  $\sigma_1$ . Die übrigen Punkte von  $u$  sind nicht Bilder von Punkten im  $R^3$ . Also:



Jeder Punkt der Ebene  $\alpha$  ausserhalb  $u$  ist Bild einer Geraden der Kongruenz  $G$ .  $U_1(U_2)$  ist Bild der Ebene  $\sigma_2 = u_2s$  ( $\sigma_1 = u_1s$ ). Die übrigen Punkte von  $u$  sind nicht Bildpunkte.

Wir wollen danach das Bild einer Geraden untersuchen, indem wir doch stets etwaige Punkte auf  $u_1$ ,  $u_2$  und  $s$  ausschliessen. Es gibt 5 Fälle:

1°. Wenn die Gerade  $p$  die Geraden  $u_1$  und  $u_2$  schneidet, jedoch von  $s$  verschieden ist, wird  $p$  in einen Punkt abgebildet.

2°. Wenn  $p$  die Geraden  $u_1$  und  $s$  schneidet, also in  $\sigma_1$  liegt, wird  $p$  in  $U_2$  abgebildet.

3°. Wenn  $p$  die Gerade  $u_1$ , aber weder  $u_2$  noch  $s$  schneidet, beschreibt, wenn  $p$  von  $P$  durchlaufen wird, der in  $T_1$  entsprechende Punkt  $P_1$  eine feste Gerade durch  $U_1$ , und  $P_3$  wird deshalb diese Gerade so durchlaufen, dass  $P$  und  $P_3$  projektive Reihen erzeugen.

4°. Wenn  $p$  die Gerade  $s$ , aber weder  $u_1$  noch  $u_2$  schneidet, werden die Ebenenbüschel  $u_1P$  und  $u_2P$  projektiv, die Geradenbüschel  $U_1P_1$  und  $U_2P_2$  aber perspektiv. Der Punkt  $P_3$  durchläuft deshalb die Perspektivachse der Geradenbüschel, so dass die Punktreihen  $(P)$  und  $(P_3)$  projektiv werden.

5°. Wenn  $p$  allgemeine Lage hat, also weder  $u_1$ ,  $u_2$  noch  $s$  schneidet, werden, wenn  $p$  von  $P$  durchlaufen wird, die Geradenbüschel  $U_1P_1$  und  $U_2P_2$  projektiv, aber nicht perspektiv.  $P_3$  durchläuft folglich einen Kegelschnitt durch  $U_1$  und  $U_2$ .

Wir fassen diese Ergebnisse zusammen:

Eine Gerade  $p$  wird im allgemeinen in einen Kegelschnitt durch  $U_1$  und  $U_2$  abgebildet. Wenn  $p$  eine der Geraden  $u_1$ ,  $u_2$ ,  $s$  schneidet, ist das Bild von  $p$  eine Gerade, und wenn  $p$  zwei dieser Geraden schneidet, wird das Bild ein Punkt.

Die Abbildung  $T_3$  wird somit eine quadratische Abbildung des Raumes auf die Ebene  $\alpha$ .

Die Geraden  $u_1$ ,  $u_2$ ,  $s$  werden als Hauptgeraden des Raumes, die Punkte  $U_1$  und  $U_2$  als Hauptpunkte, der Strahl  $u$  als Hauptgerade der Ebene  $\alpha$  bezeichnet.



Hiernach sieht man leicht, wie eine Ebene  $\gamma$  auf  $\alpha$  abgebildet wird.

1°. Wenn  $\gamma$  die Geraden  $u_1$  und  $s$  enthält ( $\gamma = \sigma_1$ ), wird sie in den Punkt  $U_2$  abgebildet.

2°. Wenn  $\gamma$  die Gerade  $u_1$ , aber nicht  $s$  enthält, ist ihr Bild eine Gerade durch  $U_1$ .

3°. Wenn  $\gamma$  die Gerade  $s$ , aber weder  $u_1$  noch  $u_2$  enthält, wird  $\gamma$  projektiv auf  $\alpha$  abgebildet. Bei der dadurch bestimmten Kollineation korrespondieren die Geraden  $s$  und  $u$ .

4°. Wenn  $\gamma$  die Hauptgeraden in den Punkten  $B_1, B_2, C_1$  schneidet, wird  $\gamma$  in  $\alpha$  durch eine quadratische Transformation abgebildet. Die Gerade  $B_1C$  wird in den Punkt  $U_2$ , die Gerade  $B_2C$  in  $U_1$  und die Gerade  $B_1B_2$  in einen Punkt  $B_3$  der Ebene  $\alpha$  abgebildet. Die Hauptpunkte in  $\alpha$  sind somit die Punkte  $U_1, U_2, B_3$ , in  $\gamma$  die Punkte  $B_1, B_2, C$ .

Die Abbildung betreffend sei noch Folgendes bemerkt. Es sei  $p$  eine Gerade, die bei  $T_3$  in den Kegelschnitt  $\kappa_p$  durch  $U_1$  und  $U_2$  abgebildet wird; und  $q$  sei eine andere Gerade, die in  $\kappa_q$  abgebildet wird. Allgemein haben  $\kappa_p$  und  $\kappa_q$  noch zwei Punkte gemein, die Bilder der zwei Transversalen der 4 Strahlen  $u_1, u_2, p, q$ . Haben die vier Geraden nur eine Transversale, berühren sich die Kegelschnitte; und wenn die vier Geraden hyperboloidische Lage haben, fallen  $\kappa_p$  und  $\kappa_q$  zusammen. Folglich wird ein Kegelschnitt in  $\alpha$  durch  $U_1$  und  $U_2$  das Bild einer Fläche zweiter Ordnung sein. Die eine zur Kongruenz  $G$  gehörige Regelschar wird so

abgebildet, dass jede Erzeugende einem Punkt des Kegelschnittes zugeordnet ist, während jede Erzeugende der anderen Schar sich in den ganzen Kegelschnitt abbildet.

Eine Gerade in  $\alpha$ , die weder  $U_1$  noch  $U_2$  enthält, ist auch das Bild einer Fläche zweiter Ordnung, wo jedoch die zu  $G$  gehörige Regelschar die Gerade  $s$  enthalten muss.

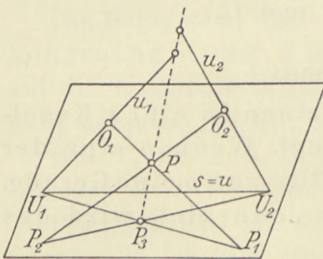


Fig. 6.

Besonders übersichtlich wird die betrachtete Abbildung, wenn beide perspektiven Abbildungen  $T_1$  und  $T_2$  nur Zentralprojektionen sind (Fig. 6). Die Sehpunkte  $O_1$  und  $O_2$  liegen ausserhalb  $\alpha$ .

$u_1$  ist die Gerade  $O_1U_1$ ,  $u_2$  die Gerade  $O_2U_2$ . Eine Gerade der Kongruenz  $G$  wird in ihren Schnittpunkt mit  $\alpha$  abgebildet, und eine beliebige Gerade  $p$  wird durch den Kegelschnitt, in dem  $\alpha$  von der Strahlenfläche zweiter Ordnung durch  $p, u_1, u_2$  geschnitten wird, abgebildet. Die quadratische Abbildung zwischen einer Ebene  $\gamma$ , die nicht  $s (= u)$  enthält, und  $\alpha$  ist die bekannte STEINER'sche »schiefe Projektion«.<sup>1)</sup>

Hieraus folgt leicht:

Wenn  $u_1$  und  $u_2$  sich nicht schneiden, kann man die Abbildung  $T_3$  aus einer schiefen Projektion des Raumes auf eine Ebene  $\gamma$  und einer projektiven Abbildung dieser Ebene auf  $\alpha$  zusammensetzen.

Man braucht nur die Ebene  $\gamma$  durch die Hauptgerade  $s$  zu wählen.

#### A<sub>II</sub>. Die Geraden $u_1$ und $u_2$ schneiden sich.

Den Schnittpunkt der Geraden bezeichnen wir mit  $O_3$ . Es sei  $P$  ein Punkt im  $R^3$  ausserhalb der Ebene  $\omega = O_1O_2O_3$ . Der Ebene  $u_1P(u_2P)$  entspricht in  $T_1(T_2)$  die Gerade  $U_1P_1(U_2P_2)$ . Wenn  $U_1P_1$  und  $U_2P_2$  nicht zusammenfallen (in  $u = U_1U_2$ ), wird  $P$  in ihren Schnittpunkt  $P_3$  abgebildet. Dieser Punkt ist zugleich das Bild aller anderen Punkte der Geraden  $O_3P$ , doch hat  $O_3$  offenbar kein Bild in  $T_3$ . Die Gerade  $u = U_1U_2$  ist bei  $T_1(T_2)$  das Bild einer Ebene  $\sigma_1(\sigma_2)$  durch  $u_1(u_2)$ . Es entstehen dann zwei verschiedene Möglichkeiten, je nachdem  $\sigma_1$  und  $\sigma_2$  (mit der Schnittgeraden  $s$  durch  $O_3$ ) verschieden sind oder in der Ebene  $\omega$  zusammenfallen. Diese kann man auch so formulieren, dass im ersten Falle die Ebene  $\omega$  verschiedene Bilder in  $T_1$  und  $T_2$  hat, im zweiten Falle aber dasselbe Bild und dann eben die Gerade  $u = U_1U_2$ .

a) Die Ebene  $\omega = O_1O_2O_3$  hat verschiedene Bilder in  $T_1$  und  $T_2$ .

Jeder Punkt  $P$  ausserhalb  $u_1, u_2$  und  $s$  hat in  $T_3$  einen bestimmten Bildpunkt  $P_3$ , der gleichzeitig der Bildpunkt der ganzen Geraden  $O_3P, O_3$  ausgenommen, ist. Jedem Punkt der Ebene  $\omega$  (ausserhalb  $u_1$  und  $u_2$ ) entspricht der Punkt  $S$ , wo die  $\omega$  in  $T_1$  und  $T_2$  entsprechenden Geraden durch  $U_1$  und  $U_2$  sich schnei-

<sup>1)</sup> vergl. [9], S. 73 ff., [11], [12], [13].



den. Einem Punkt in der Ebene  $\sigma_1(\sigma_2)$  entspricht der Punkt  $U_2(U_1)$ . Durchläuft  $P$  eine Gerade  $p$ , die keine der drei Geraden  $u_1, u_2, s$  schneidet, werden die Ebenenbüschel  $u_1P$  und  $u_2P$  bei  $T_1$  bzw.  $T_2$  in projektive, aber nicht perspektive Geradenbüschel  $U_1P_1$  und  $U_2P_2$  abgebildet. Daraus folgt, dass  $P_3$  einen Kegelschnitt durch  $U_1, U_2$  und  $S$  durchläuft. Es ist nun ersichtlich:

$T_3$  ist eine quadratische Abbildung des Geradenbündels ( $O_3$ ) auf die Ebene  $\alpha$ , wo  $u_1, u_2, s$  die Hauptgeraden des Bündels,  $U_1, U_2, S$  die Hauptpunkte der Ebene  $\alpha$  sind.

Dies kann man auch auf folgende Weise auslegen:

Wenn die Geraden  $u_1$  und  $u_2$  sich in  $O_3$  schneiden, und wenn die Ebene  $u_1u_2$  bei  $T_1$  und  $T_2$  nicht in dieselbe Gerade abgebildet wird, lässt sich die Abbildung  $T_3$  aus einer Zentralprojektion aus  $O_3$  auf eine Ebene  $\gamma$  und einer quadratischen Transformation von  $\gamma$  auf  $\alpha$  zusammensetzen.

Speziell kann  $s$  in  $u_1$  oder  $u_2$  fallen; in diesem Fall wird die quadratische Abbildung singular (mit zwei zusammenfallenden Hauptpunkten).

b) Die Ebene  $\omega = O_1O_2O_3$  hat dasselbe  
Bild in  $T_1$  und  $T_2$ .

Wie oben werden die Punkte einer Geraden  $O_3P$  bei  $T_3$  in denselben Punkt  $P_3$  abgebildet. Wenn  $P$  eine Gerade  $p$  ausserhalb  $\omega$  durchläuft, werden die oben erwähnten Geradenbüschel  $U_1P_1$  und  $U_2P_2$  diesmal perspektiv, da der Schnittpunkt der Geraden  $p$  mit  $\omega$  in  $T_1$  sowohl als in  $T_2$  einem Punkt der Geraden  $u = U_1U_2$  entspricht. Folglich wird  $P_3$  eine  $p$  entsprechende Gerade  $p_3$  durchlaufen, so dass die zugeordneten Punkt-reihen projektiv werden. Es gilt daher:

Wenn die Geraden  $u_1$  und  $u_2$  sich in  $O_3$  schneiden, und die Ebene  $u_1u_2$  bei  $T_1$  und  $T_2$  in dieselbe Gerade  $U_1U_2$  abgebildet wird, ist  $T_3$  eine neue perspektive Abbildung mit dem Sehpunkt  $O_3$ .

Bei dieser Abbildung hat die Ebene  $\omega$  kein Bild, wie die Gerade  $u$  nicht Bild einer Ebene ist; die entstehende perspektive Abbildung von  $R^3$  ausserhalb  $\omega$  wird jedoch bewirken, dass  $\omega$  und  $u$  einander zugeordnet werden.

Wir gehen jetzt zu dem besonders speziellen Fall über:



A<sub>III</sub>. Die Geraden  $u_1$  und  $u_2$  fallen zusammen.

$U_1$  ist dann in  $T_1$  das Bild der Geraden  $o = O_1O_2$ , speziell das Bild des Punktes  $O_2$ . Entsprechend für  $U_2$ . Ein Punkt  $P$  ausserhalb  $o$  wird bei  $T_3$  in einen Punkt  $P_3$  abgebildet, und man sieht, dass die ganze Ebene  $oP$  in denselben Punkt abgebildet wird. Wenn die Ebene sich um  $o$  dreht, wird der Ebenenbüschel ( $o$ ) bei  $T_1$  und  $T_2$  in projektive Geradenbüschel abgebildet werden. Der ganze Raum (die Achse  $o$  ausgenommen) wird dann in einen Kegelschnitt oder in eine Gerade abgebildet, je nachdem diese Geradenbüschel projektiv oder zugleich perspektiv sind. Welche der beiden Möglichkeiten eintritt, ist davon abhängig, ob es eine Ebene gibt, die sowohl bei  $T_1$  als bei  $T_2$  in die Gerade  $u$  abgebildet wird oder nicht. Wir haben somit:

Wenn die Geraden  $u_1$  und  $u_2$  beide in die Gerade  $o = O_1O_2$  fallen, wird  $T_3$  eine singuläre quadratische oder eine singuläre perspektive Abbildung sein. Der Raum wird auf einen Kegelschnitt oder eine Gerade abgebildet.

Wir haben hiermit die Möglichkeiten für  $T_3$  untersucht, die eintreffen können, wenn  $T_1$  und  $T_2$  beide regulär und die Projektionszentren  $O_1$  und  $O_2$  verschieden sind. Wir wollen jetzt kurz den Fall betrachten, wo  $O_1$  und  $O_2$  zusammenfallen.

In diesem Fall sind, wie in § 5 erwähnt, die Bilder  $(P_1)$  und  $(P_2)$  eines Gegenstandes projektiv. Die Geraden  $u_1$  und  $u_2$  können nicht windschief sein, so dass nur die Fälle A<sub>II</sub> und A<sub>III</sub> vorkommen können. Die Ergebnisse werden völlig wie oben, man kann sie aber hier anders erklären. Da  $(P_1)$  und  $(P_2)$  projektiv sind, bedeuten die Bedingungen b) S. 24 und a) S. 23, dass die Gerade  $u = U_1U_2$  in der Kollineation, die  $(P_1)$  in  $(P_2)$  überführt, Fixgerade ist oder nicht.

Wir erhalten dann die SEYDEWITZ'sche Erzeugung einer quadratischen Abbildung<sup>1)</sup>:

Wenn man aus zwei Punkten  $U_1$  und  $U_2$  zwei ebene projektive Figuren  $(P_1)$  und  $(P_2)$  zentralprojiziert, und die Gerade  $u = U_1U_2$  nicht Fixgerade der Kollineation  $(P_1) \rightarrow (P_2)$  ist, wird der Schnittpunkt entsprechender

<sup>1)</sup> Verg. z. B. Enzyklopädie der math. Wissensch. III C 11 S. 2012 ff.

Strahlen eine Figur  $(P_3)$  durchlaufen, die mit  $(P_1)$  oder  $(P_2)$  quadratisch verwandt ist.

Wenn dagegen  $u$  Fixgerade ist, wird  $(P_3)$  mit  $(P_1)$  und  $(P_2)$  projektiv sein.

Es ist oben eine Voraussetzung, dass  $U_1$  und  $U_2$  verschiedenen Geraden  $u_1$  und  $u_2$  durch  $O_1 = O_2$  entsprechen, welches bedeutet, dass  $U_1$  und  $U_2$  nichtentsprechende Punkte der Projektivität  $(P_1) \rightarrow (P_2)$  sind. Sind sie dagegen entsprechende Punkte, entsteht der Fall  $A_{III}$ , dem wir hier folgende Formulierung geben:

Wenn man von zwei entsprechenden Punkten  $U_1$  und  $U_2$  zwei projektive Figuren  $(P_1)$  und  $(P_2)$  zentralprojiziert, wird die Figur  $(P_3)$  auf einem Kegelschnitt oder einer Geraden liegen, je nachdem die Gerade  $u$  nicht Fixgerade oder Fixgerade der Kollineation  $(P_1) \rightarrow (P_2)$  ist.

Es bleibt noch zu untersuchen, welchen Einfluss die Wahl der Punkte  $U_1$  und  $U_2$  auf die erzeugte Abbildung  $T_3$  hat, wenn zwei Abbildungen  $T_1$  und  $T_2$  vorliegen.

Hier müssen wir auch eine Reihe von Möglichkeiten behandeln, indem die gegebenen Abbildungen verschieden gelegen sein können. Wir nehmen an, dass  $T_1$  und  $T_2$  regulär und die Zentren  $O_1$  und  $O_2$  verschieden seien. Der Punkt  $O_2$ , also die Gerade  $O_1O_2$ , wird bei  $T_1$  in einem Punkt  $V_1$  abgebildet, während  $O_1$ , also wieder die Gerade  $o = O_1O_2$ , bei  $T_2$  in  $V_2$  abgebildet wird.  $V_1$  und  $V_2$  heißen die Kernpunkte der Abbildung. Der Ebenenbüschel  $(o)$  wird bei  $T_1$  und  $T_2$  in projektive Geradenbüschel mit den Scheiteln  $V_1$  und  $V_2$  abgebildet. Dann entstehen die folgenden Fälle:

- 1°. Die Kernpunkte  $V_1$  und  $V_2$  sind verschieden, und die Büschel  $(V_1)$  und  $(V_2)$  sind projektiv, aber nicht perspektiv.
- 2°. Die Punkte  $V_1$  und  $V_2$  sind verschieden und die Büschel  $(V_1)$  und  $(V_2)$  perspektiv.
- 3°. Die Punkte  $V_1$  und  $V_2$  sind zusammenfallend, und die projektiven Geradenbüschel  $(V_1)$  und  $(V_2)$  haben 2, 1 oder 0 reelle Doppelstrahlen.



4°. Die Punkte  $V_1$  und  $V_2$  sind zusammenfallend, und die Büschel  $(V_1)$  und  $(V_2)$  sind identisch.

Wir wollen diese Fälle der Reihe nach behandeln.

1°. Die Büschel  $(V_1)$  und  $(V_2)$  erzeugen einen Kegelschnitt  $\kappa$ . Falls  $U_1$  und  $U_2$  so gewählt werden, dass die Geraden  $V_1U_1$  und  $V_2U_2$  sich nicht auf  $\kappa$  schneiden, werden die Strahlen  $u_1$  und  $u_2$  nicht in derselben Ebene liegen. Wenn dagegen die Geraden sich auf  $\kappa$  schneiden, liegen  $u_1$  und  $u_2$  in derselben Ebene. Diese Ebene hat jedoch nicht dasselbe Bild bei  $T_1$  und bei  $T_2$ . Wir sehen also, dass  $T_3$  immer eine quadratische Abbildung, entweder ohne oder mit Sehpunkt, wird. Dies gilt auch, wenn  $U_1$  in  $V_1$ ,  $U_2$  in  $V_2$  gewählt werden. Wir haben also:

Wenn man aus zwei gegebenen perspektiven Abbildungen  $T_1$  und  $T_2$  eine neue Abbildung  $T_3$  bildet, wird diese Abbildung im allgemeinen nicht perspektiv sein, wie man auch die Projektionszentren  $U_1$  und  $U_2$  wählt.

2°. In diesem Fall existiert also im Büschel  $(o)$  eine Ebene  $\pi$ , die sowohl bei  $T_1$  als bei  $T_2$  in die Gerade  $v = V_1V_2$  abgebildet wird. Die Perspektivachse der Büschel  $(V_1)$  und  $(V_2)$  bezeichnen wir mit  $k$ . Wählen wir nun  $U_1$  in  $V_1$ ,  $U_2$  in  $V_2$ , werden sämtliche entsprechenden Strahlen  $U_1P_1$  und  $U_2P_2$  sich auf  $k$  schneiden. Projiziert man die Bilder  $(P_1)$  und  $(P_2)$  aus den Kernpunkten  $V_1$  und  $V_2$ , werden entsprechende Geradenbüschel perspektiv.

Hier können bei geeigneter Wahl von  $U_1$  und  $U_2$  alle Möglichkeiten  $A_1$ ,  $A_{IIa}$  und  $A_{IIb}$  entstehen. Wir erhalten eine quadratische Abbildung ohne Zentrum, mit Zentrum oder eine perspektive Abbildung, je nachdem die Punkte  $U_1$  und  $U_2$  so gewählt werden, dass 1)  $V_1U_1$  und  $V_2U_2$  sich ausserhalb  $k$  schneiden, 2)  $V_1U_1$  und  $V_2U_2$  sich auf der Geraden  $k$  schneiden, und 3)  $U_1$  und  $U_2$  beide auf der Geraden  $V_1V_2$  liegen. Als Sehpunkt (Zentrum) der Abbildung hat man den Schnittpunkt der Geraden  $u_1$  und  $u_2$ .

Wir wollen noch untersuchen, ob sämtliche Punkte der Ebene  $\pi$  abgesehen von den Punkten der Geraden  $o$  als Sehpunkte  $O_3$  in  $T_3$  auftreten können. Lässt man einen Punkt  $Q$  die Gerade  $v = V_1V_2$  durchlaufen, werden die bei  $T_1$  und  $T_2$  entsprechenden Strahlen projektive Geradenbüschel in der Ebene  $\pi$  mit Scheiteln  $O_1$  und  $O_2$  durchlaufen. Da der Strahl  $o$  selber in die verschiede-



nen Punkte  $V_1$  und  $V_2$  abgebildet wird, werden die Geradenbündel einen Kegelschnitt in der Ebene  $\pi$  erzeugen. Wir sehen also:

Sämtliche Punkte der Ebene  $\pi$ , die Gerade  $o$  und ein gewisser Kegelschnitt durch  $O_1$  und  $O_2$  ausgenommen, können Sehpunkte in der aus  $T_1$  und  $T_2$  abgeleiteten perspektiven Abbildung  $T_3$  sein.

3°. Wir werden kurz die Resultate aufrechnen. Es ergibt sich eine quadratische Abbildung ohne Zentrum oder mit Zentrum oder eine perspektive Abbildung, je nachdem  $U_1$  und  $U_2$  auf nicht-entsprechenden Geraden der Bündel ( $V_1$ ) und ( $V_2$ ), auf entsprechenden Geraden oder auf einem Doppelstrahl gewählt werden.

4°. Diese letzte Möglichkeit ist von besonderem Interesse. Denn hier gibt es nur zwei Fälle: entweder ist die Abbildung quadratisch ohne Zentrum, oder sie ist perspektivisch. Die Fälle entstehen, je nachdem, ob die Gerade  $U_1U_2$  nicht durch den Punkt  $V_1 = V_2$  geht oder hindurchgeht.

Hier wird  $O_3$  nicht an eine bestimmte Ebene durch  $o$  gebunden sein, da jede Ebene durch  $o$  dasselbe Bild in  $T_1$  wie in  $T_2$  hat. Nicht alle Punkte des Raumes ausserhalb  $o$  können jedoch als Sehpunkte auftreten. Die Bedingung muss die sein, dass die Strahlen  $O_3O_1(u_1)$  bzw.  $O_3O_2(u_2)$  nicht bei  $T_1$  bzw.  $T_2$  in denselben Punkt der Ebene  $\alpha$  abgebildet werden. Lassen wir jetzt einen Punkt  $Q$  die Ebene  $\alpha$  durchlaufen, dann werden die entsprechenden Strahlen projektive Bündel mit Scheiteln  $O_1$  und  $O_2$  durchlaufen; da aber jede Ebene durch  $o = O_1O_2$  sich selbst entspricht, werden die Bündel perspektiv sein, und  $O_3$  muss ausserhalb der zugehörigen Perspektivebene gewählt werden. Also ergibt sich:

Sind die Kernbündel ( $V_1$ ) und ( $V_2$ ) identisch, kann jeder Punkt ausserhalb der Geraden  $O_1O_2$  und einer bestimmten Ebene Sehpunkt der perspektiven Abbildung  $T_3$  werden.

Diese Abbildung entsteht, wenn  $T_1$  und  $T_2$  Zentralprojektionen auf dieselbe Ebene  $\beta$  sind.  $V_1$  und  $V_2$  fallen dann beide in die Spur  $V$  der Geraden  $o$  in der Ebene  $\beta$ . Die erwähnte Perspektivebene ist hier  $\beta$ . Wählt man  $O_3$  ausserhalb dieser Ebene (und des Strahls  $o$ ), werden die Geraden  $O_3O_1$  und  $O_3O_2$

die Ebene  $\beta$  in den Punkten  $U_1$  und  $U_2$  schneiden, so dass die Gerade  $U_1U_2$  den Punkt  $V$  enthält. Wenn dagegen diese Gerade  $V$  nicht enthält, bekommt man die Steinersche schiefe Projektion (Fig. 6).

Hiermit haben wir die Behandlung des Falles A, wo die gegebenen perspektiven Abbildungen beide regulär sind, beendet, und wir wollen jetzt zu den Fällen übergehen, wo  $T_2$  allein oder zugleich  $T_1$  singulär ist.

### B. Die Abbildung $T_1$ ist regulär, $T_2$ singulär.

$T_1$  hat den Sehpunkt  $O_1$  und bildet  $R_3$  auf die ganze Ebene  $\alpha$  ab.  $T_2$  hat die Achse  $o_2$  und bildet den Raum auf die Gerade  $a_2$  in  $\alpha$  ab. Wir nehmen an, dass die Achse  $o_2$  nicht durch den Punkt  $O_1$  hindurchgeht. Es mögen nun  $U_1$  und  $U_2$  die Projektionszentren in  $\alpha$  sein.  $U_1$  ist bei  $T_1$  das Bild einer Geraden  $u_1$  durch  $O_1$ , während  $U_2$  entweder das Bild von keinem Punkt oder das Bild einer Ebene durch die Achse  $o_2$  ist, je nachdem  $U_2$  ausserhalb oder auf der Geraden  $a_2$  liegt. Wir nehmen vorläufig an,  $U_2$  liege ausserhalb  $a_2$ .

Es ergeben sich jetzt zwei Möglichkeiten, je nachdem  $u_1$  und  $o_2$  sich schneiden oder nicht.

#### B<sub>1</sub>. Die Geraden $u_1$ und $o_2$ schneiden sich nicht.

Es sei  $P$  ein Punkt von  $R^3$  ausserhalb  $u_1$  und  $o_2$ . Die Ebene  $u_1P$  wird bei  $T_1$  in eine Gerade  $U_1P_1$  abgebildet. Die Ebene  $o_2P$  wird in den Punkt  $P_2$  auf  $a_2$  abgebildet. Die Geraden  $U_1P_1$  und  $U_2P_2$  werden sich, wenn  $P_1$  und  $P_2$  nicht beide auf der Geraden  $u = U_1U_2$  liegen, in  $P_3$  schneiden, und  $P_3$  ist ausserdem in  $T_3$  das Bild jedes Punktes (ausserhalb  $u_1$  und  $o_2$ ) der Schnittgeraden der Ebenen  $u_1P$  und  $o_2P$ . Bei  $T_1$  ist die Gerade  $u$  das Bild einer Ebene  $\sigma_1$ , und der Schnittpunkt  $S_2$  von  $u$  und  $a_2$  ist bei  $T_2$  das Bild einer Ebene  $\sigma_2$  durch  $o_2$ . Diese Ebenen haben die Schnittgerade  $s$ . Genau wie bei dem Fall A<sub>1</sub> ergibt sich hier:

$T_3$  ist eine quadratische Abbildung von  $R^3$  auf  $\alpha$  mit den Hauptgeraden  $u_1$ ,  $o_2$  und  $s$ .

Man bemerkt, dass  $o_2$  bei der Abbildung eine feste, von der Wahl von  $U_2$  unabhängige Achse ist. Wenn man also  $U_1$  und die Gerade  $U_1S_2$  festhält, während  $U_2$  auf dieser Geraden variiert,



werden sämtliche Hauptgeraden der quadratischen Abbildung und damit die schiefe Projektion bewahrt, welches zur Folge hat, dass man durch Variation von  $U_2$  unter sich projektive Bilder ( $P_3$ ) erhält.

#### B<sub>II</sub>. Die Geraden $u_1$ und $o_2$ schneiden sich.

Bezeichnet man den Schnittpunkt mit  $O_3$ , wird eine Gerade  $O_3P$  allgemein in einen Punkt  $P_3$  abgebildet, so dass hier eine quadratische oder perspektive Abbildung mit dem Zentrum  $O_3$  entsteht. Welche der beiden Abbildungen eintreffen wird, hängt — wie im Falle A<sub>II</sub> — davon ab, ob die oben definierten Ebenen  $\sigma_1$  und  $\sigma_2$  verschieden sind oder zusammenfallen (in die Ebene  $\omega = O_1o_2$ ). Wir haben somit:

$T_3$  ist eine quadratische Abbildung mit Zentrum oder eine perspektive Abbildung.

Die dem Fall A<sub>III</sub> entsprechende Möglichkeit liegt hier nicht vor, da  $O_1$  ausserhalb  $o_2$  liegt, so dass  $u_1$  nie in  $o_2$  fallen kann.

Wir haben noch nicht den Sonderfall, wo der Punkt  $U_2$  auf der Geraden  $a_2$  liegt, behandelt; man sieht ohne Schwierigkeit, dass in diesem Fall nur singuläre perspektive Abbildungen entstehen können.

#### C. Die Abbildungen $T_1$ und $T_2$ sind beide singulär.

Die Abbildung  $T_1$  hat die Achse  $o_1$  und bildet den Raum auf die Gerade  $a_1$  ab, analog hat  $T_2$  die Achse  $o_2$  und bildet den Raum auf die Gerade  $a_2$  ab. Entscheidend für den Charakter der Abbildung ist es, ob  $o_1$  und  $o_2$  windschief sind, sich schneiden oder zusammenfallen.

#### C<sub>1</sub>. Die Geraden $o_1$ und $o_2$ schneiden sich nicht.

Wir nehmen an, der Punkt  $U_1$  bzw.  $U_2$  sei ausserhalb  $a_1$  bzw.  $a_2$  gewählt. Ist  $P$  ein Punkt im Raume ausserhalb der gegebenen Achsen, wird die Ebene  $o_1P$  in einen Punkt  $P_1$  auf  $a_1$  abgebildet, analog  $o_2P$  in  $P_2$  auf  $a_2$ , so dass  $P$  in den Schnittpunkt von  $U_1P_1$  und  $U_2P_2$  abgebildet wird. In diesen Punkt werden ausserdem die übrigen Punkte der  $o_1$  und  $o_2$  schneidenden Geraden durch  $P$  abgebildet. Die Schnittpunkte  $S_1$  und  $S_2$  von  $u$  und  $a_1$  und  $a_2$  entsprechen in  $T_1$  bzw.  $T_2$  zwei Ebenen



$\sigma_1$  und  $\sigma_2$  durch  $o_1$  bzw.  $o_2$ , deren Schnittgerade  $s$  kein Bild in  $T_3$  hat. Wie oben sieht man dann:

$T_3$  ist eine quadratische Abbildung mit den Hauptgeraden  $o_1$ ,  $o_2$  und  $s$ .

Wenn  $U_1$  auf  $a_1$  oder  $U_2$  auf  $a_2$  liegt, entstehen singuläre perspektive Abbildungen. Diesen speziellen Fall werden wir hier ausser Betracht lassen.

**C<sub>II</sub>. Die Geraden  $o_1$  und  $o_2$  schneiden sich.**

Der Schnittpunkt heisst  $O_3$ , die Ebene der Achsen  $\omega$ . Indem wir wieder  $U_1$  und  $U_2$  allgemein wählen, sehen wir wie vorher:

$T_3$  ist eine quadratische Abbildung mit Zentrum oder eine perspektive Abbildung.

Die Gerade  $u = U_1U_2$  schneidet wie oben  $a_1$  in  $S_1$ ,  $a_2$  in  $S_2$ , welche Bilder der Ebenen  $\sigma_1$  und  $\sigma_2$  (durch  $o_1$  bzw.  $o_2$ ) sind. Die Abbildung  $T_3$  wird quadratisch oder perspektivisch, je nachdem  $\sigma_1$  und  $\sigma_2$  eine Schnittgerade haben oder in  $\omega$  zusammenfallen.

**C<sub>III</sub>. Die Geraden  $o_1$  und  $o_2$  fallen zusammen.**

Der Ebenenbüschel mit der Achse  $o_1 = o_2$  wird bei  $T_1$  und  $T_2$  in projektive Reihen auf  $a_1$  und  $a_2$  abgebildet. Durch Projektion aus  $U_1$  und  $U_2$  bekommt man dann, wie bei dem Fall **A<sub>III</sub>**, als Bild von  $R^3$  entweder einen Kegelschnitt oder eine Gerade, wenn  $U_1$  bzw.  $U_2$  ausserhalb  $a_1$  bzw.  $a_2$  gewählt sind. Es lässt sich leicht entscheiden, wann die eine und wann die andere Möglichkeit entsteht. Also:

$T_3$  ist eine singuläre quadratische oder perspektive Abbildung.

---

Will man hier untersuchen, wie die Abbildung  $T_3$  bei gegebenen  $T_1$  und  $T_2$  von der Wahl von  $U_1$  und  $U_2$  abhängig ist, wird es aus dem Vorhergehenden offenbar sein, dass der Charakter der Abbildung im wesentlichen durch die Lage der Achsen  $o_1$  und  $o_2$ , die ja von der Wahl von  $U_1$  und  $U_2$  unabhängig sind, entschieden ist. Wir besprechen besonders die Verhältnisse im Fall **C<sub>II</sub>**.

Die Ebene  $\omega$  wird bei  $T_1$  bzw.  $T_2$  in den Punkt  $V_1$  bzw.  $V_2$  abgebildet. Die Abbildung  $T_3$  wird dann quadratisch oder per-

spektiv, je nachdem die Punkte  $U_1$  und  $U_2$  nicht beide oder beide auf der Geraden  $v = V_1V_2$  liegen.

Wenn  $T_3$  perspektivisch ist, kann man die Ebene  $\omega$  der Geraden  $v = u$  zuordnen.

Einem bestimmten  $O_3$  entsprechend bekamen wir, wenn  $T_1$  und  $T_2$  regulär waren, nur eine einzelne perspektive Abbildung  $T_3$ . Hier dagegen erhalten wir mehrere, indem man die Punkte  $U_1$  und  $U_2$  willkürlich auf der Geraden  $v = V_1V_2$  wählen darf. Im speziellen Fall, wo  $V_1$  und  $V_2$  zusammenfallen (im Schnittpunkt von  $a_1$  und  $a_2$ , falls diese Geraden verschieden sind), kann man die Gerade  $u = U_1U_2$  beliebig durch  $V_1 = V_2$ , wenn nur ausserhalb  $a_1$  und  $a_2$ , wählen. Wir haben somit:

Wenn aus zwei singulären perspektiven Abbildungen  $T_1$  und  $T_2$  sich eine reguläre perspektive Abbildung bilden lässt, kann man durch verschiedene Wahl von Projektionszentren  $U_1$  und  $U_2$   $\infty^2$  oder  $\infty^3$  unter sich projektive Bilder desselben Gegenstandes erhalten.

Die Projektivität der Bilder folgt daraus, dass wir stets dasselbe Zentrum  $O_3$  haben.

## § 7. Perspektivische Abbildungen.

Es ist in der geometrischen Photogrammetrie eine zentrale Aufgabe, aus zwei perspektiven Bildern ein drittes zu konstruieren. Diese Aufgabe ist von GUIDO HAUCK<sup>1)</sup> durch sein »Dreibilderverfahren« gelöst worden. Auf Grund der vorstehenden Untersuchungen werden wir ein neues Konstruktionsverfahren angeben.

Falls  $T_1$  und  $T_2$  zwei reguläre perspektive Abbildungen mit allgemeiner Lage sind, wird — wie aus dem Satz S. 27 hervorgeht — unsere Methode kein neues perspektives Bild geben, wie auch die Projektionszentren  $U_1$  und  $U_2$  gewählt werden. Aus § 6 ergibt sich folgendes: Bezeichnet man mit  $V_1$  und  $V_2$  die Kernpunkte, d. h. die Bilder von  $O_2$  bei  $T_1$  und von  $O_1$  bei  $T_2$ , muss 1) die Gerade  $v = V_1V_2$  sowohl bei  $T_1$  als bei  $T_2$  das Bild derselben Ebene  $\omega$  durch  $O_1O_2$  sein, und 2) müssen  $U_1$  und  $U_2$  auf der Geraden  $v$  gewählt werden. Wenn also die Bedingung 1) nicht für die gegebenen Abbildungen befriedigt ist, kann  $T_3$  nie eine perspektive Abbildung werden.

1) [7] und [8]. Vergl. auch [9], S. 157 ff.



Es besteht nun die Möglichkeit, zu  $T_1$  oder  $T_2$  eine einfache projektive Abbildung in der Bildebene  $\alpha$  hinzuzufügen, z. B. eine Bewegung eines oder beider Bilder  $(P_1)$ ,  $(P_2)$  einer gegebenen Figur  $(P)$ , um die obige Lage zu erreichen. Im allgemeinen ist dieses möglich.

Es sei  $O_3$  ein Punkt ausserhalb der Geraden  $O_1O_2$ , den wir als Sehpunkt der perspektiven Abbildung  $T_3$  wünschen. Die Ebene  $\omega = O_1O_2O_3$  wird bei  $T_1$  in eine Gerade  $w_1$  durch  $V_1$ , bei  $T_2$  in eine Gerade  $w_2$  durch  $V_2$  abgebildet. Nimmt man nun an,  $V_1$  und  $V_2$  liegen beide im Endlichen, kann man zu  $T_1$  bzw.  $T_2$  eine Drehung in der Ebene um  $V_1$  bzw.  $V_2$  hinzufügen, so dass der Strahl  $w_1$  bzw.  $w_2$  in den Strahl  $v$  fällt. Hiermit ist die Bedingung 1) befriedigt. Ist ein Kernpunkt unendlich fern, muss man die Drehung durch eine Parallelverschiebung ersetzen. Ist dagegen die Gerade  $v$ , also beide Kernpunkte, unendlich fern, kann man die Bedingung 1) durch Bewegungen der gegebenen Bilder nicht befriedigen.

Hat man nun die Befriedigung der Bedingung 1) erreicht, kann man durch passende Wahl der Punkte  $U_1$  und  $U_2$  fast jedes  $O_3$  der Ebene  $\omega$  als Sehpunkt erhalten (S. 28). Jeder Wahl des Projektionszentrums aber entspricht nur ein neues perspektives Bild der gegebenen Figur. Wir heben hervor:

Durch Hinzufügung von Bewegungen in der Bildebene  $\alpha$  zu  $T_1$  und  $T_2$  ist es im allgemeinen möglich, die beiden Bilder in solche Lagen zu bringen, dass neue perspektivische Bilder durch passende Wahl von  $U_1$  und  $U_2$  zu erhalten sind.

Wenn  $T_1$  und  $T_2$  nicht völlig allgemeine gegenseitige Lage haben, kann man ohne zusätzliche Bewegungen auskommen, indem z. B. die Bedingung 1) schon befriedigt sein, und die Konstruktion direkt an den vorliegenden Figuren vorgenommen werden kann. Dieses hat z. B. Gültigkeit, wenn die Kernpunkte  $V_1$  und  $V_2$  identisch sind, speziell wenn  $T_1$  und  $T_2$  nur Zentralprojektionen auf dieselbe Ebene sind (vergl. S. 28).

In dem Fall, wo  $(P_1)$  und  $(P_2)$  die MONGE'schen Bilder, d. h. Aufriss und Grundriss sind, sind die Verhältnisse sehr übersichtlich. Hier fallen  $V_1$  und  $V_2$  in dem unendlich fernen Punkt, der durch die Verbindungsgerade zweier entsprechender Punkte  $P_1$  und  $P_2$  bestimmt ist, zusammen. Eine neue perspektive Abbil-



Abbildung  $T_3$  erhält man in diesem Fall, wenn man  $U_1$  und  $U_2$  so wählt, dass die Gerade  $U_1U_2$  durch  $V_1 = V_2$  hindurchgeht. Dies bedeutet, dass  $U_1$  und  $U_2$  die MONGE'schen Bilder eines Punktes  $U$  im Raume sind. Der Schnittpunkt  $P_3$  von  $U_1P_1$  und  $U_2P_2$  wird ein zusammenfallendes Bild der Spur der Geraden  $UP$  in der Mittelebene bei beiden Abbildungen. Somit ist  $(P_3)$  die orthogonale Projektion auf eine der Bildebenen von derjenigen Figur, die durch Zentralprojektion der Figur  $(P)$  aus  $U$  auf die Mittelebene entsteht.

Werden  $U_1$  und  $U_2$  nicht so gewählt, dass sie Bilder von einem und demselben Punkt  $U$  sind, so wird die Abbildung  $T_3$  quadratisch.

Dem Verfahren bei axonometrischer Abbildung entsprechend werden wir auch hier eine andere Art der Erzeugung perspektiver Bilder aus zwei gegebenen Abbildungen (Bildern) besprechen, indem wir eine Kombination von regulären und singulären perspektiven Abbildungen versuchen. Dadurch erreichen wir, erstens die erwähnten Bewegungen der zwei gegebenen Bilder zu vermeiden, zweitens die Erzeugung von vielen verschiedenen, demselben Sehpunkt  $O_3$  entsprechenden Bildern  $(P_3)$ .

Es seien  $T_1$  und  $T_2$  gegebene reguläre perspektive Abbildungen mit Sehpunkten  $O_1$  und  $O_2$ . Wir suchen ein neues perspektives Bild mit Sehpunkt  $O_3$ , wo  $O_3$  ganz willkürlich ausserhalb  $O_1O_2$  gewählt wird. Dem Strahl  $O_1O_3$  entspricht bei  $T_1$  ein Punkt  $U_1$ , analog  $O_2O_3$  bei  $T_2$  ein Punkt  $U_2$ . Nun zentralprojizieren wir die Figuren  $(P_1)$  und  $(P_2)$  aus  $U_1$  bzw.  $U_2$  auf zwei Geraden  $a_1$  bzw.  $a_2$ . Dadurch entstehen auf  $a_1$  und  $a_2$  singuläre perspektive Bilder  $(P'_1)$  und  $(P'_2)$  von dem Objekt  $(P)$ , wobei die Geraden  $O_1O_3$  und  $O_2O_3$  die Achsen der Abbildungen sind. Wenden wir nun auf diese Bilder die auf S. 31—32 angegebene Konstruktion an, so entsteht ein Bild  $(P_3)$ , einer neuen regulären perspektiven Abbildung  $T_3$  mit Sehpunkt  $O_3$  entsprechend.

Damit sind wir zu folgendem Verfahren (Fig. 7) geführt worden:

Zu einem vorgelegten Sehpunkt  $O_3$  bestimmt man die  $O_3$  entsprechenden Punkte  $U_1$  und  $U_2$  in den Abbildungen  $T_1$  und  $T_2$ . Von  $U_1$  aus projiziert man das Bild  $(P_1)$  auf eine willkürlich gewählte Gerade  $a_1$  in  $(P'_1)$ , von

$U_2$  aus das Bild ( $P_2$ ) auf eine Gerade  $a_2$  in ( $P'_2$ ). Die Gerade  $U_1V_1$  schneidet  $a_1$  in  $S_1$ , und  $U_2V_2$  schneidet  $a_2$  in  $S_2$ . Auf der Geraden  $S_1S_2$  werden zwei beliebige Punkte  $U'_1$  und  $U'_2$  gewählt, wonach ( $P'_1$ ) von  $U'_1$  aus und ( $P'_2$ ) von  $U'_2$  aus projiziert werden. Der Schnittpunkt  $P_3$  entsprechender Geraden erzeugt ein neues perspektives Bild von ( $P$ ).

Bezüglich der Einführung der Punkte  $S_1$  und  $S_2$  ist zu bemerken, dass, indem  $V_1$  und  $V_2$  die Kernpunkte sind, die Gerade  $U_1V_1$  bei  $T_1$  das Bild der Ebene  $\omega = O_1O_2O_3$  wird, weshalb  $S_1$  in der singulären Abbildung das Bild derselben Ebene wird. Analog für  $S_2$ .  $U'_1$  und  $U'_2$  sollen dann auf der Geraden  $S_1S_2$  liegen.

Da auch  $a_1$  und  $a_2$  willkürlich wählbar sind, gibt es im ganzen 6 Parameter zur Festlegung des Bildes ( $P_3$ ), d. h. es können im ganzen  $\infty^6$  unter sich projektive, dem vorgelegten Sehpunkt  $O_3$  entsprechende Bilder entstehen. Weil eine Kollineation von 8 Parametern und eine Kongruenztransformation von 3 Parametern abhängig sind, ist zu erwarten, — einen Beweis

dafür habe ich jedoch nicht durchführen können, — dass man durch geeignete Wahl der beiden Geraden  $a_1, a_2$  und der Punkte  $U_1, U_2$  aus einer gegebenen Figur ( $P$ ) d. h. aus ( $P_1$ ) und ( $P_2$ ) sogar auf unendlich viele verschiedene Weisen ein vorgelegtes perspektives Bild ( $P_3$ ) hervorbringen kann.

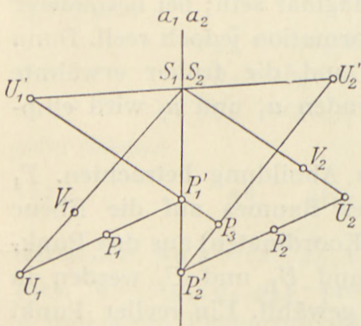


Fig. 8.

Wählt man sowohl  $a_1$  als  $a_2$  durch den Schnittpunkt  $S$  der Geraden  $U_1V_1$  und  $U_2V_2$ , braucht man nur  $U'_1$  und  $U'_2$  auf einer Geraden durch  $S$  zu wählen. Besonders einfach wird es, wenn  $a_1$  und  $a_2$  auf derselben Geraden  $a$  durch  $S$  gewählt werden. Die Konstruktion bekommt dann die in Fig. 8 angegebene relativ einfache Form.



## § 8. Imaginäre Abbildungen.

Im Vorhergehenden haben wir immer die behandelten Abbildungen als reell vorausgesetzt, wie es natürlich erscheint, da der Ausgangspunkt die axonometrischen und perspektiven Abbildungen des Raumes auf eine Ebene waren, wo man sich gewöhnlich nur für die reellen Punkte interessiert. Wenn von quadratischen Abbildungen die Rede ist, kann man indessen vorteilhaft imaginäre Punkte verwenden, indem man dadurch neue Auskünfte auch auf reellem Gebiet bekommt.

Betrachtet man die allgemeine Abbildung  $T_3$ , die aus zwei perspektiven Abbildungen  $T_1$  und  $T_2$  in Verbindung mit zwei Projektionszentren  $U_1$  und  $U_2$  hervorgeht, nämlich die quadratische Abbildung, so haben wir gesehen, dass der ganze Strahlenraum so auf die Bildebene  $\alpha$  abgebildet wurde, dass eine Gerade einem Kegelschnitt durch  $U_1$  und  $U_2$  einer neuen Geraden oder einem Punkt entspricht, je nachdem sie die Hauptgeraden nicht schneidet oder eine oder zwei von ihnen schneidet. Wählen wir nun  $U_1$  und  $U_2$  als die Kreispunkte der Ebene, wird der ganze Strahlenraum sich auf die Kreise einer Ebene abbilden lassen, indem man zu den Kreisen auch Geraden (uneigentliche Kreise) und Punkte (Punktkreise) mitrechnet.

Im allgemeinen wird die Abbildung  $T_3$ , die den Strahlenraum in die Kreise der Ebene überführt, imaginär sein; bei besonderer Wahl von  $u_1$  und  $u_2$  wird die Transformation jedoch reell. Dann müssen  $u_1$  und  $u_2$  imaginär sein, und die früher erwähnte Geradenkongruenz  $G$  mit den Leitgeraden  $u_1$  und  $u_2$  wird elliptisch.

Als Beispiel werden wir folgende Abbildung betrachten.  $T_1$  und  $T_2$  sind Zentralprojektionen des Raumes auf die Ebene  $z=0$  (in allgemeinen rechtwinkligen Koordinaten) aus den Punkten  $O_1(0, 0, i)$  und  $O_2(0, 0, -i)$ , und  $U_1$  und  $U_2$  werden in den Kreispunkten der Ebene  $z=0$  gewählt. Ein reeller Punkt  $P$  wird bei den Zentralprojektionen in konjugiert-imaginäre Punkte  $P_1$  und  $P_2$  überführt, wonach die Verbindungsgeraden mit den konjugiert-imaginären Kreispunkten einen reellen Schnittpunkt  $P_3$  geben. Die Kongruenz  $G$ , die die Geraden  $O_1U_1$  und  $O_2U_2$  als Leitgeraden hat, wird, wie ein einfaches Ausrechnen zeigt, eine Rotationskongruenz mit der  $Z$ -Achse als

Hauptachse<sup>1)</sup>, und die betrachtete Abbildung  $T_3$  wird die schiefe Projektion auf die Ebene  $z = 0$ , die durch diese elliptische Kongruenz bestimmt ist. (Einfach kann man diese Abbildung so erzeugen, dass die Gerade durch die Punkte  $(p, q, 1)$  und  $(-q, p, -1)$  in den Mittelpunkt  $\left(\frac{p-q}{2}, \frac{p+q}{2}, 0\right)$  der Strecke abgebildet wird;  $p$  und  $q$  sind unabhängige Parameter).

Diese bemerkenswerte Abbildung bildet ohne Ausnahme alle reellen Punkte des Raumes auf die reellen Punkte der Ebene ab. Die Gerade  $s$  fällt in die unendlich ferne Gerade der Ebene  $z = 0$ . Die schiefe Abbildung zwischen zwei zu  $z = 0$  parallelen Ebenen wird somit eine Ähnlichkeit (speziell eine Kongruenz), wodurch also Gerade in Gerade übergeführt wird. Dies ist damit übereinstimmend, dass eine zur Kongruenz gehörige Strahlenfläche, die eine zu  $z = 0$  parallele Gerade enthält, ein hyperbolisches Paraboloid mit der Richtungsebene  $z = 0$  ist. Da andere Geraden in Kreise abgebildet werden, schliesst man, dass für ein beliebiges Hyperboloid der Geradenkongruenz das eine System von Kreisen in Ebenen parallel zu  $z = 0$  liegt.

### § 9. Algebraische Darstellung.

Eine perspektive Abbildung  $T_1$  lässt sich durch Gleichungen der Form

$$(1) \quad \begin{aligned} \varrho y'_1 &= a_1 x_1 + a_2 x_2 + a_3 x_3 + a_4 x_4 = \alpha \xi \\ \varrho y'_2 &= b_1 x_1 + b_2 x_2 + b_3 x_3 + b_4 x_4 = \beta \xi \\ \varrho y'_3 &= c_1 x_1 + c_2 x_2 + c_3 x_3 + c_4 x_4 = \gamma \xi \end{aligned}$$

oder kürzer

$$(1) \quad \varrho \eta' = \varrho (y'_1, y'_2, y'_3) = (\alpha \xi, \beta \xi, \gamma \xi)$$

darstellen, wo  $\xi = (x_1, x_2, x_3, x_4)$  projektive Koordinaten des Raumes,  $\eta' = (y'_1, y'_2, y'_3)$  projektive Koordinaten der Bildebene  $\alpha$  und  $\varrho$  ein Proportionalitätsfaktor sind.

Der Sehpunkt  $O_1$  ist dadurch charakterisiert, dass er keinen Bildpunkt hat. Löst man also die Gleichungen

$$\alpha \xi = 0, \quad \beta \xi = 0, \quad \gamma \xi = 0,$$

<sup>1)</sup> [14], S. 168 ff.



bekommt man Koordinaten für  $O_1$ . Wir bezeichnen eine Lösung dieser Gleichungen mit  $\widehat{abc}$ , wo dieses Symbol ein Vektor ist, dessen Komponenten die Komplemente der letzten Reihe der Matrix

$$\begin{vmatrix} a_1 a_2 a_3 a_4 \\ b_1 b_2 b_3 b_4 \\ c_1 c_2 c_3 c_4 \\ 0 0 0 0 \end{vmatrix}$$

sind.

Wenn dieser Vektor eigentlich ist, d. h. wenn die Matrix den Rang 3 hat, ist die Abbildung regulär. Hat die Matrix den Rang 2, wodurch  $\widehat{abc}$  ein Nullvektor wird, ist  $T_1$  eine singuläre Abbildung, durch die der Raum auf eine Gerade abgebildet wird. Ist endlich der Rang gleich 1, bekommt man eine Abbildung des Raumes in einen einzelnen Punkt. Der Rang Null ist ausgeschlossen.

Es sei nun  $T_1$  eine reguläre Abbildung. Wir suchen die Punkte  $\xi$ , die in denselben Punkt  $\eta^0$  abgebildet werden.

Ist  $\xi^0 = (x_1^0, x_2^0, x_3^0, x_4^0)$  eine Lösung der Gleichungen (1) für  $\eta' = \eta^0$ , werden sämtliche Lösungen  $\xi$  in der Form

$$\xi = \lambda \xi^0 + \mu \widehat{abc} \quad (\lambda \neq 0)$$

dargestellt, woraus man sieht, dass alle Punkte  $\xi$  auf einer Geraden durch das Projektionszentrum (Sehpunkt)  $O_1$  liegen.

Es sei nun eine neue perspektive Abbildung  $T_2$  durch

$$(2) \quad \varrho \eta'' = (v\xi, e\xi, f\xi)$$

bestimmt, und es seien die Punkte  $U_1$  und  $U_2$  in der Ebene  $\alpha$  durch die Koordinaten  $u' = (u'_1, u'_2, u'_3)$  und  $u'' = (u''_1, u''_2, u''_3)$  gegeben. Wir suchen eine algebraische Darstellung der Abbildung  $T_3$ , die dadurch bestimmt ist, dass der Punkt  $P$  ( $\xi$ ) in den Schnittpunkt  $P_3$  der Geraden  $U_1P_1$  und  $U_2P_2$  abgebildet werden soll.

Die Linienkoordinaten dieser Geraden sind  $\widehat{u'y'}$  und  $\widehat{u''y''}$ , wonach wir zur Bestimmung von  $\eta'''$  die Gleichungen

$$\eta''' = \widehat{\widehat{u'y'}\widehat{u''y''}} = u'' | u'y'y'' | - y'' | u'y'u'' |$$

haben. Setzt man hier  $\eta' = (a\bar{x}, b\bar{x}, c\bar{x})$  und  $\eta'' = (d\bar{x}, e\bar{x}, f\bar{x})$  ein, entstehen Gleichungen einer quadratischen Abbildung des Raumes auf die Ebene.

Diese Gleichungen werden sehr einfach, wenn man z. B.  $U_1$  im Punkte  $(1, 0, 0)$  und  $U_2$  im Punkte  $(0, 1, 0)$  wählt. Man hat dann

$$u'\eta' = (0, -y'_3, y'_2), \quad u''\eta'' = (y''_3, 0, -y''_1),$$

wodurch

$$\varrho\eta''' = (y'_3y''_1, y'_2y''_3, y'_3y''_3)$$

oder

$$(3) \quad \varrho\eta''' = ((c\bar{x})(d\bar{x}), (b\bar{x})(f\bar{x}), (c\bar{x})(f\bar{x})).$$

Wir nehmen jetzt an, dass sowohl  $T_1$  als  $T_2$  reguläre Abbildungen sind, d. h. weder  $\widehat{abc}$  noch  $\widehat{def}$  Nullvektor ist. Die Gerade  $u_1$ , die bei  $T_1$  in den Punkt  $(1, 0, 0)$  abgebildet wird, muss durch die Gleichungen  $b\bar{x} = 0, c\bar{x} = 0$  bestimmt sein. Die Gerade  $u_2$  ist entsprechend durch  $d\bar{x} = 0, f\bar{x} = 0$  bestimmt. Weil die Ebene  $\sigma_1$  bei  $T_1$  der Geraden  $U_1U_2$  entspricht, muss die Gleichung dieser Ebene  $c\bar{x} = 0$  sein. Analog hat  $\sigma_2$  die Gleichung  $f\bar{x} = 0$ , so dass die dritte Hauptgerade  $s$  durch die Gleichungen  $c\bar{x} = 0, f\bar{x} = 0$  gegeben ist.

Man kann nun leicht entscheiden, wann die Abbildung  $T_3$  quadratisch ohne Sehpunkt oder mit Sehpunkt oder perspektivisch wird. Die Abbildung wird quadratisch ohne Sehpunkt, wenn  $u_1$  und  $u_2$  sich nicht schneiden, d. h.

$$|bcd\bar{f}| \neq 0.$$

Ist dagegen  $|bcd\bar{f}| = 0$ , existiert ein Sehpunkt  $O_3$  mit dem Koordinatenvektor  $\widehat{bcd}$ , und die Abbildung ist quadratisch oder perspektiv. Welche der beiden Möglichkeiten eintritt, ist davon abhängig, ob die Gerade  $s$  existiert oder nicht, also ob die Vektoren  $c$  und  $f$  linear unabhängig sind oder nicht. Wenn  $c = k \cdot f$ , ist  $T_3$  perspektiv, und wenn  $c \neq k \cdot f$  ist, wird  $T_3$  quadratisch.

Wenn  $T_3$  perspektiv ist, bekommt man aus (3) die Gleichung

$$\varrho\eta''' = (k \cdot d\bar{x}, b\bar{x}, c\bar{x}).$$



Die Ebene  $\overline{cx} = \overline{fx} = 0$  enthält die Sehpunkte  $O_1$  ( $\widehat{abc}$ ),  $O_2$  ( $\widehat{def}$ ) und  $O_3$  ( $\widehat{bcd}$ ) und ist die früher mit  $\omega$  bezeichnete Ebene, die sowohl bei  $T_1$  als bei  $T_2$  in dieselbe Gerade der Ebene  $\alpha$ , hier die  $y_3$ -Achse, abgebildet wird.

Es ist nun auch klar, dass die Kernpunkte, d. h. das Bild  $V_1$  von  $O_2$  bei  $T_1$  und das Bild  $V_2$  von  $O_1$  bei  $T_2$  auf dieser Geraden liegen. Setzt man nämlich  $\overline{x} = \widehat{abc}$  in die Gleichung (2) ein, oder  $\overline{x} = \widehat{def}$  in (1), wird in beiden Fällen die dritte Koordinate Null.

### Literaturverzeichnis.

- [1] ARVESEN, P., Zur axonometrischen Methode von L. Eckhart, Det kgl. Norske Vidensk. Selsk. Forh. XI (1938), S. 72.
- [2] — Weiteres über L. Eckharts axonometrische Methode, ebenda S. 78.
- [3] ECKHART, L., Affine Abbildung und Axonometrie, Sitzungsber. d. Akad. d. Wissensch. in Wien, mat. nat. Kl., B. 146 (1937), S. 51.
- [4] — Ein neues Schrägrissverfahren, Zeitschr. des Vereins deutsch. Ingen. (VDI) (1938), S. 447.
- [5] FABRICIUS-BJERRE, FR., Om L. Eckharts aksonometriske Metode, Mat. Tidsskr. B, (1944), S. 1.
- [6] GAUSS, Werke, B. VIII (1900), S. 345.
- [7] HAUCK, G., Neue Constructionen der Perspektive und Photogrammetrie, Journ. f. reine u. angew. Mat., B. 95 (1883), S. 1.
- [8] — Theorie der trilinearen Verwandtschaft ebener Systeme, ebenda B. 97 (1884), S. 261.
- [9] MÜLLER, E., Vorlesungen über darstellende Geometrie, Leipzig 1923.
- [10] NYSTRÖM, E. J., Zur praktischen Axonometrie, Soc. Sc. Fenn., Comm. Phys. Math. XI, 11, 1942.
- [11] STEINER, Gesammelte Werke, B. 1 (1881), S. 409.
- [12] TRANSON, A., De la projection gauche, Nouv. Ann. 2, ser. IV (1865), S. 385.
- [13] — — — (suite), ebenda, ser. V (1866), S. 63.
- [14] ZINDLER, K., Liniengeometrie mit Anwendungen, Leipzig 1902, B. 1.

DET KGL. DANSKE VIDENSKABERNES SELSKAB  
MATEMATISK-FYSISKE MEDDELELSER, BIND XXII, NR. 6

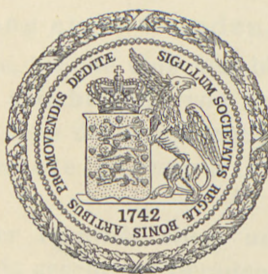
---

EINLEITUNG IN DIE  
ALLGEMEINE KONGRUENZLEHRE

VON

JOHANNES HJELMSLEV

VIERTE MITTEILUNG



KØBENHAVN

I KOMMISSION HOS EJNAR MUNKSGAARD

1945



ALLGEMEINE KOCH-REZEPTUR  
EINFÜHRUNG IN DIE KÜCHE  
VON  
FRIEDRICH WILHELM  
VON  
KÖNIGLICHEN HOCHSCHULE  
KÖLN

Die vorliegende Arbeit ist eine Zusammenfassung der  
Kochkunst, wie sie in der Gegenwart geübt wird.  
Sie ist in drei Theile eingetheilt:  
I. Die Zubereitung der Speisen.  
II. Die Zubereitung der Getränke.  
III. Die Zubereitung der Backwaren.



Printed in Denmark.  
Bianco Lunos Bogtrykkeri A/S

Diese vierte Mitteilung behandelt die allgemeine Kongruenzlehre des offenen Raumes beliebig vieler Dimensionen<sup>1</sup>.

### § 1. Totalbeschreibung des Raumes.

#### I. Punkte, gerade Linien, Transporte (Bewegungen).

Es gibt Punkte  $A, B, C, \dots$  Es gibt Punktmenge  $a, b, c, \dots$ , welche gerade Linien (Geraden) heissen. Es gibt Transformationen, welche Transporte (oder Bewegungen) heissen. Ein Transport ist eine Zuordnung, durch welche jeder Geraden und jedem auf ihr gelegener Punkt eine Gerade und ein auf ihr gelegener Punkt umkehrbar eindeutig entspricht. Die Transporte bilden eine Gruppe. Zwei Figuren, welche durch einen Transport auseinander abgeleitet werden können, sollen kongruent heissen. Alle Punkte sind kongruent. Alle Geraden sind kongruent.

#### II. Innere Bewegung einer Geraden.

Es gibt Transporte, welche eine beliebig vorgegebene Gerade  $g$  stehen lassen. Man spricht dann von kongruenten Punkt-reihen auf  $g$ , wobei man die entsprechenden Transformationen von  $g$  in sich als innere Transporte (Bewegungen) der Geraden bezeichnet.

Es gibt ausser der Identität einen und nur einen inneren Transport einer beliebig gegebenen Geraden, welche einen beliebig

<sup>1</sup> Die früher veröffentlichten Mitteilungen:

Einleitung in die allgemeine Kongruenzlehre, Erste Mitteilung, D. Kgl. Danske Vidensk. Selskab, Math.-fys. Medd. VIII, 11, 1929; Zweite Mitteilung, ibd. X, 1 1929; Dritte Mitteilung, ibd. XIX, 12, 1942, sollen im folgenden als Einl. I, II, III zitiert werden.



gegebenen Punkt  $A$  dieser Geraden stehen lässt. Dieser Transport soll als innere Spiegelung (Umwendung) um  $A$  als Zentrum bezeichnet werden.

### III. Punktspiegelung.

Einem Punkt  $O$  entspricht eine Spiegelung um  $O$ , d. h. ein involutorischer Transport, welcher  $O$  und jede Gerade durch  $O$  stehen lässt. Kein anderer Punkt als  $O$  soll bei der Bewegung stehen bleiben.

$A$  heisst Zentrum der Spiegelung. Die Spiegelung soll mit demselben Buchstaben wie das Zentrum bezeichnet werden.

### IV. Mittelpunkt.

Es gibt eine und nur eine Punktspiegelung  $M$ , welche zwei beliebig vorgegebene Punkte  $A, B$  ineinander überführt. Der Punkt  $M$  heisst Mittelpunkt der beiden Punkte  $A, B$ .

Folgerung. Jeder Transport, welcher zwei Punkte vertauscht, oder jeden von ihnen stehen lässt, muss ihren Mittelpunkt stehen lassen.

### V. Achsenspiegelung.

1. Einer Geraden  $a$  entspricht ein involutorischer Transport, welcher alle Punkte von  $a$ , und keine anderen, stehen lässt. Dieser Transport soll Achsenspiegelung (Spiegelung) um  $a$  als Achse, oder Umwendung um  $a$  heissen, und wird mit demselben Buchstaben  $a$  wie die Achse selbst bezeichnet.

2. Jede von  $a$  verschiedene Gerade, welche einen Punkt  $A$  von  $a$  enthält, und bei der Spiegelung  $a$  stehen bleibt, soll senkrecht zu  $a$  ( $\perp a$ ) oder Normale zu  $a$  in  $A$  heissen. Durch jeden Punkt ausserhalb  $a$  geht mindestens eine Senkrechte  $b$  zu  $a$ .

### Folgerungen.

1°. Jede zu  $a$  in einem Punkte  $A$  senkrechte Gerade wird nach II durch eine innere Spiegelung um  $A$  transformiert und hat demnach keinen anderen Punkt mit  $a$  gemein.

2°. Zwei Spiegelungen um verschiedene Achsen sind verschieden.

3°. Die Beziehung  $b \perp a$  ist eine reziproke; die Transformationsgleichungen  $b^a = b$ , und  $a^b = a$ , sind nämlich gleichbedeutend mit  $ab = ba$ .<sup>1</sup>

4°. Jede Verbindungsgerade  $g$  zweier Punkte  $A, B$  muss den Mittelpunkt  $M$  von  $A, B$  enthalten. Die Spiegelung  $g$  lässt nämlich  $A$  und  $B$ , und sonach  $M$ , ungeändert.

VI. Zwei kongruente Punktreihen  $ABC \dots$  und  $AB'C' \dots$ , welche auf zwei Geraden mit einem einzigen gemeinsamen Punkt  $A$  gelegen sind, können immer durch eine, und nur eine, Achsenspiegelung ineinander übergeführt werden.

VII. Eindeutiges Schneiden zweier Geraden.

Wenn eine Gerade durch den Schnittpunkt zweier Geraden, welche einander eindeutig schneiden, hindurchgeht, so muss sie jedenfalls eine von diesen Geraden eindeutig schneiden.

VIII. Eindeutige Verbindung zweier Punkte.

Wenn ein Punkt  $P$  und eine Gerade  $a$  beliebig vorgegeben sind, so gibt es immer auf der Geraden  $a$  einen Punkt  $Q$  derart, dass die beiden Punkte  $P, Q$  eine und nur eine Verbindungsgerade haben.

---

Gelegentlich wollen wir die folgenden Ausdrücke verwenden:

Nachbarpunkte sind zwei Punkte mit mehreren Verbindungsgeraden.

Fernpunkte sind solche mit einer und nur einer Verbindungsgeraden.

Schmieggeraden sind zwei Geraden mit mehreren gemeinsamen Punkten.

Kreuzgeraden sind solche mit einem und nur einem gemeinsamen Punkt.

<sup>1</sup> Wie früher bezeichnen wir die Transformation  $P^{-1}QP$  mit  $Q^P$ . Es wird dann  $(T^U)^V = T^{UV}$ , und  $T^U V^U = (TV)^U$ .



## § 2. Aufeinander senkrechte Geraden.

**Satz 1.** Zwei Kreuzgeraden  $a, b$  mit dem Schnittpunkt  $O$  haben zwei aufeinander senkrechte Spiegelungsachsen durch  $O$ .

**Beweis.** Wir betrachten (Fig. 1) zwei auf  $a$  und  $b$  gelegene kongruente Reihen  $OA\cdots$  und  $OB\cdots$ . Ihre Spiegelungsachse heie  $x$  (VI). Die Spiegelung  $O$  fhrt diese Reihen in zwei Reihen

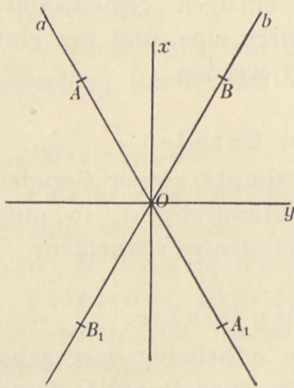


Fig. 1.

$OA_1\cdots$  und  $OB_1\cdots$  mit derselben Spiegelungsachse  $x$  ber. Die Reihen  $OA\cdots$  und  $OB_1\cdots$  haben eine andere Spiegelungsachse  $y$ , welche auch als Spiegelungsachse der beiden Reihen  $OA_1\cdots$  und  $OB\cdots$  hervortritt. Da nun die Spiegelung  $y$  die beiden Reihen  $OA\cdots$  und  $OB\cdots$  in  $OB_1\cdots$  bzw.  $OA_1\cdots$  berfhrt, muss die Achse  $x$  bei dieser Spiegelung ungendert bleiben, d. h.  $x \perp y$ .

Wenn es in einem Punkt einer Geraden  $a$  nur eine Senkrechte zu  $a$  gibt, dann kann in jedem Punkt jeder Geraden eine und nur eine Senkrechte zu dieser errichtet werden. In diesem besonders wichtigen Falle soll unser Raum als Ebene bezeichnet werden. Es soll im folgenden nachgewiesen werden, dass fr diesen Fall das in Einl. I S. 5. aufgestellte Axiomensystem erfllt ist, und dass infolgedessen die Geometrie der Ebene durch unsere frhere Darstellung erledigt ist.

**Satz 2.** Steht eine Gerade  $n$  senkrecht auf den beiden Kreuzgeraden  $a, b$  in ihrem Schnittpunkt  $O$ , so steht sie auch senkrecht auf ihren Spiegelungsachsen  $x, y$ .

Die Spiegelung  $n$  fhrt nmlich die kongruenten Reihen  $OA\cdots$  auf  $a$  und  $OB\cdots$  auf  $b$  in  $OA_1\cdots$  und  $OB_1\cdots$  ber, und jeder der beiden Achsen  $x, y$  muss deshalb bei der Spiegelung  $n$  stehen bleiben.

Unter einem  $n$ -Kreuz verstehen wir ein System von  $n$  Geraden, welche durch denselben Punkt (den Scheitel des Kreuzes) gehen und paarweise aufeinander senkrecht stehen.

Wenn in unserem Raume ein  $n$ -Kreuz existiert, das durch  $n-1$  seiner Geraden eindeutig bestimmt ist, so soll der Raum  $n$ -dimensional (ein  $n$ -Raum,  $R_n$ ) heissen.

Eine Gerade soll Normale eines  $n$ -Kreuzes heissen, wenn sie zusammen mit diesem ein  $(n+1)$ -Kreuz bildet.

Wenn ein  $(n-1)$ -Kreuz existiert, welche mehr als eine Normale aufweist, können zwei Hauptfälle eintreten:

1°. Je zwei Normalen  $p, q$  des Kreuzes sind Schmieggeraden. Durch Spiegelung von  $p$  um  $q$  und wiederholte ähnliche Spiegelungen entstehen beispielsweise andere Normalen des Kreuzes. Alle Normalen des Kreuzes bilden ein Normalenbüschel von Schmieggeraden. Der Raum soll in diesem Falle als  $R_n$ -Erweiterung oder  $R_n$ -Nachbarschaft bezeichnet werden.

2°. Es gibt zwei Normalen  $p, q$  des Kreuzes, welche nur einen Punkt gemein haben. Die Spiegelungsachsen  $x, y$  dieser Normalen sind dann auch Normalen des Kreuzes und bilden mit diesem ein  $(n+1)$ -Kreuz. Der Raum ist dann wenigstens von  $n+1$  Dimensionen.

Unsere Totalbeschreibung enthält schliesslich auch die Möglichkeit, dass der Raum unendlich viele Dimensionen aufweist, d. h. dass unendlich viele paarweise zueinander senkrecht stehende Geraden durch denselben Punkt vorkommen können.

### § 3. Die Geometrie der Ebene.

In Einl. I Axiom II wurde die Spiegelung an einer Geraden  $a$  als eine von der Identität verschiedene Bewegung, welche alle Punkte von  $a$  stehen lässt, definiert. Dass diese Eigenschaft auf Grund unserer allgemeinen Totalbeschreibung des Raumes erfüllt ist, wenn der Raum eine Ebene ist, soll nun nachgewiesen werden.

Bei einem Transport  $\tau$  in einer Ebene, wo alle Punkte einer Geraden  $a$  stehen bleiben, muss jede Normale zu  $a$  stehen bleiben. Betrachten wir eine dieser Normalen,  $n$ , mit dem Fusspunkt  $A$ . Entweder erfährt diese Normale bei der Bewegung  $\tau$  eine innere Spiegelung mit dem Zentrum  $A$ , oder alle ihre Punkte sind fest. Wenn alle Normalen von  $a$  innere Spiegelungen erfahren, ist die Bewegung  $\tau$  eine Spiegelung um  $a$ . Wenn aber alle ihre Punkte feststehen, ist die Bewegung die Identität. Man



hat also nur zu beweisen, dass wenn es für eine Normale, z. B.  $n$ , gilt, dass alle ihre Punkte fest liegen, dann ist jeder Punkt  $P$  der Ebene fest. Um dies einzusehen, fällen wir Normalen  $q, r$  von  $P$  auf  $a$  und  $n$ ; ihre Fusspunkte seien  $Q$  und  $R$ . Die Normalen  $q, r$  müssen so bei der Bewegung  $\tau$  fest liegen. Wenn sie Kreuzgeraden sind, muss also  $P$  unverändert bleiben. Wenn sie aber Schmieggeraden wären, könnte vielleicht der Fall eintreten, dass  $P$  in einen anderen gemeinsamen Punkt  $P_1$  von  $q$  und  $r$  übergehen könnte. Hierbei müsste aber das Paar  $PP_1$  seinen Mittelpunkt in  $Q$ , und zugleich in  $R$ , haben, was unmöglich ist. Wir haben also hiermit den Beweis erbracht und können den folgenden Satz aufstellen:

Satz 3. Jeder Transport der Ebene in sich, welcher alle Punkte einer Geraden in Ruhe lässt, ist entweder die Identität oder eine Spiegelung um diese Gerade.

Wir haben in der Grundtatsache VI unserer Totalbeschreibung die Bedingung gestellt, dass die in Rede stehenden Geraden nur einen Punkt gemein haben, was wir in der entsprechenden Aussage in Einl. I Axiom V nicht gefordert haben. Wir wollen aber nun zeigen, dass wir, einstweilen für die ebene Geometrie, auf den hier vorgetragenen Grundlagen die betreffende Aussage für Schmieggeraden beweisen können:

Satz 4. Wenn in der Ebene zwei kongruente Punkt-reihen  $ABC\cdots$  und  $AB'C'\cdots$  auf zwei Schmieggeraden  $p, q$  liegen, so können sie immer durch eine und nur eine Achsenspiegelung um eine Gerade durch  $A$  ineinander übergeführt werden.

Zunächst beweisen wir den folgende Hilfssatz:

Wenn  $p, q, r$  drei Gerade durch ein und denselben Punkt  $A$  bedeuten, und  $p, q$  Schmieggeraden,  $p, r$  Kreuzgeraden sind, so ist der Transport  $pqr$  einer Spiegelung gleichwertig.

Beweis. Eine der Spiegelungsachsen von  $p, r$  sei mit  $x$  bezeichnet. Durch den Transport  $pqx$  geht eine Punktreihe  $AP\cdots$  auf  $p$  in eine Punktreihe  $AP'\cdots$  auf einer Schmieggeraden  $r'$  zu  $r$  über. Die beiden Punkt-reihen haben dann eine Spiegelungsachse  $x'$  (VI), und es wird so entweder  $pqx = x'$ , oder  $pqx = px'$ ; die letztere Möglichkeit ist aber ausgeschlossen, weil  $qx$  keine Spiegelung darstellen kann. Also ist  $pqx = x'$ , und deshalb  $= xqp$ , oder

$$(qp)^x = pq. \quad (1)$$

Nun bestimmen wir eine Gerade  $s$  derart, dass  $q^x = s$ , also, da  $p^x = r$ :

$$(qp)^x = sr. \quad (2)$$

Aus (1) und (2) folgt dann  $pq = sr$ , oder

$$pqr = s, \quad \text{w. z. b. w.}$$

Um nun den Satz 4 zu beweisen, betrachten wir zunächst zwei kongruente gleich orientierte Punktreihen  $AP\cdots$  und  $AQ\cdots$  auf  $p$  und  $q$  und ausserdem eine ihnen kongruente Reihe  $AR\cdots$  auf  $r$ . Es sei ferner  $x$  die Spiegelungsachse der Reihen  $AP\cdots$  und  $AR\cdots$ , und  $y$  die Spiegelungsachse von  $AQ\cdots$  und  $AR\cdots$ . Es zeigt sich dann, dass die Reihe  $AP\cdots$  durch den Transport  $xy$ , und somit auch durch den Transport  $xyq$ , in  $AQ\cdots$  übergeht. Letzterer Transport ist aber nach dem obigen Hilfssatz einer Spiegelung  $z$  gleichwertig, weil  $x, y$  untereinander Schmiegegeraden sind, aber Kreuzgeraden zu  $q$ . Dass  $x, y$  Schmiegegeraden sind, ist sofort ersichtlich: ist nämlich  $P = Q$  und der entsprechende Punkt  $R$  auf  $r$ , so fallen die Mittelpunkte der Paare  $PR$  und  $QR$  zusammen und bestimmen dann einen von  $A$  verschiedenen gemeinsamen Punkt der Spiegelungsachsen  $x, y$ .

Es hat sich so herausgestellt, dass die Punktreihen  $AP\cdots$  und  $AQ\cdots$  durch eine Spiegelung  $xyq = z$  in einander übergehen.

Dass zwei Spiegelungsachsen  $z, z'$  nicht vorkommen können, folgt daraus, dass der Transport  $zz'$  die Reihe  $AP\cdots$  in Ruhe lassen müsste, also  $zz' = p$ , was unmöglich ist.

Der Fall, wo die Punktreihen entgegengesetzt orientiert sind, wird mittels einer Punktspiegelung  $A$  auf den vorigen zurückgeführt.

In der ebenen Geometrie gilt somit in allen Fällen der Satz:

Satz 5. Zwei kongruente Punktreihen  $ABC\cdots$  und  $AB'C'\cdots$  auf einer oder auf zwei Geraden mit dem gemeinsamen Punkt  $A$  können durch eine und nur eine Achsenspiegelung ineinander übergeführt werden.

Hieraus folgt nun für die ebene Geometrie, wie früher in Einl. I S. 10:

Satz 6. Die Aufeinanderfolge von drei Spiegelungen  $a, b, c$ , deren Achsen durch denselben Punkt  $O$  gehen,



kann durch eine einzige Spiegelung ersetzt werden. Die Achse der Spiegelung geht durch  $O$ .

Die Gleichung  $ab = xc$  ist durch  $x = abc$  befriedigt. Ist  $a \perp b$ , so wird auch  $x \perp c$ , denn aus  $ab = ba$  folgt  $xc = cx$ . Hieraus schliesst man:

Zwei beliebige zueinander senkrechte Geraden  $a, b$  durch den Punkt  $O$  bestimmen einen Transport  $ab$ , welcher jede Gerade  $c$  durch  $O$  stehen lässt. Der Transport ist involutorisch, weil  $ab = ba$ . Er lässt keinen von  $O$  verschiedenen Punkt stehen. Wäre nämlich  $P$  ein fester Punkt, könnte der Transport durch die Aufeinanderfolge von zwei Spiegelungen  $r, s$  ersetzt werden, deren Achsen  $r, s$  durch  $P$  gehen und senkrecht aufeinander stehen müssten (weil der Transport involutorisch ist), und durch  $O$  könnte man dann eine Gerade  $l \perp r$  ziehen, deren Fusspunkt und somit alle Punkte auf  $l$  fest liegen müssten, d. h. der Transport  $ab$  müsste entweder  $= l$  oder die Identität sein, was unmöglich ist. Es geht dann hieraus hervor, dass  $ab = O$ .

Einem beliebigen Punkte  $P$  ausserhalb  $a$  entspricht bei der Spiegelung  $a$  ein Punkt  $P_1$ . Der Mittelpunkt  $M$  von  $PP_1$  muss auf  $a$  liegen. Von  $P$  geht nach Voraussetzung mindestens eine Senkrechte auf  $a$ . Sie trifft  $a$  in  $M$ . Da ferner  $M$  und die Senkrechte auf  $a$  in  $M$  eindeutig sind, so ist die Senkrechte von  $P$  auf  $a$  auch eindeutig.

Nach diesen Überlegungen steht es dann völlig klar, dass für die Ebene durch unsere Totalbeschreibung das ganze Axiomsystem aus der Einl. I zur Verfügung steht, und wir können dann für den weiteren Ausbau der Geometrie der Ebene auf die frühere Darstellung verweisen.

Eine Frage müssen wir doch noch etwas ausführlicher, als wir es früher getan haben, besprechen, nämlich die Frage von den Spiegelungsachsen zweier Schmieggeraden.

Um die nötigen Hilfsmittel bereit zu haben, müssen wir auf die Untersuchung in Einl. I S. 18 zurückgreifen:

Zwei Schmieggeraden  $l, m$  Fig. 2 haben die Punkte  $A, B$  gemein. Auf  $l$  wählen wir den Punkt  $C$ , welcher nicht auf  $m$  liegt. Das Lot  $p$  von  $C$  auf  $m$  hat den Fusspunkt  $D$ .

Es wird nun  $ABD = E$  gesetzt, wo  $E$  ein Punkt von  $m$  ist. Hieraus folgt

$$ABC = EDC,$$

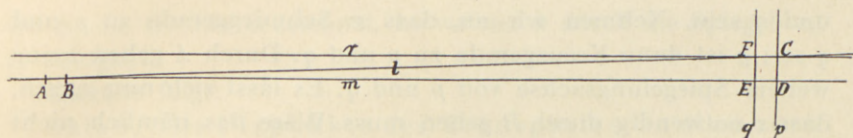


Fig. 2.

und da  $A, B, C$  einer Geraden angehören, ist  $ABC$ , also  $EDC$  ein involutorischer Transport.

Errichtet man nun das Lot  $q$  auf  $m$  in  $E$ , und das Lot  $r$  auf  $p$  in  $C$ , so wird

$$E = qm, \quad D = mp, \quad C = pr,$$

also

$$EDC = qmmprr = qr.$$

$qr$  ist also ein involutorischer Transport, d. h.  $q \perp r$ . Setzt man  $qr = F$ , gehen  $q$  und  $r$  durch  $F$ . Hieraus ersieht man, dass die beiden Linienpaare  $rm$  und  $pq$  einander senkrecht schneiden, dass also die Schnittpunkte  $EDCF$  ein »Rechteck« bilden; ferner, dass  $l$  Schmieggerade zu  $r$  und sonach (VII) Kreuzgerade zu  $q$  ist; man kann dann die naheliegende Redeweise einführen, dass  $l, q$  fast-senkrecht zueinander sind. Es gilt also der Satz:

Satz 7. Wenn eine Gerade  $l$  zwei zueinander senkrechte Geraden  $m, q$  schneidet und Schmieggerade zu einer der Geraden ist, so ist sie Kreuzgerade zu der anderen und fast-senkrecht zu dieser.

Sind  $a, b$  zwei zueinander senkrechte Geraden mit dem Schnittpunkt  $O$ , und  $c, d$  zwei Geraden durch  $O$ , welche durch jede der Spiegelungen  $a, b$  in einander übergehen, und sind  $c, d$  beide Kreuzgeraden zu  $a$  und  $b$ , so sind  $c$  und  $d$  Kreuzgeraden zueinander. Hätten nämlich  $c, d$  einen gemeinsamen Punkt  $P$  ausserhalb  $a$  und  $b$ , so müsste das Spiegelbild  $P_1$  von  $P$  bezüglich  $a$  auch den Geraden  $c, d$  gemeinsam sein, und die Normale  $n$  von  $P$  auf  $a$  müsste dann Schmieggerade zu  $c$  und dem vorigen Satz zufolge  $b$  und  $c$  Schmieggeraden zueinander sein, was unserer Annahme widerspricht.

Es seien nun  $p, q$  zwei Schmieggeraden mit den beiden gemeinsamen Punkten  $A, B$ . Es gehen dann durch  $A$  zwei zueinander senkrechte Spiegelungsachsen  $x, y$  von  $p, q$ . Sie können nach obiger Untersuchung nicht beide Kreuzgeraden zu  $p$



und  $q$  sein. Nehmen wir an, dass  $x$  Schmiegegerade zu  $p$  und  $q$  sei;  $y$  ist dann Kreuzgerade zu  $p$  und  $q$ . Durch  $A$  gehen keine weitere Spiegelungsachse von  $p$  und  $q$ . Es lässt sich nun zeigen, dass  $x$  notwendig durch  $B$  gehen muss. Wäre das nämlich nicht der Fall, so würde das Spiegelbild  $B_1$  von  $B$  bezüglich  $x$  auch den Geraden  $p, q$  angehören, und die Normale  $a$  zu  $x$  durch  $B$  hätte dann zwei Punkte  $B, B_1$  mit  $p$  und  $q$  gemein d. h.  $n$  wäre Schmiegegerade zu  $p$ , was unserer Annahme dass  $x, p$  Schmiegegeraden sind, widersprechen würde.

Also:

Satz 8. Zwei Schmiegegeraden  $p, q$  haben eine Spiegelungsachse  $x$ , welche alle gemeinsame Punkte von  $p, q$  enthält, und eine Reihe anderer Spiegelungsachsen  $\perp x$ , deren jede durch einen gemeinsamen Punkt von  $p$  und  $q$  geht.

Irgend zwei Punkte  $P, Q$  auf  $p, q$ , welche einander bei der Spiegelung  $x$  entsprechen, sind Nachbarpunkte.

#### § 4. Der dreidimensionale Raum.

Wir gehen nun daran, den dreidimensionalen Raum  $R_3$  näher zu untersuchen.

Es liege in diesem Raum ein 3-Kreuz  $npq$  mit dem Scheitel  $O$  vor, wo  $n$  also die einzige gemeinsame Normale von  $p$  und  $q$  in  $O$  ist. Es lässt sich dann leicht zeigen, dass auch  $\left\{ \begin{smallmatrix} p \\ q \end{smallmatrix} \right\}$  die einzige gemeinsame Normale von  $\left\{ \begin{smallmatrix} q \\ p \end{smallmatrix} \right\}$  und  $n$  ist. Andere 3-Kreuze lassen sich durch Bewegungen aus dem gegebenen ableiten.

Wir wollen nun das System  $\Sigma$  aller Fixpunkte des Transportes  $On$  ( $= nO$ , weil  $n^O = n$ ) ableiten. Dieses System enthält alle Punkte auf den Normalen zu  $n$  in  $O$ , und es enthält keine anderen Punkte. Es sei nämlich  $O_1$  ein Punkt von  $\Sigma$ .  $O_1$  und sein Spiegelbild  $O_2$  bezüglich  $O$  sind dann auch Spiegelbilder bezüglich  $n$ . Eine Senkrechte von  $O_1$  auf  $n$  muss auch  $O_2$  enthalten und trifft also  $n$  in  $O$ .

Es sei nun  $M$  der Mittelpunkt von  $OO_1$ . Es gilt dann

$$M^{On} = M, \quad \text{oder} \quad (On)M(On) = M,$$

also

$$On = M(On)M = O^M n^M = O_1 n_1,$$

wo  $n_1$  die Gerade bezeichnet, in welche  $n$  durch die Spiegelung  $M$  übergeht.

Hieraus folgt:

Satz 9. Alle Fixpunkte des Transportes  $On$  sind auch Fixpunkte des Transportes  $O_1n_1$ , und umgekehrt.

Ferner:

Satz 10. Das System  $\Sigma$  der Fixpunkte wird durch jeden seiner Punkte in sich selbst gespiegelt.

Satz 11. Durch  $O$  gehen unendlich viele Geraden, die in  $\Sigma$  liegen, nämlich die Normalen von  $n$  in  $O$ . Durch jeden anderen Punkt  $O_1$  von  $\Sigma$  gehen unendlich viele Geraden in  $\Sigma$ , nämlich die Normalen der entsprechenden Geraden  $n_1$  in  $O_1$ . Jedes dieser Normalenbüschel erschöpft das ganze System  $\Sigma$ .

Es folgt hieraus:

Satz 12. Je zwei Punkte von  $\Sigma$  haben wenigstens eine Verbindungsgerade, welche in  $\Sigma$  liegt.

Es sei nun  $l$  eine beliebige Gerade in  $\Sigma$  und  $P$  ein beliebiger Punkt in  $\Sigma$ . Das Spiegelbild von  $P$  bezüglich  $l$ , dargestellt durch  $P^l = lPl$ , wird dann auch  $\Sigma$  angehören. Da nämlich  $P$  und  $l$  bei dem Transport  $On$  stehen bleiben, gilt

$$P^{On} = P, \quad l^{On} = l,$$

und sonach

$$(lPl)^{On} = lPl,$$

d. h.  $P^l$  wird durch den Transport  $On$  in sich selbst transformiert, oder:

Satz 13.  $\Sigma$  wird durch Spiegelung um jede seiner Geraden in sich selbst transformiert.

Wir wollen nun den folgenden Satz beweisen:

Satz 14. In jedem Punkte einer Geraden in  $\Sigma$  kann eine und nur eine Senkrechte in  $\Sigma$  errichtet werden. Hierzu braucht man nur den Spezialfall zu betrachten, wo die in Rede stehende Gerade eine Normale  $r$  zu  $n$  in  $O$  ist, indem wir zeigen, dass wir eine und nur eine andere Normale  $s$  zu  $n$  in  $O$  auffinden können, welche senkrecht auf  $r$  steht. Die Normale  $r$  ist nun Kreuzgerade zu wenigstens einer der beiden Geraden  $p, q$ , z. B. zu  $p$ . Eine der Spiegelungsachsen



von  $p$  und  $r$  sei mit  $x$  bezeichnet. Spiegelt man  $q$  an  $x$ , erhält man die gesuchte Gerade  $S$ . Es gibt nur eine Lösung, weil  $q$  die einzige gemeinsame Normale von  $p$  und  $n$  ist.

Wir haben noch zu beweisen, dass man in  $\Sigma$  durch einen gegebenen Punkt  $P$  eine Senkrechte auf eine beliebig gegebene Gerade in  $\Sigma$  fällen kann, um danach feststellen zu können, dass  $\Sigma$  als eine Ebene im früher angegebenen Sinne bezeichnet werden muss. Wir wollen doch, schon bevor wir diesen Beweis bringen, Punktsysteme, die in ähnlicher Weise wie  $\Sigma$  als Ort der Normalen einer Geraden  $n$  in einem Punkte  $O$  von ihr erzeugt werden, Ebenen benennen, und im besonderen  $\Sigma$  als Normalebene von  $n$  in  $O$  bezeichnen. Ebenso bezeichnen wir  $n$  als Normale der Ebene  $\Sigma$  in  $O$ .

In jedem Punkte  $P$  von  $\Sigma$  gibt es eine und nur eine Normale zu  $\Sigma$ ; diese wird durch den Transport  $On$  um das Zentrum  $P$  in sich gespiegelt. Der Transport  $On$  soll deshalb als Spiegelung an der Ebene  $\Sigma$ , und mit demselben Buchstaben  $\Sigma$ , bezeichnet werden.

Durch jeden Punkt  $Q$  des Raumes kann eine und nur eine Normale zu  $\Sigma$  gezogen werden. Der Transport  $On$  führt nämlich  $Q$  in einen Punkt  $Q_1$  über, derart, dass der Mittelpunkt  $S$  von  $QQ_1$  in der Ebene  $\Sigma$  liegt. Die Normale von  $\Sigma$  in  $S$  sei mit  $s$  bezeichnet. Durch den Transport  $Ss$  geht nun  $Q_1$  in  $Q$  über; aber schon durch die Spiegelung  $S$  geht  $Q_1$  in  $Q$  über, und durch die Spiegelung  $s$  muss also  $Q$  stehen bleiben d. h.  $s$  geht durch  $Q$ . Dass nur eine Normale  $s$  existiert, folgt aus der Eindeutigkeit des Mittelpunktes  $S$ .

Satz 15. Durch jeden Punkt  $P$  des Raumes kann eine und nur eine Normalebene zu einer Geraden  $l$  gelegt werden.

Nach Voraussetzung geht nämlich durch  $P$  eine Normale  $n$  zu  $l$ ; sie schneidet  $l$  in einem Punkte  $Q$  und geht durch das Spiegelbild  $P_1$  von  $P$  bezüglich  $l$ .  $Q$  ist der Mittelpunkt von  $PP_1$  und ist also durch  $P$  und  $l$  eindeutig bestimmt. Die Normalebene  $\Sigma$  zu  $l$  in  $Q$  geht durch  $n$  und also auch durch  $P$ . Die Eindeutigkeit der Ebene folgt aus der Eindeutigkeit von  $Q$ .

Eine Ebene  $\Sigma_1$  soll senkrecht zu einer Ebene  $\Sigma$  heissen, wenn sie eine Normale  $n$  in einem Punkt  $O$  von  $\Sigma$  enthält. Die Normale  $n_1$  von  $\Sigma_1$  in  $O$  liegt dann auch in  $\Sigma$ . Die beiden Ebenen



enthalten die gemeinsame Normale  $s$  von  $n$  und  $n_1$  in  $O$ ; die Gerade  $s$  soll deshalb als Schnittlinie der Ebenen bezeichnet werden.

Die Ebenen haben keinen gemeinsamen Punkt ausserhalb  $s$ . Wäre nämlich ein solcher Punkt  $P$  vorhanden, so könnte man eine Verbindungsgerade von  $P$  nach  $O$  ziehen, einmal in  $\Sigma$  und ein andermal in  $\Sigma_1$ ; fielen diese Geraden zusammen, hätte man zwei gemeinsame Normalen zu  $n$  und  $n_1$  in  $O$ , was unmöglich ist; und fielen sie nicht zusammen, so wäre  $P$  Nachbarpunkt von  $O$ . In diesem Falle könnte man aber einen anderen Punkt,  $O_1$ , auf  $s$  statt  $O$  derart wählen, dass  $O, O_1$  Fernpunkte wären, und sodann in  $O_1$  zwei Normalen  $n'$  und  $n'_1$  zu den beiden Ebenen  $\Sigma$  und  $\Sigma_1$  errichten. Die vorhergehende Betrachtung betreffs des Systems  $snn_1OP$  liesse sich dann auf das neue System  $sn'n'_1O_1P$  anwenden, und wir sehen so, dass die Gerade  $PO_1$  mit  $s$  zusammenfallen muss, was unserer Annahme, dass  $P$  ausserhalb  $s$  liegen solle, widerspricht.

Wir gehen nun an den Beweis des früher angekündigten Satzes:

Satz 16. Wenn in einer Ebene  $\Sigma$  eine beliebige Gerade  $l$  und ein Punkt  $P$  ausserhalb  $l$  vorgegeben sind, so lässt sich immer in  $\Sigma$  eine Gerade  $g$  ziehen, welche durch  $P$  geht und zu  $l$  senkrecht ist.

Durch  $P$  geht nämlich eine Ebene  $\Sigma_1$  senkrecht zu  $l$ , und  $\Sigma_1$  schneidet dann  $\Sigma$  in der gesuchten Geraden. Wir fügen hinzu, dass die Ebene  $\Sigma_1$  eindeutig bestimmt ist, und dass die gesuchte Gerade  $g$  alsdann auch eindeutig bestimmt wird.

Wir haben somit den Beweis dafür erbracht, dass dasjenige Punktsystem  $\Sigma$ , welches wir in diesem Abschnitte schon als Ebene bezeichnet haben, wirklich alle die durch unsere Totalbeschreibung gegebenen Bedingungen erfüllt, um eine Ebene ( $R_2$ ) darzustellen.

Es folgt nun leicht der Satz:

Satz 17. Für jedes 3-Kreuz  $xyz$  gilt im  $R_3$  die Spiegelungsgleichung

$$xyz = 1.$$

Und ebenso leicht:

Satz 18. Ein Transport im  $R_3$ , welcher alle Punkte einer Ebene  $\Sigma$  stehen lässt, ist entweder die Identität oder eine Spiegelung an  $\Sigma$ .



Satz 19. Ein Transport im  $R_3$ , welcher alle Punkte einer Geraden  $a$  stehen lässt, ist entweder einer einzigen Spiegelung um eine Ebene durch  $a$ , oder der Aufeinanderfolge zweier Spiegelungen um Ebenen durch  $a$ , gleichwertig.

In letzterem Falle lässt sich die Bewegung auch durch die Aufeinanderfolge zweier Achsenspiegelungen, deren Achsen Normalen zu  $a$  in demselben Punkte von  $a$  sind, darstellen.

Satz 20. Die Aufeinanderfolge von drei Spiegelungen um Ebenen, welche durch dieselbe Gerade gehen, kann durch eine einzige Spiegelung um eine Ebene durch dieselbe Gerade ersetzt werden.

Satz 21. Die Aufeinanderfolge von drei Spiegelungen um Punkte derselben Geraden kann durch eine einzige Spiegelung um einen Punkt dieser Geraden ersetzt werden.

Satz 22. Die Aufeinanderfolge von drei Spiegelungen um Achsen, welche auf derselben Geraden senkrecht stehen, kann durch eine einzige Spiegelung um eine Achse, senkrecht auf derselben Geraden, ersetzt werden.

Eine Bewegung  $PQ$ , welche durch die Aufeinanderfolge von zwei Spiegelungen um zwei Punkte  $P, Q$  einer Geraden  $a$  bestimmt ist, soll als Schiebung längs  $a$  bezeichnet werden. Sie lässt alle Ebenen durch  $a$  fest stehen. Die Schiebung lässt sich auch durch die Aufeinanderfolge von zwei Spiegelungen um Normalebene  $\alpha$  und  $\beta$  von  $a$  in  $P$  und  $Q$  ersetzen. Man hat nämlich

$$aP = \alpha, \quad aQ = \beta,$$

also

$$PQ = \alpha\beta.$$

Eine Schiebung längs  $a$  zusammengesetzt mit einer Drehung um  $a$  (durch zwei Spiegelungen um Ebenen durch  $a$  oder zwei Spiegelungen um Normalen zu  $a$  dargestellt) ergibt eine Schraubung um  $a$ . Dieselbe kann durch die Aufeinanderfolge von zwei Spiegelungen um Normalen zu  $a$  dargestellt werden.

Zwei zueinander senkrechte Geraden bestimmen eine Ebene, welche die beiden Geraden enthält. Dasselbe lässt sich von

zwei beliebigen Kreuzgeraden aussagen, weil wir zur Bestimmung der Ebene die beiden Spiegelungsachsen der beiden Geraden wählen können. Wenn hingegen zwei Schmieggeraden  $l, m$  vorgelegt sind, dann lassen sich unendlich viele Ebenen durch die beiden Geraden legen. Um das nachzuweisen, wählen wir auf  $l$  einen Fernpunkt  $L$  zu einem gemeinsamen Punkt  $O$  der beiden Geraden. Durch  $L$  legen wir eine Ebene  $\lambda$  senkrecht zu  $m$ , welche  $m$  in  $M$  schneidet. Ferner werden  $L$  und  $l$  auf eine Ebene  $\alpha$  durch  $m$  in  $L_1$  und  $l_1$  projiziert. Die Geraden  $l, l_1, m$  sind benachbart, und aus Einl. III, 17 folgt dann, dass  $L, L_1$  sowie  $L_1, M$  also auch  $L, M$  benachbart sind.  $L$  und  $M$  haben somit in der Ebene  $\lambda$  unendlich viele Verbindungsgeraden, alle senkrecht zu  $m$  in  $M$ . Jede dieser Geraden bestimmt mit  $m$  zusammen eine Ebene, welche  $l$  und  $m$  enthält. Also:

Satz 23. Zwei Schmieggeraden  $l, m$  bestimmen ein Büschel von Schmiegebenen.

Jede Ebene senkrecht zu  $m$  (oder  $l$ ) schneidet aus diesem Büschel ein Element  $E$  aus, welches in allen Ebenen des Büschels enthalten ist. Durch Schiebung längs  $m$  beschreibt dieses Element einen Bereich, welcher allen Ebenen des Büschels angehört. Dieser Bereich soll als (ebener) Schmiegstreif und das erzeugende Element  $E$  als Breite des Streifs bezeichnet werden.

Zugleich ergibt sich, dass die beiden Schmieggeraden  $l, m$  eine Spiegelungsachse  $x$  haben, welche in allen Ebenen durch  $l, m$  enthalten ist, und ausserdem in jedem gemeinsamen Punkt ein Schmiegbüschel von Spiegelungsachsen, welche in der Normalebene zu  $x$  in diesem Punkt liegen. Dies lässt sich auch so ausdrücken:

Satz 24. Zwei Schmieggeraden  $l, m$  haben eine bestimmte Spiegelungsachse  $x$ , welche durch alle gemeinsamen Punkte der beiden Geraden hindurchgeht und in allen ihren gemeinsamen Ebenen liegt; ausserdem haben sie eine unendliche Reihe von Spiegelungsebenen, nämlich die Normalebene zu  $x$  in den gemeinsamen Punkten der beiden Geraden.

Satz 25. Zwei Ebenen, welche einen Punkt  $P$  gemein haben, haben entweder eine einzige Gerade oder einen Schmiegstreif gemein.



Die beiden Normalen in  $P$  sind nämlich entweder Kreuzlinien, und in diesem Falle haben sie eine eindeutig bestimmte gemeinsame Normale, welche die Schnittlinie der beiden Ebenen darstellt, oder sie sind Schmieggeraden, und in diesem Falle bestimmen sie ein Büschel von Schmiegeebenen, deren Normalen in  $P$  ein Büschel von Schmieggeraden ausmachen, welche alle in den beiden gegebenen Ebenen liegen.

Der Schmiegstreif ist ein Spezialfall allgemeinerer ebener Bereiche, welche wir als Schmiegebereiche bezeichnen wollen, d. h. Bereiche, welche die gemeinsamen Punkte von irgend einer Gesamtheit von Schmiegeebenen umfassen. Wenn z. B. drei Ebenen  $\alpha, \beta, \gamma$  vorliegen, welche je zwei und zwei Schmiegeebenen sind, und alle einen Punkt gemein haben, so bestimmen die Paare  $\beta\gamma, \gamma\alpha, \alpha\beta$  drei Schmiegstreife, welche einen Schmiegebereich gemein haben.

Die Schmiegebereiche können aber von sehr verschiedener Struktur sein. Einige der einfachsten, welche wir schon früher in anderem Zusammenhang (Einl. I S. 32) getroffen haben, sind solche, die bei einer Drehung um einen ihrer Punkte in sich selbst übergehen. Sie entstehen als Fixpunktmenge einer Bewegung  $ab$ , welche durch zwei Spiegelungen  $a, b$  in der Ebene erzeugt wird, wenn  $a$  und  $b$  Schmieggeraden sind (a. a. O.). Ein anderes Beispiel bildet die Menge der gemeinsamen Punkte aller Tangentenebenen eines Ovaloids, deren Berührungspunkte Nachbarpunkte eines bestimmten Punktes der Fläche sind.

Satz 26. Die Aufeinanderfolge von zwei Ebenenspiegelungen  $\alpha, \beta$  lässt sich durch eine andere,  $\alpha_1, \beta_1$ , ersetzen, wo  $\alpha_1$  (oder  $\beta_1$ ) durch einen vorgegebenen Punkt  $P$  geht.

Beweis. Durch  $P$  legen wir durch die beiden von  $P$  auf  $\alpha$  und  $\beta$  gefällten Normalen eine gemeinsame Normalebene  $\gamma$  von  $\alpha$  und  $\beta$ ; diese schneidet  $\alpha$  und  $\beta$  in zwei Geraden  $a, b$ . In der Ebene  $\gamma$  lassen sich nun zwei Geraden  $a_1, b_1$  derart bestimmen, dass  $a_1$  durch  $P$  geht, und  $a_1 b_1 = ab$  (I, 47). Die gesuchten Ebenen  $\alpha_1, \beta_1$  gehen dann durch  $a_1, b_1$  senkrecht zu  $\gamma$ .

Fallen die beiden Normalen durch  $P$  zusammen, ist die Sache besonders einfach: Die gemeinsame Normale ist dann auch Normale der beiden gesuchten Ebenen.



Unbestimmtheit trifft ein, wenn die beiden vorgegebenen Ebenen  $\alpha, \beta$  Nachbarebenen sind.

### § 5. Allgemeine Transporte im $R_3$ .

Es sei ein Transport im  $R_3$  vorgelegt, welcher einen Punkt  $O$  stehen lässt. Eine Punktreihe  $OP \dots$  auf einer Geraden  $p$  durch  $O$  gehe dabei in die Punktreihe  $OQ \dots$  auf der Geraden  $q$  über. Die beiden Punktreihen liegen in einer Ebene  $\alpha$ , welche nicht notwendig eindeutig bestimmt ist und haben in dieser die Spiegelsachse  $a$ . Durch  $a$  legen wir eine Ebene  $\alpha_1 \perp \alpha$ . Die Spiegelung  $\alpha_1$  führt nun die Reihe  $OP \dots$  in  $OQ \dots$  über, und der vorgelegte Transport kann somit durch diese Spiegelung und einen nachfolgenden Transport, welcher die Reihe  $OQ \dots$  stehen lässt, ersetzt werden. Letzterer Transport muss aber entweder einer Ebenenspiegelung  $\alpha_2$  oder der Aufeinanderfolge von zwei Spiegelungen  $\alpha, \beta$  gleichwertig sein. Der vorgelegte Transport lässt sich also entweder durch  $\alpha_1 \alpha_2$  oder durch  $\alpha_1 \alpha \beta = \alpha \beta$  ausdrücken, d. h. es gilt

Satz 27. Jeder Transport im  $R_3$ , welcher einen Punkt  $O$  stehen lässt, ist entweder durch zwei Ebenenspiegelungen  $\alpha_1, \alpha_2$  oder durch eine Achsenspiegelung  $a$  und eine Ebenenspiegelung  $\beta$  darstellbar.

Wenn im ersteren Falle  $\alpha_1$  und  $\alpha_2$  Kreuzebenen sind, ist die Bewegung eine Drehung um ihre Schnittlinie als Achse. Wenn hingegen  $\alpha_1$  und  $\alpha_2$  Schmiegebene sind, haben wir den Fall einer »Schmiegdrehung«, wo alle Punkte des gemeinsamen Schmiegestreifs der beiden Ebenen fest liegen. Aber nicht nur diese Punkte sind fest, alle Punkte des »Schmiegrohrs«, welches durch Drehung des Streifs um eine seiner Geraden entsteht müssen ebenfalls stehen bleiben.

Im letzteren Falle, wo der Transport durch  $\alpha \beta$  ausgedrückt wurde, können wir — wenn nicht schon  $a \perp \beta$ , in welchem Falle  $\alpha \beta = O$  — eine Vereinfachung der Darstellung einführen, indem wir eine Ebene  $\beta_1$  durch  $a$  senkrecht zu  $\beta$  legen und die Normale  $b$  in  $O \perp \beta_1$  errichten. Wenn nun die Schnittlinie  $\beta \beta_1$  mit  $a_1$  bezeichnet wird, lässt sich unser Transport durch des Symbol  $\alpha a_1 \beta_1$  ausdrücken, d. h. er kann durch eine Drehung  $\alpha a_1$  um die Achse  $b$  und eine Spiegelung um die Ebene  $\beta_1$  ersetzt



werden. Tritt der Sonderfall ein, dass  $\alpha$  und  $\alpha_1$  Schmieggeraden sind, so haben wir eine Schmiegdrehung  $\alpha\alpha_1$  und eine nachfolgende Spiegelung  $\beta_1$ . Die Fixpunkte unseres Transportes bilden dann einen Schmiegbereich in der Ebene  $\beta_1$ .

Satz 28. In allen Fällen gilt, dass ein Transport mit einem festen Punkt  $O$  durch 1, 2 oder 3 Ebenenspiegelungen, deren Spiegelungsebenen durch  $O$  gehen, ersetzt werden kann.

Ein Transport  $\alpha\beta\gamma\delta$ , welcher durch die Aufeinanderfolge von 4 Spiegelungen um 4 Ebenen  $\alpha, \beta, \gamma, \delta$  durch denselben Punkt  $O$  dargestellt ist, lässt sich immer auf 2 Ebenenspiegelungen reduzieren. Durch eine gemeinsame Gerade  $l$  von  $\alpha$  und  $\beta$  lässt sich nämlich immer eine Ebene  $\gamma_1$  derart legen, dass  $\gamma_1\gamma\delta$  einer Ebenenspiegelung  $\delta_1$  gleichwertig wird, d. h.

$$\alpha\beta\gamma\delta = \alpha\beta\gamma_1\delta_1.$$

Da aber  $\alpha, \beta, \gamma_1$  durch dieselbe Gerade  $l$  gehen, lässt sich hier  $\alpha\beta\gamma_1$  durch eine einzige Ebenenspiegelung  $\delta_2$  ausdrücken, d. h.

$$\alpha\beta\gamma\delta = \delta_2\delta_1.$$

Da ferner die Aufeinanderfolge von 3 Ebenenspiegelungen, deren Ebenen  $\alpha, \beta, \gamma$  durch  $O$  gehen, niemals die Identität darstellen kann (weil  $\alpha\beta\gamma$  sich immer auf die Form  $\alpha\beta_1$  abändern lässt), so folgt, dass alle Transporte mit festem Punkt  $O$  in zwei verschiedene Klassen fallen, eine, wo die Transporte sich auf 0 oder 2 Ebenenspiegelungen reduzieren lassen (die direkten Transporte, »Inbewegungen«) und eine andere, wo die Transporte sich auf 1 oder 3 Ebenenspiegelungen reduzieren lassen (die inversen Transporte, »Umbewegungen«).

Wir gehen nun daran, den allgemeinen Transport  $\tau$  in  $R_3$  zu untersuchen. Ein beliebiger Punkt  $A$  gehe durch  $\tau$  in  $A_1$  über. Der Transport lässt sich dann in eine Ebenenspiegelung  $\alpha$ , welche  $A$  nach  $A_1$  führt, und einen Transport  $\tau_1$  mit dem Fixpunkt  $A_1$  auflösen. Nach dem vorhergehenden Satz folgt dann sofort:

Satz 29. Jeder Transport im  $R_3$  lässt sich durch die Aufeinanderfolge von höchstens 4 Ebenenspiegelungen ersetzen.

Wir wollen nun den folgenden Satz beweisen:

Satz 30. Eine Folge von 5 Ebenenspiegelungen  $\alpha, \beta, \gamma, \delta, \varepsilon$  lässt sich immer auf 3 Ebenenspiegelungen reduzieren.

Zu dem Zweck wählen wir einen Punkt  $P$  in  $\alpha$  und ersetzen  $\beta\gamma$  durch  $\beta_1\gamma_1$ , wo  $\beta_1$  durch  $P$  geht (Satz 26). Das System  $\alpha\beta\gamma\delta\varepsilon$  wird so durch  $\alpha\beta_1\gamma_1\delta\varepsilon$  ersetzt, wo  $\alpha$  und  $\beta_1$  durch  $P$  gehen. In derselben Weise ersetzen wir nun  $\gamma_1\delta$  durch  $\gamma_2\delta_1$ , wo  $\gamma_2$  durch  $P$  geht. Und wir haben dann das ursprüngliche System in  $\alpha\beta_1\gamma_2\delta_1\varepsilon$  verwandelt, wo  $\alpha, \beta_1, \gamma_2$  durch  $P$  gehen. Schliesslich wird  $\delta_1\varepsilon$  durch  $\delta_2\varepsilon_1$  ersetzt, wo  $\delta_2$  durch  $P$  geht, und wir erhalten so statt der ursprünglichen Folge eine neue Folge  $\alpha\beta_1\gamma_2\delta_2\varepsilon_1$ , wo die 4 ersten Ebenen durch  $P$  gehen.

Den vorhergehenden Untersuchungen zufolge lassen sich nun diese 4 Ebenen durch zwei andere  $\xi, \eta$  ersetzen, und wir erhalten danach

$$\alpha\beta\gamma\delta\varepsilon = \xi\eta\varepsilon_1,$$

womit unser Satz bewiesen ist.

Es ergibt sich schliesslich hieraus, dass eine Folge von einer geraden Anzahl von Ebenenspiegelungen sich immer auf 4 (oder 2 oder 0) Ebenenspiegelungen reduzieren lässt; und ebenso, dass eine Folge von einer ungeraden Anzahl von Ebenenspiegelungen sich auf 3 (oder 1) Ebenenspiegelungen reduzieren lässt.

Ferner zeigt sich, dass eine Folge einer geraden Anzahl von Ebenenspiegelungen nie durch eine Folge einer ungeraden Anzahl von Ebenenspiegelungen ersetzt werden kann. Es müsste dann die Aufeinanderfolge von 3 Ebenenspiegelungen mit der Identität gleichwertig sein, was unmöglich ist.

Es zerfällt also die ganze Gruppe von Transporten im  $R_3$  in zwei verschiedene Klassen:

1°. Direkte Transporte (»In-Bewegungen«), welche durch eine gerade Anzahl Ebenenspiegelungen (4, 2, 0) dargestellt werden können, und

2°. Inverse Transporte (»Um-Bewegungen«), welche durch eine ungerade Anzahl Ebenenspiegelungen (3, 1) dargestellt werden können.

Wir wollen nun eine andere Reduktion des allgemeinen Transportes im  $R_3$  beschreiben.



Es gehe der Punkt  $A$  durch  $\tau$  in  $A_1$  über. Durch Wiederholungen des Transportes gehe  $A_1$  in  $A_2$  und  $A_2$  in  $A_3$  über, wobei wir voraussetzen wollen, dass  $A_1, A_2, A_3$  von  $A$  verschieden sind. (Die hierbei ausgeschlossenen Fälle werden immer Fixpunkte darbieten.)

Wir legen eine Gerade  $g$  durch  $A$  und  $A_1$  (eindeutig oder nicht). Diese Gerade wird durch  $\tau$  in eine Gerade  $g_1$  durch  $A_1$  und  $A_2$  übergeführt, welche durch  $\tau$  in eine Gerade  $g_2$  durch  $A_2$  und  $A_3$  weitergeführt wird. Wir legen ferner eine Ebene  $\alpha_1$  durch  $g$  und  $g_1$ . Diese wird durch  $\tau$  in eine Ebene  $\alpha_2$  durch  $g_1$  und  $g_2$  übergeführt.

In  $\alpha_1$  bestimmen wir die Spiegelungsachse  $a_1$  der beiden kongruenten Punktreihen  $A_1A \cdots$  und  $A_1A_2 \cdots$  auf den Geraden  $g$  und  $g_1$ . Die Achsenspiegelung  $a_1$  führt nun  $AA_1A_2$  in  $A_2A_1A$  über, und letzteres System lässt sich dann in  $A_1A_2A_3$  überführen durch eine weitere Achsenspiegelung  $a_2$ , deren Achse  $a_2$  durch den Mittelpunkt von  $A_1A_2$  geht, senkrecht auf der Geraden  $g_1$  steht und in einer Spiegelungsebene von  $\alpha_1$  und  $\alpha_2$  liegt, m. a. W. das System  $AA_1A_2gg_1\alpha_1$  geht durch die Transformation  $a_1a_2$  in  $A_1A_2A_3g_1g_2\alpha_2$  über. Hieraus folgt aber entweder

$$\tau = a_1a_2,$$

oder

$$\tau = a_1a_2\alpha_2 \text{ oder } \alpha_1a_1a_2.$$

Wählt man im letzteren Falle den Ausdruck  $\alpha_1a_1a_2$ , und ersetzt man dann  $\alpha_1a_1$  durch eine Spiegelung  $\alpha$ , deren Ebene durch  $a_1$  geht und senkrecht zu  $\alpha_1$  steht, hat man also das folgende Resultat:

Der allgemeine Transport  $\tau$  im  $R_3$  lässt sich durch die Aufeinanderfolge zweier Spiegelungen ersetzen, nämlich entweder zwei Achsenspiegelungen  $a_1, a_2$  oder eine Spiegelung  $\alpha$  und eine Achsenspiegelung  $a_2$ . Dass man im letzteren Falle auch die Achsenspiegelung  $a_1$  und eine nachfolgende Ebenenspiegelung  $\alpha'$  wählen kann, wo  $\alpha'$  die Spiegelungsebene von  $A_2A_1g_1$  und  $A_2A_3g_2$  ist, ist einleuchtend.

Da jede Achsenspiegelung durch zwei Ebenenspiegelungen (deren Ebenen durch die Achse gehen und senkrecht zueinander sind) ersetzt werden kann, kommen wir im Falle  $\tau = a_1a_2$  zu 4 Ebenenspiegelungen, und im Falle  $\tau = \alpha a_2$  zu 3. Also:

Satz 31. Jeder direkter Transport im  $R_3$  lässt sich auf zwei Achsenspiegelungen  $a_1, a_2$  zurückführen; jeder inverser Transport hingegen auf eine Ebenenspiegelung und eine Achsenspiegelung, oder umgekehrt.

Wir betrachten nun näher den ersteren Fall,  $\tau = a_1 a_2$ . Das Geradenpaar  $a_1, a_2$  kann nach den obigen Entwicklungen in mannigfacher Weise durch ein anderes Paar  $b_1, b_2$  ersetzt werden, wobei man verlangen kann, dass eine der Geraden, etwa  $b_1$ , durch einen gegebenen Punkt  $P$  gehen soll. Um das zu zeigen, bestimmen wir die Punkte

$$P_1 = P^{a_1 a_2}, \quad P_2 = P^{a_2 a_1}.$$

Die Spiegelungsachse von  $PP_1 \cdots$  und  $PP_2 \cdots$  liefert dann die gesuchte Gerade  $b_1$ , wobei wir jedoch der Eindeutigkeit halber voraussetzen müssen, dass  $P$  und  $P_1$  (oder  $P$  und  $P_2$ ) Fernpunkte sind, welche Bedingung immer erfüllt ist, wenn  $a_1$  und  $a_2$  nicht benachbart sind.

Gleichzeitig haben wir die Aufgabe gelöst, durch einen gegebenen Punkt  $P$  eine Gerade  $b_1$  zu ziehen, welche mit zwei gegebenen Geraden zusammen einen involutorischen Transport  $b_1 a_1 a_2$ , und zwar eine Achsenspiegelung darstellt.

Haben  $a_1, a_2$  eine gemeinsame Normale, so hat  $b_1$  (und  $b_2$ ) dieselbe Normale. Der Transport  $\tau = a_1 a_2$  ( $= b_1 b_2$ ) ist dann eine Schraubung um diese Normale, in Spezialfällen eine Drehung oder Schiebung.

## § 6. Die Geometrie des $R_n$ .

Für höhere Räume  $R_n$  ( $n > 3$ ) können wir genau dieselbe Methode wie für  $R_3$  benutzen.

Es liege im  $R_n$  ein  $n$ -Kreuz  $a_1 a_2 \cdots a_n$  mit dem Scheitel  $O$  vor, wo  $a_1$  die einzige gemeinsame Normale von  $a_2, \cdots, a_n$  ist. Durch Bewegungen lassen sich neue  $n$ -Kreuze aus dem gegebenen ableiten, und es lässt sich zeigen, dass alle  $n$ -Kreuze kongruent sind. Fassen wir in der Tat ein beliebiges  $n$ -Kreuz  $b_1 b_2 \cdots b_n$  in die Augen. Wir können gleich durch eine Punktspiegelung erzielen, dass sein Scheitel in  $O$  übergeht, und wir



denken uns deshalb das Kreuz schon in dieser Lage vorgelegt. Um dann  $b_1$  in  $a_1$  überzuführen, benützen wir eine Umwendung um eine Spiegelungsachse von  $a_1$  und  $b_1$ ; das setzt allerdings voraus, dass diese Geraden Kreuzgeraden sind, aber wenn sie Schmieggeraden wären, könnte man zuerst  $b_1$  in  $a_2$  überführen, und nachher weiter in  $a_1$ . Wir denken uns nun das Kreuz  $b_1 b_2 b_3 \cdots b_n$  schon in eine Lage gebracht, wo  $b_1 = a_1$ . Die Gerade  $b_2$  soll nun in  $a_2$  hinüber; das geschieht aber wieder durch eine Umwendung, nämlich um eine Spiegelungsachse von  $a_2$  und  $b_2$ ; bei dieser Umwendung bleibt  $b_1$  in  $a_1$  liegen, und wir haben nun eine Lage des  $b$ -Kreuzes, wo  $b_1 = a_1$ ,  $b_2 = a_2$ , erhalten. (Sollte  $a_2$  und  $b_2$  Schmieggeraden sein, führt man zuerst  $b_2$  in  $a_3$  über und dann weiter in  $a_2$ .) Dieser Vorgang lässt sich unmittelbar fortsetzen bis das Kreuz  $b_1 b_2 \cdots b_n$  schliesslich mit dem Kreuz  $a_1 a_2 \cdots a_n$  zur Deckung gebracht ist.

Wir wollen nun das System  $\Sigma$  aller Fixpunkte des Transportes  $Oa_1$  untersuchen. Unsere Betrachtungen sind den früheren ganz analog (§ 4). Das gesuchte System  $\Sigma$  ist der Ort der Normalen zu  $a_1$  in  $O$  und soll sonach als Normalraum von  $a_1$  in  $O$  bezeichnet werden. Es wird durch jeden seiner Punkte in sich selbst gespiegelt. Durch jeden Punkt  $P$  von  $\Sigma$  geht eine Normale zu  $\Sigma$ , d. h. eine Gerade, deren Normalen in  $P$  in  $\Sigma$  gelegen sind. Durch Spiegelung um eine beliebige seiner Geraden geht  $\Sigma$  in sich selbst über. Alles dies wird ganz wie die entsprechenden Tatsachen im  $R_3$  nachgewiesen.

Ebenso leicht ist es zu beweisen, dass in  $\Sigma$  in jedem Punkt einer Geraden  $g$  ein  $(n-2)$ -Kreuz von Normalen errichtet werden kann. Hierbei brauchen wir nur denjenigen Spezialfall zu betrachten, wo die in Rede stehende Gerade eine Normale  $r$  zu  $a_1$  in  $O$  ist, indem wir zeigen, dass sich ein  $(n-2)$ -Kreuz von gemeinsamen Normalen zu  $a_1$  und  $r$  in  $O$  bestimmen lässt. Das geht aber schon aus den eingangs angestellten Betrachtungen hervor.

Durch jeden Punkt  $P$  ausserhalb  $\Sigma$  kann eine und nur eine Normale zu  $\Sigma$  gezogen werden. Der Transport  $Oa_1$  führt nämlich  $P$  in einen neuen Punkt  $P_1$  über; im Mittelpunkt  $S$  von  $PP_1$  errichten wir eine Normale  $s$  zu  $\Sigma$ . Durch den Transport  $Ss$  geht nun  $P_1$  in  $P$  über; aber schon durch die Spiegelung  $S$  geht  $P_1$  in  $P$  über, und bei der Achsenspiegelung  $s$  muss also



$P$  stehen bleiben, d. h. die Gerade  $s$  geht durch  $P$ . Dass nur eine Normale von  $\Sigma$  durch  $P$  existiert, folgt aus der Eindeutigkeit des Mittelpunktes  $S$  und der Normalen  $s$ .

Durch jeden Punkt  $P$  ausserhalb einer vorgelegten Geraden  $g$  geht ein und nur ein Normalraum zu  $g$ . Nach Voraussetzung existiert nämlich eine Normale durch  $P$  zu  $g$ . Sie schneidet  $g$  in einem Punkt  $Q$ . Der Normalraum zu  $g$  in  $Q$  ist dann der gesuchte. Er ist eindeutig, weil  $Q$  eindeutig ist.

Die Normalräume  $\alpha_1, \alpha_2, \dots, \alpha_{n-1}$  der Geraden  $a_1, a_2, \dots, a_{n-1}$  des Kreuzes  $a_1 a_2 \dots a_n$  im Scheitel  $O$  haben die Gerade  $a_n$  und ausserhalb dieser keinen weiteren Punkt gemein. Durch jeden gemeinsamen Punkt  $P$  von  $\alpha_1, \alpha_2, \dots, \alpha_{n-1}$  lassen sich nämlich Senkrechten auf  $a_1, a_2, \dots, a_{n-1}$  mit demselben Fusspunkt  $O$  fällen. Sind  $O, P$  Fernpunkte, müssen also diese Senkrechten zusammenfallen, d. h. die Gerade  $OP$  fällt nach  $a_n$ . Sollten hingegen  $O, P$  Nachbarpunkte sein, so könnte man auf  $a_n$  einen neuen Punkt  $O_1$  statt  $O$  derart wählen, dass  $O_1, P$  Fernpunkte wären, und in  $O_1$  könnten dann Normalen  $a'_1, a'_2, \dots, a'_{n-1}$  auf  $\alpha_1, \alpha_2, \dots, \alpha_{n-1}$  errichtet werden, wonach wir durch Wiederholung unserer Betrachtung für das neue System sofort schliessen, dass die Gerade  $O_1 P$  mit  $a_n$  zusammenfallen muss.

In ähnlicher Weise untersuchen wir den gemeinsamen Raum der  $n-2$  Normalräume  $\alpha_1, \alpha_2, \dots, \alpha_{n-2}$  zu  $a_1, a_2, \dots, a_{n-2}$  in  $O$ . Es zeigt sich hier ganz analog, dass dieser Raum aus allen den gemeinsamen Normalen zu  $a_1, a_2, \dots, a_{n-2}$  besteht. Und ebenso leicht erhält man das allgemeine Resultat, dass der gemeinsame Raum von den  $r$  Normalräumen zu  $a_1, a_2, \dots, a_r$ , in  $O$  aus allen gemeinsamen Normalen zu  $a_1, a_2, \dots, a_r$  besteht. Der so bestimmte Raum soll als Normalraum des Kreuzes  $a_1 a_2 \dots a_r$  bezeichnet werden. Er enthält das reziproke Kreuz  $a_{r+1} a_{r+2} \dots a_n$  und soll auch  $\Sigma$ -Raum dieses Kreuzes (in Zeichen:  $\Sigma(a_{r+1} a_{r+2} \dots a_n)$ ) genannt werden. Umgekehrt wird dann natürlich der  $\Sigma$ -Raum von  $a_1 a_2 \dots a_r$  den Normalraum des Kreuzes  $a_{r+1} a_{r+2} \dots a_n$  bedeuten.

Es soll nun bewiesen werden, dass der  $\Sigma$ -Raum eines  $r$ -Kreuzes ein  $r$ -dimensionaler Raum ist. Die vorhergehenden Untersuchungen haben die meisten hierzu nötigen Grundelemente zu Wege gebracht. Es fehlt nur noch zu beweisen, dass in einem  $\Sigma$ -Raum eines jeden  $r$ -Kreuzes der Satz gültig ist, dass von jedem



Punkt  $P$  ausserhalb einer Geraden  $g$  eine Senkrechte auf  $g$  gefällt werden kann. Das haben wir schon früher (Satz 16) für den Fall  $n = 3$ ,  $r = 2$ , bewiesen. Unser Beweis lässt sich aber unmittelbar für ein beliebiges  $n$  und  $r = 2$  verallgemeinern. Und für allgemeine Werte von  $n$  und  $r$  können wir analog vorgehen:

Es sei in  $\Sigma(a_1 a_2 \cdots a_r)$  ein beliebiger Punkt  $P$  vorgelegt, von welchem eine Senkrechte auf  $a_1$  in  $\Sigma$  gefällt werden soll. Wir wissen, dass im Totalraum  $R_n$  jedenfalls eine Senkrechte  $PQ$  mit eindeutigem Fusspunkt  $Q$  auf  $a_1$  gefällt werden kann. In  $Q$  errichten wir einen Normalraum zu  $\Sigma$  und schneiden ihn mit dem Normalraum zu  $a_1$  in  $Q$ . Der Schnittraum ist ein  $\Sigma$ -Raum  $\omega$ , welcher durch  $(r-1)$  zu einander senkrechte Normalen zu  $a_1$  im Punkte  $Q$  bestimmt ist. Dieser Schnittraum enthält so eine Gerade, welcher  $P$  mit  $Q$  verbindet, und diese Gerade ist das gesuchte Lot von  $P$  auf  $a_1$ .

Wir resumieren:

Im  $R_n$  bestimmt jedes  $r$ -Kreuz  $a_1 a_2 \cdots a_r$ ,  $1 < r < n$ , einen Raum von  $r$  Dimensionen  $\Sigma$ , welcher das Kreuz enthält.

Alle Normalen des Kreuzes bestimmen einen Raum  $\Sigma'$  von  $n-r$  Dimensionen, den Normalraum des Kreuzes oder des Raumes  $\Sigma$  im Scheitel  $O$ . Die beiden Räume  $\Sigma, \Sigma'$  sind Normalräume (reziproke Räume) zueinander in  $O$ . Sie haben nur den Punkt  $O$  gemein.

In jedem Punkt von  $\Sigma$  lässt sich ein Normalraum von  $n-r$  Dimensionen errichten. Längs einer geraden Linie  $g$  in  $\Sigma$  erzeugen sonach die Normalräume zu  $\Sigma$  einen Raum von  $n-r+1$  Dimensionen, senkrecht zu  $\Sigma$  längs  $g$ . Und allgemeiner: Längs eines Raumes von  $p$  Dimensionen in  $\Sigma$  bilden die Normalräume zu  $\Sigma$  einen Raum von  $n-r+p$  Dimensionen, senkrecht zu  $\Sigma$ .

Durch jeden Punkt ausserhalb  $\Sigma$  geht eine Normale zu  $\Sigma$ .

Irgend zwei Punkte  $P, Q$  von  $\Sigma$  lassen sich durch eine gerade Linie, welche ganz in  $\Sigma$  enthalten ist, verbinden. Es folgt hieraus sofort, dass irgend zwei Punkte  $P, Q$  in  $R_n$  ( $n > 2$ ) mindestens eine Verbindungsgerade haben.

Wenn zwei Geraden einen Punkt gemein haben, gibt es mindestens eine Ebene, welche die beiden Geraden enthält. Dies wurde schon (S. 17) für den  $R_3$  bewiesen, und der Beweis ist für höhere Räume ganz analog. Der Satz lässt sich in folgender Weise verallgemeinern:

Satz 32. Wenn  $r$  Geraden  $g_1, g_2, \dots, g_r$  durch ein und denselben Punkt  $O$  gehen, so gibt es wenigstens einen Raum von  $r$  Dimensionen, welcher die Geraden enthält.

Für ein Geradensystem, welches ein  $r$ -Kreuz bildet, ist die Sache schon erledigt. In diesem Falle gibt es einen und nur einen Raum  $R_r$ , welcher die Geraden enthält. In den anderen Fällen lässt sich das Geradensystem »orthogonalisieren«, d. h. wir können es durch ein anderes System, welches ein  $r$ -Kreuz bildet, ersetzen. Dies wird in folgender Weise ausgeführt:

Durch  $g_1$  legen wir ein System von Ebenen  $g_1g_2, g_1g_3, \dots, g_1g_r$ , welche  $g_2, g_3, \dots, g_r$  enthalten. In diesen Ebenen bestimmen wir nun diejenigen Geraden  $g'_2, g'_3, \dots, g'_r$ , welche senkrecht auf  $g_1$  in  $O$  stehen. Das gegebene System wird dann zunächst durch  $g_1, g'_2, g'_3, \dots, g'_r$  ersetzt.

Danach legen wir ein neues System von Ebenen  $g'_2g'_3, g'_2g'_4, \dots, g'_2g'_r$ , welche senkrecht auf  $g_1$  stehen, und in diesen Ebenen errichten wir die Normalen  $g''_3, g''_4, \dots, g''_r$  zu  $g'_2$  in  $O$ . Hierdurch erhalten wir ein drittes Geradensystem

$$g_1g'_2g''_3g''_4 \dots g''_r,$$

wo die 3 ersten ein 3-Kreuz bilden.

Auf diese Weise gehen wir nun weiter. Das nächste Mal erhalten wir so ein System

$$g_1g'_2g''_3g'''_4 \dots g'''_r,$$

wo die ersten 4 Geraden ein 4-Kreuz bilden. Und schliesslich erhalten wir ein  $r$ -Kreuz

$$g_1g'_2g''_3 \dots g^{(r-1)}_r,$$

und der gesuchte Raum wird dann durch dieses Kreuz bestimmt.

Treten Zusammenfälle der entstehenden Geraden ein, so kann man das orthogonalisierte System mit entsprechend kleinerer Dimensionenzahl bilden, und das vorgelegte Geradensystem ist dann in einem Raum, dessen Dimensionenzahl  $< r$  ist, enthalten.

Es folgt nun ferner:



Satz 33. Durch ein System von  $r+1$  Punkten im  $R_n$ ,  $r < n$ , kann mindestens ein Raum  $R_r$  gelegt werden. Wenn nur ein Raum existiert, sollen die Punkte als freie Punkte (freies System von Punkten) bezeichnet werden.

In einem freien System von  $r+1$  Punkten haben je zwei Punkte eine eindeutige Verbindungsgerade, je 3 Punkte eine eindeutige Verbindungsebene, je 4 Punkte einen eindeutigen Verbindungsraum von 3 Dimensionen, u. s. w.

In ähnlicher Weise spricht man von einem freien System von  $r$  Geraden durch einen Punkt  $O$  ( $r$  freien Geraden durch  $O$ ), wenn die Geraden einen  $R_r$  eindeutig bestimmen.

### § 7. Involutorische Transporte im $R_n$ .

Satz 34. Wenn bei einem Transport alle Punkte der Geraden eines  $r$ -Kreuzes  $a_1a_2 \cdots a_r$  fest liegen, so liegen alle Punkte des Raumes  $\Sigma(a_1a_2 \cdots a_r)$  fest.

Der Satz ist schon im Falle  $r = 2$  bewiesen worden (Satz 3), und für höhere Werte von  $r$  lässt er sich durch Induktion beweisen. Erstens im Falle  $r = 3$ : Von einem beliebigen Punkt  $P$  fallen wir die Normalen  $PP_1, PP_2, PP_3$  auf die Ebenen  $a_2a_3, a_3a_1, a_1a_2$ . Die Fusspunkte  $P_1, P_2, P_3$  liegen dann fest, also auch die Normalen selbst, und wenn  $P$  der einzige gemeinsame Punkt dieser Normalen ist, so liegt auch  $P$  fest. Aber auch in dem Falle, wo die Normalen Nachbargeraden sind, liegt  $P$  fest; sollte nämlich  $P$  durch den vorgelegten Transport in einen andern Punkt  $Q$  übergehen, so wäre  $Q$  das Spiegelbild von  $P$  bezüglich jeder der Ebenen  $a_2a_3, a_3a_1, a_1a_2$ .  $P_1, P_2, P_3$  müssten dann alle im Mittelpunkt von  $PQ$  fallen, was ausgeschlossen ist.

Wie man nun zu höheren Werten von  $r$  weiter geht, ist klar.

Ist  $r$  eine ungerade Zahl, so lässt der Transport  $a_1a_2 \cdots a_r$  alle Punkte der Geraden des Kreuzes stehen, d. h. alle Punkte des Raumes  $\Sigma(a_1a_2 \cdots a_r)$  sind Fixpunkte dieses Transports. Jede Normale des Kreuzes wird hingegen durch den Scheitel  $O$  des Kreuzes und jede Normale des Raumes  $\Sigma$  durch ihren Fusspunkt in sich gespiegelt. Der Transport soll als Spiegelung um  $\Sigma$  bezeichnet werden.

Ist  $r$  hingegen eine gerade Zahl, so lässt der Transport  $a_1a_2 \cdots a_r$  alle Punkte im Normalraum  $\Sigma'$  des Kreuzes  $a_1a_2 \cdots a_r$ ,

fest stehen, während der Raum  $\Sigma$  durch  $O$  in sich gespiegelt wird. Der Transport ist dann eine Spiegelung um den Normalraum  $\Sigma'$  von  $\Sigma$ . Also:

Satz 35. Die Spiegelung um  $\Sigma$  ( $a_1 a_2 \cdots a_r$ ) lässt sich entweder durch die Transformation  $O a_1 a_2 \cdots a_r$  oder  $a_1 a_2 \cdots a_r$  darstellen, je nachdem  $r$  gerade oder ungerade ist.

Für den Totalraum  $R_n$  bedeutet  $a_1 a_2 \cdots a_n$ , wenn  $n$  ungerade ist, die Identität, und wenn  $n$  gerade ist, die Punktspiegelung  $O$ .

Indem wir die Spiegelungen um  $\Sigma$  und  $\Sigma'$  mit denselben Buchstaben bezeichnen wie die Räume selbst, können wir schreiben:

$$\Sigma = O^{r-1} a_1 a_2 \cdots a_r, \quad \Sigma' = O^{n-r-1} a_{r+1} a_{r+2} \cdots a_n.$$

Es folgt hieraus

$$\Sigma \Sigma' = O^n a_1 a_2 \cdots a_n = O,$$

oder

$$\Sigma' = O \Sigma.$$

Satz 36. Ausser der Identität sind die Spiegelungen (um einen Punkt, eine Achse, eine Ebene u. s. w., um einen  $R_r$ ) die einzigen involutorischen Transporte. Der Beweis wird durch Induktion geführt. In der Ebene und im  $R_3$  ist die Sache klar: für  $R_n$  brauchen wir so nur den Satz zu beweisen unter der Voraussetzung, dass der Satz schon für  $R_{n-1}$  gültig ist. Es sei nun  $\tau$  ein beliebiger involutorischer Transport in  $R_n$ , wobei ein Punkt  $A$  in einen anderen Punkt  $A_1$  übergeht. Der Mittelpunkt  $O$  von  $AA_1$  wird dann stehen bleiben. Von  $O$  aus wählen wir zwei einander entsprechende, nicht zusammenfallende Punkt-reihen  $OP \cdots$  und  $OP_1 \cdots$ . Wenn die Träger nun Kreuzgeraden sind, haben die beiden Reihen eine eindeutig bestimmte Spiegelungs-achse  $a_1$ ; wenn sie Nachbargeraden sind, und einander entsprechende Punkte Nachbarpunkte oder zusammenfallend sind, so haben die Reihen auch eine eindeutig bestimmte Spiegelungsachse  $a_1$ . Wenn die beiden Reihen hingegen eine solche Lage haben, dass die Spiegelung  $O$  die eine Reihe in eine Nachbarreihe der anderen überführt, so fügen wir die Spiegelung  $O$  zu dem vor-



gelegten Transport  $\tau$  hinzu und fassen sodann statt  $\tau$  den neuen involutorischen Transport  $O\tau$  ins Auge, um unsere Untersuchungen auf den vorigen Fall zurückführen zu können.

Die Achse  $a_1$  steht punktweise fest. Eine Hyperebene (Raum von  $n-1$  Dimensionen)  $\alpha$  durch  $O$  senkrecht zu  $a_1$  wird nun durch  $\tau$  bzw.  $O\tau$  in sich selbst übergeführt, wobei  $O$  ein fester Punkt ist. Der Transport in  $\alpha$  ist nach Voraussetzung eine Spiegelung  $\sigma$ . Es folgt aber hieraus, dass  $\tau$  bzw.  $O\tau$  mit dem Transport  $\alpha\sigma$  gleichwertig ist. Dieser Transport ist aber einer Spiegelung um den reziproken Raum  $\sigma'$  von  $\sigma$  in  $\alpha$  gleichwertig, d. h.

$$\tau \text{ oder } O\tau = \sigma',$$

also entweder  $\tau = \sigma'$  oder  $\tau = O\sigma' = \sigma''$ , wo  $\sigma''$  den reziproken Raum zu  $\sigma'$  im vorgelegten Raum  $R_n$  bedeutet. Und hiermit ist unser Beweis zu Ende gebracht.

Soll das Produkt  $\alpha\beta$  zweier involutorischer Transporte  $\alpha, \beta$  wieder ein involutorischer Transport sein, also  $\alpha\beta = \beta\alpha$ , ist hierzu notwendig und hinreichend, dass einer der beiden Räume durch Spiegelung um den anderen in sich selbst übergeht. Es können dann zwei Fälle vorkommen:

1°. Der eine Raum ist in dem anderen ganz enthalten;

2°. Die beiden Räume sind senkrecht zueinander, d. h. jeder von ihnen ist der Ort von Normalen des anderen, welche dem Sammelraum  $S(\alpha, \beta)$  angehören.

Ist insbesondere  $\alpha$  ein Punkt  $O$ , so muss dieser Punkt in  $\beta$  enthalten sein; das Produkt  $\alpha\beta$  wird dann der Spiegelung um den Normalraum zu  $\beta$  in  $O$  gleichwertig.

Ist  $\alpha$  eine Gerade,  $\beta$  eine Ebene, welche  $\alpha$  enthält, und ist der Totalraum von 3 Dimensionen, so ist das Produkt  $\alpha\beta$  eine Spiegelung um eine Ebene, welche senkrecht auf  $\beta$  längs  $\alpha$  steht. Ist der Totalraum  $R_n$ ,  $n > 3$ , so wird  $\alpha\beta$  eine Spiegelung um einen  $R_{n-1}$  darstellen, welcher längs  $\alpha$  senkrecht auf  $\beta$  steht.

Als weiteres Beispiel verweisen wir auf die früher besprochenen reziproken Räume  $\Sigma, \Sigma'$  mit dem gemeinsamen Punkt  $O$ . Hier gilt, wie wir gesehen haben,  $\Sigma\Sigma' = O$ , wenn Sammelraum und Totalraum identisch sind. Ist dies nicht der Fall, müssen wir aber schreiben:

$$\Sigma\Sigma' = OS(\Sigma, \Sigma'),$$

wo  $S(\Sigma, \Sigma')$  den Sammelraum bezeichnet.

Satz 37. Im Allgemeinen gilt, dass ein involutorisches Produkt  $\alpha\beta$  von zwei Spiegelungen  $\alpha, \beta$  eine Spiegelung darstellen muss, deren Spiegelungsraum als Normalraum des Sammelraumes  $S(\alpha, \beta)$  längs des Durchschnittsraums  $D(\alpha, \beta)$  bestimmt werden kann.

Wenn im besonderen der Sammelraum mit dem Totalraum zusammenfällt, so fällt der Spiegelungsraum mit dem Schnittraum zusammen. Einfache Beispiele hat man, wenn  $\alpha, \beta$  zwei zueinander senkrechte Ebenen sind, welche eine Gerade gemein haben und in einem  $R_n$  liegen; oder wenn  $\alpha$  eine Ebene,  $\beta$  ein  $R_3$  und  $D(\alpha, \beta)$  eine Gerade, und der Totalraum  $R_n$  ist,  $n > 3$ .

Satz 38. Die Aufeinanderfolge von drei Achsen Spiegelungen, deren Achsen  $a, b, c$  in ein und derselben Ebene  $\alpha$  liegen und durch ein und denselben Punkt  $O$  gehen, lässt sich durch eine einzige Achsen Spiegelung ersetzen, deren Achse  $d$  durch  $O$  geht und in der Ebene  $\alpha$  liegt.

Beweis. In der Ebene  $\alpha$  bestimmen wir eine Spiegelungsachse  $x$  der beiden Geraden  $a, c$ , und die Gerade  $d$  wird dann von  $b$  durch Spiegelung um  $x$  abgeleitet. Aus der Geometrie der Ebene wissen wir nämlich zunächst, dass alle Punkte in  $\alpha$  bei dem Transporte  $abcd$  Fixpunkte sind. Da ferner alle Normalen zu  $\alpha$  im Punkte  $O$  durch denselben Transport 4 mal in sich gespiegelt werden, und somit punktweise stehen bleiben, so folgt, dass der ganze Raum  $R_n$  punktweise fest bleibt. Und hiermit ist der Satz bewiesen.

Satz 39. Die Aufeinanderfolge von 4 Achsenspiegelungen, deren Achsen  $a, b, c, d$  in ein und demselben  $R_3$  liegen und durch ein und denselben Punkt  $O$  gehen, lässt sich durch eine Folge von 2 Achsenspiegelungen, deren Achsen durch  $O$  gehen und demselben  $R_3$  angehören, ersetzen.

Beweis. Wir legen zwei Ebenen, eine durch  $a, b$ , eine andere durch  $c, d$ , und bestimmen (bezw. wählen) eine gemeinsame Gerade  $e$  dieser Ebenen. Dem vorigen Satz zufolge können wir dann schreiben

$$abe = p, \quad ecd = q,$$

wo  $p, q$  zwei Geraden in den beiden Ebenen sind. Es folgt dann

$$abcd = (abe)(ecd) = pq.$$



Auf dieselbe Weise gehen wir weiter:

Satz 40. Die Aufeinanderfolge von 5 Achsenspiegelungen, deren Achsen  $a, b, c, d, e$  in einem  $R_4$  liegen und durch denselben Punkt  $O$  gehen, kann durch eine Folge von 3 Achsenspiegelungen, deren Achsen durch  $O$  gehen und in demselben  $R_4$  liegen, ersetzt werden.

Beweis. Ein 3-Raum  $abc$  und eine Ebene  $de$  haben eine gemeinsame Gerade  $f$  (eindeutig oder nicht), und den vorhergehenden Sätzen zufolge können wir dann schreiben:

$$abcf = pq, \quad fde = r,$$

wo  $p, q$  Achsen im 3-Raum  $abc$ , und  $r$  eine Achse in der Ebene  $de$  bedeuten. Hieraus folgt aber

$$abcde = (abcf)(fde) = pqr.$$

Durch Induktion erhalten wir schliesslich den Satz:

Satz 41. Die Aufeinanderfolge von  $s+1$  Achsenspiegelungen, deren Achsen in einem  $R_s$  liegen und durch einen Punkt  $O$  gehen, lässt sich durch eine Folge von  $s-1$  Achsenspiegelungen, deren Achsen durch  $O$  gehen und in demselben  $R_s$  liegen, ersetzen.

Und hieraus folgt unmittelbar:

Satz 42. Die Aufeinanderfolge von  $s$  Achsenspiegelungen, deren Achsen  $a_1, a_2, \dots, a_s$ , in einem vorgegebenen  $R_s$  liegen und durch denselben Punkt  $O$  gehen, lässt sich in diesem  $R_s$  durch eine andere Folge von  $s$  Achsenspiegelungen  $b_1, b_2, \dots, b_s$  ersetzen, wobei die erste Achse  $b_1$  beliebig durch  $O$  gewählt werden kann.

Wir können nämlich schreiben:

$$b_1 a_1 a_2 \dots a_s = b_2 b_3 \dots b_s,$$

wo  $b_2$  in einem gewissen Raum  $R_{s-1}$  frei durch  $O$  gewählt werden kann, und nach dieser Wahl  $b_3$  in einem gewissen Raum  $R_{s-2}$  frei durch  $O$  gewählt werden kann, u. s. w.

Wir möchten nun die folgende Frage untersuchen: Wann können  $s$  Achsenspiegelungen, deren Achsen  $a_1, a_2, \dots, a_s$  durch denselben Punkt  $O$  gehen und ein freies System bilden, einander aufheben?

Zunächst ersieht man, dass die Achsen notwendig paarweise auf einander senkrecht stehen müssen. Da nämlich z. B.  $a_1 = a_2 a_3 \cdots a_s$ , und dieser Transport den Raum  $a_2 \cdots a_s$  stehen lässt, so muss dieser Raum senkrecht zu  $a_1$  stehen, d. h. alle Geraden  $a_2, a_3, \cdots a_s$  sind senkrecht zu  $a_1$ . Auf diese Weise ergibt sich, dass jede der Geraden senkrecht zu den anderen steht. Diese Bedingung ist aber nicht hinreichend. Es wurde nämlich früher gezeigt, dass innerhalb des durch das  $s$ -Kreuz  $a_1 a_2 \cdots a_s$  bestimmten  $R_s$ , wenn  $s$  eine gerade Zahl ist,  $a_1 a_2 \cdots a_s = \dot{O}$ , und wenn  $s$  ungerade ist,  $a_1 a_2 \cdots a_s = 1$ . Und wir haben so die Antwort auf unsere Frage gefunden:

Satz 43. Die Achsenspiegelungen  $a_1, a_2, \cdots, a_s$ , deren Achsen ein freies Geradensystem durch denselben Punkt  $O$  bilden, können dann und nur dann einander aufheben, wenn die Achsen ein  $s$ -Kreuz bilden, und  $s$  eine ungerade Zahl ist, wozu noch die Bedingung hinzuzufügen ist, dass der Transportraum mit dem durch das Geradensystem bestimmten  $R_s$  identisch ist.

Es folgt nun hieraus, dass in einem Raum  $R_n$  von gerader Dimensionenzahl  $n-1$  Achsenspiegelungen durch denselben Punkt einander nie aufheben können.

Bilden die Achsen ein freies System, folgt diese Tatsache direkt aus dem vorigen Satz; und liegen sie in einem  $R_{n-2}$ , kann ihre Anzahl nach dem Reduktionssatz zu  $n-3$  herabgesetzt werden, und wir haben dann nur eine Wiederholung der ursprünglichen Aufgabe für eine kleinere Dimensionenzahl. Gehen wir auf diese Weise weiter, so kommen wir schliesslich zu dem Falle  $n = 2$ , und dann ist die Sache einleuchtend.

Einige Bemerkungen über Punktspiegelungen sollen hier hinzugefügt werden. Zwei Punktspiegelungen  $O, P$  erzeugen eine Transformation  $OP$ , welche jede Ebene durch  $O$  und  $P$  stehen lässt (Schiebung längs einer Geraden  $OP$ ). Zwei Normalen  $o, p$  der Geraden  $OP$  in  $O$  und  $P$  und in ein und derselben Ebene  $\varepsilon$  gelegen bestimmen zwei Spiegelungen, deren Produkt  $op$  innerhalb der Ebene gleich dem Produkt  $OP$  ist. Dieselbe Transformationsgleichung

$$op = OP$$

besteht aber auch im Totalraum  $R_n$ . Es gilt nämlich zunächst:



$$Pp = Oo,$$

weil beide Transformationen  $Pp$  und  $Oo$  eine Spiegelung um einen Hyperraum  $\perp p$  in  $P$  und  $\perp o$  in  $O$  darstellen. Hieraus folgt nun sofort  $op = OP$ , w. z. b. w.

Eine Folge von zwei Punktspiegelungen kann demnach immer durch eine Folge von zwei Achsenspiegelungen ersetzt werden. Ferner lässt sich jede Transformation  $aP$  immer auf die Form  $Qb$  bringen, indem man ein Lot  $PQ$  auf  $\alpha$  fällt und dann auf der Normalhyperebene von  $a$  durch  $P$  eine Normale  $b$  in  $P$  errichten kann. Es folgt dann  $bP = Qa$ , und also gerade  $Qb = aP$ . Es gilt also:

**Satz 44.** Jede Folge von Punkt- und Achsenspiegelungen lässt sich immer so umschreiben, dass höchstens eine Punktspiegelung (als erstes oder letztes Glied der Folge) auftritt.

### § 8. Transporte im $R_n$ mit einem Fixpunkt.

Im  $R_n$  seien zwei  $n$ -Kreuzen mit demselben Scheitel  $O$ ,  $a_1 a_2 \cdots a_n$  und  $b_1 b_2 \cdots b_n$ , vorgegeben. Wir wollen denjenigen Transport bestimmen, welcher das erste Kreuz in das andere überführt, derart, dass auf entsprechenden Geraden,  $a_1$  und  $b_1$ ,  $a_2$  und  $b_2$ ,  $\cdots$ ,  $a_n$  und  $b_n$ , vorgeschriebene von  $O$  ausgehende kongruente Punktreihen:  $OA_1 \cdots$  und  $OB_1 \cdots$ ,  $OA_2 \cdots$  und  $OB_2 \cdots$ ,  $\cdots$ ,  $OA_n \cdots$  und  $OB_n \cdots$ , in einander übergehen. Wir denken uns also kongruente Punktepaare  $OA_1$  und  $OB_1$ ,  $OA_2$  und  $OB_2$ , u. s. w. auf die Geraden abgetragen, und wir bezeichnen die zu  $A_i, B_i$  durch die Punktspiegelung  $O$  entsprechenden Punkte mit  $\overline{A}_i, \overline{B}_i$ . Der Bequemlichkeit halber soll dabei vorausgesetzt werden, dass  $O$  und  $A_i$  (und somit  $O$  und  $B_i$ ,  $O$  und  $\overline{A}_i$ ,  $O$  und  $\overline{B}_i$ ) Fernpunkte sind.

Durch eine erste Spiegelung  $x_1$  um die Spiegelungsachse  $x_1$  der beiden Reihen  $OA_1 \cdots$  und  $OB_1 \cdots$  führen wir das System  $O(A_1 A_2 \cdots A_n)$  in  $O(B_1 A'_2 \cdots A'_n)$  über. Wir bestimmen danach eine zweite Spiegelung  $x_2$  derart, dass  $OA'_2$  in  $\overline{OB}_2$  übergeht, wonach der Transport  $Ox_2$  unser System  $O(B_1 A'_2 \cdots A'_n)$  in eine neue Lage  $O(B_1 B_2 A''_3 \cdots A''_n)$  überführt. Wenn nun ferner die Spiegelung  $x_3$  das Paar  $OA''_3$  in  $\overline{OB}_3$  überführt, so wird der Trans-

port  $Ox_3$  das System  $O(B_1B_2A_3'' \cdots A_n'')$  in das neue System  $O(B_1B_2B_3A_4''' \cdots A_n''')$  überführen.

Auf diese Weise kommt man nach den Transporten

$$x_1, Ox_2, Ox_3, \dots, Ox_{n-1}$$

von dem ursprünglichen System  $O(A_1A_2 \cdots A_n)$  zum System  $O(B_1B_2 \cdots B_{n-1}B_n)$  oder  $O(B_1B_2 \cdots B_{n-1}B_n)$  d. h. man kommt von dem ersten gegebenen Kreuz zum anderen hinüber mittels eines der beiden Transporte

$$O^n x_1 x_2 \cdots x_{n-1}, \quad O^{n+1} x_1 x_2 \cdots x_n,$$

wobei  $x_n' = b_n$ .

Diese Darstellung kann noch ein wenig vereinfacht werden, indem wir jeden der beiden Fälle,  $n$  gerade oder ungerade, für sich behandeln:

1°.  $n$  gerade. Die beiden Resultate können dann so geschrieben werden:

$$x_1 x_2 \cdots x_{n-1}, \quad Ox_1 x_2 \cdots x_n.$$

Der letztere Ausdruck lässt sich aber (Satz 35) so schreiben:  $a_1 a_2 \cdots a_n x_1 x_2 \cdots x_n$ , also als eine Folge von  $2n$  Achsenspiegelungen. Nach dem Reduktionssatz (Satz 41) lässt sich aber diese Folge zu einer Folge von  $n$  Achsenspiegelungen abkürzen. Es gilt also der Satz:

Satz 45. In einem Raum  $R_n$  mit gerader Dimensionenzahl lässt sich jeder Transport mit dem Fixpunkt  $O$  als eine Folge von  $n$  oder  $n-1$  Achsenspiegelungen, deren Achsen durch  $O$  gehen, darstellen.

Die beiden Möglichkeiten schliessen einander aus, weil eine ungerade Anzahl Achsenspiegelungen durch  $O$  einander nicht aufheben können.

2°.  $n$  ungerade. Die beiden Resultate können dann so ausgedrückt werden:

$$O x_1 x_2 \cdots x_{n-1}, \quad x_1 x_2 \cdots x_n.$$

In diesem Falle ist aber  $a_1 a_2 \cdots a_n = 1$ , und der letztere Ausdruck lässt sich dann so schreiben:

$$x_1 x_2 \cdots x_n = x_1 x_2 \cdots x_n a_1 a_2 \cdots a_n,$$

also als Produkt von  $2n$  Achsenspiegelungen.



Dem Reduktionssatz zufolge ist diese Anzahl aber auf  $n-1$  reduzierbar, und es besteht somit der Satz:

Satz 46. In einem Raume  $R_n$  mit ungerader Dimensionenzahl lässt sich jeder Transport mit dem Fixpunkt  $O$  entweder als eine Folge von  $n-1$  Achsenspiegelungen, deren Achsen durch  $O$  gehen oder als eine solche Folge in Verbindung mit der Punktspiegelung  $O$  darstellen.

### § 9. Allgemeine Transporte im $R_n$ .

Als Hyperspiegelung im  $R_n$  bezeichnen wir eine Spiegelung um einen  $R_{n-1}$  (eine Hyperebene im  $R_n$ ). Ist  $O$  ein Punkt der Hyperebene und  $a$  die Normale der Hyperebene in diesem Punkt, so wird die Hyperspiegelung durch  $Oa$  oder  $aO$  dargestellt. Jeder Transport im  $R_n$  lässt sich, wie wir im folgenden zeigen werden, aus Hyperspiegelungen zusammensetzen.

Zunächst untersuchen wir die Punktspiegelung  $O$ . Ist  $n$  eine gerade Zahl, und  $a_1 a_2 \cdots a_n$  ein  $n$ -Kreuz in  $O$ , so gilt, dass  $O = a_1 a_2 \cdots a_n$ , und somit

$$O = Oa_1 \cdot Oa_2 \cdots Oa_n = a_1 a_2 \cdots a_n,$$

wo  $\alpha_i$  die Hyperspiegelung  $Oa_i$  bezeichnet. Ist hingegen  $n$  eine ungerade Zahl, so ist

$$1 = a_1 a_2 \cdots a_n,$$

also

$$O = Oa_1 \cdot Oa_2 \cdots Oa_n = \alpha_1 \alpha_2 \cdots \alpha_n,$$

d. h.

Satz 47. Die Punktspiegelung  $O$  lässt sich in allen Fällen durch eine Folge von Hyperspiegelungen um die Normalräume eines  $n$ -Kreuzes in  $O$  darstellen.

Mit Hilfe dieser Tatsache folgt unmittelbar aus den Sätzen S. 45–46, dass jeder Transport im  $R_n$  mit dem Fixpunkt  $O$  durch eine Folge von Hyperspiegelungen dargestellt werden kann, und da jeder Punkt in jeden anderen Punkt durch eine Hyperspiegelung übergehen kann, so lässt sich jeder Transport im  $R_n$  als Produkt von Hyperspiegelungen darstellen. Wir wollen nun im folgenden die möglichst kleine Anzahl dieser Hyperspiegelungen bestimmen.

Zu dem Zweck müssen wir zunächst einen Hilfssatz beweisen:

Satz 48. In einer Folge von zwei Hyperspiegelungen  $\alpha, \beta$  können die Hyperebenen  $\alpha, \beta$  durch zwei andere  $\alpha_1, \beta_1$ , von denen die erstere durch einen vorgegebenen Punkt  $P$  geht, ersetzt werden.

Der Satz ist im  $R_3$  schon bewiesen worden, und der Beweis für den  $R_n$  wird ganz analog geführt: Von  $P$  fallen wir die Normalen  $a, b$  auf  $\alpha, \beta$ . Eine Ebene  $\omega$  durch  $a, b$  (eindeutig oder nicht) schneidet  $\alpha, \beta$  in zwei Geraden  $a_1, b_1$ . Wir wissen dann, dass in dieser Ebene zwei Geraden  $g, h$  existieren, wo  $g$  durch  $P$  geht, und  $a_1 b_1 = gh$ . Längs  $g, h$  können dann zwei Hyperebenen  $\perp \omega$  gelegt werden, und hiermit haben wir die beiden gesuchten Hyperebenen  $\alpha, \beta$  gefunden.

Wenn die beiden vorgegebenen Räume  $\alpha, \beta$  einen Punkt (Raum) gemein haben, so müssen die neuen Räume  $\alpha_1, \beta_1$  denselben Punkt (Raum) gemein haben. Und wenn  $\alpha, \beta$  eine gemeinsame Normale haben, so haben  $\alpha_1, \beta_1$  dieselbe Normale.

Wir schreiten nun daran, den folgenden allgemeinen Reduktionssatz zu beweisen:

Satz 49. Die Aufeinanderfolge von  $n+2$  Hyperspiegelungen  $\alpha_1, \alpha_2, \dots, \alpha_{n+2}$  lässt sich immer durch eine Folge von  $n$  Hyperspiegelungen ersetzen.

In  $\alpha_1$  wählen wir einen Punkt  $P_1$ . Nach dem Hilfssatz können wir dann das Produkt  $\alpha_2 \alpha_3$  durch ein anderes  $\alpha'_2 \alpha'_3$  ersetzen, wo die Hyperebene  $\alpha'_2$  durch  $P_1$  geht; ferner das Produkt  $\alpha'_3 \alpha_4$  durch  $\alpha''_3 \alpha'_4$ , wo  $\alpha''_3$  durch  $P_1$  geht, u. s. w. Durch dieses Verfahren erhalten wir ein neues System von  $n+2$  Hyperebenen, von denen die ersten  $n+1$  aufeinander folgenden durch den Punkt  $P_1$  gehen, und dieses System ist dem vorgegebenen gleichwertig. Wir wollen deshalb bei unseren Überlegungen gleich voraussetzen, dass das vorgegebene System  $\alpha_1, \alpha_2, \dots, \alpha_{n+2}$  diese Eigenschaft schon besitzt, dass also die Hyperebenen  $\alpha_1, \alpha_2, \dots, \alpha_{n+1}$  den Punkt  $P_1$  gemein haben.

Die beiden Hyperebenen  $\alpha_1, \alpha_2$  haben nun einen  $R_{n-2}$  gemein, und in diesem wählen wir ein freies Punktsystem  $P_1 P_2 \dots P_{n-1}$ . Nach dem Hilfssatz können wir das Produkt  $\alpha_3 \alpha_4$  durch ein anderes  $\alpha'_3 \alpha'_4$  ersetzen, wo  $\alpha'_3$  durch  $P_2$  geht; ferner das Produkt  $\alpha'_4 \alpha_5$  durch  $\alpha''_4 \alpha'_5$ , wo  $\alpha''_4$  durch  $P_2$  geht, u. s. w., d. h. wir können das ganze Produkt  $\alpha_1 \alpha_2 \dots \alpha_{n+1}$  so umschreiben, dass die



ersten  $n-1$  Hyperebenen die beiden Punkte  $P_1, P_2$  gemein haben. Es soll deshalb gleich vorausgesetzt werden, dass die vorgegebenen Hyperebenen diese Bedingung schon erfüllen. Auf diese Weise gehen wir nun weiter. Schliesslich erhalten wir das Resultat, dass das vorgegebene System immer durch ein anderes ersetzt werden kann, in welchem die drei ersten Hyperebenen alle  $n-1$  Punkte  $P_1, P_2, \dots, P_{n-1}$ , also einen  $R_{n-2}$  gemein haben. Das Produkt der drei entsprechenden Hyperspiegelungen wird aber dann einer einzigen Hyperspiegelung gleichwertig, und unser Satz ist hiermit bewiesen.

Durch ein ähnliches Verfahren ergibt sich

Satz 50. Eine ungerade Anzahl Hyperspiegelungen können einander nicht aufheben.

Es liege nämlich eine Folge von Hyperspiegelungen  $\alpha_1, \alpha_2, \dots, \alpha_n$ , vor. Es lässt sich dann, wie wir schon gesehen haben, eine neue ihr gleichwertige Folge bilden, deren ersten  $n-1$  Hyperebenen durch ein und denselben Punkt  $P_1$  gehen. Sollen nun die Hyperspiegelungen einander aufheben, so muss die letzte der Hyperebenen auch durch  $P_1$  gehen. Wir schliessen nun weiter: Soll das Produkt  $\alpha_1 \alpha_2 \dots \alpha_n = 1$  sein, so gibt es ein gleichwertiges System  $\beta_1 \beta_2 \dots \beta_n$ , dessen Hyperebenen durch denselben Punkt  $P_1$  gehen. Wählt man dann einen neuen Punkt  $P_2$  in  $\beta_1$ , so zeigt sich durch dasselbe Verfahren, dass ein neues gleichwertiges System  $\gamma_1 \gamma_2 \dots \gamma_n$  existiert, dessen Hyperebenen alle durch die beiden Punkte  $P_1, P_2$  gehen. Durch Weiterführung dieser Betrachtung ergibt sich so ein dem ursprünglichen gleichwertiges System  $\varkappa_1 \varkappa_2 \dots \varkappa_n$ , dessen Hyperebenen durch ein und dasselbe freie Punktsystem  $P_1 P_2 \dots P_{n-1}$  gehen. Wenn aber  $n$  ungerade ist, lässt sich dieses System zu einer einzigen Hyperspiegelung reduzieren, und es kann also niemals der Identität gleichwertig sein.

Aus dem oben gefundenen Reduktionssatz (Satz 49) ergibt sich nun die allgemeine Darstellung der Transporte im  $R_n$  mittels Hyperspiegelungen:

Satz 51. Jeder Transport im  $R_n$  lässt sich aus höchstens  $n+1$  Hyperspiegelungen zusammensetzen.

Satz 52. Ist die kleinste Anzahl von Hyperspiegelungen  $p$ , kann man immer eine solche Darstellung wählen, dass die ersten (oder die letzten)  $p-1$  Spiege-

lungshyperebenen durch einen vorgegebenen Punkt hindurch gehen.

Die Transporte zerfallen in zwei Klassen: die direkten Transporte (»In-Bewegungen«), welche durch eine gerade Anzahl Hyperspiegelungen, und die inversen Transporte (»Um-Bewegungen«), welche durch eine ungerade Anzahl Hyperspiegelungen, darstellbar sind. Dass die beiden Klassen einander ausschliessen, folgt aus dem obigen Satz 50, wonach eine ungerade Anzahl Hyperspiegelungen einander nicht aufheben können.

Indem wir nun schliesslich an die Sätze 45–46, S. 35–36 erinnern, können wir die folgenden Sätze aufstellen:

Satz 53. In einem Raum  $R_n$  von gerader Dimensionenzahl lässt sich jeder  $\left\{ \begin{array}{l} \text{direkter} \\ \text{inverser} \end{array} \right\}$  Transport aus einer  $\left\{ \begin{array}{l} \text{Hyperspiegelung} \\ \text{Punktspiegelung} \end{array} \right\}$  und  $n-1$  Achsenspiegelungen, deren Achsen durch ein und denselben Punkt  $O$  gehen, darstellen. Der Punkt  $O$  kann dabei beliebig gewählt werden.

Satz 54. In einem Raum  $R_n$  von ungerader Dimensionenzahl lässt sich jeder direkte Transport aus  $n-1$  Achsenspiegelungen, von denen mindestens  $n-2$  durch ein und denselben Punkt  $O$  gehen, zusammensetzen; und jeder inverser Transport aus einer Punkt- oder Hyperspiegelung nachgefolgt von  $n-1$  Achsenspiegelungen, deren Achsen durch ein und denselben Punkt  $O$  gehen. In beiden Fällen kann der Punkt  $O$  beliebig gewählt werden.

Um diese Sätze zu beweisen, betrachten wir zunächst denjenigen Punkt  $P$ , welcher bei dem vorliegenden Transport  $\tau$  in  $O$  übergeht. Der Mittelpunkt von  $PO$  sei  $M$ . Im Falle eines direkten Transports  $\tau$  lässt sich dann schreiben:

$$\tau = MOa_1a_2 \cdots a_{n-1},$$

wo die Geraden  $a_1, a_2, \cdots a_{n-1}$  alle durch  $O$  gehen. Statt  $MO$  können wir aber (S. 33)  $pq$  schreiben, wo  $p$  und  $q$  senkrecht auf einer Verbindungsgerade von  $P$  und  $O$  in  $M$  und  $O$  sind, und in ein und derselben Ebene liegen;  $q$  kann so in der Hyper-



ebene  $\perp PO$  in  $O$  beliebig gewählt werden, und wir wählen sie dann in einer Schnittlinie von dieser Hyperebene mit einer Hyperebene durch die Geraden  $a_1, a_2, \dots, a_{n-1}$ . Es gilt dann

$$\tau = pq a_1 a_2 \cdots a_{n-1}.$$

Da aber die letzten  $n$  Geraden  $q, a_1, a_2, \dots, a_{n-1}$  dieser Folge nun in ein und demselben  $R_{n-1}$  enthalten sind, können sie durch  $n-2$  Geraden  $b_1, b_2, \dots, b_{n-2}$  ersetzt werden (Satz 41), und es folgt dann

$$\tau = pb_1 b_2 \cdots b_{n-2}$$

w. z. b. w.

Im Falle eines inversen Transports schreiben wir sofort:

$$\tau = Ma_1 a_2 \cdots a_{n-1},$$

und der Beweis ist hiermit zu Ende gebracht.

Was Beispiele anbetrifft, verweisen wir zunächst auf mehrdimensionale Koordinatengeometrien mit Koordinatenzahlen von der in Einl. III, 59 beschriebenen Art.

In einer folgenden Mitteilung beabsichtigen wir auf die weitere Beschreibung der wichtigen Nachbarfiguren zurückzukommen. Und schliesslich soll die allgemeine analytische Behandlung der singulären Geometrie (d. h. die Geometrie, wo Rechtecke beliebiger Dimensionen existieren) erledigt werden.

DET KGL. DANSKE VIDENSKABERNES SELSKAB  
MATEMATISK-FYSISKE MEDDELELSER, BIND XXII, NR. 7.

---

# METAL AMMINE FORMATION IN AQUEOUS SOLUTION V

STABILITY OF THE ZINC AND CADMIUM  
ETHYLENEDIAMINE IONS AND THE CO-ORDINATION  
NUMBERS OF THE METAL IONS

BY

JANNIK BJERRUM AND PALLE ANDERSEN



KØBENHAVN

I KOMMISSION HOS EJNAR MUNKSGAARD

1945



## CONTENTS

	page
I. Introduction and Theoretical Part.....	3
II. Experimental Part.....	8
1. Procedure in computing the formation curve for the metal ethylenediamine systems .....	8
2. Acid-base constants of the ethylenediamine at the salt concentrations used .....	10
a. Experimental.....	11
b. Measurements.....	13
3. Formation curves for the zinc and cadmium ethylenediamine ions..	16
a. Measurements .....	16
b. Discussion .....	19
4. Calculation of the complexity constants .....	21

## I. Introduction<sup>1</sup> and Theoretical Part.

WERNER and SPRUCK<sup>2</sup> have prepared a series of tri-ethylenediamine zinc and cadmium salts which, according to cryoscopic measurements, only to a slight degree split off ethylenediamine in aqueous solution. Thus they possess rather high stability and can stand recrystallization from water. Ethylenediamine has the co-ordination capacity 2, and the 3 ethylenediamine molecules must therefore be assumed to occupy 6 co-ordination positions in all, as in other salts of this type. J. BJERRUM<sup>3</sup> has previously, by means of hydrogen electrode measurements, determined the complexity constants for the formation of the tri-ethylenediamine complexes of some of the divalent metal ions of the iron group, and found that the manganous, the cobaltous, the ferrous and the nickel ions with about equal strength bind all 3 ethylenediamine molecules taken up (see Table 1). Using the terminology of J. BJERRUM<sup>4</sup> this may be expressed by saying that the characteristic and the maximal co-ordination number is the same, namely 6. The characteristic co-ordination number is defined as the number of the first firmly and uniformly bound ligand groups. In many instances it is smaller than the maximal co-ordination number which denotes the maximal number of ligand groups bound in the co-ordinatively saturated complex. In their behaviour towards

<sup>1</sup> The earlier papers in this series are: J. BJERRUM: Untersuchungen über Kupferammoniakverbindungen I, II, III, D. Kgl. Danske Vidensk. Selskab, Mat.-fys. Medd., XI, No. 5 (1931), XI, No. 10 (1932), XII, No. 15 (1934), and J. BJERRUM: Metal Ammine Formation in Aqueous Solution — Theory of the Reversible Step Reactions, Doctoral thesis, Copenhagen 1941. These papers are in the following referred to as I, II, III, and IV, respectively.

<sup>2</sup> Zeitschr. anorg. Chem. **21** (1899) 221.

<sup>3</sup> IV, pp. 198 ff.

<sup>4</sup> IV, pp. 80 ff.



Table 1. Consecutive formation constants found for a series of metal ethylenediamine systems.

The values in parenthesis are statistically corrected.

Me	log $k_1$	log $k_2$	log $k_3$	$t^\circ$	Medium
Zn <sup>++</sup> . . . .	5.92	5.15 (6.23)	1.86	25°	1 N KNO <sub>3</sub>
Cd <sup>++</sup> . . . .	5.63	4.59 (5.67)	2.07	»	»
Mn <sup>++</sup> . . . .	2.73	2.06 (2.74)	0.88 (2.53)	30°	1 N KCl
Fe <sup>++</sup> . . . .	4.28	3.25 (3.93)	1.99 (3.64)	»	»
Co <sup>++</sup> . . . .	5.89	4.83 (5.51)	3.10 (4.75)	»	»
Ni <sup>++</sup> . . . .	7.66	6.40 (7.08)	4.55 (6.20)	»	»

ammonia and many other ligands, the zinc and cadmium ions have the characteristic co-ordination number 4<sup>1</sup> (see Table 2). It might therefore be expected that they had the same co-ordination number in the ethylenediamine systems, and that the 3rd ethylenediamine molecule would be more loosely bound than the first two taken up. The formation constants determined for the zinc and cadmium tri-ethylenediamine complexes (recorded in Table 1) show that this is actually so. It will be seen that the effect is not particularly great, but, as in the corresponding ammonia systems, the zinc system more markedly than the cadmium system has the characteristic co-ordination number 4. The first 2 constants lie closer to each other, and the distance to the 3rd constant is greater than in the cadmium system. The values for log  $k_2$  given in parenthesis are statistically corrected in accordance with the characteristic co-ordination number 4, and on the assumption that the di-ethylenediamine complexes have tetrahedral configuration.<sup>2</sup> On the assumption stated, the 2nd ethylenediamine molecule may be taken up in 6 ways, and split off in 2 ways, from which it follows that log  $k_1$  for statistical reasons must be log 12 = 1.08 higher than log  $k_2$ . It is seen that the statistical correction just about explains the difference between the values found for log  $k_1$  and log  $k_2$ . With regard to the great difference between the 2nd and the 3rd constant it is reasonable to assume a rearrangement from tetrahedral to octahedral configuration at the uptake of the 3rd ethylenediamine molecule.

<sup>1</sup> Cf. IV, pp. 65 and 152 ff.

<sup>2</sup> From what is known regarding the stereochemical properties of the metal ions, the zinc and cadmium ions never show planar, but always either tetrahedral or octahedral configuration (cf. IV, p. 102).

Table 2. Consecutive formation constants for some metal ammonia systems in 2N ammonium nitrate at 30°.

The values in parenthesis are statistically corrected.\*

Me	log k <sub>1</sub>	log k <sub>2</sub>	log k <sub>3</sub>	log k <sub>4</sub>	log k <sub>5</sub>	log k <sub>6</sub>	$\frac{d \log k_n}{d t^\circ}$	$\frac{d \log k_n}{d C_{\text{NH}_4^+}}$
Zn <sup>++</sup> . . . . .	2.37	2.44 (2.87)	2.50 (3.28)	2.15 (3.36)	—	—	—0.008	0.095
Cd <sup>++</sup> . . . . .	2.65	2.10 (2.53)	1.44 (2.22)	0.93 (2.14)	—0.4	—1.7	—0.008	0.070
Co <sup>++</sup> . . . . .	2.11	1.63 (2.01)	1.05 (1.70)	0.76 (1.66)	0.18 (1.36)	—0.62 (0.94)	—0.005	0.062
Ni <sup>++</sup> . . . . .	2.795	2.24 (2.62)	1.73 (2.38)	1.19 (2.09)	0.75 (1.93)	0.03 (1.59)	—0.007	0.061

\* See IV, pp. 39 ff. and 54 ff.

For comparison, Table 1 records the previously found consecutive formation constants for the ethylenediamine systems of the divalent metal ions of the iron group. In these systems log k<sub>2</sub> and log k<sub>3</sub> are corrected for the statistical effect assuming octahedral configuration and that the 2nd ethylenediamine molecule may equally well be bound in planar and in angular position relative to the first one taken up, but that in the former case there is steric hindrance for the uptake of the 3rd ethylenediamine molecule<sup>1</sup>.

The experimentally determined constants permit us to compute the distribution of the metal ions on the particular complexes at different concentrations of ethylenediamine. Fig. 1 is a graphical representation of the ranges of existence of the different complex ions. The diagram plainly shows that the zinc and cadmium di-ethylenediamine complexes have a range of existence substantially wider than that of the other complex ions.

The available data on the complexity constants make it possible to say something regarding the extent to which the "bridge" between the 2 amino groups in ethylenediamine strengthens the bond between the amine group and the metal ions. The logarithm of the consecutive constants furnishes a direct measure

<sup>1</sup> For further details, see IV, p. 94.



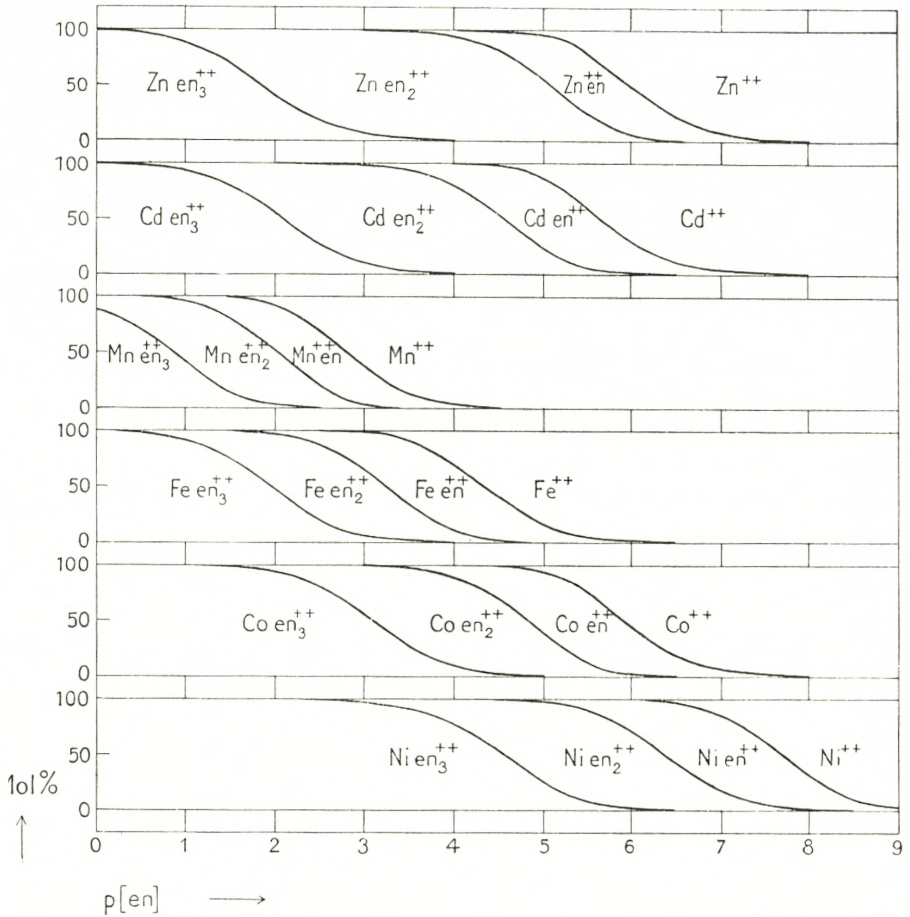


Fig. 1. Distribution of the metal ions on the different complex ions in a series of metal ethylenediamine systems. For the zinc and the cadmium systems in 1 *N* KNO<sub>3</sub> at 25°, and for the divalent metal ions of the iron group in 1 *N* KCl at 30°.

of the affinity between the metal ion and the amine molecule. The affinity, or the maximum work, at the binding of the *n*'th amine molecule in a 1 molar amine solution is thus given by the expression

$$A = RT \ln k_n. \quad (1)$$

If we denote the product of constants  $k_1 k_2 \cdots k_N$  by  $K_N$ , the following expression applies analogously to the mean affinity at the binding of the *N* first amine molecules

$$A_{\text{Mean}} = \frac{1}{N} RT \ln K_N. \quad (2)$$

Table 3. Comparison of the mean affinity (in kg. cal.) for the binding of one ethylenediamine and two ammonia molecules in some metal amine systems.

	$\frac{1}{2} RT \ln K_4 (\text{NH}_3)$	$\frac{1}{2} RT \ln K_2 (\text{en})$
Zn <sup>++</sup> . . .	6.45	7.54
Cd <sup>++</sup> . . .	4.85	6.96
	$\frac{1}{3} RT \ln K_6 (\text{NH}_3)$	$\frac{1}{3} RT \ln K_3 (\text{en})$
Co <sup>++</sup> . . .	2.36	6.38
Ni <sup>++</sup> . . .	4.03	8.59

Table 3, for the zinc, cadmium, cobaltous, and nickel ion, shows the values of the mean affinity at the binding of one ethylenediamine molecule and two ammonia molecules, calculated by means of (2), when N is put equal to the characteristic co-ordination number in the ammonia systems, and to one-half of the characteristic co-ordination number in the ethylenediamine systems. It is seen that the cobaltous and nickel ions bind one ethylenediamine molecule with a far greater affinity than two ammonia molecules, but that the difference in the case of the cadmium ion and especially the zinc ion is far smaller. Considering that the aliphatic monamines are bound less firmly than ammonia to the ions in question,<sup>1</sup> it may, however, be concluded that also in the case of the zinc ion there is a considerable "chelate" action. The particularly great "chelate" action in the case of the nickel and the cobaltous ions is perhaps explainable by the circumstance that the configuration is tetrahedral in the zinc and cadmium systems and octahedral in the cobaltous and nickel systems.<sup>2</sup> It is not a simple question of the size of the ions, as the cobaltous and nickel ions have ionic radii which lie between those of the zinc and cadmium ions.<sup>3</sup>

<sup>1</sup> A. TAMISIER, Bull. Soc. Chim. [4] **53** (1933) 97, 157.

<sup>2</sup> According to PAULING's theory, d-eigenfunctions are necessary for the establishment of strong octahedral bonds. In this connection it is of interest that the characteristic co-ordination number 6 (at least in so far as the mono- and divalent metal ions are concerned) has been found only in the case of metal ions with unsaturated d-shells.

<sup>3</sup> See IV, p. 74.



## II. Experimental Part.

### 1. Procedure in computing the formation curve for the metal ethylenediamine systems.

As in the earlier investigations of the ethylenediamine systems of the metal ions of the iron group, the formation curve —*i. e.* the relation between the average number of ethylenediamine molecules bound per metal atom ( $\bar{n}$ ), and the negative logarithm of the concentration of free ethylenediamine ( $p[en]$ ) — is established by determination of the hydrogen ion concentration and used in calculating the constants of the system. The measurements were carried out in solutions with known contents of nitric acid, zinc, or cadmium nitrate and ethylenediamine. Moreover, all solutions were made 1 N with respect to potassium nitrate, in order to establish conditions under which it was possible, with approximation, to apply the classic law of mass action.

Ethylenediamine is able to take up 2 hydrogen ions; this somewhat complicates the computation of the formation curve on the basis of hydrogen ion measurements. Following the usual practice of complex chemistry we shall denote ethylenediamine by en and its 2 acid forms by  $enH^+$  and  $enH_2^{++}$ . The 2 consecutive acid dissociation constants of the diammonium ion will be denoted by  $k_{enH_2^{++}}$  and  $k_{enH^+}$ , respectively. Concentrations of single ions or molecules are designated by the symbol being put in square brackets. In the solution we know:

$C_{HNO_3}$  total nitric acid concentration

$C_{Me}$  total concentration of the complex-forming metal ion

$C_{en}$  total ethylenediamine concentration,

and determine the hydrogen ion concentration  $[H^+]$ .

For the computation of the formation curve we shall furthermore introduce the following quantities in the acid-base system of the ethylenediamine:

$C'_{en}$  total concentration of ethylenediamine not complex-bound

$$C'_{en} = [en] + [enH^+] + [enH_2^{++}] \quad (3)$$

$C_s$  total concentration of hydrogen ions bound to ethylenediamine

$$C_s = C_{\text{HNO}_3} - [\text{H}^+] + [\text{OH}^-] = [\text{enH}^+] + 2[\text{enH}_2^{++}] \quad (4)$$

$$\alpha_{\text{en}} = \frac{[\text{en}]}{C'_{\text{en}}} = \frac{k_{\text{enH}_2^{++}} + k_{\text{enH}^+}}{k_{\text{enH}_2^{++}} + k_{\text{enH}^+} + k_{\text{enH}_2^{++}}[\text{H}^+] + [\text{H}^+]^2} \quad (5)$$

$$\bar{n}_{\text{en}} = \frac{C_s}{C'_{\text{en}}} = \frac{k_{\text{enH}_2^{++}}[\text{H}^+] + 2[\text{H}^+]^2}{k_{\text{enH}_2^{++}} + k_{\text{enH}^+} + k_{\text{enH}_2^{++}}[\text{H}^+] + [\text{H}^+]^2}. \quad (6)$$

The expression for  $\alpha_{\text{en}}$  and  $\bar{n}_{\text{en}}$ , *i. e.* the fraction of ethylenediamine in the acid-base system which is present as free ethylenediamine, and the average number of hydrogen ions bound to the ethylenediamine, are derived as usual by introducing mass action expressions for the acid dissociation constants.

The formation function for the complex system,  $\bar{n}$ , is calculated from the expression

$$C_{\text{en}} = [\text{en}] + [\text{enH}^+] + [\text{enH}_2^{++}] + \bar{n} \cdot C_{\text{Me}}. \quad (7)$$

Solving (7) with respect to  $\bar{n}$  and introducing  $\bar{n}_{\text{en}}$  and  $C_s$  by means of (3) and (6) we find

$$\bar{n} = \frac{C_{\text{en}} - \frac{C_s}{\bar{n}_{\text{en}}}}{C_{\text{Me}}}. \quad (8)$$

Combining (5) and (6) leads to the concentration of free amine

$$[\text{en}] = C_s \frac{\alpha_{\text{en}}}{\bar{n}_{\text{en}}} \quad (9)$$

or for the free ligand exponent

$$p[\text{en}] = -\log[\text{en}] = \log \frac{\bar{n}_{\text{en}}}{\alpha_{\text{en}}} - \log C_s. \quad (10)$$

It is seen that  $\bar{n}$  and  $p[\text{en}]$  are readily calculated if we know  $\bar{n}_{\text{en}}$  and  $\frac{\bar{n}_{\text{en}}}{\alpha_{\text{en}}}$ . Moreover, that these quantities may be calculated by means of (5) and (6), provided the acid-base constants of the ethylenediamine are known.



## 2. Acid-base constants of ethylenediamine at the salt concentrations used.

The majority of the zinc or cadmium ethylenediamine solutions measured had the following total concentrations<sup>1</sup>:  $C_{\text{HNO}_3} = 0.1$ ,  $C_{\text{Me}} = 0.1$ ,  $C_{\text{en}} > 0.05$ , and  $C_{\text{KNO}_3} = 1.00$ . Consequently nitric acid is bound to ethylenediamine, and it is only the excess of base which to a higher or lower degree is bound to the complex-forming metal ions. In order to carry out an accurate computation of the complex formation on the basis of the hydrogen ion concentration, it is necessary first to determine the acid-base constants of the ethylenediamine in the particular salt medium. These constants were determined by measurements of a series of ethylenediamine solutions having the same concentration of nitric acid and potassium nitrate as the complex solutions, but having the concentration of complex-forming metal ions replaced by an equivalent amount of barium salt. It is hardly to be assumed that the barium ion may bind ethylenediamine at the small concentrations of amine with which we are concerned here. A few measurements were also made of solutions with  $C_{\text{HNO}_3} = 0.1$  and  $C_{\text{KNO}_3} = 1.1$ , completely without any addition of salt of the type  $\text{MeX}_2$ .

The hydrogen ion concentration was determined by means of the glass electrode, by measuring the solution against standard acid solutions having analogous salt concentrations. Thus in the main experiments the standard acid solution had the composition  $C_{\text{HNO}_3} = 0.005$ ,  $C_{\text{BaCl}_2} = 0.1$ ,  $C_{\text{KNO}_3} = 1.1$ , and in the measurements of the solutions to which no salt of the type  $\text{MeX}_2$  had been added, the composition was  $C_{\text{HNO}_3} = 0.005$ ,  $C_{\text{KNO}_3} = 1.2$ . In the standard solutions the hydrogen ion concentration is chosen so small that we may reckon that the diffusion potential (against saturated potassium chloride) is the same as for the ethylenediamine solutions. The hydrogen ion concentration  $[\text{H}^+]$  and the hydrogen ion exponent pH may therefore (at 25°) be calculated directly from the expression

$$\text{pH} = -\log [\text{H}^+] = \frac{E_{(\text{st.})} - E}{0.591} + \text{pH}_{(\text{st.})}, \quad (11)$$

<sup>1</sup> All concentrations, here and in what follows, are given in moles per liter of solution.

where the quantities with the subscript (st.) refer to the standard solution.

#### a. Experimental.

For the glass electrode measurements we used a "Radiometer" valve potentiometer, Model PHM3, with the usual standard equipment: Glass bulb electrode with built-in silver-silver chloride electrode, and as reference electrode a saturated calomel electrode in liquid connection with the measuring vessel. The glass electrode was especially selected and proved to have theoretical pH-dependence even in rather strongly alkaline ethylenediamine solutions with pH close to 10. The glass electrode potential adjusted itself in the course of a couple of minutes, and the liquid in the measuring vessel, about 8 ml, was exchanged a couple of times before the final readings were made. Upon repetition, the potential could be reproduced with an uncertainty of about 0.3 millivolt. The whole glass electrode set-up was placed in an electrically heated air thermostat with strong circulation, so that it was possible to keep the temperature at  $25^{\circ} \pm 0.2^{\circ}$ .

As control, the glass electrode was supplemented by a hydrogen-gas electrode in the most alkaline solutions. The hydrogen electrode functioned excellently in the alkaline nitrate solutions,<sup>1</sup> but of course it was not possible to use it in the standard acid solutions containing nitric acid. Instead, the alkaline nitrate solution was measured against a standard acetate solution, which in turn was measured against the standard acid solution by means of the glass electrode. The hydrogen electrode measurements were carried out in the usual manner with a platinized platinum electrode in an electrode vessel of the type used by S. P. L. SØRENSEN. The hydrogen was obtained from a flask, washed in sulphuric acid and sodium hydroxide and further purified by being led over red-hot copper. With the aid of a thermocouple it was found that the temperature in the electric furnace was about  $500^{\circ}$ . The reference electrode was a 1 N calomel electrode, prepared according to GJALDBÆK,<sup>2</sup> in an electrode vessel of the model introduced by LEWIS, BRIGHTON, and

<sup>1</sup> See IV, p. 208.

<sup>2</sup> D. Kgl. Danske Vidensk. Selskab, Mat.-fys. Medd., V, No. 9 (1924).



SEBASTIAN,<sup>1</sup> which permits rinsing of the siphon tube. The electrodes were placed in an electrically heated water thermostat and were in liquid connection with each other through a saturated solution of potassium chloride. In all cases the temperature was  $25^{\circ} \pm 0.05^{\circ}$ . The determination of the potential was carried out by means of a Wolff potentiometer (15000 ohms resistance, smallest graduation 0.01 millivolt) and an Original Moll Galvanometer (from Kipp & Zonen). A calibrated Weston standard cell was used.

The different solutions were prepared in calibrated measuring flasks, by weighing or pipetting from stock solutions of potassium nitrate, barium chloride, nitric acid, and ethylenediamine. The stock solutions of potassium nitrate (2 molar) and barium chloride (1 molar) were made from Merck's preparations ("zur Analyse"). Solutions of the salts in question, with 0.005 mole of nitric acid added per liter, were measured by means of the glass electrode against analogous solutions with 10 times less nitric acid per liter. In this way we found a minor deviation from NERNST'S Law, corresponding to a basic impurity of 0.00004 equivalent per liter in the potassium nitrate solution without barium chloride, and 0.00006 equivalent per liter in the standard solution to which barium chloride had been added. The hydrogen ion concentration of the 0.005 molar standard solutions is therefore about 1 per cent. smaller than that corresponding to the amount of nitric acid added. The correction was made in the case of the standard solutions, but is without any significance as regards the other solutions having a substantially higher total concentration of nitric acid.

The nitric acid solutions were prepared from a boiled 5 molar solution.

The ethylenediamine was a pure commercial product of ethylenediamine hydrate, from Schuchardt. It was distilled in a "Schliff" apparatus, and the fraction  $118^{\circ}$ — $119^{\circ}$  (almost the whole portion) was collected. The specific gravity was found to be about 0.965 at  $21^{\circ}$ . By titration with 1 N hydrochloric acid (methyl orange as indicator) it was found to contain 76.2 per cent. ethylenediamine; for the hydrate the value of 76.94 per cent. was calculated. As stock solution served a solution

<sup>1</sup> Journ. Amer. Chem. Soc., **39** (1917) 2251.

of the hydrate, diluted approximately 4 times, which was kept CO<sub>2</sub>-free in a bottle with tightly fitting glass stopper. The solution was adjusted according to weight, and weighed-off portions were added to the various salt solutions.

### b. Measurements.

The acid-base constants of the ethylenediamine, determined by means of glass and hydrogen electrode, are recorded in Tables 4 and 5. The accurate composition of the standard solutions was as follows:

	C <sub>KNO<sub>3</sub></sub>	C <sub>BaCl<sub>2</sub></sub>	C <sub>HNO<sub>3</sub></sub>	pH <sub>(st.)</sub> (corr.)
Table 4	1.100	0.100	0.00499	2.307
Table 5	1.200	0	0.00500	2.304

The difference in potential between these standard solutions and the 0.1 N standard acetate solution used in the hydrogen electrode measurements was determined by means of the glass electrode, and found to be on an average 0.1400 and 0.1398 volt at 25°. In the tables, E<sub>(st)</sub>—E (4th column) shows the potential measured against the standard solutions, and pH (5th column) the hydrogen ion exponent calculated from this value with the aid of (11). In all solutions investigated, the hydrogen ion concentration and the hydroxyl ion concentration are so small that the mean number of hydrogen ions bound per molecule of ethylenediamine ( $\bar{n}_{en}$ , 3rd column) is given by the expression

$$\bar{n}_{en} = \frac{C_{HNO_3}}{C_{en}}$$

The connection between  $\bar{n}_{en}$ , the hydrogen ion concentration, and the acid dissociation constants is expressed in (6). Solving this equation with respect to  $k_{enH_2^{++}}$  and  $k_{enH^+}$  and transforming the particular expressions we arrive at

$$pk_{enH_2^{++}} = pH + \log \frac{\bar{n}_{en} - 1}{2 - \bar{n}_{en}} + \log \left( 1 + \frac{\bar{n}_{en} \cdot k_{enH^+}}{(\bar{n}_{en} - 1) [H^+]} \right) \quad (12)$$

$$pk_{enH^+} = pH + \log \frac{\bar{n}_{en}}{1 - \bar{n}_{en}} - \log \left( 1 + \frac{(2 - \bar{n}_{en}) [H^+]}{(1 - \bar{n}_{en}) k_{enH_2^{++}}} \right). \quad (13)$$



Table 4. Acid-base constants of ethylenediamine at 25° in 1 N potassium nitrate solution containing barium chloride.

$$C_{\text{KNO}_3} = 0.998, C_{\text{BaCl}_2} = 0.100$$

$$C_{\text{HNO}_3} = 0.1003 \text{ (Nos. 9, 10, 12, 13, 16) and } 0.1006 \text{ (All other Nos.)}$$

$$\text{pH}_{(\text{st.})} = 2.307.$$

$$J = \frac{\bar{n}_{\text{en}} \cdot 10^{-10.17}}{(\bar{n}_{\text{en}} - 1)[\text{H}^+]}$$

No.	$C_{\text{en}}$	$\bar{n}_{\text{en}}$	$E_{(\text{st.})} - E$	pH	$\log \frac{\bar{n}_{\text{en}} - 1}{2 - \bar{n}_{\text{en}}}$	$\log(1 + J)$	$\text{pk}_{\text{enH}_2^{++}}$ glass
1. . . . .	0.06326	1.589	0.2969	7.330	+0.156	0.002	7.488*
2. . . . .	0.07028	1.431	0.3131	7.605	-0.120	0.004	7.489
3. . . . .	0.07110	1.415	0.3143	7.625	-0.149	0.004	7.480
4. . . . .	0.07202	1.397	0.3173	7.675	-0.182	0.006	7.490*
5. . . . .	0.07273	1.383	0.3196	7.715	-0.207	0.006	7.514
6. . . . .	0.07600	1.324	0.3243	7.794	-0.319	0.008	7.478*
7. . . . .	0.08203	1.227	0.3371	8.010	-0.532	0.016	7.497*
							7.492

$$J = \frac{(2 - \bar{n}_{\text{en}})[\text{H}^+]}{(1 - \bar{n}_{\text{en}}) 10^{-7.49}}$$

No.	$C_{\text{en}}$	$\bar{n}_{\text{en}}$	$E_{(\text{st.})} - E$	pH	$\log \frac{\bar{n}_{\text{en}}}{1 - \bar{n}_{\text{en}}}$	$\log(1 + J)$	$\text{pk}_{\text{enH}^+}$ glass hydr.
8. . . . .	0.1043	0.9648	0.3950	8.991	1.438	0.287	(10.142*)
9. . . . .	0.1111	0.9028	0.4116	9.271	0.968	0.074	10.165
„ . . . . .	„	„	0.41245	9.285	„	0.073	10.180
10. . . . .	0.1206	0.8317	0.4254	9.505	0.694	0.028	10.171
„ . . . . .	„	„	0.42605	9.516	„	0.027	10.183
11. . . . .	0.1229	0.8186	0.4268	9.529	0.654	0.026	10.157*
12. . . . .	0.1373	0.7305	0.4401	9.754	0.433	0.011	10.176
„ . . . . .	„	„	0.4409	9.767	„	„	10.189
13. . . . .	0.1486	0.6750	0.4465	9.862	0.318	0.007	10.173
„ . . . . .	„	„	0.4478	9.884	„	„	10.195
14. . . . .	0.1547	0.6509	0.4491	9.906	0.270	0.006	10.170*
15. . . . .	0.1615	0.6229	0.4523	9.960	0.218	0.005	10.173*
16. . . . .	0.2524	0.3974	0.4773	10,383	-0.181	0.002	10.200

\* For the making of these measurements the authors are indebted to Mr. ERLING JUHL NIELSEN.

Expression (12) is valid only for values of  $\bar{n}_{\text{en}} > 1$ , and (13) for  $\bar{n}_{\text{en}} < 1$ . The reciprocal influence of  $k_{\text{enH}_2^{++}}$  and  $k_{\text{enH}^+}$  finds its expression in the last term, but is so small that the constants may be calculated from the first two terms alone, provided  $\bar{n}_{\text{en}} > 1.5$  or  $< 0.5$ . This is seen from Tables 4 and 5,

Table 5. Acid-base constants of ethylenediamine at 25° in 1.1 N potassium nitrate without barium chloride.

$$C_{\text{KNO}_3} = 1.099$$

$$C_{\text{HNO}_3} = 0.0995 \text{ (Nos. 1-2) and } 0.1003 \text{ (Nos. 3-4)}$$

$$\text{pH}_{(\text{st.})} = 2.304.$$

$$A = \frac{\bar{n}_{\text{en}} \cdot 10^{-10.17}}{(\bar{n}_{\text{en}} - 1)[\text{H}^+]}$$

No.	$C_{\text{en}}$	$\bar{n}_{\text{en}}$	$E_{(\text{st.})} - E$	pH	$\log \frac{\bar{n}_{\text{en}} - 1}{2 - \bar{n}_{\text{en}}}$	$\log(1 + A)$	$\text{pk}_{\text{enH}_2^{++}}$ glass
1. . . . .	0.05963	1.669	0.2874	7.167	0.306	0.001	7.474
2. . . . .	0.06559	1.517	0.3042	7.451	0.029	0.003	7.483

$$A = \frac{(2 - \bar{n}_{\text{en}})[\text{H}^+]}{(1 - \bar{n}_{\text{en}}) 10^{-7.48}}$$

No.	$C_{\text{en}}$	$\bar{n}_{\text{en}}$	$E_{(\text{st.})} - E$	pH	$\log \frac{\bar{n}_{\text{en}}}{1 - \bar{n}_{\text{en}}}$	$\log(1 + A)$	$\text{pk}_{\text{enH}^+}$ glass	hydr.
3. . . . .	0.1175	0.8536	0.4221	9.446	0.765	0.036	10.175	
„ . . . . .	„	„	0.4222	9.448	„	„		10.177
4. . . . .	0.1484	0.6759	0.4480	9.884	0.319	0.007	10.196	
„ . . . . .	„	„	0.44765	9.878	„	„		10.190

which, besides the constants found, give the values of the individual terms in the calculation.

The values of  $\text{pk}_{\text{enH}^+}$  determined by means of the hydrogen electrode are on an average a little higher than those found by means of the glass electrode, but the difference is slight, and shows that the glass electrode employed functions excellently in even the most alkaline of the solutions investigated. The variation in the values found for  $\text{pk}_{\text{enH}_2^{++}}$  is purely incidental.  $\text{pk}_{\text{enH}^+}$ , however, seems on the whole to increase a little with rising ethylenediamine concentration. J. BJERRUM<sup>1</sup> has previously determined  $\text{pk}_{\text{enH}^+}$  in 1 N potassium nitrate solution at 30°, using the hydrogen electrode, and found it to be 9.94; at salt concentrations corresponding to those in Table 1 the value is estimated to be 9.98. The value here found at 25° is 10.18. With use of these figures, a calculation is made of the heat of

<sup>1</sup> IV, p. 208.



neutralization at the uptake of the 1st hydrogen ion by the ethylenediamine, the result being 16.5 kg. cal. This value undoubtedly is too high,<sup>1</sup> but nevertheless of the right order of magnitude, and indicates the mutual agreement between the measurements concerned.

### 3. Formation curves for the zinc and cadmium ethylenediamine ions.

#### a. Measurements.

The experimental data for the establishment of the formation curves for the zinc and cadmium ethylenediamine ions are recorded in Tables 6 and 7. The solutions were prepared and the measurements were made as described in the preceding chapter. The approximately 1 molar stock solutions of zinc and cadmium nitrate (Merck, purum) were standardized according to R. BERG<sup>2</sup> by precipitation with 8-hydroxy-quinoline in weak acetic acid solution, with both weighing and bromine titration of the precipitate. pH of the stock solutions was about 4, *i. e.* a value which approximately corresponds to the hydrolysis of the pure salts and proves that the presence of acid and basic impurities in the salts employed may be ignored. The composition of the zinc and cadmium solutions investigated is recorded in the tables. In most of the solutions the concentration of zinc and cadmium nitrate is approximately 0.1 molar, and in the remaining ones 0.05 molar, to the latter solutions, however, an equivalent amount of barium chloride or barium nitrate is added, so that the total concentration of divalent metal ion in all solutions is about 0.1 molar. In some of the solutions with halved heavy metal concentration, the nitric acid concentration is likewise halved and the potassium nitrate concentration increased to 1.05; otherwise the concentrations are the usual,  $C_{\text{HNO}_3} = 0.100$  and  $C_{\text{KNO}_3} = 1.00$ .

The solutions all proved to be stable and did not show any precipitation upon standing.

<sup>1</sup> According to M. BERTHELOT, *Ann. chim. phys.* [7] **20** (1900) p. 163, the heat of neutralization at the uptake of the first hydrogen ion is 12.4 kg. cal., and for the second hydrogen ion 10.8 kg. cal.

<sup>2</sup> *Zeitschr. analyt. Chem.* **71** (1927) 174, 321.

Table 6. Glass electrode measurements of ethylenediamine containing zinc salt solutions at 25°.

Calc. with  $\text{pk}_{\text{enH}_2^{++}} = 7.49$ ,  $\text{pk}_{\text{enH}^+} = 10.17$  ( $\text{pH} < 9.30$ )  
and  $\text{pk}_{\text{enH}^+} = 10.18$  ( $\text{pH} > 9.30$ ).  $\text{pH}_{(\text{st.})} = 2.307$ .

$$C_{\text{HNO}_3} = 0.1006, C_{\text{KNO}_3} = 0.998$$

No.	$C_{\text{Zn}}$	$C_{\text{en}}$	$E_{(\text{st.})} - E$	pH	$\log \frac{\bar{n}_{\text{en}}}{\alpha_{\text{en}}}$	$\bar{n}_{\text{en}}$	$C'_{\text{en}}$	$\bar{n}$	p[en]
1	0.1001	0.0596	0.2174	5.986	5.996	1.969	0.0511	0.085	6.993
2	0.1226	0.0718	0.2264	6.137	5.697	1.958	0.0514	0.167	6.694
3	0.0993	0.1094	0.2477	6.499	4.985	1.906	0.0528	0.570	5.982
4	0.1220	0.1312	0.2503	6.542	4.901	1.899	0.0530	0.641	5.898
5	0.1000	0.1728	0.2670	6.824	4.358	1.822	0.0552	1.176	5.355
6	0.0992	0.2047	0.2777	7.005	4.017	1.753	0.0574	1.486	5.014
7	0.1218	0.2644	0.2865	7.115	3.814	1.703	0.0591	1.686	4.811
8	0.1002	0.2473	0.2969	7.331	3.428	1.590	0.0633	1.840	4.426
9	0.0997	0.2748	0.3239	7.787	2.686	1.331	0.0756	1.998	3.683
10	0.1002	0.2909	0.3437	8.122	2.214	1.181	0.0852	2.053	3.211
11	0.1000	0.3286	0.3897	8.901	1.302	0.986	0.1020	2.266	2.299
12	0.1219	0.4150	0.4131	9.297	0.886	0.897	0.1122	2.484	1.883
13	0.0995	0.3781	0.4243	9.486	0.703	0.842	0.1195	2.599	1.700
14	0.0995	0.3990	0.4340	9.650	0.530	0.768	0.1310	2.694	1.527
15	0.0993	0.4714	0.4602	10.093	0.080	0.552	0.1823	2.912	1.087

$$C_{\text{HNO}_3} = 0.0498, C_{\text{Ba}(\text{NO}_3)_2} = 0.050, C_{\text{KNO}_3} = 1.050.$$

16	0.05005	0.03508	0.2395	6.360	5.257	1.931	0.02576	0.186	6.560
17	0.04970	0.06464	0.2640	6.774	4.453	1.839	0.02706	0.756	5.756

$$C_{\text{HNO}_3} = 0.1006, C_{\text{BaCl}_2} = 0.050, C_{\text{KNO}_3} = 0.998.$$

18	0.05048	0.07516	0.2439	6.434	5.112	1.920	0.05240	0.451	6.109
19	0.04975	0.09730	0.2580	6.672	4.649	1.868	0.05385	0.873	5.646

An attempt was made to measure one of the more alkaline zinc solutions (Nr. 14) by means of the hydrogen electrode. This was considered possible, owing to the place of zinc in the electro-chemical series, but we did not succeed in obtaining definite potentials, perhaps because of the large nitrate content of the solutions. Hence the hydrogen ion concentration was determined solely by means of the glass electrode—and, corresponding to the salt concentrations employed, the standard



Table 7.

Glass electrode measurements of ethylenediamine containing cadmium salt solutions at 25°.

Calc. with  $\text{pk}_{\text{enH}_2^{++}} = 7.49$ ,  $\text{pk}_{\text{enH}^+} = 10.17$  ( $\text{pH} < 9.31$ )  
and  $\text{pk}_{\text{enH}^+} = 10.18$  ( $\text{pH} > 9.31$ ).  $\text{pH}_{(\text{st.})} = 2.307$ .

$C_{\text{HNO}_3} = 0.1006$  and  $0.0995$  (Nos. 12–14, 16, 17),  $C_{\text{KNO}_3} = 0.998$

No.	$C_{\text{Cd}}$	$C_{\text{en}}$	$E_{(\text{st.})} - E$	pH	$\log \frac{\bar{n}_{\text{en}}}{\alpha_{\text{en}}}$	$\bar{n}_{\text{en}}$	$C'_{\text{en}}$	$\bar{n}$	p [en]
1	0.0990	0.0625	0.2281	6.166	5.639	1.954	0.0515	0.111	6.637
2	0.0990	0.0787	0.2435	6.427	5.125	1.921	0.0524	0.266	6.123
3	0.0990	0.0915	0.2505	6.545	4.895	1.898	0.0530	0.389	5.892
4	0.0990	0.1098	0.2588	6.686	4.622	1.864	0.0540	0.564	5.619
5	0.0988	0.1237	0.2634	6.764	4.472	1.842	0.0546	0.700	5.469
6	0.0986	0.1859	0.2852	7.133	3.781	1.694	0.0594	1.283	4.779
7	0.0990	0.2142	0.2964	7.322	3.444	1.594	0.0631	1.528	4.441
8	0.0987	0.2431	0.3094	7.542	3.071	1.468	0.0685	1.769	4.069
9	0.0990	0.2735	0.3305	7.899	2.521	1.276	0.0789	1.968	3.519
10	0.0990	0.3070	0.3637	8.460	1.794	1.078	0.0934	2.160	2.792
11	0.0990	0.3309	0.3852	8.825	1.383	1.005	0.1000	2.332	2.381
12	0.0989	0.3377	0.3920	8.940	1.260	0.979	0.1016	2.387	2.262
13	0.0989	0.3687	0.4138	9.309	0.874	0.893	0.1114	2.601	1.876
14	0.0989	0.3935	0.4274	9.538	0.650	0.823	0.1209	2.756	1.652
15	0.0990	0.4245	0.4426	9.795	0.389	0.713	0.1412	2.865	1.387
16	0.0989	0.4562	0.4570	10.039	0.144	0.583	0.1707	2.885	1.146
17	0.0989	0.4887	0.4652	10.177	0.003	0.501	0.1985	2.933	1.005

$C_{\text{HNO}_3} = 0.0498$ ,  $C_{\text{BaCl}_2} = 0.050$ ,  $C_{\text{KNO}_3} = 1.050$

18	0.0495	0.0778	0.2843	7.118	3.809	1.702	0.0292	0.982	5.112
19	0.0495	0.1014	0.2997	7.378	3.347	1.563	0.0318	1.407	4.650
20	0.0495	0.1779	0.4137	9.307	0.876	0.895	0.0556	2.472	2.179

$C_{\text{HNO}_3} = 0.1006$ ,  $C_{\text{BaCl}_2} = 0.050$ ,  $C_{\text{KNO}_3} = 0.998$

21	0.0496	0.1063	0.2795	7.036	3.960	1.741	0.0578	0.978	4.957
----	--------	--------	--------	-------	-------	-------	--------	-------	-------

$C_{\text{HNO}_3} = 0.0498$ ,  $C_{\text{BaCl}_2} = 0.050$ ,  $C_{\text{KNO}_3} = 1.05$

22	0.0495	0.0488	0.2688	6.855	4.299	1.812	0.0275	0.430	5.602
23	0.0495	0.0778	0.2899	7.213	3.637	1.653	0.0301	0.963	4.940
24	0.0495	0.1132	0.3148	7.634	2.923	1.416	0.0351	1.579	4.226

acid solution was the same as in the experiments recorded in Table 4.

The values for the acid-base constants of the ethylenediamine which are used in calculating the auxiliary quantities  $\log \frac{\bar{n}_{en}}{\alpha_{en}}$  and  $\bar{n}_{en}$  are to be found at the top of the tables. Taking into consideration the trend of the values for  $\text{pk}_{en\text{H}^+}$  in Table 4, we use the value 10.17 for solutions with  $\text{pH} < 9.3$ , and the value 10.18 for solutions with  $\text{pH} > 9.3$ . The values found for the formation function  $\bar{n}$  and the ligand exponent  $p[\text{en}]$  are recorded in the last two columns of Tables 6 and 7; they are plotted against one another in Fig. 2.

### b. Discussion.

Fig. 2, besides the formation curves for the zinc and cadmium complexes, shows a couple of the previously determined formation curves for the ethylenediamine systems of the divalent

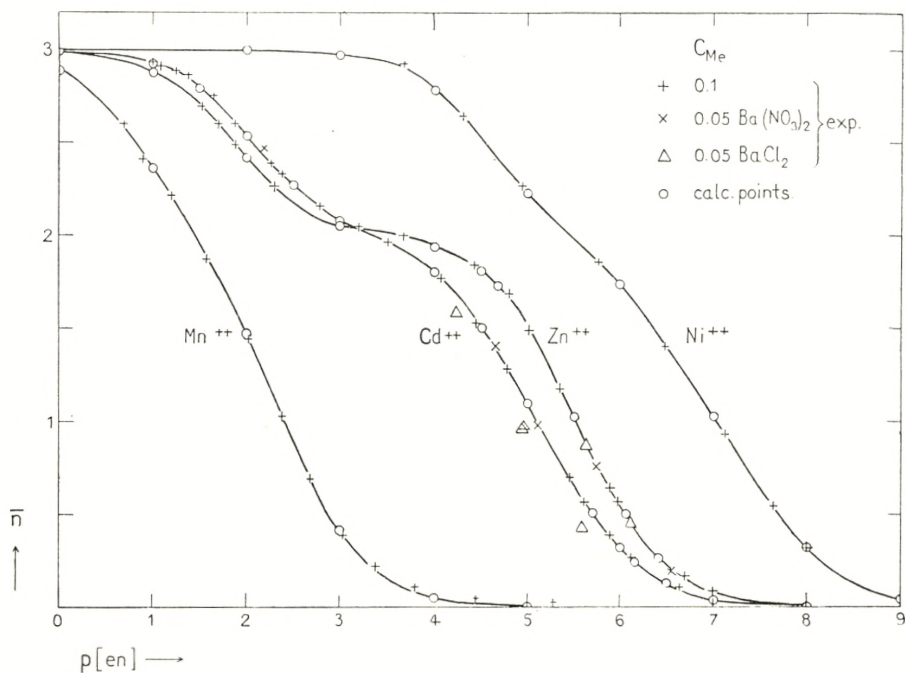


Fig. 2. Formation curves for the tri-ethylenediamine zinc and cadmium ions in 1 N  $\text{KNO}_3$  at  $25^\circ$ . For comparison the figure contains the previously determined formation curves for the tri-ethylenediamine manganous and nickel ions in 1 N  $\text{KCl}$  at  $30^\circ$ .



metal ions of the iron group. The figure shows that both the zinc and the cadmium ion bind up to 3 ethylenediamine molecules, and that the formation curves, as distinct from those of the metal ions of the iron group (most pronounced in the zinc system) are flattened out after the binding of the first 2 ethylenediamine molecules, before the 3rd molecule is taken up. The experimentally determined points corresponding to solutions with a zinc and cadmium concentration of approximately 0.1 molar are in the figure marked by + and for the concentration 0.05 by  $\times$  and  $\triangle$ , all according as the solutions are prepared with barium nitrate or chloride. In the zinc system the experimentally determined points lie almost on one and the same curve, irrespective of the different zinc concentrations and the presence of smaller amounts of chlorine ion. But in the cadmium system the tendency to chloro-complex formation<sup>1</sup> manifests itself, so that the points corresponding to the chloride-containing solutions ( $C_{Cl^-} = 0.1$ ) are distinctly displaced relative to the points corresponding to the completely chloride-free solutions; however, as might be expected in the case of 1-nuclear complexes, there is no dependence on the cadmium concentration.

In the upper part of the formation curves the points are not so nicely placed (a couple of zinc points lie close to the cadmium curve), but this circumstance is associated with the fact that the formation curve in this range is rather sensitive to errors in the hydrogen ion concentration and the values used for the acid-base constants of the ethylenediamine. For the value of the calculation it is an advantage to keep the concentration of the acid-base buffer system small in proportion to that of the complex system, but the nitric acid concentrations 0.1 and 0.05 are chosen with regard to the circumstance that still smaller acid concentrations make the solutions less defined and more basic, with all ensuing drawbacks; for one thing, the danger of hydroxo-complex formation is increased.<sup>2</sup>

It will be seen that the complex formation is almost complete at  $p[en]$  about 1, *i. e.* at ethylenediamine concentrations where it is still permissible to reckon with proportionality between concentration and activity.

<sup>1</sup> Cf. IV, p. 159.

<sup>2</sup> Cf. GROSSMANN and SCHÜCK, *Zeitschr. anorg. Chem.* **50** (1906) 9.

In the calculation of  $\bar{n}$  and  $p[en]$  we have assumed that the complex-bound ethylenediamine does not exert any basic function. This assumption is undoubtedly satisfied since the whole course of the curve towards  $\bar{n} = 2$  and 3 indicates that all the ethylenediamine is bound "chelate".<sup>1</sup>

#### 4. Calculation of the complexity constants.

The three consecutive complexity constants  $k_1$ ,  $k_2$ , and  $k_3$  of the complex systems examined are defined by the expression

$$k_n = \frac{[Me en_n]}{[Me en_{n-1}][en]}, \quad n = 1, 2, 3 \quad (14)$$

The 3rd consecutive complexity constant, owing to the flattened shape of the formation curve after the binding of the first 2 ethylenediamine molecules, is almost independent of the first 2 constants, and may therefore with good approximation be computed from each of the points of the curve with  $\bar{n} > 2$  by the equation

$$\log k_3 = p[en] + \log \frac{\bar{n} - 2}{3 - \bar{n}}. \quad (15)$$

Using the experimentally determined values for the ligand exponent and the formation function within the range  $\bar{n} = 2.3-2.7$ , we calculate with the aid of (15) the following values for  $\log k_3$  in the zinc system:

No. (in Tab. 6)	$p[en]$	$\bar{n}$	$\log k_3$
11	2.299	2.266	1.858
12	1.883	2.484	1.855
13	1.700	2.599	1.874
14	1.527	2.694	1.883
—	1.855	2.500	1.855

and for  $\log k_3$  in the cadmium system:

No. (in Tab. 7)	$p[en]$	$\bar{n}$	$\log k_3$
11	2.381	2.332	2.097
12	2.262	2.387	2.062
20	2.179	2.472	2.130
13	1.876	2.601	2.054
—	2.07	2.500	2.07

<sup>1</sup> Cf. IV, p. 216.



It is seen that the calculated values do not deviate much from one another.

The course of the formation curve up to  $\bar{n} = 2$  is almost independent of the 3rd constant, and the first 2 constants may therefore with good approximation be calculated from the ligand exponent and the slope of the curve

$$\Delta = \frac{d\bar{n}}{d \ln [\text{en}]} = -0.4343 \frac{d\bar{n}}{dp [\text{en}]}$$

for  $\bar{n} = 1$ . The relation between the particular quantities is easily found to be<sup>1</sup>

$$\left. \begin{aligned} \log k_1 &= p[\text{en}]_{\bar{n}=1} + \log \frac{2-2\Delta}{\Delta} \\ \log k_2 &= p[\text{en}]_{\bar{n}=1} - \log \frac{2-2\Delta}{\Delta} \end{aligned} \right\} (16)$$

The ligand exponent for a series of rounded-off values of  $\bar{n}$  is given in Table 8. The slope of the formation curves,  $\Delta_{\bar{n}=1}$  was found to be 0.438 and 0.379 in the zinc and the cadmium systems, respectively. The sets of constants calculated by means of (15) and (16) from  $\Delta$  and the graphically interpolated ligand exponents for  $\bar{n} = 1$  and 2.5 are recorded in the upper row of Table 9.

In order to check the correctness of the constants thus found and the accuracy of the measurements, a calculation was also made of the sets of constants satisfying the graphically interpolated values for the ligand exponent corresponding to  $\bar{n} = 0.5$ , 1.5, and 2.5, and for  $\bar{n} = 0.25$ , 1.75, and 2.5. The calculation

Table 8. Graphically interpolated values for the ligand exponent and calculated values of the formation function.

$\bar{n} =$	0.25	0.50	1.00	1.50	1.75	2.50
Zn: $p[\text{en}]$ . . . . .	6.42	6.06	5.525	5.005	4.68	1.855
Cd: $p[\text{en}]$ . . . . .	6.155	5.71	5.105	4.50	4.11	2.07
Zn: $\bar{n}$ (calc.) . . . . .	0.263	0.498	1.010	1.507	1.724	2.502
Cd: $\bar{n}$ (calc.) . . . . .	0.241	0.505	1.004	1.504	1.740	2.498

<sup>1</sup> See IV, pp. 24 ff.

Table 9. Calculated values for the consecutive complexity constants in the zinc and cadmium ethylenediamine systems.

	log $k_1$		log $k_2$		log $k_3$	
	Zn	Cd	Zn	Cd	Zn	Cd
$\Delta$ etc.	5.935	5.620	5.115	4.590	1.855	2.07
$\bar{n} = 0.5$ etc.....	5.927	5.622	5.138	4.584	1.856	2.074
$\bar{n} = 0.25$ etc.....	5.884	5.651	5.213	4.596	1.856	2.074
"Mean" .....	5.92	5.63	5.15	4.59	1.85	2.07

was carried out as a successive approximation of the constants determined by means of (15) and (16). For the approximation we used the previously derived formula<sup>1</sup>

$$k_n = \frac{1}{[en]} \cdot \frac{\sum_{t=0}^{t=n-1} \frac{\bar{n} - n + 1 + t}{[en]^t k_{n-1} k_{n-2} \cdots k_{n-t}}}{\sum_{t=0}^{t=3-n} (n - \bar{n} + t) [en]^t k_{n+1} k_{n+2} \cdots k_{n+t}}, \quad (17)$$

where the parameters are to run through all whole values between the limits fixed. As early as after one, or at the most two, insertions in (17) the constants do not change by further insertion. The constants thus calculated are recorded in the 2nd and 3rd row in Table 9.

A comparison of the constants determined by different methods shows that the 3rd constant calculated from (15), as one would expect, is practically unchanged by the successive approximation, and that the values for  $\log k_1$  and  $\log k_2$  calculated from (16) are in very nice agreement with the values calculated by means of the ligand exponents for  $\bar{n} = 0.5$  and 1.5. The agreement with the constants calculated from the ligand exponents for the more extremely located points corresponding to  $\bar{n} = 0.25$  and 1.75, however, is less satisfactory especially as regards one of the zinc constants. All the calculated constants being considered, the bottom row of Table 9 shows the sets of constants which presumably get the closest to satisfying the whole experimental material.

<sup>1</sup> In the formulae (4) and (5) in IV, pp. 37 and 38, there is an unfortunate misprint, which is easily corrected by comparison with the above formula (17).



Knowledge of the complexity constants permits us to calculate the formation function as well as the degrees of formation for the individual complexes

$$\alpha_n = \frac{[\text{Me en}_n]}{C_{\text{Me}}} \quad (18)$$

at any arbitrary concentration of ethylenediamine. If we denote the product of the constants  $k_1 k_2 \cdots k_n$  by  $K_n$ , and put  $K_0 = 1$ , the following will apply, as readily demonstrated<sup>1</sup>:

$$\bar{n} = \frac{\sum_0^3 n K_n [\text{en}]^n}{\sum_0^3 K_n [\text{en}]^n} \quad (19)$$

$$\alpha_n = \frac{K_n [\text{en}]^n}{\sum_0^3 K_n [\text{en}]^n} \quad (20)$$

$$\sum_0^3 \alpha_n = 1 \quad \text{and} \quad \sum_0^3 n \alpha_n = \bar{n} \quad (21)$$

By means of (19)–(21) and the constants found, the formation function and the degrees of formation in both the zinc and the cadmium systems are calculated for a series of ethylenediamine concentrations. The results are recorded in Table 10. The formation function is moreover calculated with the use of the graphically interpolated values for the ligand exponent corresponding to rounded-off values of  $\bar{n}$ . The values thus determined for the formation function are recorded in Table 8; it is seen that they reproduce the experimental data satisfactorily. This is also seen from Fig. 2, where all the calculated  $\bar{n}$ -values are plotted on the experimentally determined formation curves.

<sup>1</sup> Cf. IV, pp. 27 ff.

Table 10.

Distribution of the zinc and cadmium ion on the different metal ethylenediamine ions in 1 N potassium nitrate at 25°.

1. Distribution of the zinc ion calculated with:

$$\log K_1 = 5.92, \quad \log K_2 = 11.07, \quad \log K_3 = 12.93$$

p [en]	$\alpha_0$	$\alpha_1$	$\alpha_2$	$\alpha_3$	$\bar{n}$
0	0	0	0.014	0.986	2.987
1	0	0	0.121	0.879	2.877
2	0	0	0.580	0.420	2.419
3	0	0.007	0.927	0.067	2.061
4	0	0.066	0.927	0.007	1.940
5	0.048	0.395	0.557	0	1.511
6	0.514	0.427	0.060	0	0.548
7	0.922	0.077	0.001	0	0.079
8	0.992	0.008	0	0	0.008

2. Distribution of the cadmium ion calculated with:

$$\log K_1 = 5.63, \quad \log K_2 = 10.22, \quad \log K_3 = 12.29$$

p [en]	$\alpha_0$	$\alpha_1$	$\alpha_2$	$\alpha_3$	$\bar{n}$
0	0	0	0.008	0.991	2.991
1	0	0	0.078	0.922	2.922
2	0	0.001	0.459	0.540	2.538
3	0	0.023	0.874	0.103	2.080
4	0.005	0.202	0.784	0.009	1.798
5	0.144	0.616	0.240	0	1.096
6	0.693	0.296	0.012	0	0.319
7	0.959	0.041	0	0	0.041
8	0.996	0.004	0	0	0.004

A graphical presentation of the distribution of the metal ions on the particular complex ions as a function of p [en] is given in Fig. 1 (see p. 6).

Thanks are due to the Carlsberg Foundation for a grant which enabled one of the writers (P. A.) to take part in this work.

*From the Chemical Laboratory,  
University of Copenhagen.*





DET KGL. DANSKE VIDENSKABERNES SELSKAB  
MATEMATISK-FYSISKE MEDDELELSER, BIND XXII, NR. 8

---

# A NOTE ON THE FOUNDATIONS OF GEOMETRICAL OPTICS

BY

NIELS ARLEY



KØBENHAVN

I KOMMISSION HOS EJNAR MUNKSGAARD

1945



Printed in Denmark  
Bianco Lunos Bogtrykkeri A/S

## § 1.

As is well-known all the laws of geometrical optics may be deduced from FERMAT's *principle*<sup>1</sup>

$$\delta \int_{P'}^P n ds = \delta \int_{\tau'}^{\tau} n \sqrt{\left(\frac{dx}{d\tau}\right)^2 + \left(\frac{dy}{d\tau}\right)^2 + \left(\frac{dz}{d\tau}\right)^2} d\tau = 0 \quad (1)$$

or from the mathematically equivalent *principle of HUYGENS*<sup>1</sup>. In (1)  $\tau$  is an arbitrary parameter of the integration curve from  $P'$  to  $P$ , and  $n$  is the *ray index* given by

$$n = n_r = \frac{c}{v_r}, \quad (2)$$

$c$  being the velocity of light in vacuo and  $v_r$  the *velocity of the ray*, i. e. of the energy current<sup>2</sup>. Thus the integral in (1) is simply  $c$  times the time-interval from  $P'$  to  $P$ . In the most general case,  $v_r$  and thus  $n$  are functions of the point, the direction, and the colour, i. e. the frequency of the light. In geometrical optics we only consider *monochromatic light*, i. e. we abstract from *dispersion phenomena*. If for a certain medium  $n$  is independent of the point, the medium is *homogeneous*, if  $n$  is independent of the direction, it is *isotropic*.

In most textbooks on optics<sup>3</sup> FERMAT's principle is only proved to hold true for a *finite* number of reflections and refractions in an isotropic medium with piece-wise constant index of

<sup>1</sup> This is shown most completely in CARATHÉODORY (1937). In this paper the theory is developed quite generally for an inhomogeneous, anisotropic medium by means of the methods due to HAMILTON. Furthermore, it also briefly outlines the history of the two famous principles.

<sup>2</sup>  $n$  is often erroneously stated as being the *index of refraction*,  $n_n = \frac{c}{v_n}$ ,  $v_n$  being the *normal* or *phase velocity*. This statement is only true in the case of isotropic media, the normal and the ray directions as well as  $v_n$  and  $v_r$  coinciding only in this case.

<sup>3</sup> See e. g. the well-known textbook of DRUDE (1900) or the modernized version of this standard treatise: FÖRSTERLING (1928).



refraction. Furthermore, HUYGENS' principle is as a rule only stated but not proved<sup>1</sup>.

Now it is an obvious task to deduce the two fundamental principles in the *general* case of an inhomogeneous, anisotropic, absorbing medium from MAXWELL'S electro-magnetic theory of light, at the same time deducing the conditions for the validity of geometrical optics. It is the purpose of the present note to work out this programme, which surprisingly enough has not, as far as we know, been done before. We thereby proceed by combining a method due to SOMMERFELD and RUNGE<sup>2</sup> with the general theory of partial differential equations of the first order and their connection with the calculus of variations.<sup>3</sup> Although the following considerations do not, of course, yield any new results, they may perhaps be of some pedagogic interest.

## § 2.

Any propagation of light in an arbitrary non-ferromagnetic medium is governed by the four MAXWELL equations

$$\operatorname{rot} \mathbf{H} = \frac{4\pi}{c} \sigma \cdot \mathbf{E} + \frac{1}{c} \varepsilon \cdot \dot{\mathbf{E}} \quad (1)$$

$$\operatorname{rot} \mathbf{E} = -\frac{\mu}{c} \dot{\mathbf{H}} \quad (2)$$

$$\operatorname{div} \varepsilon \cdot \mathbf{E} = 0, \operatorname{div} \mu \mathbf{H} \equiv 0, \quad (3)$$

in which  $\varepsilon = \varepsilon(x, y, z)$  and  $\sigma = \sigma(x, y, z)$  are symmetric tensor-functions (indicated by a dot in all products) and  $\mu = \mu(x, y, z)$  a scalar function (no dots in the products). The main equations

<sup>1</sup> See e. g. the most modern textbook on optics: BORN (1933). In LANDÉ (1928) HUYGENS' principle is deduced from that of FERMAT, but this principle itself has not been proved.

<sup>2</sup> SOMMERFELD and RUNGE (1911). This method is also described in BORN'S textbook, in PLANCK (1927) and JENTZSCH (1927).

<sup>3</sup> See e. g. COURANT-HILBERT (1937) or CARATHÉODORY (1935). The method of SOMMERFELD and RUNGE is in fact only a special case of a general method for obtaining the characteristic equation belonging to an arbitrary partial differential equation of the second order with  $n$  variables, see COURANT-HILBERT (1937) chap. VI § 10.1. Furthermore, the same method has been used by DIRAC (1930), p. 120, to deduce the corresponding transition from wave

to classical mechanics. In this calculation a term  $-ih \sum_r \frac{\partial^2 S}{\partial q_r^2}$  has, however, erroneously been omitted; this term is just important because the condition that it may be neglected imposes the restriction that the radius of curvature of the "path" is to be large compared with the wave-length (cf. p. 8 below).

are (1) and (2), while (3) only imposes certain conditions on the direction of the field-vectors  $\mathbf{E}$  and  $\mathbf{H}$ . In fact it follows from (1) and (2) that if (3) is satisfied at the initial time, (3) will be satisfied for all times. We eliminate  $\mathbf{H}$  between (1) and (2) by taking the time derivative of (1) and rot of (2), obtaining by means of the vector identities

$$\left. \begin{aligned} \text{rot } \varphi \mathbf{A} &= \varphi \text{rot } \mathbf{A} + [\text{grad } \varphi \times \mathbf{A}] \\ \text{rot rot } \mathbf{A} &= -\Delta \mathbf{A} + \text{grad div } \mathbf{A} \end{aligned} \right\} \quad (4)$$

the general *wave equation*

$$\Delta \mathbf{E} - \text{grad div } \mathbf{E} + \left[ \frac{\text{grad } \mu}{\mu} \times \text{rot } \mathbf{E} \right] - \frac{4\pi\mu}{c^2} \sigma \cdot \dot{\mathbf{E}} - \frac{\mu}{\epsilon^2} \epsilon \cdot \ddot{\mathbf{E}} = \mathbf{0}. \quad (5)$$

Having calculated  $\mathbf{E}$  from (5) and the boundary conditions we obtain  $\mathbf{H}$  from (2). We now assume the time variation of  $\mathbf{E}$  to be strictly harmonious (otherwise we only need expand  $\mathbf{E}$  in a Fourier series) i. e. we put

$$\mathbf{E} = \mathbf{F} e^{i\omega t}, \quad \omega = 2\pi\nu, \quad (6)$$

which inserted in (5) gives the time independent wave equation, being a system of 3 simultaneous, linear, homogeneous, partial differential equations of the second order,

$$\lambda_0^2 \left( \Delta \mathbf{F} - \text{grad div } \mathbf{F} + \left[ \frac{\text{grad } \mu}{\mu} \times \text{rot } \mathbf{F} \right] \right) - \frac{4\pi\mu i}{c} \lambda_0 \sigma \cdot \mathbf{F} + \mu \epsilon \cdot \mathbf{F} = \mathbf{0}. \quad (7)$$

Here

$$\lambda_0 = \frac{c}{\omega} \quad (8)$$

is the vacuum wave-length divided by  $2\pi$ .

Now geometrical optics is just characterized as that branch of optics in which we may consider  $\lambda_0$  as infinitely small, i. e. strictly speaking obtained by making the limit  $\lambda_0 \rightarrow 0$ . In order to obtain a solution of (7) which will approximately describe a *light-ray*, i. e. a wave propagation which vanishes outside a very narrow region which in the limit  $\lambda_0 \rightarrow 0$  may be considered as a geometrical curve, we put  $\mathbf{F}$  approximately equal to a homogeneous plane wave

$$\mathbf{F} = \mathbf{A}(x, y, z) \exp \left[ \frac{i}{\lambda_0} S(x, y, z) \right], \quad (9)$$



in which the amplitude  $\mathbf{A} = \mathbf{A}(x, y, z)$  is a slowly varying vector-function, being approximately constant along the light-ray and zero outside it, and the phase function  $S = S(x, y, z)$ , describing the wave fronts, deviates but little from the linear function  $n(\mathbf{s} \cdot \mathbf{r}) = n(s_x x + s_y y + s_z z)$ . (In order to obtain the *exact* solution we had, as is well-known, to superpose plane waves with slightly different wave vectors  $\mathbf{s}$ ). Using the well-known vector identities (4),

$$\left. \begin{aligned} \text{grad}(\varphi\psi) &= \varphi \text{grad} \psi + \psi \text{grad} \varphi, \\ \text{and} \quad \text{div}(\varphi \mathbf{A}) &= \varphi \text{div} \mathbf{A} + (\mathbf{A} \cdot \text{grad} \varphi) \\ \text{grad}(\mathbf{A} \cdot \mathbf{B}) &= (\mathbf{A} \cdot \text{grad} \mathbf{B}) + (\mathbf{B} \cdot \text{grad} \mathbf{A}) + [\mathbf{A} \times \text{rot} \mathbf{B}] + [\mathbf{B} \times \text{rot} \mathbf{A}] \end{aligned} \right\} (10)$$

we obtain (using furthermore the fact that  $\text{rot grad} \equiv 0$ )

$$\left. \begin{aligned} \text{rot} \mathbf{F} &= \frac{i}{\lambda_0} \exp \left[ \frac{i}{\lambda_0} S \right] [\text{grad} S \times \mathbf{A}] + \exp \left[ \frac{i}{\lambda_0} S \right] \text{rot} \mathbf{A} \\ \mathbf{A} \mathbf{F} &= \text{div grad} \mathbf{F} = \left( \frac{i}{\lambda_0} \right)^2 \exp \left[ \frac{i}{\lambda_0} S \right] (\text{grad} S)^2 \mathbf{A} + \\ &\quad + \frac{i}{\lambda_0} \exp \left[ \frac{i}{\lambda_0} S \right] (2(\text{grad} \mathbf{A} \cdot \text{grad} S) + \mathbf{A} \mathcal{A} S) + \exp \left[ \frac{i}{\lambda_0} S \right] \mathcal{A} \mathbf{A} \\ \text{grad div} \mathbf{F} &= \left( \frac{i}{\lambda_0} \right)^2 \exp \left[ \frac{i}{\lambda_0} S \right] (\mathbf{A} \cdot \text{grad} S) \text{grad} S + \\ &\quad + \frac{i}{\lambda_0} \exp \left[ \frac{i}{\lambda_0} S \right] (\text{div} \mathbf{A} \text{grad} S + (\mathbf{A} \cdot \text{grad} (\text{grad} S)) + \\ &\quad + (\text{grad} S \cdot \text{grad} \mathbf{A}) + [\text{grad} S \times \text{rot} \mathbf{A}]) + \exp \left[ \frac{i}{\lambda_0} S \right] \text{grad div} \mathbf{A}. \end{aligned} \right\} (11)$$

(11) inserted in the wave equation (7) finally, after division with  $\exp \left[ \frac{i}{\lambda_0} S \right]$ , gives

$$\left. \begin{aligned} &(-(\text{grad} S)^2 + \text{grad} S(\text{grad} S \cdot) + \mu \varepsilon \cdot) \mathbf{A} + i \lambda_0 \left( (\text{grad} S \cdot \text{grad} \mathbf{A}) + \right. \\ &\quad \left. + \mathbf{A} \mathcal{A} S - \text{grad} S \text{div} \mathbf{A} - (\mathbf{A} \cdot \text{grad} (\text{grad} S)) - [\text{grad} S \times \text{rot} \mathbf{A}] + \right. \\ &\quad \left. + \left[ \frac{\text{grad} \mu}{\mu} \times [\text{grad} S \times \mathbf{A}] \right] - \frac{4\pi}{c} \sigma \cdot \mathbf{A} \right) + \lambda_0^2 (\mathcal{A} \mathbf{A} - \text{grad div} \mathbf{A}) = \mathbf{0}, \end{aligned} \right\} (12)$$

in which  $\text{grad} S(\text{grad} S \cdot)$  denotes the tensor product of  $\text{grad} S$  with itself. If now  $\lambda_0$  is a very small number, we see in fact that (9) is a solution of the wave equation (7) if  $S$  is a solution of the equation

$$(-(\text{grad } S)^2 + \text{grad } S(\text{grad } S \cdot) + \mu \varepsilon \cdot) \mathbf{A} = \mathbf{0}. \quad (13)$$

This equation is, however, as an equation for  $\mathbf{A}$ , a linear homogeneous vector equation. Consequently the necessary and sufficient condition for its having other solutions than  $\mathbf{A} \equiv \mathbf{0}$  consists in the determinant vanishing, i. e.

$$\left| \begin{array}{ccc} \mu \varepsilon_{xx} - (\text{grad } S)^2 + \left(\frac{\partial S}{\partial x}\right)^2, & \mu \varepsilon_{xy} + \frac{\partial S}{\partial x} \frac{\partial S}{\partial y}, & \mu \varepsilon_{xz} + \frac{\partial S}{\partial x} \frac{\partial S}{\partial z} \\ \mu \varepsilon_{yx} + \frac{\partial S}{\partial y} \frac{\partial S}{\partial x}, & \mu \varepsilon_{yy} - (\text{grad } S)^2 + \left(\frac{\partial S}{\partial y}\right)^2, & \mu \varepsilon_{yz} + \frac{\partial S}{\partial y} \frac{\partial S}{\partial z} \\ \mu \varepsilon_{zx} + \frac{\partial S}{\partial z} \frac{\partial S}{\partial x}, & \mu \varepsilon_{zy} + \frac{\partial S}{\partial z} \frac{\partial S}{\partial y}, & \mu \varepsilon_{zz} - (\text{grad } S)^2 + \left(\frac{\partial S}{\partial z}\right)^2 \end{array} \right| = 0, \quad (14)$$

in which  $(x, y, z)$  is an arbitrary *Cartesian* coordinate system. This equation is just the so-called *characteristic equation* belonging to the wave equation (7). It is a partial differential equation of the first order and the degree 6 (viz. equal to the product of the order of and the number of equations in the wave equation). We shall, however, see in a moment that the degree of (14) is in fact only 4. Before doing so we shall state under what conditions the terms in (12) with  $\lambda_0$  and  $\lambda_0^2$  may be neglected in comparison with the first term. They are, obviously, since the dimensionless quantity  $\text{grad } S$  is of the order of magnitude 1, the following:

$$\left. \begin{array}{l} \text{(a)} \quad \lambda_0 ((\text{grad } S \cdot \text{grad } \mathbf{A}) - \text{grad } S \text{div } \mathbf{A} - [\text{grad } S \times \text{rot } \mathbf{A}]) \ll \mathbf{A} \\ \text{i. e.} \quad \lambda_0 \left| \frac{\partial A_i}{\partial x_k} \right| \ll |\mathbf{A}| \quad (i, k = 1, 2, 3) \end{array} \right\} \quad (15)$$

$$\left. \begin{array}{l} \text{(b)} \quad \lambda_0 (\mathcal{A}S - (\text{grad } (\text{grad } S) \cdot)) \mathbf{A} \ll \mathbf{A} \\ \text{i. e.} \quad \lambda_0 \left| \frac{\partial^2 S}{\partial x_i \partial x_k} \right| \ll 1 \quad (i, k = 1, 2, 3) \end{array} \right\} \quad (16)$$

$$\left. \begin{array}{l} \text{(c)} \quad \lambda_0 \left[ \frac{\text{grad } \mu}{\mu} \times [\text{grad } S \times \mathbf{A}] \right] \ll \mathbf{A} \\ \text{i. e.} \quad \lambda_0 \left| \frac{\partial \mu}{\partial x_i} \right| \ll \mu \quad (i = 1, 2, 3) \end{array} \right\} \quad (17)$$



$$\begin{aligned}
 \text{(d)} \quad & \lambda_0 \frac{4\pi\mu}{c} \sigma \cdot \mathbf{A} \ll \mathbf{A} \\
 \text{i. e.} \quad & \lambda_0 \frac{4\pi\mu}{c} \sigma_i = \frac{1}{2} \left( \frac{\lambda_0}{d_i} \right)^2 \ll 1 \quad (i = 1, 2, 3),
 \end{aligned}
 \left. \vphantom{\begin{aligned} \text{(d)} \\ \text{i. e.} \end{aligned}} \right\} \quad (18)$$

in which<sup>1</sup>

$$d_i = \frac{\lambda_0}{4\pi z_i} = \frac{c}{4\pi \sqrt{\nu\mu\sigma_i}} \quad (19)$$

( $z_i$ : the coefficient of absorption in the direction of the  $i$ 'th principal axis of  $\sigma$ ,  $d_i$ : the corresponding length of penetration).

$$\begin{aligned}
 & \lambda_0^2 (\mathcal{A}\mathbf{A} - \text{grad div } \mathbf{A}) \ll \mathbf{A} \\
 \text{(e)} \quad \text{i. e.} \quad & \lambda_0^2 \left| \frac{\partial^2 A_i}{\partial x_k \partial x_l} \right| \ll |\mathbf{A}| \quad (i, k, l = 1, 2, 3).
 \end{aligned}
 \left. \vphantom{\begin{aligned} & \lambda_0^2 (\mathcal{A}\mathbf{A} - \text{grad div } \mathbf{A}) \ll \mathbf{A} \\ \text{(e)} \quad \text{i. e.} \end{aligned}} \right\} \quad (20)$$

(a) + (e) means that each component of the amplitude  $\mathbf{A}$  is to vary so slowly that both the first and the second variation of  $\mathbf{A}$  in a distance of the order of magnitude of the wave-length  $\lambda_0$  is negligibly small compared with  $|\mathbf{A}|$ . If we consider a sharply defined light ray,  $\mathbf{A}$  will obviously vary strongly in a distance of the order  $\lambda_0$  on the border between the ray and the shadow. In this region we shall, consequently, expect deviations from the laws of geometrical optics: the phenomena of diffraction.

(b) means that the phase function  $S$  is to deviate so little from linearity that its second derivatives are negligible compared with  $\frac{1}{\lambda_0}$ , i. e. the principal radii of curvature of the wave fronts given by  $S = \text{const}$  are to be large compared with  $\lambda_0$ . This statement, again, is equivalent to two other conditions: ( $\alpha$ ) the radii of curvature of the light rays themselves are to be large compared with  $\lambda_0$ . ( $\beta$ ) no points in which the light rays diverge or converge are to be considered (as in these points one or both of the principal radii of curvature vanish). Finally we see from (14) that,  $S$  being determined by the variation of the product  $\mu\varepsilon$ , our condition (16) demands that  $\mu\varepsilon$  varies so slowly that its variation in a distance of the order  $\lambda_0$  is negligible compared with  $\mu\varepsilon$  itself:

$$\lambda_0 \left| \frac{\partial (\mu\varepsilon_{ik})}{\partial x_l} \right| \ll \mu\varepsilon_{ik} \quad (i, k, l = 1, 2, 3). \quad (21)$$

<sup>1</sup> Cf. e. g. BORN (1933) p. 261.

(c) means that  $\mu$  is to vary so slowly that its variation in a distance of the order  $\lambda_0$  is negligible compared with  $\mu$  itself. From (21) it then follows that the same applies to the dielectric tensor  $\epsilon$  itself.

(d) means that the medium is to have so small a conductivity tensor  $\sigma$  that the principal lengths of penetration  $d_i$  are very large compared with the wave-length  $\lambda_0$ . This condition is, besides, obvious, as we could not otherwise speak of light rays at all, the rays being at once absorbed.

(f) Finally we see that geometrical optics is only valid so long as all questions regarding phenomena of intensity, polarization, and interference, and as already stated also of dispersion, may be disregarded.

### § 3.

Having stated the exact conditions for the validity of geometrical optics, we shall now investigate the equation § 2 (14), which contains all its laws. Firstly, we note that the equation is invariant against all coordinate transformations. Secondly, that the dielectric tensor  $\epsilon$  being always *symmetric*, it may in each point be transformed on diagonal form, and to obtain simpler formulae it will, therefore, be convenient to transform to new generalized, orthogonal coordinates

$$\left. \begin{aligned} (\xi, \eta, \zeta) &= (\xi(x, y, z), \eta(x, y, z), \zeta(x, y, z)) \\ ds^2 &= dx^2 + dy^2 + dz^2 = g_\xi d\xi^2 + g_\eta d\eta^2 + g_\zeta d\zeta^2 \\ g_\xi &= \left(\frac{\partial x}{\partial \xi}\right)^2 + \left(\frac{\partial y}{\partial \xi}\right)^2 + \left(\frac{\partial z}{\partial \xi}\right)^2, \quad g_\eta = \left(\frac{\partial x}{\partial \eta}\right)^2 + \left(\frac{\partial y}{\partial \eta}\right)^2 + \left(\frac{\partial z}{\partial \eta}\right)^2, \\ g_\zeta &= \left(\frac{\partial x}{\partial \zeta}\right)^2 + \left(\frac{\partial y}{\partial \zeta}\right)^2 + \left(\frac{\partial z}{\partial \zeta}\right)^2. \end{aligned} \right\} (1)$$

( $g_\xi, g_\eta, g_\zeta$  are the only non-vanishing elements of the fundamental metric tensor  $g_{ik}$  of the  $(\xi, \eta, \zeta)$  coordinate system).

Here the transformation matrix  $\left| \frac{\partial x^i}{\partial \xi^k} \right|$  is determined so that  $\epsilon$  is in *each* point of the  $(\xi, \eta, \zeta)$  coordinate system on diagonal form. In case the medium is homogeneous, the transformation becomes simply orthogonal with constant coefficients and  $g_\xi = g_\eta = g_\zeta = 1$ , otherwise it consists in general of non-linear functions of  $(x, y, z)$ ,



$g_{\xi}, g_{\eta}, g_{\zeta}$  being then functions of  $(\xi, \eta, \zeta)$ . Now  $\frac{\partial S}{\partial \xi} = S_{\xi}, \frac{\partial S}{\partial \eta} = S_{\eta}, \frac{\partial S}{\partial \zeta} = S_{\zeta}$  are the covariant components of  $\text{grad } S$  in the  $(\xi, \eta, \zeta)$  coordinate system, and the elements of the tensor in § 2 (14) the mixed components,  $\mu \varepsilon_k^i - \delta_k^i (\text{grad } S)^2 + (\text{grad } S)^i (\text{grad } S)_k$ . Expressed in terms of the covariant components  $S_{\xi}, S_{\eta}, S_{\zeta}$  our equation § 2 (14) thus becomes, because in case of an orthogonal coordinate system we have  $S^i = g^{ii} S_i = \frac{1}{g_{ii}} S_i$  (no summation over  $i$ ),

$$\begin{aligned} & \mu^3 \varepsilon_{\xi} \varepsilon_{\eta} \varepsilon_{\zeta} \left| \begin{array}{ccc} 1 - \frac{(\text{grad } S)^2 - \frac{1}{g_{\xi}^2} S_{\xi}^2}{\mu \varepsilon_{\xi}} & \frac{S_{\xi} S_{\eta}}{g_{\xi} \mu \varepsilon_{\xi}} & \frac{S_{\xi} S_{\zeta}}{g_{\xi} \mu \varepsilon_{\xi}} \\ \frac{S_{\eta} S_{\xi}}{g_{\eta} \mu \varepsilon_{\eta}} & 1 - \frac{(\text{grad } S)^2 - \frac{1}{g_{\eta}^2} S_{\eta}^2}{\mu \varepsilon_{\eta}} & \frac{S_{\eta} S_{\zeta}}{g_{\eta} \mu \varepsilon_{\eta}} \\ \frac{S_{\zeta} S_{\xi}}{g_{\zeta} \mu \varepsilon_{\zeta}} & \frac{S_{\zeta} S_{\eta}}{g_{\zeta} \mu \varepsilon_{\zeta}} & 1 - \frac{(\text{grad } S)^2 - \frac{1}{g_{\zeta}^2} S_{\zeta}^2}{\mu \varepsilon_{\zeta}} \end{array} \right| = \\ & \mu^3 \varepsilon_{\xi} \varepsilon_{\eta} \varepsilon_{\zeta} \left\{ \left( 1 - \frac{(\text{grad } S)^2 - \frac{1}{g_{\xi}^2} S_{\xi}^2}{\mu \varepsilon_{\xi}} \right) \left( 1 - \frac{(\text{grad } S)^2 - \frac{1}{g_{\eta}^2} S_{\eta}^2}{\mu \varepsilon_{\eta}} \right) \left( 1 - \frac{(\text{grad } S)^2 - \frac{1}{g_{\zeta}^2} S_{\zeta}^2}{\mu \varepsilon_{\zeta}} \right) + \right. \\ & \quad + 2 \frac{S_{\xi}^2 S_{\eta}^2 S_{\zeta}^2}{g_{\xi} g_{\eta} g_{\zeta} \mu^3 \varepsilon_{\xi} \varepsilon_{\eta} \varepsilon_{\zeta}} - \frac{S_{\xi}^2 S_{\zeta}^2}{g_{\xi} g_{\zeta} \mu^2 \varepsilon_{\xi} \varepsilon_{\zeta}} \left( 1 - \frac{(\text{grad } S)^2 - \frac{1}{g_{\eta}^2} S_{\eta}^2}{\mu \varepsilon_{\eta}} \right) - \\ & \quad \left. \frac{S_{\eta}^2 S_{\zeta}^2}{g_{\eta} g_{\zeta} \mu^2 \varepsilon_{\eta} \varepsilon_{\zeta}} \left( 1 - \frac{(\text{grad } S)^2 - \frac{1}{g_{\xi}^2} S_{\xi}^2}{\mu \varepsilon_{\xi}} \right) - \frac{S_{\xi}^2 S_{\eta}^2}{g_{\xi} g_{\eta} \mu^2 \varepsilon_{\xi} \varepsilon_{\eta}} \left( 1 - \frac{(\text{grad } S)^2 - \frac{1}{g_{\zeta}^2} S_{\zeta}^2}{\mu \varepsilon_{\zeta}} \right) \right\} = \\ & \mu^3 \varepsilon_{\xi} \varepsilon_{\eta} \varepsilon_{\zeta} \left\{ 1 - \left( \frac{(\text{grad } S)^2 - \frac{1}{g_{\xi}^2} S_{\xi}^2}{\mu \varepsilon_{\xi}} + \frac{(\text{grad } S)^2 - \frac{1}{g_{\eta}^2} S_{\eta}^2}{\mu \varepsilon_{\eta}} + \frac{(\text{grad } S)^2 - \frac{1}{g_{\zeta}^2} S_{\zeta}^2}{\mu \varepsilon_{\zeta}} \right) + \right. \\ & \quad \left. + (\text{grad } S)^2 \left( \frac{S_{\xi}^2}{g_{\xi} \mu^2 \varepsilon_{\eta} \varepsilon_{\zeta}} + \frac{S_{\eta}^2}{g_{\eta} \mu^2 \varepsilon_{\zeta} \varepsilon_{\xi}} + \frac{S_{\zeta}^2}{g_{\zeta} \mu^2 \varepsilon_{\xi} \varepsilon_{\eta}} \right) \right\} = 0 \quad (\text{covariant comp. of grad } S) \\ & \mu = \mu(\xi, \eta, \zeta), \quad \varepsilon_{\xi, \eta, \zeta} = \varepsilon_{\xi, \eta, \zeta}(\xi, \eta, \zeta), \quad (\text{grad } S)^2 = \frac{1}{g_{\xi}} S_{\xi}^2 + \frac{1}{g_{\eta}} S_{\eta}^2 + \frac{1}{g_{\zeta}} S_{\zeta}^2. \quad (2) \end{aligned}$$

Here  $\varepsilon_\xi, \varepsilon_\eta, \varepsilon_\zeta$  are the principal dielectric constants in the  $(\xi, \eta, \zeta)$  coordinate system. They are in the general case of inhomogeneous media functions of  $\xi, \eta, \zeta$ . We see in fact, as already announced, that (2) is a partial differential equation for the phase function  $S$ , which is of the first order and the 4<sup>th</sup> degree. We note that writing each factor of the first term in the form  $\left(1 - \frac{(\text{grad } S)^2}{\mu\varepsilon_\xi}\right) + \frac{S_\xi^2}{g_\xi\mu\varepsilon_\xi}, \dots$  we would have obtained (2) in the form

$$\frac{\frac{1}{g_\xi} S_\xi^2}{(\text{grad } S)^2 - \mu\varepsilon_\xi} + \frac{\frac{1}{g_\eta} S_\eta^2}{(\text{grad } S)^2 - \mu\varepsilon_\eta} + \frac{\frac{1}{g_\zeta} S_\zeta^2}{(\text{grad } S)^2 - \mu\varepsilon_\zeta} = 1. \quad (\text{covariant}) \quad (3)$$

If we multiply on both sides with  $(\text{grad } S)^2$  and next subtract  $(\text{grad } S)^2$  from both sides, (3) may also be written in the form

$$\frac{\mu\varepsilon_\xi \frac{1}{g_\xi} S_\xi^2}{(\text{grad } S)^2 - \mu\varepsilon_\xi} + \frac{\mu\varepsilon_\eta \frac{1}{g_\eta} S_\eta^2}{(\text{grad } S)^2 - \mu\varepsilon_\eta} + \frac{\mu\varepsilon_\zeta \frac{1}{g_\zeta} S_\zeta^2}{(\text{grad } S)^2 - \mu\varepsilon_\zeta} = 0. \quad (\text{covariant}) \quad (4)$$

We note that the two last equations are just the generalization of the well-known *normal equation of FRESNEL* (in the covariant form).

In order to prove FERMAT's and HUYGENS' principles it is now only necessary to write (2) in Hamiltonian form and then calculate the corresponding Lagrangian function  $L$ , which function shall then turn out to be equal to the integrand in § 1 (1). By this procedure there is, however, a difficulty because  $L$ , in the case of an isotropic medium, becomes homogeneous of the first degree in  $\dot{x}, \dot{y}, \dot{z}$ , the ray index being in this case only dependent on  $x, y, z$ —and furthermore equal to the index of refraction. In this case the Legendre transformation from the variables  $\dot{x}, \dot{y}, \dot{z}$  to the generalized momentum variables  $p_x, p_y, p_z$ , being necessary in order to write the equations in Hamiltonian form, becomes impossible<sup>1</sup>. In order to avoid this complication we shall, therefore, assume that all the light rays considered are of such a kind that we may as the parameter  $\tau$  in § 1 (1) choose one

<sup>1</sup> COURANT-HILBERT (1937) chap. II § 9.



of the variables  $\xi, \eta, \zeta$  themselves which will in practice always be so<sup>1</sup>. The equation for the phase function  $S$ , (2), containing only terms of the 0<sup>th</sup>, 2<sup>nd</sup> and 4<sup>th</sup> degree, we may solve it with respect to  $S_\xi$ , assuming in what follows  $\xi$  to be the parameter. We thus in general obtain two different solutions (which may be shown always to be both real) corresponding to the well-known fact that we have in general two different kinds of rays, called the *ordinary* and the *extraordinary*, respectively, which coincide only in the case of isotropic media:

$$S_\xi + H^\pm(\xi, \eta, \zeta, S_\eta, S_\zeta) = 0 \quad (5)$$

$$H^\pm(\xi, \eta, \zeta, S_\eta, S_\zeta) = -\sqrt{-\frac{1}{2}\Phi \pm \sqrt{\frac{1}{2}\Phi^2 - \Psi}} \quad (6)$$

$$\Phi = \left(\frac{\varepsilon_\eta}{\varepsilon_\xi} + 1\right) \frac{g_\xi}{g_\eta} S_\eta^2 + \left(\frac{\varepsilon_\zeta}{\varepsilon_\xi} + 1\right) \frac{g_\xi}{g_\zeta} S_\zeta^2 - \mu(\varepsilon_\eta + \varepsilon_\zeta) g_\xi$$

$$\begin{aligned} \Psi = & \frac{\varepsilon_\eta}{\varepsilon_\xi} \frac{g_\xi^2}{g_\eta^2} S_\eta^4 + \frac{\varepsilon_\zeta}{\varepsilon_\xi} \frac{g_\xi^2}{g_\zeta^2} S_\zeta^4 + \left(\frac{\varepsilon_\eta + \varepsilon_\zeta}{\varepsilon_\xi}\right) \frac{g_\xi^2}{g_\eta g_\zeta} S_\eta^2 S_\zeta^2 - \mu \left(\frac{\varepsilon_\eta \varepsilon_\zeta}{\varepsilon_\xi} + \varepsilon_\eta\right) \frac{g_\xi^2}{g_\eta} S_\eta^2 - \\ & \mu \left(\frac{\varepsilon_\eta \varepsilon_\zeta}{\varepsilon_\xi} + \varepsilon_\zeta\right) \frac{g_\xi^2}{g_\zeta} S_\zeta^2 + \mu^2 \varepsilon_\eta \varepsilon_\zeta g_\xi^2. \end{aligned}$$

Here (5) is just of the form of a HAMILTON-JACOBI partial differential equation for the phase function  $S$ , which function thus corresponds to HAMILTON'S principal action—or characteristic—function,  $\xi$  corresponding to the time variable. Next  $H^\pm = H^\pm(\xi, \eta, \zeta, p_\eta, p_\zeta)$  given in (6) are the two Hamiltonian functions corresponding to the ordinary and the extraordinary ray, respectively. Furthermore,  $p_\eta, p_\zeta$  are the generalized momentum variables defined as usual by

$$p_\eta = S_\eta, \quad p_\zeta = S_\zeta. \quad (7)$$

We note that the two signs of the first  $\sqrt{\quad}$  in (6) do not correspond to two different light propagations, but determine only the direction of the light rays. We have chosen the negative sign in order to make the normal and the ray directions point to the same

<sup>1</sup> Cf. also CARATHÉODORY (1937) p. 9.

side of the wave fronts, i. e. have an angle between them less than  $\frac{\pi}{2}$ .

From the general theory of partial differential equations of the first order (<sup>1</sup> p. 11) it follows that the equation (5) has a complete solution (i. e. a solution containing three arbitrary constants of integration), which may be written in the form

$$\left. \begin{aligned} S^\pm(\xi, \eta, \zeta) &= \int_{P_0}^P L^\pm(\xi, \eta, \zeta, \dot{\eta}, \dot{\zeta}) d\xi + S(\xi_0, \eta_0, \zeta_0), \\ P &= (\xi, \eta, \zeta), \quad P_0 = (\xi_0, \eta_0, \zeta_0). \end{aligned} \right\} (8)$$

Here  $S(\xi_0, \eta_0, \zeta_0)$  is an arbitrary function of  $P_0$  giving the initial values of  $S$  on an arbitrary boundary surface  $F(\xi_0, \eta_0, \zeta_0) = 0$ . In case this surface is a wave front, we have  $S(P_0) = \text{const}$  on this surface. (We note that  $S(P)$  corresponds to the indefinite integral,  $\int_{P_0}^P L d\xi$  to the definite integral in the case of differential equations with only one unknown.) Next it follows from the general theory that (5) is equivalent to the variation problem

$$\delta \int_{P'}^P L^\pm d\xi = 0. \tag{9}$$

The Lagrangian function  $L$  occurring in (8) and (9) is, furthermore, obtained by differentiating (8) along the integration curve and using (5) and (7)

$$L^\pm(\xi, \eta, \zeta, \dot{\eta}, \dot{\zeta}) = -H^\pm + p_\eta \dot{\eta} + p_\zeta \dot{\zeta}. \tag{10}$$

Finally  $\eta = \eta^\pm(\xi)$  and  $\zeta = \zeta^\pm(\xi)$  occurring in (8) and (9) are the coordinates of the ordinary, respectively extraordinary light ray between  $P_0$  and  $P$ . They are given uniquely as solutions of the Hamiltonian system of ordinary differential equations

$$\left. \begin{aligned} \dot{\eta} &= \frac{d\eta}{d\xi} = \frac{\partial H^\pm}{\partial p_\eta} & \dot{\zeta} &= \frac{d\zeta}{d\xi} = \frac{\partial H^\pm}{\partial p_\zeta} \\ \dot{p}_\eta &= \frac{dp_\eta}{d\xi} = -\frac{\partial H^\pm}{\partial \eta} & \dot{p}_\zeta &= \frac{dp_\zeta}{d\xi} = -\frac{\partial H^\pm}{\partial \zeta}. \end{aligned} \right\} (11)$$

In the general case the principal dielectric constants  $\epsilon_\xi, \epsilon_\eta, \epsilon_\zeta$ , the magnetic permeability  $\mu$  as well as the elements of the funda-



mental metric tensor  $g_\xi, g_\eta, g_\zeta$  of the  $(\xi, \eta, \zeta)$  coordinate system are functions of  $\xi, \eta, \zeta$  and the same, therefore, applies to  $H^\pm$ . If, especially, they are all constants,  $H^\pm$  becomes independent of  $\xi, \eta, \zeta$ , and (11) is then immediately solved to

$$\begin{aligned} \dot{p}_\eta = \dot{p}_\zeta = 0 \quad \text{i. e.} \quad p_\eta = \text{const} = c_1, \quad p_\zeta = \text{const} = c_2 \\ \dot{\eta} = \text{const} = f_\eta(c_1, c_2), \quad \dot{\zeta} = \text{const} = f_\zeta(c_1, c_2), \\ \text{i. e.} \end{aligned} \quad \left. \begin{aligned} \eta &= f_\eta(c_1, c_2) \xi + c_3 \\ \zeta &= f_\zeta(c_1, c_2) \xi + c_4. \end{aligned} \right\} (12)$$

In the generalized coordinates  $\xi, \eta, \zeta$  the light rays are thus straight lines if  $\varepsilon_\xi, \varepsilon_\eta, \varepsilon_\zeta, \mu, g_\xi, g_\eta, g_\zeta$  are constants. This is just the case for a *homogeneous* medium. Here the transformation  $(x, y, z) \rightarrow (\xi, \eta, \zeta)$  may, as already mentioned, simply be taken as a linear, orthogonal transformation, i. e. a rotation of the Cartesian coordinate system. Thus the light rays are also straight lines in the coordinates  $(x, y, z)$  of real space. For *inhomogeneous* media the light rays, however, in general are curved lines<sup>1</sup>.

Now (8) just expresses HUYGENS' principle, as it follows from this equation that if  $S^\pm = \text{const} = c$  is one wave front, then we obtain the neighbouring wave fronts  $S = c \pm dc$  by drawing through each point of the first wave front a light ray and on each of these rays mark out the distance  $\pm ds$  given by

$$\left. \begin{aligned} ds &= \sqrt{g_\xi d\xi^2 + g_\eta d\eta^2 + g_\zeta d\zeta^2} = \sqrt{dx^2 + dy^2 + dz^2} = \frac{dc}{n} \\ n &= n^\pm(\xi, \eta, \zeta, \dot{\eta}, \dot{\zeta}) = \frac{L^\pm}{\frac{ds}{d\xi}} = \frac{L^\pm}{\sqrt{g_\xi + g_\eta \dot{\eta}^2 + g_\zeta \dot{\zeta}^2}}. \end{aligned} \right\} (13)$$

<sup>1</sup> We note that a treatment of geometrical optics based on eqs. (5)–(6), which is due to HAMILTON, shows, as already stressed by HAMILTON himself, a very close analogy with classical mechanics. It was just this analogy which led SCHRÖDINGER (1926) to his discovery of wave mechanics by his idea of interpreting the mechanical principal action function of HAMILTON as a phase function of the DE BROGLIE waves (or in mathematical language, of interpreting the HAMILTON-JACOBI eq. as the characteristic equation of a wave equation). In fact, starting with the H-J eq. and carrying out, in the opposite order the calculations (with  $\lambda_0 \rightarrow \hbar$ ) which led us from the wave eq. § 2 (7) to the H-J eq. § 3 (5), just leads to the time dependent SCHRÖDINGER wave eq. Consequently, conditions corresponding to those in § 2 for the validity of geometrical optics, viz. small wave-length, apply to the validity of classical mechanics.

We may now interpret the phase function  $S^\pm(P, P') = \int_{P'}^P nds = c \int_{P'}^P dt$ , in which the integral is taken along a light ray between two arbitrary points  $P'$  and  $P$ , as a geodetic distance, equal to the time interval, between the points  $P'$  and  $P$ . ( $S$  is then called the characteristic function or the *eiconal*). Two wave fronts given by  $S = c'$  and  $S = c$ , respectively, may then be said to be geodetic parallel surfaces corresponding to the fixed distance  $S(P, P') = c - c'$ ,  $P'$  being an arbitrary point of the first wave front and  $P$  the point of intersection between the ray through  $P'$  and the second wave front; for it follows (<sup>1</sup>p. 11) that ( $\alpha$ )  $S(P, P')$  is independent of  $P'$  and ( $\beta$ )  $\delta S(P, P') = 0$  for each fixed  $P'$  and  $P$  varying in the second wave front. Hence, if we plot a geodetic 'sphere' with radius  $c - c'$  about each  $P'$ , i. e. a surface—called a *ray surface*—having the constant geodetic distance  $c - c'$  from  $P'$ , then, for each of these surfaces, we also have  $\delta S(P, P') = 0$ . This fact, however, just means that the second wave front is the envelope of all the geodetic 'spheres', which is exactly HUYGENS' principle. We note, furthermore, that because of the property  $\delta S = 0$  the light rays may in a generalized sense be said to be transverse to the wave fronts. They are, therefore, also called the transversal curves—not to be confused with the orthogonal, or normal, trajectories, the direction of which are given by  $\text{grad } S$ .

Introducing  $n$  from (13) in (9) and comparing with § 1 (1), we see that in order to establish FERMAT'S principle it now only remains to prove that  $n$  defined by (13) is identical with the ray index defined in § 1 (2). We treat isotropic and anisotropic media separately.

(A). Isotropic media.

Such media are characterized by the dielectric tensor reducing to a scalar, i. e.  $\epsilon_\xi = \epsilon_\eta = \epsilon_\zeta = \epsilon = \epsilon(x, y, z)$ . Consequently we can put  $(\xi, \eta, \zeta) = (x, y, z)$ , i. e. our fixed Cartesian coordinates. In this case the ordinary and the extraordinary rays are seen to coincide, since our equations reduce to the following

$$\left. \begin{aligned} \Phi &= 2(S_y^2 + S_z^2 - \mu\epsilon) \\ \Psi &= (S_y^2 + S_z^2 - \mu\epsilon)^2 \end{aligned} \right\} \text{i. e. } \frac{1}{4} \Phi^2 - \Psi = 0 \quad (14)$$

$$\text{i. e. } H^+ = H^- = H = -\sqrt{-\frac{1}{2} \Phi}$$



$$S_x + H = S_x - \sqrt{\mu\epsilon - S_y^2 - S_z^2} = 0 \quad \text{i. e.} \quad (\text{grad } S)^2 = \mu\epsilon \quad (15)$$

$$\dot{y} = \frac{dy}{dx} = \frac{\partial H}{\partial p_y} = \frac{p_y}{\sqrt{\mu\epsilon - p_y^2 - p_z^2}}, \quad \dot{z} = \frac{dz}{dx} = \frac{\partial H}{\partial p_z} = \frac{p_z}{\sqrt{\mu\epsilon - p_y^2 - p_z^2}} \quad (16)$$

$$L = -H + p_y \dot{y} + p_z \dot{z} = \sqrt{\mu\epsilon - p_y^2 - p_z^2} + \frac{p_y^2 + p_z^2}{\sqrt{\mu\epsilon - p_y^2 - p_z^2}} = \frac{\mu\epsilon}{\sqrt{\mu\epsilon - p_y^2 - p_z^2}} \quad (17)$$

$$\frac{ds}{dx} = \sqrt{1 + \dot{y}^2 + \dot{z}^2} = \sqrt{\frac{\mu\epsilon}{\mu\epsilon - p_y^2 - p_z^2}} \quad (18)$$

$$n = n(x, y, z) = \frac{L}{\frac{ds}{dx}} = \sqrt{\mu(x, y, z) \epsilon(x, y, z)}. \quad (19)$$

(19) is, however, just the MAXWELL relation for the index of refraction  $= \frac{c}{v}$ , q. e. d. From (16) it next follows, by means of (15) and (7), that the normal direction,  $\text{grad } S$ , and the ray direction,  $(1, \dot{y}, \dot{z})$ , coincide:

$$\text{grad } S = (-H, p_y, p_z) = \sqrt{\mu\epsilon - p_y^2 - p_z^2} (1, \dot{y}, \dot{z}). \quad (20)$$

Consequently, the index of refraction and the ray index coincide. (15) together with (19) and (20) may finally be written in the well-known form<sup>1</sup>

$$\text{grad } S = n\mathbf{s} = \sqrt{\mu\epsilon} \mathbf{s}, \quad \mathbf{s} = \frac{\text{grad } S}{|\text{grad } S|}. \quad (21)$$

### (B). Anisotropic media.

In this case it would be extremely laborious to determine  $n^\pm$  directly from (13) and verify that it is a solution of the well-known *ray equation* of FRESNEL (in the contravariant form) obtained from the normal equation (4) by making the transformation  $\mathbf{s} \rightarrow -\hat{\mathbf{s}}$ ,  $n_n \rightarrow \frac{1}{n_r}$ ,  $\epsilon_i \rightarrow \frac{1}{\epsilon_i}$  (together with  $\hat{s}_i = g_i \hat{s}^i$ )<sup>2</sup>

$$\frac{g_\xi (\hat{s}^\xi)^2}{n_r^2 - \mu\epsilon_\xi} + \frac{g_\eta (\hat{s}^\eta)^2}{n_r^2 - \mu\epsilon_\eta} + \frac{g_\zeta (\hat{s}^\zeta)^2}{n_r^2 - \mu\epsilon_\zeta} = 0 \quad (\text{contravariant}) \quad (22)$$

<sup>1</sup> BORN (1933) p. 48.

<sup>2</sup> BORN (1933) p. 225.

in which

$$\mathfrak{s} = (\mathfrak{s}^\xi, \mathfrak{s}^\eta, \mathfrak{s}^\zeta) = \frac{1}{\sqrt{g_\xi + g_\eta \dot{\eta}^2 + g_\zeta \dot{\zeta}^2}} (1, \dot{\eta}, \dot{\zeta}) \quad (\text{contravariant}) \quad (23)$$

is a unit vector in the ray direction and  $\mathfrak{s}^\xi, \mathfrak{s}^\eta, \mathfrak{s}^\zeta$  its contravariant components in the  $\xi, \eta, \zeta$  coordinate system. We may, however, make a short cut, observing that the index of refraction  $n_n = \frac{c}{v_n}$  is equal to the rate of change of the phase function  $S$  in the direction of the normal given by  $d\mathbf{s} = \text{const. grad } S$

$$dS = (\text{grad } S, d\mathbf{s}) = n_n ds, \quad (24)$$

whereas the ray index  $n_r = \frac{c}{v_r}$  is equal to the rate of change of  $S$  in the ray direction given by  $d\mathfrak{s} = \text{const. } (1, \dot{\eta}, \dot{\zeta})$

$$dS = (\text{grad } S, d\mathfrak{s}) = n_r d\mathfrak{s}. \quad (25)$$

Considering two neighbouring wave fronts  $S$  and  $S + dS$ , we have  $ds = d\mathfrak{s} \cos(\mathbf{s}, \mathfrak{s}) = d\mathfrak{s}(\mathbf{s} \cdot \mathfrak{s})$ , and the well-known relation follows:

$$n_r = n_n (\mathbf{s} \cdot \mathfrak{s}). \quad (26)$$

From (24), (5) and (7) we now have that the covariant components of  $\text{grad } S$  still satisfy (21) with  $n = n_n$ :

$$\text{grad } S = (S_\xi, S_\eta, S_\zeta) = (-H, p_\eta, p_\zeta) = n_n (s_\xi, s_\eta, s_\zeta). \quad (\text{covariant}) \quad (27)$$

Introducing (27) in (4),  $n_n = n_n^\pm(\xi, \eta, \zeta, s_\xi, s_\eta, s_\zeta)$  is thus seen to be a root in FRESNEL'S normal equation (in the covariant form)

$$\frac{\frac{1}{g_\xi} s_\xi^2}{\frac{n_n^2}{\mu \epsilon_\xi} - 1} + \frac{\frac{1}{g_\eta} s_\eta^2}{\frac{n_n^2}{\mu \epsilon_\eta} - 1} + \frac{\frac{1}{g_\zeta} s_\zeta^2}{\frac{n_n^2}{\mu \epsilon_\zeta} - 1} = 0. \quad (\text{covariant}) \quad (28)$$

Introducing (27) in (10) then just gives, with the use of (26), for the integrand in (9) of either sort of ray

$$\left. \begin{aligned} Ld\xi &= (-H + p_\eta \dot{\eta} + p_\zeta \dot{\zeta}) d\xi = (n_n s_\xi + n_n s_\eta \dot{\eta} + n_n s_\zeta \dot{\zeta}) d\xi = \\ &= n_n (s_\xi \mathfrak{s}^\xi + s_\eta \mathfrak{s}^\eta + s_\zeta \mathfrak{s}^\zeta) \sqrt{g_\xi + g_\eta \dot{\eta}^2 + g_\zeta \dot{\zeta}^2} d\xi = \\ &= n_n (\mathbf{s} \cdot \mathfrak{s}) d\mathfrak{s} = n_r d\mathfrak{s}, \end{aligned} \right\} \quad (29)$$



q. e. d.  $n_n^\pm$  satisfying the normal equation (28) it follows as usual that  $n_r^\pm$  satisfies the ray equation (22).

In conclusion we see that FERMAT'S principle has now been proved for both the ordinary and the extraordinary ray in the most general case of a non-ferromagnetic, absorbing, inhomogeneous, anisotropic medium under the one assumption that the magnetic permeability scalar  $\mu$  and the dielectric tensor  $\varepsilon$  are *continuous* functions of  $x, y, z$ . If, however, we have a discontinuity surface, i. e. two neighbouring media with different values of  $\mu$  and  $\varepsilon$ , a case which is of the utmost practical importance, then we have—for either sort of ray—in the first medium a certain Hamiltonian  $H^{(1)}$  and Lagrangian  $L^{(1)}$  and in the second medium another one,  $H^{(2)}$  and  $L^{(2)}$ , respectively. Now in both media the phase function  $S$  satisfies the HAMILTON-JACOBI equation (5) and is given by (8). Next it follows from the general theory of partial differential equations<sup>1</sup> that  $S$  is uniquely given from the equation and the boundary conditions, i. e. the functions  $F(\xi_0, \eta_0, \zeta_0) = 0$  and  $S(\xi_0, \eta_0, \zeta_0)$  in (8). Thus, if the values of  $S$  are given on a certain surface  $F(\xi_0, \eta_0, \zeta_0) = 0$  in the first medium, the values of  $S$  on the discontinuity surface will be determined by the equation. Next, these values of  $S$  being the boundary values in the second medium, we see that the behaviour of  $S$  is uniquely determined in *both* media and that  $S$  is a continuous function given by (8) throughout. From this fact, which is equivalent to the general validity of HUYGENS' principle also for discontinuously varying  $\varepsilon$  and  $\mu$ , follows the well-known law of refraction (as well as that of reflection) in the general case of both media being inhomogeneous and anisotropic, the directions of the light rays  $(1, \dot{\eta}, \dot{\zeta})$  being simply given on both sides of the discontinuity surface by (11). It may be shown<sup>2</sup> that the general law of refraction may equally well be obtained from postulating FERMAT'S principle to hold true also for discontinuity surfaces. Consequently, this principle is also generally valid.

It may be of interest to note that in the case of *isotropic* media these facts may be seen quite elementarily. It follows, namely, in this case from (21) that

$$n(\mathbf{s} \cdot d\mathbf{r}) = (\text{grad } S \cdot d\mathbf{r}) = \frac{\partial S}{\partial x} dx + \frac{\partial S}{\partial y} dy + \frac{\partial S}{\partial z} dz = dS \quad (30)$$

<sup>1</sup> COURANT-HILBERT (1937) chap. II.

<sup>2</sup> CARATHÉODORY (1937) § 23.

is a total differential, and as  $S$  is, furthermore, *continuous* throughout, we therefore have

$$\oint_C n (\mathbf{s} \cdot d\mathbf{r}) = 0 \tag{31}$$

for an arbitrary, closed curve  $C$  independent of, whether or not  $C$  passes any discontinuity surface<sup>1</sup>. From (31) it follows firstly, in the same way as in electro-dynamics, that

$$(n\mathbf{s})_{\text{tg}}^{(1)} = (n\mathbf{s})_{\text{tg}}^{(2)} \tag{32}$$

i. e. the continuity of the component  $(n\mathbf{s})_{\text{tg}}$  of the vector  $n\mathbf{s}$  in the tangent plane of the discontinuity surface. (32) is, however, just the law of refraction, which states ( $\alpha$ ) that  $\mathbf{s}^{(1)}$  and  $\mathbf{s}^{(2)}$  are both lying in the plane of incidence and ( $\beta$ ) that  $n_1 \sin \psi_1 = n_2 \sin \psi_2$ .

Secondly, it follows from (31), if  $C$  is a light ray from  $P'$  to  $P$  and  $K$  an arbitrary different curve between  $P'$  and  $P$ , that

$$\int_C n ds = \left| \int_K n (\mathbf{s} \cdot d\mathbf{r}) \right| \leq \int_K n dr \quad (|\mathbf{s}| = 1). \tag{33}$$

The curve integral of  $n$  is thus a minimum along the light ray  $C$  from  $P'$  to  $P$  and the first variation of  $\int n ds$  consequently vanishes along  $C$ , which is just FERMAT'S principle §1 (1). We note, however, that  $\delta \int n ds = 0$  does not always mean  $\int n ds = \text{min.}$ ; it may also, as is well-known, mean a relative minimum or even a maximum, e. g. by reflexions from certain curved surfaces. In fact the proof in (33) is only valid under the assumption that the light ray field  $n\mathbf{s}$  is a unique vector field, but in the case of reflexions this does not hold, two or more rays passing through each point. Nevertheless it is possible to interpret the correct formulation of FERMAT'S principle §1 (1) in terms of a minimum statement<sup>2</sup>:

*A curve  $C$  may then and only then be the path of a light ray, if every point  $P$  of  $C$  is an inner point of at least one subcurve of  $C$  with the following property: the integral  $\int n ds$  along this subcurve between its endpoints  $P'$  and  $P''$  has a lower value than the same integral taken along a different curve having the same endpoints  $P'$  and  $P''$  and lying in a certain narrow neighbourhood of  $C$ .*

We see that by this formulation the above proof in (33) is also valid for reflexions.

### Summary.

As is well-known all the laws of geometrical optics may be deduced from FERMAT'S principle or the equivalent principle of HUYGENS. It is the purpose of the present note to deduce these principles from MAXWELL'S electro-magnetic theory of light in

<sup>1</sup> We note that (31) here follows directly from the theory, whereas in BORN (1933) p. 50 it is deduced from the law of refraction.

<sup>2</sup> CARATHÉODORY (1937) p. 11.



the general case of non-ferromagnetic, absorbing, inhomogeneous, anisotropic media, at the same time obtaining the exact conditions for the validity of geometrical optics. In § 1 the problem is stated. In § 2 the equation for the phase function is deduced together with the conditions mentioned. In § 3 the phase equation is written in Hamiltonian form and FERMAT'S and HUYGENS' principles are deduced together with the generalizations of the normal and ray equations of FRESNEL. It is seen that the  $n$  occurring in FERMAT'S principle is the ray index and *not* the index of refraction, as seldom stressed in the literature. Finally the case of discontinuity surfaces is discussed.

*Institute of Theoretical Physics of the  
University of Copenhagen.*

---

### List of References.

- BORN 1933, Optik, Berlin.
- CARATHÉODORY 1935, Variationsrechnung und partielle Differentialgleichungen erster Ordnung, Leipzig.
- 1937, Geometrische Optik, Erg. d. Math. Bd. 4 Hft. 5, Berlin.
- COURANT-HILBERT 1937, Methoden d. math. Physik, Bd. II, Berlin.
- DIRAC 1930. The Principles of Quantum Mechanics, Oxford.
- DRUDE 1900, Lehrbuch der Optik, Leipzig.
- FÖRSTERLING 1928, Lehrbuch der Optik, Leipzig.
- JENTZSCH 1927, Die Beziehungen der geometrischen Optik zur Wellenoptik, Hdbuch d. Physik Bd. 18, Berlin.
- LANDÉ 1928, Optik, Mechanik und Wellenmechanik, Hdbuch d. Physik Bd. 20, Berlin.
- PLANCK 1927, Einf. in die theor. Physik Bd. 4 Optik, Leipzig.
- SCHRÖDINGER 1926, Quantisierung als Eigenwertproblem (2. Mitt.), Ann. d. Physik (4) 79, 489.
- SOMMERFELD und RUNGE 1911, Anwendung der Vektorrechnung auf die Grundlagen der geometrischen Optik, Ann. d. Physik (4) 35, 277.





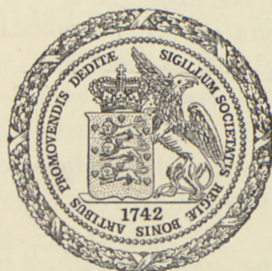
DET KGL. DANSKE VIDENSKABERNES SELSKAB  
MATEMATISK-FYSISKE MEDDELELSER, BIND XXII, NR. 9

---

# THE POTENTIAL FUNCTION OF BENZENE

BY

B. BAK



KØBENHAVN  
I KOMMISSION HOS EJNAR MUNKSGAARD  
1945



THE POTENTIAL FUNCTION  
OF BENZENE

CONTENTS

	Page
I. Introduction .....	3
II. Expression of Kinetic Energy and Potential Function. Definition of Symmetry Coordinates .....	4
III. Drawing up and Solution of the Equations for the Vibrational Movements .....	11
IV. Calculation of Some of the Force Constants of the Potential Function. 12	12
V. Calculation of Vibration Frequencies in Partly Deuterated Benzenes.. 17	17
VI. Estimate of the Error in the Force Constants .....	24
VII. The Intramolecular Forces .....	26
VIII. Summary .....	31



Printed in Denmark.  
Bianco Lunos Bogtrykkeri A/S

## I. Introduction.

Few problems have attracted the interest of chemists more than the question of setting up a correct benzene formula. A brief survey of the formulas proposed is found e.g. in WITTIG<sup>1</sup>. The final answer of chemistry is that the benzene molecule is plane and has a sixfold axis of symmetry (symmetry class  $D_{6h}$ ). But as chemical constitution proofs are produced by means of substitution processes in which the molecule to be investigated is greatly disturbed, it is very desirable to obtain confirmation of the above-mentioned result by means of physical methods. The molecule to be investigated may by such methods be exposed to minimum disturbances (e.g. by irradiation of light) so that the aspects of the structure of the molecule obtained are exceedingly reliable.

Such a physical investigation, viz. a recording of the Raman spectra of benzene and completely or partly deuterated benzenes, was made in 1936—38 in the Chemical Laboratory of the University of Copenhagen<sup>2,3</sup>. Indeed, similar investigations have been made by others,<sup>4,5</sup> but a material as great and reliable as that provided by LANGSETH, LORD, and KLIT, has not been published from other quarters. In the present work I shall therefore in the main follow LANGSETH and LORD in their interpretation of the spectra observed. The result of their investigations was that the molecule of benzene has a sixfold axis of symmetry, the same result as that appearing from the chemical

<sup>1</sup> Stereochemie, 158—60. Leipzig 1930.

<sup>2</sup> LANGSETH and KLIT. D. Kgl. Danske Vidensk. Selskab, Math.-fys. Medd. XV, No. 13 (1938).

<sup>3</sup> LANGSETH and LORD, D. Kgl. Danske Vidensk. Selskab, Math.-fys. Medd. XVI, No. 6 (1938).

<sup>4</sup> REDLICH und STRICKS. Monatshefte f. Chem. **67**, 213. **68**, 47, 374 (1936).  
<sup>5</sup> INGOLD and collaborators. Nature **135**, 1033 (1935); **139**, 880 (1937).  
Journ. Chem. Soc. London 912 (1936).



properties of the molecule. Amongst other things this means that we now know for certain that the chemical bonds from carbon atom to carbon atom is the same throughout the whole benzene ring.

LANGSETH and LORD only in one part of their work tried to utilize the values of frequency found for a quantitative determination of the valence forces of the benzene molecule. In the present work it is intended to try to utilize the available material of figures to the utmost. Even though a complete description of the potential function for the vibrations thus cannot be obtained, we are approaching appreciably to such a description, so that a single characteristic feature of the conditions of force in the molecule may be adduced. But the calculations made are also otherwise of importance, for it has proved to be possible on the basis of some of the vibration frequencies found by LANGSETH and LORD to precalculate the magnitude of others. A comparison between calculated and observed values of frequency on the whole turns out as favourable as may be expected. As LANGSETH and LORD's interpretation of the spectra of deuterated benzenes could be carried through with the greatest certainty, the agreement mentioned means confirmation of the correctness of the method of calculation used in the present work.

## II. Expression of Kinetic Energy and Potential Function. Definition of Symmetry Coordinates.

MANNEBACK and his collaborators<sup>1, 2, 3</sup> were the first to take up the question of the calculation of the intramolecular forces in benzene on a broad basis. WILSON JUNR.<sup>4</sup>, indeed, about the same time had been occupied with the potential function for the vibrational degrees of freedom, but in his calculations had only deduced formulas applying to a so-called "valence force

<sup>1</sup> Ann. Soc. Scient. Brux. LIV, 230 (1934).

<sup>2</sup> Ann. Soc. Scient. Brux. LV, 129 (1935).

<sup>3</sup> Ann. Soc. Scient. Brux. LV, 237 (1935).

<sup>4</sup> Phys. Rev. 45, 706 (1934).

model". WILSON's work includes no numerical calculations. At these it is soon proved, as will appear from what follows, that the valence force system is very little suitable for a rendering of conditions of force in the benzene molecule. In MANNEBACK's paper<sup>1</sup> some of the constants of the general quadratic potential function were calculated, but it was published three years before LANGSETH and LORD's work, so that the problem could only be subjected to a very incomplete treatment. Furthermore, the calculations seem to have been made in an unnecessarily complicated way. Finally we shall have a use for expressions of the connexion between the force constants in the potential function and the frequencies of the partly deuterated benzenes. These are completely absent in MANNEBACK's paper. So I have had to make up my mind to start all the calculations afresh.

The general quadratic potential function for the vibrations of benzene must be formulated with regard to the grouping of the vibrations in symmetry classes. The potential is expressed as a function of certain so-called symmetry coordinates  $S_i$ , found in the same number and having the same symmetry qualities as the vibrations in the symmetry class to which they belong. Here, of course, LANGSETH and LORD's classification is followed (*loc. cit.*, Table I). Table I is a survey of the symmetry coordinates.

Table I.

Symmetry class	Elements of symmetry				Number of vibrations	Zero frequencies	Symmetry coordinates
	$C_3^z$	$C_2^z$	$C_2^y$	$i$			
$A_{1g}$	+	+	+	+	2	..	$S_1 S_2$
$A_{2g}$	+	+	-	+	1	$R_z$	$S_4$
$A_{2u}$	+	+	-	-	1	$T_z$	$S_5$
$B_{1u}$	+	-	+	-	2	..	$S_7 S_8$
$B_{2g}$	+	-	-	+	2	..	$S_9 S_{10}$
$B_{2u}$	+	-	-	-	2	..	$S_{11} S_{12}$
$E_g^+$	$\varepsilon^{\pm 1}$	+	$\pm$	+	4	..	$S_{13} S_{14} S_{15} S_{16} S_{17} S_{18} S_{19} S_{20}$
$E_u^+$	$\varepsilon^{\pm 1}$	+	$\pm$	-	2	..	$S_{21} S_{22} S_{23} S_{24}$
$E_g^-$	$\varepsilon^{\pm 1}$	-	$\pm$	+	1	$R_x, R_y$	$S_{25} S_{26}$
$E_u^-$	$\varepsilon^{\pm 1}$	-	$\pm$	-	3	$T_x, T_y$	$S_{27} S_{28} S_{29} S_{30} S_{31} S_{32}$

<sup>1</sup> Ann. Soc. Scient. Brux. LV, 237 (1935).



The four last symmetry classes include degenerate vibrations, hence two symmetry coordinates must be defined for each vibration. And consequently the potential function is rendered by the equation:

$$\begin{aligned}
 2V = & a_1 S_1^2 + a_2 S_2^2 + a_3 S_1 S_2 + a_4 S_4^2 + a_5 S_5^2 + a_6 S_7 S_8 + a_7 S_7^2 + a_8 S_8^2 \\
 & + a_9 S_9^2 + a_{10} S_{10}^2 + a_{11} S_9 S_{10} + a_{12} S_{12}^2 + a_{13} S_{11} S_{12} + a_{14} S_{11}^2 \\
 & + a_{15} (S_{13}^2 + S_{17}^2) + a_{16} (S_{14}^2 + S_{18}^2) + a_{17} (S_{15}^2 + S_{19}^2) \\
 & + a_{18} (S_{16}^2 + S_{20}^2) + a_{19} (S_{13} S_{14} + S_{17} S_{18}) + a_{20} (S_{13} S_{15} + S_{17} S_{19}) \\
 & + a_{21} (S_{13} S_{16} + S_{17} S_{20}) + a_{22} (S_{14} S_{15} + S_{18} S_{19}) \\
 & + a_{23} (S_{14} S_{16} + S_{18} S_{20}) + a_{24} (S_{15} S_{16} + S_{19} S_{20}) + a_{25} (S_{21}^2 + S_{23}^2) \\
 & + a_{26} (S_{22}^2 + S_{24}^2) + a_{27} (S_{21} S_{22} + S_{23} S_{24}) + a_{28} (S_{27}^2 + S_{28}^2) \\
 & + a_{29} (S_{29}^2 + S_{30}^2) + a_{30} (S_{31}^2 + S_{32}^2) + a_{31} (S_{27} S_{29} + S_{28} S_{30}) \\
 & + a_{32} (S_{27} S_{31} + S_{28} S_{32}) + a_{33} (S_{29} S_{31} + S_{30} S_{32}) + a_{34} (S_{25}^2 + S_{26}^2).
 \end{aligned}$$

The  $a$ 's are the so-called force constants, 34 of which thus being found in the complete potential function. It is the numerical values of these 34 constants I shall try to calculate.

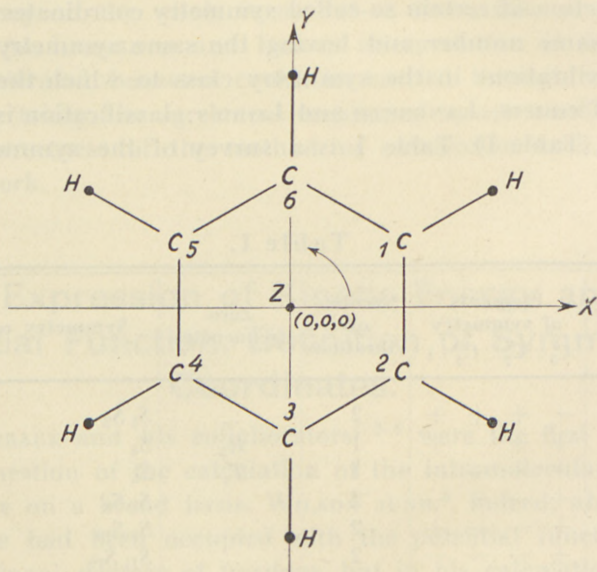


Fig. 1.

At the definition of the symmetry coordinates and the subsequent calculations the molecule is supposed to be placed in an orthogonal  $xyz$  coordinate system as shown in fig. 1.

The  $z$ -axis is perpendicular to the paper and has a positive direction towards the reader. The distance from  $(0,0,0)$  to  $C$  is denoted by  $r$  ( $= 1.40 \text{ \AA}^1$ ), the distance from  $(0,0,0)$  to  $H$  is denoted by  $R$  ( $= 2.48 \text{ \AA}^1$ ). The  $H$  and  $C$  atoms are numbered as shown in the drawing.

The components of the displacement of  $C$  atom no.  $j$  away from the position of equilibrium is denoted by

$$X_j, Y_j, Z_j \quad (j = 1, 2, 3, 4, 5, 6).$$

The components of the displacement of  $H$  atom no.  $j$  away from the position of equilibrium is denoted by

$$x_j, y_j, z_j \quad (j = 1, 2, 3, 4, 5, 6).$$

We define

$$U_j = X_j + iY_j \quad u_j = x_j + iy_j$$

$$U_j^* = X_j - iY_j \quad u_j^* = x_j - iy_j.$$

Inversely we have

$$X_j = \frac{1}{2}(U_j + U_j^*) \quad x_j = \frac{1}{2}(u_j + u_j^*)$$

$$Y = -\frac{i}{2}(U_j - U_j^*) \quad y_j = -\frac{i}{2}(u_j - u_j^*).$$

Because of the presence of the symmetry element  $C_3^Z$  it is further convenient to define the coordinates  $h_j$  and  $v_j$ , given by the equations

$$h_1 = u_1 + u_3 + u_5 \quad h_2 = u_2 + u_4 + u_6$$

$$h_3 = u_1 + \varepsilon u_3 + \varepsilon^2 u_5 \quad h_4 = u_2 + \varepsilon u_4 + \varepsilon^2 u_6$$

$$h_5 = u_1 + \varepsilon^2 u_3 + \varepsilon u_5 \quad h_6 = u_2 + \varepsilon^2 u_4 + \varepsilon u_6$$

$$v_1 = z_1 + z_3 + z_5 \quad v_2 = z_2 + z_4 + z_6$$

$$v_3 = z_1 + \varepsilon z_3 + \varepsilon^2 z_5 \quad v_4 = z_2 + \varepsilon z_4 + \varepsilon^2 z_6$$

$$v_3^* = z_1 + \varepsilon^2 z_3 + \varepsilon z_5 \quad v_4^* = z_2 + \varepsilon^2 z_4 + \varepsilon z_6$$

$$\varepsilon = -\frac{1}{2} + \frac{i}{2}\sqrt{3}$$

<sup>1</sup> The distance  $C-C = 1.40 \text{ \AA}$ , the distance  $C-H = 1.08 \text{ \AA}$ .



and analogous definitions with capital letters instead of small letters.

Inversely we have

$$\begin{aligned}
 3 u_1 &= h_1 + h_3 + h_5 & 3 u_2 &= h_2 + h_4 + h_6 \\
 3 u_3 &= h_1 + \varepsilon^2 h_3 + \varepsilon h_5 & 3 u_4 &= h_2 + \varepsilon^2 h_4 + \varepsilon h_6 \\
 3 u_5 &= h_1 + \varepsilon h_3 + \varepsilon^2 h_5 & 3 u_6 &= h_2 + \varepsilon h_4 + \varepsilon^2 h_6 \\
 3 z_1 &= v_1 + v_3 + v_3^* & 3 z_2 &= v_2 + v_4 + v_4^* \\
 3 z_3 &= v_1 + \varepsilon^2 v_3 + \varepsilon v_3^* & 3 z_4 &= v_2 + \varepsilon^2 v_4 + \varepsilon v_4^* \\
 3 z_5 &= v_1 + \varepsilon v_3 + \varepsilon^2 v_3^* & 3 z_6 &= v_2 + \varepsilon v_4 + \varepsilon^2 v_4^*.
 \end{aligned}$$

An expression of the kinetic energy  $T$  of the molecule may now be drawn up, as

$$\begin{aligned}
 2 T &= \sum_1^6 m_H (\dot{x}_j^2 + \dot{y}_j^2 + \dot{z}_j^2) + \sum_1^6 m_c (\dot{X}_j^2 + \dot{Y}_j^2 + \dot{Z}_j^2) = \\
 &\frac{1}{3} m_H (h_1 \dot{h}_1^* + h_2 \dot{h}_2^* + h_3 \dot{h}_3^* + h_4 \dot{h}_4^* + h_5 \dot{h}_5^* + h_6 \dot{h}_6^* + \dot{v}_1^2 + 2 \dot{v}_3 \dot{v}_3^* + \dot{v}_2^2 + 2 \dot{v}_4 \dot{v}_4^*) \\
 &+ \frac{1}{3} m_c (\dot{H}_1 \dot{H}_1^* + \dot{H}_2 \dot{H}_2^* + \dot{H}_3 \dot{H}_3^* + \dot{H}_4 \dot{H}_4^* + \dot{H}_5 \dot{H}_5^* + \dot{H}_6 \dot{H}_6^* + \dot{V}_1^2 + 2 \dot{V}_3 \dot{V}_3^* + \dot{V}_2^2 + 2 \dot{V}_4 \dot{V}_4^*).
 \end{aligned}$$

For the use of the coordinates  $h_j$ ,  $v_j$ ,  $H_j$ , and  $V_j$  for the definition of the symmetry coordinates it is further of importance to know how  $h_j$ ,  $v_j$ ,  $H_j$ , and  $V_j$  vary during those symmetry operations whose corresponding symmetry elements are found at the top of col. 2 in Table I.

By a rotation of  $120^\circ$  round the  $z$ -axis in the direction of the arrow we get

$$\begin{array}{llll}
 h_1 \rightarrow \varepsilon h_1 & h_2 \rightarrow \varepsilon h_2 & v_1 \rightarrow v_1 & v_2 \rightarrow v_2 \\
 h_3 \rightarrow h_3 & h_4 \rightarrow h_4 & v_3 \rightarrow \varepsilon^2 v_3 & v_4 \rightarrow \varepsilon^2 v_4 \\
 h_5 \rightarrow \varepsilon^2 h_5 & h_6 \rightarrow \varepsilon^2 h_6 & v_3^* \rightarrow \varepsilon v_3^* & v_4^* \rightarrow \varepsilon v_4^*
 \end{array}$$

and corresponding relations in capital letters.

By a rotation of  $180^\circ$  round the  $z$ -axis we get

$$\begin{array}{ll}
 h_1 \leftrightarrow -h_2 & v_1 \leftrightarrow v_2 \\
 h_3 \leftrightarrow -\varepsilon^2 h_4 & v_3 \leftrightarrow \varepsilon^2 v_4 \\
 h_5 \leftrightarrow -\varepsilon h_6 & v_3^* \leftrightarrow \varepsilon v_4^*
 \end{array}$$

By a rotation of  $180^\circ$  round the  $y$ -axis we get

$$\begin{array}{llll} h_1 \leftrightarrow -h_1^* & h_2 \rightarrow -h_2^* & v_1 \rightarrow -v_1 & v_2 \rightarrow -v_2 \\ h_3 \rightarrow -\varepsilon^2 h_3^* & h_4 \rightarrow -\varepsilon h_4^* & v_3 \rightarrow -\varepsilon^2 v_3^* & v_4 \rightarrow -\varepsilon v_4^* \\ h_5 \rightarrow -\varepsilon h_5^* & h_6 \rightarrow -\varepsilon^2 h_6^* & v_3^* \rightarrow -\varepsilon v_3 & v_4^* \rightarrow -\varepsilon^2 v_4 \end{array}$$

By inversion round  $(0,0,0)$  we finally get

$$\begin{array}{ll} h_1 \leftrightarrow -h_2 & v_1 \leftrightarrow -v_2 \\ h_3 \leftrightarrow -\varepsilon^2 h_4 & v_3 \leftrightarrow -\varepsilon^2 v_4 \\ h_5 \leftrightarrow -\varepsilon h_6 & v_3^* \leftrightarrow -\varepsilon v_4^* \end{array}$$

Corresponding relations are valid for capital letters.

Next, we may pass on to constructing the symmetry coordinates  $S_i$ .

In my doctor's thesis<sup>1</sup> I have had an opportunity to show how this is done in practice. With the symmetry class  $A_{1g}$  in benzene as an example I shall therefore only briefly state according to which criteria the symmetry coordinates  $S_1$  and  $S_2$  have been constructed.  $S_1$  and  $S_2$  are linear coordinate combinations which fulfil the following requirements:

(1)  $S_1$  and  $S_2$  must both be 0 at translational and rotational movements.

(2) As the vibrations in the  $A_{1g}$  class have the symmetry character  $C_3^z(+)$ ,  $C_2^z(+)$ ,  $C_2^y(+)$ , and  $i(+)$   $S_1$  and  $S_2$  must be invariant at the symmetry operations  $C_3^z$ ,  $C_2^z$ ,  $C_2^y$ , and  $i(0,0,0)$ .

(3) For vibrations in the  $A_{1g}$  class we have  $(S_1, S_2) \neq (0,0)$ , for vibrations in other symmetry classes  $(S_1, S_2) = (0,0)$ .

As appears, the symmetry coordinates may be selected in an infinite number of ways. The  $S_i$  chosen are rendered in Table II.

Table II.

$$\begin{array}{l} S_1 = i(\varepsilon^2 h_3 - \varepsilon h_3^* + \varepsilon^2 h_4 - \varepsilon h_4^*) \\ S_2 = i(\varepsilon^2 H_3 - \varepsilon H_3^* + \varepsilon^2 H_4 - \varepsilon H_4^*) \\ S_4 = \varepsilon^2 h_3 + \varepsilon h_3^* - \varepsilon h_4 - \varepsilon^2 h_4^* - \frac{R}{r}(\varepsilon^2 H_3 + \varepsilon H_3^* - \varepsilon H_4 - \varepsilon^2 H_4^*) \\ S_5 = v_1 + v_2 - (V_1 + V_2) \\ S_7 = i(\varepsilon h_3^* - \varepsilon^2 h_3 + \varepsilon^2 h_4^* - \varepsilon h_4) \\ S_8 = i(\varepsilon H_3^* - \varepsilon^2 H_3 + \varepsilon^2 H_4^* - \varepsilon H_4) \end{array} \quad \text{(To be continued)}$$

<sup>1</sup> B. BAK, Det intramolek. Potential. København 1943.



Table II (continued).

$S_9 = v_1 - v_2$	
$S_{10} = V_1 - V_2$	
$S_{11} = \varepsilon^2 h_3 + \varepsilon h_3^* + \varepsilon h_4 + \varepsilon^2 h_4^*$	
$S_{12} = \varepsilon^2 H_3 + \varepsilon H_3^* + \varepsilon H_4 + \varepsilon^2 H_4^*$	
$S_{13} = i(h_1 - h_1^* - h_2 + h_2^*)$	} $C_2^{II} (+)$ coordinates
$S_{14} = i(H_1 - H_1^* - H_2 + H_2^*)$	
$S_{15} = i(-\varepsilon h_5 + \varepsilon^2 h_5^* + \varepsilon^2 h_6 - \varepsilon h_6^*)$	
$S_{16} = i(-\varepsilon H_5 + \varepsilon^2 H_5^* + \varepsilon^2 H_6 - \varepsilon H_6^*)$	
$S_{17} = h_1 + h_1^* - (h_2 + h_2^*)$	} $C_2^{II} (-)$ coordinates
$S_{18} = H_1 + H_1^* - (H_2 + H_2^*)$	
$S_{19} = \varepsilon h_5 + \varepsilon^2 h_5^* - \varepsilon^2 h_6 - \varepsilon h_6^*$	
$S_{20} = \varepsilon H_5 + \varepsilon^2 H_5^* - \varepsilon^2 H_6 - \varepsilon H_6^*$	
$S_{21} = i(-\varepsilon^2 v_3 + \varepsilon v_3^* - \varepsilon v_4 + \varepsilon^2 v_4^*)$	} $C_2^{II} (+)$ coordinates
$S_{22} = i(-\varepsilon^2 V_3 + \varepsilon V_3^* - \varepsilon V_4 + \varepsilon^2 V_4^*)$	
$S_{23} = \varepsilon^2 v_3 + \varepsilon v_3^* + \varepsilon v_4 + \varepsilon^2 v_4^*$	} $C_2^{II} (-)$ coordinates
$S_{24} = \varepsilon^2 V_3 + \varepsilon V_3^* + \varepsilon V_4 + \varepsilon^2 V_4^*$	
$S_{25} = \frac{R}{r} (-\varepsilon^2 V_3 - \varepsilon V_3^* + \varepsilon V_4 + \varepsilon^2 V_4^*) + \varepsilon^2 v_3 + \varepsilon v_3^* - \varepsilon v_4 - \varepsilon^2 v_4^*$	$C_2^{II} (-)$
$S_{26} = i \frac{R}{r} (\varepsilon^2 V_3 - \varepsilon V_3^* - \varepsilon V_4 + \varepsilon^2 V_4^*) - i (\varepsilon^2 v_3 - \varepsilon v_3^* - \varepsilon v_4 + \varepsilon^2 v_4^*)$	$C_2^{II} (+)$
$S_{27} = h_1 + h_1^* + h_2 + h_2^* - (H_1 + H_1^* + H_2 + H_2^*)$	$C_2^{II} (-)$
$S_{28} = i(-h_1 + h_1^* - h_2 + h_2^*) + i(H_1 - H_1^* + H_2 - H_2^*)$	$C_2^{II} (+)$
$S_{29} = \varepsilon h_5 + \varepsilon^2 h_5^* + \varepsilon^2 h_6 + \varepsilon h_6^*$	$C_2^{II} (-)$
$S_{30} = i(\varepsilon h_5 - \varepsilon^2 h_5^* + \varepsilon^2 h_6 - \varepsilon h_6^*)$	$C_2^{II} (+)$
$S_{31} = \varepsilon H_5 + \varepsilon^2 H_5^* + \varepsilon^2 H_6 + \varepsilon H_6^*$	$C_2^{II} (-)$
$S_{32} = i(\varepsilon H_5 - \varepsilon^2 H_5^* + \varepsilon^2 H_6 - \varepsilon H_6^*)$	$C_2^{II} (+)$

Finally the possibilities of a translational and rotational movement away from the position of equilibrium are excluded by the equations

$$\begin{aligned}
 m_H (h_1 - h_1^* + h_2 - h_2^*) + m_C (H_1 - H_1^* + H_2 - H_2^*) &= 0 \\
 m_H (h_1 + h_1^* + h_2 + h_2^*) + m_C (H_1 + H_1^* + H_2 + H_2^*) &= 0 \\
 m_H (v_1 + v_2) + m_C (V_1 + V_2) &= 0 \\
 m_H R (-\varepsilon^2 v_3 - \varepsilon v_3^* + \varepsilon v_4 + \varepsilon^2 v_4^*) + m_C r (-\varepsilon^2 V_3 - \varepsilon V_3^* + \varepsilon V_4 + \varepsilon^2 V_4^*) &= 0 \\
 m_H R (\varepsilon^2 v_3 - \varepsilon v_3^* - \varepsilon v_4 + \varepsilon^2 v_4^*) + m_C r (\varepsilon^2 V_3 - \varepsilon V_3^* - \varepsilon V_4 + \varepsilon^2 V_4^*) &= 0 \\
 m_H R (\varepsilon^2 h_3 + \varepsilon h_3^* - \varepsilon h_4 - \varepsilon^2 h_4^*) + m_C r (\varepsilon^2 H_3 + \varepsilon H_3^* - \varepsilon H_4 - \varepsilon^2 H_4^*) &= 0
 \end{aligned}$$

### III. Drawing up and Solution of the Equations for the Vibrational Movements.

In what follows it is to be shown how this is done in the case of the vibrations in symmetry class  $A_{1g}$ . As regards the rest of the symmetry classes I shall content myself by stating in Table III the connexion between vibration frequencies and force constants.

The vibrations in the  $A_{1g}$  class contribute to the potential with the amount

$$A 2V = a_1 S_1^2 + a_2 S_2^2 + a_3 S_1 S_2.$$

The equations for the vibrational movements are drawn up by substitution in the formula

$$\frac{d}{dt} \left( \frac{\partial 2T}{\partial \dot{q}_K} \right) + \frac{\partial 2V}{\partial q_K} = 0.$$

For  $q_k = S_1$  we derive  $\frac{\partial 2V}{\partial S_1} = 2a_1 S_1 + a_3 S_2$  and from the expression for  $2T$ :  $\frac{\partial 2T}{\partial \dot{S}_1} = \frac{m_H}{12} \dot{S}_1$ .

Thus the equations for the movements are

$$\frac{m_H}{12} \ddot{S}_1 + 2a_1 S_1 + a_3 S_2 = 0$$

$$\frac{m_C}{12} \ddot{S}_2 + 2a_2 S_2 + a_3 S_1 = 0.$$

For harmonic vibrations we have  $\ddot{S}_1 = -\nu S_1$  and  $\ddot{S}_2 = -\nu S_2$ , so that

$$\left( 2a_1 - \frac{m_H}{12} \nu \right) S_1 + a_3 S_2 = 0$$

$$a_3 S_1 + \left( 2a_2 - \frac{m_C}{12} \nu \right) S_2 = 0.$$

The equations have only solutions  $\neq (0,0)$  for



$$\begin{vmatrix} 2a_1 - \frac{m_H}{12}z & a_3 \\ a_3 & 2a_2 - \frac{m_C}{12}z \end{vmatrix} = 0.$$

The roots of this quadratic equation in  $z$  are called  $z_1$  and  $z_2$ . We then have

$$z_1 + z_2 = 24 \left( \frac{a_2}{m_C} + \frac{a_1}{m_H} \right) \quad (1) \quad z_1 z_2 = \frac{144}{m_C m_H} (4a_1 a_2 - a_3^2) \quad (2).$$

The connexion between  $z_i$  and the frequency for the corresponding vibration  $\nu_i$  is

$$z_i = 4\pi^2 \nu_i^2.$$

Table III shows the results of corresponding calculations in the other symmetry classes. In the first column the symmetry class is stated, in the second the designation of the frequency in close accordance with LANGSETH and LORD. The third column gives the derived relations between force constants and frequencies of vibration.

#### IV. Calculation of Some of the Force Constants of the Potential Function.

In what follows this calculation is to be carried through on the basis of frequency values from LANGSETH and LORD's work. As exclusively frequencies from the molecules  $C_6H_6$  and  $C_6D_6$  are used, the formulas of Table III are immediately applicable. The results are rendered in Table IV.

It appears from the Table that in the symmetry classes  $A_{1g}$ ,  $B_{1u}$ ,  $B_{2g}$ , and  $E_u^+$  a calculation has been carried out from three constants on the basis of four frequencies.

Only in case theory and experiment completely cover one another it will be unimportant which three frequencies are used in the calculation. But here this is not so because of anharmonicity, and therefore I have, with the  $B_{2g}$  class as example, adopted the procedure of substituting the frequencies from

Table III.

Symmetry class	Frequency	Relations between frequencies and force constants
$A_{1g}$	$\nu_1 \nu_2$	$z_1 + z_2 = 24 \left( \frac{a_2}{m_C} + \frac{a_1}{m_H} \right) (1); \quad z_1 z_2 = \frac{144}{m_H m_C} (4a_1 a_2 - a_3^2) (2)$
$A_{2g}$	$\nu_3$	$z_3 = 24 a_4 \frac{m_H R^2 + m_C r^2}{m_H m_C r^2} (3)$
$A_{2u}$	$\nu_{11}$	$z_{11} = 6 a_5 \frac{m_H + m_C}{m_H m_C} (4)$
$B_{1u}$	$\nu_{12} \nu_{13}$	$z_{12} + z_{13} = 24 \left( \frac{a_8}{m_C} + \frac{a_7}{m_H} \right) (5); \quad z_{12} z_{13} = \frac{144}{m_H m_C} (4a_7 a_8 - a_6^2) (6)$
$B_{2g}$	$\nu_4 \nu_5$	$z_4 + z_5 = 6 \left( \frac{a_{10}}{m_C} + \frac{a_9}{m_H} \right) (7); \quad z_4 z_5 = \frac{9}{m_H m_C} (4a_9 a_{10} - a_{11}^2) (8)$
$B_{2u}$	$\nu_{14} \nu_{15}$	$z_{14} + z_{15} = 24 \left( \frac{a_{12}}{m_C} + \frac{a_{14}}{m_H} \right) (9); \quad z_{14} z_{15} = \frac{144}{m_H m_C} (4 a_{12} a_{14} - a_{13}^2) (10)$
$E_g^+$	$\nu_6, \nu_7, \nu_8, \nu_9$	$\begin{vmatrix} 2a_{15} - \frac{m_H}{12} z & a_{19} & a_{20} & a_{21} \\ a_{19} & 2a_{16} - \frac{m_C}{12} z & a_{22} & a_{23} \\ a_{20} & a_{22} & 2a_{17} - \frac{m_H}{12} z & a_{24} \\ a_{21} & a_{23} & a_{24} & 2a_{18} - \frac{m_C}{12} z \end{vmatrix} = 0 \quad (11)$ <p>Roots: <math>z_6, z_7, z_8, z_9</math></p>
$E_u^+$	$\nu_{16} \nu_{17}$	$z_{16} + z_{17} = 12 \left( \frac{a_{26}}{m_C} + \frac{a_{25}}{m_H} \right) (12); \quad z_{16} z_{17} = \frac{36}{m_C m_H} (4a_{25} a_{26} - a_{27}^2) (13)$
$E_g^-$	$\nu_{10}$	$z_{10} = 12 a_{34} \frac{m_C r^2 + m_H R^2}{m_H m_C r^2} (14)$
$E_u^-$	$\nu_{18}, \nu_{19}, \nu_{20}$	$\begin{vmatrix} 2a_{28} - \frac{m_H m_C}{12(m_H + m_C)} z & a_{31} & a_{32} \\ a_{31} & 2a_{29} - \frac{m_H}{12} z & a_{33} \\ a_{32} & a_{33} & 2a_{30} - \frac{m_C}{12} z \end{vmatrix} = 0 \quad (15)$ <p>Roots: <math>z_{18}, z_{19}, z_{20}</math></p>



Table IV.

Symmetry class	Experimental material		Formula used	Calculated force constants; dyn per cm.	Frequencies calculated on the basis of force constants stated	
	$C_6H_6$ ( $\text{cm}^{-1}$ )	$C_6D_6$ ( $\text{cm}^{-1}$ )			$C_6H_6$	$C_6D_6$
$A_{1g}$	$\nu_1 = 992.5$	945.2	(1) (2)	$a_1 = 2.068 \cdot 10^4$	$\nu_1 = 992.5$	934.9
	$\nu_2 = 3061.5$	2293.2		$a_2 = 5.678 \cdot 10^4$	$\nu_2 = 3061.2$	2296.5
				$a_3 = \pm 4.519 \cdot 10^4$		
$A_{2g}$	$\nu_3 = [1202]$		(3)	$a_4 = 0.2778 \cdot 10^4$		
$A_{2u}$	$\nu_{11} = 671$		(4)	$a_5 = 0.4083 \cdot 10^4$		
$B_{1u}$	$\nu_{12} = [1011.6]$	[955.2]	(5) (6)	$a_6 = \pm 4.330 \cdot 10^4$	$\nu_{12} = 1013.0$	955.7
	$\nu_{13} = [3055.1]$	[2283.8]		$a_7 = 2.078 \cdot 10^4$	$\nu_{13} = 3051.8$	2283.3
				$a_8 = 5.560 \cdot 10^4$		
$B_{2g}$	$\nu_4 = [664]$	[575]	(7) (8)	$a_9 = 1.014 \cdot 10^4$	$\nu_4 = 652.8$	587
	$\nu_5 = [1048]$	[856]		$a_{10} = 6.200 \cdot 10^4$	$\nu_5 = 1065.1$	837
				$a_{11} = \pm 1.698 \cdot 10^4$		
$E_u^+$	$\nu_{16} = 406$	350	(12) (13)	$a_{25} = 0.2757 \cdot 10^4$	$\nu_{16} = 404.8$	351.1
	$\nu_{17} = [845]$	[690]		$a_{26} = 1.859 \cdot 10^4$	$\nu_{17} = 849.7$	689.5
				$a_{27} = \pm 0.8375 \cdot 10^4$		
$E_g^-$	$\nu_{10} = 849.7$		(14)	$a_{84} = 0.2809 \cdot 10^4$		

$C_6H_6$  and  $C_6D_6$  in (7). In this way  $a_9$  and  $a_{10}$  were determined. By substitution in (8) two different values of  $(4a_9 \cdot a_{10} - a_{11}^2)$  were calculated. In the continued calculation a mean value was used. Thus the value for  $a_{11}$  of Table IV was found. Inversely we now by means of the values for  $a_9$ ,  $a_{10}$ , and  $a_{11}$  and the formulas (7) and (8) compute  $\nu_4$  and  $\nu_5$  in  $C_6H_6$  and  $C_6D_6$ . The results are rendered in col. 6 of Table IV together with results

obtained by using a similar procedure in other symmetry classes.

The experimental material in the classes  $A_{2g}$ ,  $B_{1u}$ ,  $B_{2g}$ , and  $E_u^+$  is given in square brackets. The frequencies stated are not observed in the spectra of the  $C_6H_6$  and the  $C_6D_6$  molecules, but by considerations which will be discussed below, it is possible to determine their values approximately on the basis of the partly deuterated benzenes.

The frequencies in symmetry class  $B_{1u}$  given in square brackets deviate inconsiderably from those stated by LANGSETH and LORD, *loc. cit.* p. 75. The values given there have been obtained as the result of some calculations carried out on the basis of the valence force system (pp. 29—30). In these calculations it is assumed that the potential belonging to vibrations in the symmetry classes  $A_{1g}$  and  $B_{1u}$  may be described by using three constants,  $K$ ,  $k$ ,  $q$ . We have here used six constants,  $a_1$ ,  $a_2$ ,  $a_3$ ,  $a_6$ ,  $a_7$ , and  $a_8$ , and therefore, in order not to confuse two points of view, we must find another starting-point.

We shall first try to estimate the size of  $\nu_{12}$ . The frequency is not Raman active in  $C_6H_6$  and  $C_6D_6$ , but in a number of deuterated benzenes it makes its appearance in the spectrum. The line is often displaced from its "normal" position, viz. in those deuterated benzenes in which it belongs to the same symmetry class as  $\nu_1$ . It is unperturbed in *o*- $C_6H_4D_2$  and *o*- $C_6H_2D_4$  only, and thus we may fairly well from the position of  $\nu_{12}$  in these spectra—by extrapolation—infer the position of  $\nu_{12}$  in  $C_6H_6$  and  $C_6D_6$ .

	$C_6H_6$	<i>o</i> - $C_6H_4D_2$	<i>o</i> - $C_6H_2D_4$	$C_6D_6$
Observed		992.8	974.0	
Extrapolated (1011.6)				955.2

These values only immaterially deviate from those found by LANGSETH and LORD. (1010 and 962.)

Next  $\nu_{13}$  was calculated in the following way: Those vibrations which in  $C_6H_6$  and  $C_6D_6$  are grouped in two symmetry classes  $A_{1g}$  and  $B_{1u}$ , in sym-trideuterobenzene belong to one symmetry class,  $A_1$ . All the frequencies in this symmetry class



have been measured in the Raman spectrum of sym-trideutero-benzene. Hence we may calculate  $\nu_{13}$  by means of TELLER'S product rule<sup>1</sup>

$$\frac{\nu_1 \nu_2 \nu_{12} \nu_{13} (C_6H_6)}{\nu_1 \nu_2 \nu_{12} \nu_{13} (s-C_6H_3D_3)} = 1.414 \quad \frac{\nu_1 \nu_2 \nu_{12} \nu_{13} (s-C_6H_3D_3)}{\nu_1 \nu_2 \nu_{12} \nu_{13} (C_6D_6)} = 1.414.$$

In these equations  $\nu_{13}(C_6H_6)$  and  $\nu_{13}(C_6D_6)$  are the only unknown quantities. They are calculated to be 3055.1 and 2283.8  $\text{cm.}^{-1}$ , respectively, in good agreement with LANGSETH and LORD, who record 3060 and 2290.

$a_6$ ,  $a_7$ , and  $a_8$  then could be calculated in the way stated above. It is interesting to compare the numerical values of these constants with the numerical values of  $a_1$ ,  $a_2$ , and  $a_3$ . It is seen that these constants are really with good approximation equal in twos, so that the potential in the classes  $A_{1g}$  and  $B_{1u}$  may be described by means of three different constants as assumed and shown by LANGSETH and LORD.

The frequencies in the square brackets in the  $B_{2g}$  class are estimated values as in LANGSETH and LORD'S paper. Only, in order not to confuse various points of view, the correction for anharmonicity has been omitted.

As for the frequencies in the  $E_u^+$  class, reference may be made to the chapter on The Non-Planar Vibrations p.66 ff. in LANGSETH and LORD. For the frequencies in the  $A_{2g}$  class see *ibid.* pp. 65—66.

Thus it has proved possible to calculate 15 out of the 34 constants of the potential function. The reason why not all the 34 constants can be computed is a double one, viz. partly difficulties about the calculation which have not yet been overcome, partly lack of experimental material. Difficulties of the first category are found in the symmetry classes  $E_g^+$  and  $E_u^-$ . In these classes respectively 10 and 6 constants enter. In  $C_6H_6$ ,  $C_6D_6$ , and  $s-C_6H_3D_3$  the available spectroscopically determined numerical material includes 31 frequencies, and in the spectra of the other deuterated benzenes there is also numerical material from which the values of the 16 constants mentioned depend. But so far I have not been able to overcome the dif-

<sup>1</sup> LANGSETH and LORD, *loc. cit.* pp. 14—17.

difficulties of a solution of the complicated equations (11) and (15)—that is to say, if these equations are to be utilized for the determination of the unknown force constants.

The lack of experimental material is felt particularly in the symmetry class  $B_{2u}$ ; for here the vibrations are neither active in the Raman spectrum nor in infrared absorption.

In what follows the reliability of the values of the force constants computed here is to be tried through a precalculation of vibration frequencies for the *partly* deuterated benzenes and a comparison with those determined experimentally. For three of the constants,  $a_4$ ,  $a_5$ , and  $a_{34}$ , it is already now possible to carry out a test calculation. These constants were calculated by means of frequencies from the  $C_6H_6$  spectrum. We may now by means of the values of the constants and the equations (3), (4), and (14) precalculate three of the vibration frequencies in the spectrum of  $C_6D_6$ .

Calculated frequencies	Observed frequencies
$\nu_3 = 933$	924
$\nu_{11} = 492.5$	503
$\nu_{10} = 661.0$	663.5

The agreement must be designated as good.

## V. Calculation of Vibration Frequencies in the Partly Deuterated Benzenes.

In the following considerations it is very useful to look at figs. 2 a and 2 b in LANGSETH and LORD (p. 14). Fig. 2 a is a survey of symmetry classes of the planar vibrations in  $C_6H_6$  and deuterated benzenes. Fig. 2 b is a corresponding survey of the non-planar vibrations. The symmetry classes in the  $C_6H_6$  and  $C_6D_6$  molecules are stated against the symbol  $D_{6h}$ , the designation of the symmetry qualities of these molecules. The symmetry classes in  $p$ - $C_6H_4D_2$  (symmetry class  $V_h$ ) are stated against  $V_h$ , etc. For the molecules with  $D_{6h}$  symmetry ( $C_6H_6$  and  $C_6D_6$ ) we have in the preceding section calculated numerical values for the force constants in the symmetry classes  $A_{1g}$ ,



$B_{1u}$ , and  $A_{2g}$  (planar vibrations), and  $B_{2g}$ ,  $A_{2u}$ ,  $E_u^+$ , and  $E_g^-$  (non-planar vibrations). From fig. 2a it appears that it will be possible to precalculate the frequencies in the  $A_1'$  class in molecules with  $D_{3h}$  symmetry ( $s\text{-}C_3H_3D_3$ ), because the  $A_1'$  class in  $D_{3h}$  molecules arises by a combination of the symmetry classes  $A_{1g}$  and  $B_{1u}$  in  $D_{6h}$  molecules. But the force constants in the  $A_{2g}$  class cannot be utilized for precalculations, as these must be combined with the force constants in either the  $B_{2u}$  or the  $E_g^+$  class, which we do not know.

Matters are considerably more favourable in the case of the non-planar vibrations. Here the force constants in all the four symmetry classes of the  $D_{6h}$  molecules are known. It is evident from fig. 2b that a calculation of the frequencies for all non-planar vibrations in all partly deuterated benzenes is possible. Therefore we shall in what follows calculate the vibration frequencies for the  $A_1'$  class in  $s\text{-}C_6H_3D_3$  and a selection of non-planar vibrations in deuterated benzenes specified below, everywhere comparing calculated and experimentally determined values.

### 1. Calculation of frequencies in $s\text{-}C_6H_3D_3$ . The $A_1'$ class.

The deuterium atoms being supposed to be placed in the positions 1, 3, and 5 (fig. 1), we have

$$\begin{aligned}
 2T = & \frac{1}{3}m_H (\dot{h}_2\dot{h}_2^* + \dot{h}_4\dot{h}_4^* + \dot{h}_6\dot{h}_6^* + \dot{v}_2^2 + 2\dot{v}_4\dot{v}_4^*) \\
 & + \frac{1}{3}m_D (\dot{h}_1\dot{h}_1^* + \dot{h}_3\dot{h}_3^* + \dot{h}_5\dot{h}_5^* + \dot{v}_1^2 + 2\dot{v}_3\dot{v}_3^*) \\
 & + \frac{1}{3}m_C (\dot{H}_1\dot{H}_1^* + \dot{H}_2\dot{H}_2^* + \dot{H}_3\dot{H}_3^* + \dot{H}_4\dot{H}_4^* + \dot{H}_5\dot{H}_5^* \\
 & + \dot{H}_6\dot{H}_6^* + \dot{V}_1^2 + 2\dot{V}_3\dot{V}_3^* + \dot{V}_2^2 + 2\dot{V}_4\dot{V}_4^*).
 \end{aligned}$$

The potential function is the sum of those contributions which in  $D_{6h}$  molecules are distributed to the classes  $A_{1g}$  and  $B_{1u}$ , thus

$$A^2V = a_1S_1^2 + a_2S_2^2 + a_3S_1S_2 + a_7S_7^2 + a_8S_8^2 + a_6S_7S_8$$

the  $a$ 's and the  $S$ 's of course having the same signification as above.

Next, it is easily inferred that

$$\frac{\partial 2T}{\partial \dot{S}_1} = \frac{m_H + m_D}{24} \dot{S}_1 + \frac{m_H - m_D}{24} \dot{S}_7$$

$$\frac{\partial 2T}{\partial \dot{S}_2} = \frac{m_C}{12} \dot{S}_2$$

$$\frac{\partial 2T}{\partial \dot{S}_7} = \frac{m_H - m_D}{24} \dot{S}_1 + \frac{m_H + m_D}{24} \dot{S}_7$$

$$\frac{\partial 2T}{\partial \dot{S}_8} = \frac{m_C}{12} \dot{S}_8.$$

The equations for the vibrational movements being drawn up as shown above, it is seen that the frequencies must be roots in the equation:

$$\begin{vmatrix} 2a_1 - \frac{m_H + m_D}{24}z & a_3 & \frac{m_D - m_H}{24}z & 0 \\ a_3 & 2a_2 - \frac{m_C}{12}z & 0 & 0 \\ \frac{m_D - m_H}{24}z & 0 & 2a_7 - \frac{m_H + m_D}{24}z & a_6 \\ 0 & 0 & a_6 & 2a_8 - \frac{m_C}{12}z \end{vmatrix} = 0.$$

From this the vibration frequencies may be computed. As for  $a_3$  and  $a_6$ , the sign of which is uncertain, it appears that only the squares of these enter. Below, calculated and observed (LANGSETH and LORD) frequencies are compared.

$s\text{-}C_6H_3D_3$ . ( $A'_1$  class).

Calculated	Observed
$\nu_1 = 945.0$	956.6
$\nu_2 = 3058.2$	3055.1
$\nu_{12} = 1003.5$	1003.9
$\nu_{13} = 2290.5$	2283.8



The agreement must be called excellent. The vibrations here considered are planar, so-called valence vibrations (see figs. 1, 2, 12, and 13 in LANGSETH and LORD, p. 10). It is a common experience that particularly with vibrations of this type one obtains good agreement between experiment and calculation.

## 2. Calculation of frequencies in $s\text{-C}_6\text{H}_3\text{D}_3$ . The $A_2'$ class.

The expression for  $2T$  is the same as above. The expression for  $A_2V$  is

$$A_2V = a_5 S_5^2 + a_9 S_9^2 + a_{10} S_{10}^2 + a_{11} S_9 S_{10}.$$

Further we have

$$\frac{\partial 2T}{\partial \dot{S}_5} = \frac{m_C(m_H + m_D)}{3N} \dot{S}_5 + \frac{m_C(m_D - m_H)}{3N} \dot{S}_9 \quad \frac{\partial 2T}{\partial \dot{S}_{10}} = \frac{m_C}{3} \dot{S}_{10}$$

$$\frac{\partial 2T}{\partial \dot{S}_9} = \frac{m_C(m_D - m_H)}{3N} \dot{S}_5 + \frac{2m_H m_D + m_C(m_H + m_D)}{3N} \dot{S}_9$$

$$N = 2m_C + m_H + m_D.$$

The determinant for the determination of the vibration frequencies here is

$$\begin{vmatrix} 2a_5 - \frac{m_C(m_H + m_D)}{3N}z & \frac{m_C(m_H - m_D)}{3N}z & 0 \\ \frac{m_C(m_H - m_D)}{3N}z & 2a_9 - \frac{2m_H m_D + m_C(m_H + m_D)}{3N} & a_{11} \\ 0 & a_{11} & 2a_{10} - \frac{m_C}{3}z \end{vmatrix} = 0.$$

The unknown sign of  $a_{11}$  is of no importance for the value of the solution. We find

$s\text{-C}_6\text{H}_3\text{D}_3$ . ( $A_2''$  class).

Calculated	Observed
$\nu_4 = 666$	691
$\nu_5 = 964$	914
$\nu_{11} = 525$	533

The observed values originate from the infrared spectrum.<sup>1</sup>—The vibrations are vibrations perpendicular to the plane of the benzene ring. Here the agreement between calculated and observed frequencies is considerably inferior to those for valence vibrations. The amplitude for non-planar vibrations is considerably greater than for valence vibrations. The anharmonicity therefore comes to play a great rôle, so that the assumption on which the calculations are made, viz. that it is sufficient to include square terms in the potential function, is less well fulfilled.

### 3. Calculation of frequencies in $s\text{-C}_6\text{H}_3\text{D}_3$ . The $E''$ class.

The symmetry coordinates to be used are  $S_{23}$ ,  $S_{24}$ , and  $S_{25}$ , originating from the symmetry classes  $E_u^+$  and  $E_g^-$  in the  $D_{6h}$  molecules. Thus we have

$$A2V = a_{25}S_{23}^2 + a_{26}S_{24}^2 + a_{27}S_{23}S_{24} + a_{34}S_{25}^2.$$

Finally it is inferred that

$$\begin{aligned} \frac{\partial 2T}{\partial \dot{S}_{23}} &= \frac{1}{6N} [m_D(m_C r^2 + m_H R^2) + m_H(m_C r^2 + m_D R^2)] \dot{S}_{24} + \\ &\quad + \frac{1}{6N} (m_D m_C r^2 - m_H m_C r^2) \dot{S}_{25} \\ \frac{\partial 2T}{\partial \dot{S}_{25}} &= \frac{1}{6N} [m_D(m_C r^2 + m_H R^2) - m_H(m_C r^2 + m_D R^2)] \dot{S}_{23} + \\ &\quad + \frac{1}{6N} (m_D m_C r^2 + m_H m_C r^2) \dot{S}_{25} \\ \frac{\partial 2T}{\partial \dot{S}_{24}} &= \frac{m_C}{6} \dot{S}_{24} \end{aligned} \quad N = 2m_C r^2 + (m_H + m_D) R^2.$$

After setting up the determinant, etc., as above, we get:

#### $s\text{-C}_6\text{H}_3\text{D}_3$ . The $E''$ class.

Calculated frequencies	Observed frequencies <sup>2</sup>
$\nu_{10} = 676$	712
$\nu_{17} = 848$	815
$\nu_{16} = 376$	373

<sup>1</sup> INGOLD, Nature 139, 880 (1937).

<sup>2</sup> LANGSETH and LORD, *loc. cit.*



The vibrations are non-planar vibrations. Considering this the agreement must be regarded as good.

#### 4. Calculation of frequencies in $p\text{-C}_6\text{H}_4\text{D}_2$ and $p\text{-C}_6\text{HD}_{24}$ .

##### The $B_{3g}$ class.

The deuterium atoms in  $p\text{-C}_6\text{H}_4\text{D}_2$  are supposed to be placed in the positions 3 and 6. We get

$$\begin{aligned}
 2T = & \frac{1}{3} m_C (\dot{H}_1 \dot{H}_1^* + \dot{H}_2 \dot{H}_2^* + \dot{H}_3 \dot{H}_3^* + \dot{H}_4 \dot{H}_4^* + \dot{H}_5 \dot{H}_5^* + \dot{H}_6 \dot{H}_6^* + \\
 & + \dot{V}_1^2 + 2\dot{V}_3 \dot{V}_3^* + \dot{V}_2^2 + 2\dot{V}_4 \dot{V}_4^*) \\
 & + \frac{1}{3} m_H (h_1 h_1^* + h_2 h_2^* + h_3 h_3^* + h_4 h_4^* + h_5 h_5^* + h_6 h_6^* + \\
 & + \dot{v}_1^2 + 2\dot{v}_3 \dot{v}_3^* + \dot{v}_2^2 + 2\dot{v}_4 \dot{v}_4^*) \\
 & + \frac{m_D - m_H}{9} [(\dot{h}_1 + \varepsilon^2 \dot{h}_3 + \varepsilon \dot{h}_5) (\dot{h}_1^* + \varepsilon \dot{h}_3^* + \varepsilon^2 \dot{h}_5^*) + \\
 & + (\dot{h}_2 + \varepsilon \dot{h}_4 + \varepsilon^2 \dot{h}_6) (\dot{h}_2^* + \varepsilon^2 \dot{h}_4^* + \varepsilon \dot{h}_6^*) + (\dot{v}_1 + \varepsilon^2 \dot{v}_3 + \varepsilon \dot{v}_5)^2 + \\
 & + (\dot{v}_2 + \varepsilon \dot{v}_4 + \varepsilon^2 \dot{v}_6)^2].
 \end{aligned}$$

$$\frac{\partial 2T}{\partial \dot{S}_9} = \frac{3 m_C^2 r^2 (m_D - m_H)}{9 N} \dot{S}_{25} + \frac{3 m_H R^2 (m_H + 2 m_D) + 3 m_C r^2 (2 m_H + m_D)}{9 N} \dot{S}_9$$

$$\frac{\partial 2T}{\partial \dot{S}_{25}} = \frac{m_C r^2 (m_D - m_H)}{3 N} \dot{S}_9 + \frac{m_C r^2 (m_H + 2 m_D)}{6 N} \dot{S}_{25}. \quad \frac{\partial 2T}{\partial \dot{S}_{10}} = \frac{m_C}{3} \dot{S}_{10}.$$

$$N = 3 m_C r^2 + (m_H + 2 m_D) R^2.$$

$$2V = a_9 S_9^2 + a_{10} S_{10}^2 + a_{11} S_9 S_{10} + a_{34} S_{25}^2.$$

On the basis of this the frequencies are calculated in the below table.

##### $p\text{-C}_6\text{H}_4\text{D}_2$ . The $B_{3g}$ class.

Calculated frequencies	Observed frequencies
$\nu_5 = 1040$	966
$\nu_{10b} = 700$	738
$\nu_4 = 629$	634

These vibrations, too, are non-planar vibrations.

*p*-C<sub>6</sub>H<sub>2</sub>D<sub>4</sub>. The B<sub>3g</sub> class.

Calculated frequencies	Observed frequencies
$\nu_5 = 939$	927
$\nu_{10b} = 732$	765
$\nu_4 = 606$	605

The agreement is best for *p*-C<sub>6</sub>H<sub>2</sub>D<sub>4</sub>, presumably because the molecule contains more deuterium atoms than C<sub>6</sub>H<sub>4</sub>D<sub>2</sub>. Because of the greater mass the amplitudes of the deuterium atoms are smaller than those of the hydrogen atoms. The deviation of the vibrations from the harmonic mode of vibration therefore becomes smaller. (Compare the results with *o*-C<sub>6</sub>H<sub>4</sub>D<sub>2</sub> and C<sub>6</sub>H<sub>2</sub>D<sub>4</sub>).

### 5. Calculation of frequencies in *o*-C<sub>6</sub>H<sub>4</sub>D<sub>2</sub> and *o*-C<sub>6</sub>H<sub>2</sub>D<sub>4</sub>. The B<sub>2</sub> class.

The deuterium atoms in *o*-C<sub>6</sub>H<sub>4</sub>D<sub>2</sub> are supposed to be placed in the positions 4 and 5. Thus we find

$$\frac{\partial 2 T}{\partial \dot{S}_5} = \frac{m_H + 2 m_D}{9} \dot{A} + \frac{m_H - m_D}{18} \dot{S}_{23} + \frac{m_H - m_D}{18} \sqrt{3} \dot{H}$$

$$\frac{\partial 2 T}{\partial \dot{S}_{23}} = \frac{m_H - m_D}{18} \dot{A} + \frac{m_D + 5 m_H}{36} \dot{S}_{23} + \frac{m_D - m_H}{36} \sqrt{3} \dot{H}$$

$$\frac{\partial 2 T}{\partial \dot{S}_{26}} = \frac{r m_C}{6 R} \dot{K} \qquad \frac{\partial 2 T}{\partial \dot{S}_{24}} = \frac{m_C}{6} \dot{S}_{24}.$$

$$A = \frac{1}{N} \left[ m_C \left( \frac{R\sqrt{3}}{6r} (m_H + m_D) + \frac{m_C r}{R\sqrt{3}} \right) S_5 + \frac{m_C r}{6R} (m_H - m_D) S_{26} + \right. \\ \left. + \frac{m_D - m_H}{6} \left( \frac{R\sqrt{3} m_H}{3r} + \frac{m_C r}{R\sqrt{3}} \right) S_{23} \right]$$

$$H = \frac{1}{N} \left[ \frac{R m_C (m_D - m_H)}{3r} S_5 - \frac{m_C r}{3R\sqrt{3}} (2 m_H + m_D + 3 m_C) S_{26} + \right. \\ \left. + \frac{(m_H - m_D) R}{6r} (m_H + m_C) S_{23} \right]$$



$$K = \frac{1}{N} \left[ m_C \frac{m_D - m_H}{3} S_5 + \frac{\sqrt{3}}{18} (3 m_C (m_H + m_D) + m_H^2 + 5 m_H m_D) S_{26} + \frac{(m_H - m_D)(m_H + m_C)}{6} S_{23} \right]$$

$$N = \frac{R\sqrt{3}}{18r} [m_H^2 + 5 m_H m_D + 3 m_C (m_H + m_D)] + \frac{m_C r}{3\sqrt{3}R} (2 m_H + m_D + 3 m_C)$$

$$A2V = a_5 S_5^2 + a_{25} S_{23}^2 + a_{26} S_{24}^2 + a_{27} S_{23} S_{24} + a_{34} S_{26}^2.$$

By insertion of numerical values we calculate:

*o-C<sub>6</sub>H<sub>4</sub>D<sub>2</sub>. B<sub>2</sub> class.*

Calculated frequencies	Observed frequencies <sup>1</sup>
$\nu_{10a} = 676$	782
$\nu_{11} = 571$	582
$\nu_{16b} = 369$	384
$\nu_{17b} = 841$	825

*o-C<sub>6</sub>H<sub>2</sub>D<sub>4</sub>. The B<sub>2</sub> class.*

Calculated frequencies	Observed frequencies <sup>1</sup>
$\nu_{10a} = 684$	739
$\nu_{11} = 527$	—
$\nu_{16b} = 359$	369
$\nu_{17b} = 815$	778

## VI. Estimate of the Error in the Force Constants.

It may be said at once about all the force constants that experimentally badly determined differences of frequency nowhere enter into the calculations. Hence there is practically no uncertainty originating from the measurement of the spectra as regards the numerical values. On the other hand it must

<sup>1</sup> LANGSETH and LORD, *loc. cit.*

be admitted that the values involve minor errors. For actually the equations (1)–(15) were deduced on the assumption that the vibrations were harmonic, this only being so where the amplitudes are small. This assumption is fulfilled best in the case of the planar valence vibrations, so that the constants  $a_1, a_2, a_3, a_6, a_7,$  and  $a_8,$  which describe the potential for these vibrations, are determined best. Hence it also appears that at the precalculation of the vibrations in  $s\text{-}C_6H_3D_3$  (the  $A'_1$  class), where the values of these constants are used, we find values deviating at most 1 per cent. from those found experimentally.

On the other hand the constants describing changes of potential with non-planar vibrations are less well determined. The amplitudes here are so great that the vibrations become slightly anharmonic. Let us look at e. g. (14):

$$\alpha_{10} = 4\pi^2\nu_{10}^2 = 12a_{34} \frac{m_C r^2 + m_H R^2}{m_H m_C r^2}.$$

$\nu_{10}$  is the frequency for one of the non-planar vibrations. As a rule a lower value for  $\nu_{10}$  will be determined than the one which would appear if the vibration was harmonic. In rare cases, however, also a higher value. Of course it is not possible to give a common value for the error committed for all non-planar vibrations, because, as done here, we reckon with the observed frequency instead of the "harmonic" one, but in what follows, however, we shall, in accordance with ordinary spectroscopic experience,<sup>1</sup> reckon with an error of  $\pm 2$  per cent. in frequencies belonging to non-planar vibrations. As appears from (14), this involves that  $a_{34}$  is determined with an error of about  $\pm 5$  per cent. As for the constants  $a_4^2$  and  $a_5$  we obtain the same result.

For the constants  $a_9, a_{10}, a_{11}, a_{25}, a_{26},$  and  $a_{27}$  the connexion between frequencies and constants is more complicated. (7), (8), (12), (13). In what follows we shall assume that these constants, too, are exposed to an error of  $\pm 5$  per cent. The assumption of a possible error of  $\pm 5$  per cent. in the constants, corresponding to all non-planar vibrations, gives an unstrained

<sup>1</sup> Cf. LANGSETH and LORD, *loc. cit.* p. 81.

<sup>2</sup>  $a_4$  belongs to a planar deformation vibration, but the remark on anharmonicity also applies here.



explanation of the deviations found between calculated and observed frequencies for the partly deuterated benzenes.

## VII. The Intramolecular Forces.

It is now possible to calculate the forces acting on the individual atoms of the molecule when the atoms are removed from the position of equilibrium, to the same extent as we have above succeeded in establishing numerical values for the force constants in the potential function of benzene. With a view to the possibility of later treating the mechanism of reaction in processes in which benzene is involved, it should be noted that it is of the greatest importance to study those movements away from the position of equilibrium by which the numerically smallest forces become active. Among these movements we find all the non-planar vibrations, in which the amplitudes are great, i. e. there is a much greater chance to find a hydrogen atom outside the position of equilibrium perpendicular to the plane of the benzene ring than in this plane.

According to the above considerations the changes of potential by displacements of atoms perpendicular to the plane of the benzene ring are rendered by

$$\begin{aligned} 1/2 V = & a_5 S_5^2 + a_9 S_9^2 + a_{10} S_{10}^2 + a_{11} S_9 S_{10} + a_{25} (S_{21}^2 + S_{23}^2) + \\ & + a_{26} (S_{22}^2 + S_{24}^2) + a_{27} (S_{21} S_{22} + S_{23} S_{24}) + a_{34} (S_{25}^2 + S_{26}^2). \end{aligned}$$

Measured in dyne/cm. the numerical values of the force constants were determined as

$$\begin{array}{ll} a_5 = 0.408 \cdot 10^4 & a_9 = 1.01 \cdot 10^4 \\ a_{10} = 6.20 \cdot 10^4 & |a_{11}| = 1.70 \cdot 10^4 \\ a_{25} = 0.276 \cdot 10^4 & a_{26} = 1.86 \cdot 10^4 \\ |a_{27}| = 0.837 \cdot 10^4 & a_{34} = 0.281 \cdot 10^4. \end{array}$$

The values are supposed to involve an error of  $\pm 5$  per cent.

In order to learn about the forces active between the atoms of the benzene molecule on the basis of the above values, we shall examine a particularly simple movement away from the position of equilibrium. Supposing, by means which, indeed,

cannot be realized in practice, that the 11 atoms are kept in the position of equilibrium, while the 12th, *H*-atom no. 6 in fig. 1 (*H*(6)), is supposed to be displaced perpendicular to the plane of the benzene ring towards the reader. To this constellation applies

$$z_6 > 0 \quad x_6 = y_6 = 0$$

$$(x_j \ y_j \ z_j) = (0, 0, 0) \quad (j = 1, 2, 3, 4, 5)$$

$$X_j, Y_j, Z_j = (0, 0, 0) \quad (j = 1, 2, 3, 4, 5, 6)$$

By going through the expressions for  $S_1$ , etc., we find under these circumstances

$$S_5 = z_6 \quad S_9 = -z_6 \quad S_{23} = 2z_6 \quad S_{25} = -2z_6$$

$$S_{10} = S_{21} = S_{22} = S_{24} = S_{26} = 0,$$

so that

$$A2V = a_5 S_5^2 + a_9 S_9^2 + a_{25} S_{23}^2 + a_{34} S_{25}^2.$$

On the basis of this we find

$$K_{H(6)} = -\frac{\partial V}{\partial z_6} = -z_6 (a_5 + a_9 + 4(a_{25} + a_{34}))$$

$$K_{H(1)} = -\frac{\partial V}{\partial z_1} = -z_6 (a_5 - a_9 + 2(a_{34} - a_{25})) = K_{H(5)}$$

$$K_{H(2)} = -\frac{\partial V}{\partial z_2} = -z_6 (a_5 + a_9 - 2(a_{34} + a_{25})) = K_{H(4)}$$

$$K_{H(3)} = -\frac{\partial V}{\partial z_7} = -z_6 (a_5 - a_9 + 4(a_{25} - a_{34}))$$

$$K_{C(6)} = -\frac{\partial V}{\partial Z_6} = -z_6 \left( -a_5 - 4 \frac{R}{r} a_{34} \right)$$

$$K_{C(1)} = -\frac{\partial V}{\partial Z_1} = -z_6 \left( -a_5 - 2 \frac{R}{r} a_{34} \right) = K_{C(5)}$$

$$K_{C(2)} = -\frac{\partial V}{\partial Z_2} = -z_6 \left( -a_5 + 2 \frac{R}{r} a_{34} \right) = K_{C(4)}$$

$$K_{C(3)} = -\frac{\partial V}{\partial Z_3} = -z_6 \left( -a_5 + 4 \frac{R}{r} a_{34} \right).$$

$K$  denotes the force acting on the atom used as index.



By substitution of numerical values we find

$$\left. \begin{array}{l} K_{H(1)} : K_{H(2)} : K_{H(3)} : K_{H(4)} : K_{H(5)} : K_{H(6)} : K_{C(1)} : K_{C(2)} : \\ \qquad \qquad \qquad : K_{C(3)} : K_{C(4)} : K_{C(5)} : K_{C(6)} = \\ 0.595 : -0.308 : 0.626 : -0.308 : 0.595 : -3.65 : 1.40 : -0.589 : \\ \qquad \qquad \qquad : -1.58 : -0.589 : 1.40 : 2.40. \end{array} \right\}$$

The result is illustrated in fig. 2, where the length of the arrows is proportional to the magnitude of the forces.

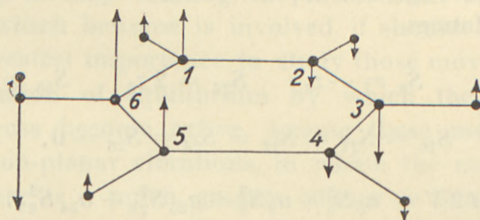


Fig. 2.

The force is of course greatest on the directly "attacked" hydrogen atom and its adjoining atom C(6). But further it is seen that forces are active on all the other atoms as well. It is seen that the forces do not decrease the longer the atom is removed from C(6) and H(6), but that e.g.  $K_{H(1)}$  and  $K_{H(3)}$  are of very nearly the same magnitude and both nearly twice as great as  $K_{H(2)}$ . Or, in other words, the hydrogen atoms in *ortho* and *para* positions to the H atom subject to force are influenced fairly in the same way, while the hydrogen atoms in *meta* positions are only influenced by nearly half the force. Nearly the same rule (applying to the numerical values of the forces) may be set up as regards the carbon atoms.

A control calculation shows that these results in the main are independent of the error of  $\pm 5$  per cent. assumed in the values of the force constants.

The above considerations may be utilized in a discussion of the usefulness of WILSON's<sup>1</sup> potential function for benzene. As mentioned, WILSON has not used the potential function

<sup>1</sup> Phys. Rev. 45, 706, (1935).

set up by him for numerical calculations. But it has been used to a limited extent by REDLICH and STRICKS<sup>1</sup> and LANGSETH and LORD<sup>2</sup>. The question is whether it may also be applied to all the vibrations of benzene.

From personal information<sup>3</sup> it is known that LANGSETH and LORD tried to carry through more extensive calculations on the basis of WILSON's potential function, but that the correspondence between calculated and observed frequencies often was so bad that they had to drop the matter. The reason why WILSON's potential system is applicable to a limited extent only is easily seen. Let us, as above, suppose  $H(6)$  to be shifted from the position of equilibrium perpendicular to the plane of the benzene ring towards the reader. Fig. 3 represents the vertical plane through  $C(6)$ ,  $H(6)$  and the shifted  $H(6)$  as placed in the horizontal plane of the benzene ring (1-2-3-4-5-6).

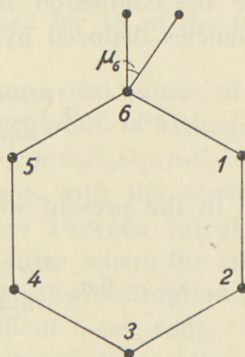


Fig. 3.

Moving  $H(6)$  requires some work, as, according to WILSON,

(a) an angle  $\mu_6$  arises between the line  $C(6)-H(6)$  and the plane defined by  $C(6)$ ,  $C(5)$ , and  $C(1)$ . Thus we have

$$\Delta V = h(R-r)^2 \mu_6^2,$$

where  $h$  is a constant.

(b) The valences  $C(5)-C(6)$  and  $C(6)-C(1)$  make a torsional movement. For this is required the work

$$\Delta V = k_2 (\varphi_{5,6}^2 + \varphi_{6,1}^2),$$

where  $k_2$  is a constant and  $\varphi_{5,6}$  is the angle by which the bond  $C(5)-C(6)$  is twisted.

As appears,  $V$  only becomes a function of the rectangular coordinates with indices 1, 5, and 6. But this means that the force acting on the  $C$  and  $H$  atoms no. 2, 3, and 4 becomes zero. We have above had an opportunity of ascertaining that the effect

<sup>1</sup> Monatshefte, *loc. cit.*

<sup>2</sup> *Loc. cit.* p. 29.

<sup>3</sup> From Professor LANGSETH.



of force on these atoms is as great as that on the atoms no. 1 and 5. WILSON in his potential function thus disregards the reciprocity of action between atoms which are not in the generally assumed structure formula connected with valence lines. Hence, WILSON's potential function is unsuitable for a rational treatment of the problems pointed out here.

This fundamental defect in WILSON's potential function must also be expected to appear at a consideration of the expressions for the connexion between force constants and vibration frequencies deduced by WILSON. According to WILSON

$$z_{11} = h \frac{m_C + m_H}{m_C m_H} \quad z_{10} = h \frac{m_C r^2 + m_H R^2}{m_H m_C r^2}.$$

In the present work it was deduced that

$$z_{11} = 6 a_5 \frac{m_C + m_H}{m_C m_H} \quad z_{10} = 12 a_{34} \frac{m_C r^2 + m_H R^2}{m_H m_C r^2}$$

WILSON uses *one* force constant,  $h$ , where *two* are used in the present work, viz.  $6 a_5$  and  $12 a_{34}$ . This approximation can be applicable only if  $6 a_5 = 12 a_{34}$ . By substitution of the numerical values found here, it appears that  $6 a_5 = 2.45$ ,<sup>1</sup> while  $12 a_{34} = 3.37$ .<sup>1</sup> Hence, it must be characterized as too rough an approximation to use one force constant only.

The results obtained in this paper seem to be of interest in another connexion. In treating problems of the electronic structure of molecules roughly two methods have crystallized out: the method of 'localized pairs' and the method of 'molecular orbitals'. It seems as if the above considerations represent a new means of deciding empirically which of the two methods should be used. In the case of the benzene molecule where a disturbance at one atom of the molecule produces a great effect on all the other atoms—independent of the distance from the atom attacked—the result is that benzene should be treated by means of the 'molecular orbitals' method, consistent with the views of E. HÜCKEL<sup>2</sup>.

<sup>1</sup> Unity:  $10^4$  dyne/cm.

<sup>2</sup> E. HÜCKEL, Z. Physik **70**, 204 (1931); **72**, 310 (1931).

## VIII. Summary.

(1) In the equations (1)–(15) the connexion is given between the vibration frequencies and the 34 force constants in the general quadratic potential function for  $C_6H_6$  and isotopic molecules.

(2) On the basis of some of the experimental material from the RAMAN spectra of  $C_6H_6$  and  $C_6D_6$  and data from infrared absorption, numerical values are established for 15 of the force constants.

(3) The correctness of the deduced numerical values of the force constants is checked through a precalculation of frequencies from the Raman spectra of  $C_6D_6$ ,  $s-C_6H_3D_3$ ,  $p-C_6H_4D_2$ ,  $p-C_6H_2D_4$ ,  $o-C_6H_4D_2$ , and  $o-C_6H_2D_4$  and a comparison with the observed values. It is estimated that the differences between calculated and observed values which are bound to arise where the vibrations are anharmonic, may be explained on the assumption that the force constants involve an error of about 5 per cent.

(4) As only 15 of the necessary 34 constants can be calculated, only an imperfect picture of conditions of force can be drawn. Only by movements perpendicular to the plane of the benzene ring a complete description of the potential may be obtained. By a specified displacement of one of the atoms fairly equal forces appear on all the atoms. The considerations advanced make it possible to demonstrate a fundamental defect in WILSON'S potential function.

The author wishes to offer his cordial thanks to Professor LANGSETH for helpful discussions on the subject.





DET KGL. DANSKE VIDENSKABERNES SELSKAB  
MATEMATISK-FYSISKE MEDDELELSER, BIND XXII, NR. 10

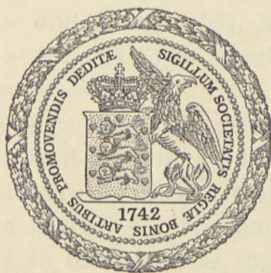
---

THE ACID DISSOCIATION OF  
THE HYDRATED LEAD ION AND THE  
FORMATION OF POLYNUCLEAR IONS

THE PRECIPITATES FORMED  
WHEN SOLUTIONS OF LEAD NITRATE AND SODIUM  
HYDROXIDE ARE MIXED

BY

KAI JULIUS PEDERSEN



KØBENHAVN

I KOMMISSION HOS EJNAR MUNKSGAARD

1945



DET KGL. DANSKE VIDENSKABENS Selskab  
MATHEMATISKE FYSIKALISKE MEDDELELSER, 22. H. Nr. 10

THE ACID DISSOCIATION OF  
THE HYDRATED LEAD ION AND THE  
FORMATION OF POLYNUCLEAR IONS

THE PRECIPITATES FORMED  
WHEN SOLUTIONS OF LEAD NITRATE AND SULFURIC  
ACID ARE MIXED

BY

K. M. JENSEN



KOBENHAVN

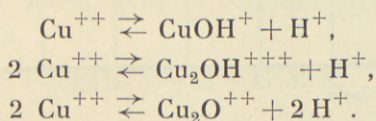
Printed in Denmark.

Bianco Lunos Bogtrykkeri A/S

## Part I.

### The Acid Dissociation of the Hydrated Lead Ion and the Formation of Polynuclear Ions.

In an earlier paper (1), the hydrogen ion concentrations of aqueous solutions of cupric nitrate were measured by means of the glass electrode. The following equilibria (omitting the water of hydration) were found:



In the present paper, a similar study of solutions of lead nitrate has been made.

The hydrogen ion concentrations of lead nitrate solutions were first measured by WALKER and ASTON (2) using the method of inversion of sucrose. The same method was applied by LONG (3) and by KULLGREN (4). The quinhydrone electrode was used by DENHAM and MARRIS (5), and the glass electrode by CRANSTON and BROWN (6). The results of the last two investigations are given in Fig. 1.

In the present paper, the hydrogen ion concentrations of aqueous solutions of lead nitrate, and of solutions containing both lead nitrate and barium nitrate, were measured by means of the glass electrode at 18.0° C. The concentration of lead nitrate varied from 0.4 to 0.005 molar, and both pure aqueous solutions and solutions containing small concentrations of sodium hydroxide or nitric acid were measured. In 0.4 and 0.1 molar lead nitrate, the greatest concentration of sodium hydroxide which gave no turbidity during the measurement was only about 0.4



per cent. of the lead ion concentration; in 0.01 molar lead nitrate, it was about 1 per cent. These examples show that only extremely weakly buffered solutions could be measured.

The preparations used were commercial pure lead nitrate, which was further recrystallized twice from water, and *pro analysi* barium nitrate, which was recrystallized once. The amount of acid or basic impurity in the recrystallized preparations was determined from the hydrogen ion concentrations of

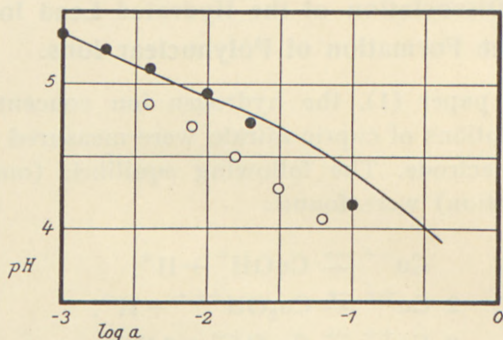
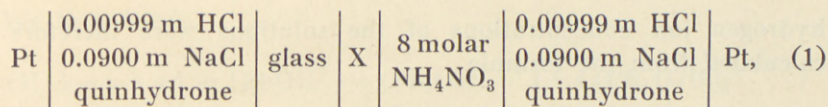


Fig. 1. Measurements of the pH of solutions of lead nitrate ( $a$  molar). Open circles: DENHAM and MARRIS, quinhydrone electrode at 25° C. Solid circles: CRANSTON and BROWN, glass electrode at 15° C. The curve represents the measurements of the present paper.

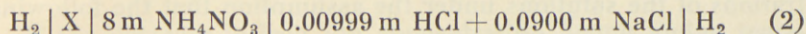
the solutions (see below). In the barium nitrate and in one of the preparations of lead nitrate, no acid or basic impurity could be detected, while two other preparations of lead nitrate contained respectively  $3 \cdot 10^{-6}$  and  $9 \cdot 10^{-6}$  equivalents of basic impurity per mole. The sodium hydroxide used for the solutions was taken from a 0.01 normal solution, which was stored in a bottle covered inside with a layer of paraffin wax and fitted out with a 5 ml. micro burette and the ordinary device for protecting the contents from the carbon dioxide of the air. It was prepared from a clear, saturated solution of sodium hydroxide *pro analysi* and carbon dioxide free water. Redistilled water was used for all the solutions.

The measurements were carried out as described in the earlier paper on cupric nitrate solutions (1). The cells measured had the composition



where X is the solution under investigation.

Every day, both before and after the measurements, X was replaced by a solution of the composition 0.00999 m HCl + 0.0900 m NaCl, and the e. m. f. (the asymmetry potential) was measured. When this small potential is subtracted from the e. m. f. of the cells (1), the potential  $E$  volts of cells of the composition



is obtained.

To a series of measurements at 18° C. in solutions X of constant lead nitrate and barium nitrate concentrations, but varying concentrations of nitric acid or sodium hydroxide, we may apply the formula

$$-\log(\text{H}^+) = A + 17.32 E, \quad (3)$$

where  $(\text{H}^+)$  is the hydrogen ion concentration of the solution X, and  $A$  includes the salt effect and the effect of the liquid-liquid junction of the left half cell (scheme 2), together with the whole effect of the right half cell, the latter having the same composition throughout the measurements. When the concentration of acid or base added is sufficiently small,  $A$  attains a constant value  $A_0$ .

In order to determine  $A_0$  for a given concentration of lead and barium nitrate, measurements were carried out on solutions containing in addition so much nitric acid that the hydrogen ion concentration produced by the dissociation of the lead ions was negligible, except, in a few cases, for a small correction. In these solutions, the hydrogen ion concentration was known, and  $A$  could be computed by means of equation 3.  $A_0$  was found by extrapolation of  $A$  to zero concentration of nitric acid. The results are given in Table 1.

In all the other solutions measured, the concentration of nitric acid or sodium hydroxide was so small compared with that of lead nitrate that we may put  $A = A_0$  in formula 3. The

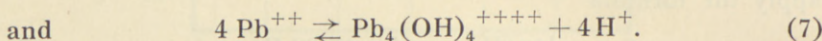
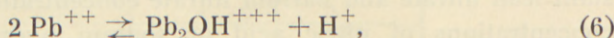
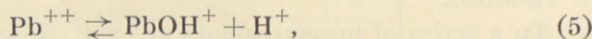


hydrogen ion concentrations of the solutions were therefore calculated from the formula

$$-\log(\text{H}^+) = A_0 + 17.32 E, \quad (4)$$

where  $A_0$  has the values given in Table 1. The results are presented in Table 2, where the second and third column give respectively  $E$  and  $-\log(\text{H}^+)$ . Before analyzing these results, we must consider the theory to be applied.

As we shall see, we may explain the hydrogen ion concentrations of the solutions under the assumption that the following three equilibria occur:



The mass action constants are

$$k_1 = \frac{(\text{PbOH}^+)(\text{H}^+)}{(\text{Pb}^{++})}, \quad (8)$$

$$k_{1,2} = \frac{(\text{Pb}_2\text{OH}^{+++})(\text{H}^+)}{(\text{Pb}^{++})^2}, \quad (9)$$

$$k_{4,4} = \frac{(\text{Pb}_4(\text{OH})_4^{++++})(\text{H}^+)^4}{(\text{Pb}^{++})^4}. \quad (10)$$

When  $n$  hydrogen ions and  $p$  metal ions take part in the equilibrium, the constant is denoted by  $k_{n,p}$ .  $p$  is left out when it is one.

We consider a series of measurements in solutions where the concentrations of lead and barium nitrate are constant, respectively  $a$  and  $b$  molar. The lead nitrate contains a small amount of basic impurity,  $\delta$  equivalents per mole.  $x$  is the concentration of sodium hydroxide added (or  $-x$  that of nitric acid).

We then have

$$\begin{aligned} (\text{H}^+) + x + a\delta &= (\text{PbOH}^+) + (\text{Pb}_2\text{OH}^{+++}) + 4(\text{Pb}_4(\text{OH})_4^{++++}) \\ &= k_1 \frac{(\text{Pb}^{++})}{(\text{H}^+)} + k_{1,2} \frac{(\text{Pb}^{++})^2}{(\text{H}^+)} + 4k_{4,4} \frac{(\text{Pb}^{++})^4}{(\text{H}^+)^4}, \end{aligned}$$

which may also be written as follows:

$$\frac{(\text{H}^+) [(\text{H}^+) + x]}{(\text{Pb}^{++})} + \frac{(\text{H}^+) a\delta}{(\text{Pb}^{++})} = k_1 + k_{1,2} (\text{Pb}^{++}) + 4k_{4,4} \frac{(\text{Pb}^{++})^3}{(\text{H}^+)^3}. \quad (11)$$

If the decrease in lead ion concentration owing to the reactions 5 to 7 is denoted by  $\mathcal{A}$ , we get

$$(\text{Pb}^{++}) = a - \mathcal{A} \quad (12)$$

and

$$\begin{aligned} \mathcal{A} &= (\text{PbOH}^+) + 2(\text{Pb}_2\text{OH}^{+++}) + 4(\text{Pb}_4(\text{OH})_4^{++++}) \\ &= (\text{H}^+) + x + a\delta + (\text{Pb}_2\text{OH}^{+++}) \\ &= (\text{H}^+) + x + a\delta + k_{1,2} \frac{(\text{Pb}^{++})^2}{(\text{H}^+)}. \end{aligned}$$

An approximation leads to

$$\mathcal{A} = (\text{H}^+) + x + k_{1,2} \frac{a^2}{(\text{H}^+)}. \quad (13)$$

From equation 11 and 12 we obtain

$$k = k_1 + k_{1,2} a + 4k_{4,4} \frac{(\text{Pb}^{++})^3}{(\text{H}^+)^3}, \quad (14)$$

where

$$k \equiv \frac{(\text{H}^+) [(\text{H}^+) + x]}{(\text{Pb}^{++})} + (\text{H}^+) \delta + k_{1,2} \mathcal{A}. \quad (15)$$

Here  $(\text{H}^+) \delta$  has been used as an approximation for  $(\text{H}^+) a\delta / (\text{Pb}^{++})$ .

In order to test the theory, we first compute  $\mathcal{A}$  from equation 13 and a preliminary value of  $k_{1,2}$ , and then  $(\text{Pb}^{++})$  from equation 12. The values of  $(\text{Pb}^{++})$  found in this way are given



in the fourth column of Table 2.  $k$  of equation 15 is a sum of three terms of which the first, and by far the most important one, may now be calculated. The third term is a very small correction, which may be estimated from a preliminary value of  $k_{1,2}$ . The relative importance of the second term, which contains the unknown  $\delta$ , decreases when  $x$  increases within a series of measurements at constant  $a$ . We therefore make the preliminary assumption that  $\delta = 0$ , calculate  $k$  from equation 15, and plot it against  $(\text{Pb}^{++})^3 (\text{H}^+)^{-3}$ . In any of the 20 series of measurements carried out, the points fall close to a straight line, in agreement with equation 14. In some cases, however, there is a small, systematic deviation from the straight line for the points corresponding to the smallest values of  $x$ . It is possible to eliminate this deviation by choosing an appropriate value of  $\delta$ , and adding the correction  $(\text{H}^+) \delta$  to the values of  $k$  first calculated. In this way, the basic impurity in the preparation of lead nitrate was estimated. The values of  $k$  computed from the measurements as explained here, are given in the last column but one of Table 2.

From the straight line obtained when  $k$  for a series of measurements is plotted against  $(\text{Pb}^{++})^3 (\text{H}^+)^{-3}$ , the constants  $(k_1 + k_{1,2} a)$  and  $4k_{4,4}$  of equation 14 are evaluated. They are presented in the third and fifth columns of Table 3.  $k$ , calculated from equation 14 by means of these values of the constants, is given in the last column of Table 2. The agreement between  $k$  found from the measurements and  $k$  calculated from formula 14 shows that  $k$  varies with the hydrogen ion concentration in the way expressed by equation 14. We shall now prove that it also depends upon the lead ion concentration in the way stated in the equation. For this purpose, we compare the results for solutions of different lead nitrate concentration, but constant ionic strength,  $\mu = 3(a + b)$ . It is seen from Table 3 that, for such solutions,  $(k_1 + k_{1,2} a)$  found from the measurements varies practically linearly with  $a$ , while  $4k_{4,4}$  is practically constant. The values of the three constants  $k_1$ ,  $k_{1,2}$  and  $k_{4,4}$  which best satisfy equation 14 are given in the three last columns of the table. The fourth column presents  $(k_1 + k_{1,2} a)$  calculated by means of these constants. The agreement with  $(k_1 + k_{1,2} a)$  found for the individual series is always good. For the last two

solutions,  $k_{1,2}$  has been calculated from formula 17 (see below), and  $k_1$  has been computed from this value and  $(k_1 + k_{1,2}a)$  found from the measurements.

The equilibrium constants found for different ionic strengths may be expressed by means of the following formulae:

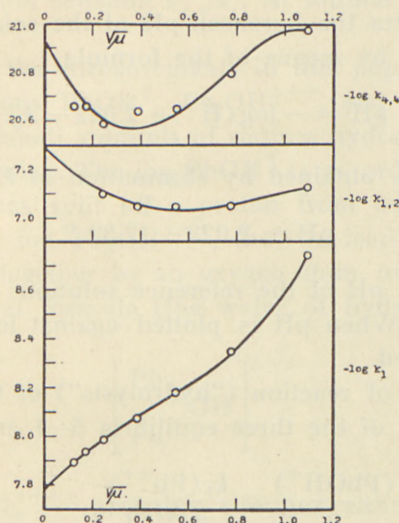


Fig. 2. The mass action constants found from the measurements. The curves represent the formulae 16–18.

$$-\log k_1 = 7.778 + 0.996 \sqrt{\mu} - 0.617 \mu + 0.432 \mu^2 \quad (16)$$

$$-\log k_{1,2} = 7.296 - 0.996 \sqrt{\mu} + 0.993 \mu - 0.189 \mu^2 \quad (17)$$

$$-\log k_{4,4} = 20.93 - 1.992 \sqrt{\mu} + 2.88 \mu - 0.854 \mu^2. \quad (18)$$

The formulae contain three empirical constants each. The fourth constant, the factor before the square root of  $\mu$ , has been deduced from the Debye-Hückel theory. In Fig. 2,  $-\log k_1$ ,  $-\log k_{1,2}$ , and  $-\log k_{4,4}$ , found from the measurements, are plotted against  $\sqrt{\mu}$ . The curves represent the formulae 16–18.

If we extrapolate to  $\mu = 0$  by means of the formulae 16–18, we obtain:

$$k_1^\circ = 1.67 \cdot 10^{-8}, \quad k_{1,2}^\circ = 5.1 \cdot 10^{-8}, \quad \text{and} \quad k_{4,4}^\circ = 1.2 \cdot 10^{-21}.$$

For the cupric ion was found (1):

$$k_1^\circ = 1.07 \cdot 10^{-8}, \quad k_{1,2}^\circ = 15.2 \cdot 10^{-8}, \quad \text{and} \quad k_{2,2}^\circ = 1.29 \cdot 10^{-11}.$$



Thus,  $k_1^\circ$  and  $k_{1,2}^\circ$  are of the same order of magnitude for the two ions.

Table 4 contains the equilibrium constants  $k_1$ ,  $k_{1,2}$ , and  $k_{4,4}$  for lead nitrate solutions, calculated from the formulae 16–18. The fifth column shows  $-\log(\text{H}^+)$  for pure lead nitrate solutions, calculated by means of the constants in the table. The next column gives the Sørensen pH of the solutions, calculated from  $-\log(\text{H}^+)$  by means of the formula

$$\text{pH} = -\log(\text{H}^+) + 2.022 - A_0.$$

This formula is obtained by elimination of  $E$  from formula 4 and

$$\text{pH} = 2.022 + 17.32 E,$$

2.022 being the pH of the reference solution: 0.00999m HCl + 0.0900m NaCl. When pH is plotted against  $\log a$ , the curve of Fig. 1 is obtained.

The degrees of reaction (“hydrolysis”) of the lead ions according to each of the three equilibria 5–7 are

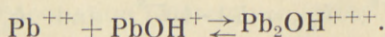
$$\alpha_1 = \frac{(\text{PbOH}^+)}{a} = \frac{k_1(\text{Pb}^{++})}{a(\text{H}^+)},$$

$$\alpha_{1,2} = \frac{2(\text{Pb}_2\text{OH}^{+++})}{a} = \frac{2k_{1,2}(\text{Pb}^{++})^2}{a(\text{H}^+)},$$

$$\alpha_{4,4} = \frac{4(\text{Pb}_4(\text{OH})_4^{++++})}{a} = \frac{4k_{4,4}(\text{Pb}^{++})^4}{a(\text{H}^+)^4},$$

respectively. The total degree of reaction is  $\alpha = \alpha_1 + \alpha_{1,2} + \alpha_{4,4}$ . The degrees of reaction for pure lead nitrate solutions have been calculated by means of the equilibrium constants and the hydrogen ion concentrations given in Table 4. They are to be found in the last four columns of the table. It is noted that  $\alpha_{4,4}$  in pure lead nitrate solutions is extremely small.

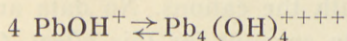
From the equilibria 5 and 6, we derive



The mass action constant of this equilibrium is  $k_{1,2}/k_1$ . At infinite dilution, it has the value 3.1. For the corresponding

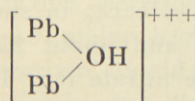
equilibrium with cupric ions instead of lead ions, the constant at infinite dilution was found (1) to be 14.

From the equilibria 5 and 7, we derive

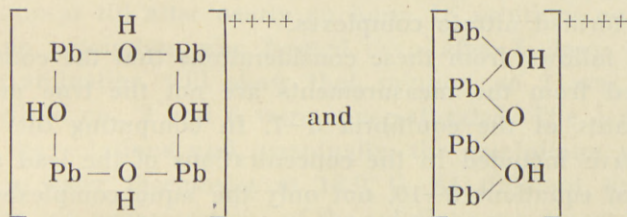


with the equilibrium constant  $k_{4,4}/k_1^4$ . At infinite dilution, it has the value  $1.5 \times 10^{10}$ .

As a result of the measurements in this paper, it has been shown that the ions  $\text{PbOH}^+$ ,  $\text{Pb}_2\text{OH}^{+++}$ , and  $\text{Pb}_4(\text{OH})_4^{++++}$  are formed when small amounts of sodium hydroxide are added to lead nitrate solution. The ion  $\text{PbOH}^+$  is an ordinary hydrated lead ion which has split off a proton from one of its water molecules. In the ion  $\text{Pb}_2\text{OH}^{+++}$ , the two lead atoms are undoubtedly bound together by an oxygen atom, as shown in the following structural formula (the water of hydration as usual being left out):



The ion  $\text{Pb}_4(\text{OH})_4^{++++}$  probably contains either a ring or a chain of alternating lead and oxygen atoms. The following structural formulae may be suggested:



It speaks in favour of the cyclic structure that a marked tendency to form tetranuclear compounds has been established, while ions containing three atoms have not been found. There is no reason to believe that a chain of four lead atoms is much more stable than one of three, but it is well known that a ring is most stable when containing a definite number of atoms.

All the computations of this paper have been carried out under the assumption that the nitrates present are completely



dissociated. However, there can be no doubt that the nitrate ions, especially in the more concentrated solutions, to a considerable extent have formed coordination compounds and association products with the cations. No data are available which make it possible to account for this effect. Only a rough estimate of the extent of complex formation of the nitrate ions with the lead and barium ions may be ventured. From measurements of the electrical conductivity of solutions of lead and barium nitrate, RIGHELLATO and DAVIES (7) have found the following constants corresponding to infinite dilution:

$$\frac{(\text{Pb}^{++})(\text{NO}_3^-)}{(\text{PbNO}_3^+)} = 0.0647 \text{ and } \frac{(\text{Ba}^{++})(\text{NO}_3^-)}{(\text{BaNO}_3^+)} = 0.121.$$

From these values and a rough estimate of the activity coefficients, we find that the constants for 0.2 m solutions are about 0.5 and 1, respectively. Hence, in such solutions about 40 per cent. of the lead ions and about 25 per cent. of the barium ions have taken up one nitrate ion. The percentage of lead and barium ions which have taken up nitrate ions is probably somewhat higher, because complexes with more than one nitrate ion may also be formed. We therefore make the rough estimate that, in the more concentrated of the solutions examined, about one half of the lead ions and one third of the barium ions have formed nitrate complexes.

It follows from these considerations that the constants calculated from the measurements are not the true mass action constants of the equilibria 5-7. In computing the constants, we have included in the concentrations of the lead containing ions of equations 8-10, not only the aquo complexes, but also the complexes in which water molecules have been exchanged with nitrate ions. The apparent equilibrium constants found in this way approach the true constants when the nitrate ion concentration decreases. Therefore, the values found by extrapolation to infinite dilution are true mass action constants for the equilibria 5-7. The formulae 16-18 and Fig. 2 give the apparent constants for solutions of lead nitrate, when  $\mu$  is calculated under the assumption that the lead nitrate is completely dissociated.

## Part 2.

### The Precipitates Formed when Solutions of Lead Nitrate and Sodium Hydroxide are Mixed.

A Preliminary Examination.

(X-ray crystal analysis by A. TOVBORG JENSEN).

In each of the experiments summarized in Table 5, 200 ml. of  $2x$  molar sodium hydroxide were poured into 200 ml. of ( $2a$  molar lead nitrate +  $2b$  molar barium nitrate), while a vigorous current of pure, carbon dioxide-free air was passed through the solution. Immediately after the mixtures were made, all the solutions were clear, but, when  $x$  was sufficiently great, a crystalline precipitate was formed after some time. In the solution containing most sodium hydroxide (no. 5), the precipitate was observed already after about one minute; in no. 3, it did not appear till after nearly an hour. In solutions nos. 1, 2, and 6, no precipitate was formed even after 5 days. The following examination will show that solution no. 1 was unsaturated, while nos. 2 and 6 were supersaturated. The bottles containing the solutions and, eventually, the precipitates were rotated in a water thermostat at  $18.0^{\circ}$  C. At different times, the hydrogen ion concentrations of the solutions were measured by means of the glass electrode in the same way as in Part 1. After two days, constant values of  $-\log(\text{H}^+)$  were found. They are presented in the fifth column of Table 5. For each of the solutions nos. 2 and 6, two values of  $-\log(\text{H}^+)$  are given. The first value refers to the clear, supersaturated solution, the second to a saturated solution obtained when the supersaturated solution was rotated with a small amount of the crystals prepared as described below (preparation A). After some days,



the lower values given in the table were measured. They remained constant on further rotation.

It follows from the analyses given below that the precipitate has the composition  $\text{Pb}(\text{OH})\text{NO}_3$ . The sodium hydroxide added ( $x$  molar) is partly used in forming the three ions  $\text{PbOH}^+$ ,  $\text{Pb}_2\text{OH}^{+++}$ , and  $\text{Pb}_4(\text{OH})_4^{++++}$ , partly in forming the precipitate. If  $y$  denotes the part of  $x$  which has been consumed by the precipitate, we have (the formation of nitrate complexes being neglected):

$$\begin{aligned} y &= x - (\text{PbOH}^+) - (\text{Pb}_2\text{OH}^{+++}) - 4(\text{Pb}_4(\text{OH})_4^{++++}), \\ (\text{Pb}^{++}) &= a - y - (\text{PbOH}^+) - 2(\text{Pb}_2\text{OH}^{+++}) - 4(\text{Pb}_4(\text{OH})_4^{++++}), \\ \text{and } (\text{NO}_3^-) &= 2a - y. \end{aligned}$$

$(\text{PbOH}^+)$ ,  $(\text{Pb}_2\text{OH}^{+++})$ , and  $(\text{Pb}_4(\text{OH})_4^{++++})$  are computed from the hydrogen ion concentrations by means of the equations 8–10 and the equilibrium constants given in Table 4. The values are inserted into the above equations, and  $y$ ,  $(\text{Pb}^{++})$ , and  $(\text{NO}_3^-)$  are calculated. They are to be found in Table 5.

For solutions saturated with the salt  $\text{Pb}(\text{OH})\text{NO}_3$ ,

$$L = \frac{(\text{Pb}^{++})(\text{NO}_3^-)}{(\text{H}^+)}$$

is the ratio between the solubility product  $(\text{Pb}^{++})(\text{OH}^-)(\text{NO}_3^-)$  and the ionization constant of water  $K_w = (\text{H}^+)(\text{OH}^-)$ .  $\log L$  is given in the last column of Table 5. For the saturated solutions,  $\log L$  is found to be practically constant (mean 3.55). The slight decrease of  $\log L$  when the amount of precipitate increases may be due to the decrease of ionic strength accompanying the formation of precipitate. The constancy of  $L$  is a confirmation of the formula  $\text{Pb}(\text{OH})\text{NO}_3$  found by chemical analysis of the crystals.  $\log L$  for solutions where no precipitate was formed is placed in parenthesis. In no. 1  $\log L$  is smaller, in nos. 2 and 6 it is greater than the value found for saturated solutions. This shows that solution no. 1 was unsaturated, while solutions nos. 2 and 6 were supersaturated.

The chemical composition of the precipitate, expressed by the formula  $\text{Pb}(\text{OH})\text{NO}_3$ , was found in the following way. Solution no. 5 was prepared again, in the same way as before,

only on a larger scale. The crystals (preparation A) were isolated and analyzed. When lead was determined gravimetrically as lead sulphate, the weight 287.6 per atom of lead was found (calculated: 286.2). The equivalent weight of the substance considered as a base was determined as follows. 0.7192 g. was dissolved in 25.01 ml. of 0.1001 m  $\text{HNO}_3$  and diluted to 50 ml. If the formula is correct, the solution is identical with a nearly 0.05 m lead nitrate. A glass electrode measurement of the solution was carried out in the usual way.  $E$  was found to be 0.1730 volts. According to Table 2, this corresponds to  $x = 0.7 \times 10^{-4}$ . Hence, 0.7192 g. of the preparation contains  $25.01 \times 0.1001 + 50 \times 0.7 \times 10^{-4} = 2.507$  milliequivalents of base, from which we obtain the equivalent weight 286.9 (calculated: 286.2). The equivalent weight was also determined acidimetrically. The substance was dissolved in an excess of nitric acid, and the excess was titrated with sodium hydroxide, methyl red being used as an indicator. Although the endpoint was not quite sharp, the equivalent weight found, 286.8, agrees well with that determined electrometrically.

In order to be able to identify the crystals, X-ray powder diagrams were taken of this preparation and the following ones. The diagram of preparation A contained an immense number of sharp, but rather weak lines. This shows that the preparation consisted of well developed crystals with a large unit cell.

Preparation B. A solution of the same composition as no. 5 in Table 5 was prepared, but instead of mixing equally great volumes of lead nitrate and sodium hydroxide solution, 200 ml. of 1.1 m lead nitrate were poured into 2 litres of 0.0121 m sodium hydroxide, while a current of pure, carbon dioxide-free air was passed through the solution. The mixture immediately turned milky, and soon a deposit was formed. The precipitate was isolated and analyzed. When lead was determined as lead sulphate, the weight 285.7 per atom of lead was found (calculated for  $\text{Pb}(\text{OH})\text{NO}_3$ : 286.2). The equivalent weight as a base determined electrometrically was 279.8. It follows from these results that the substance contains 1.02 hydroxyl groups per atom of lead, *i. e.* it has nearly the composition  $\text{Pb}(\text{OH})\text{NO}_3$ . The X-ray diagram showed that its structure was quite different from that of preparation A.



Preparation C. 500 ml. of about 0.125 m sodium hydroxide were added slowly, drop by drop, to 2 litres of 0.0625 m lead nitrate, while a current of pure, carbon dioxide-free air was passed through the solution. A permanent precipitate was not formed till nearly half of the base had been added. The analysis of the preparation gave the following results: When lead was determined as lead sulphate, the weight 286.3 per atom of lead was found. The equivalent weight found by acidimetry was 285.6. Consequently, the substance has the composition  $\text{Pb}(\text{OH})\text{NO}_3$ . The X-ray analysis showed that its structure was entirely different from that of preparation A. The two diagrams had no line in common. The diagrams of preparations B and C, however, had many lines in common. The diagrams showed that the two preparations were mixtures of the same two phases of different crystal structure. One phase consisted of rather great ( $> 2000 \text{ \AA}$ .), the other of smaller, possibly colloidal, particles. The first phase was predominant in both preparations. Preparation C, however, contained almost as much of the second phase, while only a small part of preparation B consisted of this phase.

According to Table 5, a 0.1 m lead nitrate containing  $6.9 \times 10^{-4}$  m sodium hydroxide is unsaturated with respect to the salt of the composition  $\text{Pb}(\text{OH})\text{NO}_3$  which forms the precipitate in the other solutions of the table. However, in Part 1 (see Table 2), a turbidity was observed in 0.1 m lead nitrate when the sodium hydroxide concentration was only  $4.6 \times 10^{-4}$  m. The solutions were not mixed in the same way in the two cases. In Part 1, a small volume of concentrated lead nitrate solution was pipetted into a great volume of dilute sodium hydroxide solution. When experiment no. 1 was repeated in this way, a turbidity was formed at once. After rotation of the mixture at  $18^\circ \text{C}$ .,  $-\log(\text{H}^+)$  was found to be 5.16 in one experiment, 5.12 in another. A greater volume of the mixture was made, but the amount of precipitate obtained (preparation D) was still insufficient for a chemical analysis. The X-ray diagram taken of the preparation showed few and rather diffuse lines. The substance, therefore, consists of colloidal particles of a simple crystal structure which is quite different from those of the preparations A, B, og C.

In order to prepare more of the substance, 400 ml. of 1.25 m lead nitrate were added to 4.6 litres of  $1.2 \times 10^{-3}$  m sodium hy-



droxide, while the solution was stirred by means of a current of carbon dioxide free air. This time the attempt at getting a turbidity failed. The solution was quite clear, even when having been left for a month in a closed flask. In order to test if the turbidity obtained in some cases might be lead carbonate formed from an impurity of carbonate in the sodium hydroxide solution, a little carbon dioxide was added to the clear solution. A precipitate was formed at once (preparation E). Qualitative tests showed that it contained carbonate, but no nitrate. Its equivalent weight was, by acidimetry, found to be 135.7 (calculated for  $\text{PbCO}_3$ : 133.6). The X-ray diagram of the preparation was quite different from that of preparation D. A comparison with a diagram of the mineral cerussite ( $\text{PbCO}_3$ ) showed that preparation E has the same crystal structure as this mineral, the only difference being that the particles of the preparation have colloidal size (probably between 500 Å. and 1000 Å.).

It was once more attempted to prepare the substance forming the turbidity. 80 ml. of 1.25 m lead nitrate were added to 8.6 litres of  $4 \times 10^{-4}$  m sodium hydroxide, while the solution was stirred by means of carbon dioxide-free air. A turbidity was formed at once. The flask was closed and left standing for two days. Then the turbidity had deposited, and most of the solution was siphoned off. The precipitate was isolated by means of a centrifuge. It was washed with carbon dioxide-free water and finally dried *in vacuo* over 30 per cent. potassium hydroxide. Yield: 0.16 g. (preparation F). The following analytical data show that the substance is lead carbonate,  $\text{PbCO}_3$ . When it was added to a droplet of dilute nitric acid, an effervescence was observed. No nitrate could be detected in the preparation. Lead was determined as lead oxide by heating the substance to 500° C. in an electric furnace. In this way, the weight 265.1 per atom of lead was found (calculated for  $\text{PbCO}_3$ : 267.2). The X-ray analysis shows that the preparations D and F have the same structure. Their structure is, however, different from that of the mineral cerussite and preparation E.

We have now identified the turbidity observed in some cases when a concentrated solution of lead nitrate was added to a solution of sodium hydroxide containing insufficient hydroxide for the precipitation of the salt  $\text{Pb}(\text{OH})\text{NO}_3$ . It was found to



be lead carbonate. It has not, however, been possible to explain why no turbidity is formed when a mixture of the same composition is prepared from the same stock solutions by adding a more dilute lead nitrate solution to its own volume of sodium hydroxide solution.

The turbidity observed in some of the solutions of Table 2 (denoted by an asterisk) has, at least in some cases, been lead carbonate. When the solutions were prepared, much care was taken to exclude carbon dioxide, and after the electrode vessel had been filled, a vigorous current of carbon dioxide-free air was passed for 10 minutes through the solution in order to remove any traces of carbon dioxide. In spite of these precautions, it has not been possible to avoid the formation of lead carbonate when a certain amount of sodium hydroxide had been added. Thus, the impurity of carbonate, rather than the solubility of the salt  $\text{Pb}(\text{OH})\text{NO}_3$ , has set a limit to the concentrations of sodium hydroxide added.

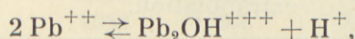
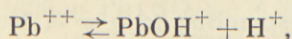
I wish to express my thanks to the head of the laboratory, Professor Dr. NIELS BJERRUM, for advice and kind interest in my work. I am also very grateful to Mr. A. TOVBORG JENSEN for carrying out the X-ray crystallography of this paper.

---

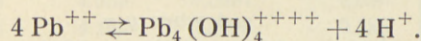
### Summary.

In Part 1, the hydrogen ion concentrations of aqueous solutions of lead nitrate, and of solutions containing both lead nitrate and barium nitrate, were measured by means of the glass electrode at 18.0° C. The concentration of lead nitrate varied from 0.4 to 0.005 molar, and the examination included both pure aqueous solutions and solutions containing small concentrations of sodium hydroxide or nitric acid.

The measurements show the presence of the following equilibria:



and



The mass action constants of the equilibria have been computed.

In Part 2, the precipitates formed when more sodium hydroxide was added to solutions of lead nitrate, were examined both by chemical and by X-ray analysis. Different modifications of the salt  $\text{Pb}(\text{OH})\text{NO}_3$  were identified. With one of them, solubility measurements were carried out.

In some cases, when solutions unsaturated with  $\text{Pb}(\text{OH})\text{NO}_3$  were prepared by adding lead nitrate to sodium hydroxide, a turbidity was formed. It was shown that the turbidity consisted of lead carbonate. Another modification of lead carbonate, identical with the mineral cerussite, was obtained when carbon dioxide was added to a clear solution of lead nitrate containing a little sodium hydroxide.

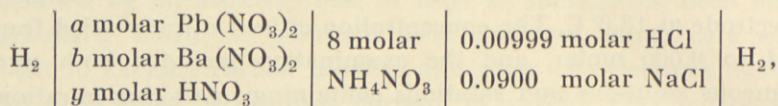
*From the Chemical Laboratory  
of the Royal Veterinary and Agricultural College.  
Copenhagen, Denmark.*



Table 1.

$$A = -17.32 E - \log (H^+),$$

where  $E$  is the e. m. f. in volts at 18.0° C. of the cell



measured by means of the glass electrode, and  $(H^+)$  is the hydrogen ion concentration of the solution in the left half cell.  $A_0$ , the value of  $A$  corresponding to  $y = 0$ , has been found by extrapolation.

$a$	$b$	$A$ when $y =$					$A_0$
		0.02	0.01	0.005	0.004	0.002	
0.400	0.000	2.038	2.038	..	2.041	2.043	2.045
0.300	0.100	..	..	..	2.045	2.047	2.048
0.200	0.200	2.043	2.042	..	2.045	2.046	2.048
0.200	0.000	2.009	2.015	2.018	..	2.022	2.024
0.150	0.050	2.010	2.013	2.014	..	2.016	2.017
0.100	0.100	2.012	2.016	2.020	..	2.021	2.022
0.050	0.150	2.013	2.016	2.021	..	2.021	2.022
0.100	0.000	2.000	2.007	2.011	..	2.012	2.014
0.075	0.025	1.999	2.005	..	2.009	2.012	2.014
0.050	0.050	1.999	2.005	..	2.008	2.011	2.012
0.025	0.075	2.000	2.006	..	2.011	2.013	2.015

$a$	$b$	$A$ when $y =$					$A_0$
		0.01	0.005	0.002	0.001	0.0005	
0.0500	0.0000	2.009	2.015	2.020	2.024	..	2.027
0.0375	0.0125	..	2.018	2.020	2.024	..	2.027
0.0250	0.0250	2.008	2.017	2.020	2.024	..	2.026
0.0125	0.0375	2.006	2.017	2.019	2.021	..	2.024
0.0200	0.0000	2.011	2.024	2.032	2.036	..	2.039
0.0100	0.0100	2.011	2.026	2.033	2.037	..	2.039
0.0050	0.0150	2.012	2.024	2.032	2.036	..	2.039
0.0100	0.0000	2.013	2.028	2.043	2.049	2.056	2.062
0.0050	0.0000	..	2.030	2.045	2.056	2.063	2.072

Table 2.

The hydrogen ion concentration ( $H^+$ ) of solutions of lead and barium nitrate containing sodium hydroxide ( $x$  molar) or nitric acid ( $-x$  molar), measured by means of the glass electrode. Comparison of  $k$  found from the measurements with  $k$  calculated from formula 14. In the solutions marked with an asterisk, a turbidity was formed either before or during the measurement.

$x \cdot 10^4$	$E$	$-\log(H^+)$	$(Pb^{++})$	$\frac{(Pb^{++})^3}{(H^+)^3} 10^{-12}$	$k \cdot 10^8$ found	$k \cdot 10^8$ formula
0.4000 m $Pb(NO_3)_2$ . $\delta = 9 \cdot 10^{-6}$ .						
-1.014	0.0993	3.765	0.3999	0.013	3.18	3.20
0.000	0.1101	3.952	0.3998	0.046	3.22	3.21
0.419	0.1148	4.033	0.3997	0.080	3.21	3.22
1.123	0.1218	4.155	0.3996	0.186	3.26	3.27
2.144	0.1300	4.297	0.3994	0.496	3.40	3.40
3.516	0.1375 <sub>5</sub>	4.427	0.3993	1.216	3.68	3.69
5.071	0.1427	4.517	0.3991	2.265	4.13	4.13
8.446	0.1490	4.626	0.3986	4.782	5.18	5.17
14.02	0.1540	4.712	0.3980	8.621	(6.96)	6.76
*17.54	0.1542	4.716	0.3976	8.839	(8.61)	6.85
0.3000 m $Pb(NO_3)_2$ + 0.1000 m $Ba(NO_3)_2$ . $\delta = 3 \cdot 10^{-6}$ .						
0.000	0.1167	4.069	0.2998	0.043	2.45	2.45
0.838	0.1283 <sub>5</sub>	4.271	0.2997	0.175	2.47	2.51
1.961	0.1390	4.455	0.2996	0.623	2.72	2.70
3.262	0.1463	4.582	0.2994	1.496	3.09	3.08
4.924	0.1516	4.674	0.2992	2.819	3.61	3.66
7.020	0.1553 <sub>5</sub>	4.739	0.2989	4.401	4.40	4.34
9.869	0.1587 <sub>5</sub>	4.798	0.2986	6.598	5.36	5.30
14.03	0.1620 <sub>5</sub>	4.855	0.2981	9.737	6.65	6.67
0.2000 m $Pb(NO_3)_2$ + 0.2000 m $Ba(NO_3)_2$ . $\delta = 3 \cdot 10^{-6}$ .						
0.000	0.1271	4.249	0.1999	0.045	1.61	1.70
0.557	0.1375	4.429	0.1998	0.154	1.74	1.74
1.260	0.1473 <sub>5</sub>	4.600	0.1997	0.502	1.91	1.89
2.245	0.1552	4.736	0.1996	1.283	2.24	2.22
3.369	0.1600	4.819	0.1995	2.274	2.68	2.64
4.930	0.1640 <sub>5</sub>	4.889	0.1993	3.680	3.28	3.23
7.010	0.1675 <sub>5</sub>	4.950	0.1990	5.579	4.02	4.03
9.82	0.1705 <sub>5</sub>	5.002	0.1987	7.953	4.98	5.04
13.47	0.1730	5.044	0.1983	10.57	6.19	6.14

(To be continued)



Table 2 (continued).

$x \cdot 10^4$	$E$	$-\log(H^+)$	$(Pb^{++})$	$\frac{(Pb^{++})^3}{(H^+)^3} \cdot 10^{-12}$	$k \cdot 10^8$ found	$k \cdot 10^8$ formula
0.2000 m $Pb(NO_3)_2$ . $\delta = 0$ .						
-0.514	0.1146	4.009	0.1999	0.009	2.28	2.28
-0.206	0.1202	4.106	0.1999	0.017	2.26	2.28
0.000	0.1237	4.166	0.1999	0.025	2.33	2.29
0.624	0.1350	4.362	0.1998	0.097	2.30	2.33
1.255	0.1434	4.508	0.1997	0.266	2.44	2.44
2.484	0.1536	4.684	0.1996	0.896	2.80	2.84
4.360	0.1604	4.802	0.1993	2.015	3.58	3.56
6.869	0.1653	4.887	0.1990	3.610	4.57	4.58
12.51	0.1707	4.981	0.1984	6.848	6.66	6.66
*22.7	..	..	..	..	..	..
0.1500 m $Pb(NO_3)_2$ + 0.0500 m $Ba(NO_3)_2$ . $\delta = 0$ .						
-0.514	0.1191	4.080	0.1499	0.006	1.77	1.73
0.000	0.1311	4.288	0.1499	0.025	1.77	1.75
0.384	0.1405 <sub>5</sub>	4.451	0.1499	0.076	1.74	1.78
0.693	0.1465	4.554	0.1498	0.154	1.81	1.83
1.152	0.1532	4.670	0.1498	0.344	1.95	1.95
1.916	0.1602	4.792	0.1497	0.798	2.24	2.24
3.464	0.1672	4.913	0.1495	1.831	2.94	2.91
4.628	0.1702	4.965	0.1493	2.613	3.44	3.41
6.961	0.1740	5.031	0.1491	4.107	4.41	4.37
9.624	0.1770	5.083	0.1488	5.842	5.40	5.48
13.49	0.1798	5.131	0.1484	8.060	6.78	6.90
0.1001 m $Pb(NO_3)_2$ + 0.1000 m $Ba(NO_3)_2$ . $\delta = 0$ .						
-0.206	0.1315 <sub>5</sub>	4.300	0.1001	0.008	1.48	1.40
0.000	0.1383	4.417	0.1000	0.018	1.47	1.40
0.248	0.1467 <sub>5</sub>	4.564	0.1000	0.049	1.42	1.42
0.624	0.1566 <sub>5</sub>	4.735	0.1000	0.160	1.49	1.49
1.248	0.1663 <sub>5</sub>	4.903	0.0999	0.510	1.72	1.72
2.236	0.1739	5.034	0.0998	1.256	2.16	2.19
4.364	0.1806 <sub>5</sub>	5.151	0.0995	2.797	3.15	3.18
7.481	0.1852 <sub>5</sub>	5.231	0.0992	4.818	4.47	4.47
12.47	0.1891 <sub>5</sub>	5.298	0.0987	7.530	6.40	6.21
*22.4	..	..	..	..	..	..
0.05000 m $Pb(NO_3)_2$ + 0.1500 m $Ba(NO_3)_2$ . $\delta = 0$ .						
0.000	0.1537	4.684	0.04997	0.014	0.86	0.90
0.280	0.1680	4.932	0.04994	0.078	0.93	0.94
0.560	0.1769 <sub>5</sub>	5.087	0.04991	0.227	1.05	1.04
1.075	0.1854 <sub>5</sub>	5.234	0.04985	0.624	1.33	1.29

(To be continued)

Table 2 (continued).

$x \cdot 10^4$	$E$	$-\log(H^+)$	$(Pb^{++})$	$\frac{(Pb^{++})^3}{(H^+)^3} 10^{-12}$	$k 10^8$ found	$k 10^8$ formula
1.750	0.1912	5.334	0.04977	1.239	1.67	1.68
2.809	0.1957	5.412	0.04966	2.107	2.23	2.24
*3.510	0.1975	5.443	0.04958	2.600	2.58	2.55
*4.203	0.1970 <sub>5</sub>	5.435	..	..	..	..
0.1000 m $Pb(NO_3)_2$ . $\delta = 3 \cdot 10^{-6}$ .						
0.000	0.1381	4.406	0.0999	0.017	1.56	1.57
0.280	0.1463	4.548	0.0999	0.044	1.60	1.60
0.447	0.1508	4.626	0.0999	0.075	1.63	1.63
0.768	0.1576 <sub>5</sub>	4.744	0.0999	0.170	1.72	1.71
1.312	0.1651 <sub>5</sub>	4.874	0.0998	0.416	1.94	1.93
2.108	0.1712	4.979	0.0997	0.855	2.34	2.33
3.178	0.1757 <sub>5</sub>	5.058	0.0996	1.474	2.88	2.89
*4.583	0.1787	5.109	0.0994	2.087	(3.65)	3.44
0.07500 m $Pb(NO_3)_2 + 0.0250$ m $Ba(NO_3)_2$ . $\delta = 3 \cdot 10^{-6}$ .						
0.000	0.1435	4.499	0.07495	0.013	1.35	1.35
0.237	0.1524	4.654	0.07493	0.039	1.37	1.37
0.420	0.1579 <sub>5</sub>	4.750	0.07491	0.075	1.42	1.41
0.722	0.1655 <sub>5</sub>	4.881	0.07488	0.185	1.50	1.50
1.122	0.1716 <sub>5</sub>	4.987	0.07483	0.383	1.69	1.68
1.561	0.1760	5.062	0.07478	0.642	1.92	1.91
2.098	0.1794 <sub>5</sub>	5.122	0.07472	0.969	2.20	2.20
2.803	0.1826	5.177	0.07464	1.412	2.56	2.59
3.507	0.1847	5.213	0.07456	1.805	2.94	2.94
0.05000 m $Pb(NO_3)_2 + 0.0500$ m $Ba(NO_3)_2$ . $\delta = 3 \cdot 10^{-6}$ .						
0.000	0.1517	4.639	0.04997	0.010	1.06	1.12
0.224	0.1623	4.823	0.04995	0.037	1.13	1.14
0.351	0.1671 <sub>5</sub>	4.907	0.04993	0.065	1.18	1.17
0.587	0.1741 <sub>5</sub>	5.028	0.04991	0.151	1.28	1.24
0.873	0.1800 <sub>5</sub>	5.130	0.04987	0.304	1.41	1.38
1.266	0.1850	5.216	0.04983	0.550	1.62	1.61
1.827	0.1892 <sub>5</sub>	5.290	0.04977	0.914	1.94	1.93
2.533	0.1926	5.348	0.04969	1.358	2.33	2.33
3.370	0.1953 <sub>5</sub>	5.395	0.04960	1.868	2.77	2.79
*4.215	0.1975 <sub>5</sub>	5.434	0.04951	2.433	(3.17)	3.30
0.02500 m $Pb(NO_3)_2 + 0.0750$ m $Ba(NO_3)_2$ . $\delta = 3 \cdot 10^{-6}$ .						
0.000	0.1631 <sub>5</sub>	4.841	0.02498	0.005	0.84	0.87
0.168	0.1757	5.058	0.02497	0.023	0.90	0.89
0.279	0.1828 <sub>5</sub>	5.182	0.02496	0.055	0.91	0.92

(To be continued)



Table 2 (continued).

$x \cdot 10^4$	$E$	$-\log(H^+)$	$(Pb^{++})$	$\frac{(Pb^{++})^3}{(H^+)^3} 10^{-12}$	$k 10^8$ found	$k 10^8$ formula
0.475	0.1908 <sub>5</sub>	5.321	0.02494	0.142	1.00	1.00
0.699	0.1963	5.415	0.02491	0.272	1.14	1.12
1.119	0.2022 <sub>5</sub>	5.518	0.02486	0.550	1.40	1.38
1.678	0.2068 <sub>5</sub>	5.598	0.02480	0.950	1.74	1.75
*2.474	0.2085	5.626	0.02473	1.142	(2.39)	1.93
$0.05000 \text{ m Pb}(\text{NO}_3)_2. \quad \delta = 3 \cdot 10^{-6}.$						
0.000	0.1480 <sub>5</sub>	4.591	0.04997	0.007	1.32	1.31
0.210	0.1581	4.765	0.04995	0.025	1.32	1.32
0.419	0.1662 <sub>5</sub>	4.906	0.04993	0.065	1.36	1.36
0.699	0.1738	5.037	0.04990	0.160	1.46	1.45
1.047	0.1799	5.143	0.04986	0.333	1.62	1.62
1.540	0.1850 <sub>5</sub>	5.232	0.04980	0.613	1.89	1.89
2.104	0.1890	5.300	0.04974	0.977	2.17	2.24
*2.816	..	..	..	..	..	..
$0.03750 \text{ m Pb}(\text{NO}_3)_2 + 0.0125 \text{ m Ba}(\text{NO}_3)_2. \quad \delta = 3 \cdot 10^{-6}.$						
0.000	0.1525 <sub>5</sub>	4.669	0.03747	0.005	1.23	1.19
0.168	0.1622 <sub>5</sub>	4.837	0.03746	0.017	1.22	1.21
0.315	0.1697 <sub>5</sub>	4.967	0.03745	0.042	1.22	1.23
0.526	0.1776	5.103	0.03742	0.107	1.28	1.29
0.786	0.1838 <sub>5</sub>	5.211	0.03740	0.225	1.40	1.39
1.155	0.1895	5.309	0.03736	0.461	1.58	1.59
*1.573	0.1933	5.375	0.03731	0.693	1.83	1.82
$0.02500 \text{ m Pb}(\text{NO}_3)_2 + 0.0250 \text{ m Ba}(\text{NO}_3)_2. \quad \delta = 0.$						
0.0000	0.1588	4.776	0.02498	0.003	1.12	1.08
0.1313	0.1689	4.951	0.02497	0.011	1.09	1.09
0.3140	0.1800	5.144	0.02496	0.042	1.11	1.11
0.4734	0.1872 <sub>5</sub>	5.269	0.02494	0.099	1.14	1.16
0.6291	0.1917 <sub>5</sub>	5.347	0.02492	0.170	1.22	1.21
0.8393	0.1965 <sub>5</sub>	5.430	0.02490	0.301	1.31	1.31
1.048	0.1997	5.485	0.02488	0.439	1.42	1.42
$0.01248 \text{ m Pb}(\text{NO}_3)_2 + 0.0375 \text{ m Ba}(\text{NO}_3)_2. \quad \delta = 0.$						
0.0000	0.1695 <sub>5</sub>	4.961	0.01247	0.001	0.96	0.95
0.0944	0.1802 <sub>5</sub>	5.146	0.01246	0.005	0.95	0.96
0.2102	0.1911	5.334	0.01245	0.019	0.96	0.97
0.3146	0.1983	5.459	0.01244	0.046	0.98	1.00
0.4204	0.2028	5.536	0.01243	0.078	1.05	1.03
0.5258	0.2072	5.613	0.01242	0.132	1.08	1.08
0.6317	0.2104 <sub>5</sub>	5.669	0.01241	0.194	1.13	1.14

(To be continued)

Table 2 (continued).

$x \cdot 10^4$	$E$	$-\log(H^+)$	$(Pb^{++})$	$\frac{(Pb^{++})^3}{(H^+)^3} \cdot 10^{-12}$	$k \cdot 10^8$ found	$k \cdot 10^8$ formula
0.02000 m $Pb(NO_3)_2$ . $\delta = 0$ .						
0.0000	0.1598	4.807	0.01998	0.002	1.22	1.20
0.1051	0.1683 <sub>5</sub>	4.955	0.01998	0.006	1.20	1.21
0.2102	0.1760	5.087	0.01997	0.015	1.20	1.21
0.3680	0.1848 <sub>5</sub>	5.241	0.01995	0.042	1.22	1.24
0.5242	0.1907	5.342	0.01994	0.084	1.30	1.28
0.6805	0.1953 <sub>5</sub>	5.422	0.01992	0.146	1.37	1.35
0.8687	0.1996 <sub>5</sub>	5.497	0.01990	0.244	1.44	1.44
*1.064	0.2026 <sub>5</sub>	5.549	0.01988	0.348	1.55	1.55
0.01000 m $Pb(NO_3)_2 + 0.0100$ m $Ba(NO_3)_2$ . $\delta = 0$ .						
0.0000	0.1697	4.978	0.00999	0.001	1.11	1.12
0.0789	0.1788	5.136	0.00998	0.003	1.11	1.12
0.1831	0.1888	5.309	0.00997	0.008	1.14	1.13
0.2892	0.1972 <sub>5</sub>	5.455	0.00997	0.023	1.14	1.14
0.4192	0.2044 <sub>5</sub>	5.580	0.00995	0.054	1.18	1.17
0.5565	0.2097	5.671	0.00994	0.101	1.24	1.22
0.6904	0.2138 <sub>5</sub>	5.743	0.00993	0.166	1.29	1.29
0.8436	0.2173 <sub>5</sub>	5.804	0.00991	0.251	1.36	1.37
*1.061	..	..	..	..	..	..
0.005000 m $Pb(NO_3)_2 + 0.0150$ m $Ba(NO_3)_2$ . $\delta = 0$ .						
0.0000	0.1785	5.131	0.004992	0.000	1.10	1.08
0.0627	0.1892 <sub>5</sub>	5.317	0.004989	0.001	1.07	1.08
0.1258	0.1984 <sub>5</sub>	5.476	0.004984	0.003	1.07	1.08
0.2101	0.2076 <sub>5</sub>	5.635	0.004976	0.010	1.09	1.09
0.2936	0.2146 <sub>5</sub>	5.757	0.004968	0.023	1.10	1.11
0.3766	0.2195 <sub>5</sub>	5.842	0.004960	0.041	1.13	1.13
0.4614	0.2241	5.920	0.004951	0.070	1.15	1.16
0.5463	0.2272	5.974	0.004943	0.101	1.20	1.19
0.6297	0.2296 <sub>5</sub>	6.017	0.004934	0.135	1.25	1.23
0.7335	0.2328 <sub>5</sub>	6.072	0.004924	0.196	1.28	1.30
*0.876	..	..	..	..	..	..
0.01000 m $Pb(NO_3)_2$ . $\delta = 0$ .						
0.0000	0.1673 <sub>5</sub>	4.961	0.00999	0.001	1.20	1.23
0.0786	0.1761	5.112	0.00998	0.002	1.21	1.23
0.1730	0.1850	5.266	0.00998	0.006	1.23	1.24
0.2625	0.1921	5.389	0.00997	0.015	1.24	1.24
0.3920	0.1998	5.523	0.00996	0.037	1.27	1.26
0.5245	0.2057	5.625	0.00994	0.074	1.31	1.30

(To be continued)



Table 2 (continued).

$x \cdot 10^4$	$E$	$-\log (H^+)$	$(Pb^{++})$	$\frac{(Pb^{++})^3}{(H^+)^3} 10^{-12}$	$k \cdot 10^8$ found	$k \cdot 10^8$ formula
0.6828	0.2110	5.717	0.00993	0.139	1.36	1.36
0.8332	0.2145	5.777	0.00991	0.209	1.43	1.42
*1.051	0.2177	5.833	0.00989	0.305	(1.58)	1.50
0.005000 m $Pb(NO_3)_2$ . $\delta = 0$ .						
0.0000	0.1740 <sub>5</sub>	5.087	0.004992	0.000	1.34	1.31
0.0627	0.1841 <sub>5</sub>	5.261	0.004988	0.001	1.29	1.31
0.1258	0.1924	5.404	0.004983	0.002	1.31	1.31
0.2097	0.2015 <sub>5</sub>	5.563	0.004976	0.006	1.30	1.32
0.2848	0.2073 <sub>5</sub>	5.663	0.004969	0.012	1.34	1.32
0.3693	0.2134 <sub>5</sub>	5.769	0.004960	0.025	1.33	1.33
0.4701	0.2186 <sub>5</sub>	5.859	0.004950	0.046	1.35	1.35
0.5469	0.2219 <sub>5</sub>	5.916	0.004943	0.068	1.37	1.37
0.6616	0.2249	5.967	0.004931	0.095	(1.47)	1.40
*0.783	..	..	..	..	..	..

Table 3.

Equilibrium constants found from the measurements in solutions of lead nitrate (*a* molar) and barium nitrate (*b* molar).

<i>a</i>	<i>b</i>	$(k_1 + k_{1,2} a) \cdot 10^8$ found	$(k_1 + k_{1,2} a) \cdot 10^8$ calcd.	$4 k_{4,4} 10^{21}$ found	$k_1 10^8$	$k_{1,2} 10^8$	$k_{4,4} 10^{21}$
0.4000	0.0000	3.19	3.18	4.14	0.18	7.50	1.06
0.3000	0.1000	2.43	2.43	4.35			
0.2000	0.2000	1.68	1.68	4.22			
0.2000	0.0000	2.27	2.24	6.41	0.45	8.96	1.60
0.1500	0.0500	1.73	1.79	6.42			
0.1000	0.1000	1.39	1.35	6.40			
0.0500	0.1500	0.89	0.90	6.4			
0.1000	0.0000	1.56	1.56	9.0	0.66	9.0	2.25
0.0750	0.0250	1.34	1.34	8.85			
0.0500	0.0500	1.11	1.11	9.0			
0.0250	0.0750	0.87	0.88	9.3			
0.0500	0.0000	1.30	1.30	9.6	0.85	9.0	2.3
0.0375	0.0125	1.19	1.19	9.1			
0.0250	0.0250	1.08	1.07	7.8			
0.0125	0.0375	0.95	0.96	10			
0.02000	0.0000	1.20	1.20	10	1.04	8	2.6
0.01000	0.0100	1.12	1.12	10			
0.00500	0.0150	1.08	1.08	11			
0.01000	0.0000	1.23	..	9	1.16	(7)	2.2
0.00500	0.0000	1.31	..	9	1.28	(6.5)	2.2



Table 4.

The equilibrium constants, hydrogen ion concentrations, and degrees of "hydrolysis" for pure aqueous solutions of lead nitrate ( $\alpha$  molar), calculated by means of the formulae 16–18.

$\alpha$	$k_1 10^8$	$k_{1,2} 10^8$	$k_{4,4} 10^{21}$	$-\log(\text{H}^+)$	pH	$\alpha_1 10^3$	$\alpha_{1,2} 10^3$	$\alpha_{4,4} 10^6$	$\alpha 10^3$
0.4000	0.18	7.50	1.06	3.947	3.92	0.016	0.530	1.6	0.55
0.2000	0.46	8.87	1.56	4.173	4.17	0.069	0.528	2.5	0.60
0.1000	0.66	9.3	2.37	4.397	4.41	0.166	0.464	3.7	0.63
0.0500	0.83	8.8	2.7	4.597	4.59	0.328	0.348	3.2	0.68
0.0200	1.03	7.7	2.4	4.812	4.80	0.668	0.201	1.4	0.87
0.0100	1.17	7.0	2.1	4.953	4.91	1.051	0.126	0.6	1.18
0.0050	1.28	6.5	1.9	5.091	5.04	1.582	0.080	0.2	1.66
0.0020	1.41	6.0	1.6	5.274	5.21	2.640	0.045	0.1	2.69
0.0010	1.48	5.7	1.5	5.414	5.34	3.838	0.015	0.0	3.85
0	1.67	5.1	1.2	..	..	..	..	..	..

Table 5.

Measurements of the hydrogen ion concentrations of lead nitrate solutions saturated with the salt  $\text{Pb}(\text{OH})\text{NO}_3$  at  $18.0^\circ\text{C}$ .

$$L = \frac{(\text{Pb}^{++})(\text{NO}_3^-)}{(\text{H}^+)}$$

No.	$\alpha$	$b$	$x$	$-\log(\text{H}^+)$	$y 10^3$	$(\text{Pb}^{++})$	$(\text{NO}_3^-)$	$\log L$
1..	0.1000	0.0000	0.00069	5.196	0	0.09916	0.2000	(3.493) <sup>1</sup>
2..	0.1000	0.0000	0.00138	5.287	0	0.09844	0.2000	(3.581) <sup>2</sup>
				5.265	0.07	0.09846	0.1999	3.559
3..	0.1000	0.0000	0.00275	5.268	1.47	0.09709	0.1985	3.553
4..	0.1000	0.0000	0.00551	5.282	4.20	0.09434	0.1958	3.549
5..	0.1000	0.0000	0.01101	5.307	9.70	0.08884	0.1903	3.535
6..	0.0500	0.0500	0.00138	5.595	0	0.04853	0.2000	(3.582) <sup>2</sup>
				5.557	0.30	0.04854	0.1997	3.546
7..	0.0500	0.0500	0.00275	5.571	1.65	0.04717	0.1984	3.542
8..	0.0500	0.0500	0.00551	5.601	4.37	0.04441	0.1956	3.540

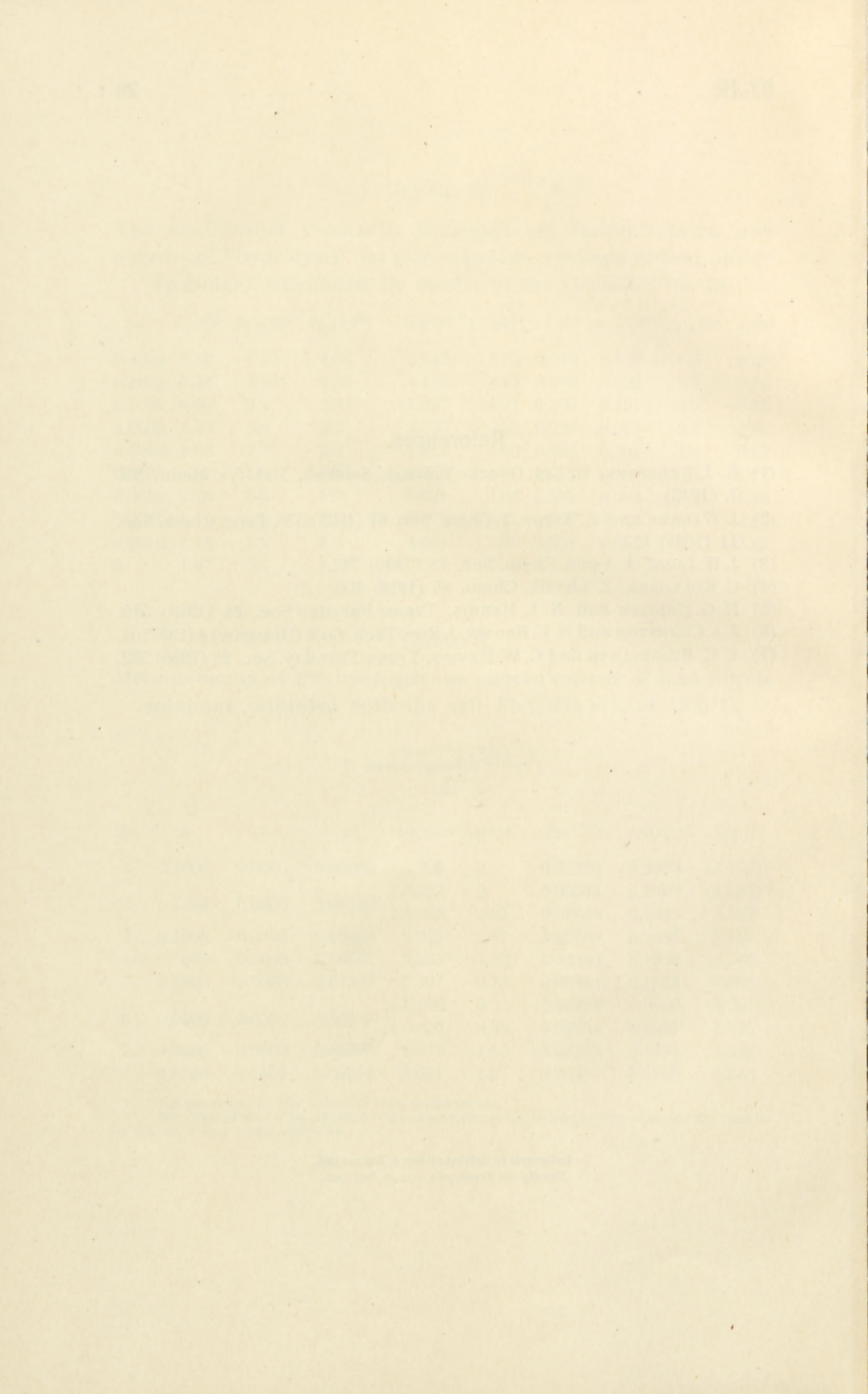
<sup>1</sup> No precipitate. The solution was unsaturated.

<sup>2</sup> No precipitate. The solution was supersaturated. When it was seeded, the results in the next line were obtained.

### References.

- (1) K. J. PEDERSEN, D. Kgl. Danske Vidensk. Selskab, Mat.-fys. Medd. **XX** 7. (1943)
- (2) J. WALKER and E. ASTON, J. Chem. Soc. **67** (1895) 576, Proc. Chem. Soc. **11** (1895) 112.
- (3) J. H. LONG, J. Amer. Chem. Soc. **18** (1896) 717.
- (4) C. KULLGREN, Z. physik. Chem. **85** (1913) 466.
- (5) H. G. DENHAM and N. A. MARRIS, Trans. Faraday Soc. **24** (1928) 515.
- (6) J. A. CRANSTON and H. F. BROWN, J. Roy. Tech. Coll. (Glasgow) **4** (1937) 54.
- (7) E. C. RIGHELLATO and C. W. DAVIES, Trans. Faraday. Soc. **26** (1930) 592.





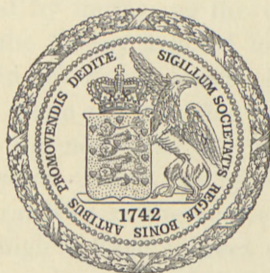
DET KGL. DANSKE VIDENSKABERNES SELSKAB  
MATEMATISK-FYSISKE MEDDELELSER, BIND XXII, NR. 11

---

# A HIGH VOLTAGE X-RAY INSTALLATION

BY

J. C. JACOBSEN



KØBENHAVN  
I KOMMISSION HOS EJNAR MUNKSGAARD  
1945



DET KÖL DÄNSKE FÖRENINGEN  
FÖR RÖNTGEN-TEKNIK

# A HIGH VOLTAGE X-RAY INSTALLATION

THE INSTITUTE



Printed in Denmark.  
Bianco Lunos Bogtrykkeri A/S

For several years the development in the production of X-rays for medical deep therapy has been governed by the demand of an increased depth dose. This has mainly been achieved by increasing the voltage, although the second alternative, increasing the current, has also been proposed. In the latter case the increase in depth dose is obtained merely as a result of the increase in intensity, which allows a larger distance from the anode to the skin, in the former both the intensity and the penetrability of the X-rays are increased. A closer consideration shows that a limit to the energy which can be applied to the anode, is soon set by the difficulties encountered in the cooling; since, however, the output of X-rays is nearly proportional to the third power of the voltage, a rapid increase of the intensity of the X-rays can be obtained by increasing the voltage without at the same time increasing the energy applied to the anode.

The development in the construction of high voltage X-ray installations which has taken place during the last 10 or 15 years, has been intimately connected with the progress in the experiments on nuclear physics. The X-ray tubes are in most cases built in the same general way as the accelerating tubes used for nuclear research; the high voltage sources show a great variety, both electrostatic high voltage (1), (2), (3) transformers with rectification (4) or without rectification (5), (6), (7) have been used.

The design to be described here employs unrectified a. c. voltage from a resonance transformer (2) giving a simple and



compact construction. The use of unrectified voltage on the other hand gives a somewhat smaller output of X-rays than a d. c. voltage. This point is considered in more detail below.

The high voltage source is a resonance transformer, where the secondary coil is built from 95 flat coils stacked on each other, separated by 6 mm. intervals for ventilation, the axis of the coil is vertical. Each of the flat coils contains 1,600 windings of 0.2 mm. copper wire, the dimensions of the winding area are height 3 mm., inner and outer diameter 45 cm. and 60 cm. Each of the flat coils is supported by a ring of cardboard, which extends about 2 cm. beyond the outer and inner edge of the winding, the whole being pasted together with paraffin wax<sup>1</sup>. The primary coil, wound from flat copper band, is placed below the secondary one. On top of the secondary coil is placed a hemispherical shield made of zinc.

The transformer is placed in a pressure tank with diameter 1.7 metres and height 2.7 metres. The tank is filled with carbon dioxide to a pressure of 3 atm.; carbon dioxide is used instead of air to prevent the insulating materials from catching fire. The tank is made in two parts, which are bolted together. The top part can be lifted by a crane.

To prevent losses in the wall of the pressure tank a laminated steel shield is placed inside the tank, the shield extends to the same height as the hemisphere on top of the transformer. The distance between the secondary coil and the inside of the laminated shield is 39 cm. When the tank is filled with carbon dioxide, a pressure of 3 atm. is sufficient to prevent sparking over at a voltage of 900 kV. The resonance frequency is 300 Hz. The current for the primary coil is delivered by a rotating converter driven by 250 volts d. c., which in turn is delivered by a second converter driven by 380 volts a. c. from the city mains. The speed of revolution of the a. c. generator connected to the primary coil can be varied by a resistance placed in the magnetizing circuit of the d. c. motor driving it, so that the frequency of the a. c. generator can be tuned to resonance with the transformer. The mechanical inertia of the rotors of the two con-

<sup>1</sup> The use of paraffin wax and cardboard involves relatively high dielectric losses; because of the war situation low loss materials such as mica were unobtainable.

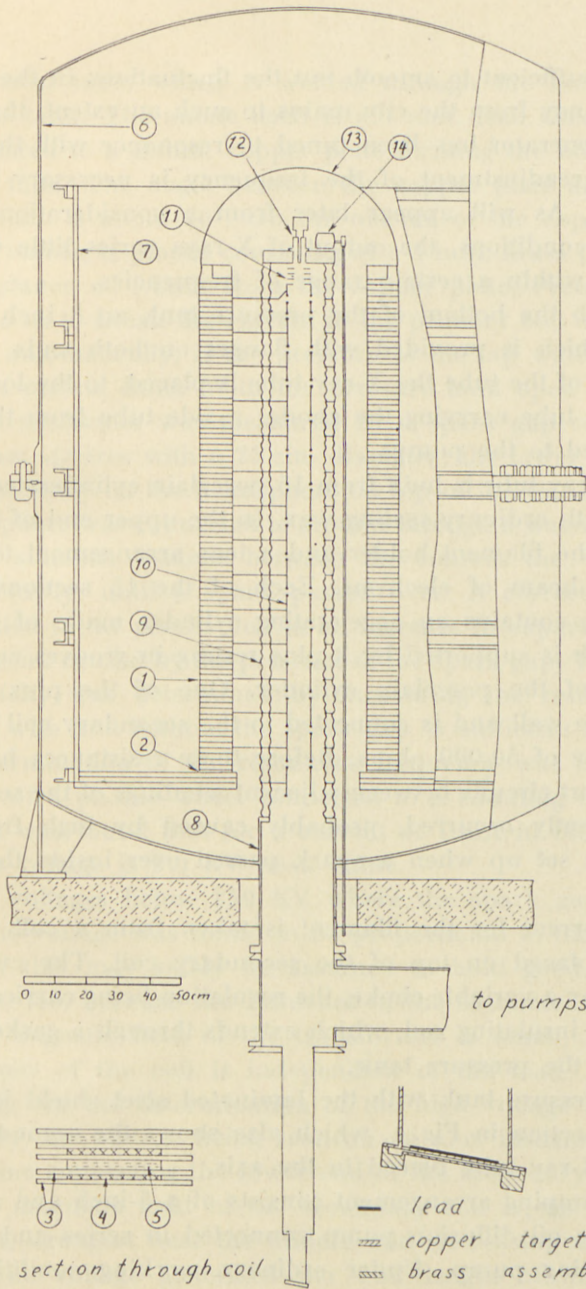


Fig. 1. (1) secondary coil. (2) primary coil. (3) cardboard rings. (4) secondary coil. (5) intermediate insulator for separating the coils. (6) pressure tank. (7) laminated shield. (8) steel tube. (9) porcelain cylinder. (10) accelerating electrode. (11) lens arrangement. (12) filament holder. (13) hemisphere. (14) variable choke.



verters is sufficient to smooth out the fluctuations in the voltage and frequency from the city mains to such an extent, that when once the generator has been tuned to resonance with the transformer, a readjustment of the frequency is necessary only in rare cases. As will appear later from a consideration of the resonance conditions, the output of X-rays varies little with the frequency within a certain range of frequencies.

Through the bottom of the pressure tank an 8 inch tube is welded, which is provided with flanges on both ends. On the upper end of the tube the X-ray tube is placed, to the lower end is bolted a tube carrying the anode; a side tube from the latter is connected to the pumps.

The X-ray tube is built from 15 porcelain cylinders cemented together with ordinary sealing wax. In the upper end of the tube is placed the filament holder and a lens arrangement to obtain a parallel beam of electrons. Each of the 15 sections of the X-ray tube contains an accelerating cylinder made of stainless steel, which is supported by 3 pins resting in grooves cut in the end face of the porcelain cylinder. One of the pins extends through the wall and is connected to the secondary coil through a resistance of 50,000 ohms. Before these resistances had been placed, short circuits between adjacent windings of the secondary coil frequently occurred, probably caused by high frequency oscillations set up when a spark passed over inside the X-ray tube.

The current for the filament is taken from a coil with 12 windings placed on top of the secondary coil. The current is regulated by a variable choke, the regulation being carried out by turning an insulating rod, which extends through a gasket in the bottom of the pressure tank.

The pressure tank with the laminated steel shield is shown partly in section in Fig. 1, which also shows the secondary coil with the X-ray tube placed in the axis.

The pumping arrangement consists of a 5-inch and a 2-inch single stage oil diffusion pump connected in series and backed by a rotating pump. Under ordinary working conditions the pressure as measured by a McLeod gauge connected to the system near the pumps is about  $10^{-6}$  mm.

The anode is placed at the bottom of a copper tube connected

to the steel tube, which is welded through the bottom of the pressure tank. The anode itself is a 1 mm. lead sheet, which is tin soldered to a 2 mm. copper plate forming the bottom of the copper tube. The angle between the copper plate and the axis of the tube is about  $70^\circ$ . On the outside of the copper plate a cooling mantle is placed consisting of a 1 mm. brass plate placed at a distance of 1 mm. from the copper plate. Precautions are taken so as to break the current in the primary coil of the transformer automatically, if the pressure of the tap water decreases below a certain limit. With the pressure tank open the voltage of the transformer was measured by a spark gap consisting of two brass spheres with a 25 cm. diameter; the lower sphere was placed directly on the hemisphere on top of the transformer, the upper sphere was connected to ground through a water resistance. With a suitable distance between the spheres the voltage was raised slowly, until a spark passed over. A correction had to be applied to the results due to an increase in capacity of about 10 per cent. caused by the presence of the spark gap. The increase in capacity was determined by measuring the resonance frequency with and without the spark gap. A sufficient accuracy in the determination of the resonance frequency was obtained by the use of a phonic wheel connected to a counting meter. As a result it was found that for a current of 1 mA in the secondary coil the voltage is 9.0 KV peak value.

For voltages below 250 KV where the spark gap could be used, the voltage was found to be proportional to the secondary current; this may safely be assumed to hold good for higher currents, too, because the influence of the laminated steel shield on the magnetic field of the transformer is small, so that the inductance of the coil is independent of the load. A separate voltmeter for the determination of the high voltage is thus unnecessary, the voltage being read on an a. c. instrument placed in the line connecting the lower end of the secondary to ground.

The magnetic field of the secondary coil is, as usual in a solenoid, strongest near the middle and decreasing against both ends. The voltage generated per unit length of the coil was measured by placing a single turn of a stiff copper wire round the coil and short circuiting the ends through an a. c. ammeter; the current in the ammeter was read with the copper wire placed



at different heights, the current in the coil being kept constant. The results are shown in Fig. 2; it is seen that the maximum and minimum voltages differ by about 25 per cent. from the mean value.

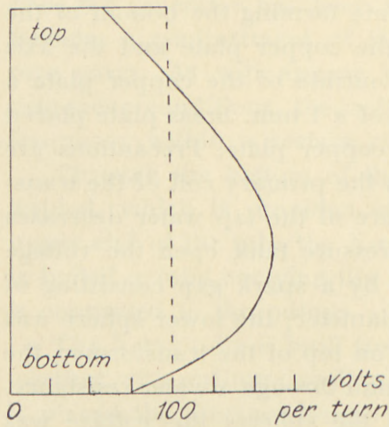


Fig. 2.

in Fig. 1) through a gasket in the wall of the pressure tank, until it makes contact with the metal hemisphere; the mean temperature of the coil can now be determined by measuring the resistance. For a more detailed knowledge it is necessary to determine the temperature rise at various points of the coil; this was done with the pressure tank open. The results are shown in Fig. 3, showing both the rise in temperature at various heights of the coil and the mean value. If the maximum permissible rise in temperature is fixed at  $20^{\circ}$  C., the measurements show that the corresponding mean rise in temperature will be  $14^{\circ}$ , or a change in the resistance of 5.3 per cent. The rise in temperature found in actual use, where the apparatus is always used intermittently, hardly exceeds half of this. No measurements of the rise in temperature with the apparatus running continuously have so far been made.

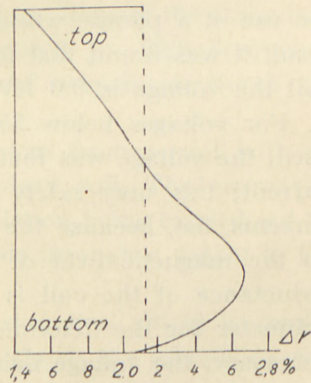


Fig. 3.

In Fig. 4a is shown the secondary current as a function of the frequency, the voltage applied to the primary coil being kept

constant. From the curve it is found that  $Q = \omega L : r_{\text{eff}}$  is 22, where  $r_{\text{eff}}$  is an effective resistance of the circuit, including all the losses.  $\omega L$  is found from  $V = i \cdot \omega L$ , where  $V$  and  $i$  are effective values of voltage and current in the secondary coil. With 9.0 KV peak value per milliamp. as found previously,  $\omega L$  becomes  $6.3 \times 10^6$ , or  $r_{\text{eff}} = 2.9 \times 10^5$  ohms. Since the resistance of the secondary coil is  $1.35 \times 10^5$  ohms, a considerable part of the losses are of dielectric origin.

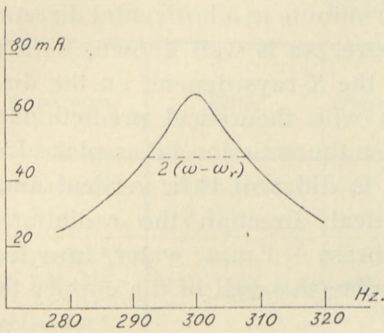


Fig. 4 a.

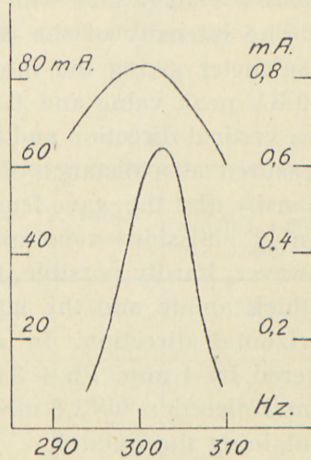


Fig. 4 b.

In Fig. 4 b are shown the secondary current and the emission from the filament as a function of the frequency. From the variation of the emission current it is seen, that to keep the emission sufficiently constant the frequency must be kept constant within less than 0.5 per cent. As already mentioned, the mechanical inertia of the rotating converters is sufficient to eliminate fluctuations of short duration in the supply from the city mains. It is seen that the maximum of emission from the filament occurs at a slightly higher frequency than the maximum of the secondary current, as was to be expected, because the filament voltage is proportional both to the secondary current and to the frequency. Inside the region of frequencies which lies between the two maxima, the changes in filament current and in the secondary voltage, resulting from a change in frequency, are in opposite directions. This means that the dependence of the output of



X-rays on the frequency is less critical than might appear from a consideration of the emission current alone.

For the purpose of screening the anode is surrounded by a cylindrical lead block with ports for a vertical and a horizontal beam of X-rays. The accessories for use in the X-ray treatment will be described elsewhere, together with the results obtained from measurements carried out in connection with the actual treatment; in this connection the output of X-rays obtained with constant voltage and with alternating voltage will be discussed.

The intensity of the X-rays was measured with a Siemens dose meter giving the intensity in *r* per minute directly. With 900 KV peak value and 1 mA the intensity was 21 *r* per minute in a vertical direction and 8 *r* per minute in a horizontal direction, measured at a distance of 1 metre. As is well known, both the intensity and the wave-length of the X-rays depend on the direction of emission; a comparison with theoretical predictions is, however, hardly possible, because the emission takes place from a thick anode and the filtering is different in a vertical and a horizontal direction. In a vertical direction the radiation is filtered by 1 mm. Pb + 3 mm. brass + 1 mm. water, in a horizontal direction by 2.6 mm. copper (the wall of the copper tube containing the anode).

The output of X-rays obtained with alternating voltage is of course smaller than with constant voltage under the same conditions, i. e. the same maximum voltage and the same current. If it is assumed that the output of X-rays is proportional to the third power of the voltage, a simple consideration shows that the output per milliamp. with constant voltage should be 2.3 times that obtained with alternating voltage. To obtain more definite information the results shown in Table 1 have been collected. In these measurements both the voltage and the filtering have varied considerably, so that corrections must be applied to make the results comparable. For the variation with voltage it will be assumed here that the output is proportional to  $V^n$  with  $n = 3$ ; this agrees quite well with the results for the variation of output with voltage, although for a heavy filtering a slightly higher value of  $n$  would be preferable. To correct for the variation in filter thickness the results given by HAENISCH, LASSER, EISL, and RUMP (4) have been used. They measured the absorption in

different materials for 1000 KV X-rays; with the aid of their results it is easy to refer the results to a standard filter thickness, provided the same absorption curves can be used in the range of voltages between 900 and 1500 KV. In Table 1 the results as given by the authors have been recalculated to correspond to a filter of 5 mm. Pb and 1000 KV.

A further correction is that due to the differences in target material. This has not been included in Table 1, partly because it is of minor importance and partly because no determination of the variation of output with target material seems to have been carried out.

Table 1.

Apparatus	Filter	r/min	Filter equiv. Pb	Target material	r/min. recalculated 1,000 KV. 5 mm. Pb
Electrostat. <sup>1</sup> 1000 KV.	3.3 Pb + 5 Cu + 2 Al	24	5.3	Au	25.3
Electrostat. <sup>2</sup> 1250 KV.	2 Pb + 5 Cu	62	3.7	Pb	26.0
Electrostat. <sup>3</sup> 1500 KV.	10.5 Pb	60	10.5	Pb	36
Transform. <sup>4</sup> 1000 KV. rectif.	5 Pb	37	5	W	37
Transform. <sup>5</sup> 1000 KV. unrectif.	1.5 W + 4.75 Ni + 15.7 brass	5.6	10.1	W	10.9
Transform. <sup>*</sup> 900 KV. unrectif.	1 Pb + 3 Cu	21.2	2.0	Pb	17.2

Intensity in r/min at 1 milliamp. and 1 meter distance; no correction for difference in target material. \*Present determination.

The results given in the last column show that the ratio between the output obtained with constant voltage and with alternating voltage probably is not far from the value 2.3, which was estimated previously, but at the same time the results are so widely scattered, that a direct comparison hardly seems



justifiable. From the corrections introduced the correction for the variation in filter thickness is likely to introduce a slight error, because the same absorption curves have been used at different voltages; this does not explain the difference between the results quoted under (1) and (4), which have been obtained under nearly identical conditions. The same applies to the results (5) and (6), although the difference in filter thickness here is considerable. DAHL and TRUMPY working with 1.5 MV, d. c. and a filter of 10.5 mm. Pb find half a value layer of 6.8 mm. Pb, a value which fits fairly well into the absorption curve for 1000 KV radiation given by HAENISCH, LASSEN, EISL, and RUMP. This agreement between values for the absorption in lead obtained under rather different conditions indicates that the error introduced by using the same absorption curves at different voltages is insignificant.

As regards the ratio (d. c. output) : (a. c. output), the results can be arranged in two groups, one containing the results (1), (2), and (5), giving the ratio 2.3, and a second group (3), (4), and (6) giving the ratio 2.1. The differences between the two groups are, however, so large, that they cannot possibly have been introduced by the corrections for filter thickness and voltage.

We have here considered the output as a function of the voltage for a constant current through the X-ray tube. It is probably more interesting to consider the output obtained when the energy supplied to the X-ray tube is kept constant, since it is the difficulties in the cooling of the anode which will usually set a limit to the output of X-rays. If this is done, the calculated ratio of 2.3 must be divided by  $\sqrt{2}$ , giving 1.6.

A quite considerable gain in intensity is thus obtained by the use of constant voltage, a gain which must be confronted with the simplicity and compactness of design of an apparatus employing alternating voltage.

The building where the X-ray tube is installed, is shown in ground plan and in section in Fig. 5 a and b. The pressure tank is placed on the upper floor with the anode tube extending into the treatment room. The height of the pressure tank is 2.7 metres, the height of the room 4 metres. Besides the treatment room the ground floor comprises a control room and a machine room. The thickness of the wall, ordinary brick wall, between the

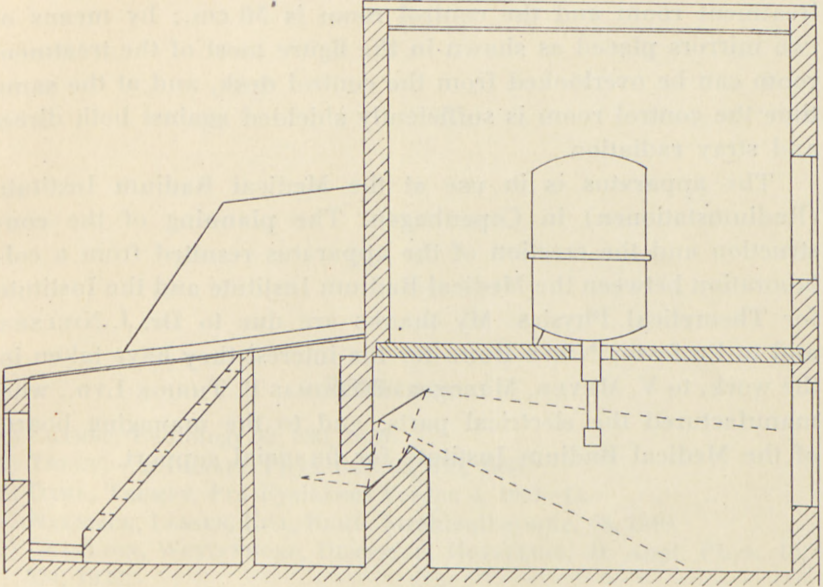


Fig. 5 a.

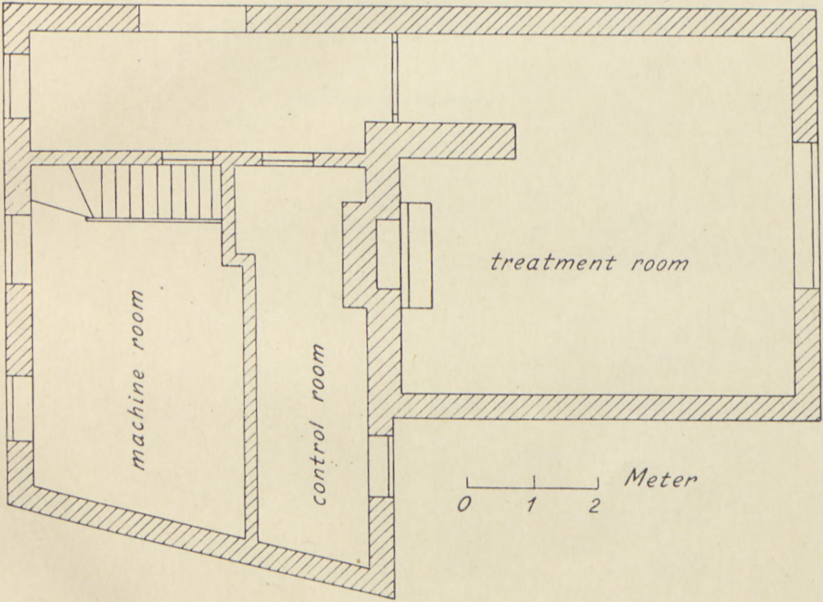


Fig. 5 b.



treatment room and the control room is 50 cm.; by means of two mirrors placed as shown in the figure most of the treatment room can be overlooked from the control desk, and at the same time the control room is sufficiently shielded against both direct and stray radiation.

The apparatus is in use at the Medical Radium Institute (Radiumstationen) in Copenhagen. The planning of the construction and the erection of the apparatus resulted from a collaboration between the Medical Radium Institute and the Institute for Theoretical Physics. My thanks are due to Dr. J. NIELSEN and to Professor NIELS BOHR for the interest they have taken in the work, to V. MEYER, Manager of THOMAS B. THRIGE LTD., who manufactured the electrical parts, and to the managing board of the Medical Radium Institute for financial support.

---

### References.

- (1) CRAMER, Radiology 32, 530, 1939.
  - (2) TRUMP, v. D. GRAAFF, Phys. Rev. 55, 676, 1939.
  - (3) DAHL, TRUMPY, Fra Fysikkens Verden 4, 1941-42.
  - (4) HAENISCH, LASSEN, EISL, RUMP, Strahlentherapie, 68, 1940.
  - (5) CHARLTON, WESTENDORP, DEMPSTER, HOTALLING, Jr. Appl. Phys. 10, 374, 1939.
  - (6) LAURITZEN, Radiology 31, 354, 1939.
-



The first part of the report is devoted to a general description of the project and its objectives. It is followed by a detailed account of the work done during the period covered by the report.

The results of the work are presented in the following sections. The first section deals with the general results, and the second section deals with the results of the various experiments conducted.

The conclusions drawn from the work are presented in the final section. It is hoped that the results of this work will be of interest to other workers in the field.

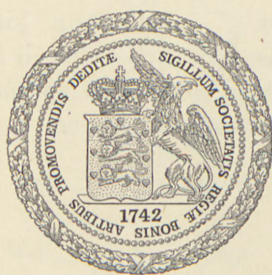
DET KGL. DANSKE VIDENSKABERNES SELSKAB  
MATEMATISK-FYSISKE MEDDELELSER, BIND XXII, Nr. 12

---

THE COMPLEX  
FORMATION BETWEEN CUPRIC  
AND ACETATE IONS

BY

KAI JULIUS PEDERSEN



KØBENHAVN

I KOMMISSION HOS EJNAR MUNKSGAARD

1945



THE COMPLEX  
FORMATION BETWEEN CLERIC  
AND ACETALDEHYDE

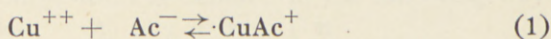
BY  
J. H. HANSEN



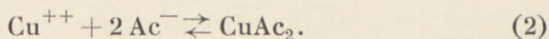
Printed in Denmark  
Bianco Lunos Bogtrykkeri A/S

Our present knowledge of the complex formation between cupric and carboxylate ions is very scanty and mostly of a qualitative nature. Although complex formation in solutions of cupric acetate has been studied by several workers (EWAN<sup>(1)</sup>, CALAME<sup>(2)</sup>, SIDGWICK and TIZARD<sup>(3)</sup>, GÜNTHER-SCHULZE<sup>(4)</sup>, FRENCH and LOWRY<sup>(5)</sup>, BRITTON and MEEK<sup>(6)</sup>), no satisfactory quantitative information of the problem is to be found in the literature.

The author of this paper has studied the complex formation in solutions containing cupric and acetate ions both by means of the glass electrode and by measurements of light absorption. The following equilibria are found (the acetate ion being denoted by  $\text{Ac}^-$ ):

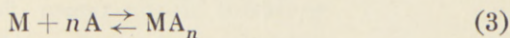


and

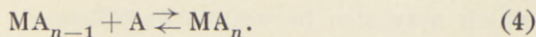


The measurements of light absorption indicate that higher complexes, such as  $\text{CuAc}_3^-$  and  $\text{CuAc}_4^{--}$ , and also polynuclear complexes, are formed in sufficiently concentrated solution.

In general, the complex formation between a central group M and ligand groups A may be expressed in one of the following ways:



and



The equilibrium constants are

$$K_n = \frac{(\text{MA}_n)}{(\text{M})(\text{A})^n} \quad (5)$$



and 
$$k_n = \frac{(MA_n)}{(MA_{n-1})(A)}, \quad (6)$$

respectively, where

$$K_n = k_1 k_2 \cdots k_n. \quad (7)$$

When only mononuclear complexes are formed, the total concentration of the central group is

$$c = \sum_0^N (MA_n) = \sum_0^N K_n (M) (A)^n, \quad (8)$$

where  $N$  is the maximum value of  $n$ , and  $K_0 = 1$ . The total concentration of ligands bound to the central group is

$$x = \sum_0^N n (MA_n) = \sum_0^N n K_n (M) (A)^n. \quad (9)$$

Into the mathematical formula

$$\sum_0^N \left( y_n \sum_0^N n y_n \right) = \sum_0^N \left( n y_n \sum_0^N y_n \right)$$

we insert

$$y_n = K_n (M) (A)^n$$

and use equations 8 and 9. We obtain

$$\sum_0^N K_n (M) (A)^n x = \sum_0^N n K_n (M) (A)^n c,$$

which may also be written as follows:

$$\sum_0^N K_n (nc - x) (A)^n = 0. \quad (10)$$

## Glass Electrode Measurements.

The method is similar to that used by J. BJERRUM<sup>(7)</sup> in his study of metal ammine formation. The concentration of free acetate ion in a solution of acetic acid, sodium acetate, and cupric nitrate may be found from the equation

$$(\text{Ac}^-) = K \frac{(\text{HAc})}{(\text{H}^+)}, \quad (11)$$

when the hydrogen ion concentration ( $\text{H}^+$ ) is measured and  $K$ , the dissociation constant of acetic acid in the solution, is known.

We make the assumption that the cupric ion concentration is sufficiently small for neglecting the formation of polynuclear complexes, and the acetate ion concentration sufficiently small for neglecting the formation of complexes with more than two acetate ions, that is, we consider only complexes formed according to the equilibria 1 and 2.

We further assume (1) that  $K$  is the same as in a solution in which the ions  $\text{Cu}^{++}$  and  $\text{CuAc}^+$  have been replaced by  $\text{Ba}^{++}$  and  $\text{Na}^+$ , respectively, and (2) that we may neglect a possible complex formation between barium and acetate ions.  $K$  is therefore determined by measuring the hydrogen ion concentration of solutions whose composition is denoted in the following way:

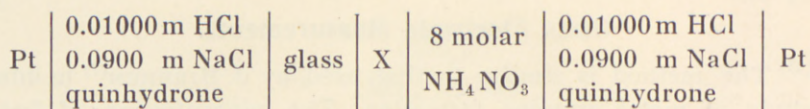
$$X = \begin{cases} d & \text{molar barium nitrate} \\ (s-b) & \text{molar sodium nitrate} \\ a & \text{molar acetic acid} \\ b & \text{molar sodium acetate.} \end{cases} \quad (12)$$

The complexity constants are found by measuring the hydrogen ion concentration of solutions composed as expressed in the following scheme:

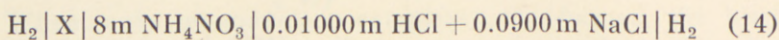
$$X = \begin{cases} c & \text{molar cupric nitrate} \\ (s-b) & \text{molar sodium nitrate} \\ a & \text{molar acetic acid} \\ b & \text{molar sodium acetate.} \end{cases} \quad (13)$$

The measurements were carried out at 18.0°C. The procedure was the same as that reported in an earlier paper<sup>(8)</sup>. The cells measured had the composition:





When a small asymmetry potential (measured daily by substituting for X the solution 0.01000 m HCl + 0.0900 m NaCl) was subtracted, the e. m. f.,  $E$  volts, of cells of the composition

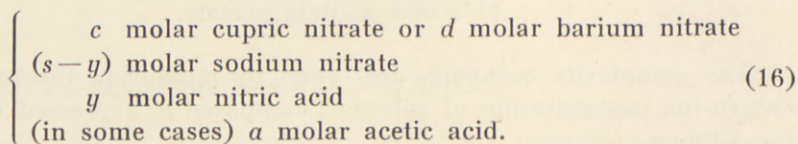


was obtained.

The hydrogen ion concentration ( $\text{H}^+$ ) of the solution X may be found from the measurements when we know  $A_0$  in the equation

$$-\log(\text{H}^+) = A_0 + 17.32 E. \quad (15)$$

$A_0$  includes the salt effect and the effect of the liquid-liquid junction of the left half cell (scheme 14), together with the whole effect of the right half cell, the latter having the same composition throughout the measurements. As an approximation to  $A_0$  for the solutions of the schemes 12 and 13 we use the values of  $A_0$  found for solutions in which the ions  $\text{Ac}^-$  and  $\text{CuAc}^+$  have been replaced by  $\text{NO}_3^-$  and  $\text{Na}^+$ , respectively. In order to determine these values,  $E$  is first measured for solutions of known hydrogen ion concentration of the composition expressed by the following scheme:



$A = -17.32 - \log(\text{H}^+)$  is calculated from the measurements, and  $A_0$  is found by extrapolation to  $y = 0$ .

Materials. — Acetic acid (glacial, free from higher homologes, for analytical purposes) was purified by partial crystallization and, finally, by distillation in an all-glass apparatus fitted out with a column containing glass beads (freezing point  $16.54^\circ$ ). — 1 molar sodium hydroxide was prepared from a clear, satu-

rated solution of sodium hydroxide (for analytical purposes) and carbon dioxide-free water. It was stored in a bottle covered inside with paraffin wax and protected from the carbon dioxide of the air.—Cupric nitrate (purest, Schering-Kahlbaum) was recrystallized from water. 1 molar solutions were stored in silica bottles. They were analyzed for copper by the iodometric titration method of HAGEN<sup>(9)</sup>. Metallic copper (electrolytically deposited) was used as a standard substance.—Barium nitrate and sodium nitrate (both for analytical purposes) were recrystallized.—Redistilled water was used for all the solutions.

Determination of  $A_0$ . The results are given in Table 1. The acid dissociation of the cupric ion being negligible<sup>(8)</sup>,  $(H^+) = y$  for all the solutions not containing acetic acid. In calculating  $(H^+)$  for the two solutions containing 0.1 and 0.5m acetic acid, respectively, the dissociation constants of acetic acid given in Table 3 have been used. It is seen that the increase of  $A_0$ , when acetic acid is added, is  $0.030 \times (HAc)$ .

The dissociation constant of acetic acid. The results of the electrometric measurements in solutions composed as expressed in scheme 12 are given in Table 2. Within each series, consisting of 4 solutions of the same ionic strength  $\mu$ ,  $d$ ,  $s$ , and  $a$  are kept constant, while  $b$  varies.  $-\log(H^+)$ , presented in the 6th column, is computed from  $E$  by means of equation 15. For  $A_0$  are used values taken from Table 1 for solutions of the same composition, except that the acetate ions have been replaced by nitrate ions (that is,  $b = 0$ ). Before use, the values are corrected for the influence of acetic acid. The last column but one of Table 2 gives the dissociation constant  $K$  of acetic acid found from the measurements. The dependence of  $-\log K$  on  $b$ , within a series at constant  $\mu$  may be expressed by the linear relationship given in the 5th column of Table 3.  $-\log K$  calculated from this formula is given in the last column of Table 2. The agreement between  $-\log K$  found and calculated is always satisfactory.

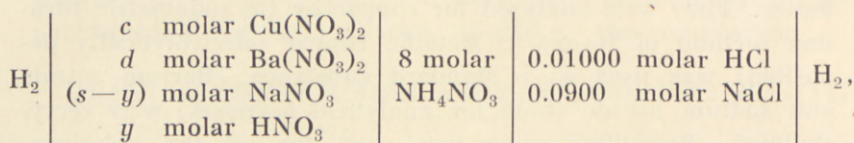
Table 3 gives a summary of the dissociation constants measured.  $-\log K$  for acetate-free solution, obtained by extrapolation to  $b = 0$  of the expression in the 5th column of the table, is free of the error introduced by using  $A_0$  for acetate-free solution



Table 1.

$$A = -17.32 E - \log(H^+),$$

where  $E$  is the e. m. f. in volts at 18.0°C. of the cell



measured by means of the glass electrode, and  $(H^+)$  is the hydrogen ion concentration of the solution in the left half cell.  $A_0$ , the value of  $A$  corresponding to  $y = 0$ , has been found by extrapolation.

c	d	s	A when y =				A <sub>0</sub>
			0.02	0.01	0.005	0.0025	
0.100	0.000	0.100	..	2.009	2.013	2.015	2.017
0.000	0.100	0.100	1.998	2.006	2.015	2.012	2.017
0.050	0.000	0.150	..	2.004	2.007	2.010	2.012
0.000	0.050	0.150	1.993	2.003	2.012	..	2.014
0.000	0.000	0.200	1.991	2.001	2.008	2.006	2.010
0.050	0.000	0.100	..	2.004	2.007	2.010	2.012
0.000	0.050	0.100	1.995	2.003	2.010	2.011	2.013
0.000	0.025	0.125	1.998	2.003	..	2.009	2.011
0.000	0.025	0.125 <sup>1</sup>	2.001	2.006	..	2.012	2.014
0.000	0.025	0.125 <sup>2</sup>	2.013	2.018	..	2.023	2.026
0.000	0.000	0.150	1.993	2.001	2.008	..	2.013
0.025	0.000	0.100	..	2.004	2.010	2.012	2.014
0.000	0.025	0.100	1.995	2.003	2.008	2.009	2.012
0.000	0.000	0.125	1.993	2.002	2.010	..	2.015
0.010	0.000	0.100	..	2.004	2.011	2.015	2.019
0.000	0.000	0.100	1.996	2.006	2.013	2.016	2.019

c	d	s	A when y =				A <sub>0</sub>
			0.008	0.004	0.002	0.001	
0.004	0.000	0.040	2.018	2.025	2.032	2.034	2.036
0.000	0.004	0.040	2.019	2.029	2.031	..	2.036
0.000	0.000	0.044	2.019	2.031	2.033	..	2.037

<sup>1</sup> The solution in addition contains 0.100 molar acetic acid.

<sup>2</sup> The solution in addition contains 0.500 molar acetic acid.

Table 2.

The electromotive force  $E$  volts at 18.0° C. of the cell

$H_2$	$d$ molar $Ba(NO_3)_2$ $(s-b)$ molar $NaNO_3$ $a$ molar $CH_3COOH$ $b$ molar $CH_3COONa$	8 molar $NH_4NO_3$	0.01000 molar HCl 0.0900 molar NaCl	$H_2$
-------	---	-----------------------	--	-------

measured by means of the glass electrode. The hydrogen ion concentration ( $H^+$ ) and the dissociation constant of acetic acid  $K$  in the solution of the left half cell.

$d$	$s$	$a$	$b$	$E$	$-\log(H^+)$	$-\log K$ found	$-\log K$ calcd.
0.1000	0.1000	0.1000	0.09984	0.1420 <sub>5</sub>	4.480	4.481	4.481
			0.04000	0.1186 <sub>5</sub>	4.075	4.472	4.472
			0.01994	0.1011 <sub>5</sub>	3.772	4.468	4.469
			0.00991	0.0843	3.480	4.468	4.467
0.0500	0.1500	0.1000	0.09984	0.1442	4.515	4.515	4.516
			0.04000	0.1205 <sub>5</sub>	4.105	4.502	4.500
			0.01994	0.1029	3.799	4.495	4.495
			0.00991	0.0858 <sub>5</sub>	3.504	4.493	4.493
0.0000	0.2000	0.1000	0.09984	0.1463	4.547	4.547	4.547
			0.04000	0.1226	4.136	4.533	4.533
			0.01994	0.1050	3.832	4.528	4.528
			0.00991	0.0878 <sub>5</sub>	3.535	4.525	4.525
0.0500	0.1000	0.1000	0.09984	0.1443	4.515	4.516	4.515
			0.04000	0.1207 <sub>5</sub>	4.107	4.504	4.504
			0.01994	0.1032	3.803	4.499	4.500
			0.00991	0.0862	3.509	4.498	4.498
0.0250	0.1250	0.1000	0.09984	0.1456 <sub>5</sub>	4.537	4.537	4.538
			0.04000	0.1220 <sub>5</sub>	4.128	4.525	4.524
			0.01994	0.1044	3.822	4.519	4.519
			0.00991	0.0873	3.526	4.516	4.516
0.0250	0.1250	0.5000	0.1005	0.1056 <sub>5</sub>	3.856	4.552	4.552
			0.04069	0.0823 <sub>5</sub>	3.452	4.538	4.538
			0.02065	0.0657	3.164	4.533	4.533
			0.01052	0.0507	2.904	4.531	4.530
0.0000	0.1500	0.1000	0.09984	0.1472	4.566	4.566	4.565
			0.04000	0.1231 <sub>5</sub>	4.149	4.546	4.548
			0.01994	0.1057	3.847	4.543	4.542
			0.00991	0.0885	3.549	4.539	4.539

(To be continued)



Table 2 (continued).

$d$	$s$	$a$	$b$	$E$	$-\log(H^+)$	$-\log K$ found	$-\log K$ calcd.
0.0250	0.1000	0.1000	{ 0.09984	0.1459	4.542	4.542	4.543
			{ 0.04000	0.1222 <sub>5</sub>	4.132	4.529	4.527
			{ 0.01994	0.1045	3.825	4.521	4.521
			{ 0.00991	0.0874 <sub>5</sub>	3.530	4.519	4.519
0.0000	0.1250	0.1000	{ 0.09984	0.1477	4.576	4.577	4.577
			{ 0.04000	0.1238 <sub>5</sub>	4.163	4.560	4.559
			{ 0.01994	0.1061	3.856	4.552	4.553
			{ 0.00991	0.0890	3.559	4.550	4.550
0.0100	0.1000	0.1000	{ 0.09984	0.1472	4.572	4.572	4.571
			{ 0.04000	0.1232 <sub>5</sub>	4.157	4.554	4.555
			{ 0.01994	0.1058	3.855	4.551	4.550
			{ 0.00991	0.0886	3.557	4.547	4.548
0.0040	0.0400	0.1000	{ 0.03986	0.1250 <sub>5</sub>	4.205	4.603	4.603
			{ 0.01597	0.1019 <sub>5</sub>	3.805	4.597	4.597
			{ 0.00796	0.0851	3.513	4.594	4.595
			{ 0.00406	0.0704	3.258	4.594	4.594
0.0000	0.0440	0.1000	{ 0.03986	0.1258 <sub>5</sub>	4.220	4.618	4.617
			{ 0.01597	0.1025	3.815	4.607	4.608
			{ 0.00796	0.0856 <sub>5</sub>	3.523	4.605	4.605
			{ 0.00406	0.0710	3.270	4.604	4.604

for the computation of  $-\log(H^+)$ . The formula at the bottom of the table expresses  $-\log K$  (when  $b = 0$ ) as a function of  $\mu$  and  $a$ . The influence of the acetic acid was estimated by comparing the 5th and the 6th series, containing 0.1 and 0.5m acetic acid, respectively. The factor before  $\sqrt{\mu}$  follows from Debye-Hückel's theory, while the other constants in the formula have been chosen so as to obtain the best fit.  $-\log K$  calculated from the formula is given in the last column of Table 3. A comparison with the values in the last column but one shows that the agreement is fairly good, although small systematic deviations owing to the individual influences of the sodium and barium ions are noticeable. The fact that equal ionic strengths of sodium and barium nitrate have nearly the same influence on the dissociation constant seems to justify the neglect of a possible complex formation between barium

Table 3.

The dissociation constant  $K$  at 18.0° C. of acetic acid

in the solution:  $\left\{ \begin{array}{l} d \text{ molar Ba(NO}_3)_2 \\ (s-b) \text{ molar NaNO}_3 \\ a \text{ molar CH}_3\text{COOH} \\ b \text{ molar CH}_3\text{COONa.} \end{array} \right.$

$d$	$s$	$a$	$\mu$	$-\log K$	$-\log K (b = 0)$ calculated
0.1000	0.1000	0.1000	0.400	$4.466 + 0.15 b$	4.465
0.0500	0.1500	0.1000	0.300	$4.490 + 0.26 b$	4.490
0.0000	0.2000	0.1000	0.200	$4.523 + 0.24 b$	4.516
0.0500	0.1000	0.1000	0.250	$4.496 + 0.19 b$	4.503
0.0250	0.1250	0.1000	0.200	$4.514 + 0.24 b$	4.516
0.0250	0.1250	0.5000	0.200	$4.528 + 0.24 b$	4.530
0.0000	0.1500	0.1000	0.150	$4.536 + 0.29 b$	4.532
0.0250	0.1000	0.1000	0.175	$4.516 + 0.27 b$	4.522
0.0000	0.1250	0.1000	0.125	$4.547 + 0.30 b$	4.543
0.0100	0.1000	0.1000	0.130	$4.545 + 0.26 b$	4.540
0.0040	0.0400	0.1000	0.052	$4.593 + 0.25 b$	4.594
0.0000	0.0440	0.1000	0.044	$4.602 + 0.37 b$	4.602

$$-\log K = 4.759_5 + 0.035a - 0.996 \sqrt{\mu} + 1.15\mu - 0.80\mu^2, \text{ when } b = 0.$$

and acetate ions. By extrapolation to infinite dilution, the activity constant  $-\log K^\circ = 4.759_5$  is obtained. There is a satisfactory agreement between this result and  $-\log K^\circ = 4.757$  found by HARNED and EHLERS<sup>(10)</sup> from electrometric measurements of cells without liquid junction at the same temperature.

The complexity constants. The results of the electrometric measurements in solutions composed as expressed in scheme 13 are given in Table 4a and b. Within each series consisting of 5 solutions,  $c$ ,  $s$ , and  $a$  are kept constant, while  $b$  varies.  $-\log(H^+)$ , presented in the last column but one of Table 4a, is found from  $E$  by means of equation 15. For  $A_0$  is used a value, found by interpolation in Table 1 for a solution containing, instead of the two ions  $\text{CuAc}^+$  and  $\text{Ac}^-$ , the ions  $\text{Na}^+$  and  $\text{NO}_3^-$ , respectively. Its composition may be expressed



Table 4a.

$c$	$s$	$a$	$b$	$E$	$A_0$	$-\log(H^+)$	$-\log K$
0.09978	0.1005	0.1000	0.1005	0.1137	2.015	3.984	4.506
			0.07536	0.1033	2.015	3.804	4.495
			0.5044	0.0908	2.016	3.589	4.486
			0.02023	0.0655	2.018	3.152	4.475
			0.00976	0.0485 <sub>5</sub>	2.019	2.860	4.470
0.04985	0.1005	0.1000	0.1005	0.1291	2.017	4.253	4.543
			0.07536	0.1191	2.016	4.079	4.532
			0.05044	0.1058	2.016	3.848	4.521
			0.02022	0.0783 <sub>5</sub>	2.015	3.372	4.507
			0.00978	0.0600	2.015	3.054	4.502
0.04985	0.1000	0.5000	0.09989	0.0889	2.029	3.569	4.556
			0.07536	0.0789 <sub>5</sub>	2.028	3.395	4.546
			0.04983	0.0653 <sub>5</sub>	2.028	3.160	4.535
			0.01963	0.0392 <sub>5</sub>	2.027	2.707	4.521
			0.00976	0.0254 <sub>5</sub>	2.027	2.468	4.516
0.02492	0.1005	0.1000	0.1005	0.1386 <sub>5</sub>	2.019	4.420	4.567
			0.07535	0.1294	2.019	4.260	4.558
			0.05043	0.1169	2.018	4.043	4.547
			0.02022	0.0893 <sub>5</sub>	2.017	3.565	4.531
			0.00975	0.0702	2.017	3.233	4.524
0.00999	0.1005	0.1000	0.1005	0.1444	2.021	4.522	4.574
			0.07535	0.1360 <sub>5</sub>	2.021	4.377	4.567
			0.05043	0.1246	2.021	4.179	4.560
			0.02022	0.0989	2.022	3.735	4.551
			0.00975	0.0796 <sub>5</sub>	2.022	3.402	4.549
0.003992	0.0398	0.1000	0.03976	0.1229	2.040	4.169	4.614
			0.02970	0.1150	2.040	4.032	4.609
			0.01975	0.1042	2.040	3.845	4.604
			0.00771	0.0801	2.039	3.426	4.598
			0.00393	0.0654	2.039	3.172	4.596

Table 4b.

(Ac <sup>-</sup> )	<i>x</i>	$\mu$	log <i>K</i> <sub>1</sub> found	log <i>K</i> <sub>1</sub> formula	log <i>K</i> <sub>2</sub> found	log <i>K</i> <sub>2</sub> formula	<i>E</i> calcd.	$\Delta 10^4$
0.03003	0.07057	0.2689	1.646	1.630	2.46	2.44	0.1138	+1
0.02034	0.05518	0.2957	1.639	1.617	2.47	2.43	0.1037	+4
0.01264	0.03806	0.3267	1.607	1.603	..	2.41	0.0909	+1
0.00472	0.01622	0.3686	1.587	1.586	..	2.39	0.0655	0
0.00242	0.00872	0.3840	1.584	1.580	..	2.38	0.0487	+1
..	..	0.400	1.577	1.575	..	..	..	..
0.05129	0.04927	0.1620	..	1.699	2.56	2.54	0.1292	+1
0.03520	0.04024	0.1760	1.678	1.688	2.51	2.52	0.1190	-1
0.02120	0.02938	0.1944	1.651	1.674	2.45	2.50	0.1054	-4
0.00730	0.01334	0.2243	1.653	1.655	..	2.48	0.0783	-1
0.00353	0.00713	0.2368	1.655	1.647	..	2.47	0.0602	+2
..	..	0.240	1.642	1.640	..	..	..	..
0.05149	0.04867	0.1625	..	1.699	2.53	2.54	0.0888	-1
0.03529	0.04047	0.1755	1.692	1.688	2.52	2.52	0.0789	-1
0.02106	0.02946	0.1944	1.661	1.674	2.47	2.50	0.0651	-3
0.00764	0.01395	0.2243	1.658	1.655	..	2.48	0.0393	+1
0.00445	0.00871	0.2358	1.651	1.648	..	2.47	0.0255	+1
..	..	0.240	1.645	1.640	..	..	..	..
0.07127	0.02927	0.1246	..	1.734	2.64	2.59	0.1389	+3
0.05032	0.02509	0.1306	..	1.728	2.61	2.58	0.1296	+2
0.03130	0.01922	0.1396	1.672	1.719	2.52	2.57	0.1167	-2
0.01078	0.00971	0.1564	1.694	1.704	..	2.55	0.0892	-2
0.00509	0.00525	0.1655	1.686	1.696	..	2.54	0.0699	-3
..	..	0.175	1.678	1.689	..	..	..	..
0.08870	0.01183	0.1098	..	1.750	2.52	2.61	0.1442	-2
0.06454	0.01085	0.1113	..	1.749	2.56	2.61	0.1360	0
0.04156	0.00894	0.1142	1.515	1.745	2.53	2.60	0.1244	-2
0.01525	0.00515	0.1207	1.714	1.738	..	2.59	0.0987	-2
0.00710	0.00305	0.1251	1.743	1.734	..	2.59	0.0798	+2
..	..	0.130	1.74	1.728	..	..	..	..
0.03587	0.00396	0.0448	..	1.859	2.87	2.76	0.1231	+2
0.02646	0.00333	0.0457	1.93	1.856	2.80	2.76	0.1151	+1
0.01739	0.00250	0.0471	1.784	1.853	..	2.75	0.1040	-2
0.00670	0.00138	0.0495	1.843	1.848	..	2.74	0.0800	-1
0.00374	0.00086	0.0507	1.838	1.845	..	2.74	0.0654	0
..	..	0.052	1.835	1.842	..	..	..	..



as follows:  $(\text{Cu}^{++})$  molar  $\text{Cu}(\text{NO}_3)_2 + [s + (\text{CuAc}^+)]$  molar  $\text{NaNO}_3 + a$  molar  $\text{HAc}$ . In order to find this value of  $A_0$ , we must have a rough knowledge of the equilibria in the solution under investigation. The method, therefore, is one of successive approximations. The value of  $A_0$  given in the 6th column of Table 4a is that finally adopted.

$(\text{Ac}^-)$ , presented in the first column of Table 4b, is found from  $(\text{H}^+)$  by means of equation 11 and

$$(\text{HAc}) = a - (\text{H}^+).$$

For  $K$  is used a value found by interpolation in Table 3 for a solution containing, instead of the two ions  $\text{Cu}^{++}$  and  $\text{CuAc}^+$ , the ions  $\text{Ba}^{++}$  and  $\text{Na}^+$ , respectively. Its composition may be expressed as follows:  $(\text{Cu}^{++})$  molar  $\text{Ba}(\text{NO}_3)_2 + [s + (\text{CuAc}^+) - (\text{Ac}^-)]$  molar  $\text{NaNO}_3 + a$  molar  $\text{HAc} + (\text{Ac}^-)$  molar  $\text{NaAc}$ . Here also, we must apply successive approximations. The value of  $-\log K$ , given in the last column of Table 4a, is that finally adopted.

$x$ , the concentration of acetate ion bound to cupric ion, is given in the second column of Table 4b. It has been computed by means of the equation

$$x = b + (\text{H}^+) - (\text{Ac}^-).$$

As already mentioned, we neglect in our computations polynuclear complexes and complexes with more than two acetate ions. We may also neglect the acid dissociation of the cupric ion. It follows from the equilibrium constants reported in an earlier paper<sup>(8)</sup> that the decrease in cupric ion concentration owing to acid dissociation is less than 0.1 per cent. at the hydrogen ion concentrations measured here. We therefore only consider the equilibria 1 and 2 with the mass action constants

$$K_1 = \frac{(\text{CuAc}^+)}{(\text{Cu}^{++})(\text{Ac}^-)} \quad \text{and} \quad K_2 = \frac{(\text{CuAc}_2)}{(\text{Cu}^{++})(\text{Ac}^-)^2}. \quad (17)$$

According to the equations 8 and 10, we have

$$c = (\text{Cu}^{++}) + K_1 (\text{Cu}^{++})(\text{Ac}^-) + K_2 (\text{Cu}^{++})(\text{Ac}^-)^2 \quad (18)$$

$$\text{and} \quad x = K_1(c-x)(\text{Ac}^-) + K_2(2c-x)(\text{Ac}^-)^2. \quad (19)$$

Equation 19 may also be written as

$$\frac{x}{(c-x)(\text{Ac}^-)} = K_1 + K_2 \frac{(2c-x)(\text{Ac}^-)}{c-x}. \quad (20)$$

From the equations 18, 19, and 17, we obtain

$$(\text{Cu}^{++}) = \frac{2c-x}{2 + K_1(\text{Ac}^-)} \quad (21)$$

and

$$(\text{CuAc}^+) = \frac{K_1(\text{Ac}^-)(2c-x)}{2 + K_1(\text{Ac}^-)}. \quad (22)$$

The concentrations of the cations in the solutions are  $(\text{Cu}^{++})$ ,  $(\text{CuAc}^+)$ ,  $(\text{Na}^+) = s$ , and  $(\text{H}^+)$ . Only univalent anions are present. By means of the equations 21 and 22 we therefore find that the ionic strength is

$$\mu = s + (\text{H}^+) + \frac{3 + K_1(\text{Ac}^-)}{2 + K_1(\text{Ac}^-)}(2c-x). \quad (23)$$

When  $(\text{Ac}^-)$  approaches 0, the last term of equation 20 vanishes. From each of the 6 series of measurements in the table, a preliminary value of  $K_1$  (corresponding to  $\mu = 3c + s$ ) may therefore be found by extrapolation of the term on the left side of equation 20 to  $(\text{Ac}^-) = 0$ . In this way, values of  $K_1$  at 5 different ionic strengths are obtained. They differ only slightly from those finally adopted. The final values, which are expressed by formula 24, are found by successive approximations, starting from the preliminary values. It is sufficient to describe the last step. We assume that we have obtained formula 24, and we shall show that the next step leads to the same formula.

$\mu$  and  $\log K_1$ , given in the 3rd and 5th column of Table 4b, are calculated from the formulae 23 and 24 by successive approximations. From  $K_1$  obtained in this way and the experimental data, we now compute  $K_2$  by means of formula 19. It follows from this formula that  $K_2$  is the less sensitive to an



error of  $K_1$  the smaller  $|c-x|$ , while, on the other hand,  $K_1$  is the less sensitive to an error of  $K_2$  the smaller  $(Ac^-)$  or  $x$ . When  $x = c$ ,  $K_1$  disappears from the equation.  $K_2$ , therefore, has only been computed for solutions where  $|c-x| < \frac{c}{2}$ . The results are to be found in the 6th column of Table 4b. They are used for developing formula 25.  $\log K_2$ , calculated from this formula, is given in the 7th column of the table. From the values of  $K_2$  obtained from formula 25 and the experimental data, we now compute  $K_1$  by means of formula 20.  $\log K_1$  found in this way is given in the 4th column of Table 4b. For the reason mentioned above, no results are given for the smallest values of  $|c-x|$ . The accuracy of  $K_1$  increases when  $x$  approaches 0, not only because the influence of complexes with two or more acetato-groups vanishes, but also owing to the disappearance of the error introduced by choosing a value of  $A_0$  corresponding to acetate-free solution. The values of  $\log K_1$  found for the smallest values of  $b$  are therefore considered the most reliable. The values printed in italics in Table 4b have been found by extrapolation to the ionic strengths corresponding to  $b = 0$  by means of the dependence on  $\mu$  expressed in formula 24. When these values are used in developing an interpolation formula, equation 24 is obtained.  $-\log K_1$  calculated from this formula is given in the 5th column of the table.

The formulae expressing the two equilibrium constants found from the measurements are

$$\log K_1 = 2.164 - \frac{1.992\sqrt{\mu}}{1 + 1.8\sqrt{\mu}} \quad (24)$$

$$\log K_2 = 3.205 - \frac{2.988\sqrt{\mu}}{1 + 2\sqrt{\mu}} \quad (25)$$

They contain two empirical constants each. The factor before the square root in the numerator has been deduced by the Debye-Hückel theory.

Equilibria 1 and 2 give a satisfactory explanation of the measurements in Table 4a, when the equilibrium constants have the values calculated from formulae 24 and 25. This is seen most directly when  $E$  is calculated by means of these

formulae and the system of equations given above, together with the values of  $A_0$  from Table 1 and  $K$  from Table 3. In this way, the values of  $E$  presented in the last column but one of Table 4b are obtained. The deviation  $\Delta$  from  $E$  observed is given in the last column. The agreement is satisfactory.

By comparison of the second and third series of Table 4a and b, it is seen that an increase of the concentration of acetic acid from 0.1 to 0.5 molar (and, consequently, the corresponding increase of the hydrogen ion concentration) has no influence on the equilibrium constants found. This shows that the acetato-complexes considered have neither split off nor taken up protons to any perceptible degree. Complexes containing hydroxyl ions or acetic acid as ligands are, therefore, of no importance in the solutions measured here.

$K_1$  of equation 24 has been found by an extrapolation to acetate-free solution. It is, therefore, essentially free of the error due to the neglect of complexes with more than two acetato-groups and to the application of values of  $A_0$  found for acetate-free solutions. On the other hand, we cannot exclude errors due to the formation of polynuclear complexes and to the use of  $K$  for solutions containing barium ions instead of cupric ions. Further, formation of nitrate-complexes may have some influence. All these errors, however, vanish when  $c$  approaches 0.  $K_2$  of equation 25 is much less accurate than  $K_1$ . None of the errors mentioned can be excluded.

If we extrapolate to  $\mu = 0$  by means of the formulae 24 and 25, we obtain

$$K_1^0 = 146 \quad \text{and} \quad K_2^0 = 1600.$$

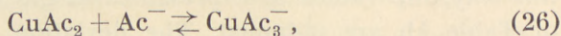
When the equilibria are written in the form of scheme 4, we find, according to equation 7:

$$k_1^0 = 146 \quad \text{and} \quad k_2^0 = 11.$$

Hence,  $k_2^0/k_1^0 = 0.075$ . If we assume that a cupric ion can take up altogether 4 acetate ions in 4 uniform co-ordinative positions,  $k_2^0/k_1^0$  should, for statistical reasons only, be  $\frac{3}{8} = 0.375$  (cf. J. BJERRUM<sup>(7)</sup>). A ligand effect is therefore responsible for



a 5 times decrease of the ratio. We may make a very rough estimate of  $k_3$ , the mass action constant of the equilibrium



when we assume that the ligand effects of  $k_2^0/k_1^0$  and  $k_3^0/k_2^0$  are equal. The statistical factor of  $k_3/k_2$  is  $\frac{4}{9}$ . Hence, we find  $k_3^0 \approx \frac{4}{9} \times \frac{1}{5} \times 11 \approx 1$ . Owing to the nature of equilibrium 26,  $k_3$  is approximately independent of the salt concentration. Using equation 7, we therefore find  $K_3 \approx K_2$ . By means of this very rough estimate of  $K_3$ , an attempt was made to correct the determinations of  $K_1$  and  $K_2$  for the influence of the formation of triacetato-complexes. As might be expected, formula 24 was unchanged. The only change of formula 25 was that the constant 3.205 fell to 3.17.

The figure illustrates the complex formation in solutions of sodium acetate containing an infinitesimal amount of cupric nitrate. The fraction of the cupric ions which has combined with  $n$  acetate ions ( $\alpha_n$ ), and the average number of acetate ions bound per atom of copper ( $\frac{x}{c}$ ), have been computed by means of the formulae

$$\alpha_n = \frac{K_n (\text{Ac}^-)^n}{\sum_0^N K_n (\text{Ac}^-)^n}$$

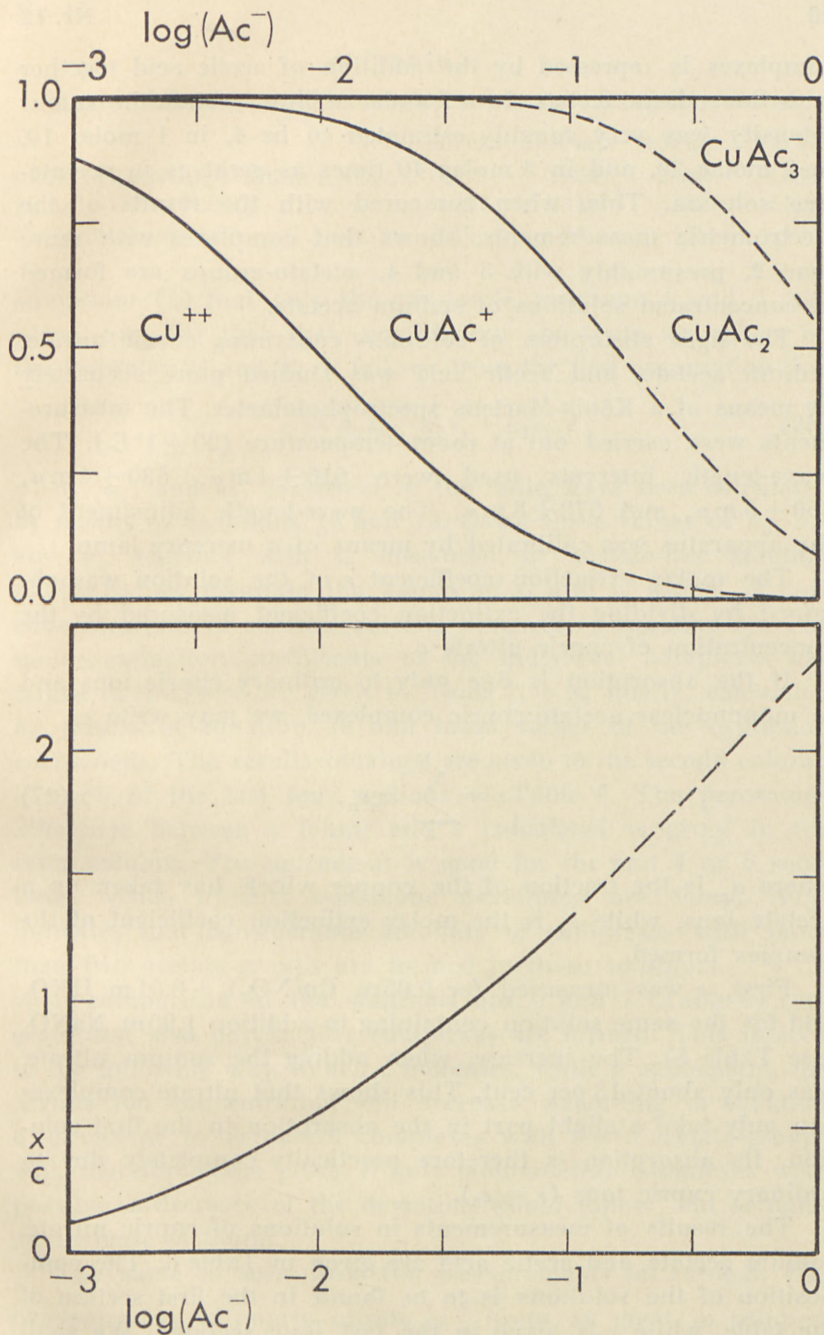
and

$$\frac{x}{c} = \sum_1^N n \alpha_n.$$

It has been assumed that complexes with more than three acetato-groups are not formed ( $N = 3$ ).  $K_1$  has been calculated from equation 24, while both  $K_2$  and  $K_3$  have been found from equation 25 modified as just mentioned.

### Measurements of Light Absorption.

When sodium acetate is added to a solution of cupric nitrate, the blue colour intensifies, even when the formation of hydroxo-



Complex formation in solutions of sodium acetate containing a small amount of cupric nitrate. In the upper graph, the parts of the ordinate falling in the areas marked  $\text{Cu}^{++}$ ,  $\text{CuAc}^+$ ,  $\text{CuAc}_2$ , and  $\text{CuAc}_3^-$ , respectively, represent the fractions of the copper which have formed the complexes stated. The lower graph shows the average number of acetate ions bound per atom of copper.



complexes is repressed by the addition of acetic acid together with the sodium acetate. In 0.1 molar sodium acetate the colour intensity was very roughly estimated to be 4, in 1 molar 10, in 2 molar 20, and in 3 molar 40 times as great as in acetate-free solution. This, when compared with the results of the electrometric measurements, shows that complexes with more than 2, presumably with 3 and 4, acetato-groups are formed in concentrated solutions of sodium acetate.

The light absorption of solutions containing cupric nitrate, sodium acetate, and acetic acid was studied more accurately by means of a König-Martens spectrophotometer. The measurements were carried out at room temperature ( $20 \pm 1^\circ \text{C}$ ). The wave-length intervals used were  $610 \pm 4 \text{ m}\mu$ ,  $630 \pm 4 \text{ m}\mu$ ,  $650 \pm 5 \text{ m}\mu$ , and  $670 \pm 8 \text{ m}\mu$ . The wave-length adjustment of the apparatus was calibrated by means of a mercury lamp.

The molar extinction coefficient  $\epsilon$  of the solution was obtained by dividing the extinction coefficient measured by the concentration of cupric nitrate  $c$ .

If the absorption is due only to ordinary cupric ions and to mononuclear acetato-cupric complexes, we may write

$$\epsilon = \sum_0^N \alpha_n \epsilon_n, \quad (27)$$

where  $\alpha_n$  is the fraction of the copper which has taken up  $n$  acetate ions, while  $\epsilon_n$  is the molar extinction coefficient of the complex formed.

First,  $\epsilon$  was measured for  $0.05 \text{ m Cu(NO}_3)_2 + 0.01 \text{ m HNO}_3$  and for the same solution containing in addition  $1.90 \text{ m NaNO}_3$  (see Table 5). The increase, when adding the sodium nitrate, was only about 13 per cent. This shows that nitrate-complexes can only take a slight part in the absorption in the first solution. Its absorption is therefore practically completely due to ordinary cupric ions ( $\epsilon = \epsilon_0$ ).

The results of measurements in solutions of cupric nitrate, sodium acetate, and acetic acid are given in Table 6. The composition of the solutions is to be found in the first section of the table, while  $\epsilon$  is given in the last four sections. We shall examine to what extent the measurements agree with the as-

Table 5.

Molar extinction coefficients of solutions of cupric nitrate.

	610 m $\mu$	630 m $\mu$	650 m $\mu$	670 m $\mu$
0.0500 m Cu(NO <sub>3</sub> ) <sub>2</sub> + 0.01 m HNO <sub>3</sub> ..	1.115	1.850	2.880	4.030
Same + 1.90 m NaNO <sub>3</sub> .....	1.257	2.110	3.252	4.514
Percentage increase .....	13	14	13	12

sumptions (1) that only the reversible reactions 1 and 2 take place, and (2) that their equilibrium constants are given by the formulae 24 and 25. It follows from the first assumption that

$$\varepsilon = \alpha_0 \varepsilon_0 + \alpha_1 \varepsilon_1 + \alpha_2 \varepsilon_2. \quad (28)$$

$\mu$ ,  $\alpha_0$ ,  $\alpha_1$ , and  $\alpha_2$ , presented in the table, have been calculated by means of equations 18 and 19. Using these values of  $\alpha_0$ ,  $\alpha_1$ , and  $\alpha_2$ , together with  $\varepsilon_0$  measured in acetate-free solution (Table 5), we compute the values of  $\varepsilon_1$  and  $\varepsilon_2$  which, at low concentrations of sodium acetate, best satisfy equation 28. The molar extinction coefficients of the individual complexes obtained in this way are given in Table 7.  $\varepsilon$  is, finally, calculated by means of equation 28 and these values of the extinction coefficients. The results obtained are given in the second column of each of the last four sections of Table 6. The percentage difference between  $\varepsilon$  found and  $\varepsilon$  calculated is given in the third column. The agreement is good for the first 4 or 5 solutions. When  $b > 0.1$ , systematic deviations are found. This indicates that considerable amounts of complexes with more than two acetato-groups are formed in these solutions.

A comparison of the solutions nos. 6 and 7 (Table 6) suggests that also polynuclear complexes are formed. This is seen in the following way. When  $c$  increases, while  $b$  is constant, the acetate ion concentration will decrease. According to equation 6, a change in favour of complexes with fewer acetato-groups will, therefore, take place. If only mononuclear complexes were possible, a decrease of the deviation would follow; but actually an increase is found.

The same is seen from the measurements in Table 8. The concentration of cupric nitrate is  $\frac{5}{2}$  times as great in solution X as in solution Y, while the concentrations of sodium acetate



Table 6.

The molar extinction coefficients  $\epsilon$  of cupric nitrate solutions containing:  
 $c$  molar  $\text{Cu}(\text{NO}_3)_2 + b$  molar  $\text{CH}_3\text{COONa} + 0.100$  molar  $\text{CH}_3\text{COOH}$ .

No.	$c$	$b$	$\mu$	$\alpha_0$	$\alpha_1$	$\alpha_2$
1	0.04976	0.02000	0.1424	0.7344	0.2538	0.0118
2	0.05035	0.04002	0.1427	0.5397	0.4169	0.0434
3	0.05035	0.07031	0.1490	0.3392	0.5428	0.1180
4	0.05035	0.0999	0.1629	0.2257	0.5729	0.2014
5	0.1003	0.04002	0.2808	0.7068	0.2765	0.0167
6	0.02042	0.1998	0.2123	0.0563	0.4407	0.5030
7	0.05035	0.1998	0.2370	0.0834	0.4888	0.4278
8	0.05035	0.2998	0.3262	0.0440	0.3941	0.5619

No.	$\epsilon$ at 610 m $\mu$			$\epsilon$ at 630 m $\mu$		
	found	calcd.	Percentage diff.	found	calcd.	Percentage diff.
1	2.071	2.074	-0.1	3.412	3.413	0
2	2.912	2.900	+0.4	4.737	4.726	+0.2
3	3.967	3.975	-0.2	6.364	6.384	-0.3
4	4.804	4.804	0	7.622	7.623	0
5	2.219	2.194	+1.1	3.639	3.602	+1.0
6	7.072	6.986	+1.2	10.90	10.76	+1.3
7	6.763	6.493	+4.0	10.53	10.06	+4.5
8	8.077	7.342	+9.1	12.46	11.26	+9.6

No.	$\epsilon$ at 650 m $\mu$			$\epsilon$ at 670 m $\mu$		
	found	calcd.	Percentage diff.	found	calcd.	Percentage diff.
1	5.208	5.201	+0.1	6.954	6.925	+0.4
2	7.072	7.086	-0.2	9.230	9.288	-0.6
3	9.344	9.366	-0.2	12.14	12.17	-0.2
4	11.02	10.99	+0.3	14.29	14.23	+0.4
5	5.473	5.471	0	7.380	7.264	+1.6
6	15.35	14.83	+3.4	19.60	19.17	+2.2
7	14.86	14.00	+5.8	18.70	18.10	+3.2
8	17.41	15.41	+11.5	21.78	19.92	+8.6

Table 7.

Molar extinction coefficients of the individual complexes.

		610 m $\mu$	630 m $\mu$	650 m $\mu$	670 m $\mu$
Cu <sup>++</sup>	$\epsilon_0$ .....	1.115	1.850	2.880	4.030
CuAc <sup>+</sup>	$\epsilon_1$ .....	4.49	7.41	11.26	14.46
CuAc <sub>2</sub>	$\epsilon_2$ .....	9.83	14.7	19.3	25.0

are the same. The sodium nitrate is added in order to keep the ionic strength nearly constant. The difference between the extinctions of 2 cm. of solution X and 5 cm. of solution Y was measured directly, and the difference between the molar extinction coefficients of the solutions,  $\epsilon_X - \epsilon_Y$ , was evaluated. When passing from solution X to solution Y, a change in favour of

Table 8.

Measurements of the difference between the molar extinction coefficients  $\epsilon_X$  and  $\epsilon_Y$  of the cupric nitrate solutions X and Y at the wave-length 630 m $\mu$ . All the solutions contain 0.200 m acetic acid.

Cu (NO <sub>3</sub> ) <sub>2</sub>	Solution X		Cu (NO <sub>3</sub> ) <sub>2</sub>	Solution Y		$\epsilon_X - \epsilon_Y$
	CH <sub>3</sub> COONa	NaNO <sub>3</sub>		CH <sub>3</sub> COONa	NaNO <sub>3</sub>	
0.0760	0.500	1.35	0.0304	0.500	1.44	0.158
0.0760	0.750	1.10	0.0304	0.750	1.19	0.399
0.0512	0.750	1.15	0.0205	0.750	1.21	0.237

complexes with a greater number of acetato-groups will take place. If only mononuclear complexes were formed,  $\epsilon_X - \epsilon_Y$  would therefore be negative; but actually positive values are found.

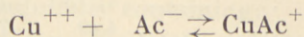
I wish to express my cordial thanks to the head of the laboratory, Professor NIELS BJERRUM, for advice and kind interest in my work.

### Summary.

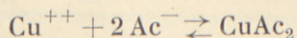
The hydrogen ion concentration of solutions containing cupric nitrate, sodium nitrate, acetic acid, and sodium acetate was measured at 18.0° C. by means of the glass electrode.



The acetate ion concentration of the solutions was calculated from the hydrogen ion concentration and the dissociation constant of acetic acid. The mass action constants of the equilibria



and



were evaluated.

The dissociation constant of acetic acid was determined from measurements of the hydrogen ion concentration of solutions containing barium nitrate instead of cupric nitrate.

Spectrophotometric measurements were carried out on solutions containing cupric nitrate, acetic acid, and sodium acetate. Although they do not allow an independent calculation of the complexity constants, they agree with the electrometric measurements at concentrations where a comparison is possible. They further indicate that both complexes with more than two acetato-groups and polynuclear complexes are formed in more concentrated solution.

*From the Chemical Laboratory  
of the Royal Veterinary and Agricultural College.  
Copenhagen, Denmark.*

---

### References.

- (1) T. EWAN, Proc. Roy. Soc. (London) **57** (1894) 117.
  - (2) P. CALOME, Z. physik. Chem. **27** (1898) 401.
  - (3) N. V. SIDGWICK and H. T. TIZARD, J. Chem. Soc. **93** (1908) 188, **97** (1910) 957.
  - (4) A. GÜNTHER-SCHULZE, Z. Elektrochem. **28** (1922) 89.
  - (5) H. S. FRENCH and T. M. LOWRY, Proc. Roy. Soc. (London) A **106** (1924) 489.
  - (6) H. T. S. BRITTON and F. H. MEEK, J. Chem. Soc. (1931) 2831.
  - (7) J. BJERRUM, Metal Ammine Formation in Aqueous Solution. Dissertation. Copenhagen (1941).
  - (8) K. J. PEDERSEN, D. Kgl. Danske Vidensk. Selskab, Mat.-fys. Medd. **XX** 7 (1943).
  - (9) S. K. HAGEN, Z. anal. Chem. **117** (1939) 26, Kemisk Maanedssblad **23** (1942) 38.
  - (10) H. S. HARNED and R. W. EHLERS, J. Amer. Chem. Soc. **55** (1933) 652.
-





DET KGL. DANSKE VIDENSKABERNES SELSKAB  
MATEMATISK-FYSISKE MEDDELELSER, BIND XXII, NR. 13

---

# EINLEITUNG IN DIE ALLGEMEINE KONGRUENZLEHRE

VON

JOHANNES HJELMSLEV

FÜNFTE MITTEILUNG



KØBENHAVN

I KOMMISSION HOS EJNAR MUNKSGAARD

1945



Früher veröffentlichte Mitteilungen I—IV:

Einleitung in die allgemeine Kongruenzlehre, Erste Mitteilung, D. Kgl. Danske Vidensk. Selskab, Math.-fys. Medd. VIII, 11, 1929; Zweite Mitteilung, ibd. X, 1, 1929; Dritte Mitteilung, ibd. XIX, 12, 1942; Vierte Mitteilung, ibd. XXII, 6, 1945.

In dieser fünften Mitteilung kehren wir zunächst zu den in der dritten Mitteilung vorgeführten Fragen über Nachbarpunkte und Nachbargeraden zurück. Die schwachen Transporte (die singulären Bewegungen) der Ebene in sich werden näher erörtert, und für die Schmiegebüschel (d. h. Büschel von Geraden, welche durch zwei vorgegebene Nachbarpunkte, und somit durch deren zugehörige Erweiterung hindurchgehen) werden die Beziehungen zwischen dem Scheitelemente und den Schnittelementen, welche von verschiedenen Transversalen aus dem Büschel ausgeschnitten werden, dargelegt. Auch werden Nachbargeraden ohne gemeinsame Punkte genauer untersucht und die Beziehungen der beiden Dimensionen eines Rechtecks auseinandergesetzt.

Schliesslich wird nachgewiesen (in § 8), dass die singuläre Geometrie (d. h. die Geometrie wo Rechtecke beliebiger Dimensionen existieren) mit Hilfe einer Erweiterung der Hilbertschen Streckenrechnung erledigt werden kann. Es geht hieraus hervor, dass die Hauptsätze der Euklidischen Geometrie tatsächlich von dem Eindeutigkeitsaxiom unabhängig bestehen.

---

### § 1. Schwache Transporte in der Ebene.

1. Unter einem schwachen Transport soll ein Transport verstanden werden, welcher jeden Punkt entweder in einen Nachbarpunkt überführt oder in Ruhe lässt. Im besonderen spricht man von einer schwachen Drehung um einen Punkt oder einer schwachen Schiebung längs einer Geraden. Jeder schwache Transport ist ein direkter Transport. Zwei Figuren,



welche durch einen schwachen Transport in einander übergehen können, sollen als Nachbarfiguren bezeichnet werden.

Einen Transport, welcher durch Zusammensetzung eines schwachen Transportes und einer Achsenspiegelung entsteht, bezeichnen wir als Nachbarspiegelung. Dieselbe lässt sich darstellen entweder als Produkt  $Aa$  einer Punktspiegelung  $A$  und einer Achsenspiegelung  $a$  derart, dass der Punkt  $A$  Nachbarpunkt der Geraden  $a$  ist, oder als Produkt einer Achsenspiegelung  $x$  und einer schwachen Schiebung längs der Geraden  $x$ .

Zwei schwache Transporte oder zwei Nachbarspiegelungen lassen sich zu einem schwachen Transport zusammensetzen.

Ein direkter Transport, welcher zwei Fernpunkte  $A, B$  in zwei zu diesen benachbarte Punkte  $A_1, B_1$  überführt, ist ein schwacher Transport. Er lässt sich nämlich aus zwei schwachen Transporten, nämlich einer schwachen Schiebung  $A \rightarrow A_1$  und einer schwachen Drehung um  $A_1$ , zusammensetzen.

2. Ein schwacher Transport mit einem Fixpunkt  $A$  besitzt unendlich viele Fixpunkte. Der Transport lässt sich nämlich als Produkt  $ab$  zweier Achsenspiegelungen darstellen, deren Achsen  $a, b$  Schmiegeraden sind, welche beide durch den Punkt  $A$  gehen, wobei die eine von diesen sonst beliebig gewählt werden kann. Die beiden Geraden  $a, b$  haben unendlich viele Punkte mit einander gemein, und jeder von diesen Punkten ist ein Fixpunkt des vorgegebenen Transportes.

Hat ein schwacher Transport eine Fixgerade  $a$ , so besitzt er unendlich viele Fixgeraden. Der Transport lässt sich nämlich darstellen als Produkt  $AB$  zweier Punktspiegelungen, deren Zentren  $A, B$  Nachbarpunkte auf der Geraden  $a$  sind, von welchen der eine sonst beliebig gewählt werden kann. Die beiden Punkte haben unendlich viele Verbindungsgeraden, und jede von diesen ist eine Fixgerade des vorgelegten Transportes.

Wenn ein schwacher Transport weder Fixpunkte noch Fixgeraden besitzt, so lässt er sich darstellen als Produkt  $ab$  zweier Achsenspiegelungen, deren Achsen  $a, b$  Nachbargeraden sind, ohne gemeinsame Punkte oder gemeinsame Normalen. Die beiden Geraden können so bestimmt werden, dass eine beliebige von ihnen durch einen vorgegebenen Punkt hindurchgeht.

## § 2. Striche und Flecke.

3. Alle Geraden, welche durch zwei vorgegebene Nachbarpunkte  $A, B$  hindurchgelegt werden können, bilden ein Schmiegbüschel  $S(A, B)$ . Sie haben eine ganze Menge von Punkten  $S(A, B)$  mit einander gemein, welche wir früher (Einl. III, 55) als Erweiterung der Strecke  $AB$  (oder als lineares Element, Schnittelement, Scheitelelement des Schmiegbüschels) bezeichnet haben. Aus diesem Elemente haben wir wiederum ein entsprechendes ebenes Element durch Drehung um einen beliebigen Punkt von  $S(A, B)$  abgeleitet. Wir gehen nun daran, diese Elemente näher zu untersuchen. Der Bequemlichkeit halber wollen wir das lineare Element  $S(A, B)$  mit dem kurzen Namen »Strich«, und das entsprechende ebene Element mit dem Namen »Fleck« bezeichnen. Die Strecke  $AB$  soll Grundstrecke der beiden Elemente heißen.

4. Für jeden direkten Transport  $\tau$ , welcher die beiden Nachbarpunkte  $A$  und  $B$  stehen lässt, sind alle Punkte von  $S(A, B)$  Fixpunkte. Der Transport lässt sich nämlich als Produkt  $ab$  zweier Spiegelungen darstellen, deren Achsen durch die Punkte  $A, B$  gehen, wobei  $a$  eine beliebig zu wählende Gerade durch diese Punkte bezeichnet. Die Geraden  $a, b$  enthalten sonach alle Punkte von  $S(A, B)$ , und infolgedessen lässt der Transport  $\tau = ab$  alle Punkte von  $S(A, B)$  in Ruhe. Umgekehrt gilt, dass jeder Punkt  $C$  einer vorgegebenen Geraden  $a$  durch  $A$  und  $B$ , welcher Fixpunkt eines jeden Transportes ist, welcher die Punkte  $A, B$  stehen lässt, dem Strich  $S(A, B)$  angehören muss. Jeder der in Rede stehenden Transporte lässt sich nämlich durch eine Spiegelungsfolge  $ab$  ersetzen derart, dass die Gerade  $b$  durch  $A$  und sonach auch durch  $B$  und  $C$  hindurchläuft, woraus folgt, dass  $C$  dem Strich  $S(A, B)$  angehört.

5. Jeder direkte Transport mit den Fixpunkten  $A, B$  besitzt aber unendlich viele Fixpunkte, welche dem Strich  $S(A, B)$  nicht angehören. Beispielsweise schneiden sich wie früher gezeigt (Einl. I, S. 31 ff.) zwei Geraden durch  $A$  bzw.  $B$ , welche nicht Nachbargeraden sind, in einem neuen Fixpunkt.

In der ganzen Ebene soll nun die Menge aller Fixpunkte, welche jedem Transport mit den beiden Fixpunkten  $A, B$  angehören, mit  $F(A, B)$  bezeichnet werden. Sie ist wie früher ange-



deutet mit der ebenen Erweiterung von  $A, B$  (oder von  $S(A, B)$ ) identisch. Dies soll nun hier näher nachgewiesen werden.

Es sei  $p$  eine beliebige Gerade durch  $A$ . Wir können dann eine ihr entsprechende gerade Linie  $q$  durch  $A$  derart bestimmen, dass  $pq = ab$  (wobei  $a, b$  dieselbe Bedeutung haben wie oben) den in Rede stehenden Transport mit den Fixpunkten  $A, B$  darstellt. Das Geradenpaar  $p, q$  wird aus  $a, b$  durch eine Drehung um  $A$  abgeleitet, wobei  $a$  in  $p$  übergeht. Es folgt hieraus, dass die Gerade  $p$  den Fleck  $F(A, B)$  in einem Strich schneidet, welcher aus  $S(A, B)$  durch Drehung um  $A$  entsteht. Also jede Gerade, welche durch  $A$  oder einen anderen Punkt von  $F(A, B)$  gelegt wird, schneidet  $F(A, B)$  in einem Strich, welcher dem Strich  $S(A, B)$  kongruent ist. Mit anderen Worten: Der Fleck  $F(A, B)$  wird aus dem Strich  $S(A, B)$  durch Drehung um einen beliebigen Punkt in diesem erzeugt.

6. Ist nun  $g$  eine beliebige Gerade, welche durch die beiden Punkte  $A, B$  und infolgedessen durch alle Punkte von  $S(A, B)$ , hindurchgeht, und ist  $C$  ein Punkt von  $F(A, B)$  ausserhalb  $g$ , ist ferner  $h$  eine Gerade, welche durch  $C$  geht und die Gerade  $g$  eindeutig in  $D$  schneidet, und ist  $g_1$  eine neue Gerade durch  $A, B$ , dann lässt sich eine Gerade  $h_1$  durch  $C$  so bestimmen, dass  $gg_1 = hh_1$ .

Hieraus folgt aber  $hgg_1 = h_1$ , d. h. die drei Geraden  $g, h, g_1$  sind in Involution, und weil die beiden ersten Geraden  $g, h$  sich eindeutig in  $D$  schneiden, muss die dritte Gerade,  $g_1$ , durch  $D$  gehen, d. h.  $D$  gehört dem Strich  $S(A, B)$  an. Es gilt also:

Ist  $g$  eine beliebige Gerade durch die beiden Nachbarpunkte  $A, B$ , und  $C$  ein Punkt von  $F(A, B)$  ausserhalb  $g$ , dann wird jeder Punkt, in welchem  $g$  von einer Geraden  $h$  durch  $C$  eindeutig geschnitten wird, dem Strich  $S(A, B)$  angehören.

Im besonderen wird also der Fusspunkt der Senkrechten von  $C$  auf  $g$  dem Strich  $S(A, B)$  angehören. Das Spiegelbild von  $C$  bezüglich  $g$  gehört sonach dem Fleck  $F(A, B)$  an.

Es folgt dann, dass in der inneren Geometrie des Flecks  $F(A, B)$  alle ursprünglich aufgestellten Axiome der ebenen Geometrie gültig sind, wenn wir unter

»Gerade« den Durchschnitt des Flecks mit einer ursprünglichen Geraden verstehen.

7. Drei Geraden  $a, b, c$  von welchen die beiden ersten,  $a, b$ , Schmieggeraden sind mit dem Schnittelelement  $S(a, b)$ , bestimmen dann und nur dann einen involutorischen Transport  $abc$ , wenn die dritte Gerade  $c$  den durch  $S(a, b)$  erzeugten Fleck durchschneidet.

Beweis. Es sei  $O$  ein Punkt des Schnittelements  $S(a, b)$  und  $P$  sein Spiegelbild in bezug auf  $c$ . Dann muss  $P$  bei dem Transport  $cbac$  fest bleiben. Ist nun  $cba = abc$ , also  $cbac = ab$ , folgt hieraus, dass  $P$  bei dem Transport  $ab$  stehen bleibt und dem von  $S(a, b)$  erzeugten Fleck angehören muss. Dies gilt aber dann auch von dem Mittelpunkt  $M$  der Strecke  $OP$ , und da  $M$  auf  $c$  gelegen ist, ist hiermit bewiesen, dass  $c$  den Fleck durchschneidet. Umgekehrt: Wenn  $c$  in den Fleck hineindrängt, muss das Spiegelbild  $P$  von  $O$  bezüglich  $c$ , und somit auch der Mittelpunkt  $M$  von  $OP$ , dem Fleck angehören. Infolgedessen muss  $M$  bei dem Transport  $abc$  fest liegen, d. h. dieser Transport ist eine Spiegelung.

8. Zwei Paare von Nachbarpunkten,  $A, B$  und  $C, D$  sollen ebenbürtig heißen, in Zeichen  $AB \infty CD$ , wenn die entsprechenden Striche  $S(A, B)$  und  $S(C, D)$  einander kongruent sind.

Gehen zwei Geraden  $h, i$ , welche einander in einem Punkt  $C$  eindeutig schneiden, durch zwei Nachbarpunkte  $A$  bzw.  $B$ , dann muss mindestens eine von diesen Geraden jede Gerade  $g$  durch  $A$  und  $B$  eindeutig schneiden (Einl. III, 12). Ist z. B. der Schnittpunkt  $A$  von  $h$  und  $g$  eindeutig bestimmt, so folgt hieraus, dass  $A$  dem Flecke  $F(B, C)$  und  $C$  dem Flecke  $F(A, B)$  angehört, und infolgedessen sind die beiden Flecke identisch, d. h. die Striche  $S(A, B)$  und  $S(B, C)$  sind einander kongruent. Kurz kann dies so ausgedrückt werden:

Wenn in einem Dreieck mit singulären Seiten zwei ordinäre Winkel vorhanden sind, dann müssen die ihnen gegenüberliegenden Seiten einander ebenbürtig sein.

Sind alle drei Winkel ordinär, so müssen alle drei Seiten einander ebenbürtig sein.

9. Ein Nachbarpunktepaar  $A, B$  soll einem anderen Nachbarpunktepaar  $C, D$  unterlegen genannt werden, in Zeichen:



$AB \prec CD$ , wenn  $S(A, B)$  durch einen Transport in einen echten Teil von  $S(C, D)$  übergeführt werden kann. Dieselbe Eigenschaft wird dadurch ausgedrückt, dass das Paar  $C, D$  dem Paar  $A, B$  überlegen genannt wird, in Zeichen  $CD \succ AB$ .

Dieselbe Beziehung wird dadurch ausgedrückt, dass wir  $S(A, B)$  und  $F(A, B)$  kleiner (oder schwächer) als  $S(C, D)$  bzw.  $F(C, D)$  nennen.

Lemma I. Ist  $AB \succ BC$ , so folgt  $AC \approx AB$ . Die Dreiecksungleichheit besagt nämlich, dass

$$AB - BC \leq AC \leq AB + BC,$$

und hieraus folgt, wegen  $BC < \frac{1}{2}AB$ ,

$$\frac{1}{2}AB < AC < \frac{3}{2}AB.$$

Lemma II. Es seien  $a, b, c$  drei Nachbargeraden, welche durch denselben Punkt gehen. Die Schnittlemente der drei Geradenpaare seien mit  $S(b, c)$ ,  $S(c, a)$ ,  $S(a, b)$  bezeichnet. Ist dann  $S(a, b) \succ S(b, c)$ , so gilt  $S(b, c) \equiv S(c, a)$ .

### § 3. Reziprozitätssatz.

10. Als Reziprozitätssatz bezeichnen wir den schon in Einl. III, S. 45—46 aufgestellten Satz über die reziproke Beziehung des Schnittlements und des Ordinatenelements zweier Schmiegenderaden. Der Satz soll hier in verallgemeinerter Form bewiesen werden.

Die beiden Schmiegenderaden  $a, b$  haben den gemeinsamen Punkt  $A$  (Fig. 1); ihre Lote in  $A$  sind  $n, n_1$ . Die Strecke  $AQ$  auf  $b$  ist ordinär; die Normale  $c$  auf  $b$  in  $Q$  schneidet  $a$  in  $P$ . Die Normale von  $a$  in  $P$  ist  $a_1$ .

Es sei nun  $c'$  eine beliebige von  $c$  verschiedene Verbindungsgerade von  $P, Q$  und  $c_1$  die ihr in der Weise zugeordnete Gerade durch  $P$ , dass  $c'c = ac_1$ , also  $c_1 = cc'a$ . Es folgt dann

$$abc_1 = abcc'a.$$

Der letztere Transport ist aber involutorisch, weil die Geraden  $b, c, c'$  durch denselben Punkt hindurchgehen. Der obigen Gleich-

ung zufolge ist dann die Bewegung  $abc_1$ , also auch die gleichwertige  $nn_1c_1$ , involutorisch. Da nun  $c_1$ , wegen  $c'c = ac_1$ , Nachbargerade von  $a$  ist, so schneidet sie die Normale  $n$  von  $a$  eindeutig in einem Punkt  $C$ ; durch diesen Punkt muss dann auch  $n_1$  hindurchgehen.

Ist umgekehrt  $C$  ein beliebiger gemeinsamer von  $A$  verschiedener Punkt der beiden Geraden  $n, n_1$ , und  $c_1$  die Verbindungsgerade der Punkte  $C, P$ , und ist ferner  $c'$  diejenige Gerade



Fig. 1

durch  $P$ , welche durch die Gleichung  $ac_1 = c'c$  bestimmt wird, so folgt wiederum, dass der Transport

$$nn_1c_1 = abc_1 = abcc'a,$$

also auch  $bcc'$  involutorisch ist, d. h. die Gerade  $c'$  geht durch den eindeutig bestimmten Schnittpunkt  $Q$  der Geraden  $b, c$ .

Es stellt sich also heraus, dass das Geradenbündel  $(c')$ , welches das Punktepaar  $PQ$  enthält, demjenigen Strahlenbündel  $P(C)$  kongruent ist, welches das gemeinsame Element der Geraden  $n, n_1$  vom Punkt  $P$  aus projiziert. Dieses Element ist aber dem gemeinsamen Element der Geraden  $a, b$  kongruent.

Diejenige Spiegelungsachse der Geraden  $a, b$  welche das Schnittelement der beiden Geraden enthält, sei nun mit  $x$  bezeichnet. Die Normale von  $P$  auf  $x$  schneidet dann  $b$  in einem Punkt  $R$  dergestalt, dass  $AP = AR$  und  $QR \prec QP$ . Wenn nun eine der Punktreihe  $AQR$  kongruente Reihe  $PQ_1R_1$  auf  $c$  abgetragen wird, so müssen die Ordinaten des Winkels  $(c, c')$  in  $Q_1$  und  $R_1$ , wegen  $Q_1R_1 \prec QP$ , kongruent ausfallen. Die Ordinate



in  $R_1$  ist aber, wegen  $c'c = ac_1$  und  $PR_1 = RA = PA$ , der Ordinate  $AC$  des Winkels  $(a, c_1)$  kongruent, und die Ordinate in  $Q_1$  ist demnach ebenfalls der Strecke  $AC$  kongruent.

Durch eine Schiebung  $P \rightarrow Q$  längs  $c$  geht  $Q_1$  in einen Punkt  $U$  über, derart, dass  $QU = AQ$ , und die Ordinate des Winkels  $(c, c')$  in  $U$  ist dann wiederum der Strecke  $AC$ , oder der entsprechenden Strecke  $AB$  des Schnittelements der beiden Geraden  $a, b$ , kongruent. Es gilt also der Satz:

Dreht man das Schnittelement der Geraden  $n, n_1$  einen rechten Winkel um  $Q$  herum, so erhält man ein Ordinatenenelement des Geradenbüschels  $(c, c')$  durch  $P, Q$ .

Da nun die Schnittelemente der beiden Geradenpaare  $a, b$  und  $n, n_1$  einander kongruent sind, ergibt sich ferner die folgende Tatsache:

Das Schnittelement  $\sigma$  und das Ordinatenenelement  $\omega$  zweier Schmieggeraden sind der Grösse nach in der Weise reziprok verbunden, dass ein anderes Paar von Schmieggeraden, dessen Schnittelement dem Element  $\omega$  kongruent ist, ein Ordinatenenelement besitzt, welches dem Element  $\sigma$  kongruent ist.

11. Was die gegenseitige Lage der Striche  $\sigma$  und  $\omega$  anbetrifft, haben wir bei unserer obigen Untersuchung vorausgesetzt, dass die Abstände  $AQ$  und  $QU$  ordinär und einander kongruent sind. Auf die Frage nach der Entbehrlichkeit dieser Voraussetzung kehren wir später zurück. Bis auf weiteres soll die Reziprozität im obigen Sinne aufgefasst werden, und die Striche  $\sigma$  und  $\omega$  sollen dann als reziprok bezüglich der Punkte  $A, Q$ , oder bezüglich des Abstandes  $AQ$ , bezeichnet werden.

Die entsprechenden Flecke  $\Sigma$  und  $\Omega$ , welche durch Drehung von  $\sigma$  und  $\omega$  um  $A$  und  $Q$  entstehen, sollen ebenfalls als reziprok bezüglich  $A, Q$ , oder bezüglich des Abstandes  $AQ$ , bezeichnet werden. Alle Geraden durch  $A$ , welche  $\Omega$  durchschneiden, bilden ein Schmiegbüschel mit dem Schnittelement  $\sigma$ , und alle Geraden durch  $Q$ , welche  $\Sigma$  durchschneiden, bilden ein Büschel mit dem Schnittelement  $\omega$ .

12. Ein Fleck, welcher seinem reziproken Fleck überlegen

(unterlegen) ist, soll Oberfleck (Unterfleck) genannt werden. Ist ein Fleck seinem reziproken Fleck kongruent, so bezeichnen wir ihn als Parifleck.

Wenn zwei Abstände bezw. in zwei einander reziproken Flecken enthalten sind, so gibt es immer ein Rechteck, dessen Seiten diesen Abständen kongruent sind (I, S. 18, IV, S. 10–11).

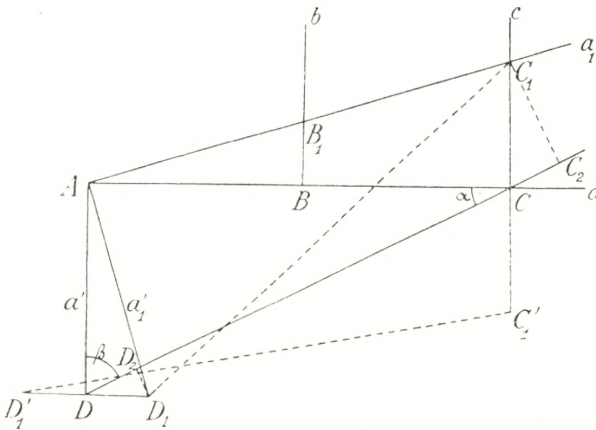


Fig. 2

Fassen wir nun eine beliebige Gerade  $m$  ins Auge, welche die Gerade  $b$  eindeutig in  $Q$  schneidet (Fig. 1). Sie schneidet  $a$ , ebenfalls eindeutig, in einem Punkt  $M$ . Das Dreieck  $QPM$  hat dann ordinäre Winkel bei  $P$  und  $M$ , und infolgedessen sind die Strecken  $QP$  und  $QM$  ebenbürtig (8). Es gilt also:

Alle Geraden, welche eine Gerade eines Schmiegbüschels in ein und demselben Punkt eindeutig schneiden, schneiden aus dem Schmiegbüschel kongruente Striche aus.

13. Wir wollen jetzt die Striche untersuchen, welche entstehen, wenn ein Schmiegbüschel mit zwei beliebigen Transversalen geschnitten wird. Wegen des vorigen Satzes können wir uns auf denjenigen Fall beschränken, wo die Transversalen auf einer Geraden des Büschels senkrecht stehen.

Es sei nun das vorgegebene Büschel durch zwei seiner Geraden  $a, a_1$  mit dem gemeinsamen Punkt  $A$  bestimmt (Fig. 2). Auf



$a$  errichten wir in zwei Fernpunkten  $B, C$  zu  $A$  die Senkrechten  $b, c$ , welche  $a_1$  in  $B_1, C_1$  schneiden. Um dann die Strecken  $BB_1$  und  $CC_1$  vergleichen zu können, drehen wir  $BB_1$  einen rechten Winkel um  $A$  herum, wobei sie in die neue Lage  $DD_1$  übergeführt wird. Wir ziehen die Geraden  $AD$  ( $\perp AB$ ),  $AD_1$  ( $\perp AB_1$ ),  $CD$  und  $C_1D_1$ , welche alle eindeutig bestimmt sind. Die Winkel  $\alpha, \beta$  im Dreieck  $ACD$  sind ordinär, weil die ihnen gegenüberliegenden Seiten,  $AD = AB$  und  $AC$ , ordinär sind.

Es soll nun gezeigt werden, dass die Projektionen  $CC_2$  und  $DD_2$  der Strecken  $CC_1$  und  $DD_1$  auf die Gerade  $CD$  einander kongruent sind. Zu dem Zwecke betrachten wir die symmetrischen Punkte  $C'_1, D'_1$  zu  $C_1, D_1$  bezüglich  $C, D$ . Die Drehung  $a_1a$  führt  $C_1$  in  $C'_1$  und dieselbe Drehung,  $a'_1a' = a_1a$ , führt  $D_1$  in  $D'_1$  über. Die Punktepaare  $C'_1D'_1$  und  $C_1D_1$  bestimmen sonach zwei kongruente Punktreihen mit der Mittellinie  $m = CD$ , und infolgedessen können sie zur Deckung gebracht werden durch die Aufeinanderfolge einer Spiegelung an  $m$  und einer Schiebung längs  $m$ , welche sowohl durch die Spiegelungsfolge  $CC_2$  als durch  $DD_2$  dargestellt werden kann. Hieraus geht dann hervor, dass die Punktepaare  $CC_2$  und  $DD_2$  einander kongruent sind.

Auf Grund dieser Tatsache gelingt es jetzt zu erweisen, dass die beiden Strecken  $DD_1$  und  $CC_1$ , und somit auch  $BB_1$  und  $CC_1$ , ebenbürtig sind. Da die beiden Winkel  $\alpha, \beta$  ordinär sind, geht nämlich aus den rechtwinkligen Dreiecken  $CC_1C_2, DD_1D_2$  hervor, dass  $CC_1 \sim CC_2$ , und  $DD_1 \sim DD_2$ , und da die Strecken  $CC_2, DD_2$  einander kongruent sind, folgt sofort  $CC_1 \sim DD_1$ , oder  $BB_1 \sim CC_1$ .

Es ist hiermit erwiesen worden, dass das vorgegebene Schmiegbüschel  $(a, a_1)$  von den beiden Transversalen  $b, c$  in einander kongruenten Strichen geschnitten wird. Dem vorigen Satz zufolge haben wir dann schliesslich das folgende Resultat:

Jedes Schmiegbüschel wird von allen Transversalen in ordinärem Abstand vom Scheitelement in kongruenten Strichen geschnitten.

Diese Striche sollen Querstriche des Büschels heissen.

Es folgt nun ferner:

Wenn zwei Elemente (Striche, Flecke) reziprok sind bezüglich irgend eines ordinären Abstandes, so

sind sie reziprok bezüglich aller ordinären Abstände (Vergl. 11).

Wird ein Nachbarpunkt  $P$  einer Geraden  $g$  mit verschiedenen auf der Geraden gelegenen Fernpunkten zu ihm verbunden, so werden die Verbindungsgeraden kongruente Striche auf  $g$  ausschneiden. Die Striche sind nämlich alle reziprok zu ein und demselben Strich  $S(P, Q)$ , welcher durch das von  $P$  auf  $g$  gefällte Lot  $PQ$  bestimmt ist.

14. Dass man auch von Reziprozität bezüglich singulärer Abstände reden kann, ist leicht verständlich. Man erkennt unmittelbar, wie die vorstehenden Entwicklungen auf den so erweiterten Begriff Verwendung finden. Z. B. lässt sich der obenstehende Satz in folgender Weise erweitern:

Wenn zwei Elemente (Striche, Flecke) reziprok sind bezüglich irgendeines Abstandes, so sind sie reziprok bezüglich aller mit ihm ebenbürtigen Abstände.

Was nicht ebenbürtige Abstände anbetrifft, sei nur hervorgehoben, dass wenn in der Fig. 2  $AB \prec AC$  ist, so folgt, dass der Winkel  $\alpha$  singulär ist, und hieraus ergibt sich:

$$CC_1 \succ CC_2 = DD_2 \infty DD_1 = BB_1,$$

also

$$CC_1 \succ BB_1.$$

15. Bei einer schwachen Drehung um einen Punkt  $O$  werden die Punkte  $A, B, C, \dots$  deren Abstände von  $O$  einander ebenbürtig sind, in Nachbarpunkte  $A', B', C', \dots$  übergeführt derart, dass die Abstände  $AA', BB', CC', \dots$  einander ebenbürtig sind. Ist  $OA \prec OB$ , so wird  $AA' \prec BB'$ .

Wenn wir im folgenden von »reziproken Elementen« reden, meinen wir stets »reziprok bezüglich ordinärer Abstände«.

#### § 4. Punktfremde Nachbargeraden.

16. Unter einer ordinären Transversale zweier punktfremden Nachbargeraden  $p, p_1$  verstehen wir eine Gerade, welche  $p$ , und somit  $p_1$ , eindeutig schneidet. Die beiden Geraden werden von allen ordinären Transversalen in ebenbürtigen Punktepaaren geschnitten. Um das zu beweisen wird es genügen, zwei



Transversalen zu betrachten, welche auf  $p$  in den beiden Punkten  $A, B$  senkrecht stehen. Diese Transversalen seien von  $p_1$  in den Punkten  $A_1, B_1$  geschnitten (Fig. 3), und es soll dann gezeigt werden, dass die Punktepaare  $AA_1$  und  $BB_1$  ebenbürtig sind.

Wir nehmen eine Gerade  $r$  zu Hilfe, welche mit  $p, p_1$  in Involution ist und durch einen Fernpunkt zu  $p$  hindurchgeht.

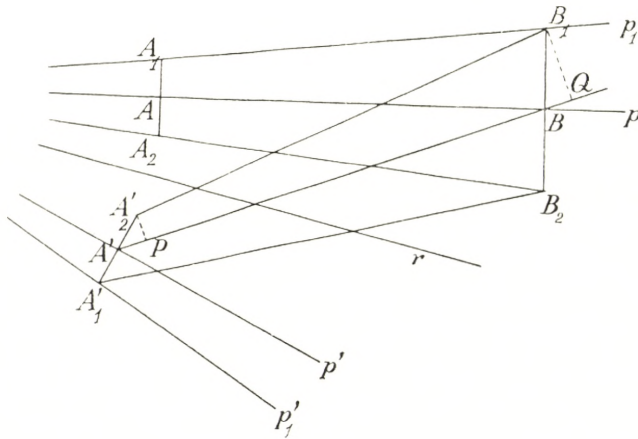


Fig. 3

Alle Punkte von  $r$  sind dann Fernpunkte zu  $p$  (und  $p_1$ ). Es seien  $p', p'_1$  die Spiegelbilder von  $p$  bzw.  $p_1$  bezüglich  $r$ . Es folgt dann

$$p' = p^r, \quad p'_1 = p_1^r,$$

und weil  $p, p_1, r$  in Involution sind:

$$p_1 p = (p p_1)^r,$$

also

$$p_1 p = p' p'_1.$$

Der Transport  $rp'$  führt  $AA_1$  in  $A'A'_2$ , und das Spiegelbild  $A_2$  von  $A_1$  bezüglich  $p$  in  $A'_1$  über, wobei  $A'_2$  das Spiegelbild von  $A'_1$  bezüglich  $p'$  bedeutet. Das Spiegelbild von  $B_1$  bezüglich  $p$  sei  $B_2$ .

Man zieht nun die Geraden  $A'_1 B_2, A'B, A'_2 B_1$ , welche alle eindeutig bestimmt sind. Da nun

$$B_2 = B_1^{p_1 p}, \quad A'_1 = (A'_2)^{p' p'_1},$$

wo die Exponenten  $p_1p$  und  $p'p'_1$ , wie oben gezeigt, gleichwertig sind, so ersieht man, dass die Punktepaare  $A'_2B_1$  und  $A'_1B_2$  einander kongruent sind. Da ferner die hierdurch bestimmten kongruenten Punktreihen die Mittellinie  $A'B$  besitzen, so können sie zur Deckung gebracht werden durch einen Transport, welcher aus einer Spiegelung an  $A'B$  und einer Schiebung längs derselben zusammengesetzt ist. Diese Schiebung lässt sich aber durch jede der beiden Spiegelungsfolgen  $PA'$  und  $QB$  darstellen, wobei  $P, Q$  die Projektionen von  $A'_2, B_1$  auf die Mittellinie bezeichnen. Es folgt also hieraus, dass die beiden Punktepaare  $A'P$  und  $BQ$  einander kongruent sind. Da nun die Gerade  $A'B$  ordinäre Winkel mit  $p$  und  $p'$  bildet, so ergibt sich aus den Dreiecken  $A'PA'_2$  und  $BQB_1$ , dass die Seiten  $A'A'_2$  und  $BB_1$  ebenbürtig sind, und hieraus folgt dann sofort, dass  $AA_1$  und  $BB_1$  ebenfalls ebenbürtig sind, w. z. b. w.

17. Bei jedem schwachen Transport, welcher durch die Aufeinanderfolge von zwei Spiegelungen an zwei Nachbargeraden ohne gemeinsame Punkte bestimmt ist, sind alle Abstände von den verschiedenen Punkten nach ihren entsprechenden Punkten einander ebenbürtig. Im besonderen gilt dies für jede schwache Schiebung. Die schwache Drehung ist im vorgehenden besprochen worden (15).

18. Zwei punktfremde Nachbargeraden  $p, p_1$  werden von jeder Nachbargeraden, welche zwei Punkte  $A, B$  der beiden Geraden verbindet, in kongruenten Strichen geschnitten.

Zum Beweis betrachten wir die beiden Punktepaare  $AA_1$  und  $BB_1$ , in welchen die beiden Geraden  $p, p_1$  von zwei ordinären Transversalen, welche durch  $A$  bzw.  $B$  gehen, geschnitten werden. Der Schnittlement bei  $A$  ist zum Strich  $S(B, B_1)$  reziprok bezüglich des Abstandes  $AB$ , und der Schnittlement bei  $B$  ist in gleicher Weise zum Strich  $S(A, A_1)$  reziprok. Wegen  $S(A, A_1) \infty S(B, B_1)$  sind dann die beiden Schnittlemente einander kongruent.

19. Die beiden Nachbargeraden  $p, p_1$  werden von einer ordinären Transversale in einem Punktepaare  $A, A_1$  geschnitten. Der entsprechende Strich  $S(A, A_1)$  soll ein Querstrich der Geraden heissen. Alle Querstriche der Geraden sind kongruent. Der von ihnen erfüllte ebene Bereich soll ein Streif  $\sigma(p, p_1)$  heissen. Der



Streif enthält unendlich viele Geraden, die Streifgeraden, z. B. jede Gerade, welche zwei Fernpunkte der Geraden  $p, p_1$  verbindet. Die Geraden, welche eine Streifgerade rechtwinklig schneiden, sollen als Normalen des Streifs bezeichnet werden. Die Querstriche der Geraden  $p, p_1$  sind auch Querstriche zweier beliebigen Streifgeraden und sollen daher schlechthin als Querstriche des Streifs bezeichnet werden.

Die Streifgeraden, welche durch einen Punkt des Streifs gehen, bilden ein Schmiegbüschel, dessen Scheitelelement den Querstrichen reziprok ist.

Der Streif geht durch folgende Transporte in sich selbst über: Spiegelungen an Streifgeraden; Spiegelungen an Normalen; Spiegelungen an beliebigen Punkten des Streifs.

20. In Einl. III, 31–32 haben wir gesehen, dass in zwei Nachbargeraden sich unendlich viele Rechtecke derart einschreiben lassen, dass zwei Gegenseiten des Rechtecks auf den beiden Geraden liegen. Ferner haben wir gezeigt, dass man ein Element angeben kann (das Schiebelelement der beiden Geraden), welches alle diejenigen Streckenlängen enthält, die bei Seitenpaaren eingeschriebener Rechtecke vorkommen können.

Hier wollen wir nun besonders den Fall betrachten, wo die beiden Geraden  $g, h$  eine gemeinsame Normale  $n$  besitzen. Die Schnittpunkte von  $n$  mit  $g, h$  seien mit  $G, H$  bezeichnet (vgl. Fig. 4, S. 18). Wenn dann  $GHH_1G_1$  ein in  $g, h$  eingeschriebenes Rechteck ist, so gilt die Transformationsgleichung

$$GG_1 = HH_1.$$

Es seien ferner  $g_1, h_1$  die Normalen zu  $g, h$  in den Punkten  $G_1, H_1$ , dann gilt:

$$GG_1 = ng_1, \quad HH_1 = nh_1,$$

also

$$ng_1 = nh_1, \quad \text{oder} \quad g_1 = h_1,$$

d. h. die beiden Geraden  $g, h$  haben ein und dieselbe Normale in den Punkten  $G_1, H_1$ . Also:

Haben zwei Nachbargeraden eine gemeinsame Normale, so haben sie unendlich viele gemeinsame Normalen. Diese schneiden auf den beiden Geraden zusammengehörige Schiebelelemente aus.

21. Wie früher erwähnt (Einl. III, 33) kann das Schiebelelement die ganze Gerade umfassen. Das bedeutet, dass jede Normale der einen Gerade auch Normale der anderen ist. In diesem Falle ist (wie a. a. O. gezeigt wurde) die Winkelsumme eines jeden Dreiecks höchstens um einen singulären Winkel von zwei Rechten verschieden. Ist die Winkelsumme genau zwei Rechte, soll unsere Geometrie als singulär bezeichnet werden. Ist die Winkelsumme von zwei Rechten verschieden, aber nur um einen singulären Winkel, so soll die Geometrie schwach singulär heissen. In der singulären Geometrie haben zwei beliebige Geraden mit einer gemeinsamen Normalen überhaupt dieselben Normalen. In der schwach singulären Geometrie gibt es zu jeder Geraden  $g$  ein System von Nachbargeraden, welche dieselben Normalen wie  $g$  besitzen. Diese Geraden erfüllen einen Streifen, den Singularitätsstreifen um  $g$ . Jede Grundstrecke des entsprechenden Querstrichs soll als Singularitätsmass bezeichnet werden.

Wenn es keine zwei Geraden gibt, welche dieselben Normalen besitzen, soll die Geometrie ordinär heissen.

### § 5. Das Rechteck.

22. Im folgenden soll nun untersucht werden, welchen Bedingungen die Seiten eines Rechtecks der Grösse nach in den verschiedenen Fällen unterworfen sind.

Zuerst betrachten wir den ordinären Fall.

Es sei wie früher  $GHH_1G_1$  ein in  $g, h$  eingeschriebenes Rechteck, welches durch die gemeinsamen Normalen  $n, n_1$  der beiden Geraden  $g, h$  ausgeschnitten wird (Fig. 4, S. 18). Es sei ferner auf der Geraden  $g$  ein Fernpunkt  $P$  zu  $G$  gewählt. Wenn wir dann auf  $g$  einen solchen Punkt  $P_1$  bestimmen, dass

$$PP_1 = GG_1 = HH_1,$$

so folgt

$$PHH_1 = P_1,$$

und hieraus schliessen wir, dass  $H_1$  und  $P_1$  auf der eindeutig bestimmten geraden Linie  $HP$  liegen müssen. Aus der Figur ergibt sich sodann, dass die Strecke  $PP_1$ , und somit auch die



Strecke  $GG_1$ , dem reziproken Elemente zu  $S(G, H)$  angehören muss. Es gilt also der Satz:

In der ordinären Geometrie existiert dann und nur dann ein Rechteck mit vorgegebenen Seitenlängen, wenn die eine von diesen dem reziproken Elemente der anderen angehört.

Aus diesem Satze schliessen wir sofort die folgenden Tatsachen:

In der ordinären Geometrie gilt, dass die Geometrie eines Unter- oder Pariflecks immer singulär ist, während die Geometrie eines Oberflecks schwach singulär ausfällt.

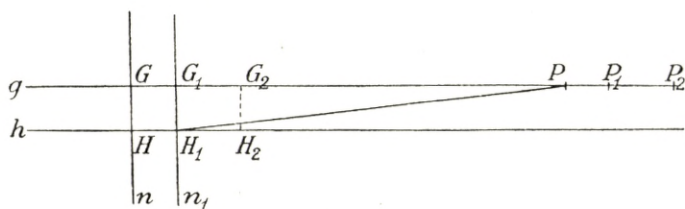


Fig. 4.

23. In der singulären Geometrie können alle Grössen der Seiten des Rechtecks angenommen werden. Wir haben deshalb nur noch die schwach singuläre Geometrie zu betrachten. Zu dem Zwecke kehren wir zur Figur 4 zurück. Es sei dann  $GHH_2G_2$  ein in  $g, h$  eingeschriebenes Rechteck. Wir setzen

$$PP_2 = GG_2 = HH_2,$$

woraus

$$PHH_2 = P_2.$$

In dem vorliegenden Falle, wo die Geometrie schwach singulär ist, lässt sich aber nicht mehr schliessen, dass  $H_2$  auf der Geraden  $PH$  liegt, sondern nur, dass der Abstand von  $H_2$  nach  $PH$  dem Singularitätsmass unterlegen oder ebenbürtig ist. Hieraus ergibt sich aber sofort für die schwach singuläre Geometrie das folgende Resultat:

Um auf der Seite  $HH_2$  ein Rechteck zu konstruieren, errichtet man das Singularitätsmass  $H_2H'$  senkrecht

auf  $h$  in  $H_2$ . Eine Gerade durch  $H$  und  $H'$  bestimmt dann mit  $h$  zusammen ein Schmiegebüschel, dessen Querstrich alle in Betracht kommenden Seitengrößen  $GH$  enthält.

24. Zwei Elemente (Striche, Flecke) sollen komplementär heißen, wenn ihre Grundstrecken zwei anstossenden Seiten eines Rechtecks kongruent sind. Die Grundstrecken selbst sollen dann ebenfalls komplementär genannt werden. In der ordinären Geometrie gilt, dass zwei reziproke Elemente stets komplementär sind, und umgekehrt. In der schwach singulären Geometrie hingegen kommt dem vorhergehenden Satz zufolge ein Unterschied zwischen den beiden Begriffen zum Vorschein: reziproke Elemente sind komplementär, aber komplementäre Elemente nicht notwendig reziprok. In der singulären Geometrie schliesslich sind alle Elemente komplementär, und diese Geometrie soll daher in der Folge ausser Betracht gelassen werden.

Aus der in 23 angegebenen Konstruktion soll jetzt eine wichtige allgemeine Beziehung komplementärer Elemente abgeleitet werden. Es seien  $a, b$  zwei vorgegebene Schmiegeraden durch den Punkt  $O$ . In zwei Punkten  $P, Q$  von  $a$  seien Lote  $p, q$  auf  $a$  errichtet, welche  $b$  in  $P_1, Q_1$  schneiden. Es gilt dann:

Wenn  $PP_1$  zu  $OQ$  komplementär ist, so wird  $QQ_1$  zu  $OP$  komplementär.

In dem Spezialfalle einer schwach singulären Geometrie, wo  $OQ$  ordinär,  $PP_1$  Singularitätsstrich, ist der Satz in 23 enthalten, und der allgemeine Satz lässt sich auf diesen Spezialfall zurückführen. Man braucht nämlich nur die Figur in der Geometrie eines Flecks mit der Grundstrecke  $OQ$  zu deuten.

Der Satz gibt uns die Mittel in die Hand, aus zwei vorgegebenen komplementären Strecken  $m, \mu$  die komplementäre Strecke  $\mu_1$  zu einer vorgegebenen Strecke  $m_1$  zu konstruieren. Man trägt  $OQ = m$ ,  $OP = m_1$  ab, errichtet in  $P$  das Lot  $PP_1 = \mu$ , und zieht eine Gerade  $OP_1$ , wodurch die gesuchte Strecke  $QQ_1 = \mu_1$  abgeschnitten wird.

In der ordinären Geometrie lassen sich auf diese Weise alle Paare reziproker Grundstrecken aus den Grundstrecken eines Maximal- und eines Minimalflecks ableiten.



## § 6. Der Kreis.

25. Es seien  $a, b$  zwei Schmieggeraden (Fig. 5) mit dem gemeinsamen Punkt  $O$  und dem Schnittlelement  $S(a, b)$ . Im Punkte  $A$  von  $a$  ausserhalb  $S(a, b)$  errichten wir das Lot  $p$  auf  $a$ . Sein Schnittpunkt mit  $b$  sei  $B$ . Die schwache Drehung  $ab$  wird dann die Gerade  $p$  in eine andere Gerade  $q$  überführen, welche durch  $B$  hindurchgeht. Auf  $p$  wählen wir einen Punkt  $P$  derart, dass

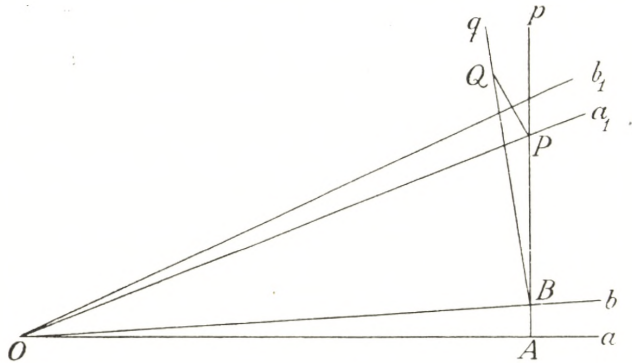


Fig. 5.

$AP \sim OA$ . Dieser Punkt geht bei der Drehung  $ab$  in einen solchen Punkt  $Q$  auf  $q$  über, dass

$$Q = P^{ab} = P^{a_1 b_1} = P^{b_1},$$

wobei  $a_1$  die Gerade  $OP$  bezeichnet und  $b_1$  dadurch bestimmt ist, dass  $a_1 b_1 = ab$ .

Es folgt nun hieraus, dass die beiden Büschel  $(p, q)$  und  $(a_1, b_1)$  den gemeinsamen Querstrich  $S(P, Q)$  bezüglich der beiden einander ebenbürtigen Abstände  $AP$  und  $OP$  haben. Wegen  $a_1 b_1 = ab$  hat das Büschel  $(a, b)$  gerade denselben Querstrich. Es folgt dann schliesslich, dass die Büschel  $(p, q)$  und  $(a, b)$  einander kongruente Schnittlemente haben. Auf diese Weise gelangen wir zu folgenden Tatsachen:

Eine schwache Drehung führt jede Gerade in eine entsprechende Schmieggerade über. Alle Schnittlemente einander entsprechender Geraden sind einander kongruent.

26. Um die Elemente eines Kreises untersuchen zu können, erinnern wir zunächst an den folgenden Satz (Einl. III, 40,1°):

In einem rechtwinkligen Dreieck  $ABC$  mit einem singulären Winkel  $A$ , dessen Scheitelement grösser als die gegenüberliegende Kathete  $BC$  ist, ist die Hypotenuse  $AB$  gleich der anderen Kathete  $AC$ . Es folgt hieraus unmittelbar:

Die Tangente in einem Punkte  $P$  eines Kreises mit Zentrum  $O$  enthält auf dem Kreis alle Nachbarpunkte  $Q$  von  $P$ , welche der Bedingung genügen, dass das Element  $PQ$  dem gemeinsamen Element der beiden Radien  $OP$  und  $OQ$  unterlegen oder ebenbürtig ist.

Das gemeinsame Element des Kreises und seiner Tangente soll Tangentenelement des Kreises heissen. Es folgt:

Das Tangentenelement eines Kreises mit ordinärem Radius ist ein Parielement oder jedenfalls allen linearen Unterelementen überlegen.

Aus dem Satze in 25 folgern wir:

Die Tangenten in zwei Nachbarpunkten  $P, Q$  eines Kreises sind Schmiegeraden. Ihr Schnittelement ist dem Schnittelement der beiden Radien  $OP, OQ$  kongruent.

Mit Hilfe des obigen Satzes von dem Tangentenelement ergibt sich dann:

Das Schnittelement der Tangenten in zwei Nachbarpunkten  $P, Q$  eines Kreises ist zum Element  $S(P, Q)$  bezüglich dem Radius reziprok.

27. Indem wir noch an den Satz 40,2° in Einl. III erinnern, formulieren wir schliesslich den folgenden Satz:

In einem Dreieck mit ordinären Seiten, wo eine Höhe einem Unter- oder Parielement angehört, ist die grösste Seite gleich der Summe der beiden anderen Seiten.

Aus 26 folgt unmittelbar:



Zwei Kreise mit ausschliessender Berührung und ordinären Radien haben ein lineares Element gemein, welches alle Unterelemente umfassen.

Für zwei Kreise mit einschliessender Berührung und ordinären Radien gilt dasselbe. In diesem Falle muss man aber beachten, dass wenn die Zentrale die Grundstrecke eines Unterelements ist, die Kreise dann ein grösseres (nicht lineares)

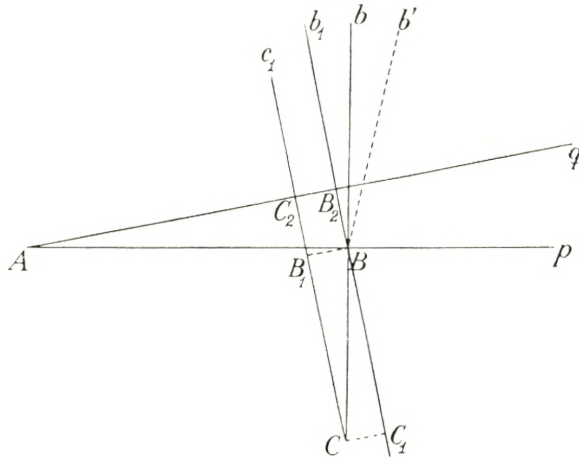


Fig. 6.

Element gemein haben, welches von demjenigen Schmiegebüschel ausgeschnitten wird, dessen Scheitelement jenes Unterelement ist.

28. Als weiteres Hilfsmittel gehen wir nun daran, einige Sätze über die gegenseitige Lage der von einem Punkt gefällten Lote auf zwei vorgegebene Nachbargeraden aufzustellen.

Es seien zunächst  $p, q$  zwei Schmieggeraden mit dem gemeinsamen Punkt  $A$  (Fig 6). Durch den Punkt  $B$  auf  $p$  ziehen wir die Normalen  $b, b_1$  zu  $p, q$ . Es lässt sich dann beweisen, dass die beiden Winkel  $(b, b_1)$  und  $(p, q)$  einander ebenbürtig sind, d. h. ihre Scheitelemente sind kongruent. Bei der schwachen Drehung  $qp$  wird nämlich  $b_1$  in das Spiegelbild  $b'$  von  $b_1$  bezüglich  $b$  übergeführt, und einem vorhergehenden Satz zufolge gilt dann

$$(b', b_1) \infty (p, q),$$

und da ferner





$\varepsilon$  um  $O$  als Scheitelement eines Büschels  $(p, q)$ . Die Gerade  $q$  schneidet den Kreis in dem zu  $P$  benachbarten Punkt  $Q$  und die Tangente  $a$  in dem Punkte  $T$ . Der zu  $\varepsilon$  reziproke Oberfleck um  $P$  schneidet aus  $\varepsilon$  ein Kreiselement  $(P, Q)$  und aus der Tangente  $a$  ein lineares Element  $(P, T)$  heraus. Der Kreisbogen  $PQ$  wird durch die »Tangentenstrecke«  $PT$  und durch die »Querstrecke«  $TQ$  bestimmt, und  $TQ$  ist zum Scheitelement des Büschels  $(a, b)$  bezüglich  $PT$  reziprok (wobei  $b$  die Verbindungsgerade von  $P, Q$  bedeutet). Ist nun  $r$  die Spiegelungsachse der beiden Radien  $OP$  und  $OQ$ , so folgt nach dem vorhergehenden Satz:  $(a, b) \infty (p, r)$ , und da  $(p, r) \infty (p, q)$ ,

$$(a, b) \infty (p, q).$$

Es lassen sich diese Tatsachen in folgenden Sätzen zusammenfassen:

Das von einem Oberfleck ausgeschnittene Element eines Kreises wird aus jedem seiner Punkte sowie aus dem Zentrum des Kreises durch kongruente Schmiegbüschel projiziert.

Hat ein rechtwinkliges Dreieck  $OPT$  einen singulären Winkel bei  $O$ , dessen Scheitelement  $\sigma$  der gegenüberliegenden Kathete  $PT$  unterlegen ist, so ist die Hypotenuse  $OT$  grösser als die andere Kathete  $OP$ . Trägt man die Differenz  $OT - OP$  als Kathete  $TS$  eines rechtwinkligen Dreiecks  $PTS$  ab, so wird das Scheitelement des singulären Winkels  $TPS$  dem Scheitelement  $\sigma$  kongruent.

### § 7. Schwache Transporte ohne Fixpunkte.

31. Ein schwacher Transport ohne Fixpunkte lässt sich immer darstellen als Produkt  $pq$  zweier Achsenspiegelungen, deren Achsen  $p, q$  ohne gemeinsame Punkte sind. Es gibt dann zwei Hauptfälle je nachdem die beiden Geraden  $p, q$  eine gemeinsame Normale haben oder keine solche Normale vorhanden ist. Die beiden Fälle sollen jetzt nacheinander betrachtet werden.

Im ersten Falle, wo  $p, q$  eine gemeinsame Normale  $n$  besitzen, ist der Transport  $pq$  eine Schiebung längs  $n$ . Diese Schiebung

lässt sich auch darstellen als Produkt  $AB$  zweier Punktspiegelungen, deren Zentren  $A, B$  in den Schnittpunkten von  $p, q$  mit  $n$  liegen. Wir wissen schon (20), dass die Geraden  $p, q$  ausser  $n$  unendlich viele gemeinsame Normalen haben. Jede solche Normale  $n_1$  ist eine Fixgerade des Transportes  $pq$ , und jede Verbindungsgerade der Schnittpunkte  $A_1, B_1$  von  $n_1$  mit  $p, q$  ist ebenfalls eine Fixgerade. Hiermit ist aber die Menge der Fixgeraden völlig erschöpft. Jede Fixgerade  $g$  soll nämlich dasselbe Spiegelbild  $g_1$  bezüglich  $p$  und  $q$  haben, d. h.  $g$  und  $g_1$  müssen  $p, q$  in ein und demselben Punktepaar schneiden, welches von einer gemeinsamen Normalen zu  $p, q$  aus-  
geschnitten wird.

Die ganze Menge der Fixgeraden wird durch jede beliebige Schiebung längs  $n$  in dieselbe Menge übergeführt.

Indem wir nun fortan den Fall ausschliessen, wo die Geraden  $p, q$  dasselbe System von Normalen besitzen, wählen wir

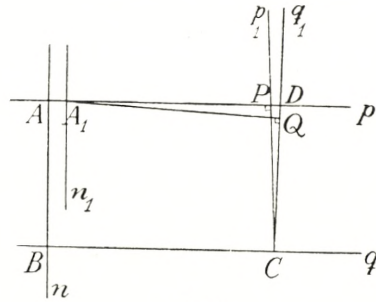


Fig. 8.

auf  $q$  einen solchen Punkt  $C$ , dass der Abstand  $BC$  ordinär ist. Die durch ihn gehenden Normalen  $p_1, q_1$  zu  $p, q$  sind dann von einander verschieden. Sie werden von  $p$  in  $P$  und  $D$  geschnitten. Durch  $A$  fallen wir die Gerade  $AQ$  senkrecht auf  $q_1$ . Diese Gerade und  $p$  sind einander benachbart. Einer ihrer von  $A$  verschiedenen gemeinsamen Punkte sei  $A_1$ , und die Normale zu  $p$  in diesem Punkt sei  $n_1$  (Fig. 8). Die Bewegung  $AA_1q_1$  ist dann involutorisch und wegen  $AA_1 = nn_1$  ist die Bewegung  $nn_1q_1$  ebenfalls involutorisch, woraus folgt, dass  $n_1 \perp q$ . Ist umgekehrt  $n_1$  eine zu  $n$  benachbarte gemeinsame Normale zu  $p, q$ , und  $A_1$  ihr Schnittpunkt mit  $p$ , so folgt, dass  $nn_1q_1 = AA_1q_1$  eine involutorische Bewegung darstellt, und hieraus ersieht man, dass eine Gerade senkrecht zu  $q_1$  durch  $A, A_1$  gelegt werden kann. Das Schnittelement  $S(p, AQ)$  ist demnach mit dem Schiebелеment  $\sigma(p, q)$  von  $p$  und  $q$  identisch. Da ferner die Schnittelemente  $S(p, AQ)$  und  $S(p_1, q_1)$  kongruent sind (28), haben wir hierdurch dargelegt, dass das Schnittelement  $S(p_1, q_1)$  dem Schiebелеment  $\sigma(p, q)$  ebenbürtig ist.

Die Untersuchung lässt sich hiernach ähnlich wie früher so



erweitern, dass man auch Punkte  $C$  ausserhalb  $q$  in Betracht nehmen kann. Wir können daher den folgenden Satz aufstellen:

Es seien  $p, q$  zwei vorgegebene Nachbargeraden mit einer gemeinsamen Normalen  $n$ . Es seien ferner  $p_1, q_1$  zwei verschiedene Normalen zu  $p, q$ , welche einen Punkt in ordinärem Abstand von  $n$  gemein haben. Dann ist das Schnittlelement  $S(p_1, q_1)$  dem Schiebelelement  $\sigma(p, q)$  kongruent.

32. Der Ort der Spiegelbilder von  $C$  bezüglich aller Normalen von  $n$  ist eine sogenannte Abstandskurve mit der Grundlinie  $n$ . Die Tangente dieser Kurve in  $C$  ist  $q_1$ , und wenn  $AB \prec \sigma(p, q)$  vorausgesetzt wird, enthält die Tangente ein Element der Kurve, welches dem Schiebelelement  $\sigma(p, q)$  kongruent ist. Hiernach ersieht man sofort, dass für die Abstandskurve ganz ähnliche Sätze wie für den Kreis gelten. Nur der einfachste soll hier formuliert werden:

Jeder Unterfleck um einen Punkt einer ordinären Abstandskurve schneidet aus dieser Kurve ein lineares Element heraus, welches allen Tangenten des Kurvenelements angehören.

Wir fügen noch hinzu, dass diese Tangenten ein noch grösseres Element gemein haben, welches reziprok zum obengenannten ist, aber dieses Element ragt über die Kurve hinaus.

33. Wir haben noch den zweiten Fall zu behandeln, wo die beiden Geraden  $p, q$  keine gemeinsamen Punkte und keine gemeinsamen Normalen aufweisen. Der Transport  $pq$  hat in diesem Falle weder Fixpunkte noch Fixgeraden. Eine Hauptaufgabe wird es dann, das Schnittlelement  $S(p_1, q_1)$  von zwei durch einen vorgegebenen Punkt  $C$  gehenden Normalen  $p_1 \perp p, q_1 \perp q$ , zu untersuchen.

Durch einen Punkt  $A$  der Geraden  $p$  legen wir zwei Geraden  $n \perp q, r \perp n$ . Der Schnittpunkt von  $n, q$  sei  $B$ . Durch einen Punkt  $C$  auf  $q$ , dessen Abstand von  $B$  ordinär ist, ziehen wir drei Geraden:  $p_1 \perp p, q_1 \perp q, r_1 \perp r$ , und wir fassen sodann die drei Schnittlelemente  $S(p_1, q_1), S(p_1, r_1), S(q_1, r_1)$  ins Auge. Von den beiden letzten bemerken wir sofort, dass  $S(p_1, r_1) = S(p, r)$  (29), und  $S(q_1, r_1) =$  dem Schiebelelement  $\sigma(q, r)$  der Geraden  $q, r$  (31). Wir prüfen zunächst die beiden

Möglichkeiten  $S(p_1, r_1) \succ S(q_1, r_1)$ . Ist  $S(p_1, r_1) \succ S(q_1, r_1)$ , so ergibt sich dem Lemma II, S. 8 zufolge, dass  $S(p_1, q_1) = S(q_1, r_1)$ , also gilt:

Wenn auf der Geraden  $p$  ein Punkt  $A$  existiert, wo  $S(p, r) \succ \sigma(q, r)$ , so wird für jeden Punkt  $C$  auf  $q$ , dessen Abstand von  $A$  ordinär ist:  $S(p_1, q_1) = \sigma(q, r)$ . Alle den verschiedenen Punkten  $C$  entsprechenden  $S(p_1, q_1)$  sind einander kongruent.

Die andere Möglichkeit  $S(p_1, r_1) \prec S(q_1, r_1)$ , oder  $S(p, r) \prec \sigma(q, r)$ , zeigt sich bei näherer Untersuchung überhaupt nicht in Betracht zu kommen. Das Schnittelement  $S(AC, r)$  ist nämlich dem Schiebelelement  $\sigma(q, r)$  kongruent (13, Schluss), und wenn dann  $S(p, r) \prec \sigma(q, r)$  wäre, würde das zur Folge haben, dass die Gerade  $p$  in das Dreieck  $ABC$  oder in das zu ihm bezüglich  $n$  symmetrische Dreieck hineindringen müsste, d. h.  $p$  und  $q$  müssten einander schneiden, was unserer Voraussetzung widerstreitet.

Es bleibt uns nur noch übrig, den Fall zu untersuchen, wo kein solcher Punkt  $A$  auf  $p$  vorhanden ist, dass  $S(p, r)$  und  $\sigma(q, r)$  von einander verschieden sind, d. h. für jeden Punkt  $A$  auf  $p$  sind die beiden Elemente  $S(p, r)$  und  $\sigma(q, r)$  einander kongruent.

Es sei nun  $D$  der Schnittpunkt von  $p, q_1$ , und  $p_2$  das Lot auf  $p$  in  $D$ ,  $r_2$  das Lot von  $q_1$  in  $D$ . Dann gilt:

$$S(p_1, q_1) = S(p_2, q_1) = S(p, r_2).$$

Hieraus folgt, dass  $S(p_1, q_1)$  dem Schiebelelement  $\sigma(q, r_2)$  kongruent und infolgedessen zum Strich  $S(C, D)$  reziprok ist. Da ferner  $S(C, D)$  mit dem Querstrich des Geradenpaares  $p, q$  gleichbedeutend ist, so folgt, dass alle  $S(p_1, q_1)$  zum Querstrich reziprok sind.

34. Bisher haben wir stets vorausgesetzt, dass der Punkt  $C$ , von welchem die beiden Normalen  $p_1, q_1$  ausgehen, auf der Geraden  $q$  gelegen ist. Nachher lässt sich aber ganz wie früher (29) zeigen, dass diese Voraussetzung ohne Belang ist. Unsere Resultate bleiben dann für jeden Punkt  $C$  gültig, im ersten Falle mit Ausnahme der Punkte eines Streifs um  $n$  mit dem Querstrich  $\sigma(q, r)$ .



35. Der Transport  $qp$  führt die Gerade  $q_1$  in eine Gerade  $q'_1$  über, welche das Spiegelbild von  $q_1$  bezüglich  $p_2$  ist. Infolgedessen gilt:

$$S(q_1, q'_1) = S(q_1, p_2) = S(p_1, q_1).$$

Versteht man unter einem offenen Kreis den Ort der Spiegelbilder eines festen Punktes bezüglich der Geraden eines Idealbüschels, so lassen sich nunmehr leicht ähnliche Sätze für offene Kreise wie früher für gewöhnliche Kreise aufstellen. Für den Spezialfall einer Abstandskurve ist dies schon erledigt worden (32).

### § 8. Die singuläre Geometrie.

36. Wenn in unserer Ebene ein Viereck mit ordinären Seiten und lauter rechten Winkeln existiert, so ist die Geometrie singulär. Die Winkelsumme des Dreiecks beträgt stets zwei Rechte. Zwei Geraden, welche eine gemeinsame Normale und somit überhaupt dasselbe System von Normalen besitzen, sollen parallel heissen. Parallele Geraden werden von jeder gemeinsamen Transversalen unter kongruenten gleichliegenden Winkeln geschnitten.

Es seien  $a, b$  zwei parallele Ferngeraden und  $s$  eine Gerade, welche  $a$  in einem Punkt  $A$  unter einem ordinären spitzen, dem rechten Winkel ebenbürtigen Winkel  $\alpha$  (d. h.  $\alpha > \frac{R}{2^n}$ , wo  $n$  eine ganze Zahl bedeutet) schneidet, dann muss  $s$  auch  $b$  schneiden, und zwar unter dem gleichen Winkel  $\alpha$ . Dies folgt aus einer sehr bekannten Schlussweise bei Legendre: Wir fällen das Lot  $AB$  auf  $b$ , tragen die Strecke  $AB_1 = AB$  auf  $b$  ab, sodann die Strecke  $B_1B_2 = AB_1$  in der Verlängerung von  $AB_1$ , ferner  $B_2B_3 = AB_2$  in der Verlängerung von  $AB_2$ , u. s. w. und gelangen auf diese Weise schliesslich an der Geraden  $s$  vorbei, weil der spitze Winkel zwischen  $AB_i$  und  $a = \frac{R}{2^i}$ , also schliesslich  $< \alpha$  wird.

37. Im folgenden soll nunmehr gezeigt werden, wie sich die von Hilbert in der Euklidischen Geometrie definierte Streckenrechnung für unsere Zwecke verallgemeinern lässt.

Zunächst wählen wir eine beliebige ordinäre Strecke  $e$  als Einheitsstrecke, und als vorläufiges Arbeitsgebiet betrachten wir den entsprechenden Eudoxischen Bereich  $E(e)$ . Dieser Bereich ist entweder als echter Teil in der vorgegebenen Ebene enthalten, oder er ist mit dieser identisch, und wenn wir unter »Gerade« in  $E(e)$  den Durchschnitt des Bereichs mit einer ursprünglichen Geraden verstehen, so sind alle ursprünglich aufgestellten Axiome der ebenen Geometrie in  $E(e)$  gültig.

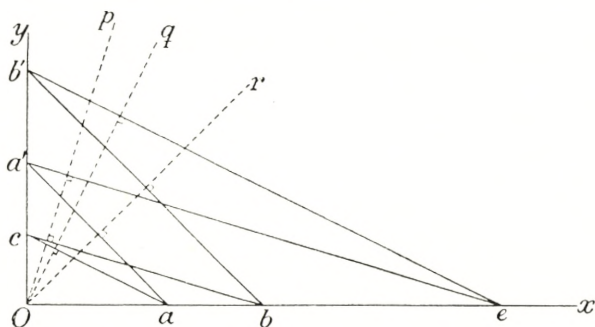


Fig. 9.

Die Summe zweier Strecken wird in gewöhnlicher Weise definiert. Um das Produkt einer Strecke  $a$  in eine Strecke  $b$  zu definieren, bedienen wir uns folgender Konstruktion (Fig. 9): Auf dem einen Schenkel  $x$  des rechten Winkels  $xy$  tragen wir vom Scheitel  $O$  aus die Strecken  $Oe = e$ ,  $Ob = b$ ,  $ab$ ; sodann tragen wir auf dem anderen Schenkel  $y$  die Strecke  $Oa' = a$  ab. Wir verbinden die Punkte  $e$  und  $a'$  durch eine Gerade und ziehen zu dieser Geraden durch den Punkt  $b$  eine Parallele. Die hierdurch auf  $y$  abgeschnittene Strecke  $Oc = c$  soll als Produkt  $ab$  bezeichnet werden. Die bei der Konstruktion benutzten Operationen sind alle eindeutig, und das Produkt ist infolgedessen eindeutig definiert.

Der besondere Fall, wo die Strecke  $0$  wird, d. h. auf einen Punkt reduziert wird, soll auch in Betracht gezogen werden. Es ist stets  $a \cdot 0 = 0 \cdot a = 0$ . Es kann aber vorkommen, dass  $a \cdot b = 0$ ,  $a \neq 0$ ,  $b \neq 0$ , nämlich in dem Falle, wo  $c$  nach  $O$  fällt. Das wird bedeuten, dass die beiden Geraden  $x$  und  $ea'$  Schmiegegeraden sind, und dass ihr Schnittelement eine Strecke gleich  $b$  enthält, also dass die Strecken  $a, b$  in reziproken Strichen enthalten sind. Also:





Einl. I, 55—56 gleichbedeutend, und hieraus folgt dann  $c' = c$ , oder  $ba = ab$ , womit wir das kommutative Gesetz für die oben definierte Multiplikation bewiesen haben.

39. Das assoziative Gesetz wird ebenso leicht nachgewiesen. Man braucht nur die Konstruktionen der Produkte  $ab$  und  $cb$  auszuführen (Fig. 10), um durch eine ähnliche Schluss-

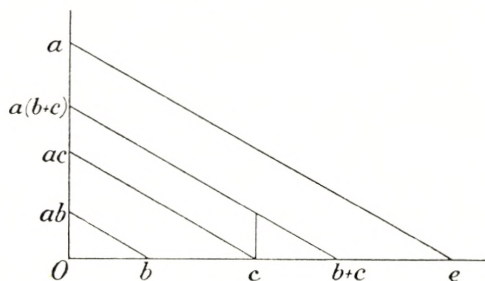


Fig. 11.

weise wie oben einzusehen, dass  $c(ab) = a(cb)$  ist, und daraus folgt mit Zuhilfenahme des kommutativen Gesetzes:

$$(ab)c = a(bc).$$

40. Endlich gilt auch das distributive Gesetz

$$a(b+c) = ab+ac,$$

was unmittelbar aus der nebenstehenden Hilbert'schen Figur (Fig. 11) hervorgeht.

41. Die Division  $a:b = \frac{a}{b}$  ist immer möglich und eindeutig, wenn der Divisor  $b$  ordinär ist. Ist  $a$  ordinär und  $b$  singulär, ist die Division unmöglich. Sind beide Strecken  $a, b$  singulär, ist die Division nur dann möglich, wenn  $a \asymp b$ ; der Quotient wird in diesem Falle unbestimmt. Ist nämlich  $a = cb$ , so ist auch  $a = c_1b$ , wenn

$$(c_1 - c)b = 0,$$

d. h. wenn

$$c_1 = c + b^*,$$

wo  $b^*$  dem zu  $b$  reziproken Strich angehört.

42. Zwei Dreiecke sollen ähnlich heißen, wenn entsprechende Winkel in ihnen kongruent sind.



Es seien  $Oab$  und  $Oa_1b_1$  zwei ähnliche rechtwinklige Dreiecke (Fig. 12), welche durch zwei Parallelen  $g, g_1$  aus dem rechten Winkel  $xy$  ausgeschnitten sind. Die Buchstaben  $a, b, a_1, b_1$  sollen sowohl die Ecken wie auch die anstossenden Katheten bezeichnen. Wir setzen voraus, dass die Winkel bei  $a$  und  $a_1$  ordinär sind. Auf  $x$  tragen wir die Einheitsstrecke  $Oe = e$  ab, und durch den Punkt  $e$  ziehen wir zu  $g, g_1$  eine Parallele, welche auf  $y$  eine Strecke  $Oc = c$  abschneidet. Es folgt dann

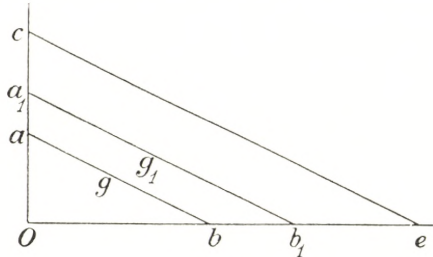


Fig. 12.

$$a = cb, \quad a_1 = cb_1,$$

also

$$ab_1 = a_1b.$$

Indem wir diese Produkte als Kreuzprodukte bezeichnen, können wir den folgenden Satz aussprechen:

In zwei ähnlichen rechtwinkligen Dreiecken sind die beiden Kreuzprodukte der Katheten einander gleich.

Aus diesem Satze leiten wir sofort den Höhensatz ab:

Im rechtwinkligen Dreieck ist das Quadrat der Höhe gleich dem Produkt der beiden Hypotenusenabschnitte.

43. Hierdurch sind wir nunmehr imstande, den allgemeinen pythagoreischen Lehrsatz zu beweisen:

Es sei  $ABC$  ein rechtwinkliges Dreieck mit den Katheten  $a, b$  und der Hypotenuse  $c$  (Fig. 13). Mit Hilfe eines Halbkreises  $DBE$ , mit dem Zentrum  $A$  und Radius  $c$ , lässt sich immer ein rechtwinkliges Dreieck  $DBE$  bestimmen, in welchem die Höhe  $BC = a$ , und die Hypotenusenabschnitte  $DC = c - b$ ,  $CE = c + b$  sind, und dem vorigen Satz zufolge gilt dann

oder

$$a^2 = c^2 - b^2,$$

$$a^2 + b^2 = c^2$$

44. Zu unserem bisherigen System von Strecken fügen wir jetzt in bekannter Weise ein entsprechendes System von negativen Strecken hinzu. Das so erweiterte System der positiven und negativen Strecken sowie der Strecke 0 gestattet dann unbeschränkt die Grund-Operationen: Addition, Subtraktion und

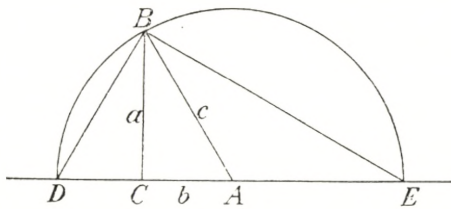


Fig. 13.

Multiplikation unter Erhaltung aller Ringpostulaten, d. h. das ganze System bildet einen Ring. In diesem Ringe sind alle singuläre Strecken Nullteiler. Zwei zu einander reziproke Strecken haben das Produkt 0.

Was die Ordnungsbeziehungen anbetriift gilt die folgende Grundregel: aus  $a > 0, b > 0$  folgt  $ab \geq 0$ .

Es liegt nun auf der Hand, wie man ein rechtwinkliges Koordinatensystem einrichten kann, in welchem jeder Punkt durch zwei Strecken  $x, y$  als Koordinaten bestimmt wird, jede Gerade durch eine lineare Gleichung

$$ax + by + c = 0,$$

in den laufenden Koordinaten  $x, y$ , wobei nicht beide Strecken  $a, b$  Nullteiler sind, und jeder Kreis durch eine Gleichung folgender Form:

$$(x - a)^2 + (y - b)^2 = r^2 \neq 0,$$

dargestellt wird.

45. Zu unserer so definierten Koordinatenebene können wir schliesslich Vektoren einführen:

Jedem Vektor  $a = (a_1, a_2)$  mit den Koordinaten  $a_1, a_2$  ent-



spricht der Quervektor  $\hat{a} = (-a_2, a_1)$ . Das Produkt  $ab$  zweier Vektoren  $a = (a_1, a_2)$ ,  $b = (b_1, b_2)$  wird so definiert:

$$ab = a_1b_1 + a_2b_2.$$

Das Quadrat  $aa = a^2$  des Vektors  $a$  ist demnach

$$a^2 = a_1^2 + a_2^2,$$

mit anderen Worten, dem pythagoreischen Lehrsatz zufolge:

Das Quadrat des Vektors ist gleich dem Quadrat der entsprechenden Strecke.

Der Vektor soll ordinär oder singular heißen, je nachdem die entsprechende Strecke ordinär oder singular ist. Die Geraden werden durch Einheitsvektoren orientiert. Seien zwei Geraden durch die Einheitsvektoren  $a, b$  orientiert, so sollen  $\cos$  und  $\sin$  ihres Winkels  $(a, b)$  so definiert werden:

$$\cos(a, b) = ab, \quad \sin(a, b) = \hat{a}b.$$

Auf Grund dieser Definitionen sind für jedes ordinäre Dreieck (d. h. ein Dreieck mit ordinären Seiten und Winkeln) die aus der traditionellen ebenen Trigonometrie bekannten Formeln ohne Schwierigkeit ableitbar.

Auch erkennen wir, dass jeder Schnittpunktsatz, der in der gewöhnlichen projektiven Geometrie gilt, ebenfalls in der hier vorgetragenen Geometrie Gültigkeit hat, unter dem Vorbehalt, dass alle in Rede stehenden Verbindungsgeraden und alle Schnittpunkte eindeutig bestimmt sind.

46. Um die Tragweite unserer Untersuchung einen Schritt weiter zu führen, betrachten wir noch den Fall, wo keine ordinären Strecken vorhanden sind, wobei stets die Voraussetzung gemacht werden soll, dass Rechtecke mit beliebig grossen Seiten existieren.

In diesem Falle wählen wir eine beliebig grosse Strecke  $a$  heraus und beschränken unsere Untersuchung auf den durch  $a$  definierten Eudoxischen Bereich  $E(a)$ . Die Geometrie dieses Bereichs gestaltet sich nun genau wie im vorhergehenden Falle, indem wir unter Geraden in  $E(a)$  die Durchschnitte der ursprünglichen Geraden mit  $E(a)$  verstehen.

In ganz ähnlicher Weise lässt sich die Geometrie eines beliebigen Flecks der singulären Ebene und die Geometrie eines Unter- oder Pariflecks der schwach singulären oder der ordinären Ebene behandeln.

47. Schliesslich erwähnen wir noch die räumliche singuläre Geometrie. Das Produkt  $ab$  zweier Vektoren  $a = (a_1, a_2, a_3)$ ,  $b = (b_1, b_2, b_3)$  ist

$$ab = a_1b_1 + a_2b_2 + a_3b_3.$$

Das Quadrat  $aa = a^2$  des Vektors  $a$  ist

$$a^2 = a_1^2 + a_2^2 + a_3^2,$$

also wiederum, dem pythagoreischen Lehrsatz zufolge:

Das Quadrat des Vektors ist gleich dem Quadrat der entsprechenden Strecke.

Sind die beiden Vektoren  $a, b$  senkrecht zueinander, so gilt, wegen des pythagoreischen Lehrsatzes:

$$a^2 + b^2 = (a - b)^2,$$

d. h.

$$ab = 0,$$

und für den Fall, wo  $a$  und  $b$  ordinär sind, gilt umgekehrt, dass  $ab = 0$  eine hinreichende Bedingung dafür ist, dass  $a \perp b$ .

Wie in der Ebene werden die Geraden durch Einheitsvektoren orientiert.

Der Quervektor  $\widehat{ab}$  (das vektorielle Produkt) zweier Vektoren  $a, b$  wird so definiert:

$$\widehat{ab} = (a_2b_3 - a_3b_2, a_3b_1 - a_1b_3, a_1b_2 - a_2b_1).$$

wonach

$$\widehat{ab} \cdot c = \begin{vmatrix} a_1 & a_2 & a_3 \\ b_1 & b_2 & b_3 \\ c_1 & c_2 & c_3 \end{vmatrix} = \widehat{abc}.$$

Durch einfache Rechnung bestätigt man die folgende Identität:

$$(\widehat{ab})^2 = a^2b^2 - (ab)^2.$$



Sind  $a, b$  zwei zueinander senkrechte Einheitsvektoren, so folgt hieraus, dass  $\widehat{ab} = c$  auch ein Einheitsvektor ist senkrecht zu den beiden anderen. Ein zweiter Einheitsvektor senkrecht zu  $a$  und  $b$  ist  $c' = -c$ . Für  $c$  und  $c'$  gelten die Gleichungen

$$\widehat{abc} = 1, \quad \widehat{abc'} = -1.$$

Für die drei Grundvektoren  $i = (1,0,0)$ ,  $j = (0,1,0)$ ,  $k = (0,0,1)$  erhalten wir:

$$\widehat{ij} = k, \quad \widehat{jk} = i, \quad \widehat{ki} = j, \quad \widehat{ijk} = 1.$$

Ein Transport um den Nullpunkt  $(0,0,0)$  als Fixpunkt wird dadurch bestimmt, dass die Grundvektoren  $i, j, k$  in vorgegebene aufeinander senkrechte Einheitsvektoren  $a, b, c$ , übergehen. Der Punkt  $x$  geht dabei in den durch die folgende Formel bestimmten Punkt  $x'$  über:

$$x' = x_1 a + x_2 b + x_3 c.$$

Der Transport ist direkt oder indirekt, je nachdem  $\widehat{abc} = \pm 1$  ist.

Für zwei beliebige Punkte  $x, y$  und deren entsprechende Punkte  $x', y'$  gilt:

$$x'y' = xy, \quad (x' - y')^2 = (x - y)^2, \quad \widehat{x'y'} = (\widehat{xy})'.$$

Für zwei Einheitsvektoren  $a, b$  definieren wir im Raume in unmittelbarem Anschluss an unsere Definitionen in der Ebene:

$$\cos(a, b) = ab, \quad \sin(a, b) = \frac{\widehat{ab}}{ef},$$

wobei  $e, f$  zwei auf einander senkrechte Einheitsvektoren der Ebene  $ab$  bedeuten. Die Normale dieser Ebene soll durch den Einheitsvektor  $\widehat{ef}$  orientiert werden. Dem Winkel  $(\alpha, \beta)$  von einer so orientierten Ebene  $\alpha$  zu einer anderen orientierten Ebene  $\beta$ , wobei auch eine Orientierung für die Schnittlinie der beiden Ebenen vorgegeben sein soll, entsprechen dann den obigen Formeln gemäss eindeutig bestimmte Werte des cosinus und sinus.

48. Betrachten wir jetzt eine dreiseitige Ecke, deren Kanten durch die Einheitsvektoren  $A, B, C$  orientiert sind, und deren Seitenebenen  $BC, CA, AB$  ebenfalls wie oben angegeben orientiert

sind. Folgende Bezeichnungen für Seiten und Raumwinkel werden eingeführt:

$$(B, C) = a, \quad (C, A) = b, \quad (A, B) = c, \\ (CA, AB) = A, \quad (AB, BC) = B, \quad (BC, CA) = C.$$

Um die allgemeinen Beziehungen dieser 6 Winkel zu finden, benutzen wir die folgenden Identitäten:

$$\widehat{CA} \cdot \widehat{AB} = \left| \begin{array}{cc} CA & CB \\ A^2 & AB \end{array} \right|, \\ \widehat{CA} \widehat{AB} = \left| \begin{array}{cc} \widehat{A} & \widehat{B} \\ \widehat{CAA} & \widehat{CAB} \end{array} \right|.$$

Aus der ersteren folgt direkt:

$$(I) \quad \cos a = \cos b \cos c - \sin b \sin c \cos A,$$

und aus der anderen ergibt sich

$$(II) \quad \sin b \sin c \sin A = \widehat{ABC},$$

und hiermit haben wir für ordinäre sphärische Dreiecke die Gültigkeit der gewöhnlichen Grundformeln nachgewiesen.





DET KGL. DANSKE VIDENSKABERNES SELSKAB  
MATEMATISK-FYSISKE MEDDELELSER, BIND XXII, NR. 14

---

# SOME LIMIT THEOREMS ON INTEGRALS IN AN ABSTRACT SET

BY

ERIK SPARRE ANDERSEN AND BØRGE JESSEN



KØBENHAVN  
I KOMMISSION HOS EJNAR MUNKSGAARD  
1946



Printed in Denmark.  
Bianco Lunos Bogtrykkeri A/S

**1. Introduction.** The present paper deals with two limit theorems on integrals in an abstract set. The first limit theorem is a generalization of the well-known theorem on differentiation on a net, the net being replaced by an increasing sequence of  $\sigma$ -fields. The second limit theorem is a sort of counterpart of the first, the sequence of  $\sigma$ -fields being now decreasing. The proofs follow the lines of the proof of the theorem on differentiation on a net.

In case of integrals in an infinite product set the theorems lead to known results, when for the  $n^{\text{th}}$   $\sigma$ -field of the sequence we take either the system of measurable sets depending on the  $n$  first coordinates only, or the system of measurable sets depending on all except the  $n$  first coordinates.

If the abstract theory of integration is interpreted as probability theory, our theorems lead to two theorems concerning conditional mean values.

For the convenience of the reader the main definitions and theorems used are stated at the beginning of the paper. For references and proofs we may refer to the book by Saks [1] or to a series of articles by Jessen [2], which we follow closely.

**2. Sets and functions.** Let  $E$  be a set containing at least one element. Elements of  $E$  will be denoted by  $x, y, \dots$  and sub-sets of  $E$  by  $A, B, \dots$ . The set  $E$  itself and the empty set  $0$  will be reckoned among the sub-sets of  $E$ . The notation  $x \in A$  means that the element  $x$  belongs to the set  $A$ , while  $x \bar{\in} A$  means that  $x$  does not belong to  $A$ . If  $A$  is a subset of  $B$  we write  $A \subseteq B$  or  $B \supseteq A$ , while  $A \subset B$  or  $B \supset A$  means that  $A$  is a proper sub-set of  $B$ . By  $\bigcirc_n A_n$  or  $A_1 \dot{+} A_2 \dot{+} \dots$  we denote the



sum of the sets  $A_1, A_2, \dots$ . If no two of the sets have elements in common the signs  $\ominus$  and  $\dot{+}$  may be replaced by  $\Sigma$  and  $+$ . By  $\bigcap_n A_n$  or  $A_1 A_2 \dots$  we denote the common part of the sets  $A_1, A_2, \dots$ . The notation  $A - B$  will be used only when  $A \supset B$ , and denotes the difference between  $A$  and  $B$ .

A real function  $f$  in  $E$  is given, when to every element  $x$  of a set  $A$  there corresponds a value  $f(x)$ ,  $-\infty \leq f(x) \leq +\infty$ . The set  $A$  is called the domain of  $f$ . Functions in  $E$  will be denoted by  $f, g, \dots$ . By  $[\dots]$ , where  $\dots$  indicates a number of expressions or relations involving functions in  $E$ , we denote the set of elements  $x$  of  $E$  for which these expressions are defined and the relations are valid. For example  $[f]$  denotes the domain of  $f$ .

**3. Systems of sets and set-functions.** Let  $\mathfrak{M}$  denote the set of all sub-sets of  $E$ . Sub-sets of  $\mathfrak{M}$  will be denoted by  $\mathfrak{F}, \mathfrak{G}, \dots$ , and will be called systems of sets, the notation 'set' being reserved for sub-sets of  $E$ .

A system  $\mathfrak{F}$  is called *additive*, if  $A_1 \dot{+} \dots \dot{+} A_n \in \mathfrak{F}$  when all  $A_i \in \mathfrak{F}$ , and *multiplicative*, if  $A_1 \dots A_n \in \mathfrak{F}$  when all  $A_i \in \mathfrak{F}$ . It is called *subtractive*, if  $A - B \in \mathfrak{F}$  when  $A \in \mathfrak{F}$ ,  $B \in \mathfrak{F}$ , and  $A \supseteq B$ . It is called *completely additive*, if  $A_1 \dot{+} A_2 \dot{+} \dots \in \mathfrak{F}$  when all  $A_i \in \mathfrak{F}$ , and *completely multiplicative*, if  $A_1 A_2 \dots \in \mathfrak{F}$  when all  $A_i \in \mathfrak{F}$ .

A system of sets is called a *field*, if it contains at least one set and is additive and subtractive (and hence also multiplicative).

A system of sets is called a  $\sigma$ -*field*, if it contains at least one set and is completely additive and subtractive (and hence also completely multiplicative).

Functions in  $\mathfrak{M}$ , i. e. functions for which the domain is a system of sets, are called *set-functions* and will be denoted by  $\mu, \nu, \dots$ .

A set-function  $\mu$  with domain  $\mathfrak{F}$  is called *additive*, if  $\mu(A_1 + \dots + A_n) = \mu(A_1) + \dots + \mu(A_n)$  when all  $A_i \in \mathfrak{F}$  and  $A_1 + \dots + A_n \in \mathfrak{F}$ . It is called *completely additive*, if  $\mu(A_1 + A_2 + \dots) = \mu(A_1) + \mu(A_2) + \dots$  when all  $A_i \in \mathfrak{F}$  and  $A_1 + A_2 + \dots \in \mathfrak{F}$ .

If two set-functions  $\mu$  and  $\nu$  have the domains  $\mathfrak{F}$  and  $\mathfrak{G}$ , we call  $\nu$  an *extension* of  $\mu$  or  $\mu$  a *contraction* of  $\nu$  and write  $\nu \supset \mu$  or  $\mu \subset \nu$  when  $\mathfrak{F} \subset \mathfrak{G}$  and  $\mu(A) = \nu(A)$  for all  $A \in \mathfrak{F}$ .

**4. Content and measure.** A set-function  $\mu$  is called a *content*, if

- (i) its domain  $\mathfrak{F}$  is a field,
- (ii)  $0 \leq \mu(A) \leq +\infty$  for any  $A \in \mathfrak{F}$ ,
- (iii)  $\mu$  is additive,
- (iv) to every  $A \in \mathfrak{F}$  there corresponds a set  $\mathfrak{S}_n A_n$  where all  $A_n \in \mathfrak{F}$ ,

such that  $A \subseteq \mathfrak{S}_n A_n$  and  $\mu(A_n) < +\infty$  for all  $n$ .<sup>1</sup>

A set-function  $\mu$  is called a *measure*, if

- (i) its domain  $\mathfrak{F}$  is a  $\sigma$ -field,
- (ii)  $0 \leq \mu(A) \leq +\infty$  for any  $A \in \mathfrak{F}$ ,
- (iii)  $\mu$  is completely additive,
- (iv) to every  $A \in \mathfrak{F}$  there corresponds a set  $\mathfrak{S}_n A_n$  where all  $A_n \in \mathfrak{F}$ ,

such that  $A \subseteq \mathfrak{S}_n A_n$  and  $\mu(A_n) < +\infty$  for all  $n$ .<sup>1</sup>

Of fundamental importance is the following

*Extension Theorem.* If  $\mu$  is a content, then there exists a measure  $\omega \supseteq \mu$  if, and only if,  $\mu$  is completely additive. If so, there exists a unique measure  $\nu \supseteq \mu$ , such that  $\omega \supseteq \nu$  for any measure  $\omega \supseteq \mu$ . The domain of  $\nu$  is the smallest  $\sigma$ -field containing the domain of  $\mu$ .

The measure  $\nu$  is called the *narrowest extension of  $\mu$  to a measure*.

For the complete additivity of a content we have the following criterion:

A *finite* content  $\mu$  with domain  $\mathfrak{F}$  is completely additive if, and only if,  $\lim_n \mu(A_n) = 0$  for any sequence of sets  $A_n \in \mathfrak{F}$ , for which  $A_1 \supseteq A_2 \supseteq \dots$  and  $\mathfrak{D}_n A_n = 0$ .

**5. Integration with respect to a measure.** By the *system of functions over a  $\sigma$ -field  $\mathfrak{F}$*  we mean the system of all functions  $f$  for which  $[f \geq a] \in \mathfrak{F}$  for any  $a$ ,  $-\infty \leq a \leq +\infty$ . If  $\mathfrak{F}$  is the domain of a measure  $\mu$ , the functions of this system are called  *$\mu$ -measurable*.

The theory of *integration* of  $\mu$ -measurable functions with respect to the measure  $\mu$  may be developed in the usual way.

<sup>1</sup> This is the definition adopted in Jessen [2]. In the sequel we shall in the main only consider contents and measures for which  $E \in \mathfrak{F}$  and  $\mu(E) < +\infty$ .



For the integral of the function  $f$  over the  $\mu$ -measurable set  $A \subseteq [f]$  we shall use the notation

$$\int_A f(x) \mu(dE).$$

If the integral of  $f$  over its domain  $[f]$  exists and is finite, the function  $f$  is called  $\mu$ -integrable. The set-function

$$\varphi(A) = \int_A f(x) \mu(dE)$$

is then defined for all sub-sets  $A \in \mathfrak{F}$  of  $[f]$  and is called the *indefinite integral* of  $f$ .

Two  $\mu$ -integrable functions  $f$  and  $g$  with  $[f] = [g]$  have the same indefinite integral if, and only if,  $\mu([f \neq g]) = 0$ .

**6. Completely additive set-functions.** Let  $\varphi$  denote a *bounded* set-function with domain  $\mathfrak{F}$ . We define two other set-functions  $\varphi^+$  and  $\varphi^-$  with the same domain by placing

$$\varphi^+(A) = \text{upper bound } \varphi(B) \quad \text{and} \quad \varphi^-(A) = \text{lower bound } \varphi(B),$$

where the upper and lower bounds are taken with respect to all sub-sets  $B \in \mathfrak{F}$  of  $A$ . We then have the following

*Decomposition Theorem.* If  $\mathfrak{F}$  is a field, and  $\varphi$  is completely additive, then  $\varphi^+$  and  $-\varphi^-$  are completely additive contents, and  $\varphi = \varphi^+ + \varphi^-$ . If moreover  $\mathfrak{F}$  is a  $\sigma$ -field, then  $\varphi^+$  and  $-\varphi^-$  are measures.

The set-functions  $\varphi^+$  and  $\varphi^-$  are called the *positive* and *negative parts* of  $\varphi$ .

Moreover we have the following

*Extension Theorem.* If  $\mathfrak{F}$  is a field, and  $\varphi$  is completely additive, then there exists a unique set-function  $\psi \supseteq \varphi$ , which is bounded and completely additive and is defined on the smallest  $\sigma$ -field containing  $\mathfrak{F}$ . Moreover  $\psi^+ \supseteq \varphi^+$  and  $\psi^- \supseteq \varphi^-$ , i. e.  $\psi^+$  and  $-\psi^-$  are the narrowest extensions of the contents  $\varphi^+$  and  $-\varphi^-$  to measures.

This theorem implies that if  $\mathfrak{F}$  is a field, and  $\mathfrak{G}$  is the smallest  $\sigma$ -field containing  $\mathfrak{F}$ , then a bounded, completely additive set-function defined on  $\mathfrak{G}$ , for which the contraction to  $\mathfrak{F}$  is non-negative, will itself be non-negative.

**7. Continuous and singular set-functions.** Let  $\mu$  denote a measure in  $E$  with domain  $\mathfrak{F}$ , and suppose that  $E \in \mathfrak{F}$ .

A bounded, completely additive set-function  $\varphi$  defined on  $\mathfrak{F}$  is called  $\mu$ -continuous, if  $\varphi(M) = 0$  for any  $M \in \mathfrak{F}$  with  $\mu(M) = 0$ . It is called  $\mu$ -singular, if there exists a set  $N \in \mathfrak{F}$  with  $\mu(N) = 0$ , such that  $\varphi(A) = 0$  for every sub-set  $A \in \mathfrak{F}$  of  $E - N$ .

We have the following

*Decomposition Theorem.* Any bounded, completely additive set-function  $\varphi$  defined on  $\mathfrak{F}$  admits of a unique representation  $\varphi = \varphi_c + \varphi_s$ , where  $\varphi_c$  and  $\varphi_s$  are bounded, completely additive set-functions defined on  $\mathfrak{F}$ , of which  $\varphi_c$  is  $\mu$ -continuous, while  $\varphi_s$  is  $\mu$ -singular.

The set-functions  $\varphi_c$  and  $\varphi_s$  are called the  $\mu$ -continuous and  $\mu$ -singular parts of  $\varphi$ .

A set-function  $\varphi$  defined on  $\mathfrak{F}$  is the indefinite integral of a  $\mu$ -integrable function  $f$  with  $[f] = E$  if, and only if, it is bounded, completely additive, and  $\mu$ -continuous.

**8. First limit theorem.** Let  $E$  be a set containing at least one element, and  $\mu$  a measure in  $E$  with domain  $\mathfrak{F}$ , such that  $E \in \mathfrak{F}$  and  $\mu(E) = 1$ . Let  $\mathfrak{F}_1 \subseteq \mathfrak{F}_2 \subseteq \dots$  be an increasing sequence of  $\sigma$ -fields contained in  $\mathfrak{F}$ , such that  $E \in \mathfrak{F}_1$ . The system  $\mathfrak{G} = \bigcup_n \mathfrak{F}_n$  is a field. The smallest  $\sigma$ -field containing  $\mathfrak{G}$  will be denoted by  $\mathfrak{F}'$ .

The contraction of  $\mu$  to  $\mathfrak{F}_n$  is a measure, which will be denoted by  $\mu_n$ . Similarly the contraction of  $\mu$  to  $\mathfrak{F}'$  is a measure, which will be denoted by  $\mu'$ .

Let  $\varphi$  be a bounded, completely additive set-function defined on  $\mathfrak{F}$ , whose contraction  $\varphi_n$  to  $\mathfrak{F}_n$  is  $\mu_n$ -continuous for any  $n$ . By § 7 this means, that  $\varphi_n$  is the indefinite integral with respect to  $\mu_n$  of a  $\mu_n$ -integrable function  $f_n$ , i.e. there exists for every  $n$  a  $\mu_n$ -integrable function  $f_n$ , such that

$$\int_A f_n(x) \mu(dE) = \varphi(A) \quad \text{for every } A \in \mathfrak{F}_n.$$

This function  $f_n$  need not be uniquely determined. In the sequel  $f_n$  denotes for every  $n$  some such function. We shall consider the functions

$$\underline{f} = \liminf_n f_n \quad \text{and} \quad \bar{f} = \limsup_n f_n.$$



Evidently these functions are  $\mu'$ -measurable. The contraction of  $\varphi$  to  $\mathfrak{F}'$  will be denoted by  $\varphi'$ .

The first limit theorem now states:

*With the above notations we have the relation*

$$\mu([\underline{f} < \bar{f}]) = 0,$$

and  $\varphi(C) = 0$  for any sub-set  $C \in \mathfrak{F}'$  of  $[\underline{f} < \bar{f}]$ .

Moreover  $\underline{f}$  and  $\bar{f}$  are  $\mu'$ -integrable, and their indefinite integrals with respect to  $\mu'$  are the  $\mu'$ -continuous part  $\varphi'_c$  of  $\varphi'$ , i. e. for any  $A \in \mathfrak{F}'$  we have

$$\varphi'_c(A) = \int_A \underline{f}(x) \mu(dE) = \int_A \bar{f}(x) \mu(dE).$$

Finally, the positive and negative parts of the  $\mu'$ -singular part  $\varphi'_s$  of  $\varphi'$  satisfy for any  $A \in \mathfrak{F}'$  the relations

$$\varphi'_s{}^+(A) = \varphi(A[\underline{f} = +\infty]) \quad \text{and} \quad \varphi'_s{}^-(A) = \varphi(A[\bar{f} = -\infty]).^1$$

9. The proof will be based on the following lemma:

Placing  $H = [\underline{f} \leq h]$  and  $K = [\bar{f} \geq k]$  for arbitrary numbers  $h$  and  $k$  we have for any  $C \in \mathfrak{F}'$  the inequalities

$$\varphi(HC) \leq h\mu(HC) \quad \text{and} \quad \varphi(KC) \geq k\mu(KC).$$

In order to prove the first inequality we put

$$H_n = [\inf_p f_{n+p} < h_n]$$

and

$$H_{np} = \begin{cases} [f_{n+1} < h_n] & \text{for } p = 1 \\ [f_{n+1} \geq h_n, \dots, f_{n+p-1} \geq h_n, f_{n+p} < h_n] & \text{for } p > 1, \end{cases}$$

where  $h_1, h_2, \dots$  denotes a decreasing sequence of numbers converging towards  $h$ . Then  $H_{np} \in \mathfrak{F}_{n+p}$  and  $H_{np} \subseteq [f_{n+p} < h_n]$ . Clearly (for a given  $n$ ) no two of the sets  $H_{np}$  have elements in common, and  $H_n = \sum_p H_{np}$ . Further  $H_1 \supseteq H_2 \supseteq \dots$  and  $H = \mathfrak{D}_n H_n$ .

<sup>1</sup> The assumption  $\mu(E) = 1$  has been introduced for the sake of convenience. The theorem may easily be extended to the case where  $E \in \mathfrak{F}$  and  $\mu(E)$  is arbitrary (finite or infinite).

Now, if  $C \in \mathfrak{G} = \mathfrak{G}_n$ , we shall have  $C \in \mathfrak{F}_n$  for all  $n > (\text{some})$   $n_0$ ; hence  $H_{np} C \in \mathfrak{F}_{n+p}$  for  $n \geq n_0$  and all  $p$ . We therefore have

$$\begin{aligned} \varphi(H_n C) &= \varphi\left(\sum_p H_{np} C\right) = \sum_p \varphi(H_{np} C) = \sum_p \int_{H_{np} C} f_{n+p}(x) \mu(dE) \\ &\leq \sum_p h_n \mu(H_{np} C) = h_n \mu\left(\sum_p H_{np} C\right) = h_n \mu(H_n C). \end{aligned}$$

Since  $H_1 C \supseteq H_2 C \supseteq \dots$  and  $HC = \bigcap_n H_n C$ , we have  $\mu(HC) = \lim_n \mu(H_n C)$  and  $\varphi(HC) = \lim_n \varphi(H_n C)$ . We therefore obtain  $\varphi(HC) \leq h \mu(HC)$ .

We now define a set-function  $\alpha$  on  $\mathfrak{F}'$  by placing

$$\alpha(C) = h \mu(HC) - \varphi(HC).$$

Clearly  $\alpha$  is bounded and completely additive. Moreover, since  $\varphi(HC) \leq h \mu(HC)$  for  $C \in \mathfrak{G}$ , the contraction of  $\alpha$  to  $\mathfrak{G}$  is non-negative. Hence, by § 6, the set-function  $\alpha$  is itself non-negative, i. e. the inequality  $\varphi(HC) \leq h \mu(HC)$  is valid for all  $C \in \mathfrak{F}'$ .

The inequality  $\varphi(KC) \geq k \mu(KC)$  is proved analogously.

**10.** By means of the lemma we shall now first prove that  $\mu(\underline{f} < \bar{f}) = 0$ , and that  $\varphi(C) = 0$  for any sub-set  $C \in \mathfrak{F}'$  of  $[\underline{f} < \bar{f}]$ .

Since  $[\underline{f} < \bar{f}] = \mathfrak{G}([\underline{f} < h, \bar{f} > k])$ , where the summation is with respect to all pairs of rational numbers  $h$  and  $k$ , for which  $h < k$ , it is sufficient to prove that  $\mu(C) = 0$  and  $\varphi(C) = 0$  for any sub-set  $C \in \mathfrak{F}'$  of  $[\underline{f} < h, \bar{f} > k]$ , when  $h < k$ .

This follows from the lemma. For, when  $C \in \mathfrak{F}'$  is a sub-set of  $[\underline{f} < h, \bar{f} > k]$ , we have  $C \subseteq H$  and  $C \subseteq K$ , and hence

$$h \mu(C) \geq \varphi(C) \geq k \mu(C).$$

Since  $h < k$ , this shows that  $\mu(C) = 0$ , and hence also  $\varphi(C) = 0$ .

**11.** Next we prove that the functions  $\underline{f}$  and  $\bar{f}$  are  $\mu'$ -integrable and that their indefinite integrals with respect to  $\mu'$  are the  $\mu'$ -continuous part  $\varphi'_c$  of  $\varphi'$ .



Placing  $N^+ = [\underline{f} = +\infty]$  and  $N^- = [\bar{f} = -\infty]$  we shall first prove that  $\mu(N^+) = 0$  and  $\mu(N^-) = 0$ .

For every  $k$  we have  $N^+ \subseteq [\underline{f} = +\infty] \subseteq [\bar{f} \geq k]$ . From the lemma it follows that when  $k > 0$  we have

$$\mu(N^+) \leq \mu([\bar{f} \geq k]) \leq \frac{1}{k} \varphi([\bar{f} \geq k]) \leq \frac{1}{k} \varphi^+(E).$$

Making  $k \rightarrow +\infty$  we obtain  $\mu(N^+) = 0$ . Analogously it is proved that  $\mu(N^-) = 0$ .

For an arbitrary finite  $d > 0$  we now put

$$f_d(x) = \begin{cases} nd & \text{for } x \in [nd \leq \underline{f} = \bar{f} < (n+1)d], -\infty < n < +\infty, \\ 0 & \text{for } x \in [-\infty < \underline{f} = \bar{f} < +\infty] \end{cases}$$

and apply for an arbitrary set  $A \in \mathfrak{F}'$  the lemma on the set  $C_n = A[nd \leq \underline{f} = \bar{f} < (n+1)d]$  together with  $H_n = [\underline{f} \leq (n+1)d]$  and  $K_n = [\bar{f} \geq nd]$ . This yields

$$nd\mu(C_n) \leq \varphi(C_n) \leq (n+1)d\mu(C_n).$$

If we choose  $A = E$ , these inequalities show that  $f_d$  is  $\mu'$ -integrable. For an arbitrary  $A \in \mathfrak{F}'$  they show, together with the relations  $\mu(A[\underline{f} < \bar{f}]) = 0$  and  $\varphi(A[\underline{f} < \bar{f}]) = 0$ , that

$$\int_{AD} f_d(x) \mu(dE) \leq \varphi(AD) \leq \int_{AD} f_d(x) \mu(dE) + d,$$

where  $D = E - (N^+ + N^-)$ .

Since in the set  $D - [\underline{f} < \bar{f}]$  we have  $f_d \leq \underline{f} = \bar{f} < f_d + d$ , it is plain that  $\underline{f}$  and  $\bar{f}$  are  $\mu'$ -integrable, and that for an arbitrary  $A \in \mathfrak{F}'$

$$\int_{AD} f_d(x) \mu(dE) \leq \left\{ \begin{array}{l} \int_{AD} \underline{f}(x) \mu(dE) \\ \int_{AD} \bar{f}(x) \mu(dE) \end{array} \right\} \leq \int_{AD} f_d(x) \mu(dE) + d.$$

Since  $d$  may be chosen arbitrarily small, the preceding inequalities show that

$$\varphi(AD) = \int_{AD} \underline{f}(x) \mu(dE) = \int_{AD} \bar{f}(x) \mu(dE).$$

The set-function  $\psi(A) = \varphi(AD)$  defined on  $\mathfrak{F}'$  is therefore  $\mu'$ -continuous, and since  $\varphi'(A) = \varphi(AD) + \varphi(A(E-D))$ , where  $\mu(E-D) = 0$ , so that  $\chi(A) = \varphi(A(E-D))$  is  $\mu'$ -singular, it follows from the decomposition theorem of §7 that  $\psi$  and  $\chi$  must be the  $\mu'$ -continuous and  $\mu'$ -singular parts of  $\varphi'$ . Since the integrals of  $\underline{f}$  and  $\bar{f}$  over  $AD$  are equal to the integrals over  $A$ , the last relations may therefore also be written

$$\varphi'_c(A) = \int_A \underline{f}(x) \mu(dE) = \int_A \bar{f}(x) \mu(dE).$$

**12.** The set-function  $\chi$  being the  $\mu'$ -singular part of  $\varphi'$ , it is plain that for any  $A \in \mathfrak{F}'$

$$\varphi'_s(A) = \varphi(A(E-D)) = \varphi(AN^+) + \varphi(AN^-).$$

Since  $AN^+ \subseteq [\bar{f} \geq 0]$ , it follows from the lemma that  $\varphi(AN^+) \geq 0$  for any  $A \in \mathfrak{F}'$ . Similarly it is proved that  $\varphi(AN^-) \leq 0$ .

For any sub-set  $B \in \mathfrak{F}'$  of  $A$  we therefore have  $0 \leq \varphi(BN^+) \leq \varphi(AN^+)$  and  $\varphi(AN^-) \leq \varphi(BN^-) \leq 0$ . Since  $\varphi'_s(B) = \varphi(BN^+) + \varphi(BN^-)$ , this shows that  $\varphi(AN^-) \leq \varphi'_s(B) \leq \varphi(AN^+)$ .

Hence by the definition of §6 we have for any  $A \in \mathfrak{F}'$

$$\varphi_s'^+(A) = \varphi(AN^+) \text{ and } \varphi_s'^-(A) = \varphi(AN^-).$$

This completes the proof of the theorem.

**13. Corollaries of the first limit theorem.** If in particular  $\mathfrak{F}' = \mathfrak{F}$ , we have  $\mu' = \mu$  and  $\varphi' = \varphi$ , so that the first limit theorem contains statements about the set-function  $\varphi$  itself.



Even if  $\mathfrak{F}' \subset \mathfrak{F}$ , we may, however, under certain additional assumptions, deduce less precise results regarding the set-function  $\varphi$ .

Let us first assume that to any set  $A \in \mathfrak{F}$  there exists a set  $B \in \mathfrak{F}'$ , such that  $B \supseteq A$  and  $\mu(B - A) = 0$ . We shall then prove two results:

(i) If  $\varphi$  is non-negative, then the indefinite integrals of  $\underline{f}$  and  $\bar{f}$  with respect to  $\mu$  are the  $\mu$ -continuous part  $\varphi_c$  of  $\varphi$ , and the  $\mu$ -singular part of  $\varphi$  satisfies for any  $A \in \mathfrak{F}$  the relation  $\varphi_s(A) = \varphi(A[\underline{f} = +\infty])$ .

Proof. We have the decomposition  $\varphi(A) = \varphi(AD) + \varphi(AN^+)$ . The set-function  $\varphi(AN^+)$  is  $\mu$ -singular, since  $\mu(N^+) = 0$ . The set-function  $\varphi(AD)$  is  $\mu$ -continuous. For if  $A \in \mathfrak{F}$  and  $\mu(A) = 0$ , there exists a set  $B \in \mathfrak{F}'$ , such that  $B \supseteq A$  and  $\mu(B - A) = 0$ , i. e.  $\mu(B) = 0$ . Hence, since  $\varphi$  is non-negative,  $0 \leq \varphi(AD) \leq \varphi(BD) = 0$ , and therefore  $\varphi(AD) = 0$ . Finally  $\varphi(AD)$  is the indefinite integral of  $\underline{f}$  and  $\bar{f}$  with respect to  $\mu$ . For to an arbitrary  $A \in \mathfrak{F}$  there exists a  $B \in \mathfrak{F}'$ , such that  $B \supseteq A$  and  $\mu(B - A) = 0$ , and we then have

$$\varphi(AD) = \varphi(BD) = \begin{cases} \int_{BD} \underline{f}(x) \mu(dE) = \int_{AD} \underline{f}(x) \mu(dE) \\ \int_{BD} \bar{f}(x) \mu(dE) = \int_{AD} \bar{f}(x) \mu(dE). \end{cases}$$

(ii) Without restriction on the sign of  $\varphi$  the indefinite integrals of  $\underline{f}$  and  $\bar{f}$  with respect to  $\mu$  are the  $\mu$ -continuous part  $\varphi_c$  of  $\varphi$ .

Proof. The statement follows from the decomposition  $\varphi = \varphi^+ + \varphi^-$ , when we apply the previous result on each of the set-functions  $\varphi^+$  and  $-\varphi^-$ .

We mention that not only the relations  $\varphi_s^+(A) = \varphi(AN^+)$  and  $\varphi_s^-(A) = \varphi(AN^-)$ , but even the relation  $\varphi_s(A) = \varphi(A(N^+ + N^-))$ , need not hold generally. This is shown by the following example:

Let  $\mathfrak{F}$  consist of all sub-sets of a set  $E$  of three elements  $a$ ,  $b$ , and  $c$ , and let  $\mu(\{a\}) = 1$ ,  $\mu(\{b\}) = \mu(\{c\}) = 0$ , and  $\varphi(\{a\}) = 0$ ,  $\varphi(\{b\}) = 1$ ,  $\varphi(\{c\}) = -1$ . Let each of the  $\sigma$ -fields  $\mathfrak{F}_1, \mathfrak{F}_2, \dots$  consist of all sets containing either both or none of the elements  $b$  and  $c$ . Then the above condition is satisfied, but  $\varphi$  is singular,

and there exists no set  $N \in \mathfrak{F}'$  for which  $\varphi(A) = \varphi(AN)$  for all  $A \in \mathfrak{F}$ .

**14.** Next, let us assume that to any set  $A \in \mathfrak{F}$  there exists a set  $B \in \mathfrak{F}'$ , such that  $\mu(A \dot{+} B - AB) = 0$ . Evidently this condition is weaker than the preceding one. We shall then prove:

*If  $\varphi$  is  $\mu$ -continuous, then  $\varphi$  is the indefinite integral of  $f$  or  $\bar{f}$  with respect to  $\mu$ .*

*Proof.* Let  $A \in \mathfrak{F}$  be arbitrary, and let  $B \in \mathfrak{F}'$  be chosen such that  $\mu(A \dot{+} B - AB) = 0$ . Since  $\mu(A - AB) = 0$  and  $\mu(B - AB) = 0$ , we have

$$\varphi(A) = \varphi(B) + \varphi(A - AB) - \varphi(B - AB) = \varphi(B),$$

and, denoting by  $f$  any of the functions  $f$  and  $\bar{f}$ ,

$$\int_A f(x) \mu(dE) = \int_B + \int_{A-AB} - \int_{B-AB} f(x) \mu(dE) = \int_B f(x) \mu(dE),$$

from which the result follows.

**15. Differentiation on a net.** Let  $E$  be a set containing at least one element, and  $\mu$  a measure in  $E$  with domain  $\mathfrak{F}$ , such that  $E \in \mathfrak{F}$  and  $\mu(E) = 1$ .

By a *partition of  $E$  with respect to  $\mu$*  we shall mean a partition  $E = \sum_p D_p$  of  $E$  into sets  $D_p \in \mathfrak{F}$ , for which  $\mu(D_p) > 0$ . These sets  $D_p$  are called the meshes of the partition. By a *net in  $E$  with respect to  $\mu$*  we shall mean a sequence of partitions  $E = \sum_p D_p^1, E = \sum_p D_p^2, \dots$  with respect to  $\mu$ , each of which is a sub-partition of the preceding one.

If we denote by  $\mathfrak{F}_n$  the  $\sigma$ -field consisting of all sums of meshes from the  $n^{\text{th}}$  partition  $E = \sum_p D_p^n$ , it is plain that the conditions  $\mathfrak{F}_1 \subseteq \mathfrak{F}_2 \subseteq \dots \subseteq \mathfrak{F}$  and  $E \in \mathfrak{F}_1$  of § 8 are satisfied. Moreover, since  $\mu(D_p^n) > 0$  for all meshes, it is plain that for any bounded, completely additive set-function  $\varphi$  defined on  $\mathfrak{F}$ , the contraction  $\varphi_n$  to  $\mathfrak{F}_n$  is  $\mu_n$ -continuous. Thus the first limit theorem is applicable. The  $\mu_n$ -integrable function  $f_n$  in this case is uniquely determined by



$$f_n(x) = \frac{\varphi(D_p^n)}{\mu(D_p^n)} \text{ for } x \in D_p^n.$$

The two functions  $\underline{f}$  and  $\bar{f}$  are called the *lower and upper derivatives of  $\varphi$  with respect to  $\mu$  on the net*.

**16. Density of a set with respect to a  $\sigma$ -field.** Let  $\mu$  be a fixed measure in  $E$  with domain  $\mathfrak{F}$ , such that  $E \in \mathfrak{F}$  and  $\mu(E) = 1$ , and let  $\mathfrak{H}$  be a  $\sigma$ -field contained in  $\mathfrak{F}$ . Let  $\nu$  denote the contraction of  $\mu$  to  $\mathfrak{H}$ .

For an arbitrary set  $A \in \mathfrak{F}$  the set-function  $\varphi$  on  $\mathfrak{F}$  defined by  $\varphi(B) = \mu(AB)$  is bounded, completely additive, and  $\mu$ -continuous. Its contraction  $\psi$  to  $\mathfrak{H}$  is therefore bounded, completely additive, and  $\nu$ -continuous, and is therefore the indefinite integral with respect to  $\nu$  of a  $\nu$ -integrable function  $f$ . By the *density* of  $A$  with respect to  $\mathfrak{H}$  (and the measure  $\mu$ ) we mean any such function  $f$ , i. e. any  $\nu$ -integrable function  $f$  with  $[f] = E$ , such that

$$\mu(AB) = \int_B f(x) \mu(dE) \text{ for any } B \in \mathfrak{H}.$$

Suppose now, as in § 8, that a sequence of  $\sigma$ -fields  $\mathfrak{F}_1 \subseteq \mathfrak{F}_2 \subseteq \dots$  contained in  $\mathfrak{F}$  is given, such that  $E \in \mathfrak{F}_1$ , and let  $\mathfrak{F}'$  denote the smallest  $\sigma$ -field containing  $\mathfrak{G} = \bigcup_n \mathfrak{F}_n$ . Let further  $A \in \mathfrak{F}$  be arbitrary. From the first limit theorem then follows:

Denoting by  $f_n$  the density of  $A$  with respect to  $\mathfrak{F}_n$  and by  $f'$  the density of  $A$  with respect to  $\mathfrak{F}'$  we have  $\mu(\lim_n f_n = f') = 1$ .

If to the set  $A$  there exists a set  $C \in \mathfrak{F}'$ , such that  $\mu(A \dot{+} C - AC) = 0$ , we have the more precise result, that  $\mu(\lim_n f_n = f) = 1$ , where  $f$  denotes the characteristic function of  $A$ .

This implies the following *nought-or-one-theorem*:

If for every  $n$  the density  $f_n$  of the set  $A$  with respect to  $\mathfrak{F}_n$  satisfies the relation  $\mu([f_n = k_n]) = 1$  for some number  $k_n$ , and there exists a set  $C \in \mathfrak{F}'$  such that  $\mu(A \dot{+} C - AC) = 0$ , then the measure of the set  $A$  is either 0 or 1.

We shall also give an independent proof of this theorem:

From the relation  $\mu(AB) = k_n \mu(B)$  for any  $B \in \mathfrak{F}_n$  we obtain, by placing  $B = E$ , the equality  $\mu(A) = k_n$ . Hence  $\mu(AB) = \mu(A)\mu(B)$  for any  $B \in \mathfrak{G}$ . By the extension theorem of § 4 the relation  $\mu(AB) = \mu(A)\mu(B)$  is then valid for any  $B \in \mathfrak{F}'$ . Choosing  $B$  such that  $\mu(A \dot{+} B - AB) = 0$ , we have  $\mu(AB) = \mu(A)$  and  $\mu(B) = \mu(A)$ . The relation therefore becomes  $\mu(A) = \mu(A)^2$ , which shows that  $\mu(A)$  is either 0 or 1.

**17. Second limit theorem.** Let  $E$  be a set containing at least one element, and  $\mu$  a measure in  $E$  with domain  $\mathfrak{F}$ , such that  $E \in \mathfrak{F}$  and  $\mu(E) = 1$ . Let now  $\mathfrak{F}_1 \supseteq \mathfrak{F}_2 \supseteq \dots$  be a decreasing sequence of  $\sigma$ -fields contained in  $\mathfrak{F}$ , such that  $E \in \mathfrak{F}_n$  for every  $n$ . The system  $\mathfrak{F}' = \bigcap_n \mathfrak{F}_n$  is a  $\sigma$ -field, and  $E \in \mathfrak{F}'$ .

The contraction of  $\mu$  to  $\mathfrak{F}_n$  is a measure, which will be denoted by  $\mu_n$ . Similarly the contraction of  $\mu$  to  $\mathfrak{F}'$  is a measure which will be denoted by  $\mu'$ .

We shall consider a  $\mu$ -integrable function  $f$  with  $[f] = E$ . Its indefinite integral

$$\varphi(A) = \int_A f(x) \mu(dE)$$

with respect to  $\mu$  is, by § 7, a bounded, completely additive and  $\mu$ -continuous set-function, in  $\mathfrak{F}$ . Since the contraction of  $\varphi$  to  $\mathfrak{F}_n$  is for every  $n$  a  $\mu_n$ -continuous set-function, there exists, by § 7, a  $\mu_n$ -integrable function  $f_n$ , such that

$$\int_A f_n(x) \mu(dE) = \varphi(A) \quad \text{for any } A \in \mathfrak{F}_n.$$

Similarly there exists a  $\mu'$ -integrable function  $f'$ , such that

$$\int_A f'(x) \mu(dE) = \varphi(A) \quad \text{for any } A \in \mathfrak{F}'.$$

The functions  $f_n$  and  $f'$  need not be uniquely determined. In the sequel  $f_n$  and  $f'$  will denote some such functions.

The second limit theorem now states:

*With the above notations we have the relation*

$$\mu([\lim_n f_n = f']) = 1.$$



To prove this it is sufficient to prove that  $\mu(\underline{f} < f') = 0$  and  $\mu(f' < \bar{f}) = 0$ , where

$$\underline{f} = \liminf_n f_n \quad \text{and} \quad \bar{f} = \limsup_n f_n.$$

For  $E - [\lim_n f_n = f'] \subseteq [\underline{f} < f'] \dot{+} [f' < \bar{f}]$ .

18. The proof will be based on the following lemma:

Placing  $H = [\inf_n f_n < h]$  and  $K = [\sup_n f_n > k]$  for arbitrary numbers  $h$  and  $k$ , we have for any  $C \in \mathfrak{F}'$  the inequalities

$$\varphi(HC) \leq h\mu(HC) \quad \text{and} \quad \varphi(KC) \geq k\mu(KC).$$

In order to prove the first inequality it is sufficient to prove, that if for an arbitrary  $n$  we put

$$H_n = [\min_{p \leq n} f_p < h],$$

we have  $\varphi(H_n C) \leq h\mu(H_n C)$  for any  $C \in \mathfrak{F}'$ . For  $H_1 \subseteq H_2 \subseteq \dots$  and  $H = \bigcup_n H_n$ . Hence  $\mu(HC) = \lim_n \mu(H_n C)$  and  $\varphi(HC) = \lim_n \varphi(H_n C)$ .

To prove the inequality  $\varphi(H_n C) \leq h\mu(H_n C)$  we put

$$H_{np} = \begin{cases} [f_p < h, f_{p+1} \geq h, \dots, f_n \geq h] & \text{for } p < n \\ [f_n < h] & \text{for } p = n. \end{cases}$$

Then  $H_{np} \in \mathfrak{F}'_p$  and  $H_{np} \subseteq [f_p < h]$ . Moreover  $H_n = \sum_{p \leq n} H_{np}$ . Since  $C \in \mathfrak{F}'_p$  for any  $p$ , this implies

$$\varphi(H_n C) = \sum_{p \leq n} \varphi(H_{np} C) = \sum_{p \leq n} \int_{H_{np} C} f_p(x) \mu(dE) \leq \sum_{p \leq n} h\mu(H_{np} C) = h\mu(H_n C).$$

The inequality  $\varphi(KC) \geq k\mu(KC)$  is proved analogously.

19. The proof of the theorem now runs as follows:

In order to prove that  $\mu(\underline{f} < f') = 0$  it is sufficient to prove that  $\mu(\underline{f} < h, f' > k) = 0$  for any pair of rational numbers  $h$

and  $k$  for which  $h < k$ . For  $[f < f'] = \mathfrak{S}[f < h, f' > k]$ , where the summation is with respect to all such pairs.

We now apply the inequality  $\varphi(HC) \leq h\mu(HC)$  to the set  $C = [f < h, f' > k]$ . Since  $f$  is  $\mu_n$ -measurable for all  $n$ , it is  $\mu'$ -measurable; hence  $C \in \mathfrak{F}'$ . As  $C \subseteq H$ , we obtain

$$\varphi(C) \leq h\mu(C).$$

On the other hand, since  $C \subseteq [f' > k]$ , we have

$$\varphi(C) \geq k\mu(C).$$

Since  $h < k$ , these two inequalities show that  $\mu(C) = 0$ .

The relation  $\mu([f' < \bar{f}]) = 0$  is proved analogously.

**20. Corollary of the second limit theorem.** If in particular  $\mu'$  only attains the values 0 and 1, i. e. if for any set  $A \in \mathfrak{F}'$  either  $\mu(A) = 0$  or  $\mu(A) = 1$ , we must have

$$\mu([f' = \int_E f(x) \mu(dE)]) = 1,$$

since otherwise one of the sets

$$[f > \int_E f(x) \mu(dE)] \quad \text{or} \quad [f' < \int_E f(x) \mu(dE)]$$

would have the measure 1, which is impossible, as

$$\int_E f'(x) \mu(dE) = \int_E f(x) \mu(dE).$$

By the second limit theorem we therefore in this case have

$$\mu([\lim_n f_n = \int_E f(x) \mu(dE)]) = 1.$$

**21. Approximation of a Lebesgue integral by Riemann sums.** Let  $E$  be the real axis  $-\infty < x < +\infty$ ,  $\mathfrak{F}$  the system of Lebesgue measurable sets  $A$  on  $E$  with period 1, and  $\mu(A)$  the measure of a period of  $A$ . Let  $\mathfrak{F}_n$  denote the system of Lebesgue measurable sets of period  $\frac{1}{2^n}$ . Then  $\mathfrak{F} \supseteq \mathfrak{F}_1 \supseteq \mathfrak{F}_2 \supseteq \dots$ , and



$E \in \mathfrak{F}_n$  for all  $n$ . The systems  $\mathfrak{F}, \mathfrak{F}_1, \mathfrak{F}_2, \dots$  are  $\sigma$ -fields. The  $\sigma$ -field  $\mathfrak{F}' = \mathfrak{D}\mathfrak{F}_n$  consists of all Lebesgue measurable sets having the period  $\frac{1}{2^n}$  for any  $n$ . Hence<sup>1</sup> for any  $A \in \mathfrak{F}'$  we have either  $\mu(A) = 0$  or  $\mu(A) = 1$ . The corollary of the second limit theorem is therefore applicable and leads to the following theorem:<sup>2</sup>

*If  $f(x)$  is a Lebesgue integrable function of period 1, then the sequence of functions*

$$f_n(x) = \frac{1}{2^n} \sum_{k=0}^{2^n-1} f\left(x + \frac{k}{2^n}\right)$$

*converges for almost all  $x$  towards the integral*

$$\int_0^1 f(x) dx.$$

**22. Product sets.** Let  $E_1, E_2, \dots$  denote a finite or infinite sequence of sets. By the finite or infinite *product*

$$E = (E_1, E_2, \dots)$$

we shall mean the set of all symbols

$$x = (x_1, x_2, \dots)$$

where  $x_n \in E_n$  for every  $n$ . The elements  $x_n$  are called the *coordinates* of  $x$ .

For every  $n$  except the last in case of a finite product we shall write

$$E'_n = (E_1, \dots, E_n) \quad \text{and} \quad E''_n = (E_{n+1}, E_{n+2}, \dots).$$

For an arbitrary element  $x = (x_1, x_2, \dots)$  of  $E$ , the corresponding elements

<sup>1</sup> By the well-known theorem, that a Lebesgue measurable set with arbitrarily small periods is either a null-set or the complement of a null-set. We mention that in case of the periods  $\frac{1}{2^n}$  this theorem is an easy consequence of the nought-or-one-theorem of § 16.

<sup>2</sup> Jessen [1].

$$x'_n = (x_1, \dots, x_n) \quad \text{and} \quad x''_n = (x_{n+1}, x_{n+2}, \dots)$$

of  $E'_n$  and  $E''_n$  are called the *projections* of  $x$  on  $E'_n$  and  $E''_n$ . We may write

$$E = (E'_n, E''_n) \quad \text{and} \quad x = (x'_n, x''_n).$$

If  $A'_n$  is a set in  $E'_n$ , the set  $(A'_n, E''_n)$  in  $E$  is called a *cylinder in  $E$  with base  $A'_n$  in  $E'_n$* ; it consists of all elements  $x \in E$  for which the projection  $x'_n$  on  $E'_n$  belongs to  $A'_n$ . Similarly, if  $A''_n$  is a set in  $E''_n$ , the set  $(E'_n, A''_n)$  is called a *cylinder in  $E$  with base  $A''_n$  in  $E''_n$* .

Suppose now that every  $E_n$  contains at least one element, and let  $\mathfrak{F}_n$  for every  $n$  be a field in  $E_n$  such that  $E_n \varepsilon \mathfrak{F}_n$ . A set  $A = (A_1, A_2, \dots)$  in  $E$ , where  $A_n \varepsilon \mathfrak{F}_n$  for every  $n$ , and  $A_n = E_n$  for all  $n$  from a certain stage in case of an infinite product, will be called a *simple set* in  $E$  with respect to the fields  $\mathfrak{F}_n$ . We notice that in case of an infinite product any simple set  $A$  is a cylinder with base in some  $E'_n$ .

The smallest field containing all simple sets will be denoted by

$$\mathfrak{F} = [\mathfrak{F}_1, \mathfrak{F}_2, \dots].$$

This field  $\mathfrak{F}$  consists of all sets in  $E$  which are a sum of a finite number of simple sets no two of which have elements in common. Hence, in case of an infinite product, any set in  $\mathfrak{F}$  is a cylinder with base in some  $E'_n$ .

The smallest  $\sigma$ -field containing all simple sets will be denoted by

$$\mathfrak{G} = (\mathfrak{F}_1, \mathfrak{F}_2, \dots).$$

On placing

$$\begin{aligned} \mathfrak{F}'_n &= [\mathfrak{F}_1, \dots, \mathfrak{F}_n], & \mathfrak{F}''_n &= [\mathfrak{F}_{n+1}, \mathfrak{F}_{n+2}, \dots], \\ \mathfrak{G}'_n &= (\mathfrak{F}_1, \dots, \mathfrak{F}_n), & \mathfrak{G}''_n &= (\mathfrak{F}_{n+1}, \mathfrak{F}_{n+2}, \dots), \end{aligned}$$

it is easily seen that

$$\mathfrak{F} = [\mathfrak{F}'_n, \mathfrak{F}''_n] \quad \text{and} \quad \mathfrak{G} = (\mathfrak{F}'_n, \mathfrak{F}''_n) = (\mathfrak{G}'_n, \mathfrak{G}''_n).$$

**23. Measure and integration in product sets.** Let  $\mu_n$  for every  $n$  be a content in  $E_n$  with domain  $\mathfrak{F}_n$ , such that  $E_n \varepsilon \mathfrak{F}_n$  and



$\mu_n(E_n) = 1$ . Then it is easily seen that there exists a unique content  $\mu$  in  $E = (E_1, E_2, \dots)$  with domain  $\mathfrak{F} = [\mathfrak{F}_1, \mathfrak{F}_2, \dots]$ , such that

$$\mu(A) = \mu_1(A_1)\mu_2(A_2)\cdots$$

for any simple set  $A = (A_1, A_2, \dots)$ . We notice that the factors of the product  $\mu_1(A_1)\mu_2(A_2)\cdots$  are 1 from a certain stage in case of an infinite product.

This content  $\mu$  will be denoted by

$$\mu = [\mu_1, \mu_2, \dots].$$

On placing

$$\mu'_n = [\mu_1, \dots, \mu_n] \quad \text{and} \quad \mu''_n = [\mu_{n+1}, \mu_{n+2}, \dots],$$

it is easily seen that

$$\mu = [\mu'_n, \mu''_n].$$

We shall now prove the following theorem:

*If the contents  $\mu_n$  are all completely additive, then the content  $\mu = [\mu_1, \mu_2, \dots]$  is also completely additive.*

By the criterion of §4 it is sufficient to prove that for any sequence  $A_1 \supseteq A_2 \supseteq \dots$  of sets  $A_m \in \mathfrak{F}$  for which  $\mu(A_m) \geq (\text{some}) k > 0$  for all  $m$ , there exists an element  $x^* = (x_1^*, x_2^*, \dots)$  of  $E$  which belongs to all  $A_m$ .

In the proof we shall use the relations

$$E''_n = (E_{n+1}, E''_{n+1}) \quad \text{and} \quad \mu''_n = [\mu_{n+1}, \mu''_{n+1}].$$

For an arbitrary set  $A$  in  $E$  and an arbitrary element  $x'_n = (x_1, \dots, x_n) \in E'_n$  we shall denote by  $A(x'_n) = A(x_1, \dots, x_n)$  the set of all elements  $x''_n \in E''_n$  for which  $x = (x'_n, x''_n)$  belongs to  $A$ .

We choose an arbitrary sequence of numbers

$$k > k_1 > k_2 > \dots > 0.$$

Corresponding to the relations  $E = (E_1, E''_1)$  and  $\mu = [\mu_1, \mu''_1]$  we begin by considering for every  $m$  the set  $B_m$  of all  $x_1 \in E_1$  for which

$$\mu''_1(A_m(x_1)) > k_1.$$

A simple consideration shows that

$$\mu_1(B_m) + k_1(1 - \mu_1(B_m)) \geq \mu(A_m) > k,$$

whence

$$\mu_1(B_m) > \frac{k - k_1}{1 - k_1}.$$

Since  $B_1 \supseteq B_2 \supseteq \dots$ , and  $\mu_1$  is completely additive, this implies the existence of an element  $x_1^* \in E_1$ , which belongs to all  $B_m$ . Thus for this  $x_1^*$  we have for all  $m$

$$\mu_1''(A_m(x_1^*)) > k_1.$$

Corresponding to the relations  $E_1'' = (E_2, E_2'')$  and  $\mu_1'' = [\mu_2, \mu_2'']$  we may now repeat the argument to the sets  $A_1(x_1^*) \supseteq A_2(x_1^*) \supseteq \dots$  in  $E_1''$ . This proves the existence of an element  $x_2^* \in E_2$ , such that

$$\mu_2''(A_m(x_1^*, x_2^*)) > k_2$$

for all  $m$ . Continuing in this manner we arrive at a sequence  $x_1^*, x_2^*, \dots$ , where  $x_n^* \in E_n$ , such that

$$\mu_n''(A_m(x_1^*, \dots, x_n^*)) > k_n$$

for every  $n$  and all  $m$ .

If the product  $E = (E_1, E_2, \dots)$  is infinite, the element  $x^* = (x_1^*, x_2^*, \dots)$  of  $E$  must belong to all  $A_m$ . For every  $A_m$  is a cylinder with base in some  $E_n'$ , and the set  $A_m(x_1^*, \dots, x_n^*)$  is not empty.

If the product  $E = (E_1, E_2, \dots)$  is finite, say  $E = (E_1, \dots, E_p)$ , the above procedure breaks off for  $n = p - 1$ , and the last relation becomes

$$\mu_p(A_m(x_1^*, \dots, x_{p-1}^*)) > k_{p-1}.$$

Since  $A_1(x_1^*, \dots, x_{p-1}^*) \supseteq A_2(x_1^*, \dots, x_{p-1}^*) \supseteq \dots$ , and  $\mu_p$  is completely additive, this implies the existence of an element  $x_p^* \in E_p$ , which belongs to all  $A_m(x_1^*, \dots, x_{p-1}^*)$ . The element  $x^* = (x_1^*, \dots, x_p^*)$  of  $E$  then belongs to all  $A_m$ .



**24.** The conditions of the previous theorem are in particular satisfied if the contents  $\mu_n$  are measures. Applying the extension theorem of § 4 we therefore obtain the following theorem:<sup>1</sup>

If  $E = (E_1, E_2, \dots)$ , and  $\mu_n$  is for every  $n$  a measure in  $E_n$  with domain  $\mathfrak{F}_n$ , for which  $E_n \in \mathfrak{F}_n$  and  $\mu_n(E_n) = 1$ , then there exists a unique measure  $\nu$  in  $E$  with domain  $\mathfrak{G} = (\mathfrak{F}_1, \mathfrak{F}_2, \dots)$ , such that

$$\nu(A) = \mu_1(A_1)\mu_2(A_2)\cdots$$

for any simple set  $A = (A_1, A_2, \dots)$ .

This measure  $\nu$  will be denoted by

$$\nu = (\mu_1, \mu_2, \dots).$$

On placing

$$\nu'_n = (\mu_1, \dots, \mu_n) \quad \text{and} \quad \nu''_n = (\mu_{n+1}, \mu_{n+2}, \dots)$$

it is easily seen that

$$\nu = (\nu'_n, \nu''_n).$$

**25.** Regarding integration in a product of two sets the usual theorem on repeated integration is valid. Applying this theorem to  $E = (E'_n, E''_n)$  and  $\nu = (\nu'_n, \nu''_n)$  we obtain the following results:

If  $f$  is a  $\nu$ -integrable function defined in  $E$ , then on placing

$$f'_n(x'_n) = \int_{E''_n} f(x'_n, x''_n) \nu''_n(dE''_n)$$

when the integral exists, we have  $[f'_n] \in \mathfrak{G}'_n$  and  $\mu'_n(E'_n - [f'_n]) = 0$ , and for every set  $A'_n \in \mathfrak{G}'_n$

$$\int_{(A'_n, E''_n)} f(x) \nu(dE) = \int_{[f'_n] A'_n} f'_n(x'_n) \nu'_n(dE'_n).$$

<sup>1</sup> Lomnicki and Ulam [1] have given an incomplete proof of this theorem (in the proof of lemma 4 the number  $N$  is chosen twice). The proof given here is taken from Jessen [2, article 4]. An analogous theorem on arbitrary measures in product sets has been given by Doob [1], but his proof seems incomplete (it is not seen how the sets  $\tilde{A}_n$  on p. 92 are chosen). The proof by Sparre Andersen of a more general theorem is incomplete (the relation  $\sup_n f_n^{(2)}(x_2) \leq 1$  on p. 21 needs not be valid).

Similarly, on placing

$$f''_n(x''_n) = \int_{E'_n} f(x'_n, x''_n) \nu'_n(dE'_n)$$

when the integral exists, we have  $[f''_n] \in \mathfrak{G}''_n$  and  $\mu''_n(E''_n - [f''_n]) = 0$ , and for every set  $A''_n \in \mathfrak{G}''_n$

$$\int_{(E'_n, A'_n)} f(x) \nu(dE) = \int_{[f''_n] A''_n} f''_n(x''_n) \nu''_n(dE''_n).$$

**26.** Let  $\mathfrak{G}^{n'}$  denote the system of all cylinders in  $E$  with a base in  $E'_n$  belonging to  $\mathfrak{G}'_n$ , i. e. the system of all sets  $(A'_n, E''_n)$ , where  $A'_n \in \mathfrak{G}'_n$ . Evidently  $\mathfrak{G}^{n'}$  is a  $\sigma$ -field,  $\mathfrak{G}^{1'} \subseteq \mathfrak{G}^{2'} \subseteq \dots$ , and  $\mathfrak{G}$  is the smallest  $\sigma$ -field containing all  $\mathfrak{G}^{n'}$ . Finally  $E \in \mathfrak{G}^{1'}$ .

Let  $f$  be a  $\nu$ -integrable function defined in  $E$ , and let

$$\varphi(A) = \int_A f(x) \nu(dE)$$

be its indefinite integral. Let  $f^{n'}$  denote the function  $f'_n$  introduced in § 25, considered as a function in  $E$  which is independent of  $x''_n$ . Then  $[f^{n'}] \in \mathfrak{G}^{n'}$  and  $\nu(E - [f^{n'}]) = 0$ , and for every set  $A \in \mathfrak{G}^{n'}$

$$\varphi(A) = \int_{[f^{n'}] A} f^{n'}(x) \nu(dE).$$

By the first limit theorem we therefore obtain the following result:<sup>1</sup>

*If  $f(x) = f(x_1, x_2, \dots)$  is a  $\nu$ -integrable function defined in  $E$ , then the sequence of integrals*

$$f^{n'}(x) = \int_{E''_n} f(x'_n, x''_n) \nu''_n(dE''_n)$$

*converges towards  $f(x)$  for all  $x$  outside a set  $N \in \mathfrak{G}$  with  $\nu(N) = 0$ .*

**27.** Let in particular  $f$  be the characteristic function of a set  $S \in \mathfrak{G}$  having the property, that any two elements  $x = (x_1, x_2, \dots)$

<sup>1</sup> This theorem, and the two which follow, have been stated without proof in Jessen and Wintner [1], where some applications are given. Proofs were given in Jessen [2, article 4].



and  $y = (y_1, y_2, \dots)$ , for which  $x_n = y_n$  for all  $n$  from a certain stage, either both belong to  $S$  or both do not belong to  $S$ . Then  $f$  is for every  $n$  actually independent of  $x'_n$ . The integral  $f^{n'}(x)$  is therefore in this case defined for all  $x$  and is a constant  $k_n$ .

The nought-or-one-theorem in § 16 therefore gives the following result:

*If  $S \in \mathfrak{G}$  is a set in  $E$ , such that any two elements  $x = (x_1, x_2, \dots)$  and  $y = (y_1, y_2, \dots)$ , for which  $x_n = y_n$  for all  $n$  from a certain stage, either both belong to  $S$  or both do not belong to  $S$ , then  $\nu(S)$  is either 0 or 1.*

28. Let  $\mathfrak{G}^{n''}$  denote the system of all cylinders in  $E$  with a base in  $E''_n$  belonging to  $\mathfrak{G}''_n$ , i. e. the system of all sets  $(E''_n, A''_n)$ , where  $A''_n \in \mathfrak{G}''_n$ . Then  $\mathfrak{G}^{1''} \supseteq \mathfrak{G}^{2''} \supseteq \dots$  is a decreasing sequence of  $\sigma$ -fields contained in  $\mathfrak{G}$ , and  $E \in \mathfrak{G}^{n''}$  for all  $n$ . The system  $\mathfrak{H} = \mathfrak{D} \mathfrak{G}^{n''}$  is the system of sets  $S \in \mathfrak{G}$ , which for every  $n$  is a cylinder with a base in  $E''_n$ , i. e. satisfying the condition of § 27. Thus  $\nu(S)$  is either 0 or 1 for any  $S \in \mathfrak{H}$ .

Let  $f$  be a  $\nu$ -integrable function defined in  $E$ , and let

$$\varphi(A) = \int_A f(x) \nu(dE)$$

be its indefinite integral. Let  $f^{n''}$  denote the function  $f''_n$  introduced in § 25, considered as a function in  $E$  which is independent of  $x'_n$ . Then  $[f^{n''}] \in \mathfrak{G}^{n''}$  and  $\nu(E - [f^{n''}]) = 0$ , and for every set  $A \in \mathfrak{G}^{n''}$

$$\varphi(A) = \int_{[f^{n''}]A} f^{n''}(x) \nu(dE).$$

By the corollary of the second limit theorem we therefore obtain the following result:

*If  $f(x) = f(x_1, x_2, \dots)$  is a  $\nu$ -integrable function defined in  $E$ , then the sequence of integrals*

$$f^{n''}(x) = \int_{E'_n} f(x'_n, x''_n) \nu'_n(dE'_n)$$

*converges towards*

$$\int_E f(x) \nu(dE)$$

for all  $x$  outside a set  $N \in \mathfrak{G}$  with  $\nu(N) = 0$ .

**29. Applications to the theory of probability.** Let  $E$  be a set containing at least one element. A measure  $\mu$  in  $E$  with domain  $\mathfrak{F}$ , for which  $E \in \mathfrak{F}$  and  $\mu(E) = 1$ , may also be called a *probability distribution* in  $E$ . The measure  $\mu(A)$  of a set  $A \in \mathfrak{F}$  is then called the *probability* of the *event*  $A$ . A  $\mu$ -measurable function  $f$  with  $[f] = E$  is called a *random variable*, and the integral

$$\mathfrak{M}(f) = \int_E f(x) \mu(dE),$$

when it exists, is called the *mean value* of  $f$ .

Besides  $E$  we shall now consider another set  $E^*$ . We suppose that to every  $x \in E$  is assigned a definite element  $x^* \in E^*$ . Let  $\mathfrak{G}^*$  be a  $\sigma$ -field in  $E^*$  such that  $E^* \in \mathfrak{G}^*$ . For every set  $A^* \in \mathfrak{G}^*$  we consider the set  $A$  of all elements  $x \in E$  for which  $x^*$  belongs to  $A^*$ . The system of all sets  $A \in \mathfrak{F}$  of this particular type will be denoted by  $\mathfrak{G}$ . As is easily proved,  $\mathfrak{G}$  is a  $\sigma$ -field, and  $E \in \mathfrak{G}$ . The contraction of  $\mu$  to  $\mathfrak{G}$  will be denoted by  $\nu$ .

Let now  $f$  be a random variable for which the mean value  $\mathfrak{M}(f)$  exists. Let

$$\varphi(A) = \int_A f(x) \mu(dE)$$

be its indefinite integral, and let  $g$  be some  $\nu$ -integrable function with  $[g] = E$ , for which

$$\varphi(A) = \int_A g(x) \mu(dE) \quad \text{for any } A \in \mathfrak{G}.$$

The function  $g$  evidently depends on  $x^*$  only, i. e. it has the same value for any two elements  $x \in E$  with the same corresponding element  $x^* \in E^*$ . We call  $g(x)$  the *conditional mean value of  $f$  by known  $x^*$* , taken with respect to the  $\sigma$ -field  $\mathfrak{G}^*$ , and shall use the notation

$$g(x) = \mathfrak{M}_{x^*}^*(f).^1$$

<sup>1</sup> If for  $\mathfrak{G}^*$  we take the system of all sets in  $E^*$ , the conditional mean value is that defined by Kolmogoroff [1, chap. V]. The modification here adopted is necessary for the results of §§ 33–34.



From the definition of  $g$  it follows, that

$$\mathfrak{M}(g) = \mathfrak{M}(\mathfrak{M}_{x^*}(f)) = \mathfrak{M}(f).$$

When  $f$  is the characteristic function of a set  $A \in \mathfrak{F}$ , the conditional mean value  $\mathfrak{M}_{x^*}(f)$  is also called the *conditional probability* of  $A$  by known  $x^*$ , taken with respect to  $\mathfrak{G}^*$ .

**30.** Let  $\mathfrak{G}_1 \subseteq \mathfrak{G}_2 \subseteq \dots$  be an arbitrary increasing sequence of  $\sigma$ -fields in  $E^*$ , such that  $E^* \in \mathfrak{G}_1^*$ , and let  $\mathfrak{G}^*$  be the smallest  $\sigma$ -field containing  $\bigcup_n \mathfrak{G}_n^*$ . Let  $\mathfrak{G}_1, \mathfrak{G}_2, \dots$ , and  $\mathfrak{G}$ , be the corresponding  $\sigma$ -fields in  $E$ . Clearly  $\mathfrak{G}_1 \subseteq \mathfrak{G}_2 \subseteq \dots \subseteq \mathfrak{G}$ . Assuming that for every set  $A^* \in \mathfrak{G}^*$  the corresponding set  $A$  in  $E$  belongs to  $\mathfrak{F}$  we shall now prove that  $\mathfrak{G}$  is the smallest  $\sigma$ -field containing  $\bigcup_n \mathfrak{G}_n$ .

Let for the moment this smallest  $\sigma$ -field be denoted by  $\mathfrak{G}'$ , and let  $\mathfrak{H}^*$  be the system of sets  $A^*$  in  $E^*$ , for which the corresponding set  $A$  in  $E$  belongs to  $\mathfrak{G}'$ . From the mere fact that  $\mathfrak{G}'$  is a  $\sigma$ -field, follows easily that  $\mathfrak{H}^*$  is a  $\sigma$ -field. Moreover, by our assumption every  $\mathfrak{G}_n^* \subseteq \mathfrak{H}^*$ . Hence  $\mathfrak{G}^* \subseteq \mathfrak{H}^*$ . Thus for every set  $A^* \in \mathfrak{G}^*$  the corresponding set  $A$  in  $E$  belongs to  $\mathfrak{G}'$ , i. e.  $\mathfrak{G} \subseteq \mathfrak{G}'$ , and hence  $\mathfrak{G} = \mathfrak{G}'$ .

**31.** Next, let  $\mathfrak{G}_1^* \supseteq \mathfrak{G}_2^* \supseteq \dots$  be an arbitrary decreasing sequence of  $\sigma$ -fields in  $E^*$ , such that  $E^* \in \mathfrak{G}_n^*$  for all  $n$ . Then  $\mathfrak{G}^* = \bigcap_n \mathfrak{G}_n^*$  is also a  $\sigma$ -field, and  $E^* \in \mathfrak{G}^*$ . Let  $\mathfrak{G}_1, \mathfrak{G}_2, \dots$ , and  $\mathfrak{G}$ , be the corresponding  $\sigma$ -fields in  $E$ . Clearly  $\mathfrak{G}_1 \supseteq \mathfrak{G}_2 \supseteq \dots \supseteq \mathfrak{G}$ . We shall now prove that  $\mathfrak{G} = \bigcap_n \mathfrak{G}_n$ .

To see this, we have to prove that any set  $A \in \bigcap_n \mathfrak{G}_n$  corresponds to some  $A^* \in \mathfrak{G}^*$ . Since  $A \in \mathfrak{G}_n$ , it corresponds to a set  $A_n^* \in \mathfrak{G}_n^*$ . These sets  $A_n^*$  will differ only by elements  $x^*$  which do not correspond to any  $x$ . Hence any set  $A^*$  in  $E^*$  for which  $\bigcap_n A_n^* \subseteq A^* \subseteq \bigcup_n A_n^*$  will have  $A$  as its corresponding set. Let us take  $A^* = \limsup_n A_n^* = \bigcap_p \bigcup_{n \geq p} A_{n+p}^*$ . For every  $m$  we have  $A_n^* \in \mathfrak{G}_m^*$  for  $n \geq m$ . Hence  $A^* \in \mathfrak{G}_m^*$  for all  $m$ , i. e.  $A^* \in \mathfrak{G}^*$ .

**32.** Let us now consider a finite or infinite sequence of random variables  $g_1, g_2, \dots$ , and let  $E^*$  be the space  $(R_1, R_2, \dots)$ ,

where each  $R_n$  is the real axis  $-\infty \leq x_n \leq +\infty$ . To every  $x \in E$ , let us assign the point

$$x^* = (g_1(x), g_2(x), \dots)$$

of  $E^*$ . Let  $\mathfrak{G}^*$  denote the system of Borel sets in  $E^*$ , i. e. the smallest  $\sigma$ -field containing all sets  $x_n \leq a_n$ . The corresponding  $\sigma$ -field  $\mathfrak{G}$  in  $E$  will then be denoted by  $\mathfrak{G}_{g_1, g_2, \dots}$ , and the corresponding conditional mean value  $\mathfrak{M}_{x^*}(f)$  will be called the *conditional mean value of  $f$  by known values of  $g_1, g_2, \dots$* , and will be denoted by

$$\mathfrak{M}_{g_1, g_2, \dots}(f).$$

If  $f$  is the characteristic function of a set  $A \in \mathfrak{F}$ , the conditional mean value  $\mathfrak{M}_{g_1, g_2, \dots}(f)$  is also called the conditional probability of  $A$  by known values of  $g_1, g_2, \dots$ .

§3. Let us now suppose that the sequence  $g_1, g_2, \dots$  is infinite. Let  $\mathfrak{G}_n^*$  for every  $n$  denote the system of Borel sets in  $E^*$ , which are cylinders with base in  $(R_1, \dots, R_n)$ . The bases of these sets being just all Borel sets in  $(R_1, \dots, R_n)$ , the  $\sigma$ -field in  $E$  corresponding to  $\mathfrak{G}_n^*$  will be  $\mathfrak{F}_{g_1, \dots, g_n}$ .

Now  $\mathfrak{G}_1^* \subseteq \mathfrak{G}_2^* \subseteq \dots$ , and  $\mathfrak{G}^*$  is the smallest  $\sigma$ -field containing  $\mathfrak{G}_n^*$ ; moreover, it is easily seen that for every set  $A \in \mathfrak{G}^*$  the corresponding set  $A$  in  $E$  belongs to  $\mathfrak{F}$ . Hence by § 30 we have  $\mathfrak{F}_{g_1} \subseteq \mathfrak{F}_{g_1, g_2} \subseteq \dots$ , and  $\mathfrak{F}_{g_1, g_2, \dots}$  is the smallest  $\sigma$ -field containing  $\mathfrak{F}_{g_1, \dots, g_n}$ . The first limit theorem is therefore applicable and yields the following result:

*The conditional mean value  $\mathfrak{M}_{g_1, \dots, g_n}(f)$  of  $f$  by known values of  $g_1, \dots, g_n$  converges for  $n \rightarrow \infty$  with the probability 1 towards the conditional mean value  $\mathfrak{M}_{g_1, g_2, \dots}(f)$  of  $f$  by known values of  $g_1, g_2, \dots$ .*

When  $f$  is the characteristic function of a set  $A \in \mathfrak{F}$ , the theorem becomes a theorem on conditional probabilities. If in particular  $A \in \mathfrak{F}_{g_1, g_2, \dots}$ , the theorem shows that the conditional probability of  $A$  by given values of  $g_1, \dots, g_n$  converges for  $n \rightarrow \infty$  with the probability 1 towards 1 in  $A$  and 0 in  $E - A$ .<sup>1</sup>

<sup>1</sup> Lévy [1, pp. 128—130].



34. Still assuming the sequence  $g_1, g_2, \dots$  to be infinite, let us now by  $\mathfrak{G}_n^*$  denote the system of Borel sets in  $E^*$ , which are cylinders with base in  $(R_{n+1}, R_{n+2}, \dots)$ . The bases of these sets being just all Borel sets in  $(R_{n+1}, R_{n+2}, \dots)$ , the  $\sigma$ -field in  $E$  corresponding to  $\mathfrak{G}_n^*$  will be  $\mathfrak{F}_{g_{n+1}, g_{n+2}, \dots}$ .

We have  $\mathfrak{G}_1^* \supseteq \mathfrak{G}_2^* \supseteq \dots$ . Let us put  $\mathfrak{G}^* = \bigcap_n \mathfrak{G}_n^*$ . Then  $\mathfrak{G}^*$  is the system of Borel sets  $A^*$  in  $E^*$  with the property that two points  $x^* = (x_1, x_2, \dots)$  and  $y^* = (y_1, y_2, \dots)$ , for which  $x_n = y_n$  for all  $n$  from a certain stage, either both belong to  $A^*$  or both do not belong to  $A^*$ .

The class of all sequences obtained from a given sequence  $x_1, x_2, \dots$  by changing only a finite number of elements will briefly be called an *end*, and will be denoted by  $\{x_1, x_2, \dots\}$ . The  $\sigma$ -field  $\mathfrak{G}$  in  $E$  corresponding to the above  $\sigma$ -field  $\mathfrak{G}^* = \bigcap_n \mathfrak{G}_n^*$  will be denoted by  $\mathfrak{F}_{\{g_1, g_2, \dots\}}$ , and the corresponding conditional mean value  $\mathfrak{M}_{x^*}(f)$  will be called the *conditional mean value of  $f$  by known end of the sequence  $g_1, g_2, \dots$* , and will be denoted by

$$\mathfrak{M}_{\{g_1, g_2, \dots\}}(f).$$

From § 31 it follows that  $\mathfrak{F}_{g_1, g_2, \dots} \supseteq \mathfrak{F}_{g_2, g_3, \dots} \supseteq \dots$ , and that  $\mathfrak{F}_{\{g_1, g_2, \dots\}} = \bigcap_n \mathfrak{F}_{g_{n+1}, g_{n+2}, \dots}$ . The second limit theorem is therefore applicable and yields the following result:

*The conditional mean value  $\mathfrak{M}_{g_{n+1}, g_{n+2}, \dots}(f)$  of  $f$  by known values of  $g_{n+1}, g_{n+2}, \dots$  converges for  $n \rightarrow \infty$  with the probability 1 towards the conditional mean value  $\mathfrak{M}_{\{g_1, g_2, \dots\}}(f)$  of  $f$  by known end of the sequence  $g_1, g_2, \dots$ .*

The corollary of the second limit theorem shows that if the probability of any event  $A \in \mathfrak{F}_{\{g_1, g_2, \dots\}}$  is either 0 or 1, then the conditional mean value  $\mathfrak{M}_{g_{n+1}, g_{n+2}, \dots}(f)$  converges for  $n \rightarrow \infty$  with the probability 1 towards the mean value  $\mathfrak{M}(f)$ . In particular, this will be so when the probability of any event  $A$  whatsoever with the property, that two elements  $x$  and  $y$  for which  $g_n(x) = g_n(y)$  for all  $n$  from a certain stage, either both belong to  $A$  or both do not belong to  $A$ , is either 0 or 1.

### References.

- E. Sparre Andersen. [1] Indhold og Maal i Produktmængder. Mat. Tidsskr. B 1944, pp. 19—23.
- J. L. Doob. [1] Stochastic processes with an integral-valued parameter. Trans. Amer. Math. Soc. 44 (1938), pp. 87—150.
- B. Jessen. [1] On the approximation of Lebesgue integrals by Riemann sums. Ann. of Math. 35 (1934), pp. 248—251.
- [2] Abstrakt Maal- og Integralteori 1—10. Mat. Tidsskr. B 1934—1947. In particular articles 1—4, 1934, pp. 73—84, 1935, pp. 60—74, 1938, pp. 13—26, 1939, pp. 7—21.
- B. Jessen and A. Wintner. [1] Distribution functions and the Riemann zeta function. Trans. Amer. Math. Soc. 38 (1935), pp. 48—88.
- A. Kolmogoroff. [1] Grundbegriffe der Wahrscheinlichkeitsrechnung. Berlin 1933.
- P. Lévy. [1] Théorie de l'addition des variables aléatoires. Paris 1937.
- Z. Łomnicki and S. Ulam. [1] Sur la théorie de la mesure dans les espaces combinatoires et son application au calcul des probabilités I. Variables indépendantes. Fund. Math. 23 (1934), pp. 237—278.
- S. Saks. [1] Theory of the integral. Second edition. Warszawa—Lwów 1937.





# PYRENSTUDIEN

III.

AMINOPYREN

IV.

ALKYLIERUNG DES PYRENS

VON

HAKON LUND UND ARNE BERG



KØBENHAVN

I KOMMISSION HOS EJNAR MUNKSGAARD

1946



Printed in Denmark.  
Bianco Lunos Bogtrykkeri A/S

## PYRENSTUDIEN III

### Aminopyren.

In Fortsetzung dieser Reihe<sup>1)</sup> soll hier über Aminopyren und seine Reaktionen berichtet werden.

3-Aminopyren wird zweckmässig nach der Vorschrift Ann. 531, 109 oder bei katalytischer Hydrierung mit Platindioxyd als Katalysator dargestellt. Nach der ersten Methode erhält man immer das Amin mit grünlicher oder braunlicher Farbe. Am besten wird es bei Destillation im Ölpumpenvakuum (etwa 0,2 mm Hg) gereinigt, wobei man es mit rein schwefelgelber Farbe erhält.

Über die Eigenschaften des Aminopyrens liegen im Schrifttum nur wenige Angaben vor. In der schon oft zitierten Arbeit von VOLLMANN, BECKER, CORELL und STREECK<sup>2)</sup> ist das Acetylaminopyren beschrieben, und es wird mitgeteilt, dass das diazotierte Amin mit Kaliumkuprocyanid in schlechter Ausbeute Cyanpyren liefert. Ferner haben diese Autoren beim Erhitzen von Pyrenylammonium-hydrosulfat 3-Aminopyren-4-sulfonsäure erhalten, und endlich wird angegeben, dass aus Acetylaminopyren beim Nitrieren in Eisessig ein Gemisch von 8- und 10-Nitro-acetylaminopyren entsteht. Aus der Patentliteratur entnimmt man, dass einige Halogenderivate des Aminopyrens dargestellt und getrennt worden sind.

Wir haben zuerst die Alkylierung des Aminopyrens untersucht. Methylbromid und -jodid und Äthylbromid addieren sich ohne Schwierigkeit zum Amin und bilden die im betreffenden Alkohol schwerlöslichen Ammoniumsalze. Keine Dialkylierung scheint dabei aufzutreten. Das Dimethylaminopyren entsteht aber glatt bei der Einwirkung von Methyljodid auf das sekundäre,

<sup>1)</sup> II. Mitt.: D. Kgl. Danske Vidensk. Selskab, Math.-fys. Medd. XXI, 5 (1941).

<sup>2)</sup> Ann. 531, 1 (1937).



freie Amin, während die Äthylierung von Monoäthylaminopyren auf Schwierigkeiten stösst.

Es ist bemerkenswert, dass Dimethylaminopyren sich — im Gegensatz zum Dimethylanilin — mit Benzaldehyd beim Erhitzen mit Zinkchlorid nicht kondensieren lässt. Auch das Verhalten des tertiärenamins gegen salpetrige Säure ist eigentümlich: Es konnte kein Nitroso-, sondern nur ein Nitrodimethylaminopyren erhalten werden. Aus den vergeblichen Versuchen, das erhaltene Produkt in verschiedene Fraktionen zu trennen, glauben wir schliessen zu können, dass eine einheitliche Nitroverbindung entstanden ist. Die Stellung der Nitrogruppe hat sich noch nicht feststellen lassen.

Die nitrierende Wirkung der salpetrigen Säure auf Pyrenabkömmlinge ist im Falle vom 3,8-Dimethoxyphenylpyren beobachtet worden<sup>1)</sup>.

Aminopyren kondensiert sich in normaler Weise mit Aldehyden zu Schiff'schen Basen und setzt sich mit Harnstoff leicht unter Bildung von Dipyrenylharnstoff um. Dagegen konnte eine Bildung von Mono-pyrenylharnstoff nicht festgestellt werden. — Mit Schwefelkohlenstoff in alkalisch-alkoholischer Lösung bildet Aminopyren Dipyrenylthioharnstoff.

Die Diazotierung des Aminopyrens bot einige Schwierigkeiten, konnte aber zuletzt unter bestimmten Bedingungen mit guter Ausbeute durchgeführt werden. Die Salze des Aminopyrens sind in Wasser schwerlöslich und müssen deshalb in feinverteilter Form suspendiert werden. Bei der Diazotierung in salzsaurer Lösung entsteht, wenn die korrekten Reaktionsbedingungen nicht eingehalten werden, in beträchtlicher Menge ein dunkelbraunes Harz. In salpetersaurer Lösung tritt Nitrierung des Amins störend auf. In schwefelsaurer Lösung verläuft die Diazotierung in befriedigender Weise, allerdings unter Ausscheidung des ziemlich schwerlöslichen Diazoniumsulfats.

Kuppelung mit Phenole und Amine liefert in guten Ausbeuten Azofarbstoffe, ein Beweis dafür, dass die Diazotierung ziemlich vollständig verlaufen ist. Trotzdem erhält man immer bescheidene Ausbeuten bei den Substitutionsreaktionen nach der allgemeinen Gleichung  $C_{16}H_9N_2^+ + X^- = C_{16}H_9X + N_2$ . Am besten gelingt die Substitution mit Jod, wobei die Ausbeute etwa 35

<sup>1)</sup> Ann. 531, 99.

Prozent d. Th. erreicht hat. Rhodanpyren konnte in einer Ausbeute von 15 Proz. und Chlorpyren bis zu 18 Proz. gewonnen werden, während Cyanpyren nur in winzigen Mengen isoliert werden konnte trotz vielfacher Abänderungen der Versuchsbedingungen. Dagegen verläuft die Reduktion mit Alkohol zu Pyren ganz glatt.

Eine Sonderstellung nimmt die Substitution der Diazoniumgruppe durch Fluor mittels des Borfluoridsalzes ein, wo die Ausbeute bei zweckmässiger Arbeitsweise sehr befriedigend wird.

Einige Versuche, Pyrenyldiazoniumsalze zu Pyrenylhydrazin zu reduzieren, scheiterten.

Bei längerem Stehen einer Eisessiglösung von Pyren in einem offenen Gefäss unterliegt das Aminopyren einer Oxydation durch den Sauerstoff der Atmosphäre. Die Lösung wird schmutzig braungrün gefärbt, und es scheidet sich nach und nach ein schwarzer Körper aus, der in den meisten Lösungsmitteln sehr schwer löslich ist. In Nitrobenzol löst er sich ein wenig. Die Analyse stimmt annäherungsweise mit der Formel  $C_{32}H_{18}ON_2$ , und es liegt wahrscheinlich ein Pyrenchinonimidderivat vor. Wir vermuten, dass es sich um einen mit der Anilinschwarzbildung analogen Oxydationsvorgang handelt. Der Körper — oder das Gemisch von Körpern — wurde nicht näher untersucht.

Dem Carlsbergfond danken wir bestens für die Unterstützung der Arbeit.

---



## VERSUCHSTEIL

### I. Methylierungsprodukte des Aminopyrens.

#### 1. Methylaminopyren, $C_{16}H_9 \cdot NHCH_3$ .

10 g Aminopyren und 8,5 g Methyljodid werden in 100 ml Methanol 2 Stunden unter Rückfluss gekocht. Das ausgeschiedene Salz kann aus Alkohol umkristallisiert werden. Nach Zersetzung mit Ammoniak oder Natronlauge wird das Amin in Äther aufgenommen und nach Verjagen des Äthers aus Benzin kristallisiert. Methylaminopyren bildet schwach gelbliche Nadeln, die bei 82-83° schmelzen. Ausbeute 8 g.

Analyse. Gef. C, 88,3; H, 5,63; N, 6,06%.

$C_{17}H_{13}N$ , ber. C, 88,6; H, 5,63; N, 5,94%.

#### 2. Dimethylaminopyren, $C_{16}H_9 \cdot N(CH_3)_2$ .

15 g Aminopyren und 12,5 g Methyljodid werden in 100 ml Alkohol eine Stunde unter Rückfluss gekocht, worauf eine Lösung von 1,6 g Natrium in etwas Alkohol zugefügt wird. Das Gemisch wird abgekühlt, mit 12,5 g Methyljodid versetzt und 1,5 Stunden wieder am Rückflusskühler erwärmt. Nach Erkalten wird abgesaugt. Die Mutterlauge gibt bei nochmaliger Behandlung mit Methyljodid einige Gramm. Gesamtausbeute 24 g Pyrenyldimethylammoniumjodid.

Die Reaktion gelingt mit derselben Ausbeute, wenn Methyljodid durch Methylbromid ersetzt wird; nur muss natürlich das Erhitzen in einer Druckflasche stattfinden.

Das mit Ammoniak freigemachte und in Äther aufgenommene Amin wird mit Essigsäureanhydrid eine halbe Stunde auf dem Wasserbade erwärmt zur Entfernung einer kleinen Menge von

Monomethylaminopyren und dann mit Wasser gekocht. Nach Zusatz von Natriumhydroxyd zu alkalischer Reaktion wird wieder in Äther aufgenommen. Das Amin wird im Vakuum bei etwa  $1/2$  mm Druck destilliert, Sp.  $205^\circ$ , Ausbeute 12 g.

Das erhaltene Öl kristallisiert langsam und schmilzt dann bei  $31^\circ$ .

Analyse. Gef. C, 88,5; H, 6,12; N, 5,71%.

$C_{18}H_{15}N$ , ber. C, 88,13; H, 6,16; N, 5,71%.

Dimethylaminopyren ist in heisser, verdünnter Salzsäure ziemlich leicht löslich; beim Erkalten kristallisiert das Hydrochlorid aus, Schmp.  $231-32^\circ$  u. Zers.

### 3. Nitro-dimethylaminopyren, $C_{16}H_8$ $\begin{matrix} \diagup NO_2 \\ \diagdown N(CH_3)_2 \end{matrix}$

Zu einer Lösung von Dimethylaminopyren in Eisessig wird gepulvertes Natriumnitrit (2 Mol) in kleinen Portionen unter Rühren gegeben. Es scheidet sich sofort ein roter Niederschlag aus. Wenn nur 1 Mol  $NaNO_2$  zugegeben wird, bildet sich dasselbe Produkt, nur in geringerer Menge. Die Kristalle lösen sich leicht in Benzol und können daraus mit Benzin gefällt werden. Nach Umkristallisieren aus Alkohol (die Kristallisation dauert mehrere Tage) schmilzt die Substanz bei  $126-27^\circ$ .

Analyse. Gef. N, 9,79; 9,71%.

$C_{18}H_{14}O_2N_2$ , ber. 9,67%.

Titrierung der Verbindung mit Titanichlorid bestätigte, dass eine Nitro- und keine Nitrosoverbindung vorlag: 1 Mol  $TiCl_3$  entsprach 49 g des Körpers. Für Nitroso-dimethylaminopyren berechnet sich 68,5 g, für Nitro 48,3 g.

Die Benzollösung des Körpers ist gelb mit leuchtend orange-farbiger Fluoreszens. Die Lösung in Benzin fluoresziert grün, in Äther orange.

Um die Stellung der Nitrogruppe zu bestimmen, wurde die Darstellung des Nitro-dimethylaminopyrens in anderer Weise versucht. Aus Formylaminopyren wurde bei Nitrierung in Eisessiglösung 8-Nitro-formylaminopyren gewonnen und zum Amin



hydrolysiert. Es gelang aber nicht, dieses Nitroamin zu methylieren.

Formylaminopyren wird leicht folgendermassen dargestellt: 20 g Aminopyren werden in 200 ml konz. Ameisensäure bei etwa 60° gelöst und bei dieser Temperatur eine Stunde gehalten. Schon nach 10-15 Minuten beginnt die Ausscheidung der Formylverbindung. Aus Eisessig umkristallisiert schmilzt sie bei 228°. Ausbeute 20 g.

Analyse. Gef. C, 83,5; H, 4,20; N, 5,75 %.  
 $C_{17}H_{11}ON$ , ber. C, 83,3; H, 4,10; N, 5,71 %.

Formylaminopyren, in etwa 60 Teilen Eisessig bei 60° gelöst und mit der berechneten Menge konz. Salpetersäure nitriert, liefert eine Nitroverbindung, die bei einige Stunden langem Kochen mit verdünnter Salzsäure (1:3) Nitroaminopyren ergab. Das Produkt wurde in Benzol gelöst und mit Benzin fraktioniert gefällt. Alle Fraktionen zeigten denselben Schmelzpunkt, 183-85°.

Analyse. Gef. C, 73,3; H, 4,06; N, 10,6 %.  
 $C_{16}H_{10}O_2N_2$ , ber. C, 73,3; H, 3,83; N, 10,6 %.

Mit NaSH reduziert lieferte das Nitroamin 3,8-Diaminopyren, Schmp. 230° unkor. In Ann. 531, 122 wird 232° angegeben. Es lag somit 3,8-Nitroaminopyren vor.

Es wurde weiter versucht, das Nitro-dimethylaminopyren mittels Natronlauge zu spalten, in der Hoffnung, Dimethylamin und ein Nitro-oxypyren zu erhalten. Dimethylamin konnte überhaupt nicht nachgewiesen werden, und das Nitroamin wurde in einen schwarzen Teer verwandelt.

Endlich wurde das Nitro-dimethylamin mit starker Jodwasserstoffsäure gekocht in der Hoffnung, die zwei Methylgruppen abspalten zu können. Auch hier entstand nur ein Teer.

Es ist wohl anzunehmen, dass 8-Nitro-3-dimethylaminopyren vorliegt, es fehlt aber noch ein Beweis dafür.

Bei der Behandlung von Dimethylaminopyren in Eisessig mit Salpetersäure konnte keine Mononitroverbindung erhalten werden; es entstand ein nicht näher untersuchtes Dinitro-dimethylaminopyren.

## II. Kondensationen mit Aminopyren.

### 1. Benzalaminopyren, $C_{16}H_9N=CH$ . $C_6H_5$

Eine Lösung von 2 g Aminopyren und 1,1 g Benzaldehyd in 20 ml Alkohol wird 40 Minuten auf dem Wasserbade erwärmt. Beim Erkalten scheidet sich ein bald erstarrendes Öl aus. Aus Benzin gelbe Kristalle, die bei  $122-23^\circ$  schmelzen.

Analyse. Gef. C, 90,7; H, 4,98; N, 4,80%.

$C_{23}H_{15}N$ , ber. C, 90,5; H, 4,96; N, 4,60%.

### 2. Pyrenalaminopyren, $C_{16}H_9N=CH$ . $C_{16}H_9$ .

Bei 4-stündigem Erwärmen von 1,5 g Aminopyren und 1,6 g Pyrenaldehyd in 50 ml Alkohol erhielt man 2,7 g rote Kristalle. Schwerlöslich in allen Lösungsmitteln. Die Kristalle sintern bei etwa  $250^\circ$  und schmelzen bei  $273-75^\circ$ .

Analyse. Gef. C, 92,0; H, 4,60; N, 3,29%.

$C_{33}H_{19}N$ , ber. C, 92,3; H, 4,43; N, 3,26%.

### 3. Versuche, Aminopyren mit Nitrosoverbindungen zu kondensieren.

Es wurde versucht, Aminopyren mit Nitrosopyren zu kondensieren, in der Hoffnung, Azopyren zu erhalten, jedoch ohne Erfolg. Erhitzen der zwei Substanzen in Eisessiglösung ergab einen unkristallisierbaren Teer. In Alkohol im Gegenwart von Calcium- oder Zinkchlorid entstand etwas Azoxypyren, aus dem Nitrosopyren gebildet.

Auch Nitrosodimethylanilin lässt sich nicht mit Aminopyren zu einer Azoverbindung kondensieren. Zwar entstand ein neuer Körper mit dem Schmelzpunkt  $92^\circ$  in Gestalt blauvioletter, schimmernder Kristalle; aber eine genauere Untersuchung zeigte, dass es sich um eine Molekülverbindung von 1 Mol Amin mit zwei Mol Nitrosodimethylanilin handelte: Eine kryoskopische Messung in Benzol ergab ein Molekulargewicht um etwa 170. Die Azoverbindung würde das Molekulargewicht 349 besitzen, während die genannte Molekülverbindung in dissoziiertem Zustand 176



entspricht. Die Zusammensetzung stimmt vollkommen mit der angegebenen Formel.

Analyse. Gef. C, 74,6; H, 6,19; N, 13,4<sup>0</sup>/<sub>0</sub>.  
 $C_{32}H_{31}O_2N_5$ , ber. C, 74,3; H, 6,00; N, 13,5<sup>0</sup>/<sub>0</sub>.

#### 4. Dipyrenylharnstoff, CO (C<sub>16</sub>H<sub>9</sub>NH)<sub>2</sub>.

3 g Aminopyren und 1 g Harnstoff werden in 20 ml Eisessig einige Stunden zum Sieden erhitzt. Die anfangs gelbe Lösung wird bald grün, und es bildet sich ein Niederschlag. Wenn dieser sich nicht mehr vermehrt, wird heiss filtriert und mit Alkohol gewaschen. Ausbeute 1,8 g. Gelbgrüne, sehr lichtempfindliche Kristalle, die bei 355° unkorrr. im vorher erhitzten Bade schmelzen. Die Substanz ist in allen gewöhnlichen Lösungsmitteln unlöslich.

Analyse. Gef. C, 86,6; H, 4,32; N, 6,18<sup>0</sup>/<sub>0</sub>.  
 $C_{33}H_{20}ON_2$ , ber. C, 86,1; H, 4,35; N, 6,09<sup>0</sup>/<sub>0</sub>.

Auch wenn Aminopyren mit einem grossen Überschuss an Harnstoff erhitzt wird, entsteht scheinbar nur Dipyrenylharnstoff.

#### 5. Dipyrenyl-thioharnstoff, CS (C<sub>16</sub>H<sub>9</sub>NH)<sub>2</sub>.

Zu 5 g Aminopyren, in Schwefelkohlenstoff gelöst, wird eine Lösung von 1 g Kaliumhydroxyd in 10 ml Alkohol gegeben. Der Kolben wird verschlossen 3-4 Tage im Dunkeln stehen gelassen. Es hat sich dann ein gelbes Pulver, etwa 4 g, abgeschieden, das nach Waschen mit Alkohol bei 219-20° schmilzt und in allen gewöhnlichen Lösungsmitteln schwerlöslich ist. Auch diese Substanz ist lichtempfindlich. Beim Kochen mit Merkurioxyd in Alkohol wird Merkurisulfid gebildet.

Analyse. Gef. N, 5,88; S, 6,74<sup>0</sup>/<sub>0</sub>.  
 $C_{33}H_{20}SN_2$ , ber. N, 5,87; S, 6,82<sup>0</sup>/<sub>0</sub>.

### III. Pyrenyldiazoniumreaktionen.

#### 1. Diazotieren des Aminopyrens.

Eine feindisperse Suspension von Aminopyrensalz erhält man beim Eingiessen einer Lösung desamins in wenig Eisessig in eine wässrige Lösung von Mineralsäure in dünnem Strahl unter starkem mechanischem Rühren. Die Essigsäure kann grösstenteils entfernt werden durch blosses Abfließen der wässrigen Lösung durch eine Nutsche (ohne Saugen) und Auswaschen mit verd. Mineralsäure. Die entstandene Paste wird dann mit Wasser, das mit einer abgemessenen Menge Mineralsäure versetzt ist, verrührt. Es ist zweckmässig, etwa 40-50 ml Wasser pro Gramm Aminopyren zu verwenden und so viel konz. Mineralsäure zuzufügen, dass die Lösung  $\frac{1}{4}$ — $\frac{1}{2}$ -normal wird. Die Diazotierung verläuft am besten bei 10-12° in schwefelsaurer, bei 4-6° in salzsaurer Lösung.

In salzsaurer Lösung entsteht bei der Diazotierung ausser dem gelösten Diazoniumchlorid in etwas schwankender Menge ein Harz, das jedoch beim Filtrieren durch einen Faltenfilter entfernt werden kann. Das Filtrat ist klar orangefarben. Während das Diazoniumchlorid relativ leicht löslich ist, ist das Sulfat ziemlich schwer löslich und fällt beim Diazotieren teilweise aus. Hier bildet sich kein Harz, und die Diazotierung verläuft praktisch quantitativ. Die Diazotierung wird am besten so ausgeführt, dass man das Nitrit in 6-7-prozentiger Lösung im Laufe einer halben Stunde unter Rühren zutropfen lässt und dann noch eine halbe Stunde weiterrührt. Die Temperatur wird während der Reaktion beim Einwerfen von Eisstückchen innerhalb der angegebenen Grenzen gehalten.

Noch schwerer löslich als das Sulfat ist das Perchlorat, das beim Fällen einer filtrierten Lösung des Chlorids mit Natriumperchlorat erhalten werden kann. Die rotbraunen Kristalle, die in einer Ausbeute von 75 Prozent der Theorie erhalten werden können, sind bei Zimmertemperatur vollkommen haltbar, explodieren aber beim Erhitzen oder starken Reiben. — In entsprechender Weise kann das Pyrenyldiazoniumborfluorid dargestellt werden. Es lässt sich aus Wasser umkristallisieren. Die Ausbeute ist dieselbe wie beim Perchlorat.



## 2. Kuppelungsreaktionen.

### a. Pyren-azo- $\beta$ -naphthol, $C_{16}H_9 \cdot N:N \cdot C_{10}H_6OH$ .

Die filtrierte Lösung des Diazoniumchlorids aus 2 g Aminopyren wird in eine Lösung von 1,5 g  $\beta$ -Naphthol in so viel verdünnter Natronlauge, dass die Reaktion alkalisch bleibt, unter gutem Rühren gegossen. Schon die ersten Tropfen erzeugen einen Niederschlag von violetten Kristallen. Nach einigem Stehen kann die Hauptmenge der Flüssigkeit abdekantiert werden, worauf man den sehr feinkörnigen Niederschlag am besten beim Zentrifugieren isoliert. Er wird dann zuerst mit verdünnter Natronlauge, dann mit Wasser mehrmals ausgewaschen. Ausbeute 2,7 g. Nach 2-3-maligem Umkristallisieren aus Xylol erhält man bronzeschimmernde Kristalle, die ohne Zersetzung bei  $256^\circ$  unkorrr. schmelzen.

Analyse. Gef. C, 83,9; H, 4,30; N, 7,53%.  
 $C_{26}H_{16}ON_2$ , ber. C, 83,5; H, 4,52; N, 7,61%.

Es ist auffallend, dass der aus der stark alkalischen Lösung gefällte Niederschlag die freie Oxy-azoverbindung und nicht ein Natriumsalz derselben ist. Man könnte deshalb bezweifeln, dass ein wahrer Oxy-azokörper vorliege. Da aber die Substanz bei der Reduktion mit Zinkstaub in Eisessig-Essigsäureanhydrid Acetylaminopyren und 1-Acetylmino-2-naphthylacetat (F. 205-06°) ergab, darf die Konstitution des Kuppelungsproduktes wohl als sichergestellt gelten. Es bleibt nur übrig, die ausserordentlich geringe Säurestärke dieser Oxy-azoverbindung zu konstatieren.

Es muss jedoch hinzugefügt werden, dass in einem Reduktionsversuch eine Verbindung isoliert wurde, die aus Wasser in glänzende weisse Kristalle fiel, F. 118-19°, und 4,80% Stickstoff enthielt. Der Körper wurde nicht identifiziert. Es handelt sich vermutlich um ein kernacetyliertes Diacetyl-aminonaphthol (Molgewicht 284, Stickstoffgehalt 4,90%).

### b. Pyren-azo-dimethylanilin, $C_{16}H_9 \cdot N:N \cdot C_6H_4 \cdot N(CH_3)_2$ .

Zur filtrierten Lösung des Diazoniumchlorids aus 2 g Aminopyren wird eine Lösung von 1,2 g Dimethylanilin in 50 ml verd. Salzsäure gegeben. Nach Abstumpfen der Salzsäure mit Natriumacetat erscheint zunächst ein brauner Niederschlag, der sofort

abfiltriert wird. Dann kristallisiert langsam aus dem Filtrat 1,4 g rein rote Substanz, die nach Waschen auf dem Filter sofort rein ist aber keinen definierten Schmelzpunkt hat.

Analyse. Gef. N, 12,04%; ber. 12,04%.

Schwer löslich in allen gewöhnlichen Lösungsmitteln.

### 3. Substitutionsreaktionen.

#### a. Jodpyren, $C_{16}H_9J$ .

Zum Diazoniumsulfat aus 5 g Aminopyren werden 5 g Kaliumjodid in wenig Wasser gegeben. Es entsteht sofort ein zinnoberroter Niederschlag, der sich unter Stickstoffentwicklung zersetzt. Wenn die spontane Reaktion aufhört, werden 2 g Naturkupfer zugefügt, und das Gemisch wird langsam unter Schütteln erwärmt, bis die Stickstoffentwicklung beendet ist. Man schüttelt nun mehrmals mit Äther aus. Die intensiv rote Ätherlösung wird beim Schütteln mit Aktivkohle ohne Erwärmen bis zu einer rein gelben Farbe entfärbt. Nach starkem Einengen der Lösung scheiden sich 3 g Jodpyren aus, Schmp.  $88^\circ$ . Als Nebenprodukt kann eine ganz kleine Menge Dipyrenyl isoliert werden.

Analyse. Gef. J, 39,2%; ber. 38,8%.

Jodpyren besitzt nur geringe Kristallisationsfähigkeit und fällt aus den meisten Lösungsmitteln gern als Öl aus. Am besten gelingt eine Kristallisation aus Methanol oder aus einem Gemisch von Alkohol-Äthylacetat (4:1) mit ein wenig Eisessig. Es wird dann als gelbliche, flache Nadeln mit Schmp.  $91^\circ$  erhalten.

Ein Pikrat, aus Benzol verfilzte, rote Nadeln, schmilzt bei  $156-57^\circ$ .

Jodpyren reagiert in Äther-Benzollösung langsam mit frisch gedrehten Magnesiumspänen. Ein Pyrenyl-magnesiumjodid konnte jedoch nicht aufgefunden werden. Als einziges Reaktionsprodukt konnte nur Dipyrenyl nachgewiesen werden:

3,3 g Jodpyren in 40 ml Äther + 15 ml Benzol, mit 0,5 g frisch gedrehten und mit Jod aktivierten Magnesiumspänen 4 Stunden



gekocht, lieferten 1,2 g gelbe Kristalle, die aus Xylol umkristallisiert bei 319-20° schmelzen und einen graugrünen Schimmer zeigen. In einem Stickstoffstrom vorsichtig erhitzt sublimiert das Dipyrenyl und bildet grosse, aber ausserordentlich dünne Blätter mit grüner Fluoreszens. Die Lösung in Benzol fluoresziert intensiv blau.

Analyse. Gef. C, 95,3; H, 4,55<sup>0</sup>/<sub>0</sub>.

C<sub>32</sub>H<sub>18</sub>, ber. C, 95,5; H, 4,48<sup>0</sup>/<sub>0</sub>.

GARVEY, jr., HALLEY und ALLEN<sup>1)</sup> geben an, bei der Einwirkung von p-Tolyljod-difluorid auf Pyren u. a. Dipyrenyl dargestellt zu haben. Ihr Produkt hatte jedoch keinen definierten Schmelzpunkt und liess sich nicht umkristallisieren. Es ist somit sehr unwahrscheinlich, dass sie 3,3'-Dipyrenyl in den Händen gehabt haben.

Wie oben erwähnt, entsteht ein wenig Dipyrenyl bei der Zersetzung des Diazoniumjodids, wahrscheinlich in der zweiten Phase (in Gegenwart von Kupferbronze).

#### b. Rhodanpyren, C<sub>16</sub>H<sub>9</sub>SCN.

5 g Aminopyren werden in schwefelsaurer Lösung diazotiert. 2,5 g Kaliumrhodanid und Kuprorhodanid aus 2,3 g Kaliumrhodanid, 5,8 g Kuprisulfat und 7 g Ferrosulfat werden hinzugefügt. (Spätere Versuche haben ergeben, dass Kupferbronze, etwa 3 g, das Kuprorhodanid ersetzen kann, ohne die Ausbeute zu verringern). Das Gemisch wird auf dem Wasserbade unter Rühren erwärmt, bis die Stickstoffentwicklung beendet ist. Es hat sich dann eine klebrige Masse gebildet, die beim Erkalten erstarrt. Das Produkt wird gepulvert und mit Äther gründlich ausgekocht. Die rote Lösung wird mit Kohle entfärbt und der Äther grösstenteils verdunstet. Ausbeute 0,7 g. Nach Umkristallisieren aus Benzol Schmp. 117-18°.

Analyse Gef. N, 5,48; S, 12,2; 12,4<sup>0</sup>/<sub>0</sub>.

Ber. N, 5,45; S, 12,4<sup>0</sup>/<sub>0</sub>.

Rhodanpyren lässt sich jedoch mit viel besserer Ausbeute, etwa 60<sup>0</sup>/<sub>0</sub> d. Th., bei direkter Rhodanierung des Pyrens mit

<sup>1)</sup> Am. Soc. 59, 1828 (1937).

freiem Rhodan darstellen. Über diese Reaktion sowie über die Umsetzungen des Rhodanpyrens wird später berichtet.

### c. Fluorpyren, $C_{16}H_9F$ .

Das Fluorpyren wurde nach dem Borfluorid-Verfahren von BALZ und SCHIEMANN<sup>1)</sup> dargestellt.

Eine filtrierte Lösung von Pyrenyl-diazoniumchlorid wird mit einem kleinen Überschuss an Borfluorwasserstoffsäure versetzt. Der dabei entstandene dicke Brei wird zwecks leichter Filtrierbarkeit auf dem Wasserbade unter Rühren auf  $60^\circ$  erwärmt und dann wieder abgekühlt. Der Niederschlag wird abgesaugt, mit Wasser, Alkohol und Äther gewaschen und dann, vor dem Lichte geschützt, an der Luft getrocknet. Das trockene und fein gepulverte Salz wird nun in kleinen Anteilen zu siedendem Xylol gegeben, wobei augenblicklich Zersetzung eintritt. (Während nach Schiemann loc. cit. dies Zersetzungsverfahren bisher keinen Erfolg gehabt hat, ist es hier ohne Vergleich das ergiebigste). Das Kochen wird fortgesetzt, bis kein weisser Nebel mehr entsteht. Ein wenig Harz wird abfiltriert, das Xylol mit Wasserdampf abgetrieben und der Rückstand in Äther aufgenommen. Nach Behandlung mit Aktivkohle wird der Äther verjagt und der Rückstand aus Eisessig kristallisiert. Das Fluorpyren wird dabei als flache gelbe Nadeln erhalten, die bei  $134-35^\circ$  schmelzen. Im Ölpumpenvakuum sublimiert es willig bei etwa  $170^\circ$ , und das sublimierte Produkt schmilzt bei  $136,5-37^\circ$ . Ausbeute 60 Prozent der Theorie, auf Aminopyren bezogen.

Die quantitative Bestimmung des Fluors im Fluorpyren bot verschiedene Schwierigkeiten. Viele Versuche, das Fluor abzuspalten, scheiterten, so auch die sonst so schöne Methode von VAUGHN und NIEUWLAND<sup>2)</sup>, nach der das Fluor in einer Lösung des fluorhaltigen Körpers in flüssigem Ammoniak mittels metallischen Natriums abgespalten wird. Mangels einer Bombe für die explosive Verbrennung der Substanz durch Natriumperoxyd haben wir die Analyse indirekt durchgeführt, indem wir das Fluorpyren in Tribrom-fluorpyren übergeführt haben und das Brom nach Stepanow (in Amylalkohol statt Äthylalkohols, vgl.

1) BALZ und SCHIEMANN, Ber. **60**, 1186 (1927).

SCHIEMANN, J. pr. **140**, 97 (1934).

2) VAUGHN und NIEUWLAND, Ind. Eng. Ch., Anal. Ed. **1931**, 273.



I. Mitteilung dieser Reihe) bestimmt haben. Das Tribromfluorpyren wurde in der folgenden Weise dargestellt.

1,1 g Fluorpyren in 15 ml Nitrobenzol wurden nach und nach mit 1 ml Brom (etwa 4 Mol) in 5 ml Nitrobenzol versetzt. Das Gemisch wurde dann langsam erhitzt und 2 Stunden bei 120° gehalten. Der gebildete Niederschlag wurde aus Xylol kristallisiert. Gelbe Nadeln, F. 316° korr.

Brombestimmung. Gef. 52,7; 52,4%;  $C_{16}H_6FBr_3$ , ber. 52,5%.

Die qualitative Nachweis des Fluors im Fluorpyren gelang glatt nach der Methode von SCHWER—FETKENHEUER—KÜHNEL HAGEN<sup>1</sup>).

GARVEY jr. und Mitarb. (loc. cit.) glauben, Fluorpyren bei der Behandlung von Pyren mit p-Tolyljod-difluorid erhalten zu haben. Der Schmelzpunkt ihrer Substanz ist 113°. Vielleicht liegt hier ein Druckfehler vor (113 statt 131?). Wir haben ohne Erfolg ihre Methode versucht.

1) Ausführung der Reaktion: KÜHNEL HAGEN, Mikrochemie, 15, 313 (1934).

---

## PYRENSTUDIEN IV.

### Die Alkylierung des Pyrens.

Über die Alkylierung des Pyrens ist bisher nichts bekannt. Zwar sind 3- und 4-Methyl- und 3-Äthylpyren beschrieben worden, aber diese Pyrenderivate sind aus Sauerstoff- oder Stickstoffabkömmlingen der Alkylpyrene dargestellt worden: 3-Methyl aus Pyrenaldehyd<sup>1)</sup> und aus Pyrenylessigsäure<sup>2)</sup>, 3-Äthyl aus Acetylpyren<sup>3)</sup> und 4-Methyl aus 4-Cyanpyren<sup>4)</sup> und durch eine ganz undurchsichtige Synthese<sup>5)</sup>.

Als wir am Anfang der Untersuchung, über die hier berichtet werden soll, Alkylhalogenide in der klassischen Weise mittels Aluminiumchlorids mit Pyren in Reaktion zu bringen versuchten, ging aus dem Ergebnis deutlich hervor, warum kein Alkylpyren bisher bei direkter Substitution dargestellt worden war: Das Pyren bildet mit Aluminiumchlorid eine in den gewöhnlichen für die Friedel-Crafts-Synthese verwendbaren Lösungsmitteln ganz unlösliche Komplexverbindung, die mit den zugeetzten Alkylhalogeniden nicht reagiert oder — wenn eine Reaktion bei Erhöhung der Temperatur erzwungen wird — nur in ein Pech oder einen schwarzen Schwamm verwandelt wird.

Das Ergebnis ist recht überraschend, weil das Pyren sich sehr willig und glatt mit Säurechloride und Säureanhydride in Gegenwart von Aluminiumchlorid umsetzt — Pyren gibt sogar mit Essigsäureanhydrid mit Zinkchlorid als Katalysator Acetylpyren in guter Ausbeute.

Wir versuchten dann, das Aluminiumchlorid mit dem Bromid zu ersetzen, nachdem es sich herausgestellt hatte, dass der

1) VOLLMANN, BECKER, CORELL und STREECK, *Ann.* **531**, 112 (1937).

2) *Ibid.* p. 113.

3) *Ibid.* p. 114.

4) *Ibid.* p. 142.

5) COOK and HEWETT, *J. Chem. Soc.* **1934**, 366.



$\text{AlBr}_3$ -Pyren-Komplex in Tetrachloräthan nicht ganz unlöslich war. Mit Methyljodid und Äthylbromid trat jedoch keine Reaktion ein; als wir aber einen Versuch mit Isopropylbromid anstellten, konnte eine allerdings träge, aber deutliche Halogenwasserstoffentwicklung beobachtet werden, und es konnte nach der üblichen Aufarbeitung ein öliges Produkt erhalten werden, das sich sowohl der Analyse wie der Molekulargewichtsbestimmung nach als ein ziemlich reines Isopropylpyren erwies. — In anderen Lösungsmitteln wie Schwefelkohlenstoff und Ligroin war die Reaktionsgeschwindigkeit so gering, dass sie nicht in Frage kommen konnten.

Endlich wurde versucht, die Alkylhalogenide selbst als Lösungsmittel zu verwenden und zwar mit gutem und zum Teil ganz überraschendem Erfolg. Man konnte unter solchen Umständen nicht erwarten, Monoalkylpyrene zu erhalten, vielmehr musste mit einem komplizierten Gemisch aller möglichen Alkylierungsprodukte bis Tetraalkylpyrene gerechnet werden, indem die Wasserstoffatome 3, 5, 8 und 10 sich in vielen Substitutionsprozessen mit anderen Atomen oder Atomgruppen ersetzen lassen. Wider Erwarten zeigte es sich, dass in der Hauptsache nur ganz wenige von den theoretischen Möglichkeiten verwirklicht wurden, und im allgemeinen liessen sich die gebildeten Produkte unschwer isolieren.

Die grösste Überraschung bestand jedoch darin, dass wir in 2 Fällen Penta-alkylpyrene isolieren konnten und in 2 Fällen neben den erwarteten Tetrasubstituten noch eine Tetraverbindung erhielten. Welche Stellung im Pyrenmolekül die fünfte, bzw. eine der vier Alkylgruppen einnimmt, ist noch nicht festgestellt worden. Wir können nur konstatieren, dass die gewöhnliche Substitutionsregel, dass nur die 3, 5, 8 und 10-Stellungen angegriffen werden, gebrochen sein muss.

Es sind sowohl primäre wie sekundäre und tertiäre Alkylhalogenide auf Reaktionsfähigkeit gegenüber Pyren-Aluminiumbromid untersucht worden. Die primären reagieren sehr träge und haben bisher nur ölige Produkte ergeben. Die sekundären liefern hauptsächlich Tetra- und Pentaalkylpyrene, während tertiäre Halogenide dem Anschein nach nur Dialkylpyrene bilden können. Die Bindungsweise des Halogens spielt also eine ausschlaggebende Rolle für den Verlauf der Substitution.

Die bisher dargestellten Dialkylpyrene sind alle einer sehr sorgfältigen fraktionierten Kristallisation unterworfen. Merkwürdigerweise ist es nicht möglich gewesen, mehr als ein Dialkylpyren nachzuweisen bei jedem Alkyl, im Gegensatz zu den Befunden bei den Di-acylierungen, wo stets 3, 8- und 3, 10-Substitution gleichzeitig auftreten.

Die hier gefundene Selektivität bei der Alkylierung des Pyrens tritt bekanntlich nicht bei Benzol auf. Aus Äthylchlorid, bzw. Propylchlorid, Benzol und Aluminiumchlorid oder -Bromid werden gleichzeitig viele Alkylierungsstufen und — wenn möglich — mehrere Isomeren gebildet.<sup>1)</sup> Es ist zwar möglich, dass die beim Pyren erhaltenen Restöle verschiedene Alkylpyrene enthalten. Da aber alle bisher aufgefundenen Polyalkylpyrene sehr willig kristallisieren, liegt es näher anzunehmen, dass diese Öle durch eine weitere Einwirkung des Aluminiumbromids auf die schon gebildeten Polyalkylpyrene entstanden sind. Gibt man zu einer Lösung von Penta-isopropylpyren in Isopropylbromid etwas Aluminiumbromid und erwärmt die Lösung einige Stunden, erhält man ausser unverändertem Kohlenwasserstoff nur ein kristallisationsunfähiges Öl, ein Hinweis darauf, dass das Aluminiumbromid in solcher Weise auf diese Kohlenwasserstoffe einwirken kann.

Es sei noch bemerkt, dass Aluminiumchlorid qualitativ ganz wie Aluminiumbromid in Alkylhalogenid-Lösungen wirkt.

In einer folgenden Arbeit soll nachgewiesen werden, dass Methylpyren und andere Alkylpyrene bei der Einwirkung von Alkylhalogenide auf Lithiumpyren dargestellt werden können.

Dem Carlsbergfond sind wir für eine Unterstützung zu Dank verpflichtet.

## VERSUCHSTEIL

### I. Reaktion in Tetrachloräthan-lösung.<sup>2)</sup>

Zur Lösung von 25 g Pyren in 125 ml Tetrachloräthan wurde eine Lösung von 33 g Aluminiumbromid (frisch destilliert) in

1) WERTYPOROCH und FIRLA, Ann. 500, 287 (1933).

2) Es wird später an anderer Stelle ein mehr eingehender Bericht über die Reaktionen in Verdünnungsmitteln gegeben werden.



100 ml Tetrachloräthan unter Rühren gegeben. Es bildete sich augenblicklich ein aus der Pyren-Aluminiumbromid-Komplexverbindung bestehender Brei. 16 g Isopropylbromid (1 Äquivalent) wurde nun zugefügt, und das Gemisch unter mechanischem Rühren 10 Stunden in einem Wasserbad, das auf 50—55° gehalten wurde, erwärmt. Nach der ersten Stunde war das Gemisch homogen geworden und bildete eine dunkelbraune Lösung, aus der langsam Bromwasserstoff entwich.

Nach Zersetzung mit Eis und Salzsäure wurde das Tetrachloräthan mit Wasserdampf abgetrieben, der Rückstand in Äther aufgenommen, mit Sodalösung und Wasser gewaschen, getrocknet und der Äther verjagt. Der dunkle, ölige Rückstand wurde dann im Ölpumpenvakuum fraktioniert. Aus 32 g Rohprodukt konnte etwa 10 g eines dicken, bernsteingelben Öls erhalten werden, das unzweifelhaft ein nur wenig verunreinigtes Isopropylpyren darstellte.

Analyse. Gef. C, 92,6%; H, 6,84%. Mol-gew. 255  
 $C_{19}H_{16}$ , ber. C, 93,4%; H, 6,60%; Mol-gew. 244.

Bei starker Kühlung (−80°) einer Lösung des Öles in Benzin konnte das Isopropylpyren in geringer Ausbeute kristallinisch erhalten werden. Es lässt sich dann ohne Schwierigkeit aus Benzol-Alkohol umkristallisieren und schmilzt bei 82°.

Analyse. Gef. C, 92,8%; H, 6,67%.  
 Ber. C, 93,4%; H, 6,60%.

## II. Reaktionen in Alkylhalogeniden als Lösungsmitteln.

Allgemeines Verfahren:

In einen mit eingeschliffenem Rührer und Rückflusskühler versehenen Kolben (100—250 ml) wird das fein gepulverte Pyren und das Alkylhalogenid gebracht. Es wurde bei diesen Versuchen immer »Pyren reinst« der Firma Fraenkel und Landau, später Heyl und Co., verwendet. Das Aluminiumbromid wurde jedesmal frisch aus einem Vorrat destilliert. Durch den Kühler wird der entstehende Halogenwasserstoff zuerst durch einen im

Kältebad stehenden Kolben geleitet und dann in eine abgemessene Menge n-Natronlauge aufgefangen. In dieser Weise kann man titrimetrisch den Reaktionsverlauf grob verfolgen. Das Erwärmen des Reaktionsgemisches erfolgt in einem Wasserbad, dessen Temperatur im folgenden als Reaktionstemperatur angegeben wird. Nach beendeter Reaktion, oder wenn eine bestimmte Halogenwasserstoffmenge entwickelt ist, wird abgekühlt und mit Eis und Salzsäure zersetzt.

Im folgenden sind die Schmelzpunkte alle korrigiert angegeben.

### 1. Reaktion mit Isopropylbromid. Bildung von Tetra- und Penta-Isopropylpyren.

Die Reaktion wurde wie oben beschrieben durchgeführt. Das Aluminiumbromid bildete im ersten Augenblick einen dicken, rotbraunen Brei, der aber beim Erwärmen gelöst wurde. Die zuerst rotbraune Lösung nahm allmählich eine tiefrote und schliesslich eine rotviolette Farbe an. Bei ungefähr  $45^{\circ}$  setzte eine lebhafte Halogenwasserstoff-Entwicklung ein.

Die Resultate einer Reihe von Versuchen werden in Tabellenform wiedergegeben (Tab. 1). Es geht daraus hervor, dass Reaktionsdauer und Temperatur entscheidenden Einfluss auf den Verlauf der Reaktion ausüben.

In den meisten Versuchen wurden angesetzt 10,1 g Pyren (0,05 Mol), 50—60 ml Isopropylbromid und etwa 3,3 g Aluminiumbromid (0,0125 Mol). Die vierte Kolonne der Tabelle gibt die in Natronlauge aufgefangene Halogenwasserstoffmenge in Mol pro Mol Pyren an. In den Fällen (Vers. 2 u. 8), wo grössere Mengen als angegeben zur Reaktion gebracht sind, sind die Ausbeuten auf 10,1 g Pyren umgerechnet.

Nach der Zersetzung mit Eis und Salzsäure wurde das überschüssige Isopropylbromid mit Wasserdampf vertrieben und der Rest mit Äther ausgezogen. In den Versuchen 1 bis 4 blieb ein Rest ungelöst, der sich als fast reines Tetraisopropylpyren erwies. Aus Benzol klare prismatische Tafeln, die eine starke violette Fluoreszenz besitzen, Schmp.  $311-12^{\circ}$ . Sehr schwer löslich in den meisten Lösungsmitteln mit Ausnahme des Benzols und seiner Homologe. Die Lösungen in Benzol und in heissem



Tabelle 1.

Vers. Nr	Bad-temp.	Zeit Stund.	Mol HBr	Tetra i-pr-Pyren, g	Penta	Restöl g
1	50–53	4,5	2,5	1,5	—	14
2	55–60	5	3,4	2,0	1,2	14,7
3	50–60	6,5	—	1,4	5,3	10,2
4	{ 45–50 50–60 }	{ 5 + 3,5 }	3,6	2,1	2,0	10,5
5 <sup>1)</sup>	{ 50–52 20–22 }	{ 12 + 12 }	4,1	0,1	13,6	4,1
6 <sup>1)</sup>	60–65	6	3,6	0,2	14,3	3,2
7 <sup>2)</sup>	60–75	6	4,4	—	14,2	4,8
8 <sup>2)</sup>	{ 65–70 70 }	{ 7 + 15 }	5,0	—	15,2	4,2

<sup>1)</sup> In den beiden Versuchen 5 und 6 wurde ausserdem etwa 1 g kristallinisches Produkt erhalten, welches wesentlich niedriger als die zwei isolierten Polyisopropylpyrene schmilzt. Die Substanz ist noch nicht identifiziert worden.

<sup>2)</sup> In Vers. 7 und 8 wurden 90, resp. 120 ml Isopropylbromid und 4,3 resp. 4,5 g Aluminiumbromid verwendet.

Alkohol fluoreszieren intensiv violett, während eine kalte alkoholische Lösung derselben Konzentration nicht fluoresziert.

Analyse. Gefunden C, 90,7; 91,1; 91,0%.

H, 9,52; 9,35; 9,37%.

C<sub>28</sub>H<sub>34</sub>, ber. C, 90,8%; H, 9,24%.

Mol-gew. (nach Rast) gef. 375, ber. 370.

Pikrat des Tetra-isopropylpyrens. Beim Abkühlen einer heissen Lösung von äquimolaren Mengen Tetra-isopropylpyren und Pikrinsäure in Benzol erhält man das Pikrat. Dunkle, violettschimmernde Nadeln, die bei 287° schmelzen.

Gefunden: N, 7,04%; ber. 7,01%.

Es liegt also unzweifelhaft ein Tetra-isopropylpyren vor, und aller Wahrscheinlichkeit nach die 3, 5, 8, 10-Verbindung.

Die Ätherlösung wurde neutral gewaschen, getrocknet und eingengt. Wenn nennenswerte Mengen der Tetraverbindung zugegen sind, bekommt man zuerst noch eine kleine Menge davon. Darauf folgt, in mehreren Kristallisationen, das Penta-

isopropylpyren, und endlich bleibt ein Öl zurück, aus dem kein kristallisierbares Material erhalten werden kann.

Das Rohprodukt des Penta-isopropylpyrens wurde mehrmals aus Eisessig, Benzol und Alkohol fraktioniert kristallisiert, um etwaige andere Produkte aufzufinden, jedoch ohne Erfolg.

Das Penta-isopropylpyren scheidet sich aus Äther oder Benzol in klare, pyramidale Kristalle aus, die bei 189—90° schmelzen. Die Lösungen fluoreszieren wie die der Tetra-Verbindung.

Analyse. Gefunden: C, 90,3; 90,3; 90,0; 90,3; 90,0%.

H, 9,68; 9,67; 9,50; 9,77; 9,73%.

$C_{31}H_{40}$ , ber. C, 90,3%; H, 9,71%.

Molgew., nach Rast: Gef. 414, ber. 412.

Pikrat. Aus Benzol oder Benzol-Alkohol, wie bei der Tetra-Verbindung, dunkelbraune Kristalle, Schmp. 210—12°. Ziemlich löslich in Benzol.

Gefunden: N, 6,64%; ber. 6,55%.

Die Stellung der fünften Isopropylgruppe ist vorläufig unbekannt.

## 2. Reaktion mit Cyklopentylbromid. Bildung von Tetra- und Penta-Cyklopentylpyrene.

Beim Zusammenbringen von Pyren und Aluminiumbromid in Cyklopentylbromid entsteht ein dicker roter Brei, der sich bei etwa 45° in eine rote Lösung verwandelt. Nach beendeter Reaktion und Zersetzung wurde mit Äther extrahiert, oder das Cyklopentylbromid wurde direkt abgehoben. Der Äther wurde verjagt und das Cyklopentylbromid unter vermindertem Druck abdestilliert. Der nur teilweise kristallisierte Rückstand wurde mehrmals mit Äther ausgekocht, wobei eine erste Fraktionierung erreicht wurde.

Es konnten bei der Aufarbeitung 3 Individuen isoliert werden, und zwar zwei Tetra- und ein Pentacyklopentylpyren. »Tetra I« schmilzt bei 295° und »Tetra II« bei 203—204°, während die Penta-Verbindung bei 246° schmilzt. — In Tabelle 2 sind die Ergebnisse einiger Versuche wiedergegeben. Die ange-



fürten Ausbeuten beziehen sich auf bis zur völligen Konstanz der Schmelzpunkte gereinigte Substanzen. Die Gesamtausbeute an kristallisiertem Produkt war wesentlich grösser, in Versuch 4 z. B. 17 g. In 1 und 2 geben die Zahlen jedoch die Gesamtausbeuten an. Tetra I ist aber sofort praktisch rein.

Tabelle 2.

Vers. Nr	Pyren g	C <sub>5</sub> H <sub>9</sub> Br ml	AlBr <sub>3</sub> g	Temp.	Zeit St	HBr Äq	Ausbeute, g		
							Tetra I	Tetra II	Penta
1	5,1	40	1,5	45°	1,5	1,0	0,55	—	—
2	5,1	40	1,7	55—70	0,5	2,2	1,18	—	0,1
3	5,1	45	2,0	50—70	0,5	2,0			
				70—80	0,5	0,8			
				80—100	0,5	0,4			
				70—100	1,0	0,2			
4	10,1	85	4,0	45—100	1,2	3,4	—	0,12	4,0
						4,1		0,35	11,0

Wie beim Isopropylbromid ist auch hier der Verlauf der Reaktion weitgehend von Temperatur und Zeit abhängig. Niedrige Substitutionsstufen konnten nicht erfasst werden. Neu beim Cyclopentylbromid ist die Bildung von 2 isomeren Tetrasubstituten. Wir vermuten, dass Tetra I (Schmp. 295°) wegen des hohen Schmelzpunktes die 3, 5, 8, 10-Verbindung ist, während die niedrigschmelzende II weniger symmetrisch gebaut zu sein scheint.

Tetra I kristallisiert nach der Zersetzung direkt aus der Reaktionslösung. Klare viereckige Tafeln.

Die Isolierung von Tetra II ist sehr mühsam und zeitraubend, und die Ausbeute an völlig reiner Substanz war nur gering. Die Fraktionierung gelang am besten mittels Essigesters. — Die Hauptmenge des Penta-cyclopentylpyrens fällt schon beim Beginn der Fraktionierung ziemlich rein aus; schon nach 3—4 Kristallisationen erreicht der Schmelzpunkt seinen Endwert, 246° bei schnellem Erhitzen.

Von den drei Polycyclopentylpyrenen fluoresziert Tetra I stark blauviolett in kaltem Benzol; Tetra II fluoresziert gar nicht

in kaltem und nur schwach in siedendem Benzol, Penta schwach in kaltem und bedeutend stärker in heissem Benzol.

Analysen.

Tetra I. Gef. C, 91,0; 90,9<sup>0</sup>%. H, 8,89; 8,96<sup>0</sup>%.

Tetra II. » C, 90,6<sup>0</sup>%. H, 8,89<sup>0</sup>%.

C<sub>36</sub>H<sub>42</sub>, ber. C, 91,1<sup>0</sup>%. H, 8,92<sup>0</sup>%.

Penta. Gef. C, 90,6; 90,2<sup>0</sup>%. H, 9,25; 9,29<sup>0</sup>%.

C<sub>41</sub>H<sub>50</sub>, ber. C, 90,7<sup>0</sup>%. H, 9,29<sup>0</sup>%.

### 3. Reaktion mit Cyklohexylbromid. Tetra-cyklohexylpyrene.

Der grünschwarze Brei, der beim Zusammenbringen von Pyren und Aluminiumbromid in Cyklohexylbromid gebildet wird, geht bei etwa 50° in Lösung mit rotbrauner Farbe. Die Reaktion mit Cyklohexylbromid vollzieht sich bei weitem nicht so glatt wie beim Isopropylbromid, und die Ausbeuten lassen viel zu wünschen übrig. Wahrscheinlich bewirkt das Aluminiumbromid eine Zersetzung der zuerst gebildeten Cyklohexylpyrene und verringert dabei die Ausbeuten.

Nach Zersetzung mit Eis und Salzsäure wurde mit Äther extrahiert. Wenn die Äthermenge nicht allzu gross war, fiel nach einigem Stehen nach dem Waschen mit Wasser eine Substanz aus, die sich als ein Tetracyklohexylpyren (I) erwies. Die ätherische Mutterlauge wurde eingeeengt und das überschüssige Cyklohexylbromid unter vermindertem Druck abdestilliert. Der Rückstand lieferte, mit Äther ausgerührt, langsam eine neue Kristallisation des erwähnten Tetracyklohexylpyrens, die auf einem Glasfilter von der ziemlich zähen Mutterlauge befreit wurde. Die gewonnenen Kristalle wurden aus Toluol umkristallisiert. Klare, bisweilen sechseckige Tafeln, Schmp. bei schnellem Erhitzen 369—70°.

Nach mehrtägigem Stehen konnte aus der öligen Mutterlauge eine neue kristallinische Substanz gewonnen werden, die aus Benzol umkristallisiert bei 239—40° schmolz. Unsere erste Annahme, dass es sich um eine Pentaverbindung handelte, bestätigte sich nicht. Die analytischen Daten deuten entschieden auf vier Cyklohexylgruppen im Molekül (Tetra II). Ein Penta-derivat konnte nicht nachgewiesen werden. In Tabelle 3 sind die Resultate einiger Versuche wiedergegeben.



Tabelle 3.

Vers. Nr	Pyren g	C <sub>6</sub> H <sub>11</sub> Br ml	AlBr <sub>3</sub> g	Zeit St	Temp	HBr Äq	Tetra I g	Tetra II g
1	5	40	1,1	{ 0,5 1,5 2,0 1,0 }	{ 50–80 80–85 85–90 90–100 }	3,2	1,55	—
2	6	40	1,9	0,75	65–70	1,2	0,5	—
3	5	50	1,4	{ 0,75 0,75 }	{ 70 80 }	2,0	1,45	2,2
4	5	45	1,8	1,5	70	2,0	1,65	1,55
5	10	85	4,0	2,5	65–75	2,5	3,5	1,5

## Analysen.

## Tetracyklohexylpyren I:

Gef. C, 89,9; 90,1; 90,1; 90,5; 90,8%.

H, 9,50; 9,36; 9,42; 9,26; 9,35%.

## Tetracyklohexylpyren II:

Gef. C, 89,8; 89,6; 90,6; 90,6; 90,1%.

H, 9,46; 9,52; 9,47; 9,49; 9,40%.

C<sub>40</sub>H<sub>50</sub>, ber. C, 90,5; H, 9,49%.

Die Verbrennung dieser Substanzen, wie übrigens auch der Cyklopentyl-derivate, bietet einige Schwierigkeiten. Die Kohlenstoffprocente schwanken deshalb bedeutend; für die Beurteilung des Substitutionsgrades sind aber die Wasserstoffprocente von grösserem Wert und lassen kaum Zweifel übrig. Ein Penta-cyklohexylpyren fordert 9,88% Wasserstoff.

Keiner der beiden Kohlenwasserstoffe ist zur Bildung von Pikrat fähig.

In kaltem Benzol fluoreszieren beide schwach violett, in heissem viel stärker.

In Cyklohexylchlorid statt Cyklohexylbromids bleibt die Friedel-Crafts-Reaktion gänzlich aus: 5 g Pyren, 3 g AlBr<sub>3</sub> und 40 ml Cyklohexylchlorid wurden 5 Stunden auf 100–140° erhitzt. Keine Halogenwasserstoffentwicklung konnte beobachtet werden, und 4,5 g Pyren wurde unverändert wiedergewonnen.

Es wurde auch versucht, Cyklohexylbromid durch Cyklohexen zu ersetzen, jedoch ohne Erfolg. Zwar setzte eine Reaktion ein, ausser unverändertem Pyren konnte aber nur ein kristallisationsunfähiges Öl erhalten werden.

Ausser den erwähnten sekundären Halogeniden wurde auch 3-Brom-n-pentan untersucht. Im Laufe einer Stunde wurde bei etwa  $70^{\circ}$  3 Mol Bromwasserstoff pro Mol Pyren entwickelt. Aus dem Produkt der Reaktion konnte aber kein kristallisiertes Material isoliert werden.

#### 4. Reaktion mit tert. Butylchlorid.

Di-tert.-butyl-pyren,  $C_{16}H_8(C_4H_9)_2$ .

Bei den Alkylierungen mit tertiären Alkylhalogeniden wurden die Chloride statt der Bromide benutzt, weil die Bromide im Gegenwart des Aluminiumbromids instabil sind. Bei einem Versuch mit tert. Butylbromid wurde nur die Hälfte der mit dem Chlorid erlangten Ausbeute erreicht.

5 g Pyren, 1,0 g  $AlBr_3$  und 40 ml tert. Butylchlorid wurden eine Stunde bei  $30-40^{\circ}$  gehalten. 2 Äquivalente  $HBr$  wurde dabei entwickelt. Nach der üblichen Aufarbeitung wurde die Ätherlösung eingengt, und in mehreren Kristallisationen wurde eine Gesamtmenge von 6,75 g Substanz erhalten, die sich als einheitlich erwies und aus einem Di-tert.-butylpyren bestand. Aus Benzol umkristallisiert schmilzt sie bei  $208-09^{\circ}$ .

Gef. C, 91,6; 91,9; 91,7%. H, 8,43; 8,34; 8,27%.

$C_{24}H_{26}$ , ber. C, 91,66%. H, 8,34%.

Ein Pikrat konnte aus Benzollösung erhalten werden. Dünne rote Nadeln, Schmp.  $253-54^{\circ}$ .

Gef. N, 7,81%; ber. 7,73%.

#### 5. Reaktion mit tert. Amylchlorid.

Di-tert.-amyl-pyren,  $C_{16}H_8(C_5H_{11})_2$ .

5 g Pyren, 1 g  $AlBr_3$  und 45 ml tert. Amylchlorid wurden 1,5 Stunden bei  $40^{\circ}$  gehalten. Nach der Hydrolyse wurde die Amylchloridschicht mit Wasser gewaschen und getrocknet. Das Amyl-



chlorid wurde dann im Vakuum destilliert, und nach Zusatz von Äther kristallisierte der Rückstand teilweise. Aus der Mutterlauge konnten noch ein paar Kristallisationen gewonnen werden, insgesamt 5 g. Das Produkt schmolz unscharf bei 155–60°. Nach Kristallisieren zuerst aus Eisessig oder Benzol-Alkohol und dann zweimal aus Essigester stieg der Schmp. auf 165–66°.

Eine Reaktionstemperatur höher als 40° oder eine Reaktionszeit länger als oben angegeben verringerte die Ausbeute.

Analyse. Gef. C, 91,1; 91,1<sup>0</sup>%. H, 8,72; 8,83<sup>0</sup>%.

C<sub>26</sub>H<sub>30</sub>, ber. C, 91,2<sup>0</sup>%; H, 8,83<sup>0</sup>%.

Das Pikrat schmilzt bei 209–10° korr.

Analyse. Gef. N, 7,43; ber. 7,49<sup>0</sup>%.

Die relativ schwierige Reinigung des Rohproduktes bis zum konstanten Schmelzpunkt deutete auf ein Gemisch, weshalb das aus 3 Präparationen gewonnene Rohprodukt einer sehr sorgfältigen fraktionierten Kristallisation unterworfen wurde. Der weitaus grösste Teil wurde mit dem Schmp. über 163° isoliert, während eine kleine Menge mit Schmp. 155–60° erhalten wurde, die aber, mit dem höher schmelzenden Produkt gemischt, kein Depression ergab. Es ist also nicht wahrscheinlich, dass mehrere Isomere bei der Reaktion entstanden sind.

Es wurden auch Versuche mit Tri-äthyl-methylchlorid angestellt. Sowohl das Pyren wie das Aluminiumbromid war in diesem Lösungsmittel überraschend schwerlöslich. Beim Erwärmen auf etwa 50° lösten sich jedoch beide im Laufe von 20 Minuten. Nach kurzer Zeit hatten sich 2 Äquivalente Halogenwasserstoff entwickelt, aber es konnte — wie im Falle des Diäthylmethylbromids — kein kristallisiertes Produkt erhalten werden.

Die primären Alkylhalogenide Äthylbromid und -jodid und das n-Butylbromid wurden auf Reaktionsfähigkeit in der beschriebenen Weise geprüft. Die beiden ersten reagierten überhaupt nicht. Mit Butylbromid trat zwar bei erhöhter Temperatur eine Reaktion ein, es konnte aber nur ein teerartiges Öl erhalten werden.

## Kryoskopische Messungen.

Da es uns wichtig erschien, die von den analytischen Daten abgeleiteten Formeln durch kryoskopische Messungen zu bestätigen, haben wir eine Reihe von Messungen in Benzol ausgeführt. Dabei wurde nun die Beobachtung gemacht, dass in sehr verdünnten Lösungen — 0,01 bis 0,02 molal — der gewöhnlich angenommene Wert der kryoskopischen Konstante des Benzols, 5,1, viel zu niedrige Werte für die Molgewichte ergab. Dasselbe war der Fall mit Pyren selbst und mit Phenanthren, wie wir feststellen konnten. In solchen Lösungen musste vielmehr mit Werten um etwa 5,6 gerechnet werden. Wurden aber die Konzentrationen auf 0,1 bis 0,15 molal erhöht, wurde etwa 5,2 gefunden. Es ist aber nicht für alle die hier untersuchten Stoffe möglich, so hohe Konzentrationen in kaltem Benzol zu erhalten.

Die angenommenen Formeln konnten überall bestätigt werden. Die Abweichungen von den theoretischen Werten sind so klein, dass etwaige andere Alkylierungsstufen ausgeschlossen werden können. Für die beiden Polyisopropyl-pyrene bestätigten sich die mit Campher ermittelten Molgewichte völlig.

Die Ergebnisse der Messungen sind in Tabelle 4 zusammengestellt. Es bedeutet:

- C: Konzentration der Lösung in Mol pro kg Benzol;
- M ber.: das M.-gew. aus den Atomformeln berechnet;
- M gef.: das M.-gew. aus der Messung berechnet, die Konstante des Benzols = 5,1 angenommen.
- k: die kryoskopische Konstante des Benzols, unter Voraussetzung des theoretischen Molgewichtes der Substanz.
- $\Delta$ : die gemessene Erniedrigung des Gefrierpunktes.



Tabelle 4.

Pyrenderivat	C	$\lambda$	M ber.	M gef.	k
Dibutyl.....	0,0175	0,097	314	290	5,53
	0,0252	0,140		292	5,50
	0,0973	0,508		308	5,22
Diamyl.....	0,0202	0,113	342	311	5,62
	0,0272	0,145		327	5,32
	0,129	0,686		330	5,3
Tetraisopropyl <sup>1)</sup> ....	0,0153	0,087	370,6	331	5,6
Pentaisopropyl.....	0,0152	0,086	412,7	379	5,55
	0,131	0,689		398	5,29
	0,147	0,775		400	5,26
Tetracyklo- penty I <sup>1)</sup> .....	0,0141	0,086	475	397	6,1
	0,0201	0,119		409	5,9
Tetracyklo- penty II <sup>2)</sup> .....	0,0156	0,086	475	441	5,5
	0,0227	0,125		428	5,66
Pentacyklopentyl...	0,0147	0,084	543	483	5,73
	0,0198	0,111		494	5,73
	0,110	0,581		523	5,29
Tetracyklohexyl II..	0,0145	0,084	531	472	5,78
	0,0200	0,110		493	5,5
	0,0848	0,439		523	5,2

<sup>1)</sup> Höhere Konzentration konnte wegen Schwerlöslichkeit der Substanz nicht erreicht werden.

<sup>2)</sup> Wegen Stoffmangels konnte in diesem Falle die Konzentration nicht erhöht werden.

Das Tetracyklohexylpyren I ist so schwerlöslich in kaltem Benzol, dass eine Messung unmöglich ist.

DET KGL. DANSKE VIDENSKABERNES SELSKAB  
MATEMATISK-FYSISKE MEDDELELSER, BIND XXII, NR. 16

---

# THE POTENTIAL FUNCTION OF METHANE

WITH AN APPENDIX ON ACETYLENE

BY

BØRGE BAK



KØBENHAVN

I KOMMISSION HOS EJNAR MUNKSGAARD

1946



## CONTENTS

	Page
I. Introduction .....	3
II. Symmetry Considerations .....	4
III. Formulation of Potential Function .....	11
IV. Relations between Force Constants and Vibration Frequencies .....	13
V. Numerical Calculation of the Force Constants of the Potential Function	19
VI. Comparison between Calculated Frequencies and Experimentally De- termined Ones .....	20
VII. Physical Significance of the Results Obtained .....	26
VIII. Brief Treatment of the Acetylene Molecule .....	29
IX. Summary .....	33

---

# THE INTRAMOLECULAR POTENTIAL OF METHANE

## I. Introduction.

The first physicist to formulate the general quadratic vibrational function of Methane was JENNY ROSENTHAL.<sup>1</sup> The complete function includes 5 constants. If the numerical values of these 5 constants are known, a precalculation of the vibration frequencies of methane and deuterated methanes can be carried out.

The first calculation of all 5 constants was published by DENNISON and JOHNSON.<sup>2</sup> At that time only insufficient experimental material from the vibrational analysis of Raman and infrared spectra was available. Hence DENNISON and JOHNSON had to use data from the fine structure of the infrared bands of methane, this resulting in a less accurate determination of the constants as shown below.

Shortly afterwards BARKER and GINSBURG<sup>3</sup> published data from the infrared absorption spectrum of  $CH_3D$ . This in connexion with the well-known vibration frequencies of methane itself enabled a first calculation of the 5 constants on a pure vibrational basis. However, the calculation could not be carried through without a certain arbitrariness. Due to the method used the constants calculated were sometimes real figures, sometimes imaginary ones.—In 1937 BENEDICT, MORIKAWA, BARNES and TAYLOR<sup>4</sup> published their great work on the infrared spectra of mixtures of deuterated methanes. In their paper a forthcoming publication is announced where a potential function, including anharmonic terms, would be used. Apparently the paper has not yet been published.

<sup>1</sup> J. ROSENTHAL, Phys. Rev. **45**, 538 (1934).

<sup>2</sup> DENNISON and JOHNSON, Phys. Rev. **47**, 93 (1935).

<sup>3</sup> BARKER and GINSBURG, Phys. Rev. **47**, 641 (1935); J. Chem. Phys. **3**, 668 (1935).

<sup>4</sup> BENEDICT, MORIKAWA, BARNES and TAYLOR, J. Chem. Phys. **5**, 1 (1937).



As will be seen from what precedes, it will be of importance to have a statement where, firstly, a survey of all the experimental material published is given, and, secondly, this material is utilized for a calculation of the 5 constants in the potential function of methane. The validity of the numerical values should be tested by precalculating the frequencies of all deuterated methanes. We shall here follow the programme sketched, thus for the first time giving a complete survey of the correctness by which we can precalculate the vibration spectra of methane and deuterated methanes, using a quadratic potential function.

Before the calculations are started some words should be said of the method used for attacking the problem. In 1934 HOWARD and BRIGHT WILSON, Jr.<sup>1</sup> demonstrated the use of a general normal-coordinate method, showing the convenience of employing the so-called 'symmetry coordinates'. To derive full advantage of this paper an elementary knowledge of group theory is necessary. This could be acquired by consulting an article by ROSENTHAL and MURPHY.<sup>2</sup> The two papers just cited should be studied, if necessary, before reading the present paper.

## II. Symmetry Considerations.

The methane molecule is placed in an orthogonal  $xyz$  coordinate system as shown in double-projection in fig. 1.

The hydrogen atoms are placed in the positions 1, 2, 3, and 4, the carbon atom in the zero point of the coordinate system. The components of the displacement of the carbon atom are denoted by  $x_0, y_0, z_0$ , the corresponding figures for hydrogen no.  $j$  are  $x_j, y_j, z_j$ .

Geometrically  $CH_4$  and  $CD_4$  belong to the point group  $T_D$ . In table I the characters for the normal modes of vibration are given.

The  $p$ -axis in the  $C_3^p$ -symbol is the line from the carbon atom to  $H(1)$ .—The symmetry element  $\sigma_1$  is the plane through  $H(1) - C - H(3)$ .—Beneath a survey is taken of the ways in

<sup>1</sup> HOWARD and WILSON, Jr., J. Chem. Phys. **2**, 630 (1934).

<sup>2</sup> ROSENTHAL and MURPHY, Rev. Mod. Phys. **8**, 317 (1936).

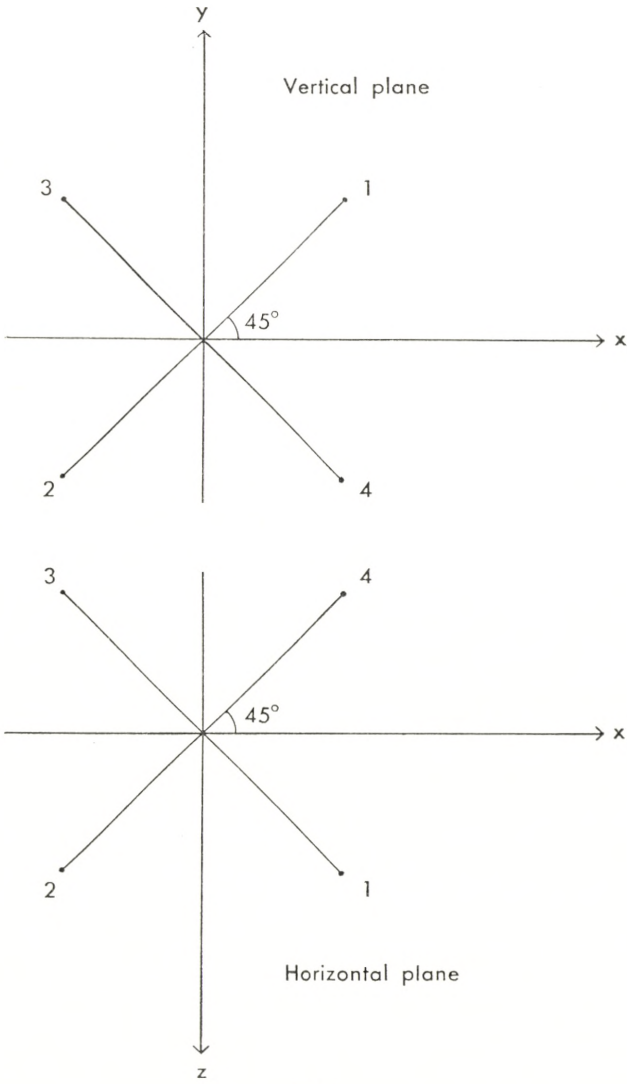


Fig. 1.



Table I.

Covering Operation	$E$	$8 C_3$	$3 C_2$	$6 \sigma_d$	$6 S_4$	Number of modes	Degree of degeneracy
Symmetry class:							
$A_1$ .....	1	1	1	1	1	1	1
$A_2$ .....	1	1	1	-1	-1	0	
$E$ .....	2	-1	2	0	0	1	2
$T_2$ .....	3	0	-1	1	1	2	3
$T_1$ .....	3	0	-1	-1	1	0	
Symmetry elements especially studied:...							
		$C_3^p$	$C_2^x$	$\sigma_I$	$S_4^y$		

which the displacement components  $x_j, y_j, z_j$  vary during the covering operations of the molecule.

By a rotation of  $120^\circ$  round the  $p$ -axis

$$\begin{array}{lll}
 x_0 \rightarrow y_0 & y_0 \rightarrow z_0 & z_0 \rightarrow x_0 \\
 x_1 \rightarrow y_1 & y_1 \rightarrow z_1 & z_1 \rightarrow x_1 \\
 x_2 \rightarrow y_4 & y_2 \rightarrow z_4 & z_2 \rightarrow x_4 \\
 x_3 \rightarrow y_2 & y_3 \rightarrow z_2 & z_3 \rightarrow x_2 \\
 x_4 \rightarrow y_3 & y_4 \rightarrow z_3 & z_4 \rightarrow x_3
 \end{array}$$

By a rotation of  $180^\circ$  round the  $x$ -axis

$$\begin{array}{lll}
 x_0 \rightarrow x_0 & y_0 \rightarrow -y_0 & z_0 \rightarrow -z_0 \\
 x_1 \rightarrow x_4 & y_1 \rightarrow -y_4 & z_1 \rightarrow -z_4 \\
 x_2 \rightarrow x_3 & y_2 \rightarrow -y_3 & z_2 \rightarrow -z_3 \\
 x_3 \rightarrow x_2 & y_3 \rightarrow -y_2 & z_3 \rightarrow -z_2 \\
 x_4 \rightarrow x_1 & y_4 \rightarrow -y_1 & z_4 \rightarrow -z_1
 \end{array}$$

By a reflexion in the plane  $\sigma_I$

$$\begin{array}{lll}
 x_0 \rightarrow z_0 & y_0 \rightarrow y_0 & z_0 \rightarrow x_0 \\
 x_1 \rightarrow z_1 & y_1 \rightarrow y_1 & z_1 \rightarrow x_1 \\
 x_2 \rightarrow z_4 & y_2 \rightarrow y_4 & z_2 \rightarrow x_4 \\
 x_3 \rightarrow z_3 & y_3 \rightarrow y_3 & z_3 \rightarrow x_3 \\
 x_4 \rightarrow z_2 & y_4 \rightarrow y_2 & z_4 \rightarrow x_2
 \end{array}$$

By a 'rotatory reflexion' of  $90^\circ$  round the  $y$ -axis

$$\begin{array}{lll}
 x_0 \rightarrow z_0 & y_0 \rightarrow -y_0 & z_0 \rightarrow -x_0 \\
 x_1 \rightarrow z_2 & y_1 \rightarrow -y_2 & z_1 \rightarrow -x_2 \\
 x_2 \rightarrow z_3 & y_2 \rightarrow -y_3 & z_2 \rightarrow -x_3 \\
 x_3 \rightarrow z_4 & y_3 \rightarrow -y_4 & z_3 \rightarrow -x_4 \\
 x_4 \rightarrow z_1 & y_4 \rightarrow -y_1 & z_4 \rightarrow -x_1
 \end{array}$$

We may now pass on to constructing the symmetry co-ordinates.

**Symmetry coordinate of the  $A_1$ -class ( $S_1$ ).**

The vibration picture of the totally symmetrical vibration (frequency  $\nu_1$ ) could be drawn immediately as shown in fig. 2 (double-projection).

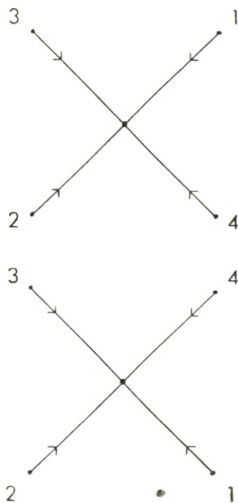


Fig. 2.

In a somewhat loose, but shorthand formulation the amplitude proportions are given by

$$\left. \begin{array}{l}
 x_0 : y_0 : z_0 : x_1 : y_1 : z_1 : x_2 : y_2 : z_2 : x_3 : y_3 : z_3 : x_4 : y_4 : z_4 = \\
 = 0 : 0 : 0 : 1 : 1 : 1 : -1 : -1 : 1 : -1 : 1 : -1 : -1 : 1 : -1. \quad \} (1)
 \end{array} \right.$$

A 'symmetry coordinate' having the symmetry properties of the  $A_1$ -class recorded in table I, is easily seen to be

$$S_1 = x_1 - x_2 - x_3 + x_4 + y_1 - y_2 + y_3 - y_4 + z_1 + z_2 - z_3 - z_4.$$



The conditions that  $S_1$  should be zero for translational and rotational movements of the molecule as a whole, are fulfilled.

### Symmetry coordinates of the $E$ -class ( $S_2$ and $S_3$ ).

According to table I there is one double degenerate vibration in this class. Our task is to find the vibration pictures of two

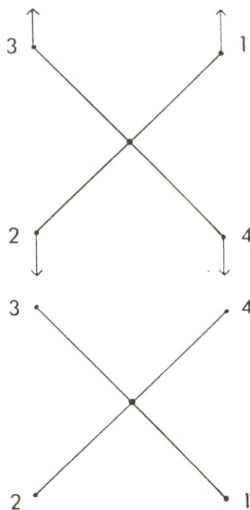


Fig. 3.

mutually orthogonal vibrations, vibrating with the same frequency ( $\nu_{2ab}$ ). To find these vibration pictures one of course makes use of the fact that  $\nu_{2ab}$  is experimentally found to be a so-called 'hydrogen deformation' frequency ( $\nu_{2ab} \sim 1500 \text{ cm}^{-1}$ ). One of these with symmetry properties as demanded by table I is easily drawn (fig. 3).

An arbitrarily chosen vibration of the  $E$ -class, as the one drawn in fig. 3, could generally be conceived as having been formed by a suitable superposition of the two fundamental frequencies  $\nu_{2a}$  and  $\nu_{2b}$  of the class + possibly normal vibrations of higher symmetry, that is, in this case the totally symmetrical vibration  $\nu_1$ . We first want to see if the vibration of fig. 3 has a totally symmetrical component. Actually it has, as the amplitude proportions

$$\left. \begin{aligned} x_0 : y_0 : z_0 : x_1 : y_1 : z_1 : x_2 : y_2 : z_2 : x_3 : y_3 : z_3 : x_4 : y_4 : z_4 = \\ = 0 : 0 : 0 : 0 : 1 : 0 : 0 : -1 : 0 : 0 : 1 : 0 : 0 : -1 : 0 \end{aligned} \right\} (2)$$

are not orthogonal to (1).

To find the pure *E*-class component

$$x'_0 : y'_0 : z'_0 : x'_1 : y'_1 : z'_1 : x'_2 : y'_2 : z'_2 : x'_3 : y'_3 : z'_3 : x'_4 : y'_4 : z'_4 \quad (3)$$

of the fig. 3 vibration, we must solve the vector equation

$$(1) + (3) = k(2).$$

$k(2)$  stands for a vector, the components of which are found from (2) by multiplying each component by  $k$ . This immediately gives the 12 equations:

$$1 + x'_1 = 0 \qquad 1 + y'_1 = k \qquad 1 + z'_1 = 0$$

and so on. The value of  $k$  is found by making use of the condition that (1) and (3) should be mutually orthogonal. We find  $k = 3$  and consequently

$$(3) = 0 : 0 : 0 : -1 : 2 : -1 : 1 : -2 : -1 : 1 : 2 : 1 : -1 : -2 : 1.$$

The vibration picture becomes (fig. 4):

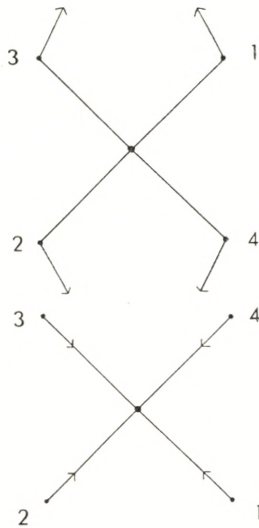


Fig. 4.



Thus, having found one pure  $E$ -class vibration we easily find another orthogonal to the first one. The vibrating molecule of fig. 4 is simply turned  $120^\circ$  round the  $p$ -axis. After the rotation the molecule of course still vibrates with the same frequency as before. The amplitude proportions are

$$0:0:0:2:-1:-1:-2:1:-1:-2:-1:1:2:1:1. \quad (4).$$

(3) and (4) do not make out a pair of normal vibrations, as they are not mutually orthogonal. But we must be able to form (4) by a superposition of (3) and the corresponding orthogonal normal vibration (5), which means that (5) can be determined by the relation

$$(5) + (3) = k(4).$$

The equation is solved as demonstrated above. The result is that  $k = -2$  and

$$(5) = 0:0:0:-3:0:3:3:0:3:3:0:-3:-3:0:-3.$$

Consequently the symmetry coordinates chosen are

$$S_2 = -x_1 + x_2 + x_3 - x_4 - z_1 - z_2 + z_3 + z_4 + 2(y_1 - y_2 + y_3 - y_4)$$

$$S_3 = 3(-x_1 + x_2 + x_3 - x_4 + z_1 + z_2 - z_3 - z_4).$$

Demonstrating that the coordinates above fulfil the requirements of table I we have:

The coordinate  $S'_2$ , having been subjected to a symmetry operation, is denoted by  $S'_i$ . By a rotation of  $180^\circ$  round the  $x$ -axis

$$S'_2 = S_2$$

$$S'_3 = -S_3,$$

that is, the character (the sum of diagonal elements) is 2, consistent with table I.—By a rotation of  $120^\circ$  round the  $p$ -axis

$$S'_2 = -0.5 S_2 + 0.5 S_3$$

$$S'_3 = -1.5 S_2 - 0.5 S_3,$$

which means that the character is  $-1$  as demanded by table I.—In an analogous manner it is shown that the characters are zero by the operations  $\sigma_1$  and  $S'_4$ .

### Symmetry coordinates of the $T_2$ -class ( $S_4, S_5, S_6, S_7, S_8, S_9$ ).

This class contains two triple-degenerate vibrations. Following a procedure quite analogous to the one sketched above we get for the three components of one of the vibrations

$$\begin{aligned} S_5 &= -4x_0 + (x_1 + x_2 + x_3 + x_4) \\ S_4 &= -4y_0 + (y_1 + y_2 + y_3 + y_4) \\ S_6 &= -4z_0 + (z_1 + z_2 + z_3 + z_4). \end{aligned}$$

The components of the second triple-degenerate vibration are chosen as

$$\begin{aligned} S_7 &= -x_1 - x_2 + x_3 + x_4 - z_1 + z_2 + z_3 - z_4 \\ S_8 &= \phantom{-x_1 - x_2 + x_3 + x_4} - z_1 + z_2 - z_3 + z_4 - y_1 - y_2 + y_3 + y_4 \\ S_9 &= -x_1 + x_2 - x_3 + x_4 \phantom{- z_1 + z_2 - z_3 + z_4} - y_1 + y_2 + y_3 - y_4. \end{aligned}$$

### III. Formulation of the Potential Function.

Wishing to formulate the potential as the quadratic expression commonest possible we write the contribution of the vibrations in the  $A_1$ -class as

$$A_2 V = a_1 S_1^2.$$

The contribution from the  $E$ -class is preliminarily written

$$A_2 V = a_2 (S_2^2 + f S_3^2).$$

The constant  $f$  can be determined by the condition that  $A_2 V$  is invariant during any covering operation of the molecule. Thus by a rotation of  $120^\circ$  round the  $p$ -axis

$$\begin{aligned} A_2 V &= a_2 (S_2^2 + f S_3^2) \rightarrow a_2 [(-0.5 S_2 + 0.5 S_3)^2 + \\ &+ f(-1.5 S_2 - 0.5 S_3)^2] = a_2 [S_2^2(0.25 + 2.25 f) + S_3^2(0.25 + 0.25 f) + \\ &+ S_2 S_3(-0.50 + 1.50 f)]. \end{aligned}$$

Identity demands that  $f = 1/3$ .

Before formulating the potential contribution from the  $T_2$ -class we shortly summarize the symmetry properties of the coordinates.



Coordinate \ Operation	$C_2^x$	$\sigma_I$	$S_4^y$	$C_3^p$
$S_4'$ .....	$-S_4$	$S_4$	$-S_4$	$S_6$
$S_5'$ .....	$S_5$	$S_6$	$S_6$	$S_4$
$S_6'$ .....	$-S_6$	$S_5$	$-S_5$	$S_5$
$S_7'$ .....	$-S_7$	$S_7$	$-S_7$	$S_9$
$S_8'$ .....	$S_8$	$S_9$	$S_9$	$S_7$
$S_9'$ .....	$-S_9$	$S_8$	$S_8$	$S_8$

Remembering that only symmetry coordinates with common symmetry properties can form 'mixed' products we get

$$A2V = a_3(S_4^2 + S_5^2 + S_6^2) + a_4(S_4S_7 + S_5S_8 + S_6S_9) + a_5(S_7^2 + S_8^2 + S_9^2).$$

The complete quadratic potential function consequently becomes

$$2V = a_1S_1^2 + a_2\left(S_2^2 + \frac{1}{3}S_3^2\right) + a_3(S_4^2 + S_5^2 + S_6^2) + a_4(S_4S_7 + S_5S_8 + S_6S_9) + a_5(S_7^2 + S_8^2 + S_9^2).$$

The simplicity, by which the problems have been solved here, should be compared with the complexity of e. g. ROSENTHAL's paper.<sup>1</sup>

---

<sup>1</sup> J. ROSENTHAL, Phys. Rev. **45**, 538 (1934).

## IV. Relations between Force Constants and Vibration Frequencies.

### 1. $CH_4$ and $CD_4$ .

Solving the problem of finding these relation in the usual way by means of the Lagrangian equations a. s. o., we get:

The  $A_1$ -class.

$$z_1 = 4 \pi^2 \nu_1^2 = \frac{12 a_1}{m_H} \quad (I)$$


---

The  $E$ -class.

$$z_2 = 4 \pi^2 \nu_{2ab}^2 = \frac{24 a_2}{m_H} \quad (II)$$


---

The  $T_2$ -class.

$$\begin{vmatrix} 2 a_3 - \frac{m_H m_C}{2 M(C H_4)} z & a_4 \\ a_4 & 2 a_5 - \frac{m_H}{4} z \end{vmatrix} = 0 \quad (III).$$

$$\text{Roots: } z_3 = 4 \pi^2 \nu_{3abc}^2; \quad z_4 = 4 \pi^2 \nu_{4abc}^2.$$


---

### 2. $CH_3D$ and $CHD_3$ . (Point group $C_{3v}$ ).

Trying to find the relations desired we should first take into consideration the fact that the number of vibrations with different frequencies (6) is another than for methane (4). The classification of the vibrations also becomes different as seen by table II, giving the characters of the normal modes.

In  $CH_3D$  the deuterium atom is placed in the 1-position (fig. 1).

As appears from table II, *nine* symmetry coordinates are to be defined. This, of course, could be done by simply starting afresh as was done in the case of  $CH_4$  and  $CD_4$ . But as methane and deuterated methanes are isotopic molecules, they all



Table II.

Covering operations	$E$	$2 C_3$	$3 \sigma_v$	Number of modes	Degree of degeneracy
Symmetry classes:					
$A_1$ .....	1	1	1	3	1
$E_1$ .....	2	-1	0	3	2
Symmetry elements especially studied:.....					
		$C_3^p$	$\sigma_I$		

have the same vibrational potential function, i. e. the one written on page 12. This means that calculations are highly facilitated if the symmetry coordinates  $U_1, U_2, \dots, U_9$  of the  $CH_3D$  and  $CHD_3$  molecules could be formulated as functions of the coordinates  $S_1, S_2, \dots, S_9$ . In trying to do this we define that  $U_1, U_2$ , and  $U_3$  should be the symmetry coordinates of the  $A_1$ -class and the rest of the  $U$ 's should represent the  $E_1$ -class.

#### Symmetry coordinates of the $A_1$ -class.

It is immediately seen that we could put  $U_1 = S_1$ .—By considering the survey of the symmetry properties of the coordinates  $S_4, S_5, \dots, S_9$  given at page 12, it is soon recognized that we can choose

$$U_2 = S_4 + S_5 + S_6$$

$$U_3 = S_7 + S_8 + S_9.$$

#### Symmetry coordinates of the $E_1$ -class.

These coordinates constitute three pairs. According to table II one member of a pair must be symmetrical (+), the other antisymmetrical (−) with respect to the symmetry element  $\sigma_I$ . We therefore arrange the coordinates  $S_2, S_3, \dots, S_9$  in the following way:

$$\begin{array}{llllll} (+) \text{ coordinates:} & S_2 & S_4 & S_7 & (S_5 + S_6) & (S_8 + S_9) \\ (-) \text{ coordinates:} & S_3 & & & (S_5 - S_6) & (S_8 - S_9). \end{array}$$

Taking into account the transformation properties of  $S_2$  and  $S_3$  given at page 10 we find that one pair of degenerate symmetry coordinates are

$$U_4 = S_2 \text{ and } U_5 = S_3.$$

Trying to find the two other pairs we find that a good proposal seems, at a first glance, to be the pair

$$S_5 + S_6 \text{ and } S_5 - S_6.$$

By the operation  $C_3^P$ , however,  $S_5 + S_6 \rightarrow S_4 + S_5$ . This shows that somehow  $S_4$  must enter. Let us try to put  $U_6 = fS_4 + (S_5 + S_6)$ .  $U_6$  must be orthogonal to the other  $U$ 's, of which only  $U_2 = S_4 + S_5 + S_6$  comes into consideration (all the other  $U$ 's do not depend upon  $S_4, S_5$ , or  $S_6$ ). The demand for orthogonality gives  $f = -2$ .  $U_6 = -2S_4 + (S_5 + S_6)$ . Let  $U_7$  be the symmetry coordinate which constitutes a pair together with  $U_6$ . We try, of course, to put  $U_7 = S_5 - S_6$ . The necessary conditions, that  $U_7$  should be orthogonal to  $U_2$  and  $U_6$ , are seen to be fulfilled. It only remains to show that the requirement of table II concerning the covering operation  $C_3^P$  is satisfied. We have

$$\begin{array}{ll} U_6 = -2S_4 + S_5 + S_6 & U'_6 = -2S_6 + S_4 + S_5 \\ U_7 = \phantom{-2S_4} S_5 - S_6 & U'_7 = \phantom{-2S_6} S_4 - S_5. \end{array}$$

This gives

$$\begin{aligned} U'_6 &= -\frac{1}{2}U_6 + \frac{3}{2}U_7 \\ U'_7 &= -\frac{1}{2}U_6 - \frac{1}{2}U_7, \end{aligned}$$

that is, the character is  $-1$  in accordance with table II.

In the same way we find

$$\begin{array}{ll} U_8 = -2S_7 + (S_8 + S_9) & \\ U_9 = \phantom{-2S_7} S_8 - S_9. & \end{array}$$

---

Being in possession of the connexion between the  $U$ 's and the  $S$ 's we can easily set up the equations of movement a. s. o. The results are :



The  $A_1$ -class.

$$\begin{array}{l}
 2 a \frac{m_C(3 m_H + m_D) + 8 m_H(m_H + m_D)}{24 M(CH_3D)} z \\
 \frac{M(CH_4)(m_D - m_H)}{24 M(CH_3D)} \\
 \frac{(m_H - m_D) m_C}{24 M(CH_3D)} z \\
 \frac{2}{3} a_3 \frac{(3 m_H + m_D) m_C}{24 M(CH_3D)} z \\
 \frac{1}{3} a_4 \frac{m_C}{24 M(CH_3D)} z \\
 \frac{2}{3} a_5 \frac{m_C(m_H + m_D) + 2 m_H(m_H + 3 m_D)}{24 M(CH_3D)} z \\
 = 0 \quad (IV)
 \end{array}$$

Roots:  $z_1, z_3, z_4$ .

The  $E_1$ -class.

$$\begin{array}{l}
 2 a_3 \frac{6(3 m_H + 5 m_D)}{m_H m_D N_1} z \\
 2 a_4 \\
 - a_4 + 18 \frac{m_D - m_H}{m_H m_D N_1} z \\
 12 a_2 + 8 a_5 - \frac{3}{2} m_H z \\
 12 a_2 - 4 a_5 \\
 - a_4 + 18 \frac{m_D - m_H}{m_H m_D N_1} z \\
 12 a_2 + 2 a_5 - 18 \frac{16 m_H m_D + m_C m_H + 3 m_C m_D}{m_H m_D m_C N_1} z \\
 = 0 \quad (V)
 \end{array}$$

where 
$$N_1 = \frac{12}{m_H^2 m_D^2} m_C (12 m_H^2 m_D + 5 m_H m_D m_C + 3 m_C m_D^2 + 20 m_H m_D^2).$$

Roots:  $z_{2,ab}, z_{3,ab}, z_{4,ab}$ .

3.  $CH_2D_2$ . (Point group  $C_{2v}$ ).

The characters of the vibrations are given in table III. The symmetry element  $\sigma_{II}$  is the plane through  $H(2) - C - H(4)$ . The deuterium atoms are placed in the 2 and 4 positions (fig. 1).

Table III.

Covering operations	$E$	$C_2$	$\sigma_v$	$\sigma_d$	Number of modes	Degree of degeneracy
Symmetry classes:						
$A_1$ .....	1	1	1	1	4	1
$A_2$ .....	1	1	-1	-1	1	1
$B_1$ .....	1	-1	1	-1	2	1
$B_2$ .....	1	-1	-1	1	2	1
Symmetry elements especially studied: .....						
		$C_2^y$	$\sigma_I$	$\sigma_{II}$		

By a rotation of  $180^\circ$  round the  $y$ -axis (symmetry element  $C_2^y$ ).

$$\begin{array}{lll}
 x_0 \rightarrow -x_0 & y_0 \rightarrow y_0 & z_0 \rightarrow -z_0 \\
 x_1 \rightarrow -x_3 & y_1 \rightarrow y_3 & z_1 \rightarrow -z_3 \\
 x_2 \rightarrow -x_4 & y_2 \rightarrow y_4 & z_2 \rightarrow -z_4 \\
 x_3 \rightarrow -x_1 & y_3 \rightarrow y_1 & z_3 \rightarrow -z_1 \\
 x_4 \rightarrow -x_2 & y_4 \rightarrow y_2 & z_4 \rightarrow -z_2
 \end{array}$$

By a reflexion in the plane  $\sigma_{II}$

$$\begin{array}{lll}
 x_0 \rightarrow -z_0 & y_0 \rightarrow y_0 & z_0 \rightarrow -x_0 \\
 x_1 \rightarrow -z_3 & y_1 \rightarrow y_3 & z_1 \rightarrow -x_3 \\
 x_2 \rightarrow -z_2 & y_2 \rightarrow y_2 & z_2 \rightarrow -x_2 \\
 x_3 \rightarrow -z_1 & y_3 \rightarrow y_1 & z_3 \rightarrow -x_1 \\
 x_4 \rightarrow -z_4 & y_4 \rightarrow y_4 & z_4 \rightarrow -x_4
 \end{array}$$

By means of these relations we are able to find out how the previously used symmetry coordinates  $S_1, S_2, \dots, S_9$  vary during the symmetry operations  $C_2^y, \sigma_I$  and  $\sigma_{II}$ , the results being recorded at the top of page 18.

If the symmetry coordinates of the  $A_1$ -class in table III are denoted by  $R_1, R_2, R_3$  and  $R_4$ , we immediately find

$$R_1 = S_1. \quad R_2 = S_2. \quad R_3 = S_4. \quad R_4 = S_7.$$



Coordinate \ Operation	$G_2^y$	$\sigma_1$	$\sigma_{II}$
$S'_1$ .....	$S_1$	$S_1$	$S_1$
$S'_2$ .....	$S_2$	$S_2$	$S_2$
$S'_3$ .....	$S_3$	$-S_3$	$-S_3$
$S'_4$ .....	$S_4$	$S_4$	$S_4$
$S'_5$ .....	$-S_5$	$S_6$	$-S_6$
$S'_6$ .....	$-S_6$	$S_5$	$-S_5$
$S'_7$ .....	$S_7$	$S_7$	$S_7$
$S'_8$ .....	$-S_8$	$S_9$	$-S_9$
$S'_9$ .....	$-S_9$	$S_8$	$-S_8$

If the symmetry coordinate of the  $A_2$ -class is called  $R_5$ , then

$$R_5 = S_3.$$

The symmetry coordinates of the  $B_1$ -class become

$$R_6 = S_5 + S_6. \quad R_7 = S_8 + S_9.$$

The symmetry coordinates of the  $B_2$ -class similarly are

$$R_8 = S_5 - S_6. \quad R_9 = S_8 - S_9.$$

The relation between vibration frequencies and force constants in the symmetry classes  $A_2$ ,  $B_1$ , and  $B_2$  are:

The  $A_2$ -class.

$$z_{2a} = 4 \pi^2 \nu_{2a}^2 = 12 a_2 \frac{m_H + m_D}{m_H m_D}. \tag{VI}$$

The  $B_1$ -class.

$$\left| \begin{array}{cc} \frac{2}{3} a_5 - \frac{8 m_H m_D + m_C (m_H + m_D)}{m_H m_D m_C N_2} z & a_4 + 3 \frac{m_H - m_D}{m_H m_D N_2} z \\ a_4 + 3 \frac{m_H - m_D}{m_H m_D N_2} z & 6 a_3 - 9 \frac{m_H + 3 m_D}{m_H m_D N_2} z \end{array} \right| = 0 \tag{VII}$$

$$N_2 = \frac{6}{m_H^2 m_D^2 m_C} (m_C m_D^2 + 4 m_D m_H^2 + 3 m_C m_H m_D + 12 m_H m_D^2).$$

Roots:  $z_{3a}$ ,  $z_{4a}$ .

The  $B_2$ -class.

$$\left. \begin{aligned} \frac{1}{27} a_5 - 6 \frac{8 m_H m_D + m_C (m_H + m_D)}{m_H m_D m_C N_3} z & - \frac{1}{18} a_4 + 18 \frac{m_H - m_D}{m_H m_D N_3} z \\ - \frac{1}{18} a_4 + 18 \frac{m_H - m_D}{m_H m_D N_3} z & \qquad \frac{1}{3} a_3 - 54 \frac{m_D + 3 m_H}{m_H m_D N_3} z \end{aligned} \right| = 0 \quad (\text{VIII})$$

$$N_3 = \frac{648}{m_H^2 m_D^2 m_C} (4 m_H m_D^2 + 3 m_H m_D m_C + 12 m_D m_H^2 + m_C m_H^2).$$

Roots:  $z_{3c}$ ,  $z_{4c}$ .

## V. Numerical Calculation of the Force Constants of the Potential Function.

This calculation we shall carry through by utilizing vibration frequencies from the spectra of  $CH_4$  and  $CD_4$ . Afterwards we shall pass on to precalculating the vibration frequencies of the partly deuterated methanes, everywhere comparing calculated and experimentally observed frequencies.

The Raman spectrum of gaseous  $CH_4$  has been taken by DICKINSON, DILLON, and RASETTI<sup>1</sup> and by BHAGAVANTAM,<sup>2</sup> the latter taking depolarisation measurements. The Raman spectrum of  $CD_4$  has been reported by McWOOD and UREY.<sup>3</sup> The infrared absorption spectrum of methane was studied by VEDDER and MECKE,<sup>4</sup> by BENEDICT, MORIKAWA, BARNES, and TAYLOR<sup>5</sup> and by NATH.<sup>6</sup> Infrared absorption of  $CD_4$  seems to have been studied by BENEDICT, MORIKAWA, BARNES, and TAYLOR.<sup>5</sup> As the best available experimental material is chosen:

	$CH_4$	$CD_4$
$\nu_1$	2915 $\text{cm}^{-1}$	2085 $\text{cm}^{-1}$
$\nu_{2ab}$	1530 —	
$\nu_{3abc}$	3020 —	2258 —
$\nu_{4abc}$	1320 —	988 —

<sup>1</sup> DICKINSON, DILLON, and RASETTI, Phys. Rev. **34**, 582 (1929).

<sup>2</sup> BHAGAVANTAM, Ind. Jour. Phys. **6**, 595 (1931).

<sup>3</sup> McWOOD and UREY, J. Chem. Phys. **3**, 650 (1935); **4**, 402 (1936).

<sup>4</sup> VEDDER and MECKE. Zeits. f. Physik **86**, 137 (1933).

<sup>5</sup> BENEDICT, MORIKAWA, BARNES, and TAYLOR, J. Chem. Phys. **5**, 1 (1937).

<sup>6</sup> NATH, Ind. Jour. Phys. **8**, 581 (1932).



For further details of experimental values see table IV below. In equation (I) page 13 we substitute  $\nu_1(CH_4) = 2915 \text{ cm}^{-1}$  and get:

$$a_1 = 4.175 \cdot 10^4 \text{ dyne cm}^{-1}.$$

Subsequently we are able to precalculate  $\nu_1(CD_4) = 2068 \text{ cm}^{-1}$ . Experimentally  $\nu_1(CD_4) = 2085 \text{ cm}^{-1}$ .

In equation (II) page 13  $\nu_{2ab}(CH_4) = 1530 \text{ cm}^{-1}$  is substituted. This gives

$$a_2 = 0.5751 \cdot 10^4 \text{ dyne cm}^{-1}.$$

This permits calculating  $\nu_{2ab}(CD_4) = 1085 \text{ cm}^{-1}$ , which has not yet been observed. (Only  $2\nu_{ab} = 2108 \text{ cm}^{-1}$  has been observed. Hence  $\nu_{2ab}(CD_4) = 1054$ ).

Equation (III) page 13 in connexion with the observed frequencies 3020 and  $1320 \text{ cm}^{-1}$  from the  $CH_4$ -spectrum and 2258 and  $988 \text{ cm}^{-1}$  from the  $CD_4$ -spectrum gives

$$a_3 = 5.354 \cdot 10^4 \text{ dyne cm}^{-1}; \quad a_4 = \pm 6.590 \cdot 10^4 \text{ dyne cm}^{-1}; \\ a_5 = 4.430 \cdot 10^4 \text{ dyne cm}^{-1}.$$

To solve the problem of the unknown sign of  $a_4$  we pass on to regard the spectra of  $CH_3D$ . Assuming  $a_4 \geq 0$  we calculate for the vibrations of the  $A_1$ -class:

$a_4 > 0$	$a_4 < 0$	Exp. determined values
1040 $\text{cm}^{-1}$	1307 $\text{cm}^{-1}$	1306.8 $\text{cm}^{-1}$
2712 —	2204 —	2205 —
3005 —	2947 —	2983 —

This definitely shows that  $a_4 < 0$ , a result which is fully confirmed by all other calculations involving  $a_4$ .

## VI. Comparison between Calculated Frequencies and Experimentally Determined Ones.

In table IV a a survey is taken of the experimental results obtained by studying the Raman spectra of methane and deuterated methanes. Table IV b is a corresponding survey of infrared absorption data. In table V experimentally determined frequencies are stated against calculated ones.

Table IV a.

Experimentally determined Raman frequencies of methane and deuterated methanes.

	$CH_4$	$CH_3D$	$CH_2D_2$	$CHD_3$	$CD_4$	Depolarisation measurements for $CH_4$
$\nu_1$	2914.8	—	2139.0	2141.1	2084.7	$\rho = 0.08$
$\nu_{2a}$	[1535.7]	[1460.8]	1332.9	1299.2	[1054]	
$\nu_{2b}$			[1458.2]			
$\nu_{3a}$	3022.1	—	2974.2	2268.6	2258.0	$\rho = 0.80$
$\nu_{3b}$			—			
$\nu_{3c}$			2199.5	—		
$\nu_{4a}$	—	1330.1	1285.6	[981.7]	—	
$\nu_{4b}$			1033.1			
$\nu_{4c}$			[1157.4]	[1038.3]		
	DICKINSON, DILLON, RASETTI, Phys. Rev. <b>34</b> , 582 (1929).	Mc WOOD and UREY, J. Chem. Phys. <b>3</b> , 650 (1935), J. Chem. Phys. <b>4</b> , 402 (1936).			BHAGAVANTAM, Ind. Jour. Phys. <b>6</b> , 595 (1931).	

The frequencies in square brackets have only been found as first over-tones.

A discrepancy between table IV a and IV b is seen in the interpretation of the spectra of  $CH_3D$ . The calculation on page 20 above together with the calculations of DENNISON and JOHNSON<sup>1</sup> support the view that the interpretation of the infrared data given by GINSBURG and BARKER is the more correct one.—For reasons to be given below it seems as if the  $\nu_{4a}$ -frequency in the Raman spectrum of  $CH_2D_2$  should be interchanged with the  $\nu_{4b}$  or  $\nu_{4c}$  frequency.—The marks of interrogation in table IV b indicate that the interpretation given is doubtful.

The infrared data of  $CH_2D_2$  found by BARKER and GINSBURG<sup>2</sup>,

<sup>1</sup> DENNISON and JOHNSON, Phys. Rev. **47**, 93 (1935).

<sup>2</sup> BARKER and GINSBURG, J. Chem. Phys. **3**, 668 (1935).



Table IVb.  
Experimentally determined infrared vibration frequencies  
of methane and deuterated methanes.

	$CH_4$	$CH_3D$	$CH_2D_2$	$CHD_3$	$CD_4$
$\nu_1$	2915	2983	—	—	—
$\nu_{2a}$	1530	1477	—	—	—
$\nu_{2b}$			1450		
$\nu_{3a}$	3020	3031	2255?	2260	2258
$\nu_{3b}$			?		
$\nu_{3c}$			2205	3020?	
$\nu_{4a}$	1320	1156.3	1235?	988	988
$\nu_{4b}$			1035?		
$\nu_{4c}$			1306.8	1035?	
	VEDDER and MECKE, Zeits. f. Phys. <b>86</b> , 137 (1933).	GINSBURG and BARKER, J. Chem. Phys. <b>3</b> , 668 (1935).	BENEDICT, MORIKAWA, BARNES, TAYLOR, J. Chem. Phys. <b>5</b> , 1 (1937).		

BENEDICT *et al.*<sup>1</sup> unfortunately are published in a manner so as to make the assignment of frequencies doubtful. In referring to vibration frequencies of methane and the isotopic molecules two systems have been used: the system of ROSENTHAL, denoting frequencies by  $\nu_1$ ,  $\nu_{2a}$  a. s. o., and, in the case of  $CH_2D_2$ , the system of DENNISON, where the frequencies are denoted in accordance with the way in which the electrical moment varies during the vibration, 'M', 'L', or 'G' being put before or after the frequency figures. Unfortunately none of these systems was employed in the papers of BARKER and BENEDICT.—Another circumstance contributing to the confusion as regards the  $CH_2D_2$ -spectrum lies in the fact that undoubtedly the early precalculation of frequencies made by DENNISON has played a more dominant rôle than has purely experimental studies (fine struc-

<sup>1</sup> BENEDICT, J. Chem. Phys. **5**, 1 (1937).

ture of the single bands a. s. o.) by the assignment of frequencies. It seems, however, as if some sort of mistake has got into the paper of DENNISON and JOHNSON. As mentioned the vibrations are classified as 'M', 'L', or 'G' vibrations, this being convenient, because the  $CH_2D_2$  molecule has three unequal moments of inertia. The axis about which the moment of inertia is the least, is denoted by 'L', the axis of middle moment of inertia by 'M' and the axis of greatest moment of inertia by 'G'. A vibration by which the electrical moment varies along the 'L' axis, is called an 'L' vibration a. s. o.—In their paper DENNISON and JOHNSON state that

'L'-frequencies should be at 3013 and 1082  $cm^{-1}$ .  
 'G'- — - - - 2227 and 1228 -

It is easy to show that 'L'-frequencies are the frequencies of the  $B_2$ -class (here denoted by  $\nu_{3c}$  and  $\nu_{4c}$ ), while the 'G'-frequencies are the frequencies of the  $B_1$ -class (here denoted by  $\nu_{3a}$  and  $\nu_{4a}$ ). By the precalculation of  $CH_2D_2$ -frequencies made in this paper, it is found that

'L'-frequencies should be at 2258 and 1230  $cm^{-1}$ .  
 'G'- — - - - 3021 - 1093 -

Fig. 5 a shows the  $CH_2D_2$  molecule in the  $M, L, G$  coordinate system, figs. 5 b and 5 c show a 'G' and an 'L' vibration.

As will be seen we must expect to find a hydrogen 'valence' vibration among the 'G'-vibrations, that is, one of the 'G'-vibrations should be located in the neighbourhood of 3000  $cm^{-1}$ . Similarly a deuterium 'valence' vibration must be among the 'L'-vibrations, that is, one of the 'L' vibrations must be near 2200  $cm^{-1}$ . These facts are reproduced best by the calculation made in this paper, while DENNISON and JOHNSON, in their paper, come to the opposite conclusion.

In table V theoretically computed and experimentally found frequency values are compared. By the assignment of frequencies of the  $CH_2D_2$ -spectrum, one has been chosen which is consistent with the frequency values calculated here.



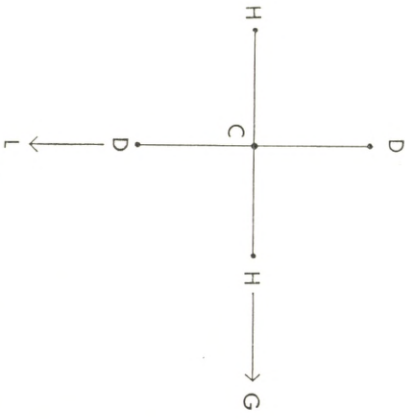
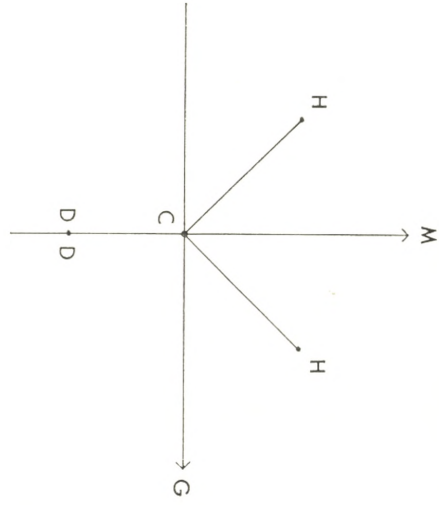


Fig. 5 a.

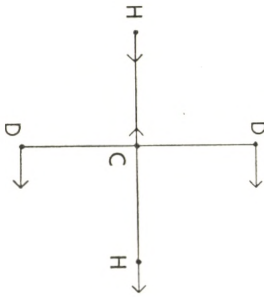
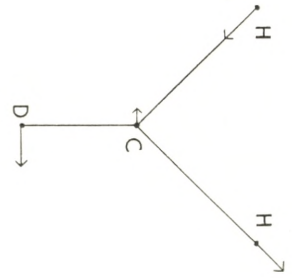


Fig. 5 b.

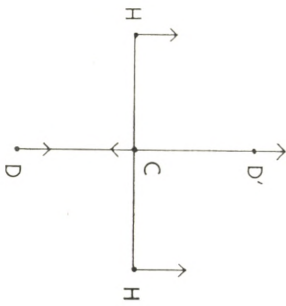
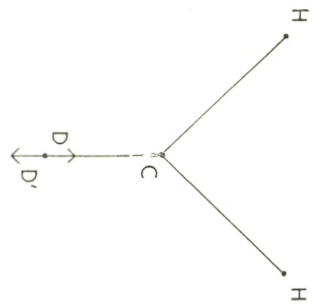


Fig. 5 c.

Table V.

		Calculated by DENNISON	Experimentally determined	Calculated in this paper
$CH_4$	$\nu_1$	2914	2915	2915
	$\nu_2$	1520	1530	1530
	$\nu_3$	3014	3020	3023
	$\nu_4$	1304	1320	1312
$CD_4$	$\nu_1$	2061	2085	2068
	$\nu_2$	1075	1054	1085
	$\nu_3$	2227	2258	2258
	$\nu_4$	987	988	988
$CH_3D$	$\nu_1$	2944	2983	2947
	$\nu_{2\ ab}$	1460	1477	1458
	$\nu_{3\ ab}$	3013	3031	3022
	$\nu_{3\ c}$	2183	2205	2204
	$\nu_{4\ ab}$	1151	1156	1177
	$\nu_{4\ c}$	1300	1307	1307
$CDH_3$	$\nu_1$	2101	2141	2114
	$\nu_{2\ ab}$	1286	1299	1264
	$\nu_{3\ ab}$	2222	2260	2292
	$\nu_{3\ c}$	2992	3000	2998
	$\nu_{4\ ab}$	1020	988	1020
	$\nu_{4\ c}$	994	988	1002
$CH_2D_2$	$\nu_1$	2141	2139	—
	$\nu_{2\ a}$	1317	1333	1326
	$\nu_{2\ b}$	1424	1458	—
	$\nu_{3\ a}$	2227	2974	3021
	$\nu_{3\ b}$	2969	—	—
	$\nu_{3\ c}$	3013	—	2258
	$\nu_{4\ a}$	1228	1038   1090	1093
	$\nu_{4\ b}$	1019	1033   —	—
	$\nu_{4\ c}$	1151	1285   1235	1230
			(Raman <sup>1</sup> )   (Infrared <sup>2</sup> )	

<sup>1</sup> MCWOOD and UREY, *loc. cit.*<sup>2</sup> BARKER and GINSBURG, *loc. cit.*



## VII. Physical Significance of the Results Obtained.

In order to be able to give an account of the above results in a lucid form—which will, at the same time, enable us to make comparisons between methane and other molecules—it is necessary to study the intramolecular forces in some perspicuous cases. In what follows two cases of special simplicity will be examined.

### Case 1.

In this case the carbon atom and  $H(1)$  are thought to be bound to their equilibrium positions by some imaginary forces.  $H(2)$ ,  $H(3)$ , and  $H(4)$  are given the same displacement along the direction carbon-hydrogen. The situation is illustrated in fig 6.

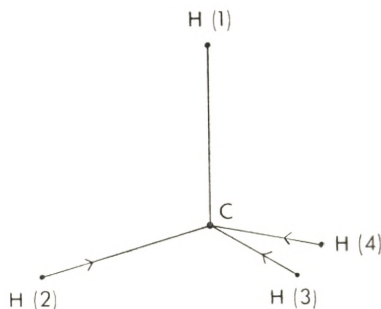


Fig. 6.

The displacements have been chosen so that

$$\begin{array}{llll}
 x_0 = 0 & y_0 = 0 & z_0 = 0 & \\
 x_1 = 0 & y_1 = 0 & z_1 = 0 & S_1 = 9 \quad S_4 = -1 \quad S_7 = 2 \\
 x_2 = -1 & y_2 = -1 & z_2 = 1 & S_2 = 0 \quad S_5 = -1 \quad S_8 = 2 \\
 x_3 = -1 & y_3 = 1 & z_3 = -1 & S_3 = 0 \quad S_6 = -1 \quad S_9 = 2 \\
 x_4 = 1 & y_4 = -1 & z_4 = -1 &
 \end{array}$$

The force acting upon hydrogen atom no.  $j$  in the direction of the  $X$ -axis (fig. 1) being denoted as  $K_{H(j)}(X)$  it is easily shown that

$$K_{H(1)}(X) = -9 a_1 + a_3 - 2 a_4 + 4 a_5 = K_{H(1)}(Y) = K_{H(1)}(Z).$$

$$K_{H(2)}(X) = 9 a_1 + a_3 - a_4 = K_{H(2)}(Y).$$

$$K_{H(2)}(Z) = -9 a_1 + a_3 - 4 a_5$$

$$K_C(X) = 4(a_4 - a_3) = K_C(Y) = K_C(Z).$$

In units of  $10^4$  dyne  $\text{cm}^{-1}$  the values of the constants are

$$a_1 = 4.175 \quad a_2 = 0.5751 \quad a_3 = 5.354 \quad a_4 = -6.590 \quad a_5 = 4.430.$$

By insertion of these values we get

$$K_{H(1)}(X) = -1.321 = K_{H(1)}(Y) = K_{H(1)}(Z).$$

By  $K_{H(1)}$  we denote the resulting force acting upon  $H(1)$ . Consequently

$$K_{H(1)} = +1.321\sqrt{3} = 2.288.$$

$$K_{H(2)} = 82.14$$

$$K_C = 79.29$$

The calculation shows that the movements of the hydrogen atoms along the direction carbon-hydrogen take place approximately independently of each other.

### Case 2.

As appears from fig. 7  $H(1)$  is displaced perpendicularly to the  $C-H(1)$ -direction. All the other atoms are kept in their equilibrium positions. For this displacement  $x_1 = z_1 = 1$ .  $y_1 = -2$ .  $S_1 = S_3 = 0$   $S_2 = -6$ .  $S_4 = S_7 = -2$   $S_5 = S_6 = S_7 = S_8 = 1$ .

$$\begin{array}{ll} K_{H(1)}(X) = -6 a_2 - a_3 - a_4 - a_5 & K_{H(1)}(Y) = 12 a_2 + 2 a_3 + 2 a_4 + 2 a_5 \\ K_{H(2)}(X) = 6 a_2 - a_3 - 2 a_4 - 3 a_5 & K_{H(2)}(Y) = -12 a_2 + 2 a_3 + a_4 \\ K_{H(3)}(X) = 6 a_2 - a_3 + a_4 + 3 a_5 & K_{H(3)}(Y) = 12 a_2 + 2 a_3 - 2 a_5 \\ K_{H(4)}(X) = -6 a_2 - a_3 + a_5 & K_{H(4)}(Y) = -12 a_2 + 2 a_3 + a_4 \\ K_C(X) = 4 a_3 + 2 a_4 & K_C(Y) = -8 a_3 - 4 a_4 \end{array}$$

$$K_{H(1)}(Z) = -6 a_2 - a_3 - a_4 - a_5$$

$$K_{H(2)}(Z) = -6 a_2 - a_3 + a_5$$

$$K_{H(3)}(Z) = 6 a_2 - a_3 + a_4 + 3 a_5$$

$$K_{H(4)}(Z) = 6 a_2 - a_3 - 2 a_4 - 3 a_5$$

$$K_C(Z) = 4 a_3 + 2 a_4$$

By substitution of numerical values we find

$$K_{H(1)} = 16.27. \quad K_{H(2)} = 5.55. \quad K_{H(3)} = 11.0. \quad K_{H(4)} = 5.55. \quad K_C = 20.18.$$

Movements of the hydrogen atoms perpendicular to the carbon-hydrogen bond could not be considered as being independent of each other.

At the present stage the study of general quadratic potential functions of polyatomic molecules is hardly possible because of the great number of constants involved in the potential function. At present it seems impossible to avoid the use of empirical rules stated with certainty in the case of simple molecules. Such rules would give some relations between the (theoretically independent) force constants. Let us e. g. consider the rule

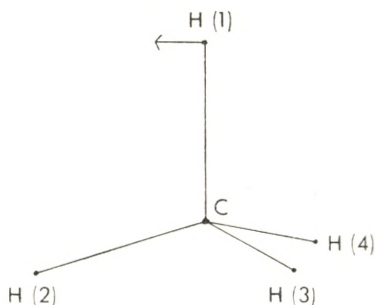


Fig. 7.

stated in *Case 1* for methane. If a more general validity of this rule could be secured, it would be a great help, e. g. in the study of the ethane molecule. It seems natural to assume, however, that deviations from the above rule are more likely to occur in dealing with molecules possessing an electronic structure essentially different from the electronic structure of methane. Here the *acetylene molecule* represents a good test example. In the following chapter a brief treatment of the acetylene molecule is given. The result is that the validity of the rule, stated in *Case 1* for methane, is shown in the case of acetylene, too. The writer hopes to be able to demonstrate the use of this and similar valuable empirical rules in future work.



## VIII. Brief Treatment of the Acetylene Molecule.

The distribution of the vibrations of  $C_2H_2$  and  $C_2D_2$  (point group  $D_{\infty h}$ ) has been given by GLOCKLER and MORRELL.<sup>1</sup>

Table VI.

Class	Sym.	Antisym.	Number of frequencies	Degree of degeneracy	Vibration frequencies
$A_1$ .....	$C_{\infty}, \sigma_v, i$		2	1	$\nu_1 \nu_2$
$A_2$ .....	$C_{\infty}, \sigma_v,$	$i$	1	1	$\nu_3$
$B_1$ .....	$\sigma_v, i$	$C_{\infty}$	1	2	$\nu_{4, 5}$
$B_2$ .....	$\sigma_v$	$C_{\infty}, i$	1	2	$\nu_{6, 7}$

Corresponding to the frequency denotation the symmetry coordinates are defined as follows:

$$S_1 = x_0 - x_1.$$

$$S_2 = x_2 - x_3.$$

$$S_3 = x_0 + x_1 - x_2 - x_3.$$

$$S_4 = \frac{r}{R} (y_0 - y_1) - y_2 + y_3.$$

$$S_5 = \frac{r}{R} (-z_0 + z_1) + z_2 - z_3.$$

$$S_6 = y_0 + y_1 - y_2 - y_3.$$

$$S_7 = z_0 + z_1 - z_2 - z_3,$$

the acetylene molecule being placed in the coordinate system as demonstrated in fig. 8.

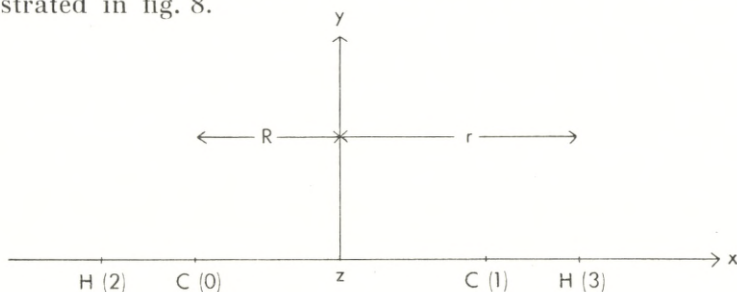


Fig. 8.

<sup>1</sup> GLOCKLER and MORRELL, J. Chem. Phys. 4, 15 (1936).

### Relations between force-constants and vibration frequencies.

The potential contribution of the  $A_1$ -class is formulated as

$$A_2 V = a_1 S_1^2 + a_2 S_2^2 + a_3 S_1 S_2.$$

Consequently the secular equation becomes

$$\begin{vmatrix} 2 a_1 - m_C z & a_3 \\ a_3 & 2 a_2 - m_H z \end{vmatrix} = 0. \quad (1)$$

Roots:  $z_1$  and  $z_2$ .

The  $A_2$ -class.

$$A_2 V = a_4 S_3^2, \quad a_4 = \frac{m_C m_H}{2(m_H + m_C)} z_3. \quad (2)$$

The  $B_1$ -class.

$$A_2 V = a_5 (S_4^2 + S_5^2), \quad a_5 = \frac{m_H m_C}{2 \left( m_C + m_H \left( \frac{r}{R} \right)^2 \right)} z_{4,5}. \quad (3)$$

The  $B$ -class.

$$A_2 V = a_6 (S_6^2 + S_7^2), \quad a_6 = \frac{m_H m_C}{2(m_H + m_C)} z_{6,7}. \quad (4)$$

The numerical values of the above-mentioned force constants will now be calculated on the basis of data from Raman and infrared spectra of  $C_2 H_2$  and  $C_2 D_2$ . A good survey of the experimental material available is given by STITT.<sup>1</sup> Beneath the experimentally determined vibration frequencies are stated.

#### $C_2 H_2$ .

$\nu_1 = 1974$  BHAGAVANTAM and RAO, Proc. Ind. Acad. Sci. 3 A, 135 (1936) (R).

GLOCKLER and MORRELL, J. Chem. Phys. 4, 15 (1936) (I).

$\nu_2 = 3372$  The same references as for  $\nu_1$ .

$\nu_3 = 3288$  } LEVIN and MEYER, J. Opt. Soc. Am. 16, 137 (1928) (I).

$\nu_{6,7} = 730$  }

$\nu_{4,5} = 612$  MECKE and ZIEGLER, Zeits. f. Phys. 101, 405 (1936) (I).

#### $C_2 D_2$ .

$\nu_1 = 1762$  } GLOCKLER and MORRELL, J. Chem. Phys. 4, 14 (1936) (I).

$\nu_2 = 2700$  }

$\nu_3 = 2428$  } FRED STITT, J. Chem. Phys. 8, 56 (1940) (I).

$\nu_{6,7} = 539$  }

$\nu_{4,5} = 506$  }

(I) = Infrared absorption; (R) = Raman spectrum.

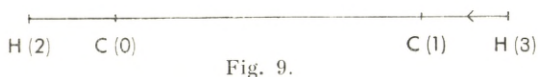
<sup>1</sup> FRED STITT, J. Chem. Phys. 8, 56 (1940).





The table at the bottom of page 31 shows the result of precalculating the complete vibration spectra of  $C_2H_2$ ,  $C_2HD$ , and  $C_2D_2$ , using the numerical values of the force constants just given. As will be seen from (5) the spectrum of  $C_2DH$  does not help us to find the correct sign of  $a_3$ , as only  $a_3^2$  enters.

Having thus demonstrated the correctness of the force-constants we proceed to study the intramolecular forces.  $H(3)$  is displaced from its equilibrium position as shown in fig. 9.



We choose  $x_3 = -1$  and get  $S_1 = S_4 = S_5 = S_6 = S_7 = 0$ ,  $S_2 = S_3 = 1$ .

By means of the usual procedure we find

$$K_{C(0)} = -\frac{1}{2}a_3 - a_4; \quad K_{C(1)} = \frac{1}{2}a_3 - a_4; \quad K_{H(2)} = -a_2 + a_4;$$

$$K_{H(3)} = a_2 + a_4.$$

Substituting the numerical values for the force-constants we get

	$a_3 < 0$	$a_3 > 0$
$K_{C(0)} \dots \dots$	0.0989	-5.9761
$K_{C(1)} \dots \dots$	-5.9761	0.0989
$K_{H(2)} \dots \dots$	0.0455	0.0455
$K_{H(3)} \dots \dots$	5.8317	5.8317

Independently of the sign of  $a_3$  it is seen that  $K_{H(2)}:K_{H(3)}$  has about the same value as found by the corresponding displacement by methane. The two hydrogen atoms move independently.—As it seems correct to assume that the force acting upon the carbon atom beside the displaced hydrogen atom, is the greater, we see that  $a_3 < 0$ . This means, however, that beyond the neighbour carbon atom scarcely any effect is exerted by the hydrogen atom attacked. As already mentioned this is the same rule as developed by methane, and it should be mentioned that it is also valid in the case of  $H-C \equiv N$ , as shown in the present writer's doctor's thesis.<sup>1</sup>

<sup>1</sup> B. BAK, Det indremolekylære Potential, Kbhvn. 1943.

## IX. Summary.

(1) The equations between vibration frequencies of methane and deuterated methanes have been deduced. It is proposed that the ideas of HOWARD and WILSON in connexion with the group-theoretical tables by ROSENTHAL should be more commonly used in solving vibrational problems.

(2) By means of vibration frequencies from the spectra of  $CH_4$  and  $CD_4$ , numerical values of 5 'harmonic' force constants have been calculated. This makes it possible to precalculate the entire spectra of all the partly deuterated methanes. The agreement between observed and calculated values as a rule is excellent.

(3) Empirical rules which might be of use in dealing with more complex molecules have been looked for, and it is shown that the displacement of a hydrogen atom towards its adjoining carbon atom produces little effect on all the other atoms of the molecule. It is demonstrated that the rule holds good, too, in the case of  $C_2H_2$  and  $HCN$ .

*Universitetets kemiske Laboratorium,*  
*Copenhagen.*





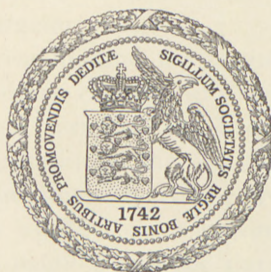
DET KGL. DANSKE VIDENSKABERNES SELSKAB  
MATEMATISK-FYSISKE MEDDELELSER, BIND XXII, NR. 17

---

THE THERMODYNAMIC  
PROPERTIES OF PARAFFIN  
MIXTURES. I

BY

J. N. BRØNSTED AND JØRGEN KOEFOED



KØBENHAVN

I KOMMISSION HOS EJNAR MUNKSGAARD

1946

## CONTENTS

	Page
1. Introduction .....	3
2. Previous Investigations .....	4
3. The Deviation of Paraffin Vapour from the Ideal Gas Laws .....	6
4. Application of Vapour Pressure Measurements for Determination of the Activity Coefficient in Solutions .....	8
5. Experimental Method .....	11
6. Materials .....	15
7. Experimental Results .....	16
8. Mathematical and Graphical Representation of the Experimental Results	23
9. The Complete Curve System .....	26
10. The Concept of Congruence. The General Equation for the Activity Coefficients of Normal Paraffins .....	29
11. Summary .....	31

---



## 1. Introduction.

The present paper contains an investigation on some thermodynamic properties of mixtures of normal paraffins at constant temperature. It forms a continuation of previous work on the influence of the size of molecules upon their thermodynamic behaviour in solution.<sup>1</sup> This influence is clearly demonstrated when comparing molecules approximately identical in chemical respect and deviating from each other only regarding magnitude. Molecules of this kind have been described as "isochemical" molecules.

The normal paraffins constitute a series in which the isochemical relationship is particularly conspicuous. On the thermodynamics of these mixtures there exists only little information. The general opinion undoubtedly is to regard them as ideal or almost ideal solutions. The present investigation does not support this view. They cannot be described as perfect solutions nor do they belong to the group of so called "regular" solutions. Nevertheless they possess, in their own way, properties of a singularly simple character.

A direct and obvious method for testing the thermodynamic nature of paraffin solutions consists in determining the solubility of a solid paraffin in a series of the lower liquid homologues. In the case of ideal conditions the solubility in terms of mole fractions should remain constant, irrespective of the individuality of the liquid paraffin applied as a solvent. With the paraffin  $C_{34}H_{70}$  as saturating substance and the paraffins from hexane to cetane as solvents it was shown in this laboratory already in 1938 that great deviations from ideality actually existed in these

<sup>1</sup> J. N. BRØNSTED: C. r. d. Lab. Carlsberg. **22**, 99 (1938) (with further references).



mixtures, but as the investigations in question are not yet concluded, the results are being reserved for later publication.

Another method for testing the character of the solution and for quantitatively determining their deviations from the ideal laws consists in measuring the vapour pressure of a volatile component in dependence of its concentration in the liquid mixture. It must be recognized, however, that a satisfactory utilization of this principle demands a very considerable increase in the accuracy of the experimental methods so far in existence. Furthermore the question of the deviations of the paraffin vapours from the laws of perfect gases has to be considered. The present article deals with the problem indicated from these points of view.

## 2. Previous Investigations.

Very few data of significance to the problem in hand can be obtained from existing literature. LESLIE and CARR<sup>1</sup> have determined concentration-boiling point diagrams for the systems hexane-heptane, hexane-octane, and heptane-octane, but their results are too inaccurate to be of any value for our calculations. CALINGAERT and HITCHCOCK<sup>2</sup> determined the volume-pressure relations in the heterogeneous vapour-liquid systems of butane-pentane, butane-heptane, and pentane-heptane, and were able from these determinations without a special analysis of the vapour to calculate the composition of the co-existing phases. In the case of butane-heptane they found conformity with the laws of perfect solutions, whereas in the two other cases the vapour pressures came out considerably below the ideal values. This result must be looked upon as subject to doubt since the butane-heptane system consists of the more dissimilar components and therefore should give the greater deviation from ideality. It must be assumed, therefore, that the accuracy of these measurements is insufficient. Also the assumption of the validity of the gas laws at the rather high pressures applied is hardly permissible. For

<sup>1</sup> E. H. LESLIE a. A. R. CARR: *Ind. Eng. Chem.* **17**, 810 (1925).

<sup>2</sup> G. CALINGAERT a. L. B. HITCHCOCK: *J. Am. Chem. Soc.* **49**, 750 (1927).  
Cf. also H. A. BEATTY a. G. CALINGAERT: *Ind. Eng. Chem.* **26**, 304 (1934), G. L. MATHESON a. L. W. T. CUMMINGS: *Ibid.* **25**, 724 (1943).

similar reasons the work of SAGE and LACEY<sup>1</sup> on propane-pentane and other mixtures is of no value for our purpose.

Of greater interest are the careful and accurate measurements by HILDEBRAND<sup>2</sup> of the vapour pressure in the hexane-cetane system at 25° C. In this system the vapour pressure is exerted solely by the volatile component, and the measurements for that reason lend themselves to a much simpler interpretation. By plotting the ratio of the vapour pressure  $p/p_0$  against the mole fraction in the liquid mixture an almost straight line comes out. Or, in the words of the author, "The ratio of the vapour pressure of hexane from the solution to that from the pure liquid,  $p/p_0$ , agrees with its mole fraction  $N$ , within what is doubtless the experimental error." This result undoubtedly suggests the presence of ideal conditions in the liquid mixture of hexane and cetane. From a few measurements at lower temperatures (14° C. —23° C.) yielding the same value for  $p/p_0N$  as the measurements at 25° C. HILDEBRAND infers that also the entropy of the mixture follows Raoult's law, i. e. has the ideal value.

A close inspection of HILDEBRAND's data in the region dilute in hexane shows vapour pressures somewhat below those calculated from the straight line relationship. The method employed, however, does not permit of accurate determinations in this region. It is not surprising, therefore, that no attention is paid by the author to these small deviations, even though the region in which they seem to appear is undoubtedly the most interesting from a theoretical point of view.

The problem of the thermodynamic properties of n-paraffin mixtures from the standpoint of statistical mechanics was dealt with in a previous paper by HILDEBRAND.<sup>3</sup> On the assumption that the entropy in the mixture depends mainly on the possible configurations, and assuming that an idealization of the mixture as a parallel arrangement of the long paraffin molecules is permissible as an approximation, the ideal value —  $R \ln x_i$  for the entropy of a paraffin component  $i$  in the mixture was derived. This again on certain simplifying assumptions leads to ideal thermodynamic properties for the mixture in general. The results

<sup>1</sup> B. H. SAGE and W. N. LACEY: *Ind. Eng. Chem.* **32**, 442 (1940). Cf. also W. B. KAY: *ibid.* **30**, 459 (1938).

<sup>2</sup> J. HILDEBRAND: *J. Phys. Chem.* **43**, 109, 297 (1939).

<sup>3</sup> J. HILDEBRAND: *J. Am. Chem. Soc.* **59**, 794 (1937).



of the measurements are looked upon as a corroboration of this theory.

FOWLER and RUSHBROOKE<sup>1</sup> have made an attempt to extend the statistical theory of perfect solutions<sup>2</sup> to mixtures in which the molecules are distinctly unequal in size. They reduce the liquid arrangements to those of a simple regular lattice and represent a change of size by taking one molecule twice the other and requiring it to occupy two adjacent lattice points. Furthermore all configurations are assumed to have the same energy. On the basis of these simplifying assumptions they show that deviations from the ideal vapour pressure curves may be due to the components of the mixture differing widely in molecular size and not necessarily due to intermolecular forces.

In the paper just mentioned HILDEBRAND also refers to some solubility determinations with dicetyl as a solute and various liquid paraffins as solvents. Similar determinations are reported by SEYERS.<sup>3</sup> We shall, however, postpone the discussion of these measurements, which are of no great accuracy, to a subsequent communication.

### 3. The Deviation of Paraffin Vapour from the Ideal Gas Laws.

An imperfect gas, within small pressure intervals, may in many cases obey the following equation of state<sup>4</sup>:

$$p(v + \Delta) = RT, \quad (1)$$

where  $\Delta$ , the residual volume, is a positive constant independent of pressure, but dependent on temperature. When the ideal mole volume is  $v^*$ ,  $\Delta$  evidently is given by:

$$v^* - v = \Delta. \quad (2)$$

If by  $\mu$  and  $a$ , respectively, we denote the chemical potential and activity of the gas considered, we have at constant temperature:

<sup>1</sup> R. H. FOWLER a. G. S. RUSHBROOKE: *Trans. Far. Soc.* **33**, 1272 (1937).

<sup>2</sup> Cf. E. A. GUGGENHEIM: *J. Phys. Chem.* **34**, 1751 (1930), *Proc. Royal Soc. A* **135**, 181 (1932), **148**, 304 (1935), *Trans. Far. Soc.* **33**, 151 (1937).

<sup>3</sup> W. F. SEYERS: *J. Am. Chem. Soc.* **60**, 827 (1938).

<sup>4</sup> LEWIS a. RANDALL: *Thermodynamics*, 197 (1923).



$$\mu - \mu_0 = RT \ln a, \quad (3)$$

or:

$$d\mu = RT d \ln a = v dp. \quad (4)$$

By introducing (1) in (4) we get:

$$d\mu = RT d \ln a = RT d \ln p - \Delta dp, \quad (5)$$

or:

$$\mu - \mu_0 = RT \ln a = RT \ln \frac{p}{p_0} + \Delta(p_0 - p). \quad (6)$$

In this equation  $\mu_0$  is obviously the potential of the gas in a standard state in which  $a = a_0 = 1$  and  $p = p_0$ .

Equation (6) expresses the chemical loss of work connected with the differential and isothermal transfer of one mole from  $p$  to  $p_0$ . The last term of the equation is the correction caused by the deviation of the gas from the ideal equation of state.

Measurements by S. YOUNG<sup>1</sup> at various temperatures gave densities of saturated hexane vapour corresponding to the following values of  $\Delta$ :

t (C°)	$\Delta$ (L)
56.4	1.97
77.6	1.42
103	1.10
124.5	0.99

An uncertain extrapolation from these temperatures to 20° results in a value about 3 L for  $\Delta$ . YOUNG's data, however, are hardly very exact. A greater accuracy is obtained by extrapolating with regard to  $v$ , i. e. the number of carbon atoms in the paraffin molecule on the basis of the following more recent information.

From the data of SAGE, WEBSTER a. LACEY<sup>2</sup> and SAGE, SCAAFSMA a. LACEY<sup>3</sup>, who have determined the ratio of fugacity to pressure of some normal paraffins, the expression:

$$\log \frac{a}{p} = -\alpha p + \beta, \quad (7)$$

<sup>1</sup> S. YOUNG: J. Chem. Soc. 1895, 1082.

<sup>2</sup> B. H. SAGE, D. C. WEBSTER a. W. N. LACEY: Ind. Eng. Ch. **29**, 1188 (1937).

<sup>3</sup> B. H. SAGE, J. G. SCAAFSMA a. W. N. LACEY: Ibid. **26**, 1218 (1934), **27**, 49 (1935).

where  $a$  stands for activity, is derived for propane, butane, and pentane at  $21^{\circ}.1$  C. The values of  $a$  for these paraffins, which are also in conformity with DESCHNER a. BROWN'S<sup>1</sup> measurements on propane at  $30^{\circ}$  and  $50^{\circ}$  C. and with the value found for hexane in the present investigations (see p. 15) are given in Table 1, the pressure being reckoned in cm Hg.

Table 1.

n-Paraffin	$a$	$\log a$	$\Delta$
C <sub>3</sub> H <sub>8</sub>	$0.95 \cdot 10^{-4}$	$\bar{5}.978$	0.4
C <sub>4</sub> H <sub>10</sub>	1.67 -	$\bar{4}.223$	0.7
C <sub>5</sub> H <sub>12</sub>	2.98 -	$\bar{4}.474$	1.3
C <sub>6</sub> H <sub>14</sub>	5.0 -	$\bar{4}.699$	2.1
C <sub>7</sub> H <sub>16</sub>	8.7 -	$\bar{4}.94$	3.7

By plotting  $\log a$  against  $\nu$  we obtain a straight line for the 4 paraffins, and an extrapolation from this line gives the  $a$ -value for heptane stated in the table. The corresponding  $\Delta$ -values computed from (6) and (7) by the equation:

$$a = \frac{\Delta}{RT} \cdot \frac{0.4343}{76},$$

where  $R = 0.08206$ , and expressed in L, are also given in the table.

#### 4. Application of Vapour Pressure Measurements for Determination of the Activity Coefficient in Solutions.

In applying equation (6) for the determination of activity and activity coefficients in the liquid mixture, we shall assume the liquid system to consist of a volatile component  $K_1$  and a non-volatile component  $K_2$ . The activity of  $K_1$  in the solution is defined by the equation:

$$\mu_1 - \mu_{1(l)} = RT \ln a_1, \quad (8)$$

analogous to (3), but in contradistinction to the latter (8) is based on the presupposition of constant pressure as well as

<sup>1</sup> W. W. DESCHNER a. G. G. BROWN: Ibid. 32, 840 (1940).



constant temperature. The equation includes the convention that the activity = 1 for the pure component at the given experimental conditions.

The change in  $a_1$  due to the change of pressure is expressed by:

$$\left(\frac{\partial \ln a_1}{\partial p}\right)_T = \frac{V_1 - V_{1(l)}}{RT}. \quad (9)$$

The difference  $V_1 - V_{1(l)}$  in the mixtures here considered, however, hardly exceeds  $2 \cdot 10^{-3}$  L. Consequently we shall not introduce any traceable error if the terms in (8) are considered independent of pressure, and the equation is applied in the pressure intervals of the actual experiments. The potential difference in (8) may therefore be identified with the potential difference in (6), when this equation is applied to the component  $K_1$  in states where the gaseous and liquid phases are in equilibrium with one another.

Thus for  $K_1$  in the solution we may write:

$$\mu_1 - \mu_{1(l)} = RT \ln a_1 = RT \ln \frac{p_1}{p_{1(l)}} + \Delta (p_{1(l)} - p_1), \quad (10)$$

where  $p$  is the vapour pressure of  $K_1$  in the solution and  $p_{1(l)}$  the vapour pressure of  $K_1$  in a pure state.

For the activity coefficient of  $K_1$  defined by:

$$a_1 = x_1 f_1 \quad (11)$$

we thus obtain:

$$\ln f_1 = \ln \frac{p_1}{p_{1(l)} x_1} + \frac{\Delta}{RT} (p_{1(l)} - p_1), \quad (12)$$

or writing:

$$\frac{p_1}{p_{1(l)} x_1} = f'_1 \quad (13)$$

where  $f'_1$  may be called the "pressure activity coefficient":

$$\ln f_1 = \ln f'_1 + \frac{\Delta}{RT} (p_{1(l)} - p_1). \quad (14)$$

$f'_1$  is the activity coefficient, calculated under the presupposition of the applicability of the gas laws to the vapour, and the last term of (14) represents the correction in  $\ln f_1$  for the



existing deviations. If the correction is small, equation (14) might be written:

$$\ln f_1 = \ln f'_1 + \frac{\Delta}{RT} p_{1(i)} x_2, \quad (15)$$

the correction term:

$$\frac{\Delta}{RT} (p_{1(i)} - p_1) = A \quad (16)$$

being replaced by:

$$\frac{\Delta}{RT} p_{1(i)} x_2 = B. \quad (17)$$

The difference between the 2 quantities A and B is easily obtained by means of (13) as:

$$A - B = \frac{\Delta}{RT} p_{1(i)} x_1 (1 - f'_1). \quad (18)$$

For hexane according to Table 1  $\Delta = 2.1$  L. For the mixture of hexane and cetane, as will be shown below, the following equation holds true:

$$-\log f'_1 = 0.048 x_2^2 + 0.0060 x_2. \quad (19)$$

Thus from (17), (18), and (19) the following data of Table 2 are computed:

Table 2.

$x_1$	$-\log f'_1$	$f'_1$	A - B
0	0.054	0.8831	0
0.1	0.04428	0.9031	0.000135
0.2	0.03552	0.9215	0.000218
0.3	0.02772	0.9382	0.000257
0.4	0.02088	0.9531	0.000260
0.6	0.01008	0.9771	0.000191
0.8	0.00312	0.9928	0.000080
1.0	0	1.0	0

The error in using the simpler expression (15) instead of (14) is thus seen to be less than 0.00026 in  $\log f'_1$ , corresponding to 0.06 per cent. in  $f'_1$ .

The magnitude of the difference A - B for the various paraffins is mainly determined by the product  $p_{1(i)} \Delta$ . As the value of this product for hexane and heptane is:

$$p_{6(6)}\Delta_6 = 12.11 \cdot 2.1 = 25.43$$

$$p_{7(7)}\Delta_7 = 3.54 \cdot 3.7 = 13.10,$$

the error involved in applying the simplified equation (15) instead of the correct equation (14) to heptane is only half of that in the case of hexane.

### 5. Experimental Method.

The method described below is generally applicable for the determination of the relation between vapour pressure and concentration of mixtures in which one component only is volatile. With certain reservations it is also applicable to binary mixtures fulfilling the condition that the vapour pressure of one component is small as compared to that of the other. In the present investigations the method is applied to the 3 binary systems: hexane-cetane, heptane-cetane, and hexane-dodecane.

In the apparatus constructed for the measurements and illustrated in Fig. 1 the mixture was contained in a glass flask A holding about 100 ml, which was shaken mechanically in a water thermostat for establishment of the liquid-vapour equilibrium, the pressure being read from one or two manometers B and C sealed into a system of glass tubes, with which the flask was connected by a thin capillary D. A known quantity of the non-volatile component was introduced in A before sealing and freed from air by evacuation. The system of glass tubes was communicating with reservoirs E, F, and G containing the volatile component, which was freed from air by evacuation at low temperature and distilling off from one reservoir to the other. The concentration of the mixture in A was altered by distilling the volatile component between A and the reservoirs, and it was determined by direct weighing of the flask, the thermostat being emptied of water, and the rinsed and dried flask released from the clamp by which it was attached to the shaking device and suspended by means of a metal wire under the scale of a balance solidly fixed on the wall above the thermostat.

The procedure of determining the concentration of the mixture directly by weighing a container in tight connection with the manometer system is made possible by the flexibility of the



connecting capillary and is the essential feature of the method described. A further advantage of this method consists in the possibility it offers of changing the concentration of the solution at will by distilling the volatile component to and from the solution. This makes possible the detection and removal of any trace of air in the liquid and the determination of any number of corresponding concentrations and pressures with the same air-free charges of material without opening the system or otherwise admitting the atmosphere.

When cetane is used as the "non-volatile" substance, it appears from an easy calculation that the quantity which may be distilled off from the flask by this process in the course of a series of experiments covering about 20 single determinations averages 1 mg only by a total quantity of 20–30 g.

As regards further details of the method, it may be mentioned that the capillary chosen after many experiments was drawn from an 8 mm cylinder tube to an external diameter of 0.45–0.55 mm and a length of ab. 50 cm. With this capillary the sensitiveness of the balance was about 0.5 mg. A capillary of a diameter of 0.8 mm interfered with the weighing too much, and a thinner capillary would impede a rapid vapour transmission and distillation. Naturally the whole construction had to be arranged with the greatest care and fixed accurately to prevent a change in the state of tension of the capillary during the experiment. The reproducibility of the experiments, however, proved that this requirement could be complied with.

The effect of varying buoyancy of the flask used in the experiment was eliminated by placing a bulb of the same size in the other scale. The weight of the vapour above the liquid, which is necessary for the calculations, was determined from the total volume of the flask and the known densities of the vapours.

The glass construction including manometers and reservoirs for the volatile component was blown all in one piece without stopcocks. Communication between the various portions was established by mercury valves operated by means of the two air reservoirs R—R, as indicated in the figure. The reservoirs and the manometer system could be cut off from the capillary and the quartz-mercury pump P by means of the long valves H and I, thereby making it possible to admit the atmosphere to



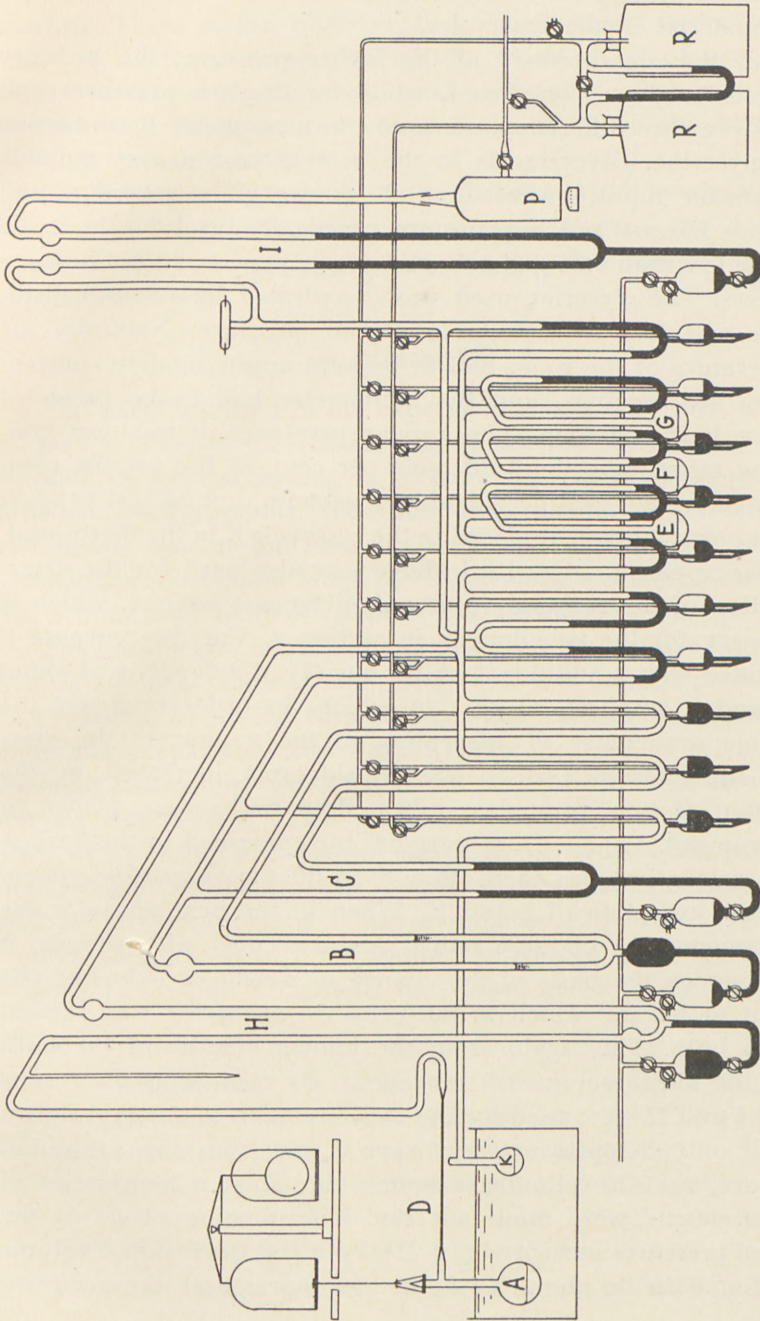


Fig. 1.

A when changing the charges without contamination of the air-free material in the reservoirs.

For the measurement of the higher pressures the mercury manometer C was employed, while for the low pressures and small pressure differences we used the manometer B containing dry glycerine. Glycerine is in the present case a very suitable manometer liquid on account of its negligible volatility, and because hexane and heptane are practically insoluble in it. Of hexane less than 0.01 g dissolves in 1 kg glycerine, and of heptane still less. The glycerine used was dehydrated by vacuum distillation and had no detectable vapour pressure. Naturally the temperature of the room had to be kept approximately constant during the readings, and the manometer had to be protected against heat radiation. The vapour pressures of mixtures containing more than about 80 mole per cent. of the volatile component were not measured against a vacuum, but against vapours of the pure component placed in the reservoir K in the thermostat.

The apparatus described above was also used for the determination of the residual volume  $\Delta$  of hexane vapour, which is necessary for the calculations in section 3. For this purpose it was fitted with 2 additional bulbs, one (I) of a capacity of about 2 L and a smaller one (II) in which—in order to detect the possible occurrence of adsorption of the vapour to the glass wall—the internal surface was considerably increased by the insertion of numerous glass tubes. Both bulbs were placed in a thermostat. Vapour from pure hexane contained in the flask A after evacuation was then allowed to fill the remaining system with the exception of I and II. When in the next phase of the experiments one of these bulbs was also filled with vapour, it was easy on the basis of the change in weight of A to find the weight of hexane which at the pressure measured was present in the bulb. This again from the known volume of the bulb gives the molar volume of the vapour. By comparing the results when I and II were used for the measurements it was first shown that if only the pressure was kept  $\frac{1}{4}$  cm from the saturation pressure, no adsorption was noticeable. Then a long series of measurements were made for the determination of  $\Delta$ . At the highest pressures measured (10—11.7 cm Hg) the residual volume was found to be about 2.1 L, at lower pressures the accuracy



is of course smaller, and the spreading of the values was more marked. There seems, however, to be good reason to accept the value of 2.1 L as correct through the whole range of pressures from 0 to 12 cm Hg. As mentioned above this value is in conformity with the results of calculations made on the basis of previous measurements.

For heptane vapour the above method is too uncertain on account of the much lower vapour pressure, and the  $\Delta$ -value stated in Table 1 was applied to this paraffin without further experimental test.

## 6. Materials.

The paraffins used in the experiments were of a high degree of purity. They were obtained by fractional distillation in a 60-plate column according to A. KLIT<sup>1</sup> and showed completely constant boiling points. The raw material for the fractional distillation was in the case of hexane, dodecane, and cetane synthetic products, and in the case of heptane a preparation from TH. SCHUCHARDT named "Heptan aus Petroleum".

The hexane and heptane preparations by progressive evaporation at 20°.00 C. showed completely constant vapour pressures, 12.11 and 3.54 cm Hg respectively. The melting point of the dodecane preparation was -9°.75 C. In the case of cetane the column distillation was carried out at a pressure of about 15 mm Hg and 150° C. The sample showed a constant melting point of 18°.15 C. P. C. CAREY and J. C. SMITH<sup>2</sup> give the melting point of pure cetane as 18°.13, while melting points between 16° and 20° are reported by other investigators.<sup>3</sup>

For the density  $d_4^{20}$  we found the values given below in column 1. Column 2 contains the values given by EGLOFF.<sup>3</sup>

	1	2
Hexane . . . . .	0.65940	0.65942
Heptane . . . . .	0.68389	0.68375
Dodecane . . . . .	0.74933	0.7493
Cetane . . . . .	0.77340	0.77499

<sup>1</sup> A. KLIT: Theses, Copenhagen 1943.

<sup>2</sup> P. C. CAREY and J. C. SMITH: J. Ch. Soc. 1933, 346.

<sup>3</sup> G. EGLOFF: Physical Constants of Hydrocarbons, p. 95 (1939).



### 7. Experimental Results.

Hexane-Cetane. Following some measurements more in the nature of an orientation, four independent series of determinations were carried out, the results of which are given in Table 3.

The 2nd column, headed  $g_{16}$ , contains the weight of cetane in grammes corrected for dissolved air, ab. 0.2 mg/g cetane. Column 3 contains the weight of hexane vapour,  $g_v$ , calculated

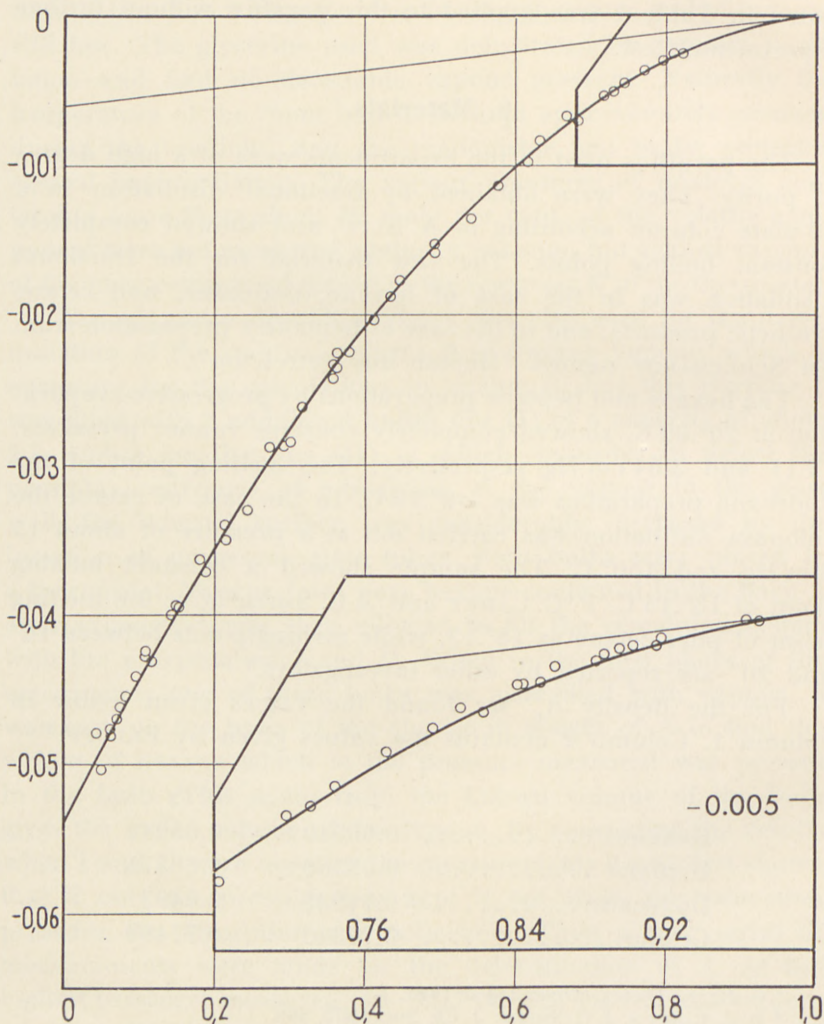


Fig. 2. Hexane-Cetane.  $\text{Log } f'_6$  against  $x_6$ .

Table 3.

Series	$g_{16}$	$g_v$	$g_6$	$x_6$	$p_6$ (Hg)	$p_6$ (Gl)	$\log f'_6$	
2	29.219	0.0116	6.7634	0.3781	p		$\bar{1}.9774$	
		.0070	3.0080	.2129	4.36			
		.0059	2.4396	.1799		25.79		.9660
		.0050	1.9905	.1518		21.68		.9637
		.0026	0.9024	.0751		18.16		.9605
					8.84	.9538		
3	1.2844	.0469	2.2673	.8226	p <sub>0</sub> - p			
		.0456	1.9044	.7958		23.89	.9973 <sub>5</sub>	
		.0443	1.6440	.7708		27.50	.9969	
		.0427	1.4232	.7443		30.81	.9963	
		.0413	1.2447	.7181		34.52	.9954	
		.0392	1.0498	.6823		38.10	.9946	
		.0480	2.6482	.8442		43.08	.9928	
		.0444	15.5584	.9695		20.89	.9981	
		.0464	12.9538	.9636		4.05	.9998	
		.0499	5.3001	.9156		4 82	.9998	
		.0500	4.5389	.9028		11.30	.9991	
		.0496	3.8534	.8874		12.97	.9991	
		.0489	2.9098	.8542		15.04	.9989	
		.0478	2.5995	.8418		19.32	.9981 <sub>5</sub>	
		.0468	2.2288	.8202		21.21	.9981	
		.0501	5.4667	.9179		24.13	.9977	
		.0499	4.2846	.8976		10.93	.9993	
		.0494	3.7031	.8834		13.67	.9991	
		.0487	3.0268	.8610		15.62	.9987	
		.0464	2.1011	.8114		18.58	.9986	
.0421	1.3285	.7309		25.34	.9975			
.0386	0.9881	.6675		36.36	.9948 <sub>5</sub>			
				44.70	.9933			
4	14.4027	.0120	2.0466	.2718	p			
		.0138	2.5322	.3159		33.33	.9712	
		.0158	3.1060	.3617		38.97	.9738	
		.0187	4.1967	.4336	4.17	44.86	.9763	
		.0208	5.2876	.4910		5.04	.9774	
		.0252	9.3498	.6305		5.76	.9812	
		.0247	8.7906	.6160		7.51	.9847	
		.0237	7.4604	.5765		7.31	.9917	
						6.82	.9902	
				.9886				



Table 3 (continued).

Series	$g_{16}$	$g_V$	$g_6$	$x_6$	$p_6$ (Hg)	$p_6$ (Gl)	$\log f'_6$
4	14.4027	0.0225	6.4185	0.5394	<p style="text-align: center;">p</p> 6.35 5.75 5.20 4.76 4.11 44.26 35.70 25.92 17.80 12.84 8.31 <sub>5</sub> 7.36 <sub>5</sub> 12.68 5.91		1.9863
		.0222	5.2836	.4908			.9841
		.0192	4.4149	.4462			.9823
		.0181	3.8182	.4106			.9796
		.0155	3.0487	.3575			.9766
		.0128	2.2520	.2912			.9756
		.0090	1.4967	.2145			.9712
		.0065	0.9577	.1487			.9649
		.0047	0.6639	.1080			.9607
		.0031	0.4172	.0707			.9576
		.0027	0.3673	.0628			.9530
		.0047	0.6544	.1068			.9519
		.0022	0.2924	.0505			.9572
							.9496
		5	23.7470	.0023			0.5940
.0031	0.8038			.0817		9.64	.9545
.0043	1.1813			.1156		13.72	.9569
.0052	1.4935			.1418		16.95	.9600
.0067	2.0938			.1881		22.62	.9628
.0098	2.8964			.2428		29.47	.9669
.0124	3.8728			.3000		36.80	.9714
.0036	0.9389			.0941		11.14	.9559

from the pressure. Column 4 gives the weight  $g_6$  of hexane in the liquid mixture, i. e. the total weight of hexane less the weight of hexane vapour. In the 5th column is given the mole fraction of hexane calculated from:

$$x_6 = \frac{1}{1 + 0.3806 \frac{g_{16}}{g_6}},$$

where the numerical factor in the denominator is the ratio of the molecular weight of hexane  $M_6 = 86.17$  to that of cetane  $M_{16} = 226.43$ .

Column 6 and 7 contain the pressures measured as the absolute vapour pressure  $p$  when this is directly determined, or as the vapour pressure lowering,  $p_0 - p$ , where  $p_0 = p_{6(6)} =$  the



vapour pressure of pure hexane. The figures in column 6 indicate the pressure in cm of mercury, and those in column 7 the pressure in cm of glycerine, both at a temperature of 22°. For pure hexane at  $t = 20^{\circ}.00$  we found:

$$\begin{aligned} p_{6(6)} &= 131.0 \text{ cm glycerine } (22^{\circ}) \\ &= 12.145 \text{ cm Hg } (22^{\circ}), \end{aligned}$$

corresponding to the ratio 10.78<sub>5</sub> between the readings of the two manometers.

Finally column 8 gives the activity coefficient  $f'_6$  calculated from (13) as:

$$f'_6 = \frac{P_6}{p_{6(6)} x_6}.$$

Heptane-Cetane. Table 4 contains the corresponding data for the heptane-cetane system at  $t = 20^{\circ}.00$ , obtained from two series of independent determinations. On account of the much lower vapour pressure all the readings could be made by means of the glycerine manometer. Otherwise the methods and calculations are quite analogous to those employed in the hexane-cetane series. For pure heptane at  $t = 20^{\circ}.00$  C. we found:

$$\begin{aligned} p_{7(7)} &= 39.23 \text{ cm glycerine } (22^{\circ}) \\ &= 3.55 \text{ cm Hg } (22^{\circ}). \end{aligned}$$

These figures give the ratio 10.77 between the readings of the two manometers. The slight deviation of this figure from the ratio given above is due to the use of different glycerine samples in the two cases.

The mole fraction is calculated from:

$$x_7 = \frac{1}{1 + 0.4425 \frac{g_{16}}{g_7}},$$

where the numerical factor in the denominator is the ratio of the molecular weight of heptane  $M_7 = 100.20$  to that of cetane  $M_{16} = 226.43$ .

Table 4.

Series	$g_{16}$	$g_V$	$g_7$	$x_7$	$p_7$ (Gl)	$\log i'$
1	4.2291	0.0026	0.3251	0.1480	5.24 <sub>5</sub>	1.9670
		.0023	0.2868	.1329	4.71	.9668
		.0032	0.4125	.1806	6.46	.9714
		.0030	0.3871	.1714	6.10	.9687
		.0028	0.3573	.1603	5.70	.9686
		.0042	0.5860	.2384	8.59	.9743
		.0039	0.5288	.2203	7.90	.9722
		.0050	0.7268	.2797	10.15	.9774
		.0047	0.6660	.2625	9.50	.9762
		.0058	0.9096	.3270	11.96 <sub>5</sub>	.9798
		.0055	0.8277	.3066	11.18 <sub>5</sub>	.9796
		.0063	1.0238	.3536	12.94 <sub>5</sub>	.9811
		.0074	1.3139	.4125	15.24 <sub>5</sub>	.9851
		.0081	1.5339	.4504	16.70	.9867
		.0076	1.3835	.4250	15.72	.9856
		.0087	1.7610	.4848	18.01 <sub>5</sub>	.9876
		.0098	2.2628	.5473	20.48	.9907
		.0108	2.8582	.6043	22.71	.9925
		.0115	3.4444	.6480	24.43 <sub>5</sub>	.9940
		.0130	5.0183	.7284	27.61	.9963
		.0137	10.1482	.8526	32.20	.9989
		.0130	15.5072	.8923	34.08	.9995
		.0119	21.3659	.9194 <sub>5</sub>	35.14	.9996
		.0120	20.8186	.9174	35.03	.9994
		.0121	20.3640	.9158	34.97	.9994 <sub>5</sub>
		.0128	16.7936	.8997	34.36	.9995
		.0134	12.9445	.8737	33.33	.9990
.0136	10.2380	.8455	32.24	.9989		
.0134	7.4375	.7990	30.40	.9979		
.0126	4.7833	.7187	27.23	.9960		
.0110	3.0009	.6159	23.16	.9929		
.0096	2.1366	.5332	19.90	.9897		
.0081	1.5306	.4499	16.64	.9857		
.0061	0.9811	.3440	12.57	.9805		
2	5.5555	.0019	0.2882	.1049	3.71	.9658
		.0024	0.3987	.1395	4.95 <sub>5</sub>	.9679
		.0023	0.3851	.1354	4.83	.9701
		.0032	0.5574	.1848	6.62	.9716
		.0031	0.5246	.1759	6.30	.9715
		.0037	0.6533	.2099	7.54 <sub>5</sub>	.9731
		.0046	0.8678	.2609	9.45	.9764
		.0055	1.1300	.3149	11.50	.9802



Table 4 (continued).

Series	$g_{16}$	$g_v$	$g_7$	$x_7$	$p_7$ (G1)	$\log f'$
2	5.5555	0.0066	1.4846	0.3765	13.86	1.9836
		.0075	1.8167	.4249	15.68	.9845
		.0083	2.1684	.4686	17.45	.9880
		.0092	2.7065	.5240	19.55	.9894
		.0097	3.1107	.5586	20.93	.9912
		.0106	3.8549	.6106	23.00	.9935
		.0113	4.6952	.6563	24.80	.9949
		.0123	6.9794	.7395	28.08	.9970
		.0111	4.5118	.6473	24.42	.9942

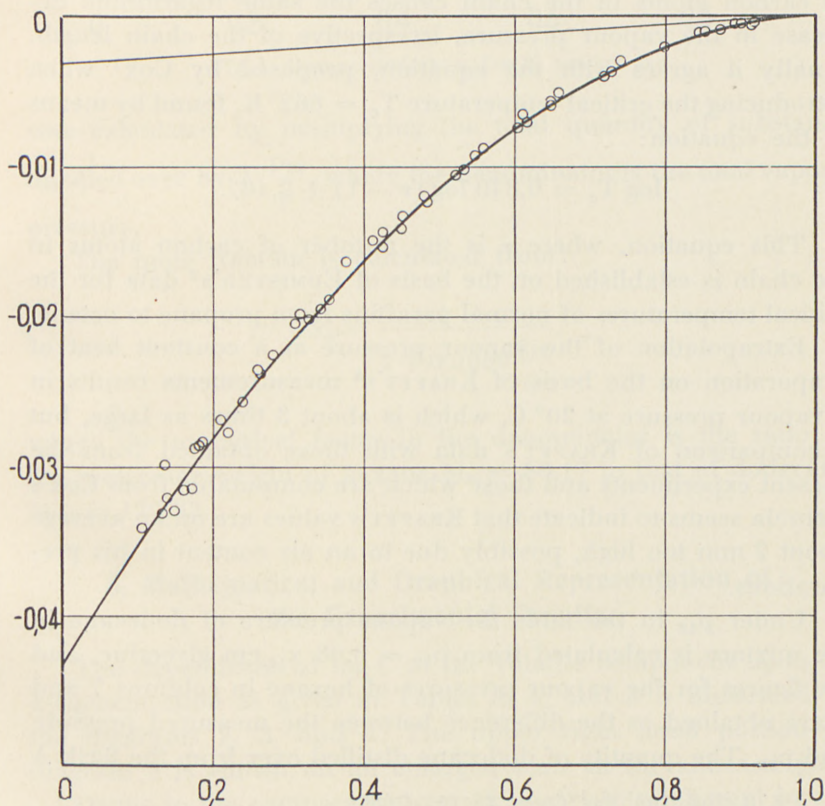


Fig. 3. Heptane-Cetane.  $\log f_7$  against  $x_7$ .



Hexane-Dodecane. The results of similar measurements with the hexane-dodecane system are listed in Table 5. In these experiments, however, the vapour pressure of the "non-volatile" component could not be disregarded.

For the vapour pressure of dodecane we found by direct measurement at 20°.00 the value  $p_{12(12)} = 0.08$  cm glycerine = 0.0075 cm Hg. This value is confirmed by the amount of dodecane carried by the hexane vapour on distillation from the flask A into the reservoirs. It is also consistent with the formula

$$p_{12(12)} = p_{6(6)} \left( \frac{p_{7(7)}}{p_{6(6)}} \right)^6 = 12.11 \cdot 0.2923^6 = 0.0076 \text{ cm Hg}$$

based upon the assumption that an increase by one in the number of carbon atoms in the chain causes the same logarithmic decrease in the vapour pressure, irrespective of the chain length. Finally it agrees with the equation, proposed by Cox<sup>1</sup> when introducing the critical temperature  $T_c = 662^\circ \text{K}$ . found by means of the equation:

$$\log T_c = 0.340 \log (\nu - 1) + 2.467.$$

This equation, where  $\nu$  is the number of carbon atoms in the chain is established on the basis of EDMISTER's<sup>2</sup> data for the critical temperatures of normal paraffins from propane to octane.

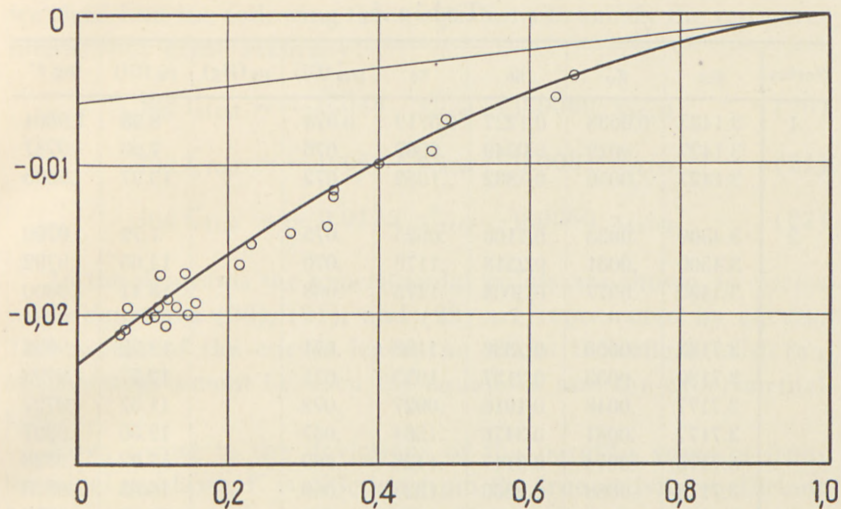
Extrapolation of the vapour pressure at a constant heat of evaporation on the basis of KRAFFT's<sup>3</sup> measurements results in a vapour pressure at 20° C. which is about 3 times as large, but a comparison of KRAFFT's data with those obtained from the present experiments and those which are computable from Cox's formula seems to indicate that KRAFFT's values are on an average about 2 mm too high, possibly due to an air content in his preparations.

Under  $p_{12}$  in the table the vapour pressure of dodecane in the mixture is calculated from  $p_{12} = 0.08 x_{12}$  cm glycerine, and the figures for the vapour pressures of hexane in columns 7 and 8 are obtained as the difference between the measured pressure and  $p_{12}$ . The quantity of dodecane distilled over from the flask A

<sup>1</sup> E. R. COX: Ind. Eng. Chem. **28**, 613 (1936).

<sup>2</sup> W. C. EDMISTER: Ind. Eng. Chem. **30**, 353 (1938).

<sup>3</sup> F. KRAFFT: Ber. d. d. chem. Ges. **15**, 1687 (1882).

Fig. 4. Hexane-Dodecane.  $\log f'_6$  against  $x_6$ .

was calculated by multiplying the total quantity of substance distilled over by  $2 \cdot \frac{P_{12}}{P}$ , where the denominator is the total vapour pressure.

The mole fraction is calculated from:

$$x_6 = \frac{1}{1 + 0.5059 \frac{g_{12}}{g_6}}$$

where the numerical factor in the denominator is the ratio of the molecular weight of hexane  $M_6 = 86.17$  to that of dodecane  $M_{12} = 170.33$ .

### 8. Mathematical and Graphical Representation of the Experimental Results.

The dependence of  $\log f'$  of the volatile component upon its  $x$ -concentration as given in Tables 3, 4, and 5 is illustrated in the diagrams 2, 3, and 4. The upper right hand portion of diagram 2 is shown on an enlarged scale in the annexed plot.

Owing to the comparatively great uncertainty inherent in the method of measuring small vapour pressures, the data at  $x$ -values



Table 5.

Series	$g_{12}$	$g_V$	$g_6$	$x_6$	$p_{12}$ (Gl)	$p_6$ (Hg)	$p_6$ (Gl)	$\log f'$
1	3.1433	0.0038	0.1227	0.0719	0.074		8.98	$\bar{1}$ .9804
	3.1427	.0029	0.0949	.0567	.076		7.06	.9787
	3.1427	.0056	0.1882	.1062	.072		13.27	.9805
2	3.4500	.0033	0.1160	.0625	.075		7.79	.9790
	3.4500	.0061	0.2318	.1176	.070		14.65	.9792
	3.4490	.0077	0.3008	.1475	.068		18.41	.9800
3	3.7182	.0058	0.2336	.1108	.071		13.92	.9826
	3.7180	.0053	0.2137	.1023	.071		12.77 <sub>5</sub>	.9798
	3.7177	.0048	0.1916	.0927	.072		11.57	.9797
	3.7177	.0081	0.3476	.1564	.067		19.56	.9807
	3.7175	.0074	0.3117	.1426	.069		17.92	.9828
	3.7173	.0069	0.2856	.1322	.069		16.53	.9805
	3.7173	.0113	0.5179	.2165	.063		27.27	.9838
	3.7173	.0147	0.7365	.2822	.057		35.71	.9859
	3.7173	.0177	0.9630	.3394	.053	4.01	43.15 <sub>5</sub>	.9879
	3.7173	.0212	1.2537	.4008	.05		4.76	.9883
	3.7173	.0262	1.8010	.4901	.04	5.86	.9901	
	3.7172	.0338	3.6451	.6605	.02	7.95	.9930	
	3.7170	.0326	3.2687	.6356	.03	7.62	.9960	
	3.7158	.0245	1.6573	.4694	.04	5.58	.9945	
	2.7146	.0172	0.9338	.3327	.05	3.91	42.10	.9909
	3.7135	.0120	0.5577	.2296	.061		28.98	.9858
	3.7117	.0062	0.2553	.1201	.068		15.02	.9848
							15.02	.9810

below 0.06 in the case of hexane and 0.1 in the case of heptane are not sufficiently accurate and have been omitted.

Regarding the quantitative relation between  $f'$  and  $x$  it has already been mentioned in section 4 that  $\log f'$  in the hexane-cetane system can be represented as a sum of two members one of which is linear, the other quadratic in  $x$ . The same is true of all the systems investigated. If for reasons to be stated below we choose the linear terms:

$$0.0060 x_{16(6)}$$

$$0.0031 x_{16(7)}$$

$$0.0060 x_{12(6)},$$



we shall find the following three equations to satisfy the measurements with great accuracy:

$$\log f'_{6(16)} = -0.048 x_{16(6)}^2 - 0.0060 x_{16(6)} \quad (20)$$

$$\log f'_{7(16)} = -0.040 x_{16(7)}^2 - 0.0031 x_{16(7)} \quad (21)$$

$$\log f'_{6(12)} = -0.0175 x_{12(6)}^2 - 0.0060 x_{12(6)} \quad (22)$$

In the diagrams the experimental points are shown as circles while equations (20), (21), and (22) are represented by curves. The course of the curves leaves no doubt that there exists an excellent agreement between the equations and the experimental data.

Now, owing to the deviations of the paraffin vapours from the ideal gas laws,  $f'$  is different from the true activity coefficient  $f_1$  as expressed by equation (15). The relation between the two coefficients can be determined from this equation by means of the known values of  $\Delta$  and  $p_0$  for the two volatile components. Introducing these values from table 1 and Section 7 we get:

$$\frac{\Delta_6}{RT} P_{6(6)} = 0.0139 = \frac{0.0060}{0.4343} \quad (23)$$

$$\frac{\Delta_7}{RT} P_{7(7)} = 0.0072 = \frac{0.0031}{0.4343} \quad (24)$$

Hence, when natural logarithms are replaced by decadic logarithms, equation (15) becomes:

$$\log f_{6(6)} = \log f'_{6(16)} + 0.0060 x_{16(6)} \quad (25)$$

$$\log f_{7(16)} = \log f'_{7(16)} + 0.0031 x_{16(7)} \quad (26)$$

$$\log f_{6(12)} = \log f'_{6(12)} + 0.0060 x_{12(6)}, \quad (27)$$

or, inserting equations (20), (21), and (22):

$$\log f_{6(16)} = -0.048 x_{16(6)}^2 \quad (28)$$

$$\log f_{7(16)} = -0.040 x_{16(7)}^2 \quad (29)$$

$$\log f_{6(12)} = -0.0175 x_{12(6)}^2. \quad (30)$$

We have thus attained the very remarkable result that the linear terms in equations (20), (21), and (22) can be accounted for as due to the effect of the deviations of the vapours from the laws of perfect gases. Removing these linear terms we arrive at expressions for the true activity coefficients  $f$  which are purely quadratic in  $x$ .

In the figures the linear member is shown by a straight line which is a tangent to the  $\log f'$ -curve at  $\log f' = 0$ .  $\log f$  is read as the vertical distance between the curve and the tangent. It is seen that the significance of the linear member is decreasing in the order: hexane-dodecane, hexane-cetane, heptane-cetane.

The data submitted convincingly show that the *n*-paraffin mixtures investigated are by no means ideal. On the contrary they manifest a clear deviation from the condition of ideality, as the activity coefficient of the volatile components shows a marked decrease with decreasing values of their concentration.

At infinite dilution the values calculated are:

$$\begin{aligned} \log f_{6(16)} &= -0.048 & f_{6(16)} &= 0.895 \\ \log f_{7(16)} &= -0.040 & f_{7(16)} &= 0.912 \\ \log f_{6(12)} &= -0.0175 & f_{6(12)} &= 0.961, \end{aligned}$$

showing in the case of hexane in pure cetane an activity coefficient more than 10 per cent. below the ideal value.

### 9. The Complete Curve System.

The possibility of expressing the logarithm of the activity coefficient of the volatile components in the paraffin mixtures by means of a parabolic equation is a fact of great consequence to the thermodynamics of the paraffin group on the whole. For it is known that the expression:

$$\ln f_1 = kx_2^2 \quad (31)$$

for one component  $K_1$  in a binary mixture by virtue of GIBBS-DUHEM's equation between the chemical potentials entails that the symmetric equation:

$$\ln f_2 = kx_1^2 \quad (32)$$



holds for the other component  $K_2$ . It is also known that the parabolic form is the only one to permit of a complete symmetry of the curves. The ideal case follows from (31) and (32) when  $k = 0$ .

On account of these particularly simple conditions the following expressions result directly from expressions (28), (29), and (30):

$$-\log f_{16(6)} = 0.048 \quad x_6^2_{(16)} \quad (33)$$

$$-\log f_{16(7)} = 0.040 \quad x_7^2_{(16)} \quad (34)$$

$$-\log f_{12(6)} = 0.0175 \quad x_6^2_{(12)}. \quad (35)$$

In addition to the activity coefficients  $f_1$  and  $f_2$  for the two components  $K_1$  and  $K_2$  we shall define a composite or integral activity coefficient  $f_i$  by the equation:

$$\log f_i = x_1 \log f_1 + x_2 \log f_2. \quad (36)$$

This activity coefficient is related to the deviation of the integral work of mixing from its ideal value in the same way as  $f_1$  and  $f_2$  are related to the corresponding difference in the differential process of mixing. In the present case the curve representing  $\log f_i$  is of course completely symmetrical with regard to the two  $x$ -concentrations, since in correspondence with (31) and (32) we have:

$$\ln f_i = kx_1x_2. \quad (37)$$

The maximum value of  $\ln f_i$  is obviously  $\frac{1}{4}$  of the maximum value of  $\ln f_1$  or  $\ln f_2$ .

In Fig. 5  $\log f_i$  is shown by the curves I, II, and III for the three systems investigated along with  $\log f_{6(12)}$  and  $\log f_{12(6)}$  for the hexane-dodecane system.

It cannot, however, be imagined that this simple relation should be limited to the 3 mixtures here considered. It must be assumed that it will hold good of normal paraffins generally if the number of carbon atoms in the molecules of the constituent components does not materially exceed the limits fixed by the present investigations. If we pass over to paraffins with a small number of carbon atoms, the deviation from the isochemical



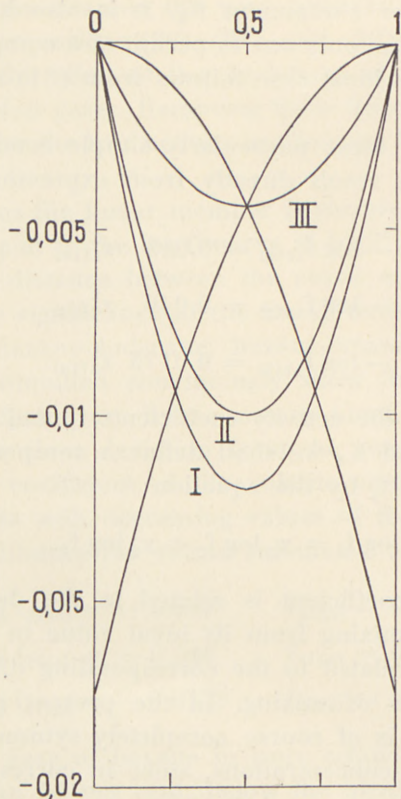


Fig. 5.  $\text{Log } f_i$  (I, II, III).  $\text{Log } f_{6(12)}$  and  $\text{Log } f_{12(6)}$  against  $x$ .

relation will become fairly considerable, and similarly deviations are to be expected in case of very great chain length of a component.

Equations (28)—(30) and (33)—(35) may be considered special forms of the general expression:

$$\text{log } f_{1(2)} = A \cdot x_2^2, \quad (38)$$

where  $A$  is a coefficient which at a given pressure and temperature is a function only of  $\nu_1$  and  $\nu_2$ , i. e. of the number of carbon atoms in the two paraffin chains. It is a problem of special significance to determine this coefficient.

## 10. The Concept of Congruence. The General Equation for the Activity Coefficients of Normal Paraffins.

The concept of congruence of mixtures of normal paraffins is proposed as the basis for a general determination of their thermodynamic properties.

A mixture of the components  $K_1, K_2, \dots$  containing  $\nu_1, \nu_2, \dots$  carbon atoms per molecule, respectively, and present in the mixture in mole fractions  $x_1, x_2, \dots$  may be characterized by an index  $\nu$ , given by:

$$\nu = x_1\nu_1 + x_2\nu_2 + \dots \quad (39)$$

Mixtures with the same index are designated as congruent. They may be derived theoretically from a given mixture by transferring  $\text{CH}_2$ -groups from one paraffin molecule into another.

The theory of congruence assumes that the thermodynamic properties of a mixture of normal paraffins are determined by the index of the mixture, and that congruent solutions therefore will show the same values, e. g. for the activity coefficients of dissolved substances, irrespective of the individuality of the components.

For a pure paraffin the index is of course equal to the number of carbon atoms in the chain. In dodecane for instance we have  $\nu = 12$ . A mixture congruent with dodecane may be produced in an infinite number of ways. If hexane and cetane are taken as the constituent components, the composition of the mixture will be determined by the equation:

$$6x_6 + 16x_{16} = 12,$$

whence:

$$x_6 = 0.4, \quad x_{16} = 0.6.$$

The experiments which form the chief basis of the theory of congruent paraffin systems differ in nature from those submitted here, and will be dealt with in a subsequent paper. We shall here apply the theory for the purpose of determining the coefficient  $A$  in (38).

Applying (39) to a system of 2 components we have  $x_1 + x_2 = 1$ , and therefore:



$$x_1 = \frac{\nu - \nu_2}{\nu_1 - \nu_2}, \quad x_2 = \frac{\nu - \nu_1}{\nu_2 - \nu_1}, \quad (40)$$

which combined with (38) gives:

$$\log f_{1(2)} = \frac{A_{1,2}}{(\nu_1 - \nu_2)^2} (\nu - \nu_1)^2 \quad (41)$$

$$\log f_{2(1)} = \frac{A_{1,2}}{(\nu_1 - \nu_2)^2} (\nu - \nu_2)^2. \quad (42)$$

By the theory of congruence  $f_1$  depends only upon  $\nu$  and  $\nu_1$ . The factor:

$$\frac{A_{1,2}}{(\nu_1 - \nu_2)^2} = B$$

appearing in (41) is therefore independent of  $\nu_2$ . Similarly, as  $f_2$  depends only upon  $\nu$  and  $\nu_2$ , the same factor appearing in (42) is independent of  $\nu_2$ . Consequently in the equation:

$$\log f_1 = B (\nu - \nu_1)^2, \quad (43)$$

where  $f_1$  is the activity coefficient of a component  $K_1$  in an arbitrary mixture of index  $\nu$ ,  $B$  is a universal constant for paraffin mixtures at constant temperature and pressure. By introduction of (40) equation (43) may be written:

$$\left. \begin{aligned} \log f_{1(2)} &= B (\nu_1 - \nu_2)^2 x_2^2 \\ \log f_{2(1)} &= B (\nu_1 - \nu_2)^2 x_1^2 \end{aligned} \right\} \quad (44)$$

and from this equation in conjunction with (28), (29), and (30) the value of the constant can be determined. The three equations in the order indicated, give the following value for  $B$ :

$$B = -\frac{0.048}{(6-16)^2} = -0.00048 \quad (\text{hexane-cetane})$$

$$B = -\frac{0.040}{(7-16)^2} = -0.00049 \quad (\text{heptane-cetane})$$

$$B = -\frac{0.0175}{(6-12)^2} = -0.00049 \quad (\text{hexane-dodecane})$$



These values show a very satisfactory agreement. However, as the results obtained in the hexane-cetane system are probably the more reliable of the three, we shall take  $B = -0.00048$  as probably the best value. Accordingly we propose to represent the activity coefficients in normal paraffin mixtures at atmospheric pressure and  $t = 20^\circ \text{C}$ . by the expression:

$$\log f_1 = -0.00048 (\nu - \nu_1)^2. \quad (45)$$

Although this formula, as we are now justified in assuming, holds very closely to systems of normal paraffins from  $\nu = 6$  to  $\nu = 16$ , it is obvious that it cannot hold by unlimited increase in the chain length. Further measurements are therefore required to test the formula outside these limits. The complete solution of the problem of the activity coefficient within the domain in which the formula is applicable naturally requires a determination of the dependence of the coefficient  $B$  on temperature. As the method used in the present work is not suited for temperatures materially above room temperature, experiments at higher temperatures based on a different principle and also including paraffins of a higher index and a correspondingly higher melting point are necessary. Such measurements are now in progress in this laboratory.

## 11. Summary.

1. Within certain limits of pressure and temperature paraffin vapours obey the equation:

$$p(\nu + \Delta) = RT,$$

where  $\Delta$  is a constant.

2. An accurate method has been devised for determining the relation between composition and vapour pressure in binary mixtures in case the two partial pressures are very different.

3. Vapour pressure determinations have been made over the whole range of concentrations in the binary paraffin mixtures 6-16, 7-16, and 6-12.

4. The activity coefficient of a component  $K_1$  in a mixture of normal paraffins containing from 6 to 16 carbon atoms is determined by the equation:

$$\log f_1 = B (\nu - \nu_1)^2,$$

where B is a constant at constant temperature,  $\nu_1$  the index of the component, i. e. the number of carbon atoms in the chain,  $\nu$  the index of the mixture, defined as  $\nu = \sum x_1 \nu_1$ , and x the mole fraction.

5. The measurements mentioned under 3. gave the value  $-0.00048$  for B at  $20^\circ \text{C}$ .

6. Mixtures with the same  $\nu$  are called congruent. On the basis of the theory of congruence the thermodynamic properties of a paraffin mixture are determined by its index  $\nu$ .

DET KGL. DANSKE VIDENSKABERNES SELSKAB  
MATEMATISK-FYSISKE MEDDELELSER, BIND XXII, NR. 18

---

# STUDIES ON ACIDO COMPLEX FORMATION. I.

OPTICAL INVESTIGATIONS OF CUPRIC  
CHLORIDE IN MIXTURES WITH  
OTHER CHLORIDES

BY

JANNIK BJERRUM



KØBENHAVN  
I KOMMISSION HOS EJNAR MUNKSGAARD  
1946



## CONTENTS

	Page
1. Introduction .....	3
2. Discussion of previous investigations.	
a. Light absorption of the cupric chloride system .....	4
b. Estimation of the formation function on the basis of DOEHLEMANN and FROMHERZ'S measurements .....	6
c. SPACU and MURGULESCU'S measurements in the blue mercury line....	8
d. An application of P. JOB'S "Méthode des variations continues" .....	12
3. Theoretical remarks on the calculation of complex equilibria in concentrated chloride solutions.	
a. Variation of the activity coefficient with the concentration .....	12
b. The basis of the calculation of the cupric chloride system .....	15
4. Extinction measurements on mixtures of cupric chloride with other chlorides.	
a. Measurements and experimental details (in collaboration with PALLE ANDERSEN) .....	17
b. The influence of the salt concentration on the light absorption ....	23
5. Calculation of the experimental material.	
a. The activity constant B and the formation function $\bar{n}$ .....	25
b. Distribution of the copper on the different chloro complexes .....	31
c. The order of magnitude of the temperature effect .....	36
6. On the auto complex formation in concentrated cupric chloride solutions.	
a. Transference number of the cupric ion .....	37
b. Estimation of the formation function and the distribution of complexes	38
c. Estimation of the true mean activity coefficient of the cupric chloride	41
7. Summary .....	42

## 1. Introduction.

The complex formation in solutions of metal salts has only in a few cases been investigated in such a way that the available measurements give sure information on the composition and stability of the complex ions in question. It is the aim of the present series of investigations on acido complex formation to provide a more comprehensive material of quantitatively investigated systems, and thereby to find general rules for the complex formation. Simultaneously, the author considers it important to attempt an improvement of the methods used for the investigation of complex systems.

In systems of comparatively great complexity it is possible to carry through the investigations at a high and constant concentration of a highly dissociated neutral salt and at low concentrations of the complex-forming substances. Thus, the classical law of mass action can be applied, and the consecutive complexity constants can be established by methods similar to those used by the author in his studies on metal ammine formation.<sup>1</sup> In systems of very slight complexity it is unfeasible to perform the investigations in a constant salt medium, since the complex formation itself involves the application of high and greatly varying anion concentrations. This renders quantitative information much more difficult, but, nevertheless, an examination can be made also in the range of very high concentrations, if the experimental method used permits a direct determination of the concentration of at least one of the complexes involved. A

<sup>1</sup> Untersuchungen über Kupferammoniakverbindungen I, II und III: D. Kgl. Danske Vidensk. Selskab, Mat.-fys. Medd. **11**, No. 5 (1931), **11**, No. 10 (1932), **12**, No. 15 (1934). Metal Ammine Formation in Aqueous Solution. —Theory of the Reversible Step Reactions. Doctoral thesis, Copenhagen 1941 (Publ. by P. Haase & Son). Metal Ammine Formation in Aqueous Solution V: D. Kgl. Danske Vidensk. Selskab, Mat.-fys. Medd. **22**, No. 7 (1945).

closer account of this problem is given in the present paper, which deals with the complex formation in cupric chloride solutions, particularly in mixtures of cupric chloride and easily soluble chlorides (hydrochloric acid, lithium-, magnesium-, and calcium chloride); the complex formation was studied by means of light absorption measurements. The complexity of the cupric chloride system is only very low (cf. Table 1, where the order of magnitude of the first complexity constant of some metal chloride systems is recorded) and, therefore, it is remarkable that, under certain approximative assumptions as to conditions of activity, a determination of the whole curve of the complex formation is possible, *viz.* from the tetraquo cupric ion to the tetrachloro complex. Moreover, the concentration of the different complexes in the various chloride solutions can be accounted for semiquantitatively.

Table 1. First complexity constant in some metal chloride systems.

$$k_1 = \frac{[\text{MeCl}^{+v-1}]}{[\text{Me}^{+v}][\text{Cl}^-]}$$

Metal ion	$k_1$	
$\text{Cu}^{++}$ .....	$\lesssim 1$	The present paper.
$\text{Fe}^{++}$ .....	$\sim 2$	OLERUP, Dissertation, Lund 1944.
$\text{Fe}^{+++}$ .....	$\sim 5$	»                   »                   »
$\text{Pb}^{++}$ .....	$\sim 25$	GÜNTEMBERG, Dissertation, Copenhagen 1938.
$\text{Cd}^{++}$ .....	$\sim 100$	LEDEN, Dissertation, Lund 1943.
$\text{Hg}^{++}$ .....	$\sim 3 \cdot 10^7$	MORSE, Z. physik. Chem. <b>41</b> (1902) 727.

## 2. Discussion of Previous Investigations.

### a. Light Absorption of the Cupric Chloride System.

As is wellknown, the colour of cupric chloride solutions changes from blue to green with increasing concentration and, after addition of easily soluble chlorides to high concentration, it may turn almost purely yellow. Fig. 1 shows how this appears in the absorption spectrum of the solutions. The logarithm of the molar extinction coefficient  $\varepsilon$  calculated from the total copper concentration of the solutions (the absorption of the chlorine ion



being very small for wave-lengths  $> 200 \text{ m}\mu$ ) is plotted as ordinates, and the wave number in  $\text{cm}^{-1}$  as abscissae; for orientation purposes, the wave-length in  $\text{m}\mu$  is also plotted. The measurements represented in Fig. 1 are mainly taken from a

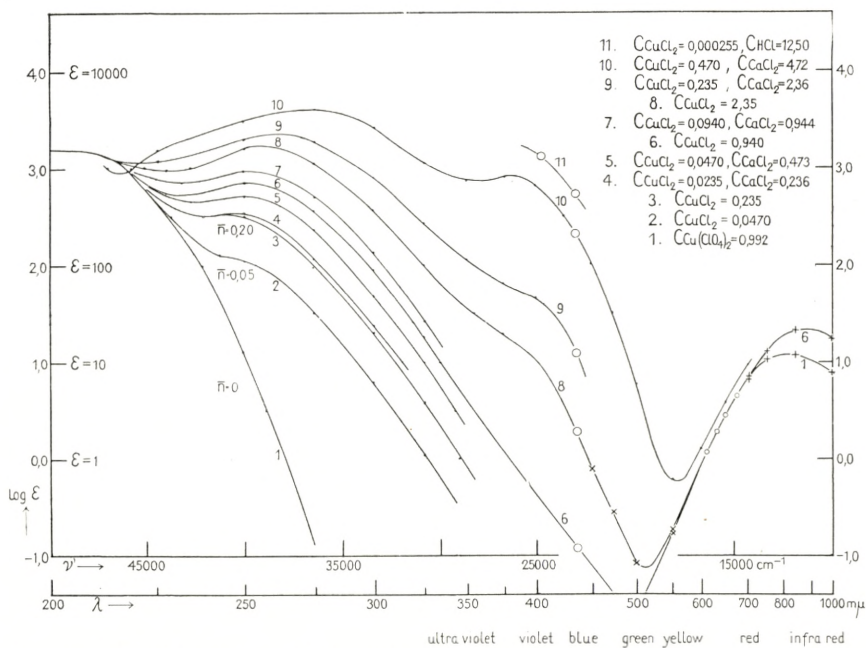


Fig. 1. Extinction curves of a number of cupric chloride solutions with and without calcium chloride (or hydrochloric acid). —  $\epsilon$  = the molar extinction coefficient,  $\nu'$  the wave number in  $\text{cm}^{-1}$ , and  $\lambda$  the wave-length in  $\text{m}\mu$ .

paper by DOEHLEMANN and FROMHERZ.<sup>1</sup> Thus, the absorption curves in the ultraviolet (corresponding to the solutions Nos. 1—10) were drawn on the basis of these authors' photographic measurements with a sector photometer. DOEHLEMANN and FROMHERZ continued the curve for solution No. 10 through the visible spectrum by measurements with a König-Martens spectrophotometer. The other curves have been continued on the basis of measurements by VAN DER GON<sup>2</sup> (marked with  $\times$ ) and the present author<sup>3</sup> ( $\circ$ ), and in the infrared on the basis of measurements by MECKE and LEY<sup>4</sup> ( $+$ ).

<sup>1</sup> DOEHLEMANN and FROMHERZ, Z. physik. Chem. A **171** (1934) 371.

<sup>2</sup> VAN DER GON, Arch. Néerlandaises des Sciences Exactes [3] A **7** (1924) 140.

<sup>3</sup> Kupferammoniakverb. II, p. 55, and Table 3 in the present paper.

<sup>4</sup> MECKE and LEY, Z. physik. Chem. **111** (1924) 391.

From Fig. 1 it appears that the complex formation in dilute cupric chloride solutions manifests itself in the ultraviolet absorption long before the absorption in the visible and the infrared spectrum is noticeably changed. DOEHLEMANN and FROMHERZ assume that the absorption band at about  $250\text{ m}\mu$ , which appears even at small chlorine ion concentrations, must be ascribed to the tetra- or trichloro complex, and that the displacement of the band in the direction of higher wave-lengths with higher chlorine ion concentrations may be attributed to the formation of polynuclear chloro complexes. This assumption is quite improbable and directly at variance with the fact that the extinction curves of the mixtures with a low copper concentration conform well to the corresponding extinction curves of the pure cupric chloride solutions. This observation indicates that there are on the whole mononuclear complexes only and, furthermore, this fact is of interest because it makes an estimation of the complexity of the system possible. In the following sections the problem will be considered in greater detail.

#### b. Estimation of the Formation Function on the Basis of DOEHLEMANN and FROMHERZ'S Measurements.

For some of the mixtures represented in Fig. 1 it is possible by interpolation to choose a cupric chloride solution of such a concentration that its molar extinction coefficient is the same as that of the mixed solution throughout the investigated part of the spectrum. This means that we have two solutions with the same complex distribution and the same concentration of free ligand, although their total concentrations are different. Such solutions have been termed corresponding by the author,<sup>1</sup> and they are important because from their total concentrations we may calculate both the mean number of bound ligands per metal atom, the so-called formation function  $\bar{n}$ , and the concentration of free ligand. Since a detailed discussion of this problem may be found in the mentioned work by the author, the method will only be outlined here.<sup>2</sup>

<sup>1</sup> D. Kgl. Danske Vidensk. Selskab, Mat.-fys. Medd. **21**, No. 4 (1944).

<sup>2</sup> The method, which is of fundamental importance for the calculation of step equilibria on the basis of optical measurements, has been applied, inde-

The formation function  $\bar{n}$  is given by the expression

$$\bar{n} = \frac{C_{\text{Cl}^-} - [\text{Cl}^-]}{C_{\text{Cu}}}. \quad (1)$$

$C_{\text{Cl}^-}$  and  $C_{\text{Cu}}$  denote the total concentrations of chlorine ion and cupric copper, respectively, and  $[\text{Cl}^-]$  the concentration of free chlorine ion. In two corresponding solutions the formation functions are identical, and if this is expressed in an equation, we easily find

$$\bar{n} = \frac{C_{\text{Cl}^-}^0 - C_{\text{Cl}^-}}{C_{\text{Cu}}^0 - C_{\text{Cu}}}. \quad (2)$$

$$[\text{Cl}^-] = \frac{C_{\text{Cu}}^0 C_{\text{Cl}^-} - C_{\text{Cu}} C_{\text{Cl}^-}^0}{C_{\text{Cu}}^0 - C_{\text{Cu}}}. \quad (3)$$

The total concentrations without indices refer *e. g.* to the mixed solutions, and the indexed concentrations to corresponding pure cupric solutions. Thus,

$$C_{\text{Cl}^-}^0 = 2 C_{\text{Cu}^{++}}^0 = 2 C_{\text{CuCl}_2}^0.$$

Table 2. Formation function and concentration of free chlorine ion calculated according to the theory of corresponding solutions from the measurements of DOEHLEMANN and FROMHERZ.

No.	$C_{\text{Cu}^{++}}$	$C_{\text{Cl}^-}$	$C_{\text{CuCl}_2}^0$ 275 m $\mu$	$C_{\text{CuCl}_2}^0$ 300 m $\mu$	$C_{\text{CuCl}_2}^0$ 325 m $\mu$
4.....	0.0235	0.519	0.288	0.282	—
5.....	0.0470	1.038	0.563	0.575	0.616
7.....	0.0940	2.076	1.260	1.260	1.175

No.	$[\text{Cl}^-]$	$\bar{n}$	$\epsilon_{275}$	$\epsilon_{300}$	$\epsilon_{325}$
4.....	0.515	$0.19 \pm 0.03$	114	23.6	—
5.....	1.03	$0.25 \pm 0.06$	224	47.5	10.0
7.....	2.04	$0.34 \pm 0.05$	490	133	26.1

pendently of the present author, by Olerup in his thesis (Järnkloridernas Komplexitet, Lund 1944, p. 65) to the particular case that one of the corresponding solutions is so dilute that the concentration of free ligand becomes identical with the total ligand concentration.



Table 2 shows the result of a calculation of the formation function for mixtures Nos. 4, 5, and 7. The calculation has been made for three wave-lengths by interpolation on curves, where  $\log \varepsilon$  of the measured pure cupric chloride solutions has been plotted against the logarithm of their concentration. The table comprises the interpolated values for  $C_{\text{CuCl}_2}^0$  and the mean values of the formation function and of the concentration of free chlorine ion, calculated by means of (2) and (3). For the solutions examined, not quite the same corresponding cupric chloride concentration is determined at each of the wave-lengths used. The influence of this uncertainty on the formation function appears in the table as a mean uncertainty of the calculated values. The application of formulae (2) and (3) is underlaying the assumption that the classical law of mass action is valid. This condition is presumably fulfilled for the most dilute solutions of Fig. 1, where the ionic strengths of the corresponding cupric chloride and calcium chloride solutions do not deviate essentially from one another, however, in this range the calculation of  $\bar{n}$  depends particularly on the accuracy of the measurements. It appears from the extinction coefficients given in the table that the light absorption at 275 and 300  $m\mu$  is almost proportional to the concentration of free chlorine ion for concentrations up to about 1 molar. Hence, it may be concluded that in the respective wave-length and concentration range mainly the monochloro complex is decisive for the light absorption.

#### c. SPACU and MURGULESCU'S Measurements in the Blue Mercury Line.

Using the visible Hg-lines and a König-Martens spectrophotometer, SPACU and MURGULESCU<sup>1</sup> performed some accurate measurements of the light absorption of cupric chloride solutions with varying potassium chloride contents at 20° C. The light absorption shows only a slight variation with the chlorine ion concentration in the Hg-lines 578 and 546  $m\mu$ , but, on the other hand, a very marked variation in the blue Hg-line 436  $m\mu$ . SPACU and MURGULESCU'S measurements at 436  $m\mu$  are repre-

<sup>1</sup> SPACU and MURGULESCU, Z. physik. Chem. A **170** (1934) 71.

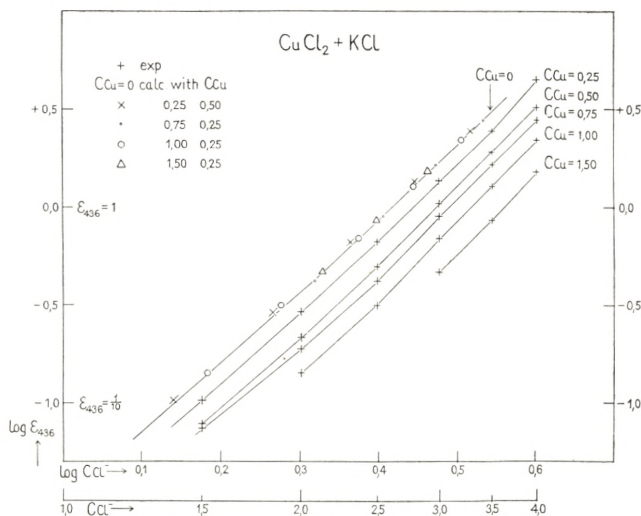


Fig. 2. SPACU and MURGULESCU's measurements of the light absorption in cupric chloride solutions with and without potassium chloride added. The figure gives the molar extinction coefficient in the Hg-line 436 m $\mu$  at various copper concentrations as a function of the total chlorine ion concentration.

sented graphically in Fig. 2. These authors measured at five different copper concentrations, and for each of these concentrations the logarithm of the molar extinction coefficient is plotted against the logarithm of the total chlorine ion concentration of the solution. For each copper concentration the slope of the curve  $\frac{\Delta \log \epsilon_{436}}{\Delta \log C_{Cl^-}}$  is very near 4 or, in other words, in the concentration range examined the molar extinction coefficient increases with almost the fourth power of the chlorine ion concentration.

SPACU and MURGULESCU observed this fact, and they realized that it is in favour of a highly absorbing tetrachloro complex present in the solution in a low concentration. On the other hand, SPACU and MURGULESCU give much reflexion to the question why BEER'S law is not valid at a constant total chlorine ion concentration. This is, of course, due to the fact that the total chlorine ion concentration and the concentration of free chlorine ions at finite copper concentrations are two different things owing to the complex-bound chlorine. A quantitative calculation of the prevailing conditions can easily be carried through by means of the above-mentioned principle, according to which solutions with

the same molar extinction coefficients have the same formation function and the same concentration of free chlorine ions. An example for the calculation of the respective magnitudes on the basis of SPACU and MURGULESCU's measurements is given in Table 3.

Table 3. Formation function, concentration of free chlorine ion, and the power with which the extinction coefficient depends on the chlorine concentration calculated from the measurements of SPACU and MURGULESCU.

$C_{Cl^-}$ ( $C_{Cu} = 0.75$ )	$\epsilon_{436}$	$\log \epsilon_{436}$	$\log C_{Cl^-}$ ( $C_{Cu} = 0.25$ )	$\bar{n}$	$[Cl^-]$	$\log [Cl^-]$	$\frac{A \log \epsilon_{436}}{A \log [Cl^-]}$
1.50	0.0741	-1.130	0.134	0.28	1.29	0.111	
2.00	0.1880	-0.726	0.250	0.44	1.67	0.223	3.60
2.50	0.4227	-0.374	0.346	0.56	2.08	0.318	3.70
3.00	0.8965	-0.047	0.432	0.60	2.55	0.407	3.67
3.50	1.637	+0.214	0.498	0.71	2.97	0.473	3.95
4.00	2.791	+0.446	0.557	0.79	3.41	0.533	3.87

In the first columns of Table 3 are given the total chlorine ion concentration and the experimentally determined extinction coefficients for all solutions with a copper concentration 0.75. The logarithm of the  $C_{Cl^-}$  concentration corresponding to the reported extinction coefficients and the copper concentration 0.25 are to be found in column 4 (determined graphically by means of Fig. 2). In the following columns are given the values for the formation function and the concentration of free chlorine ion calculated by means of (2) and (3). SPACU and MURGULESCU's measurements at other copper concentrations have been combined in an analogous manner with their measurements at the copper concentration 0.25. All corresponding values of  $\bar{n}$  and  $\log [Cl^-]$  calculated in this way are represented graphically in Fig. 5 (marked as  $\blacktriangle$  points) and together with the values calculated from DOEHLEMAN and FROMHERZ's measurements (marked as  $\blacktriangledown$  points) they determine the first part of the formation curve of the cupric chloride system. In Fig. 2  $\log \epsilon_{436}$  is plotted against the logarithm of the calculated values for the concentration of free chlorine ions. In the graph this is the curve



calculated for an infinitely small copper concentration, and it is seen that the calculated points fall very nearly on one and the same curve, independent of the copper concentration in the solutions used for the calculation. The slope of the curve

$$\frac{\Delta \log \varepsilon_{436}}{\Delta \log [\text{Cl}^-]}$$

calculated from point to point on the basis of the small circular points, representing the values of  $\log \varepsilon_{436}$  and  $\log [\text{Cl}^-]$  in Table 3, are given in the last column of the table. At chlorine ion concentrations in the range 1.5 to 2 N the slope of the curve is about 3.60, and the corresponding value for  $\bar{n}$  is about 0.40. Consequently,

$$\frac{\Delta \log \varepsilon_{436}}{\Delta \log [\text{Cl}^-]} \cong 4 - \bar{n}. \quad (4)$$

On the supposition that we may apply the concentration law of mass action, the relation between the concentration of the single complex ions and the concentration of free chlorine ions is given by the extended Bodländer formula.<sup>1</sup> According to this formula the change in the concentration of the tetrachloro complex is given by

$$\frac{d \log \frac{[\text{CuCl}_4^-]}{C_{\text{Cu}}}}{d \log [\text{Cl}^-]} = 4 - \bar{n}. \quad (5)$$

Comparing (4) and (5) it is obvious that there is an approximate proportionality between  $\varepsilon_{436}$  and the relative concentration of the tetrachloro complex. It appears from Table 3 that  $\frac{\Delta \log \varepsilon_{436}}{\Delta \log [\text{Cl}^-]}$  with increasing chlorine ion concentration exceeds the value  $4 - \bar{n}$ . This is hardly due to a formation of complexes with more than four chlorine ions, but is naturally explained by the fact that we have entered a concentration range where the activity coefficients of the ions begin to increase with increasing concentration. An increasing ligand concentration will always favour the formation of the complex richest in ligand and, hence, for sufficiently high concentrations of chlorine ion it seems justified

<sup>1</sup> See Metal Ammine Formation in Aqueous Solution, p. 28.

to calculate the concentration of the tetrachloro complex from the expression

$$[\text{CuCl}_4^{--}] = \frac{\varepsilon_{436}}{\varepsilon_{436}^0} C_{\text{Cu}}, \quad (6)$$

where  $\varepsilon_{436} \approx 500$  denotes the limiting extinction coefficient of the cupric chloride system at very high chlorine ion concentration.

#### d. An Application of P. JOB'S "Méthode des Variations Continues".

The validity of an expression like (6) is confirmed in a paper by T. MOELLER,<sup>1</sup> who, using P. JOB'S méthode des variations continues in the form modified by VOSBURGH and COOPER,<sup>2</sup> found that copper chloride solutions contain a tetrachloro complex. MOELLER mixed equimolecular solutions of cupric nitrate and various chlorides, and in that part of the spectrum where a change in absorption takes place (blue and green light) he found a maximum for the optical density at a proportion of the mixture corresponding to the tetrachloro complex, *i. e.* four volumes of chloride solution and one volume of cupric nitrate solution. According to the method this is a criterion for the existence of a tetrachloro complex.

Obviously MOELLER'S measurements do not preclude the existence of other chloro complexes, but they support the validity of (6), which will be used in what follows for the determination of the concentration of the tetrachloro complex in the cupric chloride solutions at high chlorine ion concentrations.

### 3. Theoretical Remarks on the Calculation of Complex Equilibria in Concentrated Chloride Solutions.

#### a. Variation of the Activity Coefficient with the Concentration.

In previous rough calculations the validity of the classical law of mass action was considered a supposition. This, of course,

<sup>1</sup> T. MOELLER, Journ. Physic. Chem. **48** (1944) 111.

<sup>2</sup> VOSBURGH and COOPER, Journ. Amer. Chem. Soc. **63** (1941) 437.

is not correct in the case of high and varying concentrations, and therefore we shall first discuss the question how for a number of chlorides the activity coefficient varies with the concentration. This interdependence is shown in Fig. 3. The mean activity coefficient is denoted by  $\gamma$  (and not by  $f$ ) in order to indicate

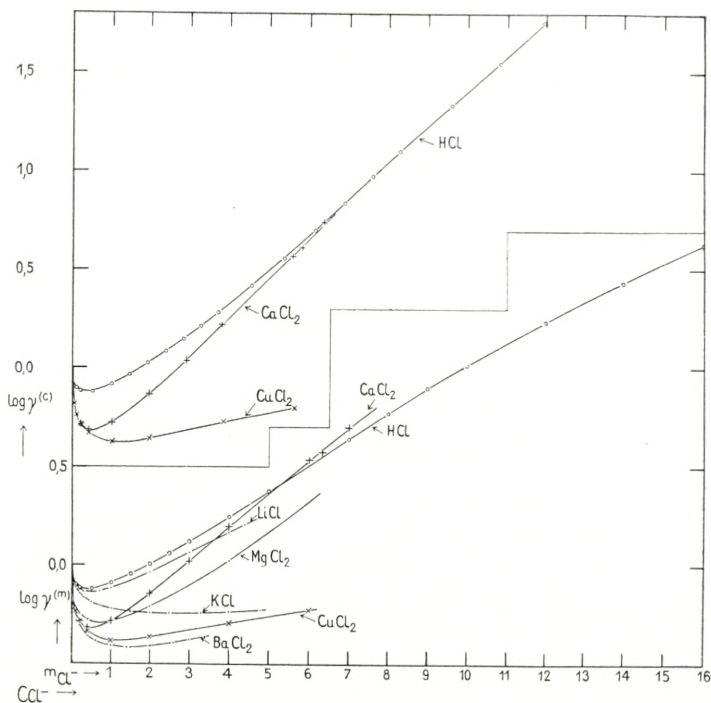


Fig. 3. The apparent mean ion activity coefficient of some chlorides as a function of the concentration. Above  $\gamma^{(c)}$  as a function of the molar chlorine ion concentration  $C_{Cl^-}$  in mols per litre solution, and below  $\gamma^{(m)}$  as a function of the chlorine ion molality  $m_{Cl^-}$  in mols per 1000 g.  $H_2O$ .

that a possible complex formation has not been taken into account. The indications  $\gamma^{(m)}$  and  $\gamma^{(c)}$  refer to the concentration scale used. In the lower part of the figure,  $\log \gamma^{(m)}$  is plotted against  $m_{Cl^-}$  or the chlorine ion normality per 1000 g. of water. These values are taken directly from LANDOLT-BÖRNSTEIN'S Tables<sup>1</sup> and are calculated thermodynamically either from cryoscopic measurements or from electrical chains without diffusion potential. In order to obtain a suitable basis of comparison for the

<sup>1</sup> II. Erg.-bd., p. 1111 and III. Erg.-bd., p. 2138.



chlorides examined in highly concentrated solutions, the upper part of the figure contains both the activity coefficients and the chlorine ion normality converted into the units used in the present investigation, *viz.* the concentration per litre solution.

It is seen that the activity coefficients decrease rapidly in the Debye-Hückel range (where mainly the type of the salt determines the course of the curve), passing through a minimum in the range of moderate concentrations where the classical law of mass action therefore holds approximately, and finally increasing at high chlorine ion concentrations. Thermodynamically we determine the activity of the non-hydrated salts; the increase in  $\gamma$  is due to the fact that the concentration of the non-hydrated ions increases with the decreasing water tension of the solution, the increase being more pronounced the more hydrated the salts.<sup>1</sup> Setting aside the cause of the increase in the activity coefficients, it is remarkable that  $\log \gamma^{(c)}$  for hydrochloric acid and calcium chloride (the only chlorides examined at very high concentrations) increases almost linearly with the ion normality for concentrations above 3 N up to the highest concentrations measured. The following formulae apply with approximation:

$$\begin{aligned}\log \gamma_{(\text{HCl})}^{(c)} &= -0.42 + 0.18 C_{\text{Cl}^-} \\ \log \gamma_{(\text{CaCl}_2)}^{(c)} &= -0.55 + 0.20 C_{\text{Cl}^-}.\end{aligned}$$

Our knowledge of the activity of the electrolytes in highly concentrated solution is indeed still very poor; however, it cannot be excluded that we have to do with a rather general rule.<sup>2</sup> The Debye-Hückel expression with a term of the first order added<sup>3</sup> formally leads to a rule of this kind; the square root expression  $\frac{1 + \sqrt{I}}{\sqrt{I}}$  being almost a constant for high values of the ionic strength  $I$ .<sup>4</sup>

<sup>1</sup> N. BJERRUM, Med. Vetenskapsakad. Nobelinst. **5**, No. 16 (1919).

<sup>2</sup> Cf. AKERLÖF, Journ. Amer. Chem. Soc. **56** (1934) 593, 1439.

<sup>3</sup> Cf. GUGGENHEIM, Phil. Mag. [7] **19** (1935) 588.

<sup>4</sup> In Fig. 3, the logarithm of the activity coefficients is deliberately plotted against the ion normality and not against the ion strength. A concept like ion strength, which is based on the supposition that the charge of the ions is of decisive importance for the activity coefficient, is of minor significance in the range of high concentration and is here naturally replaced by the total ion normality of the solution.

### b. The Basis of the Calculation of the Cupric Chloride System.

In all hitherto examined complex systems the cupric ion has the characteristic coordination number 4. This fact together with the optical finding of a monochloro and tetrachloro complex and, finally, the observation that the absorption spectra are independent of the copper concentration, which excludes polynuclear complexes, renders it probable that in cupric chloride solutions we have equilibria between the ions



The consecutive complexity constants  $k_1$ ,  $k_2$ ,  $k_3$ , and  $k_4$  corresponding to the formation of the four chloro complexes are defined by the expressions

$$\left. \begin{aligned} \frac{[\text{CuCl}^+]}{[\text{Cu}^{++}][\text{Cl}^-]} &= k_1 \frac{f_{\text{Cu}^{++}} \cdot f_{\text{Cl}^-}}{f_{\text{CuCl}^+}} \\ \frac{[\text{CuCl}_2]}{[\text{CuCl}^+][\text{Cl}^-]} &= k_2 \frac{f_{\text{CuCl}^+} \cdot f_{\text{Cl}^-}}{f_{\text{CuCl}_2}} \\ \frac{\text{CuCl}_3^-}{[\text{CuCl}_2][\text{Cl}^-]} &= k_3 \frac{f_{\text{CuCl}_2} \cdot f_{\text{Cl}^-}}{f_{\text{CuCl}_3^-}} \\ \frac{[\text{CuCl}_4^{--}]}{[\text{CuCl}_3^-][\text{Cl}^-]} &= k_4 \frac{f_{\text{CuCl}_3^-} \cdot f_{\text{Cl}^-}}{f_{\text{CuCl}_4^{--}}} \end{aligned} \right\} \quad (7)$$

For brevity, the water molecules have been omitted in the formulae and  $f_X$  denotes the activity coefficient of the molecule or ion X. In the mass action expressions (7) we find, besides the four unknown complexity constants, four activity coefficient expressions whose dependence on the concentration is unknown. It is therefore *a priori* obvious that a knowledge of the tetrachloro complex concentration  $[\text{CuCl}_4^{--}]$  (optically determined by means of (6)) and the chlorine ion concentration  $[\text{Cl}^-]$  is insufficient for an exact treatment of the cupric chloride system. Only an approximate treatment can be attempted with the aim to arrive at the essential features. Let us assume that the system

(7) may be described by a single mean activity coefficient  $F$  defined by the relations

$$F = \frac{f_{\text{Cu}^{++}} \cdot f_{\text{Cl}^-}}{f_{\text{CuCl}^+}} = \frac{f_{\text{CuCl}^+} \cdot f_{\text{Cl}^-}}{f_{\text{CuCl}_2}} = \frac{f_{\text{CuCl}_2} \cdot f_{\text{Cl}^-}}{f_{\text{CuCl}_3^-}} = \frac{f_{\text{CuCl}_3^-} \cdot f_{\text{Cl}^-}}{f_{\text{CuCl}_4^{--}}}. \quad (8)$$

This approximation corresponds to the assumption that  $\log f_{\text{CuCl}_n^{2-n}}$  changes evenly from  $f_{\text{Cu}^{++}}$  to  $f_{\text{CuCl}_4^{--}}$  and therefore is not quite unreasonable in the case of concentrated solutions, where chemical similarity between the ions rather than the charge of the ions determines the activity coefficients. As to the dependence of  $F$  on the concentration, we shall assume, in accordance with the above considerations, that in a concentrated solution

$$\log F = A + B \cdot C_{\text{ion}}, \quad (9)$$

where  $A$  and  $B$  are individual constants and  $C_{\text{ion}}$  is the total ion normality of the solution.

The validity of the classical law of mass action is a necessary condition for the application of the extended Bodländer formula

$$\frac{d \log \alpha_n}{d \log [\text{Cl}^-]} = n - \bar{n}, \quad (10)$$

where  $\alpha_n = \frac{[\text{CuCl}_n^{2-n}]}{C_{\text{Cu}}}$ . However, if only one mean activity coefficient is introduced, this formula may be written<sup>1</sup>

$$\frac{d \log \alpha_n}{d \log F + d \log [\text{Cl}^-]} = n - \bar{n}. \quad (11)$$

In expression (9) the total ion normality appears instead of the chlorine ion concentration; since, however, the experimental investigation was carried out at low copper concentrations and high chloride concentrations, and disregarding other complex formation, we may put

$$C_{\text{ion}} = [\text{Cl}^-]. \quad (12)$$

If (9) is differentiated, applying (12), with regard to the

<sup>1</sup> This is seen at once when, at the derivation of the formula, the expression for  $\alpha_n$  is differentiated with regard to  $F[\text{Cl}^-]$  instead of  $[\text{Cl}^-]$ .



chlorine ion concentration, and substituted in (11), this formula may be written

$$\frac{d \log \alpha_n}{d [\text{Cl}^-]} = \left( \frac{0.4343}{[\text{Cl}^-]} + B \right) (n - \bar{n}), \quad (13)$$

the constant A disappearing on differentiation. In this expression putting  $n = 4$  and, moreover, taking into account the proportionality between  $\alpha_4$  and  $\epsilon_{436}$ , according to (6), we obtain

$$\frac{d \log \epsilon_{436}}{d [\text{Cl}^-]} = \left( \frac{0.4343}{[\text{Cl}^-]} + B \right) (4 - \bar{n}). \quad (14)$$

In what follows, expression (14) has been used to determine the formation function  $\bar{n}$  and the constant B from  $\frac{d \log \epsilon_{436}}{d [\text{Cl}^-]}$  at various chlorine ion concentrations.

#### 4. Extinction Measurements of Mixtures of Cupric Chloride with other Chlorides.

##### a. Measurements and Experimental Details (in Collaboration with PALLE ANDERSEN).

Table 4 contains the measurements of the extinction coefficients of cupric chloride in concentrated solutions of hydrochloric acid, lithium-, magnesium-, and calcium chloride. The majority of the measurements in lithium- and magnesium chloride solutions has been carried out by Mr. PALLE ANDERSEN, the other measurements were performed by the author. The molar total concentrations of cupric chloride and of the chlorides added are recorded in columns 2 and 3 of the respective sections of the table; the last column but two gives the molar extinction coefficients found. The extinction coefficient of the wave-length  $\lambda$  was calculated according to the formula

$$\epsilon_\lambda = \frac{\log \frac{I_0}{I}}{C_{\text{Cu}} \cdot d}, \quad (15)$$

where  $I_0$  and  $I$  denote the intensity of the incident and the trans-

Table 4. Light absorption measurements of cupric chloride solutions containing an other chloride at 22–23° C.

## a. Cupric chloride + hydrochloric acid.

No.	C <sub>CuCl<sub>2</sub></sub>	C <sub>HCl</sub>	[Cl <sup>-</sup> ]	ε <sub>436</sub>	log ε <sub>436</sub>	$\frac{A \log \epsilon_{436}}{A t^\circ}$
1	0.001602	13.32	13.32	538	2.731	
2	0.001602	12.80	12.80	532	2.726	
3	0.002004	11.85	11.85	507	2.705	
4	0.002004	10.87	10.87	477	2.678	
5	0.001607	10.05	10.05	447	2.650	
6	0.002006	9.67	9.67	439	2.642	0.004
7	0.00401	8.59	8.59	369	2.567	
8	0.00397	8.52	8.52	359	2.555	
9	0.002004	8.21	8.21	332	2.521	
10	0.001990	7.82	7.82	297	2.473	
11	0.00401	7.51	7.51	272	2.434	
12	0.00399	7.02	7.02	217	2.337	
13	0.00998	6.44	6.44	167.0	2.223	0.008
14	0.01001	6.025	6.025	122.2	2.088	
15	0.00597	5.92	5.92	115.5	2.063	
16	0.00597	5.448	5.448	78.6	1.896	
17	0.003006	5.37	5.37	75.0	1.875	
18	0.01002	5.35	5.35	74.33	1.871	
19	0.01996	4.83	4.83	43.2	1.636	
20	0.0499	4.388	4.388	26.63	1.425	
21	0.01595	4.288	4.288	24.04	1.381	
22	0.02989	4.142	4.142	19.69	1.294	
23	0.02989	3.788	3.788	12.11	1.084	0.018
24	0.0499	3.625	3.625	9.63	0.984	
25	0.0499	3.625	3.625	9.95	0.998	
26	0.0995	3.313	3.313	6.64	0.822	
27	0.0299	3.222	3.222	5.50	0.740	
28	0.0499	3.203	3.203	4.77	0.679	∞ 0.02
29	0.0995	2.954	2.954	3.73	0.572	
30	0.0499	2.954	2.954	3.50	0.544	
				ε <sub>405</sub>	log ε <sub>405</sub>	$\frac{A \log \epsilon_{405}}{A^\circ t}$
31	0.000255	12.50	12.50	1290	3.11	0.004

Table 4 (continued).

## b. Cupric chloride + lithium chloride.

No.	C <sub>CuCl<sub>2</sub></sub>	C <sub>LiCl</sub>	$d_{40}^{-20}$	[Cl <sup>-</sup> ]	$\epsilon_{436}$	log $\epsilon_{436}$	$\frac{\Delta \log \epsilon_{436}}{\Delta t^{\circ}}$
1	0.003134	12.09 III	1.257	12.09	421	2.624	$\approx 0.004$
2	0.003129	11.01 III	1.237	11.02	407	2.610	
3	0.003339	10.31 III	1.220	10.32	383	2.583	
4	0.002786	9.75 II	1.207	9.76	358	2.554	
5	0.005012	9.22 II	1.198	9.24	331	2.520	
6	0.004218	8.64 III	1.185	8.65	291	2.463	
7	0.003921	7.88 I	1.169	7.90	234	2.370	
8	0.004338	7.81 III	1.168	7.81	216	2.334	
9	0.004941	7.76 II	1.167	7.77	218	2.338	
10	0.004572	7.18 III	1.155	7.19	172	2.235	
11	0.007135	6.86 III	1.148	6.86	140	2.147	
12	0.01723	6.79 III	1.148	6.80	150	2.175	
13	0.01065	6.26 II	1.137	6.29	93.2	1.970	
14	0.01005	6.24 III	1.135	6.24	94.2	1.974	
15	0.01824	5.75 III	1.128	5.76	64.8	1.812	
16	0.02837	5.22 III	1.115	5.22	40.3	1.605	
17	0.05291	4.77 III	1.109	4.78	26.2	1.419	
18	0.02358	4.76 II	1.105	4.76	23.8	1.377	
19	0.04217	4.50 III	1.104	4.50	17.0	1.231	
20	0.07404	4.26 III	1.104	4.27	14.8	1.170	
21	0.07111	3.92 II	1.095	3.93	9.30	0.967	
22	0.07710	3.77 III	1.094	3.77	7.72	0.888	
23	0.1014	3.22 II	1.084	3.23	3.73	0.572	
24	0.000246	13.34 I	1.284	13.34	$\epsilon_{405}$ 813	log $\epsilon_{405}$ 2.91	



Table 4 (continued).

## c. Cupric chloride + magnesium chloride.

No.	$C_{CuCl_2}$	$C_{MgCl_2}$	$d_{40}^{\sim 20}$	$[Cl^-]$	$\epsilon_{436}$	$\log \epsilon_{436}$	$\frac{\Delta \log \epsilon_{436}}{\Delta t^\circ}$
1	0.003427	5.080	1.340	10.16	308	2.489	
2	0.003431	4.976	1.331	9.95	307	2.487	
3	0.003313	4.897	1.327	9.79	280	2.447	0.007
4	0.003306	4.720	1.320	9.44	255	2.406	
5	0.005109	4.557	1.309	9.11	229	2.360	0.008
6	0.005743	4.331	1.292	8.66	204	2.310	
7	0.005757	4.185	1.285	8.37	182	2.260	0.010
8	0.006974	3.994	1.270	7.99	162	2.210	
9	0.008567	3.813	1.259	7.63	133	2.124	
10	0.01276	3.580	1.246	7.16	105	2.021	0.013
11	0.02905	3.330	1.232	6.66	80.1	1.904	
12	0.01592	3.205	1.222	6.41	65.7	1.818	
13	0.02399	3.056	1.213	6.11	52.6	1.721	
14	0.06732	2.695	1.195	5.39	30.1	1.479	
15	0.04829	2.480	1.180	4.96	19.1	1.281	0.017
16	0.07691	2.221	1.172	4.44	11.1	1.045	
17	0.08479	2.021	1.152	4.04	6.94	0.841	0.019
18	0.1021	1.815	1.140	3.63	4.07	0.610	
					$\epsilon_{405}$	$\log \epsilon_{405}$	
19	0.000255	4.908	1.327	9.82	740	2.87	

## d. Cupric chloride + calcium chloride.

No.	$C_{CuCl_2}$	$C_{CaCl_2}$	$d_{40}^{\sim 20}$	$[Cl^-]$	$\epsilon_{436}$	$\log \epsilon_{436}$	$\frac{\Delta \log \epsilon_{436}}{\Delta t^\circ}$
1	0.003333	7.025 II	1.522	14.05	297	2.473	
2	0.003333	6.76 II	1.506	13.52	302	2.480	$\infty$ 0.007
3	0.004004	6.365 II	1.482	12.73	296	2.472	
4	0.003333	5.71 II	1.440	11.42	275	2.440	
5	0.003212	5.25 II	1.407	10.50	249	2.396	
6	0.01002	4.725 I	1.372	9.51	208	2.318	
7	0.00600	4.378 II	1.350	8.76	169	2.227	
8	0.008034	4.160 II	1.333	8.32	145	2.160	
9	0.00804	3.875 I	1.305	7.62	103	2.013	
10	0.009998	3.435 II	1.279	6.87	70.5	1.848	
11	0.02006	3.14 I	1.260	6.34	49.4	1.694	
12	0.02415	2.895 I	1.242	5.84	35.0	1.544	
13	0.03309	2.674 II	1.227	5.35	22.8	1.358	
14	0.0400	2.49 I	1.210	5.03	16.6	1.220	
15	0.06662	2.244 II	1.194	4.49	9.73	0.988	
16	0.06662	2.043 II	1.177	4.09	6.15	0.789	
17	0.06662	1.883 II	1.164	3.77	4.26	0.630	

mitted light, respectively,  $C_{\text{Cu}}$  the total copper concentration, and  $d$  the thickness of the absorbing layer in cm. The extinction measurements were made by means of a König-Martens spectrophotometer, an Uviol mercury lamp being used as light source. The measurements were performed mainly with the mercury line  $436 \text{ m}\mu$  but, as appears from the table, a few were also made in the violet line  $405 \text{ m}\mu$ . However, the  $405$ -line is of very low visual intensity and, therefore, the latter measurements are encumbered with a considerably higher uncertainty than those at  $436 \text{ m}\mu$ . As absorption vessels were applied almost exclusively the standard cell of the "kleine Beleuchtungseinrichtung" of the König-Martens apparatus with its appurtenant "Schulzkörper" and glass cover. The effective thickness of layer of the cell is  $1 \text{ cm}$  (determined by the thickness of the Schulz body). Handling of the cell is most convenient, as it permits a rapid exchange of the solution by pipetting. It must furthermore be considered advantageous that the temperature of the solution can be checked relatively easily. The completely closed absorption tubes which are provided with screwed-on brass caps and are used in the "grosse Beleuchtungseinrichtung" of the König-Martens apparatus offer other advantages, thus the apparatus is well shielded against injurious vapours from the solutions. These tubes were therefore used for the measurement of the strongest hydrochloric acid solutions.

The absorption of blue light of cupric chloride solutions is rather dependent on temperature and, hence, the temperature had to be kept constant. The whole apparatus was therefore placed in an electrically regulated thermostat room. During the determination of the extinction coefficients recorded in Table 4 the temperature was kept at  $22$ – $22.5^\circ \text{C}$ . Generally, the solutions were a little warmer, but direct checking revealed that their temperature never exceeded  $23^\circ \text{C}$ . In some cases, the temperature dependence was determined by first measuring the extinction coefficient at the temperature of the unheated thermostat room ( $16$ – $20^\circ$ ) and, subsequently, at maximum heating of the room ( $27$ – $30^\circ$ ). The measurements at the two temperatures are comprised in the values for the temperature coefficient  $\frac{\Delta \log \epsilon_\lambda}{\Delta t^\circ}$  given in the last column of Table 4. The values marked by

*circa* are determined either at a considerably smaller temperature interval or they are less certain for other reasons.

For the preparation of the solutions, Merck's cupric chloride and magnesium chloride *pro analysi* were used; the hydrochloric acid was a completely colourless commercial product (37 per cent.). Two calcium chloride preparations were applied, *viz.* (I) an ordinary crystallized commercial product and (II) Merck's *pro analysi* preparation. Three lithium chloride preparations were used, *viz.* (I) an ordinary commercial product, (II) a recrystallized laboratory preparation, and (III) a Kahlbaum preparation. In Table 4, the Roman numerals after the lithium and calcium chloride concentrations refer to the respective salt preparation used. The solutions were made in measuring flasks from stock solutions of the different chlorides. The stock solutions were made dust-free by filtration through hard squeezed cotton. The concentration was determined by Volhard titration and, in the hydrochloric acid solutions, moreover acidimetrically. Generally, hydrochloric acid and cupric chloride were pipetted, while the concentrated viscous solutions of lithium-, magnesium-, and calcium chloride were always weighed into the measuring flasks. The specific gravity of the solutions was determined by weighing the contents of the measuring flasks, and are given in the fourth column of Table 4. Only the specific gravity of the hydrochloric acid solutions was not determined.

Solutions of the calcium chloride preparations I and the lithium chloride preparations I and II showed slight turbidity on addition of cupric chloride; however, the precipitate was dissolved after addition of a small quantity of hydrochloric acid. The hydrochloric acid thus added is included in the chlorine ion normality recorded in the fifth column of Table 4.

Three of the hydrochloric acid solutions measured are stronger than the usual commercial product and were prepared from a saturated solution of hydrogen chloride. Two of the magnesium chloride solutions and three of the calcium chloride solutions are supersaturated with regard to the respective salts.



## b. The Influence of the Salt Concentration on the Light Absorption.

The experimental material is given in Fig. 4.  $\log \epsilon_{436}$  is plotted as ordinates and the chlorine ion normality of the chloride used, *viz.* hydrochloric acid, lithium-, magnesium-, and calcium chloride as abscissae. The normality of the salts added is denoted

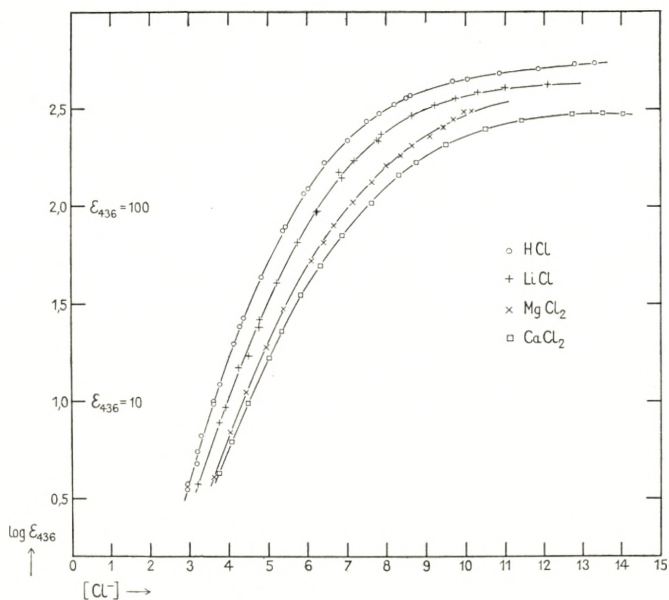


Fig. 4. Light absorption measurements of mixed cupric chloride solutions in the Hg-line 436  $m\mu$  at low copper concentration and high chloride concentrations.

as  $[Cl^-]$  because it approximates the concentration of free chloride (in the sense of chloride which is not complex-bound to copper); notably  $[Cl^-]$  does not deviate much from the total ion normality of the solution, since the copper concentration in all measured solutions is rather low. It is seen that the experimental points fall on smooth curves. The four curves are displaced rather much relative to each other. They become more flat with increasing chlorine ion concentration, and at very high chlorine ion concentrations above 10 N they are nearly horizontal. In this range it can be assumed that the tetrachloro complex is the only one existing, and therefore it is remarkable that the limiting absorption has not quite the same value in the different

chloride solutions. Of course this complicates the problem, but it is a natural consequence of the fact that the light absorption is determined in quite different salt media. HALBAN<sup>1</sup> has shown that this involves a considerable change (deformation) of the absorption spectrum as compared with the absorption in dilute solution. HALBAN and his coworkers investigated the absorption of the nitrate ion and found that generally the addition of salt causes an ultraviolet displacement of the absorption band, which depends in a specific way on the cation of the salt. HALBAN, and recently also KORTÜM,<sup>2</sup> brought the displacement of the absorption band in connection with the formation of an ion-associate between the cation and the nitrate ion in equilibrium with the original ions,<sup>3</sup> and it is natural to assume that the negatively charged tetrachloro complex forms similar ion-associates with the cations present. The extinction curves in Fig. 4 are determined at 436 m $\mu$ , only. This wave-length is found on the long-wave side of the absorption band of the chloro complex (cf. Fig. 1), and an ultraviolet displacement therefore means that the limiting absorption in the concentrated solutions is smaller than the absorption of the tetrachloro complex in dilute solution. This agrees well with the fact that the absorption in concentrated calcium chloride solutions after reaching a maximum in a *c.* 13 N solution by further increase in concentration shows a tendency to decrease. The extrapolated limiting absorption has the following values in the respective salt solutions (see p. 28):

	HCl	LiCl	MgCl <sub>2</sub>	CaCl <sub>2</sub>
log $\epsilon_{436}^0$ .....	2.742	2.65	2.66	2.50

To judge from this sequence, the deformation of the absorption curve is considerably greater in the calcium chloride- than in the alkali chloride and magnesium chloride solutions, and this is in qualitative agreement with the findings of HALBAN and KORTÜM as regards the influence of the same salts on the absorption of the nitrate ion.

According to KORTÜM,<sup>4</sup> the influence of the temperature on

<sup>1</sup> HALBAN, Z. Elektrochem. **34** (1928) 489.

<sup>2</sup> KORTÜM, Z. Elektrochem. **50** (1944) 144.

<sup>3</sup> Cf. N. BJERRUM, D. Kgl. Danske Vidensk. Selskab, Mat.-fys. Medd. **7**, No. 9 (1926).

<sup>4</sup> loc. cit., p. 149.

the absorption spectrum is also specific and inverse to the salt effect. With increasing temperature, most absorption bands are displaced towards red; the same holds here, however, it is worth noting that the temperature coefficient of the limiting absorption in calcium- and magnesium chloride solutions is higher than in lithium chloride and hydrochloric acid solutions (cf. Table 4). In all cases, the temperature coefficient increases markedly with decreasing chlorine ion concentration owing to the fact that the equilibrium between the complex ions is dependent on temperature (for further details, cf. p. 36).

In concentrated solutions of the alkali and the earth-alkali chlorides, not only the chloro complex ions, but also the chlorine ions probably form ion-associates with the metal ions, and in concentrated hydrochloric acid solutions we have a few per cent. of undissociated hydrogen chloride.<sup>1</sup>

Thus, the conditions are very complicated: if we shall altogether attempt a calculation of the concentration of the individual cupric chloride complexes as a function of the total chlorine ion concentration, this is due to the fact

(1) that the secondary salt effect on the light absorption as a whole is only small, and

(2) that by setting the concentration of the free chlorine ions equal to the total chlorine concentration of the chlorides added, an error appears which is, at least partly, neutralized by the application of the empirical activity function.

## 5. Calculation of the Experimental Material.

### a. The Activity Constant $B$ and the Formation Function $\bar{n}$ .

For the calculation of the formation function  $\bar{n}$  of the cupric chloride system we have the previously derived formula (14) (p. 17), where  $\frac{d \log \epsilon_{436}}{d [\text{Cl}^-]}$  is the slope of the extinction curves in Fig. 4, and  $B$  is the proportionality factor of the ion concentration in expression (9) for the mean activity coefficient  $F$ .  $B$  is

<sup>1</sup> Cf. ROBINSON, Trans. Faraday Soc. **32** (1936) 743.



*a priori* unknown, but fortunately it can be determined from the upper part of the extinction curves, since the limiting absorption can be roughly estimated by extrapolation of the curves of Fig. 4. According to (6), the following equation applies to the degree of formation of the tetrachloro complex

$$\alpha_4 = \frac{[\text{Cu Cl}_4^{--}]}{C_{\text{Cu}}} = \frac{\varepsilon_{436}}{\varepsilon_{436}^0}; \quad (16)$$

if  $\alpha_4 \gtrsim 0.5$ , it moreover holds that

$$1 - \alpha_4 \approx 4 - \bar{n}. \quad (17)$$

Consequently, an approximate value for B can be calculated by means of (14), and introducing this value into the same formula it becomes possible to calculate  $\bar{n}$  from the slope of the extinction curves over the whole range examined. By this method, a preliminary knowledge of the formation curve of the cupric chloride system was obtained, and it was estimated that the system had a positive ligand effect<sup>1</sup> of the order of magnitude of 0.2 to 0.3. This calculation was improved through successive approximations

(1) by finding a better value for the limiting absorption on the basis of our knowledge of B, and

(2) by substituting a better approximation for (17) on the basis of our knowledge of the ligand effect.

*ad* (1) For the fourth consecutive complexity constant the following equation applies in the range of high concentrations:

$$k_4 = \frac{\alpha_4}{(1 - \alpha_4)F \cdot [\text{Cl}^-]}. \quad (18)$$

By means of (9) and (16) this expression may be converted into

$$\varepsilon_{436}^0 - \varepsilon_{436} = \frac{1}{k_4 \cdot 10^A} \cdot \frac{\varepsilon_{436}}{[\text{Cl}^-] \cdot 10^{B[\text{Cl}^-]}}. \quad (19)$$

(19) is linear in  $\varepsilon_{436}$  and  $\frac{\varepsilon_{436}}{[\text{Cl}^-] \cdot 10^{B[\text{Cl}^-]}}$ , and the limiting absorption may therefore be determined by linear extrapolation

<sup>1</sup> See Metal Ammine Formation in Aqueous Solution, p. 39.

of a graph where  $\varepsilon_{436}$  is plotted against  $\frac{\varepsilon_{436}}{[\text{Cl}^-] \cdot 10^{B[\text{Cl}^-]}}$ . If we apply this method, the limiting absorption in the hydrochloric acid and lithium chloride solutions can be extrapolated with considerable certainty to an infinitely great chlorine ion concentration; however, it should be kept in mind that the values obtained are not corrected for the Halban salt effect. The extrapolation was more uncertain in the case of magnesium chloride solutions and was without any appreciable value in the case of calcium chloride solutions, where the salt effect is so great that the absorption passes a flat maximum already in the range studied experimentally. The values of the limiting absorption used for the final calculation are given on p. 24 and in Table 5.

*ad* (2) For a system with the characteristic coordination number 4 and a constant ligand effect  $L$  the interdependence between  $\bar{n}$  and  $\alpha_4$  is given by the formulae<sup>1</sup>

$$\alpha_4 = \frac{p^4}{1 + 4x^3p + 6x^2p^2 + 4x^3p^3 + p^4} \quad (20)$$

$$\bar{n} = \frac{4x^3p + 12x^2p^2 + 12x^3p^3 + 4p^4}{1 + 4x^3p + 6x^2p^2 + 4x^3p^3 + p^4}, \quad (21)$$

where  $x = 10^{L/2}$  is the spreading factor of the system, and  $p$  a parameter which, for  $\bar{n} = 2$ , has the value 1. The application of (20) and (21) presupposes our knowledge of the ligand effect. However, on the basis of only an approximate knowledge of this quantity the formulae offer a much better approximation than (17) which holds the worse the smaller the ligand effect. Formulae (20) and (21) are most easily applied graphically by substituting rounded-off values for  $p$  and by plotting against each other the calculated values for  $\alpha_4$  and  $\bar{n}$ . This method was used for the final calculation of the constant  $B$ ,  $L$  being tentatively put at 0.2 ( $x = 1.26$ ); and, in order to arrive at an estimation of the significance of a variation in  $L$ , the latter was also put at 0.3 ( $x = 1.41$ ).

The results of the final calculation in the four different salt media, hydrochloric acid, lithium-, magnesium-, and calcium chloride are recorded in Table 5.

<sup>1</sup> See Metal Ammine Formation in Aqueous Solution, pp. 29 ff.

Table 5. Calculation of the constant B in the expression for the mean activity coefficient of the cupric chloride system.

## a. Hydrochloric acid solutions.

$$\log \varepsilon_{436}^0 = 2.742$$

[Cl <sup>-</sup> ]	$\alpha_4 = \frac{\varepsilon_{436}}{\varepsilon_{436}^0}$	$4 - \bar{n}$		$\frac{d \log \varepsilon_{436}}{d [Cl^-]}$	0.4343 [Cl <sup>-</sup> ]	B	
		x = 1.26	x = 1.41			x = 1.26	x = 1.41
10.87	0.865	0.135	0.135	0.030	0.0400	0.182	0.182
10.05	0.810	0.202	0.20	0.042	0.0432	0.165	0.167
9.67	0.796	0.215	0.213	0.050	0.0449	0.187	0.190
8.59	0.670	0.36	0.355	0.095	0.0506	0.213	0.217
8.21	0.602	0.45	0.44	0.116	0.0529	0.205	0.211
7.82	0.538	0.535	0.52	0.138	0.0556	0.202	0.210
7.51	0.493	0.60	0.58	0.160	0.0578	0.209	0.218
						0.195	0.199

B = 0.20

## b. Lithium chloride solutions.

$$\log \varepsilon_{436}^0 = 2.65$$

9.5	0.777	0.237	0.234	0.069	0.0457	0.245	0.249
9.0	0.711	0.317	0.309	0.088	0.0482	0.229	0.237
8.5	0.631	0.411	0.401	0.112	0.0511	0.222	0.229
8.0	0.543	0.529	0.511	0.149	0.0543	0.228	0.237
7.5	0.447	0.671	0.647	0.190	0.0579	0.225	0.236
						0.230	0.238

B = 0.23

## c. Magnesium chloride solutions.

$$\log \varepsilon_{436}^0 = 2.66$$

9.5	0.575	0.487	0.473	0.110	0.0457	0.180	0.187
9.0	0.504	0.581	0.565	0.131	0.0482	0.177	0.184
8.5	0.427	0.704	0.680	0.160	0.0511	0.177	0.184
8.0	0.349	0.836	0.806	0.188	0.0543	0.171	0.179
7.5	0.275	0.98	0.945	0.222	0.0579	0.169	0.177
						0.175	0.182

B = 0.18

## d. Calcium chloride solutions.

$$\log \varepsilon_{436}^0 = 2.50$$

10.50	0.788	0.225	0.222	0.059	0.0413	0.221	0.225
9.51	0.657	0.378	0.370	0.100	0.0457	0.219	0.224
8.76	0.533	0.543	0.528	0.142	0.0496	0.212	0.219
8.32	0.458	0.652	0.631	0.168	0.0522	0.206	0.214
7.62	0.326	0.88	0.85	0.210	0.0570	0.182	0.190
						0.208	0.214

B = 0.21



It appears from the table that the computed values for B only to a slight degree depend on the value for x, which has been made the basis of the calculation, and that for one and the same salt they are almost independent of the salt concentration. The B-values found are of the same order of magnitude as in the expressions for  $\gamma_{\text{HCl}}^{(c)}$  and  $\gamma_{\text{CaCl}_2}^{(c)}$  (p. 14). B is highest (0.23) in the lithium chloride solutions and lowest (0.18) in the magnesium chloride solutions. A high B-value involves a faster convergency towards the limiting absorption, and this is seen to be in qualitative agreement with the course of the extinction curves of Fig. 4. The calculations in hydrochloric acid- and calcium chloride solutions were carried out by using the directly determined values for  $\epsilon_{436}$  and  $[\text{Cl}^-]$  given in Table 4. In the cases of lithium- and magnesium chloride solutions, however, for which the points in Fig. 4 are not quite so nicely placed, the calculations were performed with interpolated values for the extinction coefficients corresponding to rounded-off chlorine ion concentrations.  $\frac{d \log \epsilon_{436}}{d[\text{Cl}^-]}$  is always determined graphically from the slope of the levelled curves in Fig. 4.

With the values found for B substituted in (14), the formation function is estimated for rounded-off chlorine ion concentrations in the rest of the experimental range. Moreover, the degree of formation of the tetrachloro complex is computed, and in Table 6 a selection of the calculated values is given.

When applying (14) it was not taken into consideration that the absorption of the tetrachloro complex is not quite independent of the concentration. This necessarily involves an error in the calculated data. In order to correct for this omission or at least to obtain an idea of the order of magnitude of this error, B and  $\bar{n}$  in the calcium chloride medium, where the salt effect is highest (cf. p. 24), were calculated on the following basis. It is assumed that we may completely disregard the salt effect in the hydrochloric acid solutions, and that  $\epsilon_{436}$  in the calcium chloride solutions varies linearly with the concentration. This leads to the following formula:

$$\epsilon_{436}^0 = 550 - 18 [\text{Cl}^-], \quad (22)$$

Table 6. Calculation of the formation function and the degree of formation of the tetrachloro complex in the range from about 4 to 7 N.

a. Hydrochloric acid solutions.

$$B = 0.20, \quad \log \varepsilon_{436}^0 = 2.742.$$

$[\text{Cl}^-]$	$\frac{d \log \varepsilon_{436}}{d [\text{Cl}^-]}$	$\frac{0.4343}{[\text{Cl}^-]}$	$\bar{n}$	$\log \varepsilon_{436}$	$\alpha_4$	$\log [\text{Cl}^-] + B[\text{Cl}^-]$
7.0	0.202	0.0620	3.23	2.340	0.396	2.25
6.0	0.308	0.0724	2.87	2.089	0.222	1.98
5.0	0.440	0.0869	2.47	1.711	0.0931	1.70
4.25	0.540	0.1021	2.21			1.48
3.50	0.660	0.124	1.96			1.24

a. Lithium chloride solutions.

$$B = 0.23, \quad \log \varepsilon_{436}^0 = 2.65.$$

7.0	0.231	0.0620	3.21	2.192	0.348	2.46
6.0	0.322	0.0724	2.93	1.899	0.177	2.16
5.0	0.413	0.0869	2.70	1.501	0.071	1.85
4.0	0.540	0.1086	2.41	1.010	0.0229	1.52

c. Magnesium chloride solutions.

$$B = 0.18, \quad \log \varepsilon_{436}^0 = 2.66.$$

7.0	0.266	0.0620	2.90	1.985	0.211	2.11
6.0	0.350	0.0724	2.61	1.690	0.107	1.86
5.0	0.455	0.0869	2.29	1.300	0.0437	1.60
4.0	0.560	0.1086	2.06	0.806	0.0140	1.32

d. Calcium chloride solutions.

$$B = 0.21, \quad \log \varepsilon_{436}^0 = 2.50.$$

7.0	0.242	0.0620	3.11	1.878	0.239	2.32
6.0	0.324	0.0724	2.85	1.595	0.125	2.04
5.0	0.436	0.0869	2.53	1.210	0.0513	1.75
4.29	0.497	0.1012	2.40	0.890	0.0245	1.53

where 550 is the limiting absorption in hydrochloric acid solutions, and the factor 18 is chosen so that putting  $[\text{Cl}^-] = 13.5$  we arrive at the found maximum absorption in the calcium chloride solutions. Substituting (22) in (16) and differentiating with regard to the chlorine ion concentration, we get

$$\frac{d \log \alpha_4}{d [\text{Cl}^-]} = \frac{d \log \varepsilon_{436}}{d [\text{Cl}^-]} + \frac{0.4343 \cdot 18}{550 - 18 [\text{Cl}^-]}. \quad (23)$$

A combination of (23) with (13) and (14) leads to the expression

$$\frac{d \log \epsilon_{436}}{d [\text{Cl}^-]} = \left( \frac{0.4343}{[\text{Cl}^-]} + B \right) (4 - \bar{n}) - \frac{0.4343 \cdot 18}{550 - 18 [\text{Cl}^-]}. \quad (24)$$

By means of (22) and (24)  $B$ ,  $\bar{n}$ , and  $\alpha_4$  are calculated from the measurements in the calcium chloride solutions as in the previous calculations. The corrected values are recorded in Table 7. It is seen that the correction results in somewhat lower values for both  $B$  and  $\bar{n}$ .

Table 7. Recalculations in the calcium chloride medium paying due regard to the change in the limiting absorption according to the expression:

$$\epsilon_{436}^0 = 550 - 18 [\text{Cl}^-]$$

a. Calculation of  $B$  ( $x = 1.26$ )

$[\text{Cl}^-]$	$\alpha_4 = \frac{\epsilon_{436}}{\epsilon_{436}^0}$	$4 - \bar{n}$	$\frac{d \log \epsilon_{436}}{d [\text{Cl}^-]}$	$\frac{-0.4343 \cdot 18}{550 - 18 [\text{Cl}^-]}$	$\frac{0.4343}{[\text{Cl}^-]}$	$B$
9.51	0.548	0.522	0.100	0.0206	0.0457	0.185
8.76	0.430	0.697	0.142	0.0199	0.0496	0.182
8.32	0.361	0.813	0.168	0.0195	0.0522	0.179
						0.182

b. Calculation of  $\bar{n}$  and  $\alpha_4$  ( $B = 0.18$ )

$[\text{Cl}^-]$	$\frac{d \log \epsilon_{436}}{d [\text{Cl}^-]}$	$\frac{-0.4343 \cdot 18}{550 - 18 [\text{Cl}^-]}$	$\frac{0.4343}{[\text{Cl}^-]}$	$\bar{n}$	$\log \epsilon_{436}$	$\alpha_4$	$\log [\text{Cl}^-] + B [\text{Cl}^-]$
7.0	0.242	0.0185	0.0621	2.93	1.878	0.178	2.11
6.0	0.324	0.0177	0.0724	2.64	1.595	0.089	1.86
5.0	0.436	0.0170	0.0869	2.30	1.210	0.0353	1.60
4.29	0.497	0.0165	0.1012	2.17	0.890	0.0164	1.40

b. Distribution of the Copper on the Different Chloro Complexes.

Fig. 5 represents a survey of the result of the investigations performed. In the lower section the formation curve for the cupric chloride system is drawn. In the more dilute range around 1 N, where the formation function is estimated on the basis of the theory for corresponding solutions from the measurements of DOEHLEMANN and FROMHERZ and SPACU and MURGULESCU (cf. p. 10), the abscissa represents the logarithm of the free



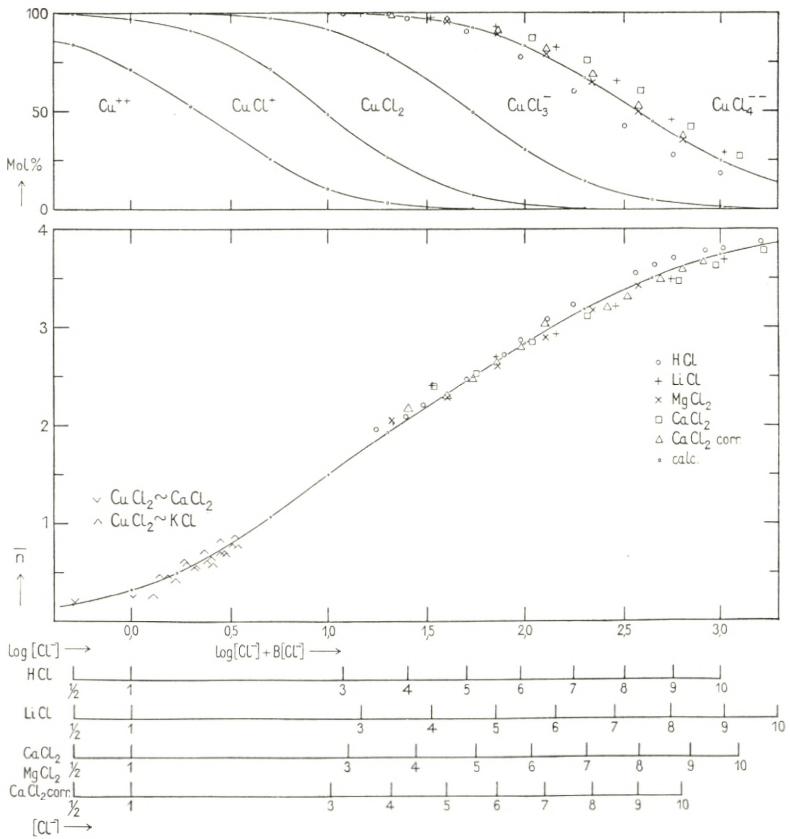


Fig. 5. Survey of the results obtained in the investigations of the cupric chloride system. The main graph shows the formation function  $\bar{n}$  as a function of  $\log [\text{Cl}^-]$  up to moderate salt concentrations, and as a function of  $\log [\text{Cl}^-] + B[\text{Cl}^-]$  at high salt concentrations. The upper part of the figure referring to the same abscissa shows the distribution of the copper on respective complexes. Finally, a number of concentration scales corresponding to each of the chlorides used are plotted below.

chlorine ion concentration. The points of this section of the curve are marked with  $\nabla$  and  $\blacktriangle$ . In the more concentrated solutions, where the  $\bar{n}$ -values are calculated according to (14) or (24),  $\log [\text{Cl}^-] + B[\text{Cl}^-]$  is plotted as abscissa, the unknown constant  $A$  in the expression for  $\log F$ , which only gives a parallel displacement of the activity scale, being put equal to 0. Putting  $A = 0$  is justified by the fact that the parts of the curve which are determined experimentally fall properly in continuation of each other. From another point of view it is most reasonable to

assume that A, corresponding to the square root term of the Debye-Hückel formula, is of the order of magnitude  $-0.5$  (cf. Fig. 3), and perhaps the whole course of the curve should be displaced correspondingly.

Below the activity scale are plotted a number of concentration scales for the chlorides used, which independent of the value chosen for A correspond directly to the values for the formation function calculated by means of (14) or (24). The  $\bar{n}$ -values of the various chloride solutions are denoted by the following signatures, *viz.* HCl  $\circ$ , LiCl  $+$ ,  $\text{MgCl}_2$   $\times$ , and  $\text{CaCl}_2$   $\square$  or  $\triangle$ , if the values are corrected for the change of absorption of the tetrachloro complex with the concentration. In the present graph it has been possible to depict the whole experimental material in one and the same curve. The points determined for hydrochloric acid fall above, and those for the other salt solutions below the curve, but the spreading is so small that it seems justified to render all the measurements by a single set of mean values for the complexity constants. On the basis of the present formation curve a set of constants has been calculated by successive approximation from a set of preliminary constants. As preliminary values for the consecutive constants the reciprocal values of  $[\text{Cl}^-]$  or  $[\text{Cl}^-] \cdot 10^{B[\text{Cl}^-]}$  at all half  $\bar{n}$ -values (see Table 8) are used. The activity correction does not give rise to any complication, since  $[\text{Cl}^-] \cdot 10^{B[\text{Cl}^-]}$  under the given assumption (8) directly replaces the ligand concentration in the previously derived formulae.<sup>1</sup>

Table 8. Calculation of a set of consecutive complexity constants corresponding to the assumption of  $A = 0$ .

$\bar{n}$	$\log [\text{Cl}^-]$ ( $F \sim 1$ )	$\frac{1}{[\text{Cl}^-]}$	$k_n = \frac{[\text{CuCl}_n^{2-n}]}{[\text{CuCl}_{n-1}^{3-n}][\text{Cl}^-]} \cdot \frac{1}{F}$
0.50	0.23	0.59	$k_1 = 0.366$
	$\log [\text{Cl}^-] + B[\text{Cl}^-]$	$\frac{1}{[\text{Cl}^-] \cdot 10^{B[\text{Cl}^-}]}$	
1.50	1.00	0.10	$k_2 = 0.114$
2.50	1.73	0.0186	$k_3 = 0.0189$
3.50	2.64	0.00229	$k_4 = 0.00315$

<sup>1</sup> Kupferammoniakverb. I, p. 18; Metal Ammine Formation in Aqueous Solution, pp. 35 ff.

From the consecutive constants the following values for the ligand effect are determined:

$$L_{1,2} = 0.08, \quad L_{2,3} = 0.43 \quad \text{and} \quad L_{1,4} = 0.35.$$

It is seen that the mean value  $L = 0.29$  is just of the order of magnitude assumed in the calculation of the constant  $B$ . By means of the estimated constants, the percentage distribution of the respective complexes is calculated with rounded-off values for  $[\text{Cl}^-] \cdot 10^{\text{B}[\text{Cl}^-]}$  (or in the more dilute range  $[\text{Cl}^-]$ ) and is represented graphically in the upper section of Fig. 5. The graph permits a direct reading of the percentages of the various complexes present in any solution. Thus, in a 4 N hydrochloric acid solution with  $\bar{n} = 2.05$  there are 2 per cent.  $\text{Cu}^{++}$ , 18 per cent.  $\text{CuCl}^+$ , 52 per cent.  $\text{CuCl}_2$ , 25 per cent.  $\text{CuCl}_3^-$ , and 2 per cent.  $\text{CuCl}_4^{--}$ .

The points drawn around the curve defining the range of existence of the tetrachloro complex are calculated directly from the optical measurements by means of (16). The same signature is used as in the lower part of the figure, and it appears that the points fall nicely around the calculated mean curve. The agreement at low chlorine ion concentrations does not appear from the figure, but Table 9 shows that it is still fairly good in 3 N chloride solutions.

Table 9.

	3 N HCl		3 N LiCl		3 N KCl
$\log \epsilon_{436}$	0.566		0.42		0.24
$\log [\text{Cl}^-] + B[\text{Cl}^-]$	1.08		1.17		
	found	calc.	found	calc.	found
Mol % $\text{CuCl}_4^{--}$ = 100 $\alpha_4$	0.67	0.40	0.59	0.65	0.32

In Table 9 are given the values for  $\alpha_4$  in 3 N hydrochloric acid and 3 N lithium chloride, both those found directly and those calculated by means of the complexity constants. For the sake of comparison, a value for  $\alpha_4$  in 3 N potassium chloride is also recorded. This value is determined on the basis of SPACU and MURGULESCU'S measurements of the extinction coefficient in solutions with  $[\text{Cl}^-] = 3$  (see Table 3), the limiting extinction



coefficient being put at 550. The corresponding value for  $\alpha_4$  in potassium chloride solutions with  $[\text{Cl}^-] = 1$  is as low as  $5.6 \cdot 10^{-5}$  (extrapolated from SPACU and MURGULESCU's measurements by means of Fig. 2), but nevertheless this value is much higher than the value  $\alpha_4 = 0.18 \cdot 10^{-5}$  calculated from the estimated formation constants, disregarding any activity correction. The discrepancy might be due to the assumption that the tetrachloro complex is not the only complex absorbing in the blue Hg-line at an  $\alpha_4$  considerably below 0.01. Ordinary cupric chloride with two molecules of crystal water is undoubtedly a dichloro compound<sup>1</sup>, and the fact that this salt is of a faint blue-green colour<sup>2</sup> indicates that the dichloro complex, and probably also the trichloro complex, have a not quite negligible absorption in blue light. The discrepancy may, however, also be due to the fact that the calculated value for  $\alpha_4$  is too low, because the activity constant A was set equal to 0. If  $A = -0.5$  (cf. p. 32) we arrive at about three times higher values for the consecutive constants  $k_3$  and  $k_4$ . It is more difficult to predict the influence on  $k_1$  and  $k_2$ , since the first part of the formation curve (Fig. 5) plotted against the chlorine ion concentration is not quite correct, either. After a displacement of the activity scale, the two sections of the curve no longer are in continuation of each other; in this connection it should, however, be taken into consideration that the  $\bar{n}$ -values which are determined from corresponding solutions containing potassium chloride and calcium chloride, are probably too low. At least, the use of hydrochloric acid or lithium chloride obviously results in higher  $\bar{n}$ -values (cf. p. 39). If all the consecutive constants of Table 8 are multiplied by  $10^{0.5}$ , the same distribution of complexes is obtained at high chlorine ion concentrations, since the displacement of the activity scale just corresponds to the change of the constants. However, this does not apply beyond the concentration range where  $\log F$  varies linearly with the chlorine ion concentration. If we put  $\log F$  in a 1 N chloride solution equal to  $-0.2$  (cf. Fig. 3), and using the constants corresponding to  $A = -0.5$ , we find  $\alpha_4$  to assume the value  $2.1 \cdot 10^{-5}$

<sup>1</sup> According to an X-ray examination by HARKER (Z. Krist. A **93** (1936) 136) the cupric chloride dihydrate is a trans-diaquo dichloro compound with four ligands in a plane square configuration round the cupric ion.

<sup>2</sup> Cf. J. BJERRUM, Kemisk Maanedstidsskrift **26** (1945) 29.

in moderate agreement with the directly determined and probably too high value  $5.6 \cdot 10^{-5}$ .

The conclusion to be drawn from the above discussion is that the consecutive activity constants for the cupric chloride system presumably lie somewhere between the constants which correspond to the two assumptions  $A = 0$  and  $A = -0.5$ , *i. e.*

$$k_1 \lesssim 1, \quad k_2 \approx 0.1 - 0.4, \quad k_3 \approx 0.02 - 0.06, \quad k_4 \approx 0.003 - 0.01.$$

### c. The Order of Magnitude of the Temperature Effect.

On heating, blue cupric chloride solutions turn green, and the minimum solubility of cupric chloride in hydrochloric acid at  $0^\circ \text{C}$ . is found at a much higher hydrochloric acid concentration (about  $8 \text{ N}^1$ ) than corresponds to the formation curve valid at room temperature. Qualitatively, this shows that the complex formation increases with increasing temperature. More quantitative information may be obtained in connection with the temperature coefficients  $\frac{\Delta \log \varepsilon_{436}}{\Delta t^\circ}$  recorded in Table 4.

In blue light the tetrachloro complex solely determines the absorption, and the temperature coefficients corrected for the temperature dependence of the limiting absorption must, therefore, mainly be due to changes in the concentration of this complex. Consequently, we may put

$$\frac{\Delta \log \varepsilon_{436} - \Delta \log \varepsilon_{436}^\circ}{\Delta t^\circ} \approx \frac{d \log \alpha_4}{dT}. \quad (25)$$

In the range  $\bar{n} \approx 2$ , the change in concentration of the tetrachloro complex is of the same order of magnitude as that in the corresponding complexity constant

$$k_3 k_4 = \frac{[\text{CuCl}_4^{--}]}{[\text{CuCl}_2][\text{Cl}^-]^2}.$$

Thus we have

$$\left( \frac{d \log \alpha_4}{dT} \right)_{\bar{n}=2} \approx \frac{d \log k_3 k_4}{dT} = 0.4343 \frac{\Delta H}{RT^2}, \quad (26)$$

<sup>1</sup> According to ENGEL, Ann. chim. phys. [6] 17 (1889) 350.

where  $\Delta H$  denotes the increase in heat content for the reaction



In the range in question ( $\bar{n} \cong 2$ ,  $[\text{Cl}^-] \cong 4$ )  $\frac{\Delta \log \varepsilon_{436}}{\Delta t^\circ}$  was determined in both hydrochloric acid and magnesium chloride solutions (cf. Table 4) and in both cases the corrected temperature coefficient may be put at 0.012. Applying this value,  $\Delta H$  turns out to be 4.8 kcal.

STACKELBERG and FREYHOLD<sup>1</sup> carried out some thermochemical measurements of the heat of reaction on mixing 0.2 molar cupric sulphate with 1 to 3 molar sodium chloride solutions; to judge from these measurements the increase in heat content during the reaction  $\text{Cu}^{++} + \text{Cl}^- \rightarrow \text{CuCl}^-$  is about 1.2 kcal. or considerably less than the average value per chlorine ion in reaction (27).

## 6. On the Auto Complex Formation in Concentrated Cupric Chloride Solutions.

### a. Transference Number of the Cupric Ion.

In concentrated cupric chloride solutions, the cupric ion migrates towards the anode and, according to quantitative experiments by KOHLSCHÜTTER<sup>2</sup> and DENHAM,<sup>3</sup> the cupric ion in such solutions shows even a considerably negative transference number. This is *a priori* surprising, because the formation function in pure cupric chloride solutions is necessarily below 2, from which it follows that the sum of the concentrations of the copper cations  $[\text{Cu}(\text{H}_2\text{O})_4^{++}] + [\text{Cu}(\text{H}_2\text{O})_3\text{Cl}^+]$  is higher than the corresponding sum of the copper anions:



That the transference number nevertheless is negative may

<sup>1</sup> Stackelberg and Freyhold, Z. Elektrochem. **46** (1940) 128.

<sup>2</sup> KOHLSCHÜTTER, Ber. deutsch. chem. Ges. **37** (1904) 1160.

<sup>3</sup> DENHAM, Z. physik. Chem. **65** (1909) 641; WATKINS and DENHAM, J. Chem. Soc. **115** (1919) 1269.



most naturally be explained by assuming that the cations transport more water than do the anions. The aquo cupric ion and the monochloro cupric ion contain more water of constitution than the complex anions; moreover, cations are more hydrated than anions. In the author's opinion, this may explain the negative transference number in concentrated cupric chloride solutions, where the quantity of water bound to the complexes is considerable, relative to the total amount of water.<sup>1</sup>

#### b. Estimation of the Formation Function and the Distribution of Complexes.

In order to estimate the tetrachloro complex content and the magnitude of the formation function, the light absorption of the blue Hg-line was measured for a number of cupric chloride solutions of different concentrations. The measurements were performed by means of the König-Martens spectrophotometer and are given in Table 10. The extinction of the most concentrated solutions was measured in the 2 cm tubes with inserted 1.9 cm glass cylinders, a combination which by gauging with a spherometer showed a layer thickness of 0.0950 cm.

Table 10. Molar extinction coefficients of some cupric chloride solutions.

$$\lambda = 436 \text{ m}\mu, t = 20-22^\circ.$$

$C_{\text{CuCl}_2}$ .....	1.20	1.60	1.92	2.42	2.88	3.60
$\epsilon_{436}$ .....	0.249	0.564	1.15	2.04	3.41	6.23
$\log \epsilon_{436}$ .....	-0.604	-0.249	0.061	0.310	0.533	0.795

The measurements recorded in Table 10 are represented graphically in Fig. 6 and here they are compared with SPACU and MURGULESCU'S measurements of some more dilute cupric chloride solutions. It is seen that  $\log \epsilon_{436}$  increases continuously with the cupric chloride concentration, more slowly, however, with increasing concentration.

Applying (6) or (16), the degree of formation of the tetrachloro complex may be calculated on the basis of the material

<sup>1</sup> Cf. SILLÉN and ANDERSSON, *Svensk kemisk Tidskrift* **55** (1943) 13.

given in Table 10, and by means of this quantity we may also calculate the formation function, as the relation between  $\bar{n}$  and  $a_4$  is exclusively determined by the ligand effect or, in other words, by the relative magnitude of the consecutive constants. Consequently, it is all the same whether the calculation is carried through with the set of constants corresponding to  $A = 0$  or to  $A = -0.5$ . Table 11 shows the result of such a calculation for three cupric chloride solutions.

In the calculation the limiting extinction coefficient is put at 550. For purposes of comparison, the table moreover contains the values for the formation function determined by comparing the pure cupric chloride solutions with corresponding mixed

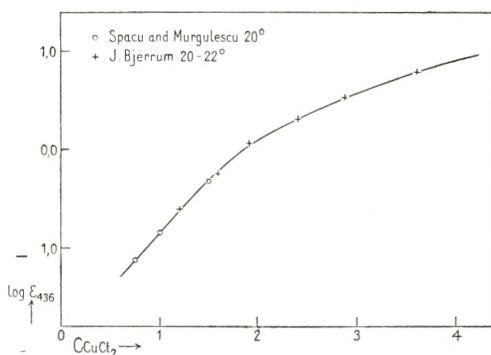


Fig. 6. Some light absorption measurements of pure cupric chloride solutions in the blue Hg-line.

Table 11. Values for the formation function in some cupric chloride solutions estimated in different ways.

$C_{\text{CuCl}_2}$	$\log \epsilon_{436}$	$a_4$	$\bar{n}$ (calc. from $a_4$ )		$\bar{n}$ (HCl)		$\bar{n}$ (LiCl)		$\bar{n}$ (CaCl <sub>2</sub> )	
			sp.	col.	sp.	col.	sp.	col.		
1.62	-0.21	0.00112	1.29	—	0.67	—	0.58	—	0.44	—
2.98	0.566	0.0067	1.75	0.99	—	0.92	—	0.78	—	
4.06	0.92	0.0151	1.98	1.13	1.21	1.05	1.04	0.93	0.92	

solutions containing hydrochloric acid, lithium- or calcium chloride. The  $\bar{n}$ -values recorded are calculated either by means of the extinction curves of Fig. 4 (the columns sp.) or on the basis of a colorimetric titration (the columns col.). The latter values originate from the author's previous paper<sup>1</sup>). The spectroscopic-

<sup>1</sup> D. Kgl. Danske Vidensk. Selskab, Mat.-fys. Medd. **21**, No. 4 (1944) 10.

ally and the colorimetrically determined values are in pretty good agreement, but otherwise the  $\bar{n}$ -values are greatly dependent on the method and the chloride used for their determination. In this connection, the values of the formation function rendered in Tables 2 and 3 should be kept in mind; these values are presumably somewhat less dependent on the chloride used, because of the lower copper concentration and because (Table 3) both corresponding solutions are mixtures.

The  $\bar{n}$ -values calculated from the light absorption by means of (16) and from our knowledge of the ligand effect undoubtedly are too high (cf. the value in the 4.06 molar cupric chloride solution according to which all the chlorine is complex-bound). This must directly or indirectly be due to the high copper concentration, as the light absorption, at least in the two strongest cupric chloride solutions, is so great that we may reckon with the validity of (16) (see Table 9). It appears from the absorption spectra that the formation of polynuclear complexes plays a minor part and, hence, it is most probable that the main discrepancy between the  $\bar{n}$ -values calculated in different ways must be ascribed to the fact that in concentrated cupric chloride solutions we have a distribution of complexes which corresponds to a smaller ligand effect (greater dismutation of the intermediary complexes) than in corresponding mixtures with a low copper concentration. This explanation involves not only that the values for the formation function calculated by means of (16) and the estimated sets of constants are too high, but moreover that the values determined by means of corresponding solutions are too low.

Table 11 shows the distribution of complexes calculated for the three cupric chloride solutions; tentatively, not only  $L_{1,2}$ , but the whole ligand effect is put at 0.08 (cf. p. 33). This value, which is considerably lower than the mean value found for the mixed solutions ( $L = 0.29$ ), seems to account satisfactorily for the distribution of the complexes in the concentrated cupric chloride solutions. The calculated values for  $\alpha_4$  agree fairly well with those found experimentally and, moreover, the  $\bar{n}$ -values and the concentrations of free chlorine ion calculated from the total chlorine ion concentrations are of a reasonable order of magnitude.  $\alpha_4$  increases with a very high power of the chlorine



ion concentration (higher than  $4 - \bar{n}$ ), but this, too, is characteristic of the mixtures in the range where F begins to increase with the concentration (see p. 11 and Fig. 4).

### c. Estimation of the True Mean Activity Coefficient of the Cupric Chloride.

The curves of Fig. 3 representing the apparent activity coefficient of cupric chloride are calculated thermodynamically without taking the complex formation into consideration. For the calculation of the true mean activity coefficient of the cupric chloride  $f_{\text{CuCl}_2}^{(e)}$  we have the relation

$$\left(f_{\text{CuCl}_2}^{(e)}\right)^3 \cdot \alpha_0 \cdot C_{\text{CuCl}_2} \cdot [\text{Cl}^-]^2 = \left(\gamma_{\text{CuCl}_2}^{(e)}\right)^3 \cdot 4 C_{\text{CuCl}_2}^3, \quad (28)$$

in which  $\alpha_0 \cdot C_{\text{CuCl}_2}$  denotes the concentration of the aquo cupric ion. The values of  $\log \gamma_{\text{CuCl}_2}^{(e)}$  which may be read from Fig. 3 and the values of  $f_{\text{CuCl}_2}^{(e)}$  computed on this basis by means of (28) for the 1.62 and 2.98 molar cupric chloride solution are recorded in Table 12.

Table 12. The distribution of the complexes and the apparent and true mean activity coefficients of cupric chloride in some concentrated cupric chloride solutions.

$C_{\text{CuCl}_2}$	$\bar{n}$	$[\text{Cl}^-]$	$\alpha_0$	$\alpha_1$	$\alpha_2$	$\alpha_3$	$\alpha_4$	$\log \gamma_{\text{CuCl}_2}^{(e)}$	$\log f_{\text{CuCl}_2}^{(e)}$
1.62	0.83	1.90	0.39	0.44	0.16	0.01	$0.97 \cdot 10^{-4}$	-0.304	-0.02
2.98	1.20	2.38	0.20	0.45	0.32	0.04	$7.2 \cdot 10^{-4}$	-0.186	+0.31
4.06	1.35	2.64	0.13	0.41	0.40	0.06	$1.74 \cdot 10^{-3}$	-	-

The estimated values for  $\log f_{\text{CuCl}_2}^{(e)}$ , when compared with Fig. 3, show that the true activity coefficient is little lower than the apparent activity coefficient of the calcium chloride at the same total concentration. This is a reasonable result and agrees with our presumption that cupric chloride is a greatly hydrated salt.

## 7. Summary.

In the present paper the complex formation in solutions of cupric chloride in the absence and in the presence of other chlorides has been investigated on the basis of light absorption measurements. The main results of the work may be summarized as follows.

A. In cupric chloride solutions there are mainly mononuclear complexes, only, and the system has a formation curve of normal appearance in accordance with the characteristic coordination number four.

B. The complexity is only slight, but nevertheless it is possible, especially in more concentrated solutions, semiquantitatively to express the contents of the different complexes as a function of the chloride concentration. Exact values for the complexity constants cannot be given, but no doubt the following set of consecutive constants corresponds fairly well to the prevailing conditions  $k_1 \lesssim 1$ ,  $k_2 \approx 0.1 - 0.4$ ,  $k_3 \approx 0.02 - 0.06$ ,  $k_4 \approx 0.003 - 0.01$ .

The more special results of the investigations may be summarized as follows.

1. In blue light, the tetrachloro complex is the only cupric complex showing any measurable light absorption and, if the concentration of free chlorine ion  $[\text{Cl}^-]$  is sufficiently high ( $> 1 \text{ N}$ ), the concentration of the tetra complex can be calculated by means of the expression

$$[\text{CuCl}_4^{--}] = C_{\text{Cu}} \frac{\varepsilon_{436}}{\varepsilon_{436}^{\circ}},$$

where  $C_{\text{Cu}}$  denotes the total copper concentration,  $\varepsilon_{436}$  the extinction coefficient in the blue mercury line, and  $\varepsilon_{436}^{\circ}$  the limiting extinction coefficient at high chlorine ion concentrations.

2. The limiting absorption, *i. e.* the light absorption of the tetrachloro complex, depends to some degree on the salt concentration and on the chloride used, and  $\varepsilon_{436}^{\circ}$  assumes the following values in the respective chloride solutions:

	HCl	LiCl	MgCl <sub>2</sub>	CaCl <sub>2</sub>
$\log \varepsilon_{436}^{\circ}$	2.742	2.65	2.66	2.50

3. The formation curve of the system was calculated (1) by means of the author's optical principle, which is based upon the

supposition that solutions with the same extinction coefficient have also the same distribution of complexes, irrespective of the total concentration of metal ion and of ligand in the solutions and, (2) on the basis of the extended Bodländer formula, applying our knowledge of the change in the concentration of the tetrachloro complex.

4. For the calculation of the formation function  $\bar{n}$  in mixtures poor in copper, but with very high chloride concentrations, the following formula was used:

$$\frac{d \log \varepsilon_{436}}{d [\text{Cl}^-]} = \left( \frac{0.4343}{[\text{Cl}^-]} + B \right) (4 - \bar{n}).$$

This formula has been derived under the tacit assumption that the system in the range of concentrations  $3.5 < C_{\text{ion}} < 10-12 \text{ N}$  is ruled by only one mean activity coefficient  $F$ , which varies with the total ion normality in accordance with the expression

$$\log F = A + B \cdot C_{\text{ion}},$$

where  $A$  and  $B$  are individual constants for the different salt media.

5. In the cupric chloride system, the constant  $B$  in the expression for  $F$  was found to assume on an average the following values in the respective chloride media:

	HCl	LiCl	MgCl <sub>2</sub>	CaCl <sub>2</sub>
B	0.20	0.23	0.18	0.21 corr. 0.18

6. In pure concentrated cupric chloride solutions the dismutation of the dichloro cupric complex to the neighbouring complexes and, further, to the aquo cupric- and the tetrachloro complex to some degree depends on the copper concentration, the dismutation of the intermediary complexes being considerably higher than in mixed solutions poor in copper.

The author is greatly obliged to the Carlsberg Foundation for a grant which enabled Mr. PALLE ANDERSEN to carry out some of the light absorption measurements recorded in this paper.





DET KGL. DANSKE VIDENSKABERNES SELSKAB  
MATEMATISK-FYSISKE MEDDELELSER, BIND XXII, NR. 19

---

GENERAL PROPERTIES  
OF THE CHARACTERISTIC MATRIX  
IN THE THEORY  
OF ELEMENTARY PARTICLES II

BY

C. MØLLER



KØBENHAVN

I KOMMISSION HOS EJNAR MUNKSGAARD

1946

Printed in Denmark  
Bianco Lunos Bogtrykkeri A/S



## INTRODUCTION

In the first paper<sup>1)</sup> (in the following quoted as I) we especially considered those general properties of HEISENBERG's characteristic matrix  $S$  which, in all essentials, are a consequence of the connection between the matrix elements of  $S$  and the cross sections for all kinds of collisions between elementary particles. In the present paper we shall in the first place treat the question how the discrete energy values in closed stationary states of a system of elementary particles are determined by the characteristic matrix. In I it was shown that new fundamental assumptions regarding the characteristic matrix are necessary for the solution of this problem.

Besides the energy values of closed stationary states there are, however, another group of quantities which are so closely connected with the experimental data obtained in laboratories that they must be considered "observable" in any theory, viz. the decay constants for systems of particles which can emit one of the particles. An  $\alpha$ -radioactive nucleus represents a typical case of this kind. If, as claimed by HEISENBERG, the characteristic matrix is to give a complete description of all "observable" quantities for any atomic system, the energies of the particles emitted in a radioactive process as well as the decay constants of the systems must be derivable from the characteristic matrix of the system.

The clue to the solution of these problems was given by KRAMERS<sup>2)</sup>, who remarked that the Schrödinger wave function  $\psi_{W^0}$  belonging to a continuous energy value  $W^0$  in all physically important cases in ordinary quantum mechanics is an analytic function of the variable  $W^0$ . By the process of analytic continuation  $\psi_{W^0}$  may then be given an unambiguous meaning also for complex values of the variable  $W^0$  as well as

for real values  $W^0$  smaller than the minimum value  $W_m^0$  of the energy in a continuous state. In any case  $\psi_{W^0}$  will be a solution of the Schrödinger equation but it is not possible to give a physical interpretation of this solution for all values of  $W^0$ . Consider, for instance, the case of a real  $W^0 < W_m^0$ ; then the asymptotic expression of  $\psi_{W^0}$  for large values of the relative distance between the particles consists of two terms, the first of which vanishes for large distances while the other increases exponentially with increasing distance. This last term contains an eigenvalue  $S^0$  of the characteristic matrix as factor. Thus  $\psi_{W^0}$  will be an eigenfunction corresponding to a closed stationary state only for those real values of  $W^0 < W_m^0$  which make  $S^0$  equal to zero.

Therefore, in order that the energy values in closed stationary states are to be derivable from the characteristic matrix, we must assume that the characteristic matrix in all cases is an analytic function of the total kinetic energy  $W$  of the system. The energy values of the closed stationary states are then simply given by the zero points of the eigenvalue of  $S$  on the real axis in the complex  $W^0$ -plane, the eigenvalue  $W^0$  of  $W$  being regarded as a complex variable.

In the first section of the present paper the extension of the ordinary quantum mechanical transformation theory to the case of complex eigenvalues of  $W$  is treated in detail. In section 2 the asymptotic expression for the wave functions of a two particle system in the case of complex values of  $W^0$  is explicitly written down, and in section 3 the "observable" quantities of the discrete stationary systems are derived from the eigenvalues of the characteristic matrix. Since  $S$  is an invariant matrix, the treatment of the discrete states may be performed in any Lorentz frame of reference with equal ease. In section 4 a new general condition regarding the character of the zero points of  $S^0$  is derived, and the question is discussed whether it is possible from a given characteristic matrix  $S$  to construct a Hamiltonian which by means of the Schrödinger equation gives the same values for the cross sections and for the discrete energy values as those derived from the matrix  $S$ .

In section 5 it is shown that also the energy  $E$  and the decay constant  $\lambda$  of a radioactive system may be calculated

from the eigenvalues of the characteristic matrix. In fact, these quantities are given as the real and imaginary parts, respectively, of those complex values  $W^0 = E - i \frac{\lambda}{2}$  of  $W^0$  in the lower half plane for which  $S^0 = S(W^0)$  is infinite. Finally, in the last section, we shall treat a few simple familiar atomic systems by means of the characteristic matrix in order to illustrate the general theory.

It thus seems that all experimental results may be described by means of HEISENBERG'S characteristic matrix without making use of the wave functions of ordinary quantum mechanics, and the way is open for a relativistic description of atomic phenomena which does not involve the difficulties inherent in all relativistic quantum field theories of the Hamiltonian form.

---

## 1. On the Use of Complex Variables in Quantum Mechanics.

In the first place we shall treat a simple system of two spinless particles with the rest mass  $\kappa$  according to quantum mechanics. If we introduce the total momentum  $\mathbf{K}$  and the "relative" momentum  $\mathbf{k}$  defined by

$$\mathbf{K} = \mathbf{k}_1 + \mathbf{k}_2, \quad \mathbf{k} = \frac{\mathbf{k}_2 - \mathbf{k}_1}{2}, \quad (1)$$

we get for the total kinetic energy

$$\begin{aligned} W &= W_1 + W_2 = \\ &= \sqrt{\kappa^2 + \left| \frac{1}{2} \mathbf{K} - \mathbf{k} \right|^2} + \sqrt{\kappa^2 + \left| \frac{1}{2} \mathbf{K} + \mathbf{k} \right|^2}, \end{aligned} \quad (2)$$

where

$$\mathbf{n} = \frac{\mathbf{k}}{k} \quad (3)$$

is a unit vector in the direction of the relative momentum  $\mathbf{k}$ . For a given value  $\mathbf{K}'$  of the total momentum the eigenvalue



$W'$  of the total kinetic energy may take on all real values of the interval

$$W'_m < W' < \infty, \quad (4)$$

where

$$W'_m = \sqrt{(2K)^2 + |\mathbf{K}'|^2} \quad (5)$$

represents the minimum value of  $W$  attained for  $k = 0$ .

From (2) we get

$$\left. \begin{aligned} \frac{\partial W}{\partial k} &= \frac{k - \frac{1}{2}(\mathbf{K}\mathbf{n})}{\sqrt{K^2 + \left|\frac{1}{2}\mathbf{K} - k\mathbf{n}\right|^2}} + \frac{k + \frac{1}{2}(\mathbf{K}\mathbf{n})}{\sqrt{K^2 + \left|\frac{1}{2}\mathbf{K} + k\mathbf{n}\right|^2}} = \\ &= \frac{\mathbf{k}_2\mathbf{n}}{W_2} - \frac{\mathbf{k}_1\mathbf{n}}{W_1} = (\mathbf{v}_2 - \mathbf{v}_1)\mathbf{n}, \end{aligned} \right\} (6)$$

which is zero for  $k = 0$ , but positive for any other value of  $k > 0$ . Further, by solving the equation (2) with respect to the variable  $k$ , we get,

$$k = \frac{W}{2} \sqrt{\frac{W^2 - (2K)^2 - |\mathbf{K}'|^2}{W^2 - (\mathbf{K}\mathbf{n})^2}}. \quad (7)$$

If  $(\mathbf{k}'_1 \mathbf{k}'_2)$  and  $(\mathbf{K}' \mathbf{k}')$  are the representatives of the same state in two representations where the variables  $(\mathbf{k}_1, \mathbf{k}_2)$  and  $(\mathbf{K}, \mathbf{k})$  are on diagonal form, respectively, we have simply

$$(\mathbf{k}'_1 \mathbf{k}'_2) = (\mathbf{K}' \mathbf{k}'), \quad (8)$$

since the functional determinant  $\frac{\partial(\mathbf{K}', \mathbf{k}')}{\partial(\mathbf{k}'_1, \mathbf{k}'_2)} = 1$ . Furthermore, if we introduce the variables  $(x) = (\zeta, \varphi)$  defined by the equations

$$\left. \begin{aligned} (x) &= (\zeta, \varphi) \\ \zeta &= \cos \theta = n_z, \quad \varphi = \operatorname{arctg} \frac{n_y}{n_x}, \end{aligned} \right\} (9)$$

we get for the representative of the state in a  $(\mathbf{K}, W, x)$ -representation

$$(\mathbf{K}' \mathbf{k}') = \sqrt{J'}(\mathbf{K}' W' x'), \quad (10)$$

where the positive functional determinant is given by

$$A' = \frac{\partial(\mathbf{K}', W', \mathbf{x}')}{\partial(\mathbf{K}', \mathbf{k}')} = \frac{(\mathbf{v}'_2 - \mathbf{v}'_1) \mathbf{n}'}{k'^2} = \frac{1}{k'^2} \frac{\partial W'}{\partial k'} \quad (11)$$

on account of (6).

Now, if  $\mathbf{X}$  and  $\mathbf{x}$  denote the coordinates of the centre of gravity and the relative coordinates, respectively, we have

$$\left. \begin{aligned} \mathbf{X} &= \frac{\mathbf{x}_1 + \mathbf{x}_2}{2} \\ \mathbf{x} &= \mathbf{x}_2 - \mathbf{x}_1, \end{aligned} \right\} (12)$$

and, since the functional determinant  $\frac{\partial(\mathbf{X}, \mathbf{x})}{\partial(\mathbf{x}_1, \mathbf{x}_2)} = 1$ , the transformation function connecting the  $(\mathbf{X}, \mathbf{x})$ -representation with the  $(\mathbf{K}, \mathbf{k})$ -representation is identical with the function (I, 80) expressed in terms of the new variables. However, the relative coordinate vector  $\mathbf{x}$  commutes with  $\mathbf{K}$ , we may therefore also use a  $(\mathbf{K}, \mathbf{x})$ -representation and, for a suitable choice of the phases in the  $(\mathbf{K}, W, \mathbf{x})$ -representation, the transformation function connecting these two representations is simply\*

$$(\mathbf{K}'' \mathbf{x}'' | \mathbf{K}' W' \mathbf{x}') = (2\pi)^{-\frac{3}{2}} \delta(\mathbf{K}'' - \mathbf{K}') \frac{e^{i(\mathbf{x}'' \mathbf{n}') K'}}{\sqrt{A'}}. \quad (13)$$

From now on, we shall have to do exclusively with states where  $\mathbf{K}$  has a well-defined value  $\mathbf{K}^0$ . All wave-functions will thus contain a factor  $\delta(\mathbf{K}' - \mathbf{K}^0)$ , which will be omitted in the following. In the same way we shall omit the factor  $\delta(\mathbf{K}' - \mathbf{K}^0)$  occurring in all matrices like  $\psi, T, U, V$  (cf. I, 16). In the  $(\mathbf{K}, W, \mathbf{x})$ -representation the wave matrix  $\psi$ , defined by the equations (10), (15), and (16) in I, then takes the form

$$\left. \begin{aligned} (W' \mathbf{x}' | \psi | W^0 \mathbf{x}^0) &= \\ = \delta(W' - W^0) \delta(\mathbf{x}' - \mathbf{x}^0) + \delta_+(W' - W^0) (W' \mathbf{x}' | U | W^0 \mathbf{x}^0) \end{aligned} \right\} (14)$$

with

\* The variables  $x$  and  $\mathbf{x}$  should not be confused! While  $x$  denotes the angle variables (9) determining the direction of the relative momentum, the heavily printed  $\mathbf{x}$  throughout this paper denotes the coordinate vector in the relative configuration space.

$$(W' x' | U | W^0 x^0) = (W' x' | U_{\mathbf{K}^0} | W^0 x^0).$$

The function (14) is a solution of the Schrödinger equation (I, 7).

If  $\alpha = (\mathbf{K}, W, \beta)$  is a complete set of collision constants, the transformation function connecting the  $(\mathbf{K}, W, x)$ -representation with a  $(\mathbf{K}, W, \beta)$ -representation is of the form

$$(W' x' | W^0 \beta^0) = \delta(W' - W^0)(x' | \beta^0), \quad (15)$$

where

$$(x' | \beta^0) = (x' | \beta^0)_{\mathbf{K}^0, W^0} \quad (16)$$

also depends on  $\mathbf{K}^0$  and  $W^0$ . In a mixed representation we get for the representative of the wave matrix  $i\mathcal{U}$

$$\begin{aligned} & (W' x' | i\mathcal{U} | W^0 \beta^0) = \\ & = \delta(W' - W^0)(x' | \beta^0) + \delta_+(W' - W^0)(W' x' | U | W^0 \beta^0). \end{aligned} \quad \left. \vphantom{\begin{aligned} & (W' x' | i\mathcal{U} | W^0 \beta^0) = \\ & = \delta(W' - W^0)(x' | \beta^0) + \delta_+(W' - W^0)(W' x' | U | W^0 \beta^0). \end{aligned}} \right\} (17)$$

On account of the equation

$$\delta_+(W' - W^0) + \delta_-(W' - W^0) = \delta(W' - W^0), \quad (18)$$

following from (I, 14), this may be written

$$\begin{aligned} & (W' x' | i\mathcal{U} | W^0 \beta^0) = \\ & = \delta_-(W' - W^0)(x' | \beta^0) + \delta_+(W' - W^0)(W' x' | A | W^0 \beta^0), \end{aligned} \quad \left. \vphantom{\begin{aligned} & (W' x' | i\mathcal{U} | W^0 \beta^0) = \\ & = \delta_-(W' - W^0)(x' | \beta^0) + \delta_+(W' - W^0)(W' x' | A | W^0 \beta^0), \end{aligned}} \right\} (19)$$

with

$$(W' x' | A | W^0 \beta^0) = (x' | \beta^0) + (W' x' | U | W^0 \beta^0).$$

By means of the equations (23), (49), and (26) in I we get for  $W' = W^0$

$$\begin{aligned} (W^0 x' | A | W^0 \beta^0) &= \int [\delta(x' - x^0) + (x' | R | x^0)] dx^0 (x^0 | \beta^0) \\ &= \int (x' | S | x^0) dx^0 (x^0 | \beta^0) = S^0(x' | \beta^0), \end{aligned} \quad \left. \vphantom{\begin{aligned} (W^0 x' | A | W^0 \beta^0) &= \int [\delta(x' - x^0) + (x' | R | x^0)] dx^0 (x^0 | \beta^0) \\ &= \int (x' | S | x^0) dx^0 (x^0 | \beta^0) = S^0(x' | \beta^0), \end{aligned}} \right\} (20)$$

where  $S^0$  is the eigenvalue of  $S$ , corresponding to the values  $\alpha^0 = (\mathbf{K}^0, W^0, \beta^0)$  for the collision constants in the complete set.

When the equation (I, 7) is written in a mixed representation it is seen that the function



$$\psi_{\alpha^0}(W'x') = \psi_{W^0\beta^0}(W'x') = (W'x' | \psi | W^0\beta^0) \quad (21)$$

is a solution of the Schrödinger equation

$$\begin{aligned} (W^0 - W') \psi_{W^0\beta^0}(W'x') &= \\ = \int (W'x' | V | W''x'') dW'' dx'' \psi_{W^0\beta^0}(W''x'') &\end{aligned} \quad \left. \vphantom{\int} \right\} (22)$$

for all real values of  $W^0$  in the interval

$$\begin{aligned} W_m^0 < W^0 < \infty \\ W_m^0 = \sqrt{(2K)^2 + |\mathbf{K}^0|^2} \end{aligned} \quad \left. \vphantom{W_m^0} \right\} (23)$$

Until now, the variables  $W^0, W', W''$  as eigenvalues of the total kinetic energy have been considered real quantities which could take on all values of the interval (23). In what follows, this "original interval" will be denoted by the symbol  $J_1$ . Following KRAMERS' idea we shall now consider solutions of the Schrödinger equation corresponding to a complex value of the energy  $W^0$ . If all the functions occurring in (22) are analytic functions of the variables  $W^0, W', W''$ , they will have a meaning also in a certain region outside the original interval and all integral relations, such as the "Schrödinger equation" (22), will hold also in this extended region. From now on, the "eigenvalues"  $W^0, W', W''$  of  $W$  will be regarded as complex variables, while the eigenvalues of  $\mathbf{K}, x, \beta \dots$  in general are real variables as before.

Now, we shall first give a meaning to the functions  $\delta_{\pm}(W' - W^0)$  occurring in (14) for complex values of  $W'$  and  $W^0$ . In the original interval  $J_1$  these functions are defined by (I, 14), and the integral  $\int f(W') \delta_{\pm}(W' - W^0) dW'$  is understood to mean the Cauchy principle value of the integral extended from  $W_m^0$  to  $\infty$ . If  $f(W')$  is an analytic function these integrals, as mentioned by HEISENBERG, are equal to the complex integrals

$$\int_{C_{\pm}(W^0)} \frac{\pm f(W') dW'}{2\pi i (W' - W^0)},$$

where the paths of integration  $C_+(W^0)$  and  $C_-(W^0)$  are two curves consisting of the portions of the real axis joining the

points  $(W_m^0, W^0 - \varepsilon)$  and  $(W^0 + \varepsilon, +\infty)$  and of small semi-circles with centre in  $W^0$  and radius  $\varepsilon$  below and above the real axis, respectively. The curves  $C_{\pm}(W^0)$  may, of course, be arbitrarily deformed inside the region of the  $W'$ -plane, where the integrand is analytic.

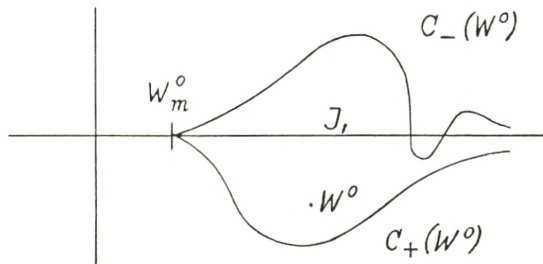


Fig. 1.

If  $W^0$  has a complex value, we may now define the functions  $\delta_{\pm}(W' - W^0)$  by the equations

$$\int_{C_{\pm}(W^0)} f(W') \delta_{\pm}(W' - W^0) dW' = \pm \int_{C_{\pm}(W^0)} \frac{f(W') dW'}{2\pi i (W' - W^0)}, \quad (24)$$

$$\int_{C_{\pm}(W^0)} \delta_{\pm}(W^0 - W') f(W') dW' = \pm \int_{C_{\pm}(W^0)} \frac{f(W') dW'}{2\pi i (W^0 - W')}, \quad (25)$$

where the paths of integration  $C_{+}(W^0)$  and  $C_{-}(W^0)$  are two curves connecting the points  $W_m^0$  and  $\infty$  in such a way that  $W^0$  lies to the left of  $C_{+}(W^0)$  but to the right of  $C_{-}(W^0)$ . Further,  $C_{+}$  and  $C_{-}$  must be chosen such that  $f(W')$  is analytic at all points on the curves and inside the region bounded by the curves  $C_{\pm}$  and  $J_1$  (see Fig. 1). Strictly speaking, the functions  $\delta_{+}$  and  $\delta_{-}$  thus have a rigorous meaning only when they appear as a factor in an integrand, just as in the case of real  $W'$  and  $W^0$ . For  $W^0 \prec J_1$  ( $W^0$  inside  $J_1$ ) the equations (24) and (25) are easily seen to be in accordance with the definitions (I, 14).

By means of (24), the equation (25) may be written

$$\begin{aligned} \int_{C_{\pm}(W^0)} \delta_{\pm}(W^0 - W') f(W') dW' &= \mp \int_{C_{\mp}(W^0)} \frac{f(W') dW'}{2\pi i (W' - W^0)} = \\ &= \int_{C_{\mp}(W^0)} f(W') \delta_{\mp}(W' - W^0) dW'. \end{aligned} \quad (26)$$

This result, which holds for an arbitrary (analytic) function  $f$ , can be expressed by the equation

$$\delta_{\pm}(W^0 - W') = \delta_{\mp}(W' - W^0). \tag{27}$$

Further, we may define the functions  $\delta(W' - W^0)$  and  $\delta(W^0 - W')$  by the equations

$$\left. \begin{aligned} \int f(W') \delta(W' - W^0) dW' &= \int \delta(W^0 - W') f(W') dW' = \\ &= \int_{C(W^0)} \frac{f(W') dW'}{2\pi i (W' - W^0)} = f(W^0), \end{aligned} \right\} \tag{28}$$

where  $C(W^0)$  is a contour encircling the point  $W^0$  in the counter-clockwise sense in such a way that  $f(W')$  is analytic at any point inside  $C$ . From (24) we then get

$$\left. \begin{aligned} \int f(W') [\delta_{+}(W' - W^0) + \delta_{-}(W' - W^0)] dW' &= \\ = \int_{C(W^0)} \frac{f(W') dW'}{2\pi i (W' - W^0)} = \int f(W') \delta(W' - W^0) dW', \end{aligned} \right\} \tag{29}$$

a result which may be expressed by the equation

$$\delta_{+}(W' - W^0) + \delta_{-}(W' - W^0) = \delta(W' - W^0) = \delta(W^0 - W'). \tag{30}$$

In the same sense we have, according to (24), (25), and (28),

$$\left. \begin{aligned} 2\pi i (W' - W^0) \delta_{+}(W' - W^0) &= -2\pi i (W' - W^0) \delta_{-}(W' - W^0) = 1 \\ (W' - W^0) \delta(W' - W^0) &= 0, \end{aligned} \right\} \tag{31}$$

just as in the case of real arguments.

Now, let  $f(W')$  be an arbitrary analytic function originally given in the interval  $J_1$  and defined in a larger region  $\Omega$  of the  $W'$ -plane by the process of analytic continuation. In the following,  $\Omega$  will be a common notation for the regions where the functions considered are analytic.  $\Omega$  may very well contain singular points where the functions have poles of any order. The extension of the region  $\Omega$  will thus depend on the kind of



function considered. By the "adjoint" function  $f(W)^\dagger$  we mean that (uniquely determined) analytic function, which in  $J_1$  is identical with the conjugate complex function  $f(W)^*$ . Outside  $J_1$  the functions  $f^\dagger$  and  $f^*$  will not be identical and the regions  $\Omega$ , where the functions  $f$  and  $f^\dagger$  are analytic, generally will also not be identical. The functions  $f$  and  $f^\dagger$  will be identical only if  $f$  is real in the original interval. In particular, we have

$$W^\dagger = W'. \quad (32)$$

Let  $g_\pm(W^0)$  be the functions connected with  $f$  by the equations

$$g_\pm(W^0) = \int f(W') \delta_\pm(W' - W^0) dW'. \quad (33)$$

For  $W^0 \prec J_1$  we then, according to (I, 14) and (24) have,

$$\begin{aligned} g_\pm(W^0)^* &= \left\{ \int_{W_m^0}^{\infty} f(W') \delta_\pm(W' - W^0) dW' \right\}^* = \\ &= \int_{W_m^0}^{\infty} f(W')^* \delta_\mp(W' - W^0) dW' = \mp \int_{C_\mp(W^0)} \frac{f(W')^\dagger dW'}{2\pi i (W' - W^0)}. \end{aligned}$$

By "analytic continuation" of this relation we thus get

$$g_\pm(W^0)^\dagger = \mp \int_{C_\mp(W^0)} \frac{f(W')^\dagger dW'}{2\pi i (W' - W^0)} = \int f(W')^\dagger \delta_\mp(W' - W^0) dW'. \quad (34)$$

The result of comparison of (33) and (34) may be expressed by the equations

$$\delta_\pm(W' - W^0)^\dagger = \delta_\mp(W' - W^0) = \delta_\pm(W^0 - W'), \quad (35)$$

where we have used the equations (27), also. Further, we get from (30) and (35)

$$\delta(W' - W^0)^\dagger = \delta(W' - W^0). \quad (36)$$

Consider now an arbitrary transformation function connecting two representations in the quantum mechanical transformation theory, e. g. the functions  $(W'x' | W^0\beta^0)$  in (15). Since

$(W^0 \beta^0 | W' x')$  is equal to  $(W' x' | W^0 \beta^0)^*$  for  $W'$  and  $W^0$  inside  $J_1$  we have quite generally

$$(W^0 \beta^0 | W' x') = (W' x' | W^0 \beta^0)^\dagger \tag{37}$$

for  $W'$  and  $W^0$  inside  $\Omega$ . All integral relations between these functions which hold inside  $J_1$  will hold also inside the wider region  $\Omega$ , i. e. we have e. g.

$$\int (W' \beta' | W'' x'') dW'' dx'' (W'' x'' | W^0 \beta^0) = \delta(W' - W^0) \delta(\beta' - \beta^0), \tag{38}$$

or by (15),

$$\int (\beta' | x'')_{W^0} dx'' (x'' | \beta^0)_{W^0} = \delta(\beta' - \beta^0). \tag{39}$$

If  $(W' x' | A | W^0 x^0)$  denotes the representative of an operator  $A$  in the  $(W, x)$ -representation, this function is defined for all values of  $W'$  and  $W^0$  inside  $J_1$ . Supposing that this function is an analytic function of  $W'$  and  $W^0$ , the “matrix elements”  $(W' x' | A | W^0 x^0)$  may, by the process of analytic continuation, be defined in a larger region  $\Omega$  comprising also complex values of  $W'$  and  $W^0$ . We now define the “adjoint” matrix  $A^\dagger$  by the equation

$$(W^0 x^0 | A^\dagger | W' x') = (W' x' | A | W^0 x^0)^\dagger. \tag{40}$$

For  $W'$  and  $W^0$  inside  $J_1$  the equation (40) is identical with the ordinary definition (I, 17) of the Hermitian conjugate matrix  $A^\dagger$ . For matrices of the form (I, 15) and (I, 30), i. e.

$$(W' x' | T_\pm | W^0 x^0) = \delta_\pm (W' - W^0) (W' x' | U_\pm | W^0 x^0), \tag{41}$$

we get, by (40) and (35),

$$(W' x' | T_\pm^\dagger | W^0 x^0) = \delta_\pm (W' - W^0) (W' x' | U_\pm^\dagger | W^0 \beta^0). \tag{42}$$

The ordinary rule for “matrix multiplication”

$$(W' x' | AB | W^0 x^0) = \int (W' x' | A | W'' x'') dW'' dx'' (W'' x'' | B | W^0 x^0) \tag{43}$$

may be extended to the case of complex values of the variables  $W$ . The path of integration in  $\int dW''$  may then be arbitrarily deformed inside the region  $\Omega$ . From (40) and (43) we get

$$\begin{aligned}
 (W^0 x^0 | (AB)^\dagger | W' x') &= (W' x' | AB | W^0 x^0)^\dagger = \\
 &= \int (W' x' | A | W'' x'')^\dagger dW'' dx'' (W'' x'' | B | W^0 x^0)^\dagger = \\
 &= \int (W^0 x^0 | B^\dagger | W'' x'') dW'' dx'' (W'' x'' | A^\dagger | W' x') = \\
 &= (W^0 x^0 | B^\dagger A^\dagger | W' x').
 \end{aligned}
 \tag{44}$$

Thus, the ordinary matrix rule

$$(AB)^\dagger = B^\dagger A^\dagger \tag{45}$$

is seen to hold also for the generalized matrices with complex values of the  $W$ -variables. From (34) or (35) and (42) it follows that the equation (44) is true also in the case where one of the functions, say  $(W' x' | B | W^0 x^0)$ , contains a factor  $\delta_\pm (W' - W^0)$  like the matrix  $T_\pm$  in (41).

If  $A$  is a Hermitian matrix in the original interval the equation

$$A^\dagger = A \tag{46}$$

will hold also in the larger region  $\Omega$ , i. e.  $A$  is a self-adjoint matrix. Similarly, if  $A$  is a unitary matrix in the original sense the generalized matrix will also satisfy the generalized equations

$$A^\dagger A = AA^\dagger = 1. \tag{47}$$

Thus the matrices  $\eta$  and  $S$ , connected by the equation (I, 43), will satisfy the generalized equations (46) and (47), respectively. In a representation where the collision constants  $(W, \beta)$  are diagonal we have

$$\begin{aligned}
 (W' \beta' | \eta | W^0 \beta^0) &= \eta^0 \delta(W' - W^0) \delta(\beta' - \beta^0) \\
 (W' \beta' | S | W^0 \beta^0) &= S^0 \delta(W' - W^0) \delta(\beta' - \beta^0).
 \end{aligned}
 \tag{48}$$

The "eigenvalues"  $\eta^0, S^0$  are functions of the variables  $(W^0, \beta^0)$  and they will satisfy the equations

$$\begin{aligned}
 \eta^{0\dagger} &= \eta^0 \\
 S^{0\dagger} &= \frac{1}{S^0},
 \end{aligned}
 \tag{49}$$



respectively. All matrix equations derived in I for the original region also hold in the wider region  $\Omega$ , provided, of course, that the representative of the potential energy  $V$  in the  $(W, \mathbf{x})$ -representation is an analytic function of the energy-variables in the original interval. This restriction is, however, not serious. It does not mean that the potential function in *configuration space* must be an analytic function or even a continuous function of the position coordinates. From FOURIER'S theorem it follows that, if the potential vanishes sufficiently rapidly with increasing distance of the particles, the representative of the potential energy  $V$  in momentum space will always be an analytic function of the momentum variables.

## 2. The Asymptotic Form of the Wave Functions.

We shall now consider the wave function  $\psi_{\alpha^0}(\mathbf{x}')$  in a  $(\mathbf{K}, \mathbf{x})$ -representation where  $\mathbf{x}$  is the relative coordinate vector defined by (12). Omitting again the factor  $\delta(\mathbf{K}' - \mathbf{K}^0)$ , we get from (13) and (19)

$$\left. \begin{aligned} \psi_{\alpha^0}(\mathbf{x}') &= \psi_{W^0, \beta^0}(\mathbf{x}') = (\mathbf{x}' | \psi | W^0 \beta^0) = \\ &= (2\pi)^{-\frac{3}{2}} \left\{ \int_{\bullet} \frac{e^{i(\mathbf{x}'\mathbf{n}')k}}{\sqrt{\mathcal{A}'}} dW' dx' \delta_-(W' - W^0)(\mathbf{x}' | \beta^0) \right. \\ &\quad \left. + \int \frac{e^{i(\mathbf{x}'\mathbf{n}')k}}{\sqrt{\mathcal{A}'}} dW' dx' \delta_+(W' - W^0)(W'x' | A | W^0 \beta^0), \right\} \end{aligned} \right\} (50)$$

where  $\mathbf{n}' = \mathbf{n}(\mathbf{x}')$  is the unit-vector corresponding to the values  $(\mathbf{x}')$  of the variables (9). Further,  $k' = k(\mathbf{K}^0, W', \mathbf{x}')$  is the value of  $k$  obtained from (7) by putting  $\mathbf{K} = \mathbf{K}^0$ ,  $\mathbf{n} = \mathbf{n}'$ , and  $W = W'$ , and  $\mathcal{A}' = \mathcal{A}(\mathbf{K}^0, W', \mathbf{x}')$  is the corresponding value of the functional determinant (11). Thus, using (23), we have

$$k' = \frac{W'}{2} \sqrt{\frac{W'^2 - W_m^0{}^2}{W'^2 - (\mathbf{K}^0 \mathbf{n}')^2}}. \quad (51)$$

On account of the square root occurring in the expression for  $k'$  we shall have to make a cut in the  $W'$ -plane along a

suitable curve connecting the singular point  $W_m$  and  $(\mathbf{K}^0 \mathbf{n}')$  on the real axis in order to make  $k'$  analytic and one-valued throughout the cut plane. Since we are particularly interested in the real values of  $W' < W_m^0$ , we cannot make the cut along

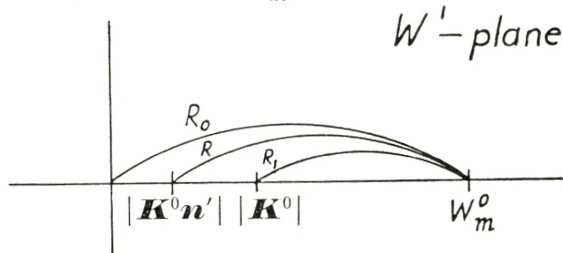


Fig. 2.

the real axis, but we can make it as close to the real axis, as we like. Putting  $U = \frac{W'^2 - W_m^{02}}{W'^2 - (\mathbf{K}^0 \mathbf{n}')^2}$  we shall define the square root of  $U$  by the equation

$$\sqrt{U} = \sqrt{\rho} e^{i \frac{\varphi}{2}} \quad (52)$$

if

$$\left. \begin{aligned} U &= \rho e^{i\varphi} \\ -\pi - \varepsilon &< \varphi < \pi - \varepsilon. \end{aligned} \right\} (53)$$

Here  $\varepsilon$  is a finite positive number which may be chosen as small as we like. This definition corresponds to a cut along the radius vector  $\varphi = \pi - \varepsilon$  in the  $U$ -plane. The corresponding cut in the  $W'$ -plane is easily seen to have the form of the curve  $R$  in Fig. 2.

Now, let  $R_0$  and  $R_1$  be the  $R$ -curves corresponding to  $|\mathbf{K}^0 \mathbf{n}'| = 0$  and  $|\mathbf{K}^0 \mathbf{n}'| = |\mathbf{K}^0|$ , respectively. Outside the region  $\omega$  circumscribed by the curves  $R_0$ ,  $R_1$  and the part of the real axis joining the points 0 and  $|\mathbf{K}^0|$ ,  $k'$  will thus, for any value of  $\mathbf{n}'$ , be an analytic and one-valued function of  $W'$ , and we shall in what follows consider such values of  $W'$ , only. If  $\varepsilon$  is made sufficiently small, the forbidden region  $\omega$  can be made as small as we like. Also the functions  $\mathcal{A}'$  and  $\sqrt{\mathcal{A}'}$  are then seen to be analytic functions of  $W'$  outside  $\omega$ .

We shall now calculate the asymptotic value of the function  $\psi_{W_0 \beta^0}(\mathbf{x}')$  in (50) for large values of the relative distance

$r' = |\mathbf{x}'| = |\mathbf{x}'_2 - \mathbf{x}'_1|$ . If we introduce the unit vector  $\mathbf{e}' = \frac{\mathbf{x}'}{r}$ , the integrals in (50) are of the form

$$X = \int e^{ir'k'(\mathbf{e}'\mathbf{n}')} f(W', x') dW' dx'. \tag{54}$$

For  $r' \rightarrow \infty$  we get, if terms of higher order in  $\frac{1}{r'}$  than the first are neglected,

$$X = \frac{2\pi}{ir'} \left\{ \int \frac{e^{ir'k'}}{k'} f(W', x') dW' - \int \frac{e^{-ir'k'}}{k'} f(W', x'_-) dW' \right\}, \tag{55}$$

where  $(x') = (\zeta', \varphi')$  are the values of the variables (9) corresponding to the direction  $\mathbf{n}' = \mathbf{e}'$ , while  $(x'_-) = (-\zeta', \varphi' + \pi)$  correspond to the opposite direction  $\mathbf{n}' = -\mathbf{e}'$ . Similarly,  $k'$  in (55) is the value of  $k'$  in (51) for  $\mathbf{n}' = \pm \mathbf{e}'$ . The equation (55) follows at once by a partial integration if we temporarily introduce  $(k', x')$  instead of  $(W', x')$  as integration variables.

Since the functions  $f$  in our case contain a factor  $\delta_{\pm}(W' - W^0)$ , we have to calculate for  $r' \rightarrow \infty$  integrals of the type

$$Y_{\pm} = \int e^{ir'k'} \delta_{\pm}(W' - W^0) g(W') dW' = \int_{C_{\pm}(W^0)} \frac{e^{ir'k'} g(W') dW'}{\pm 2\pi i (W' - W^0)}, \tag{56}$$

$$Z_{\pm} = \int e^{-ir'k'} \delta_{\pm}(W' - W^0) g(W') dW' = \int_{\pm 2\pi i (W' - W^0)} \frac{e^{-ir'k'} g(W') dW'}{\pm 2\pi i (W' - W^0)}. \tag{57}$$

Now, let  $R(z)$  and  $I(z)$  denote the real and imaginary parts of a complex number  $z$ , respectively. From the definitions (51), (52), and (53) it then follows immediately that the imaginary part of  $k'$  is positive for  $R(W') > 0$  if  $W'$  lies above the real axis and outside  $\omega$ . Further, we have  $I(k') < 0$  for  $R(W') > 0$  if  $W'$  lies below the forbidden region  $\omega$ . Let  $\Omega_+$  and  $\Omega_-$  be those parts of the region  $\Omega$  for which  $I(k')$  is positive and negative, respectively. For  $W' \in \Omega_+$  the exponential functions in (56) contain a factor  $e^{-\alpha r'}$ , where  $\alpha$  is real and positive. Those parts of the paths of integration in (56) which lie inside  $\Omega_+$  will thus give a vanishing contribution to  $Y_{\pm}$  in the limit  $r' \rightarrow \infty$ .\* Similarly, those parts of the integration curves which lie inside  $\Omega_-$  will give a vanishing contribution to  $Z_{\pm}$  for

\* Provided the interchange of the limiting process  $r' \rightarrow \infty$  and the operation of integration is allowed.



$r' \rightarrow \infty$ . If we choose the curves  $C_+$  and  $C_-$  as in Fig. 3, we get for  $r' \rightarrow \infty$  the asymptotic expressions

$$Y_{\pm} = \left\{ \begin{array}{l} \int_{C(W^0)} \frac{e^{ir'K} g(W') dW'}{2\pi i (W' - W^0)} = e^{ir'k^0} g(W^0) \\ 0, \end{array} \right\} \quad (58)$$

where  $k^0$  denotes the value of  $k'$  following from the 'theorem of conservation of energy', i. e.

$$k^0 = \frac{W^0}{2} \sqrt{\frac{W^{02} - W_m^2}{W^{02} - (\mathbf{K}^0 \mathbf{e}')^2}} \quad (59)$$

By a suitable choice of the curves  $C_+$  and  $C_-$  in (57) we similarly get the asymptotic expressions

$$Z_{\pm} = \left\{ \begin{array}{l} 0 \\ e^{-ir'k^0} g(W^0). \end{array} \right\} \quad (60)$$

Thus, by means of the equations (54)–(60) and by (20), we obtain the following asymptotic expression for the wave function (50) in the limit  $r' \rightarrow \infty$

$$\begin{aligned} \Psi_{W^0, \beta^0}(\mathbf{x}') &= (\mathbf{x}' | \Psi | W^0 \beta^0) = \\ &= \frac{(2\pi)^{-\frac{1}{2}}}{ir'k^0 \sqrt{\mathcal{A}^0}} \left\{ -e^{-ir'k^0} (x'_- | \beta^0) + e^{ir'k^0} S^0(x' | \beta^0) \right\} \end{aligned} \quad (61)$$

with

$$\mathcal{A}^0 = \mathcal{A}(\mathbf{K}^0, W^0, x') = \mathcal{A}(\mathbf{K}^0, W^0, x'_-). \quad (62)$$

For a system consisting of two particles only, we may take for the collision constants  $\beta$  the variables  $L$  and  $m$  defined by (173), (183), (163), and (160) in I, and in the following sections the symbol  $\beta$  is used simply as an abbreviation for the two quantities  $L$  and  $m$ , which have the discrete eigenvalues  $L^0 = l^0 (l^0 + 1)$ ,  $l^0 = 0, 1, 2 \dots$  and  $m^0 = -l^0, -l^0 + 1, \dots + l^0$ , respectively. Since  $I^{\mu}$  is a pseudo-four-vector the variables  $L$  and  $m$  are invariant under spatial reflections at the origin. However,  $L$  and  $m$  are invariant also under the transformation  $(x') \rightarrow (x'_-)$  or  $\mathbf{K}' \rightarrow -\mathbf{K}'$ , which corresponds to a reflection in the relative space only; for this transformation is equivalent to a permutation of the two particles, as is seen

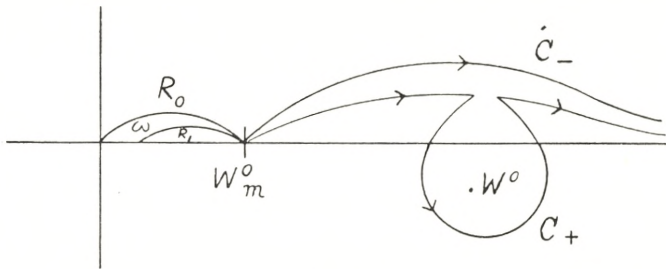


Fig. 3.

from (1), and the variables  $L$  and  $m$  are symmetrical in the particles. Thus, if  $\tau$  denotes the operator corresponding to this transformation,  $\tau$  commutes with  $L$  and  $m$  and the eigenfunctions  $(x' | l^0 m^0)$  of  $L$  and  $m$  will also be eigenfunctions of  $\tau$ . Now, since  $\tau^2 = 1$ , the eigenvalues of  $\tau$  are  $\pm 1$ , hence we get

$$\tau(x' | l^0 m^0) = (x'_- | l^0 m^0) = \pm (x' | l^0 m^0). \tag{63}$$

In the centre of gravity system the variables  $L$  and  $m$  are identical with  $M^2$  and  $M_z$ , and the functions  $(x' | l^0 m^0)$  are the usual spherical harmonics  $Y_{l^0 m^0}(\zeta', \varphi')$ . Thus we have in this frame of reference

$$(x'_- | l^0 m^0) = (-1)^{l^0} (x' | l^0 m^0). \tag{64}$$

However, since  $\tau$  commutes with the variables  $\mathbf{N}$  and  $\mathbf{M}$  defined by (132) and (139) in I,  $\tau$  is a relativistic invariant on account of (I, 135) and (I, 138), and the equations (64) will, therefore, hold in all frames of reference.

The asymptotic expression (61) for the wave function thus takes the form

$$\left. \begin{aligned} \Psi_{\alpha^0}(\mathbf{x}') &= \Psi_{W^0 l^0 m^0}(\mathbf{x}') = \\ &= \frac{(2\pi)^{-\frac{1}{2}}}{i r' k^0 \sqrt{J^0}} \left\{ e^{-i r' k^0} (-1)^{l^0+1} + e^{i r' k^0} S^0 \right\} (x' | l^0 m^0), \end{aligned} \right\} \tag{65}$$

where  $S^0 = S(\alpha^0)$ , according to (I, 185), is a function of  $K^0 = \sqrt{W^{02} - |\mathbf{K}^0|^2}$  and  $l^0$  only:

$$S^0 = S(K^0, l^0). \tag{66}$$

$\Psi_{\alpha^0}(\mathbf{x}')$  is a solution of the Schrödinger equation, i. e.  $\Psi_{\alpha^0}(\mathbf{x}')$  is an eigenfunction of the Hamiltonian  $H$ . However, since  $H$  does not commute with the variables  $L$  and  $m$ ,  $\Psi_{\alpha^0}(\mathbf{x}')$  is not

in general an eigenfunction of  $L$  and  $M$ . This is seen also from the asymptotic expression (65), since  $k^0$  and  $\mathcal{A}^0$  occurring in the factor of the eigenfunction ( $x' | l^0 m^0$ ) depend on  $(x')$ . Nevertheless, the eigenvalues  $l^0$  and  $m^0$  of the collision constants  $L$  and  $m$  may be used for labelling the eigenfunctions of  $H$  instead of the eigenvalues of a set of constants of motion which are customarily used for this purpose.

Only in the centre of gravity system, i. e. for  $\mathbf{K}^0 = 0$ , where  $L$  and  $m$  are essentially equal to  $M^2$  and  $M_z$ , respectively,  $k^0$  and  $\mathcal{A}^0$  will be independent of  $(x')$ , and  $\psi_{\alpha^0}(\mathbf{x}')$  will be an eigenfunction of  $L$  and  $m$ , also. In fact, in this case we get from (59), (23), (62), (11), and (6)

$$\left. \begin{aligned} k^0 &= \sqrt{\left(\frac{W^0}{2}\right)^2 - K^2} \\ \mathcal{A}^0 &= \frac{2}{k^0 \sqrt{K^2 + k^{02}}} \end{aligned} \right\} (67)$$

which are independent of  $(x')$ . The same is approximately true also in the 'non-relativistic' case where  $\mathbf{K}^0$  may be treated as small compared with  $W^0$ .

The adjoint wave matrix  $\psi^\dagger$  satisfies the equation

$$W \psi^\dagger - \psi^\dagger W = \psi^\dagger V, \quad (68)$$

as is seen from (I, 7) when it is noticed that  $W$  and  $V$  are self-adjoint matrices. If (68) is written in the mixed representation, we find that the adjoint wave function

$$\psi_{\alpha^0}^\dagger = \psi_{W^0 \beta^0} (W' x')^\dagger = (W' x' | \psi | W^0 \beta^0)^\dagger = (W^0 \beta^0 | \psi^\dagger | W' x') \quad (69)$$

satisfies the adjoint Schrödinger equation

$$\left. \begin{aligned} &\psi_{\alpha^0} (W' x')^\dagger (W^0 - W') = \\ &= \int \psi_{\alpha^0} (W'' x'')^\dagger dW'' dx'' (W'' x'' | V | W^0 x^0). \end{aligned} \right\} (70)$$

In the  $(\mathbf{K}, \mathbf{x})$ -representation the adjoint wave function  $\psi_{\alpha^0}(\mathbf{x}')^\dagger$  has the asymptotic form (for  $r' \rightarrow \infty$ )



$$\psi_{\epsilon^0}(\mathbf{x}')^\dagger = \frac{(2\pi)^{-\frac{1}{2}}}{-ir'k^0\sqrt{\mathcal{A}^0}} \left\{ e^{ir'k^0}(-1)^{l^0+1} + e^{-ir'k^0}S^{0\dagger} \right\} (l^0m^0 | \mathbf{x}'), \quad (71)$$

as is seen from (65) when we consider the fact that  $k^0$  and  $\sqrt{\mathcal{A}^0}$  are real for  $W^0 \prec I$ , i. e.

$$\left. \begin{aligned} k^{0\dagger} &= k^0 \\ \sqrt{\mathcal{A}^{0\dagger}} &= \sqrt{\mathcal{A}^0} \end{aligned} \right\} (72)$$

for  $W^0 \prec \Omega$ .

### 3. Determination of the Discrete Stationary States.

The function  $\psi_{\epsilon^0} = \psi_{W^0 l^0 m^0} = \psi_{W^0}$  is a solution of the Schrödinger equation (22) for all values of  $W^0$  inside  $\Omega$ , i. e. also for real values of  $W^0$  in the interval  $J_2$ , defined by

$$|\mathbf{K}^0| < W^0 < W_m^0, \quad (73)$$

provided that the region  $\Omega$ , where  $\psi_{W^0}$  is analytic, contains this interval. However,  $\psi_{\epsilon^0}$  is not an eigenfunction of  $H$ , unless  $\psi_{\epsilon^0}$  is everywhere regular, and this does not apply to all values of  $W^0$  in  $J_2$ . From the definitions (59), (52), and (53) we get for  $W^0 \prec J_2$

$$k^0 = -i|k^0| = -i \frac{W^0}{2} \sqrt{\frac{W_m^{02} - W^{02}}{W^{02} - (\mathbf{K}^0 \mathbf{e}')^2}}, \quad (74)$$

and the curled bracket in the asymptotic expression (65) becomes

$$e^{-|k^0|r'}(-1)^{l^0+1} + e^{|k^0|r'}S^0.$$

While the first term vanishes for  $r' \rightarrow \infty$ , the last term increases exponentially with  $r'$ . Hence, the condition for  $\psi_{\epsilon^0}$  being an eigenfunction is that  $S^0$  is zero and the energy values of the system in the closed stationary states are determined as the values  $W_n^0(l^0)$  of  $W^0$  inside  $J_2$ , which make  $S^0 = 0$ . They are thus determined by the equations

$$\left. \begin{aligned} S^0 &= S(K_n(l^0), l^0) = 0 \\ K_n(l^0) &= \sqrt{W_n^0(l^0)^2 - |\mathbf{K}^0|^2}, \end{aligned} \right\} (75)$$

where  $n$  is an index labelling the zero points of  $S^0$  corresponding to a fixed value of  $l^0$ . The quantity  $K_n(l^0)$  simply denotes the value of the rest mass of the system as a whole in the stationary state considered. It has a well-defined physical meaning independently of the frame of reference.

This general result from quantum mechanics may now be assumed to hold also in cases where no Hamiltonian of the system exists. Thus, in the special case of a system of two particles we shall postulate<sup>3)</sup> that *the characteristic matrix*  $S = S(\mathbf{K}, L)$  *is an analytic function of*  $\mathbf{K}$  *for all values of*  $L$  *and that the values of the rest mass*  $\mathbf{K}$  *of the system in the discrete stationary states are determined by the equation (75). The determination of the closed stationary states in the new theory may therefore be performed in any Lorentz frame of reference with equal ease. This is a particularly beautiful feature of the new theory, which is due to the extremely simple transformation properties of the characteristic matrix.*

In order to find further general conditions for the characteristic matrix we shall now return to the case where a Hamiltonian and a Schrödinger equation exist. Using (17), (16), (18), and (I, 23), (I, 26), we get for the wave function  $\psi_{\alpha^0}(W'x')$  in (21)

$$\left. \begin{aligned} \psi_{\alpha^0}(W'x') &= \psi_{W^0\beta^0}(W'x') = (W'x' | \psi | W^0\beta^0) = \\ &= (W'x' | S | W^0\beta^0) - \delta_-(W' - W^0)(W'x' | U | W^0\beta^0). \end{aligned} \right\} (76)$$

If  $W^0$  is one of the zero values  $W_n^0(l^0)$  defined by (75), we have

$$(W'x' | S | W^0\beta^0) = (W'x' | W^0\beta^0) \cdot S^0 = 0, \quad (77)$$

and if  $r = (n, l^0, m^0)$  is an index labelling the closed stationary states, we get for the normalized eigenfunction  $\psi_r(W'x')$  belonging to the discrete energy value

$$E_r = W_n^0(l^0) \quad (78)$$

the following expression:

$$\begin{aligned} \psi_r(W'x') &= N_r \cdot \psi_{W^0=E_r, \beta^0}(W'x') = \\ &= -N_r \delta_-(W' - E_r)(W'x' | U | r), \end{aligned} \quad \left. \vphantom{\psi_r(W'x')} \right\} (79)$$

where  $N_r$  is a normalization factor and

$$(W'x' | U | r) = (W'x' | U | W^0 = E_r, \beta^0). \quad (79')$$

For  $W' \prec J_1$  the difference  $W' - E_r$  is real and positive, and we have simply

$$\psi_r(W'x') = \frac{N_r}{2\pi i(W' - E_r)}(W'x' | U | r), \quad (80)$$

since the interval  $J_1$  has the character of a  $C_-(E_r)$ -curve.

The corresponding function  $\psi_r(\mathbf{x}')$  in configuration space has the asymptotic form, following from (65), (74), and (75)

$$\psi_r(\mathbf{x}') = \frac{(2\pi)^{-\frac{1}{2}} N_r}{|k_r^0| \sqrt{\mathcal{A}_r^0}} (-1)^{l^0+1} \cdot \frac{e^{-|k_r^0|r'}}{r'} (x' | l^0 m^0), \quad (81)$$

where  $k_r^0$  and  $\mathcal{A}_r^0$  are the values of  $k^0$  and  $\mathcal{A}^0$  for  $W^0 = E_r$ . The eigenfunction  $\psi_r(W'x')$  in (80) is a regular normalized solution of the Schrödinger equation (22) with  $W^0 = E_r$ .

While  $\psi_{W^0, \beta^0}$  is regular for  $W^0 = E_r$  the adjoint wave function  $\psi_{W^0, \beta^0}(W'x')^\dagger$  in (69) diverges for  $W^0 \rightarrow E_r$ . This is seen, for instance, from the asymptotic expression (71) when account is taken of the equation (49) which shows that

$$\begin{aligned} S^{0\dagger} &= \frac{1}{S^0} \rightarrow \infty \\ &\text{for} \\ &W^0 \rightarrow E_r. \end{aligned} \quad \left. \vphantom{S^{0\dagger}} \right\} (82)$$

Let us, therefore, consider the function

$$\Phi_{\alpha^0}(W'x') = S^0 \psi_{\alpha^0}(W'x')^\dagger, \quad (83)$$

which is also a solution of the adjoint Schrödinger equation (70). (The wave matrix  $S \psi^\dagger$  occurring in (83) is closely connected with



the matrix  $\Psi_-$  defined by the equations (29)–(31) in I). From (I, 10) and (I, 21) we get for  $\Psi^\dagger$  in the mixed representation

$$\left. \begin{aligned} (W^0 \beta^0 | \Psi^\dagger | W' x') = \\ (W^0 \beta^0 | 1 | W' x') + \delta_+ (W^0 - W') (W^0 \beta^0 | U^\dagger | W' x'). \end{aligned} \right\} (84)$$

Hence, on account of (27),

$$\left. \begin{aligned} \Phi_{\alpha^0} (W' x') = \\ = (W^0 \beta^0 | S | W' x') + \delta_- (W' - W^0) (W^0 \beta^0 | S U^\dagger | W' x'). \end{aligned} \right\} (85)$$

For  $W^0 = E_r = W_n(l^0)$  the first term is zero and the function

$$\Phi_r(W' x') = \Phi_{W^0=E_r, \beta^0}(W' x') = \delta_- (W' - W^0) (r | S U^\dagger | W' x') \quad (86)$$

is a regular solution of the adjoint Schrödinger equation (70). While  $(W' x' | U | W^0 \beta^0)$  was regular for  $W^0 \rightarrow E_r$ , we see that  $(W^0 \beta^0 | U^\dagger | W' x')$  diverges for  $W^0 \rightarrow E_r$ , since  $(W^0 \beta^0 | S U^\dagger | W' x') = S^0 \cdot (W^0 \beta^0 | U^\dagger | W' x')$  remains finite and  $S^0 \rightarrow 0$  for  $W^0 \rightarrow E_r$ . If  $W' \notin J_1$ , we have simply

$$\Phi_r(W' x') = -\frac{1}{2\pi i (W' - E_r)} (r | S U^\dagger | W' x'), \quad (87)$$

since the Interval  $J_1$  is a  $C_-(E_r)$ -curve. The corresponding function  $\Phi_r(x')$  in configuration space has the asymptotic form, following from (71), (49), (74), and (75),

$$\Phi_r(x') = -\frac{(2\pi)^{-\frac{1}{2}}}{|k_r^0| \sqrt{\mathcal{A}_r^0}} \cdot \frac{e^{-|k_r^0| r'}}{r'} (l^0 m^0 | x'). \quad (88)$$

Now, for  $W^0 = E_r$  we have

$$\left. \begin{aligned} (l^0 m^0 | x') &= (x' | l^0 m^0)^* \\ \sqrt{\mathcal{A}_r^0}^* &= -i \sqrt{\mathcal{A}_r^0}. \end{aligned} \right\} (89)$$

In the centre of gravity system, i. e. for  $\mathbf{K}^0 = 0$ , these relations are obviously true, since the functions  $(x' | l^0 m^0)$  in this

case are ordinary spherical harmonics  $Y_{l^0 m^0}(x') = P_{l^0}(\zeta') \frac{e^{im^0\eta'}}{\sqrt{2\pi}}$  and  $A_r^0$ , by (67), is given by

$$A_r^0 = \frac{4i}{|k_r^0| E_r}. \tag{90}$$

The second equation (89) then follows immediately from the definitions (52), (53) of the square root. Using the connection (I, 175) between the transformation functions  $(x'|l^0 m^0)$  in two different Lorentz frames of reference as well as the general definition (62), (11), and (6) for  $l_r^0$ , we may easily prove the equation (89) to hold in an arbitrary Lorentz frame.

A comparison of (88) with (81) then shows that the asymptotic expression of  $\psi_r^*$  and  $\Phi_r$  deviate only by a factor  $i(-1)^{l^0} N_r^*$ , i. e.

$$\psi_r^* = i(-1)^{l^0} N_r^* \cdot \Phi_r \tag{91}$$

for  $r' \rightarrow \infty$ . But, since both  $\psi_r^*$  and  $\Phi_r$  are solutions of the conjugate complex Schrödinger equation, (91) must hold for all values of  $r'$ . For  $W' \prec J_1$  we thus from (91) and (87) get

$$\psi_r^* = \frac{-i(-1)^{l^0} N_r^*}{2\pi i(W' - E_r)} (r|SU^\dagger|W'x'), \tag{92}$$

and from (80) and (92)

$$(W'x'|U|r)^* = i(-1)^{l^0} (r|SU^\dagger|W'x') \tag{93}$$

for  $W' \prec J_1$ .

#### 4. A New General Condition for the Characteristic Matrix.

Consider the General equation (I, 20), which holds for any form of the Hamiltonian. By means of (I, 15) and (I, 21) and by the definitions (24) and (25) the equation (I, 20) may be written in a  $(W, \beta)$ -representation as follows:

$$\left. \begin{aligned} (W' \beta' | U + U^\dagger | W^0 \beta^0) + \int_{C_-(W')} \frac{(W' \beta' | U^\dagger | W'' x'') dW'' dx'' (W'' x'' | U | W^0 \beta^0)}{2 \pi i (W' - W'')} \\ + \int_{C_+(W^0)} \frac{(W' \beta' | U^\dagger | W'' x'') dW'' dx'' (W'' x'' | U | W^0 \beta^0)}{2 \pi i (W'' - W^0)} = 0, \end{aligned} \right\} (94)$$

or

$$\left. \begin{aligned} (W' \beta' | U + U^\dagger | W^0 \beta^0) + \\ + (W' - W^0) \int_{[C_+(W^0), C_-(W')]} \frac{(W' \beta' | U^\dagger | W'' x'') dW'' dx'' (W'' x'' | U | W^0 \beta^0)}{2 \pi i (W' - W'') (W'' - W^0)} = 0. \end{aligned} \right\} (95)$$

In the last integral the path of integration in the  $W''$ -plane must be a curve which is simultaneously a  $C_+(W^0)$ -curve and a  $C_-(W')$ -curve, i. e. the points  $W^0$  and  $W'$  must lie to the left and to the right of the path, respectively. In the equation (95) as it stands we cannot, therefore, let  $W' \rightarrow W^0$ , and in a subsequent integration over  $W'$  the point  $W^0$  must lie to the left of the path of integration. Thus, if (95) is divided by  $2 \pi i (W' - W^0)$ , the matrix elements of  $U + U^\dagger$  will be multiplied by the function  $\delta_+(W' - W^0)$ . Hence, by (24), (25), (I, 15), and (I, 21), we get

$$(W' \beta' | T + T^\dagger + T^\dagger T | W^0 \beta^0) = 0, \quad (96)$$

or by (I, 10)

$$(W' \beta' | \psi^\dagger \psi | W^0 \beta^0) = (W' \beta' | 1 | W^0 \beta^0). \quad (97)$$

This is a new and very much simpler derivation of the equations (61) and (62) in I, holding now for all values of  $W'$  and  $W^0$  inside  $\Omega$ . For  $W'$  and  $W^0$  inside the original interval  $J_1$  the equation (97) may be written

$$\left. \begin{aligned} \int_{J_1} (W' \beta' | \psi^\dagger | W'' x'') dW'' dx'' (W'' x'' | \psi | W^0 \beta^0) = \\ = \delta(W' - W^0) \delta_{\beta', \beta^0}. \end{aligned} \right\} (98)$$

It then simply expresses the orthogonality and normalization conditions for the continuous eigenfunctions



$$\left. \begin{aligned} \psi_{E^0\beta^0}(W''x'') &= (W''x'' | \psi | E^0\beta^0) \\ \psi_{E'\beta'}(W''x'')^* &= (E'\beta' | \psi^\dagger | W''x'') \end{aligned} \right\} (99)$$

of the Hamiltonian.

We shall now see that the equation (95) (or (97)) contains the orthogonality conditions (I, 72) for the discrete eigenfunctions, too. Let us multiply (95) by  $\frac{S'}{W' - W^0}$  and afterwards let  $W' \rightarrow W_n(l') = E_r$ ,  $W^0 \rightarrow E^0$ , where  $E_r$  is one of the values of  $W' \prec J_2$  which make  $S' = 0$ , while  $E^0 \prec J_1$ . Then we get

$$\left. \begin{aligned} &\frac{(r | SU^\dagger | E^0\beta^0)}{E_r - E^0} + \\ \int_{J_1} \frac{(r | SU^\dagger | W''x'') dW'' dx'' \delta_+(W'' - E^0) (W''x'' | U | E^0\beta^0)}{E_r - W''} &= 0 \end{aligned} \right\} (100)$$

$r = (n, l', m')$ .

By (92), (99), and (14) this may be written

$$\int_{J_1} \psi_r^*(W'x') dW' dx' \psi_{E^0\beta^0}(W'x') = 0, \tag{101}$$

which is the second equation (I, 72). Further, since

$$\int_{[C_+(W^0), C_-(W')] } dW'' = \int_{C_-(W^0, W')} dW'' + \int_{C(W^0)} dW'', \tag{102}$$

where  $C_-(W^0, W')$  is a path with both  $W^0$  and  $W'$  to the right and  $C(W^0)$  is a contour encircling the point  $W^0$  in the counter-clockwise sense, the equation (95) after multiplication with  $S'$ , may be written

$$\left. \begin{aligned} &S'(W'\beta' | U | W^0\beta^0) + (W'\beta' | SU^\dagger | W^0\beta^0) S^0 + \\ + (W' - W^0) \int_{C_-(W^0, W')} \frac{(W'\beta' | SU^\dagger | W''x'') dW'' dx'' (W''x'' | U | W^0\beta^0)}{2\pi i (W' - W'')(W'' - W^0)} &= 0. \end{aligned} \right\} (103)$$

Here, we have used the relations

$$\begin{aligned} & \int (W' \beta' | U^\dagger | W^0 x'') dx'' (W^0 x'' | U | W^0 \beta^0) = \\ & = \int (W' \beta' | U^\dagger | W'' x'') dW'' dx'' (W'' x'' | R | W^0 \beta^0) = \\ & = (W' \beta' | U^\dagger R | W^0 \beta^0) = (W' \beta' | U^\dagger | W^0 \beta^0) R^0 \end{aligned}$$

and  $S^0 = 1 + R^0$  following from (23) and (26) in I.

If  $W' \rightarrow E_r$  and  $W^0 \rightarrow E_s$  with  $E_r \neq E_s$ , we have  $S' \rightarrow 0$ ,  $S^0 \rightarrow 0$ , and, on account of (80) and (92), (103) becomes

$$\int_{J_1} \psi_r^* (W' x') dW' dx' \psi_s (W' x') = 0 \quad (104)$$

in accordance with the first equation (I, 72).

For  $E_r = E_s$  a closer investigation is necessary. Since  $W^0$  and  $W'$  lie on the same side of the path of integration in (103), we can here let  $W' \rightarrow W^0$  and we get, first

$$\delta_{\beta', \beta^0} \cdot S^0 [R^0 + R^{0\dagger} (1 + R^0)] = 0,$$

or

$$S^{0\dagger} S^0 = 1 + R^0 + R^{0\dagger} + R^{0\dagger} R^0 = 1,$$

i. e. the equation (49). Further, if we differentiate (103) with respect to  $W'$  and afterwards let  $W' \rightarrow E_r$  and  $W^0 \rightarrow E_s$  with  $E_r = E_s$ ,  $r = (n', \beta') = (n', l', m')$ ,  $s = (n^0, \beta^0) = (n^0, l^0, m^0)$ , we get

$$\left. \begin{aligned} & - \frac{dS(K_r, l^0)}{dK_r} \cdot \frac{E_r}{K_r} \cdot \delta_{\beta', \beta^0} = \\ & = 2\pi i \int_{J_1} \frac{(r | SU^\dagger | W' x') dW' dx' (W' x' | U | S)}{(2\pi i)^2 (W' - E_r) (W' - E_s)} \end{aligned} \right\} \quad (105)$$

since  $S' = S^0 = 0$  and  $R^0 = -1$  for  $W' = E_r = E_s = W^0$ . On account of (80) and (92) this may be written

$$\left. \begin{aligned} \int_{J_1} \psi_r^* (W'x') dW' dx' \psi_s (W'x') = \\ = \frac{(-1)^l N_r^* N_r}{2\pi} \cdot \frac{E_r}{K_r} \cdot \frac{dS(K_r, l^0)}{dK_r} \cdot \delta_{rs} \end{aligned} \right\} (106)$$

Thus (106) together with (104) is identical with the first equation (I, 72) if we put

$$|N_r|^2 = 2\pi (-1)^l \cdot \frac{K_r}{E_r} \frac{1}{\frac{dS(K_r, l^0)}{dK_r}}, \quad r = (n, l^0, m^0). \quad (107)$$

Since  $S_r = S(K_r, l^0)$  does not depend on  $m^0$ ,  $N_r$  is a function of  $n$  and  $l^0$  only. Further, since  $K_r$ ,  $E_r$  and  $|N_r|^2$  are real and positive quantities,  $\frac{dS_r}{dK_r}$  must be real and satisfy the general condition

$$(-1)^l \frac{dS_r}{dK_r} = (-1)^l \cdot \frac{dS(K_r, l^0)}{dK_r} > 0. \quad (108)$$

The inequality (108) represents a *new general condition for the characteristic matrix* which holds in quantum mechanics independently of the form of the Hamiltonian and which may, therefore, be supposed to hold also in the new theory even in cases where no Hamiltonian of the system exists. The condition (108) implies that the zero points of the eigenvalues of  $S$  in the interval  $J_2$ , which are defined by (75), have the multiplicity one, i. e. in the neighbourhood of  $K_r$  the function  $S(K^0, l^0)$  has the form

$$S(K^0, l^0) = a_r (K^0 - K_r), \quad (109)$$

where

$$a_r = \frac{dS_r}{dK_r} \neq 0$$

is a real positive or negative number, according as  $l^0$  is even or odd, respectively.



If  $S_1$  is a unitary matrix satisfying all the general conditions of a characteristic matrix, in particular the condition (108),  $S_1$  defines a certain atomic system. The matrix  $S_2 = S_1^\dagger$  is then also a unitary invariant matrix, but in general it will not satisfy the condition (108) and therefore may not always be taken as a characteristic matrix. However, if  $S_2$  satisfies all the general conditions, it defines a new atomic system which may be called the 'adjoint' system. Since  $R_2 = S_2 - 1 = S_1^\dagger - 1 = R_1^\dagger$ , all cross-sections in the two adjoint systems are equal, but the two systems will have no closed stationary states which are identical, since  $S_1$  and  $S_2$  can have no common zero points.

By use of the equation (I, 26), the 'condition of completeness' (Vollständigkeitsrelation) (I, 74) of the eigenfunctions of the Hamiltonian may be written

$$(W'x' | T + T^\dagger + TT^\dagger | W''x'') + \sum_r \psi_r(W'x') \psi_r(W''x'')^* = 0, \quad (110)$$

where the variables  $W'$  and  $W''$  are values of the original interval  $J_1$ . By means of (80), (92), and (107) the sum in (110) becomes

$$\left. \begin{aligned} \sum_r \psi_r(W'x') \psi_r(W''x'') &= \sum_r \frac{(W'x' | U | r)(r | U^\dagger | W''x'')}{2\pi i (W' - E_r)(E_r - W'')} \cdot \frac{S_r}{\frac{dS_r}{dE_r}} \\ &= \sum_{\beta^0} \int_{C(0)} \frac{(W'x' | U | W^0\beta^0) dW^0 (W^0\beta^0 | U^\dagger | W''x'')}{(2\pi i)^2 (W' - W^0)(W^0 - W'')}, \end{aligned} \right\} (111)$$

where the path of integration  $C(0)$  in the  $W^0$ -plane is a series of contours encircling in a counter-clockwise sense all the zero points (75) of  $S^0$  in such a way that the integrand has no singularities inside  $C(0)$ . Here, we have used CAUCHY'S theorem and the fact that  $S^0$  in the neighbourhood of any zero point  $W^0 = E_r$  is of the form

$$S^0 = \frac{dS_r}{dE_r} (W^0 - E_r).$$

If we multiply (110) by  $2\pi i (W' - W'')$ , we get, by means of (111),

$$\left. \begin{aligned} & (W'x' | U + U^\dagger | W''x'') + \\ & + (W' - W'') \sum_{\beta^0} \int_{[C_+(0, W'') C_-(W')] } \frac{(W'x' | U | W^0\beta^0) dW^0 (W^0\beta^0 | U^\dagger | W''x'')}{2\pi i (W' - W^0)(W^0 - W'')} = 0, \end{aligned} \right\} (112)$$

where the path of integration is a  $C_+$ -curve for all the zero points and for the point  $W''$  and, simultaneously, a  $C_-$ -curve for the point  $W'$ . The equation (112) is a general condition for the matrix  $U$ , holding in quantum mechanics for any system and for all values of  $W'$  and  $W''$  inside  $\Omega$ . (112) has a similar form as the equation (95).

We shall now discuss the question how far the atomic system is defined in the quantum mechanical sence, if only the characteristic matrix  $S$  is given. Assuming that the given matrix  $S$  satisfies all the general conditions (I, 27), (I, 28), and (108), we can try to find a matrix  $U$  which satisfies the general equations (95) and (112), and which, further, is connected by the given matrix  $R = S - 1$  by the equation (I, 23). If we have found such a matrix  $U$ , we can define a wave matrix  $\Psi$  by (I, 10) and (I, 15). Furthermore, we can define a set of functions  $\Psi_r$  by (80), where  $r$  is an index enumerating the zero points of the eigenvalues of  $S$ , and  $N_r$  may be taken as the square root of the right hand side of (107). The functions  $\Psi_r$  together with the functions (99) are then the eigenfunctions of a 'Hamiltonian'  $H$  defined by

$$\left. \begin{aligned} & (W'x' | H | W''x'') = \\ & = \sum_{\beta^0} \int (W'x' | \Psi | E^0\beta^0) E^0 dE^0 | E^0\beta^0 | \Psi^\dagger | W''x'') + \\ & \quad + \sum_r \Psi_r(W'x') E_r \Psi(W''x'')^* \end{aligned} \right\} (113)$$

with the discrete eigenvalues  $E_r = W_n^0(I^0)$  given by (75) and the continuous eigenvalues  $E^0$  in the interval  $J_1$ , i. e.  $W_m^0 < E^0 < \infty$ . If the operator (113) is used as Hamiltonian in a Schrödinger equation, we get the same result as regards the 'observable' quantities of HEISENBERG as that following directly from the given  $S$ -matrix. However, if there is a solution at all of the equations (95), (112), and (I, 23) for the matrix  $U$ , it is easily seen that there are many solutions. This means that there are

many Hamiltonians (113) which give the same result as regards the 'observable' quantities of HEISENBERG, but the wave functions corresponding to the different Hamiltonians will only be identical for large distances apart of the particles and they will, thus, in general lead to different results regarding, for instance, the probability of the particles being in small distances from each other.

To see this, let us consider the simple case where the eigenvalues of  $S$  have no zero points in  $J_2$ , which means that the system has no closed stationary states. In this case the equations (95) and (112), expressing the orthogonality properties and the completeness of the eigenfunctions, may be expressed in terms of the wave matrix  $\Psi$  by the simple matrix equations

$$\left. \begin{aligned} \Psi^\dagger \Psi &= 1 \\ \Psi \Psi^\dagger &= 1 \end{aligned} \right\} \quad (114)$$

showing that the wave matrix  $\Psi$  is a unitary matrix in this case. (Cf. (I, 62) and (I, 63)). Now, let us assume that we have found a solution of (114) of the form (I, 10)

$$\Psi = 1 + T \quad (115)$$

$$(\Psi' x' | T | W^0 x^0) = \delta_+ (W' - W^0) (W' x' | U | W^0 x^0), \quad (116)$$

where  $U$  is a matrix satisfying (I, 23), i. e.

$$\left. \begin{aligned} (W^0 x' | U | W^0 x^0) &= (x' | R | x^0) \\ R &= S - 1. \end{aligned} \right\} \quad (117)$$

The Hamiltonian (113) is then given by the matrix equation

$$H = \Psi W \Psi^\dagger. \quad (118)$$

However, the matrix

$$\check{\Psi} = \Psi A \quad (119)$$

with

$$A^\dagger A = A A^\dagger = 1 \quad (120)$$

will also satisfy (114), i. e.

$$\check{\Psi}^\dagger \check{\Psi} = \check{\Psi} \check{\Psi}^\dagger = 1. \quad (121)$$



Putting

$$A = 1 + B \tag{122}$$

we get from (120) for  $B$

$$\left. \begin{aligned} B + B^\dagger + B^\dagger B &= 0 \\ B^\dagger B &= BB^\dagger. \end{aligned} \right\} \tag{123}$$

Since the new wave matrix must have the same form (115), (116) as the old one we have

$$\check{\Psi} = 1 + \check{T} \tag{115'}$$

$$(W'x' | \check{T} | W^0x^0) = \delta_+ (W' - W^0) (W'x' | \check{U} | W^0x^0). \tag{116'}$$

Thus, from (115'), (119), (122), and (115), we get

$$\check{T} = \check{\Psi} - 1 = \Psi A - 1 = \Psi - 1 + \Psi B = T + B + TB. \tag{124}$$

On account of (31) we then get from (116'), (116), and (25),

$$\left. \begin{aligned} &(W'x' | \check{U} | W^0x^0) = \\ &= (W'x' | U | W^0x^0) + 2\pi i (W' - W^0) (W'x' | B | W^0x^0) + \\ &+ 2\pi i (W' - W^0) \int_{C_-(W)} \frac{(W'x' | U | W''x'') dw'' dx'' (W''x'' | B | W^0x^0)}{2\pi i (W' - W'')} \end{aligned} \right\} \tag{125}$$

Now, we are only interested in those matrices  $U$  which satisfy also the equation (117) with the given  $R$ . This means that the matrix elements of  $\check{U}$  and  $U$  must be equal for  $W' = W^0$ . From (125) this is seen to be the case if  $(W'x' | B | W^0x^0)$  has no singularity for  $W' = W^0$ .

Thus, if  $B$  is any matrix whose matrix elements are finite for  $W' = W^0$  and which satisfies (123), the matrix  $\check{U}$  defined by (125) will satisfy the conditions (95), (112), and (I, 23) provided that  $U$  is a solution of these equations, and the Hamiltonian

$$\check{H} = \check{\Psi} W \check{\Psi}^\dagger \tag{118'}$$

will give the same results as regards HEISENBERG's 'observable' quantities as the Hamiltonian  $H$  defined by (118). This means that for a given characteristic matrix  $S$  we can either define a

large number of different Hamiltonians or we can find no Hamiltonian at all for the system considered.

### 5. Non-Stationary States. New General Conditions for S. Determination of the Decay Constant of Radioactive Systems by means of the Characteristic Matrix.

Since the function  $\psi_{W^0, \beta^0}(W'x')$  defined by (21) satisfies the time independent Schrödinger equation (22) for all values of  $W^0$  inside  $\Omega$ . the function

$$\psi' = \psi_{W^0, \beta^0} e^{-iW^0 t} \quad (126)$$

satisfies the time dependent Schrödinger equation

$$i \frac{\partial \psi'}{\partial t} = H \psi' \quad (127)$$

for all values of  $W^0$  inside  $\Omega$ . However, for complex values of  $W^0$  the function (126) does not correspond to a stationary state. If  $W^0$  lies in the lower half plane inside  $\Omega$ , we may write

$$W^0 = E_1 - i \frac{\lambda}{2} \quad (128)$$

with  $E_1$  and  $\lambda$  real and positive, and the time factor in (126) takes the form

$$e^{-iE_1 t - \frac{\lambda}{2} t},$$

which means that the amplitude of the wave function (126) decreases exponentially. The asymptotic expression for the wave function (126) is obtained from (65) by multiplication with  $e^{-iW^0 t}$ . In the centre of gravity system we get for this asymptotic expression

$$C \left[ \frac{e^{-ir'k^0}}{r'} (-1)^{l^0+1} + \frac{e^{ir'k^0}}{r'} S^0 \right] Y_{l^0 m^0} e^{-iW^0 t}, \quad (129)$$

where  $C$  and  $k^0$  are constants determined by (67), i. e.

$$k^0 = \frac{1}{2} \sqrt{E_1^2 - 4K^2 - \left(\frac{\lambda}{2}\right)^2} - iE_1 \lambda = k_1^0 - ik_2^0 \quad (130)$$

with  $k_1^0$  and  $k_2^0$  real and positive for  $\lambda > 0$ . The first term in (129) corresponds to an ingoing spherical wave in the relative coordinate space and the corresponding current density in the direction of increasing  $r'$  is proportional to  $-2k_1^0 e^{-2k_1^0 r'} |Y_{l^0 m^0}|^2$ . Similarly, the second term in (129) is an outgoing spherical wave with the corresponding current density equal to  $2k_1^0 e^{2k_1^0 r'} |Y_{l^0 m^0}|^2$ . From this it follows at once that

*A the eigenvalues of  $S$ , i. e.  $S^0$ , cannot have any zero points for  $W^0 \prec \Omega$  in the lower half plane, where  $E_1$  and  $\lambda$  are positive,*

for this would correspond to a state in which we have an ingoing current through the surface of a large sphere while, simultaneously, the total probability of the system, having an  $r'$  smaller than the radius of the sphere, decreases exponentially with time, the rate of decrease being determined by the damping constant  $\lambda$ . But this would obviously be in contradiction with the continuity equation following from the Schrödinger equation for any form of the Hamiltonian. Thus, the statement *A* represents a further general condition for the matrix  $S$ .

If we multiply (126) by  $S^{0\dagger} = (S^0)^{-1}$ , we get a solution of the Schrödinger equation with the asymptotic expression

$$C \left[ \frac{e^{-ir'k^0}}{r'} (-1)^{l^0+1} S^{0\dagger} + \frac{e^{ir'k^0}}{r'} \right] Y_{l^0 m^0} e^{-iW^0 t} \quad (131)$$

Considering now a value of  $W^0 \prec \Omega$  in the lower half plane for which  $S^{0\dagger} = 0$ , i. e. where  $S^0$  has a singular point, the wave function (131) corresponds to a radioactive decay process, since we have then an outgoing wave only, for large values of  $r'$ . Thus, if  $S^0$  has singular points inside  $\Omega$  in the lower half of the  $W^0$ -plane, this means that our system may undergo a radioactive disintegration. The decay constant  $\lambda$  for this process is equal to twice the numerical value of the imaginary part of the value of  $W^0$  for which  $S^0$  is singular, and the real part  $E_1$  of  $W^0$  may be interpreted as the energy of the decaying system. Of course the energy of the system is only defined with a definite uncertainty given by the constant  $\lambda$  which also determines the breadth of the energy level.

Considering now a value of  $W^0 \prec \Omega_+$ , i. e. in the upper half of the  $W^0$ -plane, where



$$W^0 = E_1 + i \frac{\lambda}{2}, \quad E_1 > 0, \quad \lambda > 0 \quad (132)$$

we find from (131) in a similar way as before

$B = S^{0\dagger}$  has no zero points, i. e.  $S^0$  has no singular points for  $W^0 \prec \Omega$  in the upper half of the  $W^0$ -plane, where the real and imaginary parts of  $W^0$  are positive;

for this would contradict the continuity equation. Further, introducing (132) into (129), we see that the zero points of  $S^0$  in the upper half plane correspond to states where we have in-going spherical waves only, and an exponential increase in time of the probability of finding the particles in distances  $r'$  smaller than a given value. These states thus correspond to processes which are the reverse of a decay process, and the imaginary parts of  $W^0$  in such cases determine the probabilities of capture processes.

Throughout this section we have worked in the centre of gravity system where the total momentum is zero. Let us now consider a decaying system from the point of view of an observer in a Lorentz system, where the total momentum is  $\mathbf{K}^0 \neq 0$ . If  $\mathbf{v}$  is the velocity of the centre of gravity system relative to the Lorentz system of the observer, the total momentum  $\mathbf{K}^0$  and energy  $E_1$  are connected with the energy  $\bar{E}_1$  in the centre of gravity system by the equations

$$\mathbf{K}^0 = \frac{\bar{E}_1 \cdot \mathbf{v}}{\sqrt{1-v^2}}, \quad E_1 = \frac{\bar{E}_1}{\sqrt{1-v^2}}. \quad (133)$$

Here, we have assumed the decay constant to be so small compared with the energy that the system has practically a well defined energy.

Now, let

$$K^0 = \sqrt{W^{02} - |\mathbf{K}|^2} = \bar{W}^0 \quad (134)$$

be a complex value of the invariant  $K^0$  for which the invariant function  $S^0 = S(K^0, l^0)$  is infinite. If we put  $W^0 = E_1 - i \frac{\lambda}{2}$  and  $\bar{W}^0 = \bar{E}_1 - i \frac{\bar{\lambda}}{2}$  the quantities  $\lambda$  and  $\bar{\lambda}$  represent the decay constants of our system in the two Lorentz systems of reference,

and the equation (134) gives, by means of (133), a relation between  $\lambda$  and  $\bar{\lambda}$ . To be consequent, we have here to neglect all terms of the order  $\lambda^2$  and  $\bar{\lambda}^2$ , thus we get, if (134) is squared,

$$E_1^2 - i\lambda E_1 - \frac{\bar{E}_1^2 v^2}{1-v^2} = \bar{E}_1^2 - i\bar{\lambda} \bar{E}_1.$$

The real part of this equation gives just the second equation (133), while the imaginary part yields

$$\lambda E_1 = \bar{\lambda} \bar{E}_1$$

i. e.

$$\lambda = \bar{\lambda} \cdot \sqrt{1-v^2},$$

which leads to the well-known formula

$$\tau = \frac{\bar{\tau}}{\sqrt{1-v^2}}, \tag{135}$$

for the lifetimes of the system in the two Lorentz frames.

### 6. Examples Illustrating the General Theory.

In all cases, where the system considered has a Hamiltonian, the characteristic matrix is determined by the solution of the Schrödinger equation and, from (65), we see that the eigenvalues  $S^0$  of  $S$  may be obtained from the asymptotic expressions for the continuous stationary solutions. In the simple case of a non-relativistic two particle system, we have in the centre of gravity system of reference the following differential equation for the radial part  $\frac{\chi(r)}{r}$  of the wave function in the relative coordinate space

$$\frac{d^2\chi}{dr^2} + \left( k^{0^2} - \kappa V(r) - \frac{l^0(l^0 + 1)}{r^2} \right) \chi = 0, \tag{136}$$

where  $V(r)$  is the interaction potential.  $k^0$  is the relative momentum given by (67)

$$k^0 = \frac{1}{2} \sqrt{W^{0^2} - (2\kappa)^2}, \tag{137}$$

which, in the non-relativistic approximation considered here, reduces to

$$k^0 = \sqrt{K \varepsilon} \quad (138)$$

with

$$W^0 = 2K + \varepsilon. \quad (139)$$

Now, let us assume that the potential  $V$  is zero for  $r > R$ , where  $R$  is a finite, but possibly very large distance. In the region  $r > R$  the solution  $\chi_{II}(r)$  of the equation (136) is given by

$$\chi_{II} = \varphi^{(2)} + \varphi^{(1)} S^0 \quad (140)$$

with

$$\left. \begin{aligned} \varphi^{(1)} &= i^{l^0+1} \sqrt{\frac{\pi}{2} k^0 r} \cdot H_{l^0+\frac{1}{2}}^{(1)}(k^0 r), \\ \varphi^{(2)} &= i^{l^0+1} \sqrt{\frac{\pi}{2} k^0 r} \cdot H_{l^0+\frac{1}{2}}^{(2)}(k^0 r). \end{aligned} \right\} \quad (141)$$

Here  $S^0 = S(W^0, l^0)$  is an eigenvalue of  $S$  which, in the centre of gravity system where  $K^0 = W^0$ , is a function of  $W^0$  and  $l^0$  only. Further,  $H^{(1)}$  and  $H^{(2)}$  are the Hankel functions of the first and second kind, respectively.  $\chi_{II}$  is obviously a solution of (136) for  $r > R$  and the asymptotic expression of  $\chi_{II}$  for  $r \rightarrow \infty$  has the right form

$$e^{-ik^0 r} (-1)^{l^0+1} + e^{ik^0 r} S^0, \quad (142)$$

as is seen if we use the known asymptotic expressions for the Hankel functions. In the region  $r < R$ , our solution may be written

$$\chi_I = C \cdot \chi(r), \quad (143)$$

where  $\chi(r)$  is a solution of (136) which is zero for  $r = 0$ , and  $C$  is a constant.

The condition that our solution and its first derivative must be continuous for  $r = R$  gives us at once two equations from which we can determine the constants  $C$  and  $S^0$ . For  $S^0$  we get

$$S^0 = S(W^0, l^0) = -\frac{\varphi^{(2)}(R) \chi'(R) - \varphi^{(2)'}(R) \chi(R)}{\varphi^{(1)}(R) \chi'(R) - \varphi^{(1)'}(R) \chi(R)}. \quad (144)$$

Let us now consider the simple case where the potential is a negative constant for  $r < a$  and zero for  $r > a$ , i. e.



$$V = \begin{cases} -V_0 = \text{constant} & \text{for } r < a \\ 0 & \text{for } r > a. \end{cases} \quad (145)$$

In this case, we may put  $R = a$  and the function  $\chi$  in (143) is simply

$$\chi(r) = \sqrt{\frac{\pi}{2}} k_1^0 r \cdot J_{l^0 + \frac{1}{2}}(k_1^0 r), \quad (146)$$

where  $J_{l^0 + \frac{1}{2}}$  is a Bessel function of the first kind and

$$k_1^0 = \sqrt{\kappa V_0 + k^0{}^2} \quad (147)$$

If we introduce (146) and (141) into (144), we get a general expression for the eigenvalues  $S^0 = S(W^0, l^0)$  and, from this, we easily obtain the matrix elements of  $S$  in a  $(W, x)$ -representation. Omitting the factor  $\delta(W' - W^0)$  we get for these matrix elements

$$(x' | S | x^0) = \sum_{l^0 m^0} (x' | l^0 m^0) S^0 (l^0 m^0 | x^0), \quad (148)$$

which directly determine all scattering cross-sections. Since

$$J_{l^0 + \frac{1}{2}}^\dagger = J_{l^0 + \frac{1}{2}}, \quad H_{l^0 + \frac{1}{2}}^{(1)\dagger} = H_{l^0 + \frac{1}{2}}^{(2)} \quad \text{and} \quad H_{l^0 + \frac{1}{2}}^{(2)\dagger} = H_{l^0 + \frac{1}{2}}^{(1)},$$

we see that the function  $S^0$ , defined by (144), (141), and (146), satisfies the equation (49), i. e.

$$S^{0\dagger} = \frac{1}{S^0}.$$

For  $l^0 = 0$  we get from (141) and (146)

$$\left. \begin{aligned} \chi &= \sin k_1^0 r \\ \varphi^{(1)} &= e^{ik^0 r}, \quad \varphi^{(2)} = -e^{-ik^0 r} \end{aligned} \right\} \quad (149)$$

and, thus, by (144)

$$S^0 = S(W^0, 0) = \frac{1 + \frac{ik^0}{k_1^0} \operatorname{tg} k_1^0 a}{1 - \frac{ik^0}{k_1^0} \operatorname{tg} k_1^0 a} \cdot e^{-2ik^0 a} \quad (150)$$

To get the energy values of the system in the closed stationary states corresponding to  $l^0 = 0$ , we have to determine the

zero points of  $S^0$  in (150) for  $W^0 < 2\kappa$ , i. e. for  $\varepsilon < 0$ . Since we have, in this case,  $k^0 = -i|k^0| = -i\sqrt{-\kappa\varepsilon}$  the zero points are determined by the equation

$$1 + \frac{|k^0|}{k_1^0} \operatorname{tg} k_1^0 \alpha = 0. \quad (151)$$

The values of  $W^0$  or  $\varepsilon$ , given by (151), are equal to the discrete eigenvalues of the Hamiltonian following from the Schrödinger equation.

It is easily verified that the function (150) satisfies the general condition (108) and the conditions  $A$  and  $B$  on p. 35 and p. 36, respectively. The function (150) has no singular points in the lower half of the  $W^0$ -plane, which means that our system cannot undergo spontaneous disintegrations. Further, we see that our system has no adjoint system, since the function  $S_2^0 = S^{0\dagger}$  does not satisfy the conditions (108).

It is now possible in an infinite number of ways to define the  $S$ -matrix of a relativistic system which, in the non-relativistic approximation, is identical with the system just considered. In the centre of gravity system of reference we may, for instance, take the  $S$ -matrix defined by (150) (or, more generally, by (141), (144), and (146)) with  $k^0$  given by (137) or with  $k^0$  equal to any other analytic function  $f(W^0)$  of  $W^0$ , which, in the non-relativistic approximation, becomes identical with (138). The only condition for  $f(W^0)$  is that  $S$  must satisfy the general conditions (108) and  $A, B$  on p. 35 and p. 36. In order to get the expression for the characteristic matrix in an arbitrary frame of reference, we have then merely to replace  $W^0$  by  $K^0$  in the expression for  $S^0$ . For a system defined in this way, it will not in general be possible to define a Hamiltonian of the system.

In his third paper in the *ZS. f. Phys.*, HEISENBERG<sup>2)</sup> considered a system defined by a characteristic matrix with the eigenvalues

$$\left. \begin{aligned} S(K^0, 0) &= \frac{1 + \frac{i\alpha}{\kappa} k^0}{1 - \frac{i\alpha}{\kappa} k^0} \\ S(K^0, l^0 > 0) &= 1, \end{aligned} \right\} \quad (152)$$

where  $\alpha$  is a constant, and

$$k^0 = f(K^0) = \kappa \sqrt{1 - \frac{4K^2}{K^0{}^2}}. \quad (153)$$

It is easily seen that this system may be obtained as a limiting case from the system defined by (144), (141), and (146) with  $k^0 = f(K^0)$  given by (153). For, if  $\alpha \rightarrow 0$  and  $V^0 \rightarrow \infty$  in such a way that

$$\lim \frac{\operatorname{tg}(\sqrt{\kappa V_0} \alpha)}{\sqrt{\kappa V_0}} = \alpha,$$

we just get the expressions (152) for the eigenvalues of the characteristic matrix. The system defined by (152) has only one bound state if  $\alpha$  is negative, and for the rest mass of the system in this state we get from (152) and (153)

$$K^0 = \frac{2\kappa}{\sqrt{1 + \frac{1}{\alpha^2}}} \quad (154)$$

Let us now consider the case of a non-relativistic system of two particles interacting according to the Coulomb law. Since our formalism applies only to cases where the potential goes to zero faster than  $\frac{1}{r}$  as  $r$  tends to infinity, we shall assume the Coulomb potential to break off at a large distance  $R$ , i. e.

$$V(r) = \begin{cases} \frac{e_1 e_2}{r} & \text{for } r < R \\ 0 & \text{for } r > R \end{cases} \quad (155)$$

where  $e_1$  and  $e_2$  are the charges of the two particles. The eigenvalues of  $S$  are again determined by (144) and (141), where  $\chi(r)$  is the ordinary solution of the Schrödinger equation for the Coulomb case. If  $R$  is chosen sufficiently large, we may use the asymptotic expressions for  $\varphi^{(1)}$ ,  $\varphi^{(2)}$  and  $\chi$  in (144) and we get<sup>4)</sup>

$$S^0 = S(W^0, l^0) = (2k^0 R)^{-\frac{2i}{k^0 a}} \frac{\Gamma\left(l^0 + 1 + \frac{i}{k^0 a}\right)}{\Gamma\left(l^0 + 1 - \frac{i}{k^0 a}\right)} \quad (156)$$



where  $k^0$  is given by (138) and (139), and

$$a = \frac{2}{\kappa e_1 e_2}. \quad (157)$$

The closed stationary states are determined by the zero points of (156) for  $k^0 = -i|k^0|$ , i. e. by the equation

$$l^0 + 1 + \frac{1}{|k^0|a} = -\nu, \quad \nu = 0, 1, 2, \dots \quad (158)$$

Thus, we have only closed stationary states if  $a$  is negative, i. e. in the case of attraction. Putting  $n = \nu + l^0 + 1 \geq l^0 + 1$ , we get for the energy  $\epsilon$  the formula

$$\epsilon^0 = -\frac{1}{\kappa a^2 n^2}, \quad (159)$$

which gives BOHR's formula for the energies of a Coulomb system if we introduce the ordinary units. The condition (108) as well as the conditions  $A$  and  $B$  in Section 5 are easily seen to be satisfied by the expression (156). The adjoint system is, in this case, simply a system in which the sign of  $a$  is reversed, i. e. where we have repulsion instead of attraction. All cross sections are identical in these two cases, but in the case of positive  $a$  we have, of course, no bound states.

As in the case of a rectangular potential well, we also here get a relativistic generalization of the non-relativistic Coulomb system by replacing  $k^0$  in (156) by an arbitrary analytic function  $f(W^0)$  which, in the non-relativistic approximation, reduces to (138), (139). In order to determine the function  $f(W^0)$  we need some information about the scattering of charged particles in the relativistic region. Now, in the approximation where  $e_1, e_2$  may be treated as small, the cross section for the scattering of fast charged particles may be determined in a relativistically invariant and unambiguous way by a simple correspondence treatment<sup>5)</sup>. The condition that our  $S$ -matrix shall give this scattering cross section in the limit of small  $e_1 e_2$  uniquely determines the function  $f(W^0)$ . The  $S$ -matrix determined in this way then represents a relativistic system which, in the non-relativistic region of velocities, corresponds to a Coulomb po-

tential and which, for large velocities but small values of  $e_1 e_2$ , gives the right scattering cross section as determined by the correspondence principle.

Finally, we shall consider a non-relativistic two particle-system with the potential

$$V = \begin{cases} 0 & \text{for } r < a \\ U = \text{const.} & \text{for } a < r < a + l \\ 0 & \text{for } r > a + l. \end{cases} \quad (160)$$

For  $l^0 = 0$ , we in this case get from (144)

$$\left. \begin{aligned} S^0 &= S(W^0, l^0 = 0) = \\ &= e^{-2ik^0(a+l)} \frac{(\gamma + 1)(ik_1^0 + ik^0) - (ik_1^0 - ik^0)e^{-2ik_1^0 l}}{(\gamma + 1)(ik_1^0 - ik^0) - (\gamma - 1)(ik_1^0 + ik^0)e^{-2ik_1^0 l}} \end{aligned} \right\} \quad (161)$$

Here,

$$\gamma = \frac{ik_1^0}{k^0} \operatorname{tg} k^0 a, \quad (162)$$

$k^0$  is given by (138), (139), and

$$k_1^0 = \sqrt{k^{02} - \kappa U}. \quad (163)$$

For real values of  $W^0 < W_m^0$ , i. e. for  $k^0 = -i|k^0|$ ,  $S^0$  has no zero points, i. e. the system has no closed stationary states. But  $S^0$  is singular for certain complex values of  $W^0$  in the lower half of the  $W^0$ -plane, i. e. for

$$\left. \begin{aligned} W^0 &= E - i \frac{\lambda}{2} \\ E &= 2\kappa + \varepsilon > 0, \quad \lambda > 0. \end{aligned} \right\} \quad (164)$$

This indicates that the system has radioactive states in which the system disintegrates. According to the general theory in Section 5, these states are determined by the singular points of (161), i. e. by the equation

$$\gamma + 1 = (\gamma - 1) \frac{ik_1^0 + ik^0}{ik_1^0 - ik^0} e^{-2ik_1^0 l}. \quad (165)$$

(165) is a complex equation from which we can determine the real and the imaginary part of  $W^0$ , i. e.  $E$  and  $\lambda$ . For  $U > \varepsilon$ , the exponential on the right hand side contains a real factor  $e^{-2\sqrt{\kappa(U-\varepsilon)}l}$  which in all practical cases is a very small quantity. This makes the solution of (165) very easy to perform. For the real part  $E$  of  $W^0$ , we get the equation

$$\operatorname{tg}(\sqrt{\kappa \varepsilon} a) = -\sqrt{\frac{U-\varepsilon}{\varepsilon}} \quad (166)$$

and for the imaginary part

$$\lambda = \frac{16 \varepsilon^{\frac{3}{2}} (U-\varepsilon)^{\frac{3}{2}}}{U^2 (1 + a \sqrt{\kappa (U-\varepsilon)})} e^{-2\sqrt{\kappa(U-\varepsilon)}l}. \quad (167)$$

The equation (166) determines the energy values  $E$  of the system in the radioactive states, while (167) gives the relation between the decay constant  $\lambda$  and the energy. Both formulae are, of course, in agreement with the results obtained from the theory of GAMOW and CONDON and GURNEY for the potential (160)<sup>6)</sup>. The expression (161) is in accordance with the conditions  $A$  and  $B$  in Section 5.

### Conclusion.

In the present paper we have investigated in detail only simple systems consisting of two particles with no possibilities for creation and annihilation processes. It has been shown that the closed stationary states may be obtained by analytic continuation of the functions  $S^0 = S(W^0, \beta^0)$  representing the 'eigenvalues' of the characteristic matrix in a representation where the variables  $(W, \beta)$  of the complete set of collision constants are on diagonal form. In this analytic continuation  $W^0$  is considered a complex variable, while the eigenvalues  $\beta^0$  of the other collision constants are regarded as real variables.



If  $S^0$  has any zero points for real values of  $W^0$  smaller than the minimum value  $W_m^0$  of the total kinetic energy, the system considered has closed stationary states with energies equal to the values of  $W^0$  in these zero points, i. e. the energy values are determined by the equation (75). These zero points have the multiplicity one in accordance with the general condition (108).

Further more, if  $S^0$  has any poles in the lower half of the  $W^0$ -plane, this indicates that the system has radioactive states with energies and decay constants determined by the real and imaginary parts of the complex values of  $W^0$  in these singular points. Finally, the functions  $S^0$  satisfy the conditions *A* and *B* in Section 5, stating that  $S^0$  has no zero points in the lower half plane and no singular points in the upper half plane inside the region  $\Omega$  where  $S^0$  is analytic.

The results obtained for two particle systems in this paper may be supposed to hold also in the general case of a many particle system with possibilities for creation and annihilation processes, the only difference probably being that the number of collision constants  $\beta$  which together with  $W$  constitute a complete set is then larger than in the case of a simple two particle system.

**Added in proof:** After completion of the present paper, S.T.MA<sup>7)</sup> has published a note in which he points out that the condition (75) for the energy values in closed stationary states is only a necessary condition, i. e. that, in some cases,  $S^0$  may have zero points which do not correspond to closed stationary states. A subsequent investigation by D. TER HAAR<sup>8)</sup> shows that, anyway in the case considered by MA, the condition (108) may be used in order to discard these redundant zeros.

---

### References.

- 1) C. MØLLER, General Properties of the Characteristic Matrix in the Theory of Elementary Particles. I. D. Kgl. Danske Vidensk. Selskab, Mat.-fys. Medd. XXIII, Nr. 1 (1945).
- 2) Cf. W. HEISENBERG, Die "beobachtbaren Grössen" in der Theorie der Elementarteilchen. III. ZS. f. Phys. in (1944).
- 3) W. HEISENBERG, *loc. cit.* 2).
- 4) W. GORDON, Ueber den Stoss zweier Punktladungen nach der Wellenmechanik. ZS. f. Phys. **48**, 180 (1928).
- 5) C. MØLLER, Ueber den Stoss zweier Teilchen unter Berücksichtigung der Retardation der Kräfte. ZS. f. Phys. **70**, 786 (1931).
- 6) See J. KUDAR, Zur Quantenmechanik der Radioaktivität. ZS. f. Phys. **53**, 96 (1929) and C. MØLLER, ZS. f. Phys. **55**, 451 (1929). The equation in the middle of p. 466 of the last mentioned paper is identical with the formula (167) in the present paper.
- 7) S. T. MA, Phys. Rev. **69**, 668 (1946).
- 8) D. TER HAAR, On the Redundant Zeros in the Theory of the Heisenberg Matrix. *Physica*, to appear presently.